Andreas Wanninger *Editor*

Evolutionary Developmental Biology of Invertebrates

Vol. 6 Deuterostomia

Springer

Evolutionary Developmental Biology of Invertebrates 6

Andreas Wanninger
Editor

Evolutionary Developmental Biology of Invertebrates 6

Deuterostomia

Springer

Editor
Andreas Wanninger
Department of Integrative Zoology
University of Vienna
Faculty of Life Sciences
Wien
Austria

ISBN 978-3-7091-1855-9 ISBN 978-3-7091-1856-6 (eBook)
DOI 10.1007/978-3-7091-1856-6

Library of Congress Control Number: 2015947925

Springer Wien Heidelberg New York Dordrecht London

Cover illustration: Scanning electron micrograph of a tornaria larva (Metschnikoff stage) of a hemichordate, the acorn worm *Balanoglossus misakiensis*. See Chapter 2 for details

Printed on acid-free paper

Springer-Verlag GmbH Wien is part of Springer Science+Business Media (www.springer.com)

Preface

The evolution of life on Earth has fascinated mankind for many centuries. Accordingly, research into reconstructing the mechanisms that have led to the vast morphological diversity of extant and fossil organisms and their evolution from a common ancestor has a long and vivid history. Thereby, the era spanning the nineteenth and early twentieth century marked a particularly groundbreaking period for evolutionary biology, when leading naturalists and embryologists of the time such as Karl Ernst von Baer (1792–1876), Charles Darwin (1809–1882), Ernst Haeckel (1834–1919), and Berthold Hatschek (1854–1941) realized that comparing ontogenetic processes between species offers a unique window into their evolutionary history. This revelation lay the foundation for a research field today commonly known as Evolutionary Developmental Biology, or, briefly, EvoDevo.

While for many of today's EvoDevo scientists the principle motivation for studying animal development is still in reconstructing evolutionary scenarios, the analytical means of data generation have radically changed over the centuries. The past two decades in particular have seen dramatic innovations with the routine establishment of powerful research techniques using micromorphological and molecular tools, thus enabling investigation of animal development on a broad, comparative level. At the same time, methods were developed to specifically assess gene function using reverse genetics, and at least some of these techniques are likely to be established for a growing number of so-called emerging model systems in the not too distant future. With this pool of diverse methods at hand, the amount of comparative data on invertebrate development has skyrocketed in the past years, making it increasingly difficult for the individual scientist to keep track of what is known and what remains unknown for the various animal groups, thereby also impeding teaching of state-of-the-art Evolutionary Developmental Biology. Thus, it appears that the time is right to summarize our knowledge on invertebrate development, both from the classical literature and from ongoing scientific work, in a treatise devoted to EvoDevo.

Evolutionary Developmental Biology of Invertebrates aims at providing an overview as broad as possible. The authors, all renowned experts in the field, have put particular effort into presenting the current state of knowledge as comprehensively as possible, carefully weighing conciseness against level of detail. For issues not covered in depth here, the reader may consult additional textbooks, review articles, or web-based resources,

particularly on well-established model systems such as *Caenorhabditis elegans* (www.wormbase.org) or *Drosophila melanogaster* (www.flybase.org).

Evolutionary Developmental Biology of Invertebrates is designed such that each chapter can stand alone, and most chapters are dedicated to one phylum or phylum-like taxonomic unit. The main exceptions are the hexapods and the crustaceans. Due to the vast amount of data available, these groups are treated in their own volume each (Volume 4 and Volume 5, respectively), which differ in their conceptual setups from the other four volumes. In addition to the taxon-based parts, chapters on embryos in the fossil record, homology in the age of genomics, and the relevance of EvoDevo for reconstructing evolutionary and phylogenetic scenarios are included in Volume 1 in order to provide the reader with broader perspectives of modern-day EvoDevo. A chapter showcasing developmental mechanisms during regeneration is part of Volume 2.

Evolutionary Developmental Biology of Invertebrates aims at scientists that are interested in a broad comparative view of what is known in the field but is also directed toward the advanced student with a particular interest in EvoDevo research. While it may not come in classical textbook style, it is my hope that this work, or parts of it, finds its way into the classrooms where Evolutionary Developmental Biology is taught today. Bullet points at the end of each chapter highlight open scientific questions and may help to inspire future research into various areas of Comparative Evolutionary Developmental Biology.

I am deeply grateful to all the contributing authors that made *Evolutionary Developmental Biology of Invertebrates* possible by sharing their knowledge on animal ontogeny and its underlying mechanisms. I warmly thank Marion Hüffel for invaluable editorial assistance from the earliest stages of this project until its publication and Brigitte Baldrian for the chapter vignette artwork. The publisher, Springer, is thanked for allowing a maximum of freedom during planning and implementation of this project and the University of Vienna for providing me with a scientific home to pursue my work on small, little-known creatures.

This volume is dedicated to the Deuterostomia, comprising the Echinodermata and Hemichordata (usually united as Ambulacraria) as well as the Cephalochordata and the Tunicata.

Tulbingerkogel, Austria Andreas Wanninger
January 2015

Contents

1 Echinodermata 1
Maria Ina Arnone, Maria Byrne, and Pedro Martinez

2 Hemichordata 59
Sabrina Kaul-Strehlow and Eric Röttinger

3 Cephalochordata 91
Linda Z. Holland

4 Tunicata 135
Alberto Stolfi and Federico D. Brown

Index 205

Echinodermata

1

Maria Ina Arnone, Maria Byrne, and Pedro Martinez

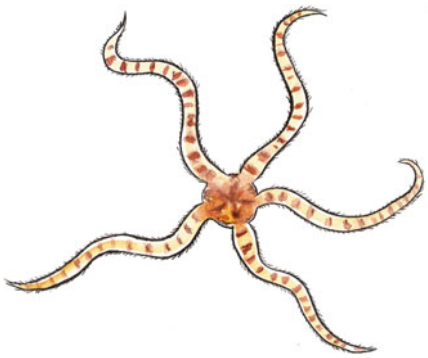

Chapter vignette artwork by Brigitte Baldrian.

M.I. Arnone
Stazione Zoologica Anton Dohrn,
Villa Comunale, Napoli 80121, Italy
e-mail: miarnone@szn.it

M. Byrne
Schools of Medical and Biological Sciences,
University of Sydney, Sydney, NSW 2006, Australia
e-mail: mbyrne@anatomy.usyd.edu.au

P. Martinez (✉)
Departament de Genètica, Universitat de Barcelona,
Av. Diagonal, 643, Barcelona 08028, Spain

ICREA (Institut Català de Recerca i Estudis
Avancats), Barcelona, Spain
e-mail: pedro.martinez@ub.edu

A. Wanninger (ed.), *Evolutionary Developmental Biology of Invertebrates 6: Deuterostomia*
DOI 10.1007/978-3-7091-1856-6_1, © Springer-Verlag Wien 2015

INTRODUCTION

The Echinoderm Body Plan

Echinoderms are a phylum of invertebrate deuterostomes that are morphologically characterized by a fivefold (pentameric) symmetric adult body plan. There are five extant subtaxa, Crinoidea (e.g., sea lilies and feather stars), Asteroidea (e.g., sea stars), Ophiuroidea (e.g., brittle stars), Echinoidea (e.g., sea urchins), and Holothuroidea (e.g., sea cucumbers) (Fig. 1.1). Studies of morphology and molecules (Janies et al. 2011) demonstrate the existence of two higher-order subphylum clades: Pelmatozoa (Crinoidea) and Eleutherozoa (the remaining classes). Echinodermata together with Hemichordata form the clade Ambulacraria (to which some authors add the enigmatic Xenacoelomorpha group). This grouping is the sister to the Chordata.

A series of autapomorphies defines the Echinodermata, including the pentameral body plan and the water vascular system (WVS). The WVS derives from the hydrocoel during develop-

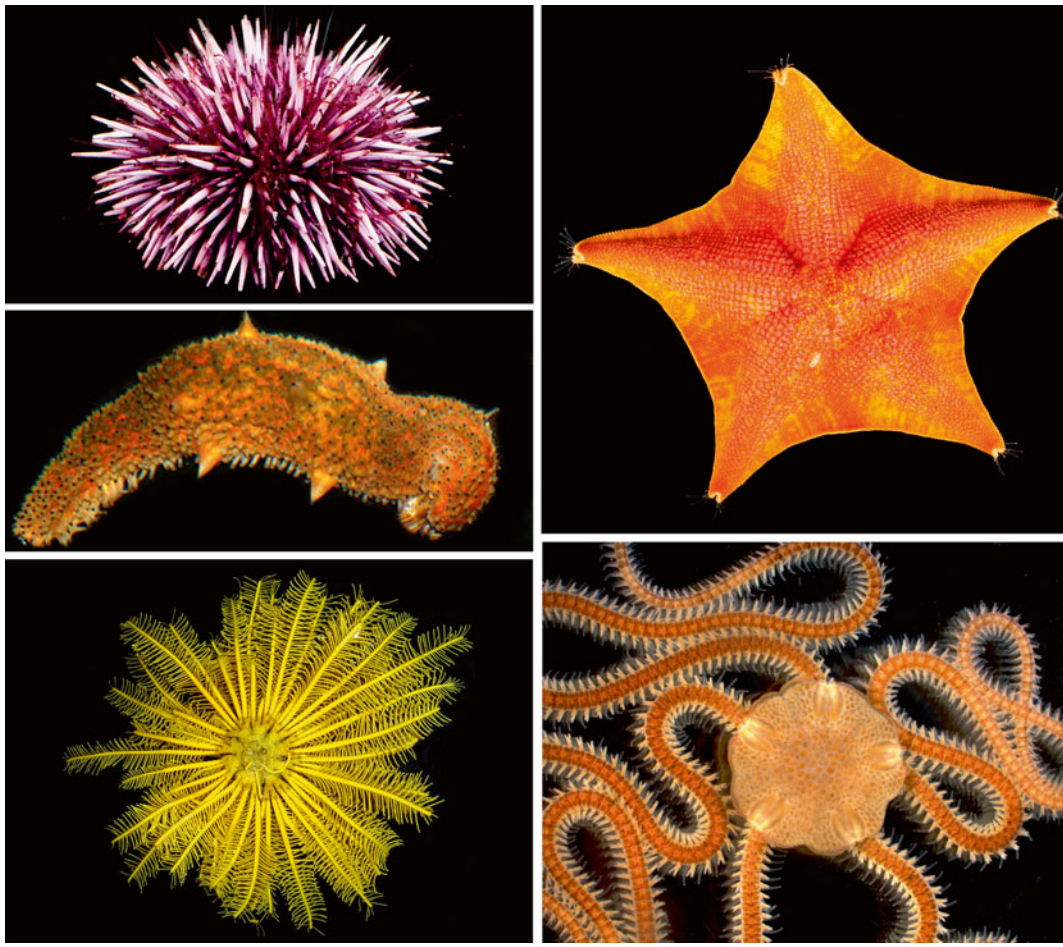

Fig. 1.1 Representatives of the five different classes of extant echinoderms. *Left column*, *top* to *bottom*: the echinoid *Strongylocentrotus purpuratus* (Courtesy of Mattias Ormestad), the holothuroid *Parastichopus parvimensis* (Courtesy of Peter Bryant), and the crinoid *Oxycomanthus intermedius* (Courtesy of Hisanori Kohtsuka). The *upper right image* shows the asteroid *Patiria miniata* (Courtesy of Mattias Ormestad) and the *lower right image* the ophiuroid *Amphiura filiformis* (Courtesy of Anna Czarkwiani and Paola Oliveri)

ment and consists of a system of fluid-filled canals and reservoirs that are used for locomotion and internal transport. Generally, the system consists of an oral water ring and five canals, each with small side branches to the locomotory tube feet and their ampullae.

The echinoderm body is formed from radial (= ambulacral) and interradial (= interambulacral) regions with the side housing the mouth defining the oral surface and the opposite side the aboral surface. The ambulacra of most echinoderms have a radial water canal which gives rise to the tube feet. The water vascular system in echinoids, asteroids, and ophiuroids opens to the exterior through the madreporite: a special skeletal plate on the body surface. In crinoids the WVS system communicates with the external medium through minute pores in the body wall. Holothuroids have an isolated WVS system that does not directly communicate with the external medium. There are a series of small madreporitic plates attached to the oral water ring. Overall, the composition of the echinoderm coelomic fluid is similar to that of seawater and also includes coelomocytes and dissolved proteins. The perivisceral coelom also functions as internal transport system. The hemal system, a diffuse extracellular matrix, is situated between the basal membranes of the epithelia of epidermis, coeloms, and gut.

The echinoderm endoskeleton is made from calcite and the skeletal elements (ossicles, plates, or spicules) have a unique porous, lattice-like organization called the stereom (another echinoderm apomorphy). Each element is a crystalline unit that develops as a stereomic structure with cells (the stroma) filling the open spaces. In echinoderms where the apposition of the plates is tight (e.g., echinoids), the body is rigid, with the plates interconnected by connective tissue ligaments. In other groups, the plates are more loosely associated and embedded in connective tissue. Some connective tissue structures are of a special type, the so-called "mutable" form, which changes their mechanical properties through nervous control (Wilkie 1984; Birenheide et al. 1998; Byrne 2001). The skeleton derives from the mesoderm and is secreted by mesenchymal cells in the embryo.

As in other "radially organized" animals, the nervous system does not coalesce into an anterior centralized structure (e.g., brain). This may allow echinoderms to interact with the environment in all directions (Yoshimura et al. 2012), although bilateral tendencies in locomotion are also reported (Ji et al. 2012). The major nerves are the circumoral nerve ring around the esophagus and the radial nerves along the ambulacra. The nerves are composed of two tissue regions: the outer ectoneural and the inner hyponeural system. A basement membrane runs between these nerve cord regions and neurons connect the two systems along the cord (Cobb 1995; Hoekstra et al. 2012). The functions of these ecto- and hyponeural systems are poorly understood. Sensory receptors are scattered around the body and are restricted to simple epithelial structures innervated by a nerve plexus of the ectoneural system (e.g., Hendler and Byrne 1987). These receptors respond to touch, chemicals, water currents, and light (see, e.g., Ullrich-Luter et al. 2011).

The gut is complete from mouth to anus, except where the anus has been lost secondarily as in all ophiuroids. No excretory systems have been described although the axial organ is usually interpreted as an excretory (although not osmoregulatory) organ. Echinoderms are mostly gonochoristic.

The origin of the germ cells in development has been determined for echinoids, where these cells have been identified to express conserved specific germ line genes – e.g., *nanos* (Wessel et al. 2013). The so-called genital rachis – associated with the hemal system – is thought to be the site where the gonads originate from. The gonads are distinct organs covered by a peritoneum on the outer side and with a germinal epithelium as the innermost tissue layer. Most taxa (exceptions being the Crinoidea and many ophiuroids) have gonoducts that open through gonopores in the genital plates, although these are not always distinctive.

The mechanisms of germ line determination in echinoderms are diverse. While echinoids appear to use an inherited mechanism of germ line formation, the sea stars appear to use an inductive mechanism (which involves the interaction with

neighboring cells; a mechanism most probably used by the majority of echinoderms; see Wessel et al. 2013; Fresques et al. 2014).

Echinoderm Diversity

Echinoderms live in all climatic zones, from shallow coastal waters to the abyssal depths. Recent surveys of the global diversity of species have revealed that there are more than 7,000 extant (nominal) species of echinoderms living on earth (Appeltans et al. 2012). All of them are marine, with most individuals, as adults, forming part of the benthos. The distribution of genera and species within the five commonly recognized echinoderm classes is shown in Table 1.1. Detailed studies of museum collections and molecular analyses suggest that there are a substantial number of species that remain undescribed; for asteroids, see (Mah and Blake 2012). The recently compiled register of marine species (Appeltans et al. 2012) estimates the total number of extant echinoderm species to range between 9,617 and 13,251.

Table 1.1 Total number of genera and species known for all echinoderm classes

Class	No. of genera	No. of nominal species described	Source of the tabulated data
Crinoidea	115	620; 623	Appeltans et al. (2012), Rouse et al. (2013)
Asteroidea	343	1,890; 1,922	Appeltans et al. (2012), Mah and Blake (2012)
Ophiuroidea	270	2,064; 2,064	Appeltans et al. (2012), Stohr et al. (2012)
Holothuroidea	200	1,250; 1,683	Smiley et al. (1991), Appeltans et al. (2012)
Echinoidea	258	999	Kroh and Mooi (2011), Appeltans et al. (2012)

The Fossil Record and the Origin of Recent Forms

More than 13,000 echinoderm species have been recognized in the fossil record with their first appearance dated to the Cambrian (Fig. 1.2). Several body sub-plans can be distinguished: pentaradiate forms (stromatocystitids and gogiids), asymmetric forms (ceratocystitid stylophorans), bilateral forms (ctenocystoids), and spiral forms (helicoplacoids) (Smith 2005). These originated in a short period of time, perhaps as short as 10–15 My, in the waters off both Gondwana and Laurentia (Smith et al. 2013). Using molecular clock estimates, Pisani and colleagues (2012) place the origin of Echinodermata (the time of the divergence between Echinodermata and their proposed sister taxon, Hemichordata) in the late Precambrian, around 570 My ago. Given that stereom skeletal elements appear in the fossil record around 525 My ago, we should assume a diversification period of some tens of My before the articulated forms were established. It is important to note that the earliest record of a stereom almost coincides with the first articulated specimens (Zamora et al. 2013).

Fossil species have been incorporated into modern phylogenetic analyses to generate a more complete picture of echinoderm evolution using different methodologies. The groundbreaking study of Smith (1984) proposes that Echinodermata comprise two major monophyletic assemblages: the eleutherozoans and the pelmatozoans (these ones represented by forms with stalks and calyces). Sumrall's cladistic analysis on a similar data set suggests an alternative arrangement (Sumrall 1996). He was the first to consider carpoids (homalozoans) as a monophyletic group and derived from modern echinoderm clades. At the same time it was considered that the variety of symmetries existing in the Cambrian is due to paedomorphic reductions from a pseudofivefold symmetric ancestor (Sumrall and Wray 2007). More recently, David and Mooi (1998) and David and colleagues (2000) have suggested another alternative topology, introducing blastozoans, a subphylum that includes all brachiole-bearing forms (i.e., eocrinoids). Importantly,

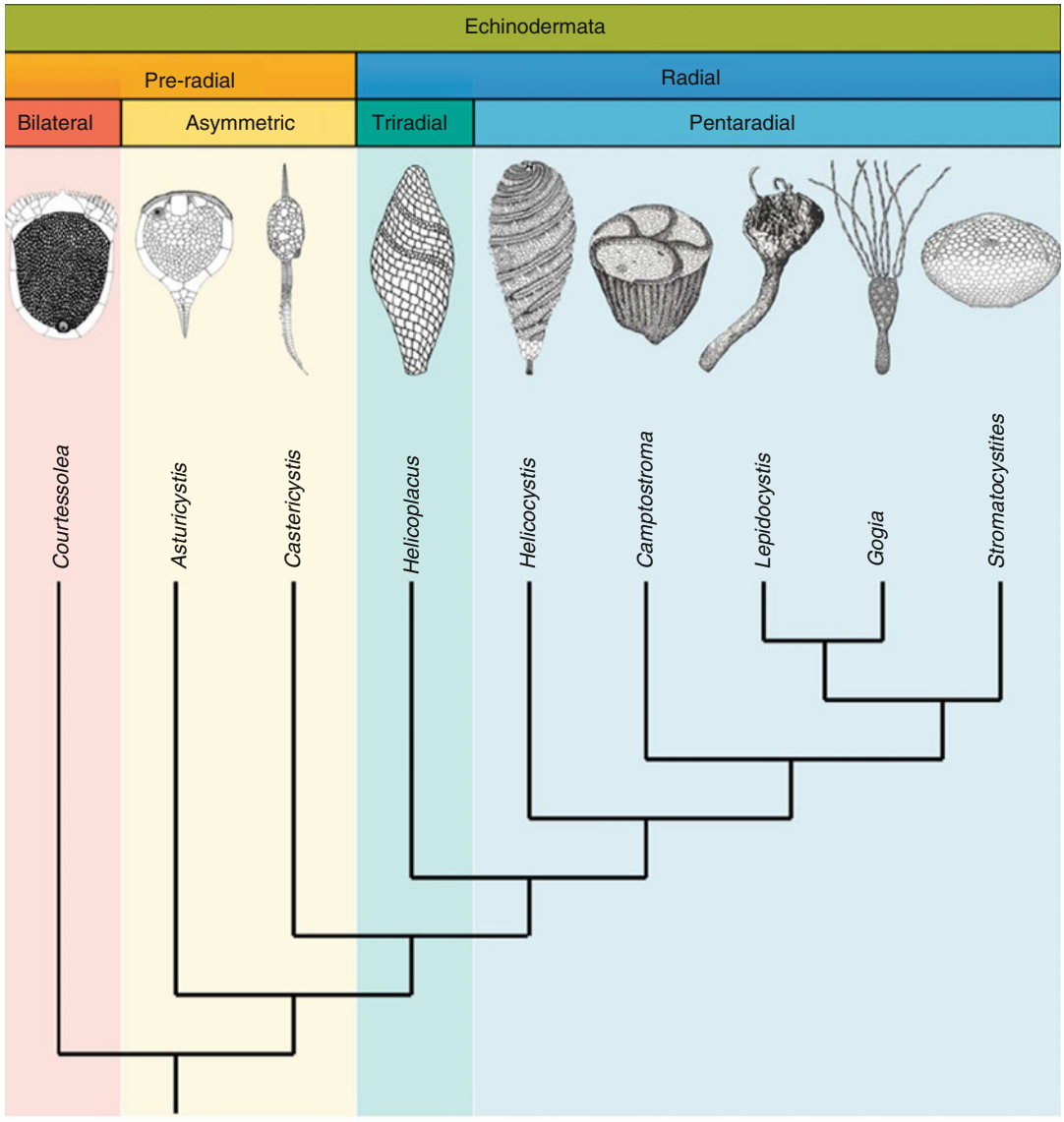

Fig. 1.2 A phylogenetic tree showing various Cambrian echinoderms, including the early bilateral representative *Courtessolea* and the most primitive pentaradial form *Helicocystis* (Figure taken from Smith and Zamora (2013)©)

they specifically propose that edrioasteroids would represent good proxies for the earliest echinoderms. A recent hypothesis suggests that the bilateral echinoderm Ctenoimbricata would represent the plesiomorphic condition for echinoderms (Zamora et al. 2012). This is based on the ontogeny and sister group relationships of modern echinoderms that suggest a bilateral species at the base of the echinoderm tree. Ctenocystoids would represent a next step, some of them having retained the primitive condition of the group while others became slightly asymmetric. In this scenario, the cinctans and solutes were more derived forms and represent the asymmetric condition before the appearance of radial forms. Radial echinoderms started with the helicoidal three ambulacra-bearing helicoplacoids. Pentaradial echinoderms also appeared in the Cambrian represented by edrioasteroids and some blastozoan groups.

Among the Paleozoic fossils, four groups of non-pentameric forms, the "homalozoans," have been at the center of intense, sometimes bitter, debate concerning the origin of a phylum related to the Echinodermata, the Chordata. The position and nature of some echinoderm structures, such as mouth, anus, or the ambulacra, have been used by many authors as arguments to suggest that homalozoans were stem taxa to all the chordates (Jefferies 1968) or early echinoderms (Ubaghs 1975; Parsley 1991). Most modern authors tend to align themselves with this latter position (Ruta 1999; Smith 2008).

However, as it happens for other fossil groups, the debates still revolve around the placement of a few key fossil groups, for instance, the carpoids within the subphylum Homalozoa. While some authors regard some of these groups as primitive, others consider them to be secondarily derived.

All extant echinoderms are derived from a few taxa that survived the Permo-Triassic extinction event. This has been clearly established for the crinoids, asteroids, and echinoids. However, all of these originated in the early Ordovician. Molecular clock analysis has allowed to estimate the times of divergence for the different classes, ranging from 509 My for the divergence of crinoids to 480 My for the eleutherozoan echinoderms (Pisani et al. 2012). The phylogenetic relationships among all extant echinoderm classes have been the subject of debate for many years. While there is consensus concerning the position of Crinoidea as the sister group to the remaining echinoderms (Eleutherozoa), there are clearly divergent opinions regarding the interrelationships of the remaining taxa. While some molecular analyses have suggested a clade that includes ophiuroids + echinoids + holothuroids (Littlewood et al. 1997; Pisani et al. 2012), there is an alternative view, supported mostly by comparative morphologists and paleontologists, which assumes a close association between asteroids and ophiuroids (Mooi and David 2000; Janies 2001). These two hypotheses are known as the "Cryptosyringida" and "Asterozoa-Echinozoa" hypothesis, respectively (Fig. 1.3).

More, and probably different, data sets are needed to resolve disputes regarding the relationships. It has become clear that the results that lead to the establishment of specific relationships are highly dependent on the choice of parameters and methods (Janies et al. 2011). Interestingly, a very recent multigene analysis (219 genes from all echinoderm classes) using Bayesian methodologies and dealing with some older methodological biases seems to clearly support Asterozoa (Telford et al. 2014). The clarification of the internal phylogeny of Echinodermata is of key relevance, since it will provide important insights into the evolutionary history of both the adult and the larval forms.

Life History Diversity, Larval Forms, and Evolution of Development

Most echinoderms spawn freely with fertilization occurring in the water column. Development proceeds through a dispersive larva, although a few species brood their embryos. Species that have small eggs (approx. <150 μm diameter) develop through feeding (planktotrophic) larvae. In contrast, species with large eggs (approx. >300 μm diameter) have nonfeeding (lecithotrophic) larvae fully provisioned by the egg (Raff and Byrne 2006). The feeding planktotrophic larva is considered to be a plesiomorphic character for modern echinoderms (Strathmann 1985; Smith 1997; McEdward and Miner 2001; Raff and Byrne 2006). Possession of a larval phase is suggested to have arisen through intercalation between the gastrula and juvenile life phases in an ancestral form (Sly et al. 2003). The feeding bipinnaria larvae of asteroids and the auricularia larvae of holothuroids are very similar to the tornaria larva of the Hemichordata (see Chapter 2). These larval forms – the so-called dipleurula-type larvae – are considered to represent the basal-type larva for the Ambulacraria (Peterson et al. 2000b; Raff and Byrne 2006).

Planktotrophic larvae feed on phytoplankton and the ciliary bands that loop around the body are used for capturing food and for locomotion (Strathmann 1985). Evolution of a large egg freed larvae from the necessity to feed, resulting in the reduction and loss of superfluous feeding structures (Raff and Byrne 2006). As a result, lecithotrophic echinoderm larvae lack a functional

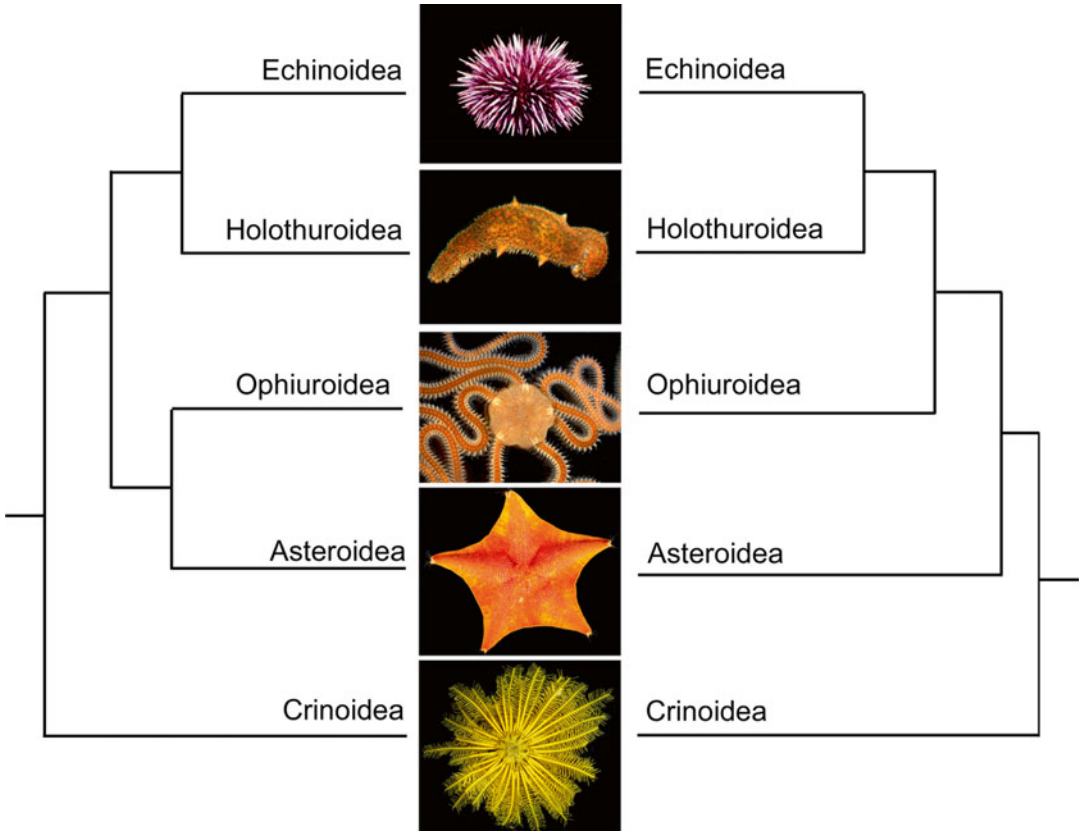

Fig. 1.3 Alternative hypotheses proposed for the relationships among extant echinoderm classes. The *left side* of the figure corresponds to the Asterozoa-Echinozoa hypothesis and the *right side* to the Cryptosyringida hypothesis

gut and have a simplified pattern of ciliation and may be planktonic or benthic. Lecithotrophy is considered to be the derived larval form for modern echinoderms and appears to have arisen independently and frequently in many echinoderm clades. Moreover, once lecithotrophic development evolved, subsequent radiation may have generated new species with this life history mode (Jeffery et al. 2003; Hart et al. 2004). The presence of lecithotrophic larvae with nonfunctional feeding structures also supports the hypothesis that these larvae arose from an ancestral adult form with a feeding larva (Raff and Byrne 2006). After 500 million years of larval evolution, approximately 68 % of echinoderms with known development have the supposedly derived, lecithotrophic larval type (Uthicke et al. 2009).

Rapid evolution of development, as seen in *Heliocidaris* sea urchins and asterinid sea stars, has resulted in diverse larval phenotypes. The two *Heliocidaris* species, one with a feeding (*H. tuberculata*) and one with a nonfeeding (*H. erythrogramma*) larva, are used as a model comparative system to investigate the developmental and genetic mechanisms underlying the evolutionary switch to a lecithotrophic larva (Wray 1996; Raff and Byrne 2006). The full range of larval types in the Echinodermata is evident in the asterinids (Byrne 2006). These asteroids include taxa with feeding (e.g., *Patiria*, *Patiriella*) and nonfeeding (e.g., *Meridiastra*) planktonic larvae, species with strange-looking nonfeeding benthic larvae (*Parvulastra*, *Asterina*) that maintain a tenacious hold on the seafloor, and species with larvae that swim in the gonad followed by metamorphosis and birth as nearly sexually mature asteroids.

Generally, the zygotes of species with small eggs give rise to two types of feeding larvae: the pluteus-like larvae of sea urchins and brittle stars and the auricularia-like larvae of sea cucumbers

and sea stars (Hyman 1955; Raff and Byrne 2006). The Echinoidea, Ophiuroidea, Holothuroidea, and Asteroidea also include species with various types of nonfeeding (lecithotrophic) larvae. Crinoidea (sea lilies and feather stars) are the only echinoderm class that does not have a feeding larva. Their embryos develop typically into a secondarily derived nonfeeding larva, the barrel-shaped doliolaria. Interestingly, one species has an auricularia-like ciliary band indicating an ancestral form with feeding larvae (Nakano et al. 2003). Figure 1.4 displays representative larval types for each echinoderm class, along with their adult forms, arranged according to one of the alternative phylogenetic arrangements currently suggested for this phylum (see Fig. 1.3 for the alternatives). The great diversity of larval forms in echinoderms with feeding and nonfeeding modes are illustrated for each class (Balser 2002; Byrne and Selvakumaraswamy 2002; Emlet et al. 2002; McEdward et al. 2002; Sewell and McEuen 2002).

At the end of the planktonic phase, larvae settle and the juvenile pentaradial form arises through a series of marked changes during metamorphosis. The adult rudiment arises on the left side of the larva. The origin of adult tissues and organs is complex and in many cases unknown. The details of the developmental process involved in the genesis of the different structures will be discussed in other sections of this chapter.

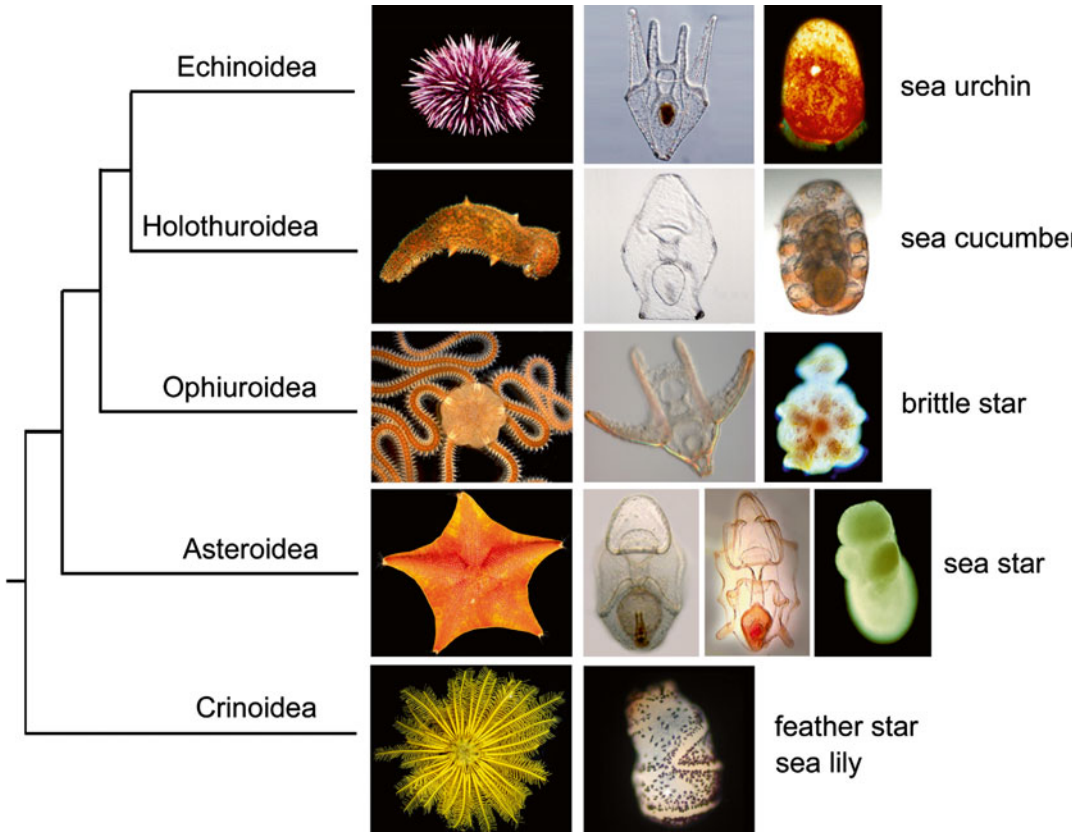

Fig. 1.4 One scenario of echinoderm interrelationships, after Janies (2001), used to illustrate adults and larvae. *From left*, each column displays, for each class, representatives of adult phenotypes (for species names and image credits see Fig. 1.1), the most representative type of planktonic larvae and adult common names. The larvae are *from left to right*: *Strongylocentrotus purpuratus* echinopluteus and *Heliocidaris erythrogramma* reduced pluteus for Echinoidea; *Parastichopus parvimensis* auricularia (Courtesy of Veronica Hinman) and *Holothuria scabra* doliolaria for Holothuroidea; *Amphiura filiformis* ophiopluteus (Courtesy of David Dylus and Paola Oliveri) and *Clarcoma pulchra* vitellaria (Courtesy of Paula Cisternas) for Ophiuroidea; *Meridiastra calcar* bipinnaria, brachiolaria, and vitellaria for Asteroidea; *Metacrinus rotundus* doliolaria (Courtesy of Hiroaki Nakano) for Crinoidea

Echinoderm Genomes: A Window into the Regulatory Landscape

Our understanding of the development of animals and some evolutionary trends within taxa is now being enhanced by our knowledge of genomes and this is also true for the Echinodermata (Kondo and Akasaka 2012). The ongoing generation of genomic data from different animal systems is providing unprecedented access to the mechanisms that control morphogenesis and its changes over evolutionary time.

After a first wave of sequencing efforts, concentrated on the so-called "model" organisms (*Drosophila melanogaster*, *Caenorhabditis elegans*, *Mus musculus*), the focus has shifted to other systems, including marine invertebrates. The sequencing of the genome of the sea urchin *Strongylocentrotus purpuratus* (814 megabases) was pioneering work and allowed the comprehensive characterization of genes in a species with a long tradition as a model system for developmental biology and a key reference for investigation of the genetic control of embryogenesis; see (Davidson 2006). The sequencing and annotation of the sea urchin genome, carried out by an international team of scientists (Sea Urchin Genome Consortium), allowed gene families to be characterized and, by comparison with other taxa, their evolutionary dynamics to be traced within the Bilateria and Deuterostomia. Some unexpected findings such as the expanded innate immunity repertoire or the huge numbers of genes devoted to sensory systems (including vision and hearing) highlight once more the importance of having access to complete genome sequences if we are to understand developmental and evolutionary processes.

Important as knowledge of genome sequences is, the best way to follow development – and to infer evolution (see Domazet-Loso and Tautz 2010) – is through the characterization of the transcriptomes and proteomes of different species. The former provides detailed information on global changes of transcription in time and/or space and the latter on similar changes but at the level of proteins. Detailed transcriptome analyses have been performed on some echinoderms, but in no case do they match the detailed characterization of transcript variations that have occurred during the development of *Strongylocentrotus purpuratus*. *S. purpuratus* transcriptomes have been analyzed at 22 different developmental times (Materna et al. 2010; Tu et al. 2012). The extent of the analysis has also allowed the definition of structural parameters for all protein-coding genes (such as intron/exon sizes, intergenic distances, numbers of introns/exons per gene, etc.). These data are incorporated into accessible databases (e.g., EchinoBase: http://mandolin.caltech.edu/Echinobase/). Other echinoderms for which transcriptome data have been generated are the echinoid *Heliocidaris erythrogramma* (mixed developmental stages) (Wygoda et al. 2014), the holothurians *Holothuria glaberrima* (intestinal regeneration) (Rojas-Cartagena et al. 2007; Du et al. 2012) and *Apostichopus japonicus* (mixed developmental stages (Du et al. 2012) or adult regenerating tissues (Sun et al. 2011)), as well as the ophiuroids *Ophiocoma wendtii* (gastrula) (Vaughn et al. 2012) and *Amphiura filiformis* (regenerating arms) (Burns et al. 2012). Many other species are currently being sequenced and analyzed; some of the results are accessible through different websites. Methodologies and the depth of sequence information vary between studies.

Most recently, other echinoderm genomes have been sequenced, most of which are from echinoids. We have complete genomic and extensive transcriptomic data for the first asteroid species, *Patiria miniata* (http://blast.hgsc.bcm.tmc.edu/blast.hgsc?organism=Pminiata). These data should prove especially useful for understanding echinoderm genome evolution and the changing patterns of gene expression associated with the diversification of the echinoderm groups. Other echinoid genomes currently being sequenced are *Paracentrotus lividus* (European consortium), *Lytechinus variegatus*, *Eucidaris tribuloides*, *Strongylocentrotus franciscanus*, and *Strongylocentrotus fragilis* (Baylor College of Medicine Human Genome Sequencing Center, Houston, and Caltech, Pasadena, USA) and the two *Heliocidaris* species with feeding (*H. tuberculata*) and nonfeeding (*H. erythrogramma*) larvae. For *H. erythrogramma* a complete developmental transcriptome is available from early embryogenesis to the juvenile stages (Wygoda et al. 2014).

An alternative approach to understanding echinoderm developmental processes is the use

of high-throughput proteomic tools, which allows researchers to follow hundreds of proteins (and their post-transcriptional modifications) at once. These techniques have been introduced recently, and their full potential is realized in organisms for which the genomes are already sequenced, for instance, in *Strongylocentrotus purpuratus* (Mann et al. 2010; Adams et al. 2012). Some of the pioneering studies involved the use of different techniques. For instance, the radial nerve cord and coelomocyte protein complements of the asteroids have been characterized using combinations of 1 and 2D electrophoresis plus MALDI-TOF (*Marthasterias glacialis*) (Franco et al. 2011a, b); techniques that were incorporated to the study of phosphorylation patterns during neuronal regeneration (Franco et al. 2012). These are just a few examples of a growing number of comprehensive analyses of protein complements.

In the near future, new genome sequences, in combination with high-throughput transcriptomic and proteomic data, will change the way we see and analyze developmental processes in echinoderms. Moreover, as mentioned above, the comparison of patterns across taxa should also revolutionize the study of evolutionary change.

The use of echinoderms in developmental biology has a long and fertile tradition. In fact, it was through working with these alluring marine creatures that fundamental concepts were made and incorporated into our current knowledge on the function of cells and embryos. These include understanding the role of cyclins in the animal cell cycle, chromosomes as determinants of development, the plasticity of blastomere fates, and the presence of maternal messages in embryos. Our understanding of the molecular control of development, the structure of the gene regulatory apparatus, and recent advances in gene regulatory networks (GRN) as control factors of animal development also stem from the use of echinoderm model systems. Echinoderms present biologists many practical features, including ready access to fertile gametes, the transparency of their embryos, and their relative ease of manipulation in the laboratory. Coupled with the recent sequencing of the genomes of several members of the phylum, it is clear that use of this group of animals as model organisms will continue to be at the center of our advances in understanding, not only of the intricate processes controlling the development of individual animals but also of the fascinating mechanisms that underlie the diversification of body plans over evolutionary time. Our future endeavors will also benefit from the long tradition of observational studies of echinoderms in ecology and in the fossil record and from in-depth studies of the evolution of their life stories. The integration of this traditional research with more modern approaches based on genomic regulatory systems should prove especially fruitful in providing us with a better understanding of specific micro- and macro-evolutionary processes. Among the echinoderms used in developmental biology, the sea urchin *Strongylocentrotus purpuratus* deserves special mention. This species, from North America's west coast, was instrumental to the incorporation of molecular techniques to the study of animal development. From the original characterization of the dynamic changes of transcription in embryogenesis to recent analyses of gene regulatory networks, *S. purpuratus* has been an important model in our modern understanding of developmental processes. The ease of obtaining billions of gametes for synchronous embryo culture, the transparency of the embryo, and the ability to introduce foreign DNA or RNA into the embryos have made of this urchin an ideal model for the study of developmental mechanisms and their molecular control. Given the rich history in research with echinoderms and the recent incorporation of a wide array of new technologies, echinoderms will undoubtedly continue to be center stage within the EvoDevo field.

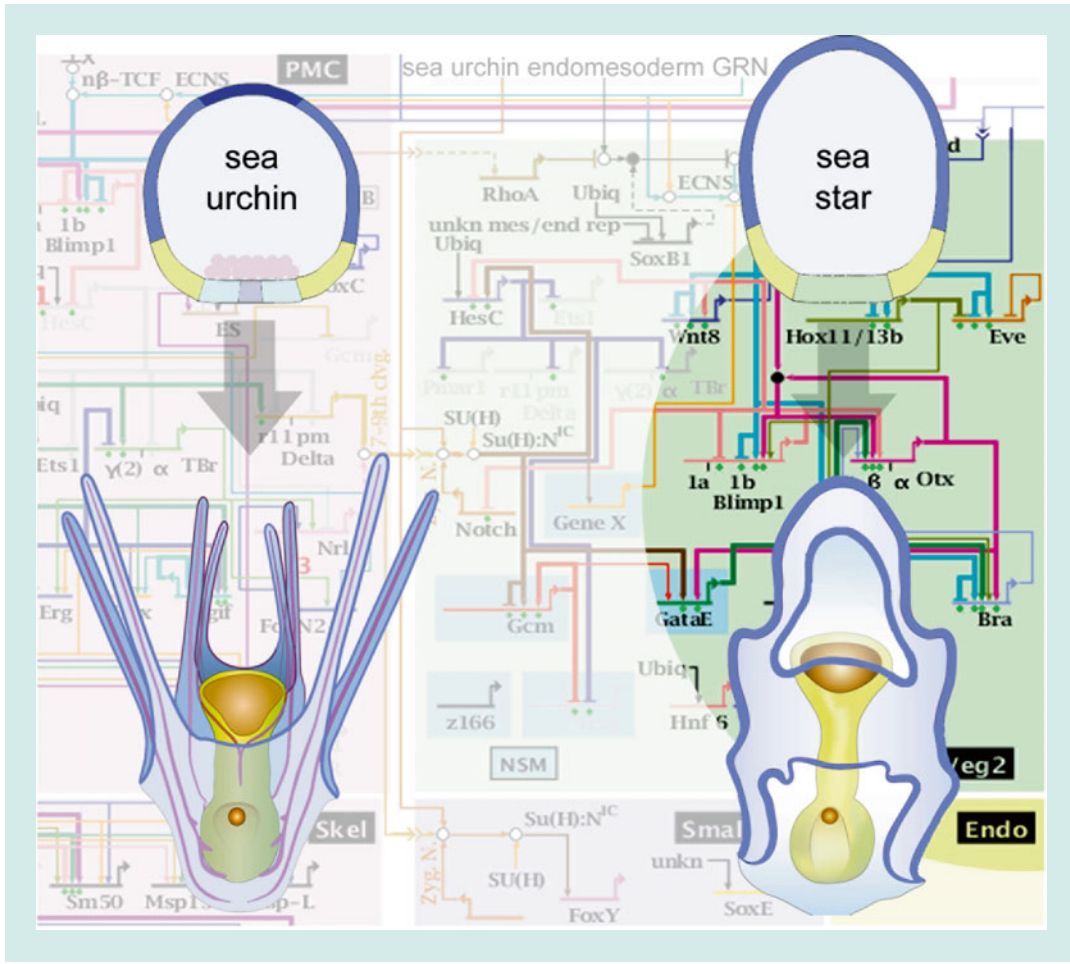

EMBRYONIC AND LARVAL DEVELOPMENT

While the implications of these alternative phylogenies on the evolution of larval types will be discussed at the end of this section, we will focus first on embryogenesis, i.e., the development from egg up to larva, for each of the five echinoderm classes, highlighting, where possible, commonalities and differences.

Since the classical studies of Derbès (1847) on the formation of the archenteron, the sea urchin embryo has served as a model system for developmental biology. Sea urchin gastrulation is considered as the archetypal model for a deuterostome morphogenetic process (McClay et al. 2004). Starting with the discovery of pronuclear fusion by Fol (1877) and Boveri's experiments on the developmental fate of polyspermic eggs (Boveri 1902), the sea urchin embryo has provided a powerful tool for the study of the role of genome activities during development (reviewed in Davidson et al. 1998). In particular, the process of specification of the endomesodermal territories is extraordinarily well known in the sea urchin *Strongylocentrotus purpuratus* and has led to the most exhaustive characterization of a gene regulatory network (GRN) for any developmental system. As a consequence, there is an extensive literature on sea urchin embryos compared to what has been published for other echinoderms, and thus, the organization of this section reflects this knowledge bias. We need to point out here that the study of regulatory mechanisms in

echinoderms, particularly in sea urchins, has been facilitated by the routine use of knockdown methodologies, particularly those using morpholino-modified oligonucleotides. This, with the regular use of transgenesis, shows the sharp contrast between the gene analysis in echinoderms and those performed in most other phyla.

Development of Echinoidea (Sea Urchins)

Many sea urchin species have been used to characterize the basic processes involved in their embryonic development. Starting with the Mediterranean *Paracentrotus lividus*, which appeared on the scientific scene associated with the abovementioned early studies and the spectacular blastomere recombination experiments of Hörstadius (1939, 1973), important insights have been obtained using the Atlantic *Lytechinus variegatus*, the Western Pacific *Hemicentrotus pulcherrimus*, and the Eastern Pacific *Strongylocentrotus purpuratus*, the latter being the first echinoderm species with a sequenced genome (Sodergren et al. 2006) and for which the first GRN that controls the specification of an embryo was established (Davidson et al. 2002). Figure 1.5 displays adult specimens of all these species. The following description of sea urchin embryonic development represents a summary of the knowledge obtained by studying these species and, thus, provides an overview for sea urchin development, keeping in mind that differences exist among the species.

The eggs of sea urchins with feeding larvae range from 80 to 180 μm in diameter. The meiotic divisions associated with oogenesis are completed while the eggs are still in the ovary. The egg has a small, clear, eccentrically located pronucleus. This is relatively homogeneous and contains uniformly distributed yolk granules and numerous small lipid vesicles and other organelles (Byrne et al. 1999). Together, these granules and the lipids supply the embryo and early larva with the energy sources and precursor molecules needed prior to feeding (Scott and Lennarz 1989). Two envelopes surround the sea urchin egg: the inner vitelline envelope and the outer jelly coat (Glabe and Vacquier 1977).

Fertilization involves two fusion events: gamete fusion, the fusion of the sperm and egg plasma membranes, and pronuclear fusion, the fusion of the male and female haploid pronuclei. As the surfaces of the gametes approach each other, a specific interaction takes place between the sperm protein bindin (Vacquier and Moy 1977) and a receptor located on the egg surface (Giusti et al. 1997; Stears and Lennarz 1997). The sperm-egg binding reaction causes the exocytosis of the sperm's acrosomal vesicle, with proteolytic enzymes being released that allows the sperm cell to penetrate the jelly coat and establish contact with the vitelline envelope (Dan and Hagiwara 1967; Franklin 1970; Levine et al. 1978). At this point, the first fusion event of fertilization, sperm-egg plasma membrane fusion, or gamete fusion takes place, facilitating that the sperm pronucleus moves towards the egg pronucleus. Sperm-egg fusion triggers a complex series

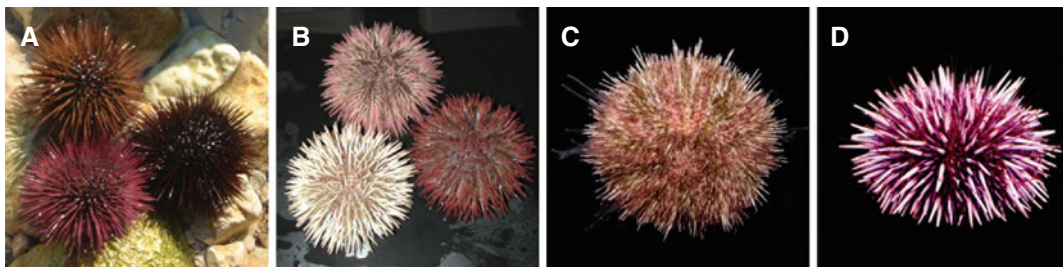

Fig. 1.5 Sea urchin species most commonly used in developmental biology. *From left to right*, *Paracentrotus lividus* (**A**, Courtesy of Christian Gache), *Lytechinus variegatus* (**B**, Courtesy of David McClay), *Hemicentrotus pulcherrimus* (**C**, Courtesy of Koji Akasaka), and *Strongylocentrotus purpuratus* (**D**, Courtesy of Mattias Ormestad). Adult specimen sizes range from about 50 to 100 mm in diameter for all 4 species

of responses. Among the most important are processes that prevent polyspermy. These start about 20 s after sperm attachment and are complete already by the end of the first minute of fertilization. Two complementary processes prevent polyspermy in sea urchins: a fast reaction, accomplished by a transient depolarization of the egg's plasma membrane (Jaffe 1976; Schuel and Schuel 1981), and a slower reaction, involving the more permanent production of a physical barrier caused by the exocytosis of cortical granules (Just 1919). Cortical granules of sea urchins contain many different components necessary to accomplish their varied tasks. Proteases dissolve the connection between the vitelline envelope and the cell membrane; they clip off the bound receptor and any sperm attached to it (Vacquier et al. 1973; Glabe and Vacquier 1978). Mucopolysaccharides produce an osmotic gradient that causes water to enter the space between the plasma membrane and the vitelline envelope, causing the envelope to expand and become the fertilization envelope (Hall 1978). A peroxidase enzyme hardens the fertilization envelope by cross-linking tyrosine residues on adjacent proteins (Foerder and Shapiro 1977; Mozingo and Chandler 1991). Finally, the cortical granules release a sticky protein, hyaline, which forms a tough extracellular matrix around the embryo (Hylander and Summers 1982). This hyaline layer holds the cells of the early embryo together until they develop cell junctions at the blastula stage. The second fusion event in fertilization, pronuclear fusion, usually occurs within 30–45 min after gamete fusion; through it the two pronuclei merge and a diploid zygote nucleus is formed.

Figure 1.6 displays the development of the sea urchin embryo from the 4-cell to the pluteus larva stage. Cleavage of sea urchin embryos is holoblastic, radial, and in the majority of stages equal. The exception is the fourth cleavage, which is unequal and thus a unique feature of echinoids with small eggs and feeding larvae. The first and second cleavages are both longitudinal, intersecting the animal and vegetal poles. These divisions lie at right angles to one another, dividing the embryo into four cells of equal size. The third cleavage is equatorial, perpendicular to the first two cleavage planes. This cleavage separates the animal and vegetal hemispheres from one another, giving rise to the eight-cell stage. Because all the cells of the embryo in each of the first three cleavages are equal in size, cleavage up to this point is said to be equal. The fourth cleavage, however, is very different from the first three. The upper four cells divide meridionally, forming equal-sized cells called mesomeres. The lower four cells divide unequally and horizontally to produce four larger macromeres and below them four smaller cells called micromeres, located at the vegetal pole of the embryo (Summers et al. 1993). At the fifth cleavage the eight mesomeres divide equally and horizontally, forming two tiers of cells in the animal hemisphere (an1 and an2), one staggered above the other. The four macromeres divide meridionally, forming a tier of eight cells, while the micromeres divide unequally once more, generating four large micromeres and four small micromeres (Okazaki 1975; Pehrson and Cohen 1986; Cameron and Davidson 1991). At sixth cleavage all the cells divide horizontally, producing the 60-cell stage embryo. At this point the subdivision of the embryo, from the animal to the vegetal pole, is as follows: 16 an1, (two layers of eight cells each), 16 an2 (two layers of eight cells each), eight veg1 (vegetal tier one), eight veg2 (vegetal tier one), and 12 micromeres (eight large micromeres and four small micromeres) (Fig. 1.6A).

The blastula stage of sea urchin development begins at the 128-cell stage. Cleavage continues, producing progressively smaller and smaller cells. The cells form a hollow sphere surrounding a central cavity or blastocoel and they become organized as a true epithelium, with permanent cell junctions and a complex extracellular matrix on both the interior and exterior surfaces.

The formation of the blastocoel is accomplished by the adhesion of the blastomeres to the hyaline layer and by an influx of water that results in an expansion of the internal cavity (Dan 1960; Wolpert and Gustafson 1961; Ettensohn and Ingersoll 1992). The cells at the vegetal pole of the blastula begin to thicken, forming a vegetal

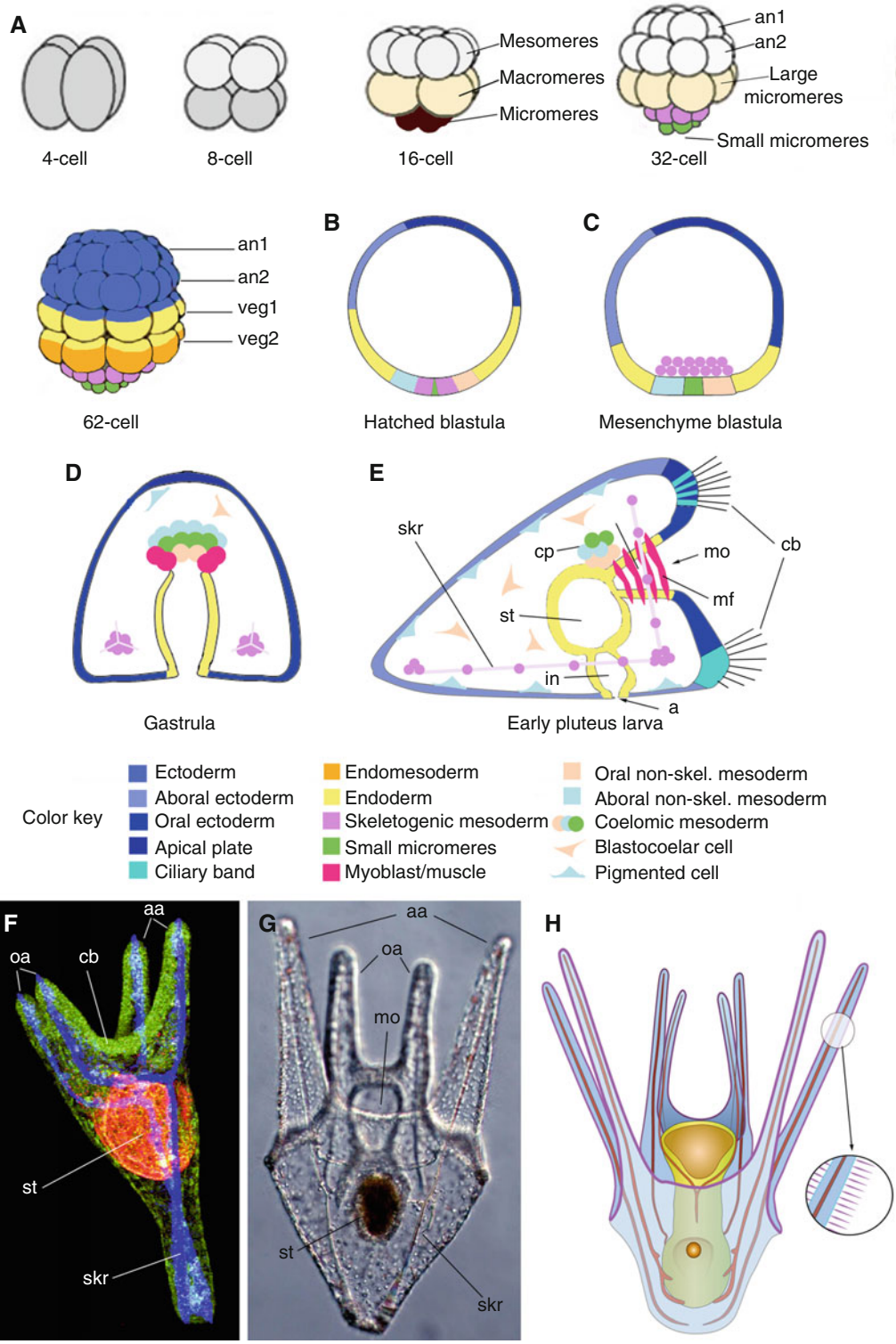
A
4-cell
8-cell
Mesomeres
Macromeres
Micromeres
16-cell
an1
an2
Large micromeres
Small micromeres
32-cell
an1
an2
veg1
veg2
62-cell
B
Hatched blastula
C
Mesenchyme blastula
D
Gastrula
E
skr
cp
mo
cb
mf
st
in
a
Early pluteus larva
Color key
Ectoderm
Aboral ectoderm
Oral ectoderm
Apical plate
Ciliary band
Endomesoderm
Endoderm
Skeletogenic mesoderm
Small micromeres
Myoblast/muscle
Oral non-skel. mesoderm
Aboral non-skel. mesoderm
Coelomic mesoderm
Blastocoelar cell
Pigmented cell
F
aa
oa
cb
st
skr
G
aa
oa
mo
st
skr
H

plate. A small tuft of long cilia forms at the animal pole of the blastula. This allows the embryo to start rotating inside the fertilization membrane. At this point an enzymatic complex is secreted by the cells of the animal half, by which the blastula hatches and starts to swim freely (Lepage et al. 1992; Reynolds et al. 1992; Ghiglione et al. 1994).

Starting from the late cleavage and blastula stages, the sea urchin embryo can be considered as composed of "territories." These territories are distinguished by specific, differential patterns of gene expression, individual cell lineage histories, and cell fates. Five major embryonic territories can be distinguished by the 60-cell stage: the small micromere, the skeletogenic mesenchyme, the vegetal plate, the aboral ectoderm, and the oral ectoderm territories (Fig. 1.6A; Davidson 1989, 1990; Cameron and Davidson 1991; Davidson et al. 1998).

The four small micromere founder cells arise at the unequal fifth cleavage; they divide only once more during embryogenesis and contribute to the coelomic pouch and adult rudiment (Juliano et al. 2010). The skeletogenic cells are the sister cells of the small micromeres and they give rise to the skeleton in the larva.

The vegetal plate territory generates the archenteron during gastrulation and all mesodermal elements. The aboral ectoderm produces a squamous epithelium that forms the wall of the late embryo and the larva, except for the oral and ciliated band domains. The oral ectoderm territory produces a variety of cell types and structures: the mouth, the oral hood, the ciliated bands, and most or all components of the larval nervous system.

Once cells have acquired unique identities and begin to express different sets of genes, the stage is set for morphogenesis and differentiation. Morphogenesis begins shortly after cleavage in echinoderms, quickly establishing the three primary germ layers. Morphogenetic events have been extensively studied in sea urchins because of the easiness with which it is possible to experimentally manipulate embryos in various informative ways. The advanced blastula consists of a single layer of about 500 cells that has the shape of a hollow ball, flattened and thickened at the vegetal side (Fig. 1.6B).

The first overt morphogenetic event is the ingression of a subset of mesenchyme cells from the vegetal pole region of this late blastula (Fig. 1.6C). The primary mesenchyme cells (PMCs), which are derived from the large micromeres and are located approximately in the center of the vegetal plate region (Burke et al. 1991), begin to change. They start extending and contracting long filopodia from their inner surface. Then, they lose their affinity for the apical lamina and for their epithelial neighbors, gaining an affinity for the extracellular matrix and the basal lamina that lines the blastocoel (Fink and McClay 1985; Amemiya 1989). This cell movement is termed ingression. Ingressing cells are

Fig. 1.6 Sea urchin development. (**A**) Cleavage stages seen along the animal (*top*)-vegetal (*bottom*) axis. At the 16-cell stage there are four micromeres (*brown*) at the vegetal pole, four central macromeres (*light yellow*), and eight mesomeres (*gray*) at the animal pole. The colors indicate when the cells begin to be specified towards ectoderm, endoderm, and mesoderm (see color key). (**B**) Hatched blastula stage, midsagittal section. The ectoderm is already subdivided (as indicated by different shades of *blue*) and the non-skeletogenic mesoderm (oral and aboral) has separated from the endoderm. (**C**) Mesenchyme blastula stage, midsagittal section. Primary mesenchyme cells have ingressed into the blastocoel while small micromeres stay behind. (**D**) Midsagittal section of a mid-gastrula stage, showing the gut invaginating, the skeletogenic cells beginning to synthesize the skeleton, and non-skeletogenic mesoderm at the tip of the archenteron subdividing into domains occupying different positions along the oral/aboral and animal/vegetal axes (different cell types are indicated following the color key). (**E**) Pluteus larva, lateral view, showing the definite structures and cell types generated during embryogenesis. (**F**) *Paracentrotus lividus* pluteus larva stained to show the gut (*red*), the skeleton (*blue*), and the ectoderm (*green*) (Courtesy of David McClay). Length of larva, from posterior end to anterior tip = 120 μm. (**G**) *Strongylocentrotus purpuratus* at the four-arm stage larva. Length of larva = 200 μm. (**H**) Scheme of the eight-arm pluteus stage larva (Courtesy of Santiago Valero-Medranda) highlighting internal skeleton (*brown*) and digestive system (*yellow*/*orange*). The inset shows details of the ciliary band on one larval arm (*purple*). Abbreviations: *a* anus, *aa* anal arm, *an* animal, *cb* ciliary band, *cp* coelomic pouch, *es* esophagus, *in* intestine, *mf* muscle fiber, *mo* mouth, *oa* oral arm, *skr* skeletal rod, *st* stomach, *veg* vegetal

bottle-shaped with their basal end protruding into the blastocoel and their apical end narrowed into the form of a thin strand. The embryo at this early stage of gastrulation is referred to as a mesenchyme blastula (Fig. 1.6C).

Once inside the blastocoel, PMCs migrate seemingly at random for a brief period, actively making and breaking filopodial connections to the wall of the blastocoel. These filopodia are not thought to function in locomotion; rather they appear to explore and sense the blastocoel wall and may be responsible for receiving dorsoventral and animal-vegetal patterning cues from the ectoderm (Malinda et al. 1995). Eventually, PMCs congregate in the vegetal half of the embryo, in a ring pattern, with two major aggregates of cells (the ventrolateral clusters). Here, PMCs become round, retract their cilia, and fuse into syncytial strands (Hodor and Ettensohn 1998), which will form the axis of the calcium carbonate spicules of the larval skeleton (for a recent review, see McIntyre et al. 2014).

As the ring of primary mesenchyme cells leaves the vegetal region of the blastula, the remaining cells at the vegetal plate move to fill in the gaps, fold inwards, and become elongated in a process called "invagination." This process has been conventionally divided into two distinct temporal phases, primary and secondary invagination (Dan and Okazaki 1956; Kinnander and Gustafson 1960). Within a few hours, the thickened vegetal plate bends inwardly. As shown by serial reconstructions of *Lytechinus pictus* embryos, relatively few cells (about 100) take part in this first step (Ettensohn 1984). At the time of invagination, the vegetal plate cells (and only these cells) secrete a chondroitin sulfate proteoglycan into the inner lamina of the hyaline layer, located directly beneath them. This hygroscopic molecule swells the inner lamina, but not the outer lamina, causing the vegetal region of the hyaline layer to buckle (Lane et al. 1993). Slightly later, a second force arising from the movements of epithelial cells adjacent to the vegetal plate facilitates this invagination by pushing the buckled layer. The invaginated region is called the archenteron (primitive gut), and the opening of the archenteron at the vegetal region is called the blastopore. Sea urchins are deuterostomes and thus the blastopore, later in development, will form the anus of the larva. By the end of this primary invagination, the archenteron, which is roughly cylindrical in shape, has extended between one-fourth and one-half of its total length across the blastocoel. When the primary invagination is completed, the length of the gut rudiment scarcely changes during a couple of hours. Meanwhile, secondary mesenchyme cells (SMCs) become visible at the tip of the gut rudiment. These cells are also called non-skeletogenic mesoderm (NSM) and are the descendants of the veg2 blastomeres formed at the sixth cleavage (Horstadius 1973; Cameron et al. 1991). SMCs begin to extend long, thin filopodia into the blastocoel and towards the area of the animal pole, exploring putative attachment sites, while they remain attached to the gut rudiment (Hardin 1988; Hardin and McClay 1990). After a brief pause, the second phase of archenteron formation begins. During this time, the archenteron extends dramatically, sometimes triplicating its length. The embryo now has reached the mid-gastrula stage (Fig. 1.6D). In this process of extension, the wide, short gut rudiment is transformed into a long, thin tube. It has been proposed that contraction of the filopodia interconnecting the archenteron tip and the apical plate pulls the gut rudiment upward (Takata and Kominami 2004). At this point, the existence of tension in SMC filopodia is evident. Further, elongation of the archenteron is blocked when the pseudopodia are broken by expanding the blastocoel (Dan and Okazaki 1956) or with the use of a laser beam (Hardin 1988). Together with the help of forces exerted by SMC filopodia, cellular rearrangements lead to the formation of a slender archenteron. These cells of the archenteron rearrange themselves by migrating over one another and, at the same time, they flatten (Ettensohn 1985; Hardin and Cheng 1986). This phenomenon, wherein cells intercalate to narrow the tissue and at the same time move it forwards, is called convergent extension. Cell division continues to produce more endodermal and secondary mesenchyme cells while the archenteron extends (Martins et al. 1998).

As the archenteron elongates, secondary mesenchyme cells delaminate from its tip and disperse

within the blastocoel, where they proliferate to form four types of non-skeletogenic mesoderm (NSM) cells (Ettensohn and Ruffins 1993): pigment cells (Gibson and Burke 1985, 1987), blastocoelar cells (Tamboline and Burke 1992), coelomic pouch cells, and circumesophageal muscle cells (Ishimoda-Takagi et al. 1984; Burke and Alvarez 1988; Andrikou et al. 2013). These cell types are specified long before delaminating from the tip of the archenteron where they are arranged spatially to occupy different positions along the animal/vegetal and oral/aboral axis (see different color cells in Fig. 1.6D, E; for the specification state of these NSM cells at the tip of the archenteron see Luo and Su 2012 and Andrikou et al. 2013).

Soon after elongation starts in *S. purpuratus* embryos, the archenteron bends ventrally, towards the prospective oral region, while in *L. variegatus* embryo this event occurs later on, as the tip of the archenteron approaches the animal pole of the blastocoel. The oral epithelium and cells at the tip of the archenteron make contact, and an opening is produced in the epithelia, which will become the larval mouth. The blastopore will develop into the anal opening of the digestive tract. Just before the archenteron makes contact with the prospective oral field, another important morphogenetic movement, coelom formation, begins. This is the time when myoblasts from each coelomic pouch extend pseudopodia towards the outer surface of the esophagus, eventually forming muscle fibers. After full elongation of the archenteron, constrictions subdivide the endoderm into foregut, midgut, and hindgut, and this regionalization not only becomes evident morphologically but also is clearly reflected in patterns of region-specific gene expression (Cole et al. 2009; Annunziata and Arnone 2014; Annunziata et al. 2014). During this period, termed prism stage, the embryo takes on the shape of a rounded, truncated pyramid. The side of the embryo where the mouth will open (stomodeum) becomes flattened, forming the oral surface of the developing larva. The blastopore side of the embryo also becomes flattened and forms the anal surface of the developing larva. A ciliary band develops around the stomodeum. Ciliary band cells are interspersed with neurons that begin to differentiate at this stage to, eventually, form the complex neuronal network typical of the pluteus larva (for a review of the sea urchin larva nervous system, see Burke et al. 2006). Also at this stage, the apical organ, where serotonergic and other type of neurons that remain to be characterized will develop, becomes morphologically evident as a disk of thick ciliated epithelium at the animal pole of the embryo (indicated as a dark blue region in Fig. 1.6B–E; see Byrne et al. 2007).

As development proceeds, the embryo elongates slightly along the dorsoventral axis and two arms, the oral arms, appear and extend outwards from the oral lobe. Two additional arms, the anal arms, appear and extend outwards at the junction of the oral and anal surfaces. The embryo has reached the pluteus stage (Fig. 1.6E). The triradiate spicules develop into skeletal rods that extend through the body and inside the arms. The myoblasts have fused to form circumesophageal muscle fibers and the coelomic pouches are fully shaped. From a portion of the left coelomic pouch, a duct-like structure, the hydroporic canal, extend to the aboral ectoderm where the hydropore forms, thus showing the first morphological signature of left-right asymmetry of the pluteus larva (Luo and Su 2012).

Because of the morphogenetic changes of the larva, the developing digestive tract is bent into a J-shape structure. The stomach enlarges and fills a large part of the body of the pluteus while the arms elongate. When completely formed, the anal arms are longer than the oral ones. A pluteus larva at this stage of development is referred to as the four-armed pluteus larva (Fig. 1.6F, G). Sequential elongation of additional arms (up to eight; Fig. 1.6H) and important modifications of the mesoderm occur during the various planktonic larval stages (see Smith et al. 2008b for progression of *Strongylocentrotus purpuratus* larval stages). A period of extensive feeding and continued larval development is required before metamorphosis to a miniature sea urchin juvenile occurs (see below).

A vast diversity of echinoids develops through nonfeeding larvae (an example is shown in Fig. 1.7). Details of embryology and larval development in these echinoids are available for several species (Raff 1992; Morris 1995; Emlet et al. 2002). Some species such as *Holopneustes*

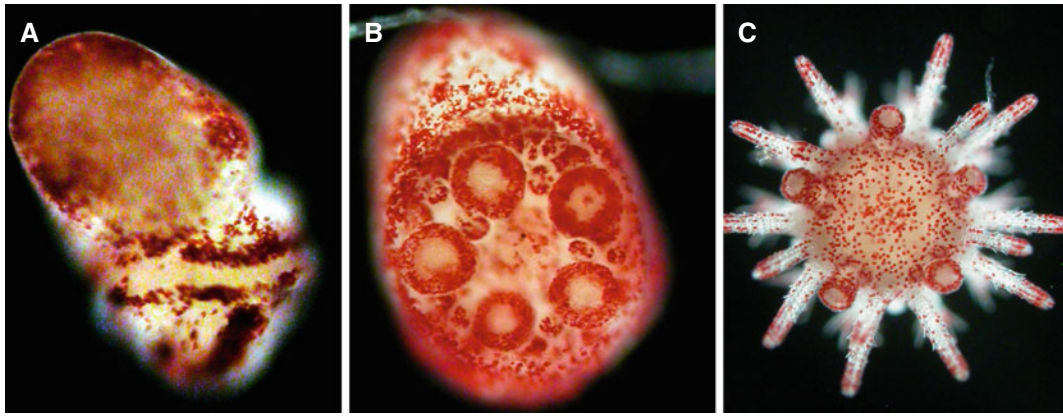

Fig. 1.7 Developmental stages of *Heliocidaris erythrogramma*, a species with nonfeeding larvae. (**A**) Seventy-two-hour-old reduced pluteus. (**B**) Ninety-six-hour-old metamorphosing larva. (**C**) Seven-day-old juvenile. Length of larvae in (**A**) and (**B**) is 400 μm; diameter of juvenile in (**C**) is 500 μm. (courtesy of Paula Cisternas)

purpurescens completely lack any pluteal features (Morris 1995), while *Heliocidaris erythrogramma* has a vestigial pluteal arm skeleton; here, band segments are interpreted as expressions of epaulets (specialized ciliated swimming structures) rather than the feeding ciliated band of the pluteus (Emlet 1995). *Phylacanthus imperialis* has a yolky nonfeeding pluteus with a reduced number of arms (Olson et al. 1993).

Many studies in the last decade have been performed to elucidate the molecular basis of territory specification in the sea urchin embryo (see diagram of basic tenets in Fig. 1.6). These studies have demonstrated the interplay between signaling events and gene regulatory interactions which underlie the specification and patterning of the sea urchin larval nervous system in species with feeding larvae (for review, see Angerer et al. 2011); the specification of the embryo left-right axis (Molina et al. 2013); the specification, formation, and patterning of the larval skeleton (for review, see McIntyre et al. 2014); and, possibly at an even deeper level of detail, the specification of the endomesoderm and its derived structures. Because the regulation of morphogenesis of the gastrointestinal system is a key innovation in metazoan evolution, endoderm specification is described in detail here, both for sea urchin and for other echinoderm embryos.

Endodermal and mesodermal cell types often share a common cell lineage in bilaterian animals, forming the so-called endomesoderm, and sea urchins are no exception. The endomesoderm precursor cells initially have the potential to develop either as mesodermal or endodermal cells until their cell fates become spatially segregated by the exclusive activation of different specification programs activated in different subsets of them.

The endomesoderm lineages emerge from the vegetal plate and form four distinct embryonic lineages: small micromeres, skeletogenic mesoderm, non-skeletogenic mesoderm, endoderm. The fourth cleavage, as already mentioned (see also Fig. 1.6A), is uneven and results in small and large tiers of cells, the micromeres and macromeres, respectively. At fifth cleavage, the micromeres divide further, giving rise to small and large micromeres. The small micromeres, which reside at the polar center of the vegetal plate where they will divide only once more during the blastula stage, remain as "set aside cells" at the tip of the archenteron during gastrulation. At a later larval stage, these cells move into the coelomic pouches, where they seem to contribute to the formation of the adult rudiment (Cameron and Davidson 1991; Juliano et al. 2010). The sister cells of the small micromeres, the large micromeres or skeletogenic mesenchyme cells, give rise to the skeletogenic mesoderm which will eventually form the skeleton of the pluteus larva.

The macromere descendants will give rise to non-skeletogenic mesoderm, endoderm, and

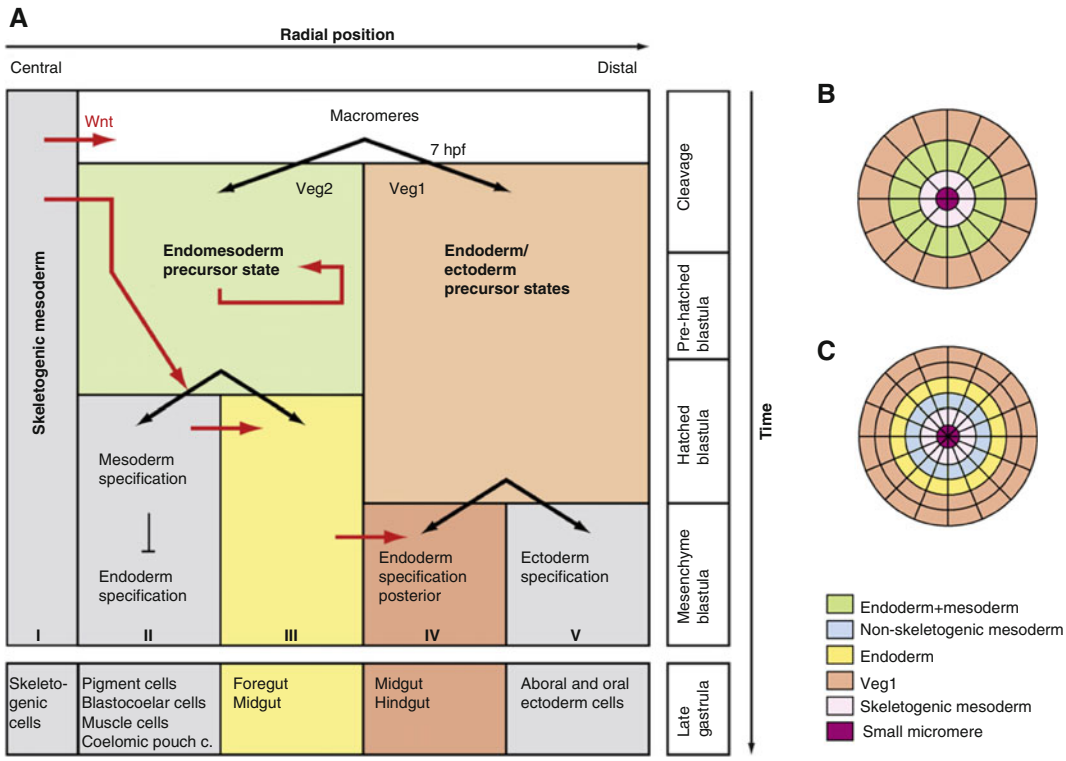

Fig. 1.8 Sea urchin endomesoderm specification. (**A**) Diagram showing the flow of information during the process of endoderm specification. Different embryonic territories are color-coded. Signaling processes occurring between different territories are marked with *arrows*. Next to the *arrows*, the temporal frames in which these interactions happen are given. The horizontal axis represents the spatial organization of the different territories, from central (*left side*) to distal domains (*right side*). The temporal arrangement of embryonic stages is represented along the vertical axis. (**B**, **C**) Schematic representation of embryonic domains seen from a vegetal view. Different colors label rings of cells with similar embryonic fates. (**B**) Territorial fates of cells at 7th cleavage. (**C**) Cellular fates at 8th cleavage. The color codes are indicated in the *bottom right* legend (Adapted and modified from Peter and Davidson (2010))

some ectodermal cells, with very complex molecular events driving the specification of each of these germ layers. The first segregation event leads to the veg1 and veg2 lineages at the sixth cleavage stage. The veg2 layer of cells will give rise to the non-skeletogenic mesoderm and the endoderm, whereas from the veg1 parts of the endoderm and the ectoderm will be formed (Fig. 1.8A). When they are born, the circular eight-cell veg2 tier abuts the polar micromere-derived cells and the eight-cell veg1 tier overlies the veg2 tier. In these embryos the veg2 lineage consists of two concentric rings of cells, the inner ring destined to become mesoderm and the outer ring destined to become oral endoderm.

At the blastula stage, the cells of the four lineages which form four concentric domains within the vegetal plate can be distinguished. At the center are the small micromere descendants, surrounding them are the skeletogenic cells, and abutting them are the veg2 and, more peripherally, the veg1 rings of cells (Davidson et al. 2002; Peter and Davidson 2010). The tier of cells closer to the micromere descendants becomes the non-skeletogenic mesoderm and will, eventually, give rise to three distinct mesodermal lineages: pigment cells, blastocoelar cells, and muscle cells. These mesodermal cells are also called secondary mesenchyme cells (SMCs) (Fig. 1.8B, C; Cameron et al. 1991).

The next event, at around 20 h post fertilization (at 15 °C) in *S. purpuratus*, is the ingression of the 16 descendants of the large micromeres into the blastocoel, which will fuse later on and form the skeleton. These cells are called primary mesenchyme cells (PMCs), because they are the first ones to ingress into the blastocoel (Burke et al. 1991). As the PMCs ingress, the SMC precursors, which encircle the PMCs, move to occupy the space vacated by these ingressing cells. The movements displace the SMC precursors towards the center of the vegetal plate (Fig. 1.6C). During gastrulation, together with the small micromeres, these cells will be part of the tip of the archenteron (Fig. 1.6D).

According to a detailed fate map study, performed in the species *Lytechinus variegatus* (Ruffins and Ettensohn 1996) and in part confirmed by gene expression studies in both *Lytechinus variegatus* and *Strongylocentrotus purpuratus*, the SMC precursors are partially segregated and differentially distributed in the vegetal plate of the mesenchyme blastula stage embryo. This suggests that developmental decisions regarding the specification of SMC precursors are being made during the interval between the stages of the hatched blastula and the late mesenchyme blastula. The pigment cell and the blastocoelar cell precursors show an asymmetric distribution within the vegetal plate, with the first to be found usually facing the future aboral ectoderm and the second facing the future oral ectoderm. When it comes to the muscle cell progenitors, a less clear distribution is observed, mostly due to the failure of scoring myoblasts independently from nearby foregut cells (Ruffins and Ettensohn 1996). Recent studies suggest that myoblast precursors are indeed specified later on, soon after having undergone epithelial mesenchyme transition at the very early gastrula stage (Andrikou et al. 2013).

Development of Asteroidea (Sea Stars)

Although sea stars are not as extensively studied as the sea urchins, the embryo of the sea star *Patiria miniata*, a species with a feeding larva, has been investigated over the last decade for analysis of gene expression during embryogenesis (Hinman et al. 2003a; Hinman and Davidson 2007; McCauley et al. 2010). Given that its genome is currently being sequenced, *Patiria* may now be considered a sea star developmental model organism. Here, a review on the development of *Patiria miniata* is provided based on Hinman et al. (2003b). Figure 1.9 shows the developmental progression of *P. miniata* from oocyte to bipinnaria and brachiolaria larvae. As is typical for echinoderms, cleavage is equal (although in *P. miniata* it is not strictly stereotypic) and the 16-cell embryo generally consists of equal-sized blastomeres (Fig. 1.9B). Also like sea urchins, sea star early

Fig. 1.9 Development of Asteroidea. (**A**, **B**) Early cleavage stages, animal pole towards the *top*. As in sea urchins, vegetal blastomeres give rise to endomesoderm (*yellow* and *red*), while the animal blastomeres become ectoderm (*blue*). Cleavage is equal in sea stars, as typical of most echinoderms, and micromeres are not formed. (**C**) Blastula, lateral view. A thickening at the vegetal pole, the vegetal plate, is noticeable. Unlike sea urchins, no mesoderm has ingressed before gastrulation starts. (**D**) Mid-gastrula, mesenchyme cells (*red*) migrate from the top of the archenteron. (**E**) Lateral view of an early bipinnaria larva; oral surface is to the *right*. The archenteron curves towards the involuting ectoderm of the oral plate, the anterior coeloms (*orange*) extend vegetally. (**F**) *Patiria miniata* bipinnaria larva, lateral view after 3 days of development. Regionalization of the digestive tube is evident from both morphology and ParaHox gene expression patterns: *PmLox* expression (*green*) marks the anterior part and *PmCdx* (*magenta*) the posterior part of the intestine. Length of larva = 300 μm. (**G**) Fluorescence immunostaining with an antibody against acetylated tubulin (*magenta)* which reveals the distribution of cilia in the 8-day-old bipinnaria larva, oral view. Length of larva = 400 μm. (**H**) Schematic depiction of a brachiolaria larva (Courtesy of Santiago Valero-Medranda), highlighting the digestive system (*yellow*/*orange*) and ciliary bands (*purple*; see inset). Abbreviations: *ac* anterior coelom, *an* anus, *cb* ciliary band, *in* intestine, *mo* mouth, *es* esophagus, *st* stomach

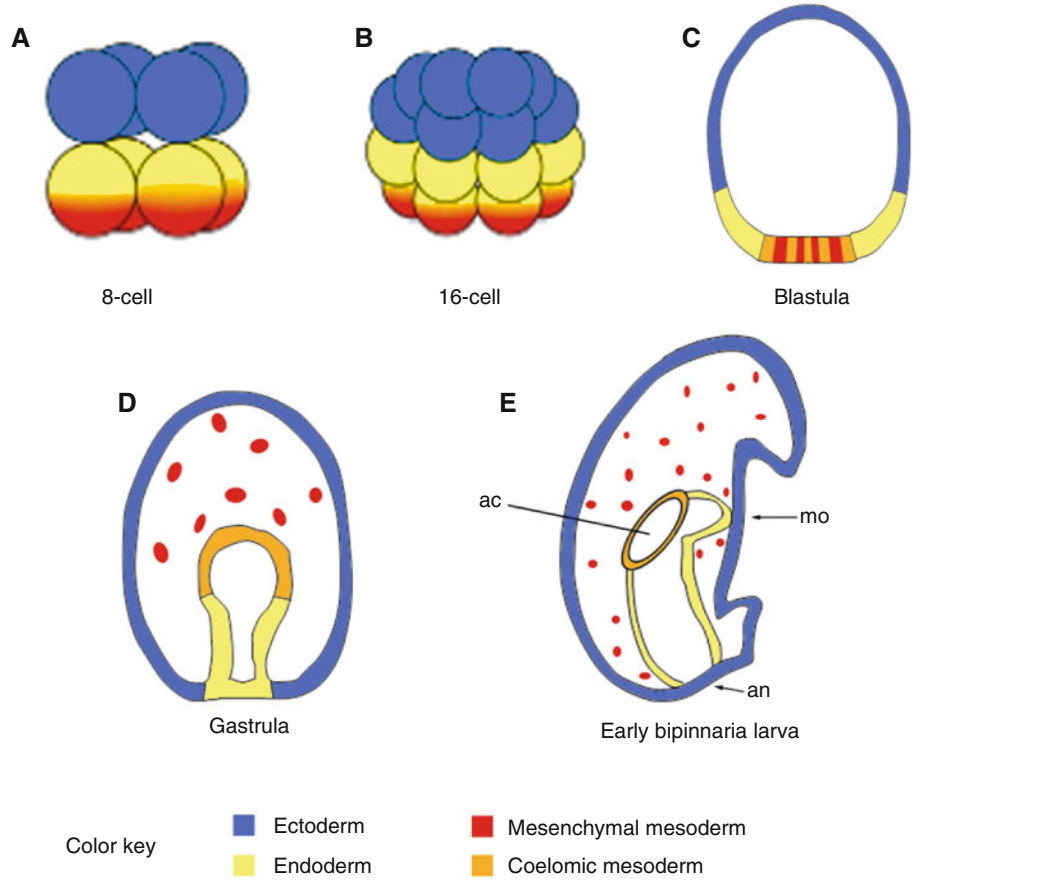
A
B
C
8-cell
16-cell
Blastula
D
E
ac
mo
an
Gastrula
Early bipinnaria larva
Color key
Ectoderm
Endoderm
Mesenchymal mesoderm
Coelomic mesoderm

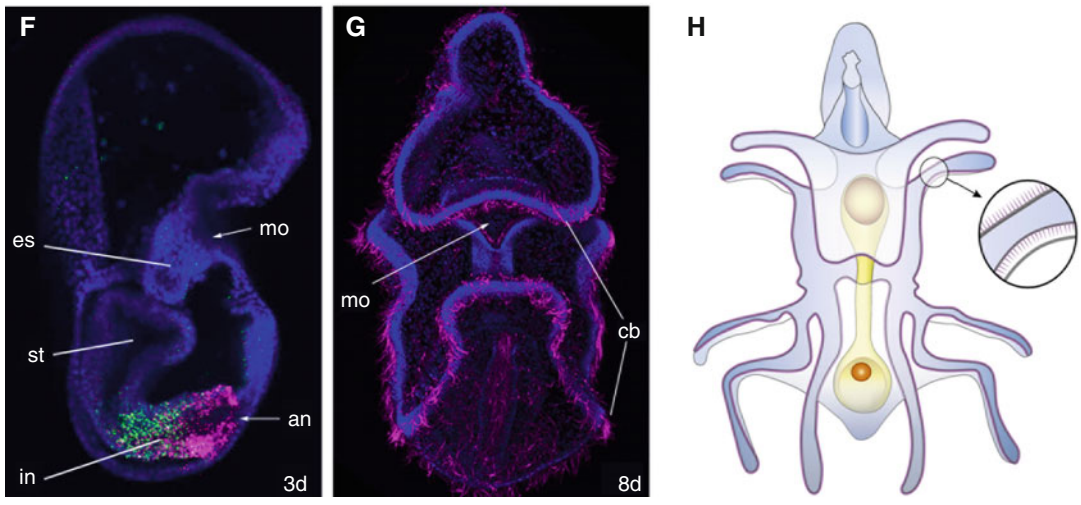
F
es
mo
st
an
in
3d
G
mo
cb
8d
H

embryos can be seen as divided into an1, an2, veg1, and veg2 cell lineages. Because cleavage is equal, sea star embryos do not form micromeres. In the fully formed blastula, the ectoderm is covered with cilia and the embryos start to rotate within the fertilization envelope, about 1 h before hatching, which is at around 26 h at 15 °C. Prior to gastrulation, a thickened vegetal plate appears (Fig. 1.9C). Similar to sea urchins, this is the region from which all endodermal- and mesodermal-derived structures will develop. Remarkably, gene orthologs of many of the regulatory genes expressed in the sea urchin endomesodermal territories are also expressed in the presumptive endoderm and mesoderm of sea stars (Hinman et al. 2003a; Hinman and Davidson 2007; McCauley et al. 2010). However, because sea star larvae do not form a skeleton, the genes that control skeletogenic mesoderm formation in sea urchin larvae are found to be absent, or expressed very differently, in sea star larvae. See Table 1.2 for details.

Gastrulation occurs via sequential invagination from the inner- to outermost cells in the vegetal plate. Cell labeling experiments in *Asterina pectinifera* indicate that the early part of the invaginating archenteron, which derives from the veg2 lineage, contributes to the formation of the rounded top of the archenteron in mid to late gastrulae and also to the anterior coeloms plus the esophagus of the bipinnaria larva. Later invaginating veg2 cells will contribute to the formation of the stomach, while the hindgut derives, in part, from the still later invagination of the veg1 cells (Kuraishi and Osanai 1992). Mesenchyme cells migrate from the top of the archenteron during gastrulation, but unlike in sea urchins, many presumptive mesoderm cells remain associated with the archenteron for a longer period (Fig. 1.9D), developing later on into prominent anterior coeloms on either side of the bipinnaria larval esophagus (Fig. 1.9E; Byrne and Barker 1991). While several blastocoelar cells are generated during gastrulation and remain as scattered cells into the blastocoel at later stages, pigment cells do not form in sea star embryos, which thus develop into completely transparent larvae.

In the late bipinnaria larva, the mouth is fully formed and the gut tube is clearly divided into esophagus, stomach, and intestine, which opens posteriorly through the anus (Fig. 1.9F). In *Patiria miniata*, similarly to *Strongylocentrotus purpuratus*, patterning of the gut tube is evident before any morphological signs are evident: for instance, two ParaHox genes, *PmLox* and *PmCdx,* are expressed in staggered domains of the early intestine, with only partial overlap (Annunziata et al. 2013; see Table 1.2 for comparison). By the late bipinnaria larval stage, ciliated cells distributed over the ectoderm at earlier stages have coalesced into two distinct bands, one that loops above the mouth and one below it, the latter extending from the ventral surface to the anterior, dorsal margins of the ectoderm. As in all echinoderm larvae, cilia can be visualized using an antibody against acetylated α-tubulin (Fig. 1.9G). It is interesting to note that similarly to echinopluteus larvae, bipinnaria larvae have an apical concentration of serotonergic neurons (Byrne et al. 2007). Neurons lie beneath the two loops of the ciliated epithelium and innervate the bands (Nakajima et al. 2004). These neurons coordinate the action of the cilia to enable the larvae to swim and feed in response to the environmental cues provided in the water column. Recently, the specification process and the gene regulatory network that describes the distribution of ciliary band-associated neurons in the sea star bipinnaria larva have been described (Yankura et al. 2013). This process involves genes such as *soxB1*, *soxC*, *nk2.1*, and *six3*, as well as the involvement of Delta-Notch signaling, which can be regarded as common features of nephrozoan neurogenesis (Burke et al. 2014; see also Table 1.2).

Taken together, both asteroid and echinoid feeding larvae form morphologically similar digestive tracts. While endomesoderm is derived from the vegetal pole of both sea star and sea urchin embryos, the formation of mesoderm differs remarkably in these two echinoderm representatives: sea urchins have at least two mesodermal cell types, pigment cells and micromere-derived skeletogenic mesoderm, which are absent in the larval sea star. However, the major difference between sea star and sea urchin feeding larvae is that the latter produces

Table 1.2 Main domains of expression of genes in echinoderm development based on data from in situ hybridization with a focus on transcription factors involved in axial patterning, endomesoderm specification, and neurogenesis

Gene	Class				
	Echinoidea	Asteroidea	Holothuroidea	Ophiuroidea	Crinoidea
hox3	Oral mesoderm of juvenile: dental sacs, spines and beneath epineural folds (Arenas-Mena et al. 1998; Morris and Byrne 2005)	N.A.	N.A.	N.A.	N.A.
hox4	N.P.	Anterior coelom, right and left coelom, hydrocoel; Juvenile coelomic epithelium (Cisternas and Byrne 2009)	N.A.	N.A.	N.A.
hox5	Juvenile rudiment epithelium of epineural folds, primary podia (Morris and Byrne 2005; 2014)	N.A.	N.A.	N.A.	Endomesoderm of auricularia larva (Hara et al. 2006)
hox7	Somatocoel and epineural canal of presumptive juvenile (Peterson et al. 2000a)	N.A.	N.A.	N.A.	Endomesoderm of auricularia larva (Hara et al. 2006)
hox8, hox9/10	Somatocoel of presumptive juvenile (Arenas-Mena et al. 2000)	N.A.	N.A.	N.A.	Endomesoderm of auricularia larva (Hara et al. 2006)
hox11/13a	Somatocoel of presumptive juvenile (Arenas-Mena et al. 2000); Vestibule roof epithelium (Morris and Byrne 2005)	N.A.	N.A.	N.A.	N.A.
hox11/13b	Most posterior embryonic endoderm (Arenas-Mena et al. 2006); anterior endoderm and mesoderm of late larva and somatocoel, anus, and spines of presumptive juvenile (Arenas-Mena et al. 2000)	Most posterior embryonic endoderm (Hinman et al. 2003a)	N.A.	N.A.	N.A.

(continued)

Table 1.2 (continued)

Gene	Class				
	Echinoidea	Asteroidea	Holothuroidea	Ophiuroidea	Crinoidea
gsx	Embryonic ectoderm (scattered cells) (Arnone et al. 2006)	Not expressed during embryonic development (Annunziata et al. 2013)	N.A.	N.A.	N.A.
xlox	Posterior embryonic endoderm (Arnone et al. 2006)	Posterior embryonic endoderm (Annunziata et al. 2013)	N.A.	N.A.	N.A.
cdx	Most posterior embryonic endoderm (Arnone et al. 2006)	Most posterior embryonic endoderm (Annunziata et al. 2013)	N.A.	N.A.	N.A.
otx	Embryonic endoderm and ciliary cells(Gan et al. 1995; Yuh et al. 2002; Nielsen et al. 2003); juvenile nerve ring and podia (Morris et al. 2004; Morris and Byrne 2005)	Embryonic and larval endoderm, coeloms, and ciliary cells (Shoguchi et al. 2000; Elia et al. 2010)	Embryonic endoderm and ciliary cells (Hinman et al. 2003b)	Embryonic ectoderm, gut, and ciliary cells (D.V. Dylus and P. Oliveri, 2014 unpublished); blastema and regenerating arm (A. Czarkwiani and P. Oliveri, 2014 unpublished)	Endoderm (enteric sac) of the auricularia larva (Omori et al. 2011)
gata1/2/3 (gatac)	Embryonic non-skeletogenic mesoderm (Davidson et al. 2002; Solek et al. 2013)	Embryonic mesoderm (Hinman et al. 2003a)	Embryonic non-skeletogenic mesoderm (McCauley et al. 2012)	Embryonic non-skeletogenic mesoderm (D.V. Dylus and P. Oliveri, 2014 unpublished); blastema of regenerating arm (Czarkwiani et al. 2013)	N.A.
gata4/5/6 (gatae)	Embryonic endomesoderm (Lee and Davidson 2004)	Embryonic endomesoderm (Hinman et al. 2003a)	Embryonic endomesoderm (McCauley et al. 2012)	Embryonic endoderm and non-skeletogenic mesoderm (D.V Dylus and P. Oliveri, 2014 unpublished)	N.A.
foxa	Embryonic endoderm (David et al. 1999; Oliveri et al. 2006)	Embryonic endoderm (Hinman et al. 2003a)	Embryonic endoderm (McCauley et al. 2012)	Embryonic endoderm (D.V Dylus and P. Oliveri, 2014 unpublished)	N.A.

tbr	Embryonic skeletogenic mesoderm (Croce et al. 2001)	Embryonic mesoderm (Hinman et al. 2003a)	Embryonic non-skeletogenic mesoderm (McCauley et al. 2012)	Embryonic endomesoderm (Dylus and Oliveri, unpublished)	N.A.
ets1/2	Embryonic mesoderm (Kurokawa et al. 1999; Rizzo et al. 2006)	Embryonic mesoderm (Hinman et al. 2003a)	Embryonic mesoderm (McCauley et al. 2012)	Embryonic endomesoderm (Dylus and Oliveri, unpublished); blastema of regenerating arm (Czarkwiani et al. 2013)	N.A.
pax6	Embryonic coelomic mesoderm (Yankura et al. 2010); Juvenile base of podia (Ullrich-Luter et al. 2011)	Embryonic apical ectoderm and coelomic mesoderm (Yankura et al. 2010)	N.A.	N.A.	Mesoderm (posterior axiocoel) of the auricularia larva (Omori et al. 2011)
six3	Embryonic animal pole ectoderm (Poustka et al. 2007; Wei et al. 2009)	Embryonic apical ectoderm (Yankura et al. 2010)	N.A.	N.A.	Mesoderm (anterior axiocoel) of the auricularia larva (Omori et al. 2011)
soxC	Embryonic animal pole and oral neurogenic ectoderm (Howard-Ashby et al. 2006; Poustka et al. 2007)	Embryonic neurogenic ectoderm (Yankura et al. 2013)	N.A.	N.A.	N.A.
nk2.1	Embryonic animal pole ectoderm (Takacs et al. 2004)	Embryonic animal pole ectoderm (Yankura et al. 2013)	N.A.	N.A.	N.A.
eng	Embryonic mesoderm, ciliary band; juvenile podia (Nielsen et al. 2003)	Larval coeloms, hydrocoel; juvenile nerve ring, radial nerve chord, and podia (Byrne et al. 2005)	N.A.	N.A.	N.A.

N.A. data not available, *N.P.* gene not present

a skeleton during embryogenesis, on which larval shape depends, whereas asteroid embryos and larvae entirely lack this structure.

A vast diversity of asteroids develop through nonfeeding larvae. Details of embryology, larval development and larval plus juvenile nervous system formation in these asteroids are also available for several species (Byrne 1996, McEdward et al. 2002 and Elia et al. 2009). Asteroids with nonfeeding larvae completely lack the bipinnaria stage and are generally divided into the barrel-shaped larvae as seen in *Astropecten* species or the yolky brachiolaria larvae of some asterinid species (e.g., *Meridiastra calcar*) (Byrne 1996; McEdward et al. 2002). Some of the strangest larvae are the benthic brachiolaria of *Leptasterias hexactis* and *Parvulastra exigua* where the brachiolarial arms appear as three feet-like structures that maintain a tenacious attachment to the substratum (Byrne 1996; McEdward et al. 2002).

Development of Holothuroidea (Sea Cucumbers)

Several sea cucumber species have been the subject of embryological studies (reviewed in Hyman 1955; Smiley et al. 1991), in particular species of the Stichopodidae (e.g., *Stichopus*, *Apostichopus*, and *Parastichopus* species) (Holland 1981; Smiley 1986; Shoguchi et al. 2000). A comprehensive gene expression analysis during development in *Parastichopus parvimensis* is available (McCauley et al. 2012), rendering this species a reference model for the development of holothurians. Thus, development of this species is reviewed here.

Cleavage of *Parastichopus parvimensis* is equal and little cell-cell adhesion is seen between the blastomeres (Fig. 1.10A, B). Divisions are not synchronous. Blastulae are formed by 16 h (at 15 °C) after fertilization and hatch from the fertilization envelope at around 26 h. Prior to gastrulation, the embryos elongate along the animal-vegetal axis, with a thickening observed at the vegetal pole, which is termed the vegetal plate. The shape of the sea cucumber blastula closely resembles the one in sea stars, but unlike the latter, mesenchyme cells ingress from the vegetal plate before invagination of the archenteron occurs (Fig. 1.10C). During gastrulation, while most mesenchyme remains associated with the tip of the archenteron, a few cells migrate to take up positions near the blastopore. At the mid-gastrula stage, around 48 h of development, the gut has elongated, the mesenchyme has begun to migrate, and additional mesenchymal cells delaminate from the tip of the archenteron (Fig. 1.10D). At this stage, three distinct populations of mesenchyme cells can be identified by their specific regulatory signatures (McCauley et al. 2012): a skeletogenic mesenchyme cell type, which, as in sea urchins, uniquely expresses the gene *alx1* (a gene expressed in all mesodermal precursors of the sea star embryo) and two types of blastocoel cells which differ from each other by the expression of *gcm*, a gene which is exclusively expressed in pigmented cell precursors in the sea urchin embryo.

Fig. 1.10 Sea cucumber development. (**A**) As in sea urchins and sea stars, the vegetal blastomeres give rise to endomesoderm (*yellow* and *red*) in holothurians, while the animal blastomeres are destined to become ectoderm (*blue*). (**B**) Cleavage is equal in *Parastichopus parvimensis* and little cell-cell adhesion is seen between blastomeres. (**C**) Mesenchyme cells ingress into the blastocoel before gastrulation begins. In the vegetal plate of the mesenchyme blastula, presumptive endoderm (*yellow*) and mesoderm (*red* and *orange*) territories are already segregated. (**D**) At the mid-gastrula stage (around 48 h post fertilization at 15 °C in *P. parvimensis*), the mesenchyme has begun to migrate, with additional mesenchymal cells ingressing from the archenteron. Different colors indicate the different mesodermal cell types: skeletogenic cells (*purple*) and blastocoelar cells, expressing (*red*) or not (*pink*), the *gcm* gene. Early 3-day (**E**) and 6-day (**F**, *P. parvimensis,* courtesy of Veronica Hinman) auricularia larvae display regionalized tripartite digestive tracts. Length of larva in (**F**) = 400 μm. A posterior coelom is evident near to the *left* side of the midgut, but no obvious anterior coeloms are detected. A small skeletal spicule is evident in the posterior part of the larva. (**G**) Schematic representation of an apodid auricularia larva (Courtesy of Santiago Valero-Medranda), highlighting the digestive system (*yellow*/*orange*), ossicles (*brown*), and ciliary band (*purple*; see inset for details). Abbreviations: *cb* ciliary band, *in* intestine, *mo* mouth, *es* esophagus, *pc* posterior coelom, *sk* skeletal spicule, *st* stomach

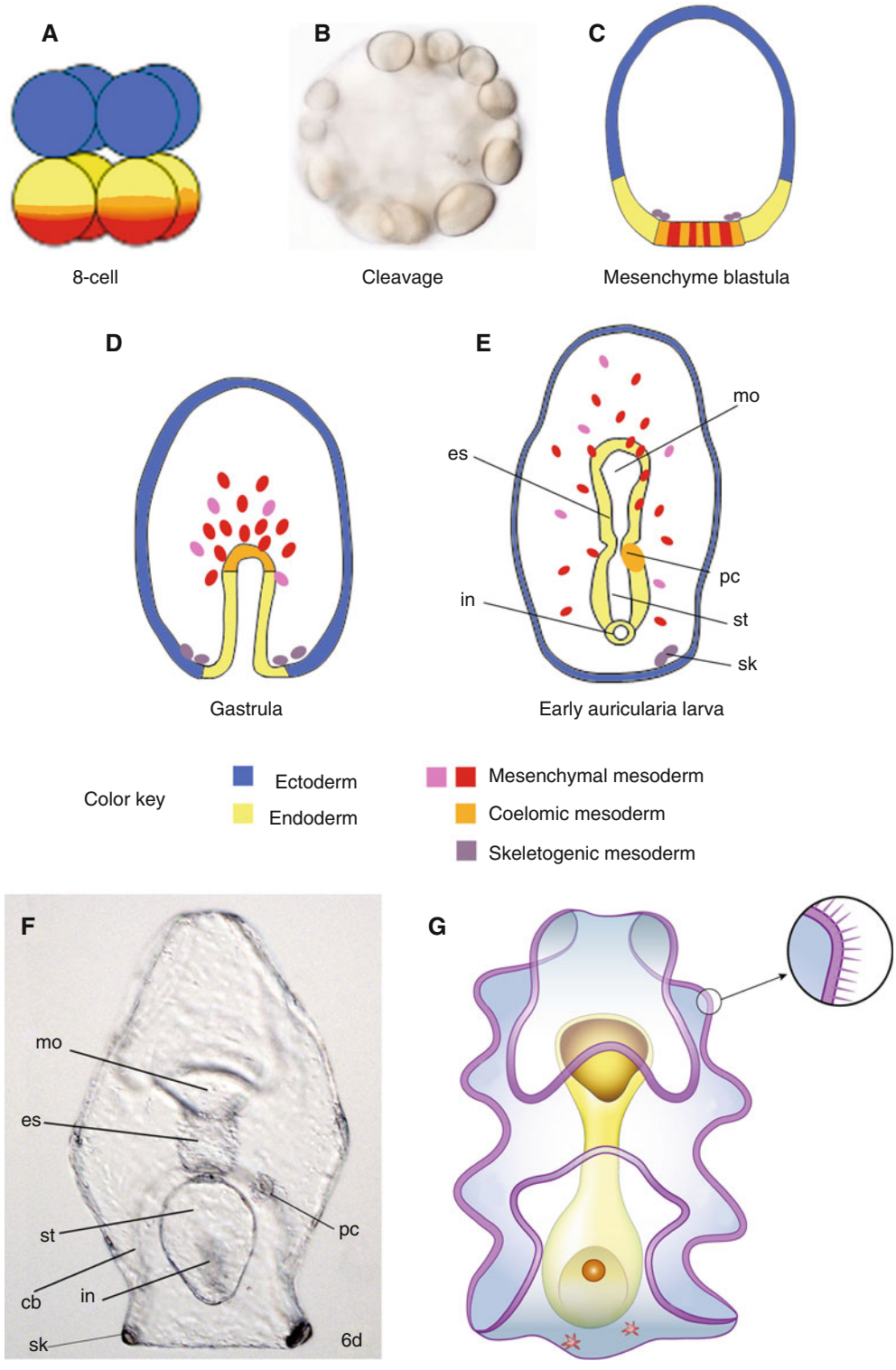
A
B
C
8-cell
Cleavage
Mesenchyme blastula
D
E
mo
es
pc
in
st
sk
Gastrula
Early auricularia larva
Color key
Ectoderm
Endoderm
Mesenchymal mesoderm
Coelomic mesoderm
Skeletogenic mesoderm
F
G
mo
es
st
pc
cb
in
sk
6d

By 72 h of development at 15 °C, the mouth has formed and the embryo reaches the early auricularia larval stage (Fig. 1.10E). The archenteron has differentiated into morphologically distinct fore-, mid-, and hindgut regions which later give rise to the esophagus, stomach, and intestine, respectively, as seen in the 6-day auricularia larva (Fig. 1.10F). Starting at the early auricularia larva stage, presumptive muscle cells can be seen associated with the foregut and a thickened ciliary band is evident in the oral hood, looping above the anus. Also visible at these stages are the coelomic sacs: in particular and from the early auricularia larva stage, a posterior coelom is evident at the left side of the midgut. Auricularia larvae also display a hydroporic canal connecting the left coelomic sac with the dorsal surface of the larva, where the hydropore opens. In some species, such as *Stichopus tremulus*, the coelomic (distal) part of the archenteron sends tubular projections towards the dorsal surface to form the hydroporic canal as early as in the gastrula stage (Hyman 1955). The shape of the larval skeleton varies in auriculariae including the single posterior spicule such as seen in *Stichopus* and *Holothuria* and the wheel-shaped ossicles in apodid larvae (Sewell and McEuen 2002; Ramafofia et al. 2003; McCauley et al. 2012).

The auricularia larva further develops by incorporation of an elaborate ciliated band that extends around the body and projecting lobes (Fig. 1.10G). The lobes formed by the band can become very numerous, although they never develop into distinct larval arms as in the later bipinnaria larvae of asteroids or the plutei of echinoids and ophiuroids (compare larvae in Fig. 1.4). The auricularia superficially resembles the bipinnaria of asteroids, but the ciliary band in the former is organized as a continuous loop over the body, with a structure very similar to that in the tornaria larva of hemichordates (see Chapter 2), while in the bipinnaria of asteroids, it forms two unconnected loops, one smaller than the other (compare with Fig. 1.9G). The auricularia larva also displays in its anterior-most region an apical organ which contains two groups of serotonergic neurons associated with the right and left portions of the anterior ciliary band (Byrne et al. 2007). These neurons are flask-shaped and give rise to a serotonin-positive process.

A vast diversity of holothuroids develops through nonfeeding larvae. Details of their embryology and larval development are available for several species (reviewed in Smiley et al. 1991; Sewell and McEuen 2002). All dendrochirotid sea cucumbers have a barrel-shaped doliolaria larva with rings of cilia (Sewell and McEuen 2002).

Development of Ophiuroidea (Brittle Stars)

In ophiuroids with small eggs, the embryos develop into a pluteus larva (the ophiopluteus) that superficially resembles the echinopluteus larva of echinoids. Several other morphological aspects of these embryos, such as the early ingression of mesenchyme before gastrulation and the prismatic shape of the late gastrula displaying two lateral clusters of mesenchymal cells producing triradiate spicules, are similar to sea urchin embryos. However, cladistic analyses indicate that the pluteus larva may have arisen independently in ophiuroids and echinoids through a process of convergent evolution (Littlewood et al. 1997; Smith 1997). In fact, a closer look at the development of brittle star embryos suggests that there are probably more differences than similarities between these two echinoderm clades.

Artificial fertilization generally fails in ophiuroids and hence material for studying their early development must be obtained from natural spawning. This difficulty, together with the opacity of the embryos, explains the few available accounts of development in ophiuroids and why so little is known about the developmental processes and the mechanisms that underlie their regional specification. A recent study using fluorescent dyes and confocal imaging examined in great detail the early embryogenesis and cell fate specification in *Ophiopholis aculeata* (Primus 2005). This species is therefore used herein as an example of brittle star development. However, the following description also takes into account some general features of brittle star embryos (see Hyman 1955; Hendler 1991).

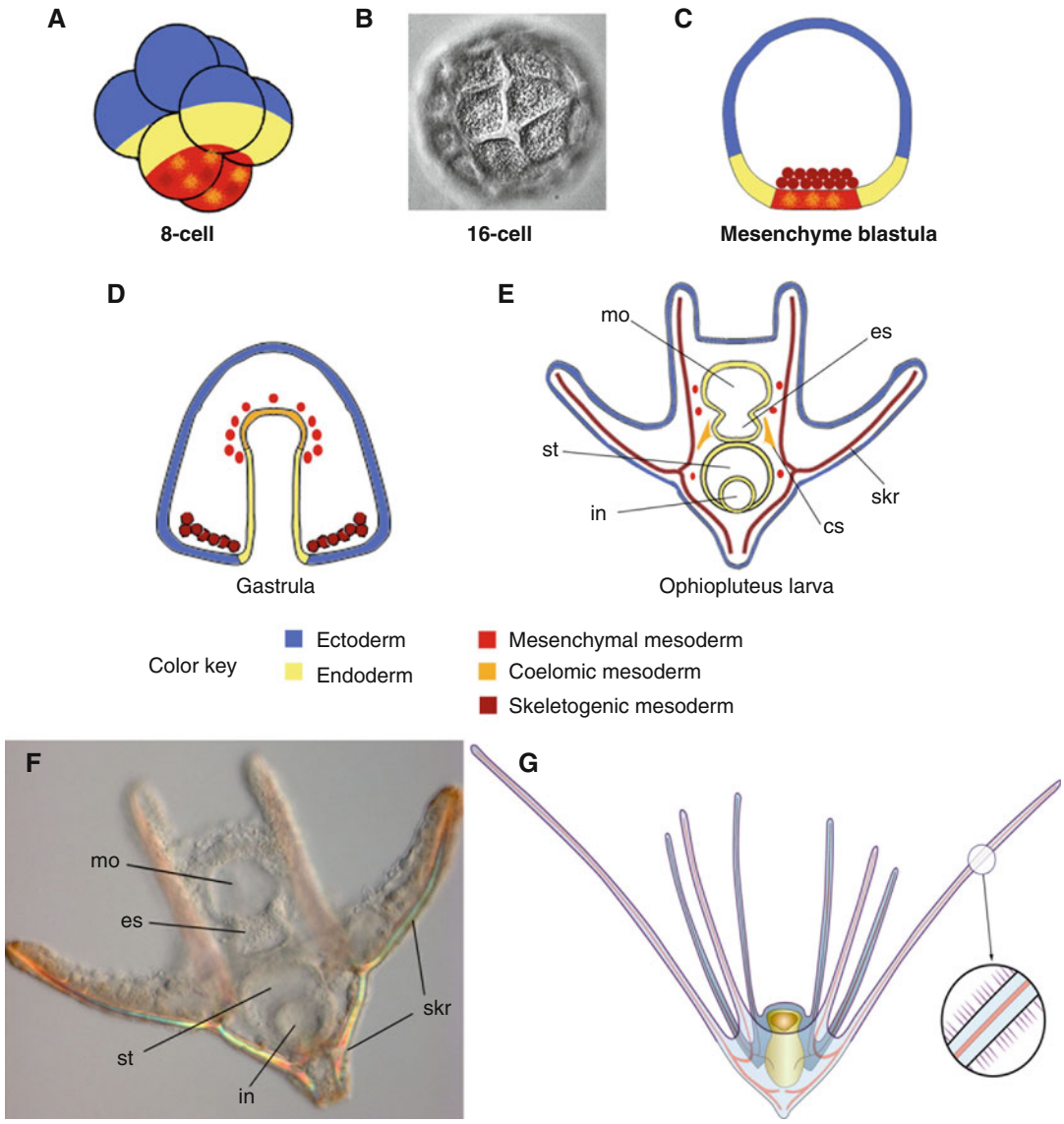

Fig. 1.11 Brittle star development. (**A**) Eight-cell stage showing unusual germ layer-specific contributions of each lineage (see *color code*). Vegetal pole is down. (**B**) *Ophiopholis aculeata* 16-cell stage showing the close association between blastomeres (Primus 2005). (**C**) Mesenchyme blastula stage showing early ingression of skeletogenic mesenchyme cells prior to gastrulation. (**D**) Late gastrula stage. Two lateral clusters of skeletogenic mesenchyme cells are present at the site where triradiate spicules will form. (**E, F**) Ophiopluteus larva showing tripartite gut and elongated arms supported by skeletal rods. The larva in (**F**) is a 4-day-old *Amphiura filiformis* larva (Courtesy of David Dylus and Paola Oliveri). Length of larva = 300 µm. (**G**) Schematic representation of the eight-arm ophiopluteus larva (Courtesy of Santiago Valero-Medranda) highlighting internal skeleton (*brown*) and digestive system (*yellow/orange*). The inset shows a detail of the ciliary band (*purple*). Abbreviations: *cs* coelomic sac, *es* esophagus, *in* intestine, *mo* mouth, *skr* skeletal rod, *st* stomach

Ophiopholis aculeata oocytes average 100–105 µm in diameter when shed. Polar bodies are produced between 30 and 60 min after spawning at 12 °C. The first three embryonic divisions in *O. aculeata* are equal (Fig. 1.11A). A fate map constructed using microinjected lineage tracers indicates that there is a major segregation of ectodermal from endomesodermal fates at first

cleavage, thus highlighting a first major difference between this embryo (and probably in general ophiuroid embryos) and the other echinoderms. Cleavage is equal in ophiuroids (Fig. 1.11B). Cell divisions are synchronous. The cell lineage of the *O. aculeata* embryo has been determined through the 64-cell stage. Cleavage in *O. aculeata* also differs from that of sea urchins with regard to the spatial arrangement of blastomeres in the early cleavage stages. Rather than being organized in orderly tiers, as is the case in sea urchins, early cleavage-stage embryos are typically arranged in a more compact manner (see close contact between blastomeres in Fig. 1.11B).

The *Ophiopholis aculeata* embryo forms a hollow blastula, the vegetal end of which flattens to form a vegetal plate where the blastopore will open, which ultimately becomes the anus of the larva. Similarly to sea urchins and sea cucumbers, mesenchyme cells ingress from the vegetal plate into the blastocoel prior to the onset of gastrulation (Fig. 1.11C). Following invagination, mesenchyme cells continue to be produced at the tip of the elongating archenteron, as in all the echinoderm classes examined so far. During gastrulation, numerous mesenchyme cells become localized in two lateral clusters and they will produce triradiate calcareous spicules that ultimately become the larval skeleton (Fig. 1.11D). Similarly to what was done with the sea urchin embryo, in experiments performed as early as at the time of Hans Driesch (Driesch 1892), the distribution of developmental potential in the early *O. aculeata* embryo was also examined by isolating different regions of the early embryo and following these isolates through larval development (Primus 2005). These analyses indicate that endomesodermal potential segregates unequally at the first, second, and third cleavages in *O. aculeata*. As a result, the unusual fate map reported in Fig. 1.11 was constructed; this highlights the differences in early development that exist between *O. aculeata* (and most likely other ophiuroids) and other Echinodermata. It is interesting to note that also the embryos of hemichordates with feeding larvae share the same early segregation of endomesodermal developmental potential observed in other echinoderm classes, thus making the early embryogenesis of ophiuroids an exceptional case within the Ambulacraria.

After gastrulation is completed, the tip of the archenteron differentiates as a thin-walled sac (Fig. 1.11D) from which two coelomic sacs are formed. The gastrula broadens its blastoporal surface and the ventral side becomes flattened. From the ventral surface, and near the animal pole, a stomodeal invagination is produced that, once fused with the archenteron, will establish the usual L-shaped digestive tract that soon will differentiate into esophagus, stomach, and intestine. By the fourth day of development, a pluteus larva with a tripartite gut and arms supported by calcareous spicules has formed (Fig. 1.11E, F). This larval morphology becomes more complex by further elongation of the primary four arms and the development of others, all supported by skeletal rods, and a well-defined ciliated band (Fig. 1.11G). As previously pointed out, ophioplutei superficially resemble echinoplutei (Fig. 1.4); thus, a similar nomenclature is used for their arms. However, the arms are not necessarily homologous between the two groups. Both generally have four pairs of arms, but there appears to be less variation in body form and number of larval arms in ophioplutei and the skeleton is generally less complex. Some additional morphological differences are seen in the larval body. While the bodies of ophioplutei are generally dorsoventrally flattened, those of echinoplutei are often laterally flattened. A striking difference between the ophioplutei and all other echinoderm larvae is that the ophioplutei do not present a clear apical concentration of serotonergic neurons, which here are distributed in two lateral ganglia with few cell bodies located within the ciliary band (Byrne et al. 2007).

A vast diversity of ophiuroids develops through nonfeeding larvae. The details of embryology and larval development in these brittle stars are available for several species (reviewed in Selvakumaraswamy and Byrne 2006). The nonfeeding larvae of ophiuroids are morphologically diverse, ranging from species with nonfeeding yolky ophioplutei with a reduced number of arms to vitellaria larvae with patches or rings of cilia (Selvakumaraswamy and Byrne 2006).

Development of Crinoidea (Sea Lilies and Feather Stars)

Crinoidea is the only echinoderm class that does not have any species with a feeding larva. Their early development, therefore, cannot be easily compared with the above descriptions. Crinoids include the feather stars and sea lilies. Feather stars lose their stalk during development, but sea lilies retain it throughout adulthood (Holland 1991).

Development of crinoids has been reported for several species (Holland 1991; Balser 2002; Nakano et al. 2003; Kohtsuka and Nakano 2005). The embryos and larvae of stalked crinoids (sea lilies), which are considered the most basal group of extant echinoderms (Foote 1999; Janies 2001), have been described only recently (Nakano et al. 2003), including several gene expression studies (Hara et al. 2006; Nakano et al. 2009; Omori et al. 2011). Due to the relevance of this group of animals for studies on the origin of the larval and adult body plan of echinoderms and all deuterostomes and because of the availability of these recent molecular studies, they have been chosen here as reference for crinoids development.

The sea lily *Metacrinus rotundus* develops through two successive larval stages: the first is a nonfeeding auricularia stage with ciliary bands similar to those present in the auricularia and bipinnaria larvae of holothurians and asteroids (the dipleurula-type larva of the Ambulacraria); the second is a barrel-shaped doliolaria larva containing circumferential ciliary bands (similar to the earliest larval stage of stalkless crinoids, the doliolaria of holothuroids, and the vitellaria of ophiuroids). Cleavage in *Metacrinus rotundus* is holoblastic, radial, and equal. By the 32-cell stage, a large pore forms in the vegetal area (arrowhead in Fig. 1.12B), possibly equivalent to the pore found at the vegetal side of feather star embryos (Holland 1991). By 24 h (at 15 °C), a gastrula results from invagination at this vegetal pole (Fig. 1.12C). During the next few hours the blastopore closes, while the embryo becomes uniformly ciliated and begins to rotate inside the fertilization envelope. The *M. rotundus* embryo hatches at the late gastrula stage (Fig. 1.12D). Unlike what is observed for the gastrulae of the feather star *Antedon* (reviewed in Hyman 1955), no mesenchymal cells are detected in the blastocoel of *M. rotundus* at the early gastrula stage.

A few hours after closure of the blastopore, a circular constriction in the middle of the archenteron appears, that can now be regarded as a closed sac. Several rearrangements of this archenteral sac occur, which ultimately give rise to three separate sacs: the anterior "axo-hydrocoel" (Hara et al. 2006), which is the first one to differentiate; the central "enteric sac"; and the posterior lobe, also called "presumptive somatocoel". At this point, the embryo has reached the early auricularia larval stage (Fig. 1.12E). A few putative mesenchymal cells are observed in the blastocoelar space, which contains the axo-hydrocoel, the middle part, and the posterior lobe. Thirty hours (at 15 °C) after blastopore closing, the presumptive somatocoel separates into left and right somatocoels, and the enteric sac elongates posteriorly, moving into a space between the left and right somatocoels. This larva, after 3 days of development, has reached the auricularia stage (Fig. 1.12F). The overall shape of this larva, possessing an anterior and a posterior ciliated band, is reminiscent of that of the sea cucumber auricularia and the starfish bipinnaria larvae. In fact, although the ventral side of this larva is indented by a vestibular invagination, in the roof of which is a mouth invagination (Fig. 1.12F), this is not connected with the rest of the gut. Similarly to what is observed in other echinoderm larvae, the left side of the axo-hydrocoel establishes communication with the exterior via a hydropore.

The expression patterns of genes known to have important roles in patterning metazoan embryos have been recently analyzed during *Metacrinus rotundus* development. These are the homologs of the Hox genes *hox5*, *hox7*, *hox8*, and *hox9/10* (Hara et al. 2006) as well as *six3*, *pax6*, and *otx* (Omori et al. 2011). All these genes appear to have a role in patterning the larval endomesoderm during early development in stalked crinoids (Fig. 1.12D–F; see Table 1.2 for comparison with other echinoderms).

The *Metacrinus rotundus* auricularia larva has a short life and within a few days undertakes

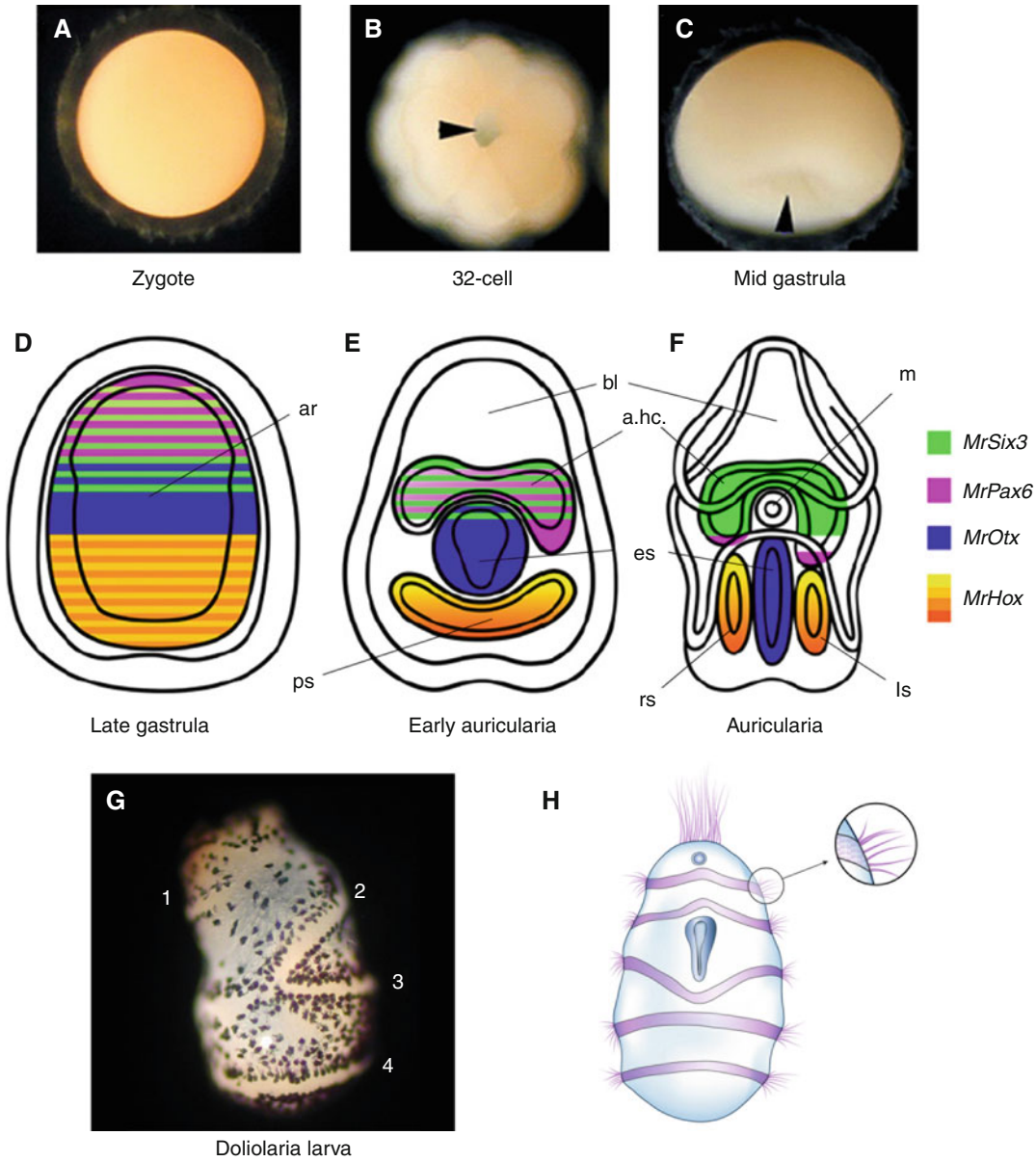

Fig. 1.12 Sea lily (*Metacrinus rotundus*, **A–G**) and feather star (*Antedon*, **H**) development. (**A**) Fertilized egg within a rough fertilization envelope. (**B**) Thirty-two-cell embryo with putative vegetal pore (*arrowhead*). (**C**) Approximate side view of a mid-gastrula (27.5 h post fertilization) showing the blastopore (*arrowhead*). (**D–F**) Development and expression of Hox genes (represented as *yellow*, *pale orange*, *orange*, and *dark orange* areas, corresponding to *MrHox5*, *MrHox7*, *MrHox8*, and *MrHox9/10*, respectively), *MrSix3* (*green*), *MrPax6* (*pink*), and *MrOtx* (*blue*) in the endomesoderm of *M. rotundus* from late gastrula to auricularia larva. (**G**) Ten-day *M. rotundus* doliolaria larva (Courtesy of Hiroaki Nakano) showing circumferential ciliary bands (1–4). Length of larva = 500 μm. (**H**) Schematic representation of a feather star (*Antedon*) doliolaria larva (Courtesy of Santiago Valero-Medranda), highlighting adhesive pit (*top blue circle*), vestibule (*blue oval*), and ciliary bands (*purple*; see inset for details). Abbreviations: *a.hc.* axo-hydrocoel, *ar* archenteron, *bl* blastocoel, *es* enteric sac, *ls* left somatocoel, *m* mouth, *ps* presumptive somatocoel, *rs* right somatocoel (Modified and adapted from Nakano et al. (2003) (**A–C**) and Omori et al. (2011) (**D–F**))

several morphogenetic transformations. The mouth invagination closes, the overall dimensions of the larvae shrink, and the ciliary bands become rearranged as the auricularia transforms into the doliolaria. Some parts of the bands break up, whereas others fuse, eventually forming four circumferential ciliary bands. The 10-day-old larva has reached the typical barrel shape of a doliolaria larva and the doliolaria plus vitellaria of sea cucumbers and brittle stars, respectively (Fig. 1.12G, H), similar to feather stars, (Holland 1991) and the dololaria and vilellaria of sea cucumbers and brittle stars, respectively (Byrne and Selvakumaraswamy 2002; Sewell and McEuen 2002).

Gene Regulatory Networks in Echinoderm Evolution and Development

The circuitry of endomesoderm specification in the sea urchin embryo has been studied in detail and has led to the elaboration of a complex gene regulatory network (GRN) model that displays how endomesoderm development progresses from fertilization until 30 h post fertilization (hpf) at 15 °C (in *Strongylocentrotus purpuratus*), when the tissue has already been segregated into definitive endoderm and mesoderm (Davidson et al. 2002; Ransick and Davidson 2006; Croce and McClay 2010; Peter and Davidson 2010, 2011; Lhomond et al. 2012; Materna and Davidson 2012). This is possibly the best GRN so far described which accounts for a complex developmental process, in space and time, and it is here used as an example of how this functional approach can be applied to gain a better understanding of the development of an entire embryo or parts of it (see Vol. 1, Chapter 2).

The endomesoderm in the sea urchin embryo *Strongylocentrotus purpuratus*, as mentioned above, derives at the sixth cleavage (about 7 hpf) in the vegetal half of the embryo from the veg2 lineage, whereas from the veg1 lineage only the most part of the oral endoderm and ectoderm will form (see also Figs. 1.6 and 1.8). Then, at 18hpf, the veg2 lineage consists of two concentric rings of cells, the inner ring (veg2L) destined to become mesoderm and the outer ring (veg2U) destined to become endoderm. Using a system-wide perturbation analysis approach, Davidson and collaborators have been able to provide a causal explanation for the dynamic process underlying the separation of the regulatory state leading to the different fates of the veg2 and veg1 lineages plus the further partitioning of the veg2 lineage in two distinct domains (rings), with their specific regulatory states. The dynamics of gene interactions happening in time and space within the endomesoderm is reflected in a complex GRN that describes the process in unprecedented detail (http://sugp.caltech.edu/endomes) (Fig. 1.13).

Within this GRN, three molecular components constitute the core machinery of endomesoderm segregation: the Delta/Notch pathway and the transcription factors *Sp-FoxA* and *Sp-Gcm*. The Delta/Notch pathway regulates non-skeletogenic mesoderm (NSM) specification (Sherwood and McClay 1999; Sweet et al. 2002). *Sp-Delta*, the ligand of the pathway, is first expressed in the skeletogenic mesoderm, the derivative of the large micromeres, at around 8–9hpf, where it has been demonstrated that it signals to the neighboring ring of veg2 endomesodermal cells, turning on *Sp-Gcm* transcription (Ransick and Davidson 2006). After the veg2 tier of cells segregates into an inner and outer tier, Sp-Delta signal is only received in the inner tier, adjacent to the skeletogenic cells, becoming the mesoderm precursors. There, Sp-Delta activates *Sp-GataE* (Lee and Davidson 2004) and subsequently the transcription factors *Sp-Prox1, Sp-Ese,* and *Sp-GataC* (and others) in the oral and *Sp-Six1/2* (plus others) in the aboral mesoderm (Materna and Davidson 2012). After ingression of the primary mesenchyme cells (PMC), *Sp-Delta* ceases to be expressed there and turns on in the non-skeletogenic mesoderm (NSM). This second wave of Sp-Delta does not affect the surrounding presumptive endoderm cells, although they are now in direct contact with the Sp-Delta source. On the contrary, it serves to deactivate endodermal genes in the NSM

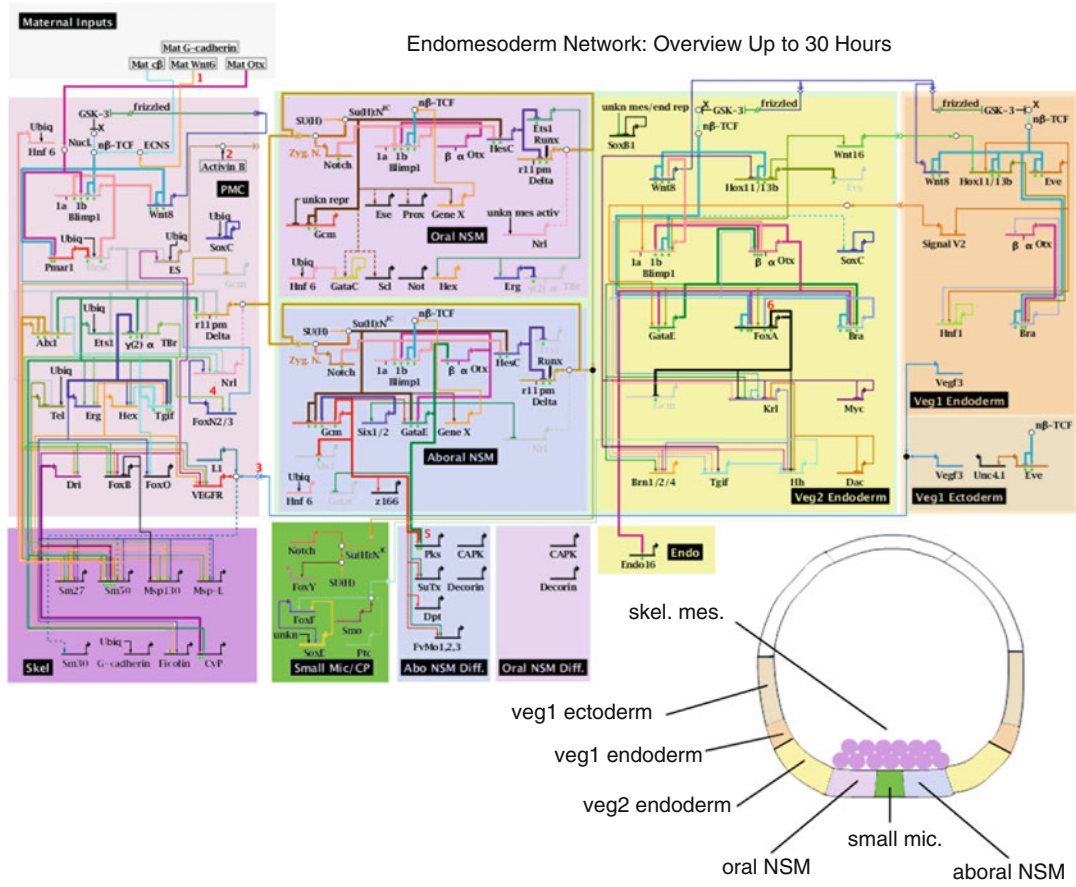

Fig. 1.13 Biotapestry diagram summarizing the gene regulatory interactions occurring during endomesoderm specification in *Strongylocentrotus purpuratus*. The last updated diagram is schematized (11/2011). The diagram is also available on the E. H. Davidson's laboratory webpage (http://sugp.caltech.edu/endomes). Colors label the different embryonic territories. Connecting lines indicate gene interactions

precursors (see below) (Croce and McClay 2010; Peter and Davidson 2011; Materna and Davidson 2012). It is known that mesodermal Sp-Delta provides a "switch" input to small micromeres and particularly to *Sp-FoxY* expression and that this later Sp-Delta signal is required for the specification of late mesoderm derivatives such as coelomic pouches and muscles (Sweet et al. 2002; Materna and Davidson 2012).

One of the first known direct outcomes of the first Delta/Notch pathway is the activation of the transcription factor *Sp-Gcm*. The *Sp-Gcm* promoter contains several Suppressor-of-Hairless (SuH) binding sites that mediate *Sp-Gcm* activation (Ransick and Davidson 2006), and the Notch pathway is known to directly activate *SuH* (Fortini and Artavanis-Tsakonas 1994). *Sp-Gcm* is later required for the development of the pigment cells by becoming involved in a positive intergenic feedback loop with *Sp-Six1/2* (Ransick and Davidson 2006). In the process of progressive segregation of fates within the endomesoderm, other transcription factors are relevant, for instance, *Sp-FoxA*. Reports on this gene indicate that *Sp-FoxA* is expressed in the definitive endoderm, where it promotes endoderm specification (Oliveri et al. 2006).

The endodermal regulatory state is dependent on a Wnt/β-catenin signaling under the spatial control of genes mediated by TCF regulatory sites. This Wnt/TCF system, together with a maternal/early zygotic form of *Sp-Otx*, activates

the endodermal regulatory genes *Sp-Blimp1b, Sp-Eve,* and *Sp-Hox11/13b* (Yuh et al. 2002; Arenas-Mena et al. 2006; Smith et al. 2008a), which will then activate *Sp-Brachyury, Sp-FoxA,* and *Sp-GataE. Sp-Gcm* at that time (12–16hpf) is coexpressed with *Sp-FoxA* in the veg2 tier and until a few hours later (18 h), when the expression domains of the two become exclusive, with *Sp-Gcm* being expressed only in the veg2L and *Sp-FoxA* in the veg2U cells. The repression of the endodermal genes in the mesodermal ring of cells (veg2L) occurs through an elegant regulatory-state exclusion mechanism: the same TCF sites that are used to initiate the endoderm GRN in the veg2 lineage are used again to extinguish it in the mesoderm precursors. The mechanism seems to depend on Delta/Notch signaling, via a MAP kinase pathway (Rottinger et al. 2006).

On the other hand, *Sp-FoxA* represses mesoderm development in the endoderm tier by preventing *Sp-Gcm* expression (Oliveri et al. 2006). All these molecular events driving the initial segregation of fates within the endomesoderm show the complexity of regulatory events needed to ensure the proper development of tissues and cell types within embryos.

The approach to study GRNs in development can obviously be applied to any developmental process in any embryo that allows for high-throughput gene perturbation analyses. Several studies are emerging which use this approach, for instance, and within echinoderms, the GRN which controls gut regionalization in the post-gastrular sea urchin embryo (Annunziata and Arnone 2014), the network responsible for oral and aboral ectoderm differentiation and ecto-endoderm boundary formation (Su et al. 2009; Li et al. 2014), or the network that defines the distribution of ciliary band-associated neurons in the bipinnaria larva of the sea star (Yankura et al. 2013). Other recent examples of the use of the same approaches outside echinoderms are the deciphering of the primary cardiac gene regulatory network in the invertebrate chordate *Ciona intestinalis* (Woznica et al. 2012) or the GRNs that underlie the compartmentalization of the *Ciona* central nervous system (Imai et al. 2009) (see Chapter 4).

GRN studies not only provide explanation of how regulatory states are established in particular cells during development and how these states eventually determine the final morphology of the embryo but also provide a powerful tool, through comparisons of GRN architectures, to reveal the molecular evolution of developmental programs among different organisms (Hinman et al. 2003a; Hinman and Davidson 2007; McCauley et al. 2010).

As previously described, in both sea urchin and sea star embryos, the endomesodermal territories arise from the vegetal plate, where the invagination movements of gastrulation start. Mesoderm progenitors are located in the center of this plate and are the first to invaginate. The outer tiers of cells will progressively invaginate to form the fore-, mid- and hindgut. In this processes, the sea urchin and the starfish are very similar. However, sea urchins have a micromere set of cells that will give rise to the larval skeleton (this territory, missing in sea star, is represented in pink in Fig. 1.14A). When the sea urchin and sea star GRNs for endomesoderm specification are compared, an almost perfectly conserved five-gene network subcircuit, required for endoderm specification, becomes evident (highlighted in red in Fig. 1.14B). However, beyond this so-called "conserved regulatory kernel" (Davidson and Erwin 2006), the GRN structure, upstream and downstream of the kernel, has diverged extensively. These changes are translated into specific phenotypic effects. For example, mesoderm specification occurs quite differently: in sea urchins, mesoderm specification is induced by the Delta-Notch signal (originated from the micromere lineage at the center of the vegetal pole) which impinges on the cis-regulatory apparatus of the *gcm* gene, while in the sea star the Delta-Notch signal has the contrary effect of preventing mesoderm specification. A second type of change observed in GRN structure is mediated by regulatory gene co-option, the redeployment of network regulatory genes in new locations, and/or different times leading to new functions. For instance, instead of the skeletogenic functions executed by the *tbrain* regulator in the micromere lineages of the sea urchin (Oliveri et al. 2002), the *tbrain* gene is required in the sea

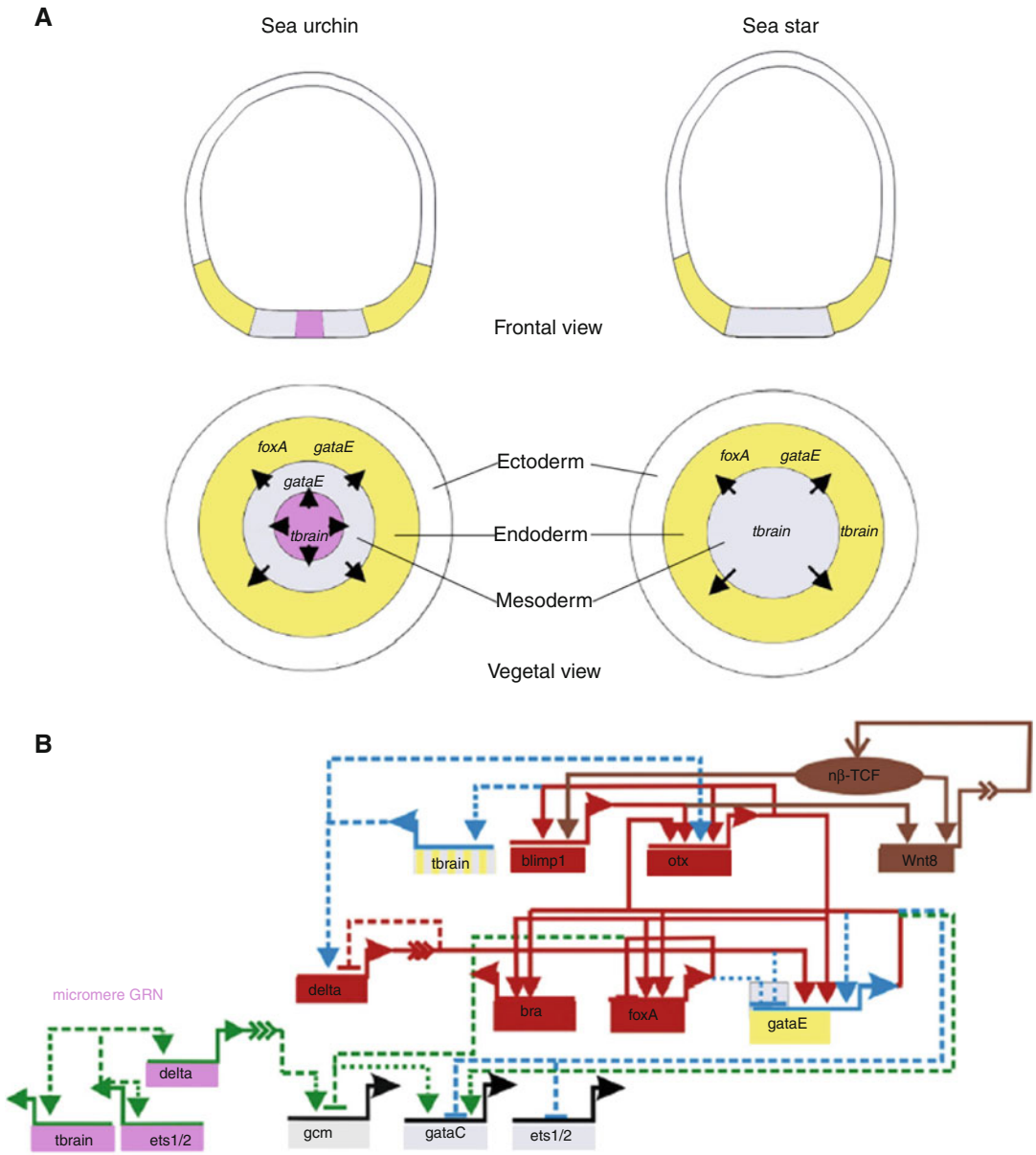

Fig. 1.14 Conservation and divergence in endomesoderm specification in sea urchins and sea stars. (**A**) Schematic representation of sea urchin and sea star blastulae. In the vegetal view of the embryos (*lower* part of the panel), some gene names are overlaid on their domains of expression, e.g., *tbrain* is expressed in the micromere cell lineage (*pink*) in the sea urchin and in the mesodermal and endodermal territories (*gray*) in the sea star and *gataE* is expressed within the endoderm and mesoderm in sea urchin but only in the endoderm in sea star. The *black arrows* represent Delta-Notch signaling from one cell territory to another. (**B**) The GRN depicting endomesoderm specification in sea urchins and sea stars at blastula stage. The regulatory interactions found in common in both taxa are shown in *red* (*solid lines*), while those occurring in the sea urchin only are shown in *dashed green lines*, and those only occurring in the sea star are shown in *dashed blue lines*. In sea urchins, the nuclearization of β-catenin is critical for the establishment of endomesoderm and forms a positive feedback loop with blimp1 (shown in *brown*). The role of nuclear β-catenin has not been examined in sea stars, but is likely to be conserved (Modified and adapted from Hinman et al. (2009))

star embryo for archenteron formation, a role performed under the control of endodermal regulators (*otx* and *gatae*), genes that do not affect the sea urchin *tbrain* gene expression at any time of development (see blue dashed arrows in Fig. 1.14B). A third difference between networks is the use of the *foxa* gene to repress mesoderm formation in sea urchin, a role taken by *gatae* in sea star embryos (compare blue and green dashed arrows in Fig. 1.14B); see Table 1.2 for comparison.

These observations demonstrate that GRNs are formed by discrete functional subcircuits which are affected by diverse selective pressures. Comparative GRN analyses provide us with key insights into the evolutionary processes that model body plans at the DNA regulatory level. As a general rule, it is assumed that the GRN subcircuits involving positive feedback tend to be conserved, generating constraints during development. This conservation may reflect a specific arrangement of transcription factor binding sites in cis-regulatory modules.

For quite a long time echinoderm biology has been greatly contributing to shed light on fundamental questions in developmental biology. The experimental availability of embryos belonging to different species, all separated by various evolutionary distances and accessible to the tools of modern regulatory biology, has proven invaluable. In the last two decades, this group of animals has been instrumental in addressing key biological questions such as how gene regulatory networks control development and how they evolved. In other words, echinoderm models have the potential to greatly contribute to solve central questions in the evolution of development, particularly from a gene regulation point of view. The larvae of echinoderms provide the rich source of morphological variation necessary to address relevant questions such as the evolution of novelties. There are many differences among echinoderm larval forms, but perhaps the most dramatic and obvious is the larval skeleton, which provides the structural material that gives the larva its typical morphology. Larval skeletons are found in the sea urchin echinoplutei and in the brittle star ophioplutei, but not in sea star larvae (see previous sections). Small larval spicules and ossicles are also found in the auricularia larvae of holothurians (see above). All the echinoderm embryos that produce larval skeletal elements share an early ingression of the mesenchyme cells, prior to gastrulation, although it appears that only sea urchins establish their skeletogenic cell lineage via an asymmetric blastomere cleavage that leads to micromere formation. The micromere skeletogenic lineage can therefore be considered a novelty in echinoids. However, it is important to point out that due to some unresolved uncertainties in echinoderm evolution, it is not clear when a larval skeleton was first invented (see Fig. 1.15 for alternative scenarios). It has been proposed, for instance, that the gene regulatory network that controls larval skeleton formation in sea urchins was co-opted from its adult skeletogenic program (Gao and Davidson 2008; Koga et al. 2014). However, it is not clear when this happened. One way to address this question would be to analyze the molecular mechanisms which control specification of larval skeletogenic lineages in other echinoderm taxa, particularly in brittle stars. This approach would shed light on the question of whether the echinoplutei and the ophioplutei are homologs or not. Additionally, and perhaps more importantly, approaching this or other developmental questions, at a deep gene regulatory network level, will provide us with new insights into the understanding of GRN evolution. The example given here is, perhaps, one of the most obvious, but questions from polarity to the specification of different cell lineages or the morphological arrangement of tissues are putative targets for undertaking similar approaches.

LATE DEVELOPMENT

Echinoderms are unique among bilaterians in that the adults have a pentameral radial body plan, the phylotypic character of the Echinodermata. The larvae, however, are bilateral with some asymmetry conveyed by the expansion of the coeloms on the left side (Hyman 1955; David and Mooi 1998). This “asymmetrical

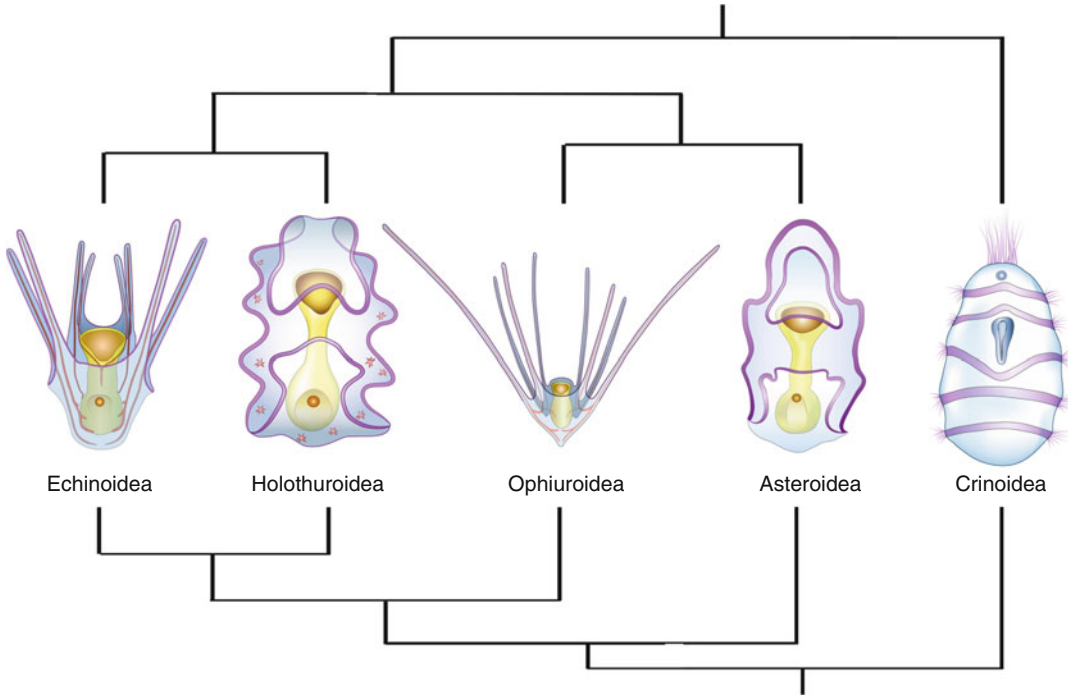

Fig. 1.15 Distribution of larval types in echinoderm phylogeny. Representative echinoderm larvae are displayed according to the two alternative phylogenetic scenarios illustrated in Fig. 1.3

bilaterality" is particularly prominent in species with nonfeeding larvae (Smith et al. 2009; Morris 2011, 2012; Morris et al. 2011). At metamorphosis, the bilateral larva transforms into the radial juvenile with a new main body axis, the oral-aboral axis. This change from a bilateral larva to a radial adult is of great interest and there are many reviews on echinoderm metamorphosis and the morphological changes that occur (Bury 1895; Hyman 1955; Chia and Burke 1978; Burke 1989).

From Bilateral to Radial Symmetry: Larval and Adult Polarities

Transformation from the larval to the adult echinoderm involves two major phases: (i) coelomogenesis, including formation of the hydrocoel and the origin of the pentameral plan, and (ii) metamorphosis. Coelomogenesis starts early, shortly after gastrulation. Although details of coelom development differ among groups, in most echinoderms the left coelom gives rise to the adult hydrocoel and somatocoel. The hydrocoel and its five lobes are the core of the body plan. These lobes form the primary podia. In juvenile development these podia give rise to the radial canals of the adult water vascular system. Each radial canal extends from a growth zone at the base of the primary podium (Morris 2012). In all echinoderms coelomic development on the larval left side is the basis for construction of the adult. The left somatocoel becomes the body coelom of the adult echinoderm (Burke 1989), while the right coelom of the sea star larva also contributes to the adult body coelom (Morris et al. 2011).

The interaction between the hydrocoel and overlying ectoderm is important during development of the juvenile body – called the juvenile rudiment. In euechinoid sea urchins, crinoids, and holothuroids, an ectodermal invagination, the vestibule, forms adjacent to the hydrocoel and the juvenile develops within the vestibule-like invagination (Smiley 1986; Burke 1989; Holland 1991; Smiley et al. 1991; Ramafofia et al. 2003). In other groups, such as the cidaroid sea urchins,

asteroids, and ophiuroids, the juvenile develops on the external surface of the larva (Emlet 1988; Byrne and Barker 1991; Selvakumaraswamy and Byrne 2006).

The timing of development of the coeloms and the rudiment differs in species with development through a feeding larva and those that develop through a nonfeeding larva. In species with feeding larvae, the time between the initiation of coelomogenesis and rudiment development can be days to months, as the larva accrues sufficient nutrients to support metamorphosis (Byrne and Barker 1991; Smith et al. 2008b). Species with nonfeeding larvae, in contrast, have considerable maternal nutrients and start building the rudiment shortly after gastrulation (Minsuk and Raff 2002; Raff and Byrne 2006; Smith et al. 2009; Morris 2012). The rapid formation of the juvenile in species with nonfeeding larvae is facilitated by a heterochronic shift in the early development of the left coelom (Raff and Smith 2009; Smith et al. 2009).

Morphogenesis of the developing juvenile is complex. This is best documented for sea urchins, in an species with planktotrophic larvae, *Strongylocentrotus purpuratus* and *Paracentrotus lividus* (Gosselin and Jangoux 1998; Smith et al. 2008b), and in species with lecithotrophic larvae, *Heliocidaris erythrogramma* (Minsuk and Raff 2002; Morris 2011) and *Holopneustes purpurascens* (Morris 2012). There are also good descriptions of metamorphosis in the other echinoid groups with feeding larvae (Emlet 1988; Vellutini and Migotto 2010). Rapid development (3–5 days) of a comparatively large rudiment in echinoids with lecithotrophic larvae has been particularly important in generating insights into coelomogenesis and metamorphosis (Minsuk and Raff 2002; Minsuk et al. 2009; Smith et al. 2009; Morris 2011, 2012).

In euechinoids, the vestibule and invagination of the ectoderm forms on the left side of the larvae. This structure forms from ectoderm overlying the region where the hydrocoel forms. The ectoderm in this region thickens and invaginates to form the vestibule. The vestibule floor develops an intimate contact with the primary podia. This mesoderm-ectoderm communication is important in development of the adult rudiment centered on the oral pole of the future oral-aboral axis (Burke 1989; Minsuk and Raff 2002; Smith et al. 2008b; Minsuk et al. 2009). The center of the vestibule becomes the adult mouth. Inductive signals from the left coelom are important for development of the rudiment (Minsuk et al. 2009). The five primary podia and the developing spines that develop between the podia project into the vestibule so that the thickened epithelium of the vestibule floor forms the external outer cover of these structures. The vestibule ectoderm also forms the nervous system, as indicated by the expression of neural genes such as *otx* in this region (Morris et al. 2004). Between the podia a thickening of tissue forms, the epineural folds. These rise up and fuse to close over the developing neural tissue (von Ubisch 1913). The skeleton is formed by associated mesoderm. Prior to metamorphosis, the vestibule and the developing rudiment dominate the left side of the euechinoid larva. In contrast, cidaroid larvae do not form a vestibule. In these echinoids the rudiment is exposed on the left side of the larva (Emlet 1988). In echinoids, the oral-aboral axis of the future adult is positioned on the respective left-right axis of the larva.

Morphogenesis of the developing juvenile asteroid is described for species with planktotrophic larvae, particularly *Asterias rubens* and *Patiriella regularis* (Gemmill 1914; Byrne and Barker 1991; Gondolf 2000) and with lecithotrophic larvae, for instance, *Asterina gibbosa*, *Leptasterias hexactis*, and *Parvulastra exigua* (Chia 1968; MacBride 1896; Morris et al. 2009). The hydrocoel and rudiment develops on the left side of the larva, and as in echinoids, the oral-aboral axis of the juvenile is positioned on the respective left-right axis of the larva. The juvenile asteroid develops as the larval body is absorbed into the future oral region of the sea star.

In holothuroids and ophiuroids, the hydrocoel originates on the left side but shifts in position during rudiment development. In holothuroids, a vestibule-like structure forms at the anterior end of the larva in the oral region and the oral-aboral axis of the future adult is positioned on the anterior-posterior axis of the larva (Hyman 1955; Smiley 1986; Smiley et al. 1991). In ophiuroids, the juvenile oral-aboral axis develops along the dorsoventral axis of the larvae (Hyman 1955; Hendler 1991). The juvenile ophiuroid develops externally. Crinoids differ from the other groups

in that the hydrocoel and vestibule originate ventrally and then become positioned at the anterior end of the larvae as the rudiment develops (Holland 1991). Thus, the juvenile crinoid oral-aboral axis is positioned along the anterior-posterior axis of the larvae.

The patterning mechanisms underlying development of the pentameral body plan are poorly understood. Several studies document expression of signaling and homeobox genes in the coeloms (e.g., *eng*, *wnt*, *hox4*), indicating a role for these genes in early development of the juvenile (Peterson et al. 2000a; Ferkowicz and Raff 2001; Byrne et al. 2005; Cisternas and Byrne 2009). Hox genes are expressed in a spatial and collinear sequence in the coeloms of sea urchin and crinoid larvae (Table 1.2; see Peterson et al. 2000a; Hara et al. 2006). The initial specification of the left coelomic pouch seems to depend on the activation of the BMP signaling pathway (Luo and Su 2012; Warner et al. 2012).

In the developing juvenile of the echinoid *Holopneustes purpurescens*, oral-aboral identity appears to be specified by Hox genes as indicated by the oral expression of *hox3* and aboral expression of *hox11/13* (Morris and Byrne 2014).

Once the rudiment has formed, expression patterns of several genes reflect different aspects of the typical echinoderm body plan (Arenas-Mena et al. 1998; Ferkowicz and Raff 2001; Lowe et al. 2002; Sly et al. 2002; Morris and Byrne 2005; Wilson et al. 2005; Morris and Byrne 2014). The developing five-rayed central nervous system has a distinct pentameral expression of many neural genes (Sly et al. 2002; Morris et al. 2004; Byrne et al. 2005; Morris and Byrne 2005). Some of these genes (e.g., *otx*) are also expressed in development of the peripheral nervous system of the tube feet, indicating a potential role in patterning a so-called "metameric-type" series of outgrowths from the radial canals (Table 1.2; see Byrne et al. 2005; Morris and Byrne 2005).

Metamorphosis

Metamorphosis can occur in the water column (e.g., in ophiuroids) or following settlement of competent larvae (e.g., in echinoids). In echinoids, ophiuroids, and holothuroids, the primary podia are used to select settlement sites and attach to the substrate. In many asteroid and crinoid species, the larvae have specialized attachment structures that they use for settlement. Metamorphosis involves degeneration of the larval body and can take minutes to hours (Chia and Burke 1978). The larval tissue of most echinoderms is discarded or resorbed. In holothuroids, however, the larval body is retained as the ectoderm of the juvenile (Smiley et al. 1991).

In euechinoids, the primary podia extend through the vestibule opening to attach to the substrate, and metamorphosis ensues with eversion of the vestibule. The vestibular ectoderm thus becomes the juvenile epidermis. What remains of the larval tissue becomes positioned as a clump of tissue on the aboral surface of the juvenile and is eventually resorbed. In asteroids, as the juvenile develops in the attached larva, the larval body bends so that the left side of the larva – the oral side of the juvenile – is directed towards the substrate and the right side becomes the upper one. The larval body degenerates into a stalk and is resorbed into the oral region of the young sea star and then the tube feet take over the role of attachment and benthic locomotion.

The bilateral larval axis of holothuroid larvae is congruent with the bilateral axis of the juvenile and adult (Smiley 1986). These echinoderms have a bilateral symmetry as adults superimposed on pentamery (Hyman 1955). The feeding larva transforms into a bilateral juvenile with the primary podia at the anterior end giving rise to the buccal tentacles that are later used for feeding (Smiley et al. 1991; Ramofafia et al. 2001). Pentamery is evident in the five buccal tentacles, which are in a radial position. In holothuroids the canals of the water vascular system form directly from the ring canal in an interradial position and thus are not homologous to the ambulacral canals of other echinoderms.

The larval gut serves as a primordium of parts of the adult echinoderm gut. During metamorphosis there is considerable degeneration of digestive tract cells and reorganization of other digestive tract cells (Chia and Burke 1978). The larval stomach forms the adult stomach. The

mouth appears to form through perforation of the hydrocoel (Gemmill 1914; Bury 1989; Minsuk et al. 2009; Morris et al. 2011). Later, growth of the digestive tract in the perimetamorphic period (sensu Gosselin and Jangoux 1998) is required to complete its morphogenesis. Formation of a functional gut to development of the anus can take days or weeks, depending on the species, and has been described in detail for *Paracentrotus lividus* (Gosselin and Jangoux 1998). The final development of the gut marks the end of metamorphosis.

EVOLUTION OF RADIAL (PENTAMERAL) SYMMETRY: POTENTIAL AXIAL HOMOLOGIES WITH OTHER DEUTEROSTOMES

The most conspicuous characteristic of extant Echinodermata is their adult pentameral (five-fold) symmetry. This symmetry evolved secondarily, as revealed by the presence of bilateral fossils (Smith 2005; Zamora et al. 2012) and the last common ancestor of Bilateria which predates the origin of Echinodermata by many millions of years. The adult echinoderm body is organized along the major body axis, the oral-aboral axis.

It is not clear how this echinoderm body plan relates to the bilaterian anterior-posterior (AP) axis. There are two main hypotheses on echinoderm body plan evolution: (1) the bilateral AP axis in echinoderms is derived from the stacking of the coeloms in development (Mooi and David 2008; Peterson et al. 2000a) and (2) the rays are in line with the chordate AP axis – the rays as the chordate body axis (Raff and Popodi 1996; Heinzeller and Welsch 1999; Morris 2011, 2012).

Coelomic Stacking Hypothesis

Several lines of evidence suggest that the bilateral AP axis in adult echinoderms is derived from the stacking of coelomic compartments that occurs during development (Peterson et al. 2000a; Mooi and David 2008; Smith et al. 2008b). These arguments are based on the expression of regulatory genes (e.g., Hox genes) during postembryonic development, comparative analysis of coelom development in echinoderms, and the analysis of skeletal plate morphology in both extant and fossil echinoderms. This hypothesis uses mesoderm derivatives as the key structures for understanding axial homologies. It is expressed in three steps, along the following lines:

(i) The coelomic stacking theory suggests that the coeloms in sea urchin larvae stack in the order: left hydrocoel-left somatocoel-right somatocoel. This arrangement is seen in development of echinoids with a feeding larva. These coeloms in an oral-aboral direction are hydrocoel, somatocoel, and right coelom. Morris (2012) also derives the AP axis from the oral-aboral arrangement of the coeloms in echinoids with a nonfeeding larva. In this case, the arrangement is derived by bending the chordate AP axis at the junction between the head of the archenteron and the forming coeloms. Thus, both Peterson et al. (2000a) and Morris (2012) get a similar sequence of coeloms from oral to aboral and both homologize this echinoderm adult axis with the AP axis of the deuterostome ancestor.

(ii) The Hox genes seem to work as a vectorial system in all bilaterian animals, providing cells along the major (AP) body axis with positional information. Their regulatory activities extend to all germ layers, although preferentially to the ectoderm and mesoderm. The main feature that characterizes this group of genes is that they are expressed in nested domains along the AP axis, with gene expression domains following the order of the genes on the respective chromosome. It is particularly relevant that some Hox genes are expressed only in the larval somatocoels, again with nested domains of expression, where the most "anterior" Hox genes are expressed in more apical/anterior domains and the "posterior" Hox genes in more blastoporal/posterior domains (Table 1.2; see Arenas-Mena et al. 2000; Hara et al. 2006).

These expression domains indicate the organization of axial domains within the somatocoels and hence in their derivatives. The use of Hox genes in both the specification of the bilaterian AP axis and in the coeloms suggests that the stacking of coeloms might be the best evidence we have for the orientation of the major echinoderm body axis (although co-option cannot be ruled out). During this part of development, there is no expression of Hox genes in the gut or nervous system.

(iii) It has been recognized that all echinoderms, extant and fossil, have body walls with two areas of skeletons, the so-called axial and extraxial skeletons (Mooi and David 1997, 2008). Although both types are composed of the same biomineral matrix, it is suggested that they may be patterned by different sets of regulatory genes (Mooi et al. 2005; Mooi and David 2008). While the axial skeleton is associated with the water vascular system, the extraxial is formed outside the axial system and comprises two subregions: the perforate extraxial (including, for instance, the anus and gonopores in sea urchins) and the imperforate extraxial, covering the coeloms in the most aboral parts (see Fig. 1.16). While the perforate axial skeleton may be associated with the left somatocoel, the imperforate one is associated with the right somatocoel. Strikingly,

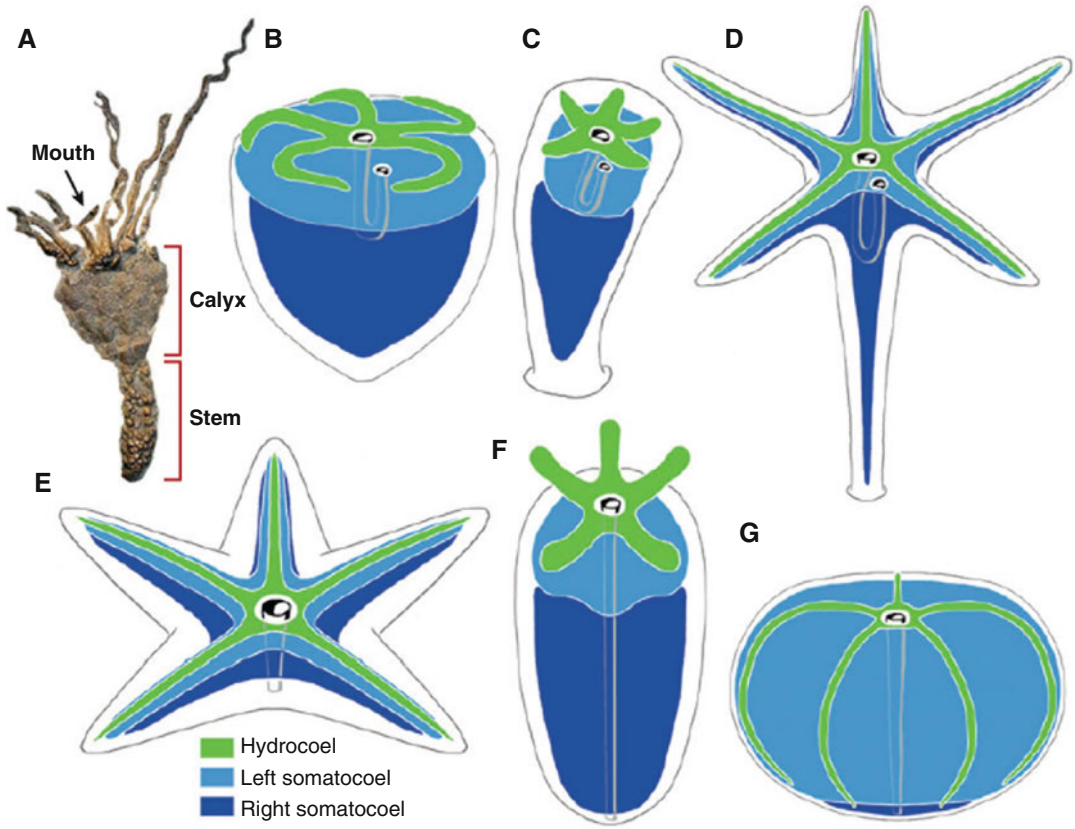

Fig. 1.16 Stacking of coelomic derivatives in all extant (but also in fossil) echinoderm classes. Different colors mark derivatives of the three coelom compartments. The arrangement of derivatives is a manifestation of the AP axis of animals, following the extraxial-axial theory (*EAT*). (**A**) Cambrian fossil *Gogia spiralis*, showing the sequential arrangement of mouth, calyx, and stem. (**B**) Cambrian fossil *Camptostroma*. (**C**) Crinoid larva. (**D**) Extant adult crinoid. (**E**) Extant asteroid. (**F**) Extant holothuroid. (**G**) Extant echinoid (The diagram is taken from Mooi and David (2008)©)

when these different skeletons are mapped onto the adult morphology of all echinoderms, we see that their relative disposition in the animal follows the stacking of the coelomic compartments, such that the hydrocoel derivatives are oral with respect to left somatocoel derivatives, which at the same time occupy oral positions with respect to the derivatives of the right somatocoel (see Fig. 1.4). The commonalities in the organization (and the ontogenies) of the different parts of the adult echinoderm body have allowed the elucidation of body wall homologies across different extant and also fossil groups (see below). These architectural and ontogenetic principles were termed extraxial-axial theory (EAT) (Mooi et al. 1994).

The EAT explains very well the anatomy of adult echinoderms with respect to the ambulacral and interambulacral regions and homologies between these body regions in the different classes. This hypothesis unites the disparate forms of the five extant echinoderm classes and some echinoderm fossils. A recent study (Hotchkiss 2012), however, reinterprets the designation of axial and extraxial skeletons in the asteroid arm by Mooi and David (2000), and this has implications for the rays as axis hypothesis (see below).

The coelomic stacking and the EAT hypotheses have been taken to suggest that the ambulacra are outgrowths, perpendicular to the major AP axis, and thus appendages. Two lines of evidence support this scenario. The first is derived from the theoretical models of Hotchkiss (Hotchkiss 1998), in which he suggests that the consideration of "rays as appendages" best explains the origin of the pentameral symmetry. Accordingly, a suggested characteristic of all echinoderms is the clear organization of structural elements along a major body axis, running from the anterior mouth (oral side = anterior) to the derivatives of the right somatocoel (aboral side = posterior). The adult echinoderm mouth thus corresponds to the anterior pole of other bilaterians. The relationship between the sequences of coelom development along the oral-aboral axis appears to be a basic feature of echinoderm anatomy (Peterson et al. 2000a; Mooi and David 2008; Morris 2012). However, the question concerning the evolution of a pentamerous arrangement of the arms remains unanswered in this scenario.

Insights into the affinity of the echinoderm ambulacrum are provided by data on expression of some regulatory genes during development, in particular the homologs of *distal-less*, which is normally expressed in the growing tips of several bilaterian appendages (e.g., annelid parapodia, tunicate ampullae, vertebrate limb buds) and in the podia of larval and juvenile echinoderms (Lowe and Wray 1997; Panganiban et al. 1997), although these expression data alone do not sufficiently argue for homology of echinoderm podia to other bilaterian appendages (e.g., (Winchell et al. 2010).

The "Rays as the Chordate Body Axis" Hypothesis

In this hypothesis the rays are axial in line with the chordate AP axis with one ambulacrum being the homolog of the chordate body axis (Fig. 1.17; see Raff and Popodi 1996; Heinzeller and Welsch 1999; Morris 2012). The echinoderm ambulacra are also interpreted as a metameric series (Turner 1998; Morris 2011, 2012). The other four ambulacra are thus hypothesized to be an evolutionary duplication from an ancestor with a single ambulacrum (Raff and Popodi 1996; Hotchkiss 1998; Heinzeller and Welsch 1999; Minsuk et al. 2009).

The "rays as the chordate body axis" hypothesis stems from development of coelom derivatives (Morris 2012; Morris and Byrne 2014) and the morphology of the adult nervous system (Heinzeller and Welsch 2001). Using the relative positions of mesodermal derivatives in both groups of animals, specific homologies between the hydrocoel and the notochord on the one hand and the secondary podia and somites on the other were suggested. The expression of some regulatory genes in coeloms would be compatible with this set of proposed homologies (however limited the number of genes is). Morris (2012) suggested that the five ambulacra arose as duplications of a

posterior growth zone – a series of duplications from an ancestor with a single ambulacrum. Thereby, the presence of repeated blocks of muscles and ossicles along the ambulacra is indicative of "segmentation," which also occurs along the major body axis (AP) of chordates. Accordingly, the posterior growth zones seen in the growth of the juvenile and adult echinoderm are the regions behind the primary podia, following the "ocular plate rule" of Mooi et al. (1994) with the oldest ossicles next to the mouth and the youngest at the end of the ambulacra. In echinoids the ocular plate is at the aboral pole and thus AP is readily seen to be parallel to oral-aboral. In asteroids, the equivalent growth zone at the terminal plate is at the end of the arms (see Hotchkiss 2012) and accordingly the AP axis would best be termed proximal-distal with regard to mouth and arm tip. Thus, the ray or ambulacrum in both echinoids and asteroids is interpreted as the chordate anterior-posterior axis (see Fig. 1.17).

Other arguments are based on the functional analogies between the chordate spinal and the echinoderm ectoneural chords, to the extent that a nervous system is required to control the movement of serial muscles and podia and its formation from ectodermal domains overlying these mesodermal structures. In fact, some authors have suggested that the radial nerves and the circumoral ring of the adult are "strong candidates" for a homolog of the chordate CNS (Haag 2005), a position that is also opposed by some (Nielsen 2006). Analysis of Hox gene expression in the adult rudiment of the direct-developing sea urchin *Holopneustes purpurascens* seems to lend support to this assumption, stressing the concept that echinoderms and chordates share structural homologies and that an echinoderm arm is organized metamerically (Morris and Byrne 2014), as is the main vertebrate axis. The reiterated expression of other genes involved in segmentation (e.g., *engrailed*) in some echinoderm arms may be interpreted in the same context. However, as for the first hypothesis, one has to be cautious about using patterns of gene expression as signs of homology due to the potential of basically all known developmental genes for having been co-opted into novel functions (Nielsen and Martinez 2003).

The homology of the ambulacrum of echinoderms to the AP axis could be interpreted as being supported by fossil data, which indicates that the earliest echinoderms have one ambulacrum and were bilaterally symmetric (Smith 2005; Zamora et al. 2012).

All in all, the axial homologies of echinoderms with other deuterostomes and the origins of the radial symmetry have generated much discussion

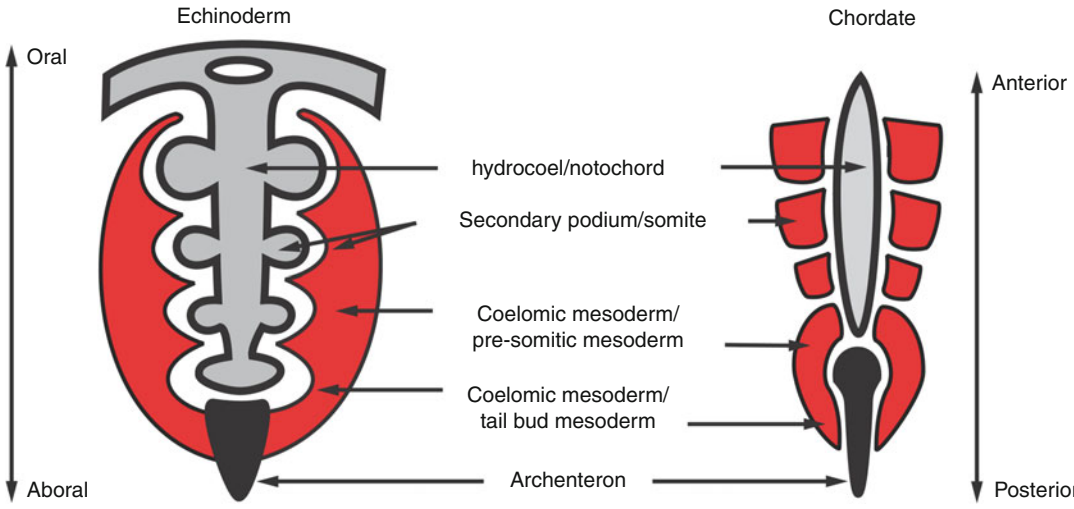

Fig. 1.17 Comparison of coelomic compartments of an echinoderm arm and the metameric anterior-posterior axis of a chordate (Courtesy of Valerie Morris)

and controversies with varying hypotheses proposed. The expected increase in comparative data on the ontogeny of adult structures and how gene regulatory networks specify them will undoubtedly continue to provide us with important insights in the future.

ADULT DEVELOPMENTAL PROCESSES: REGENERATION IN ECHINODERMS

Regeneration may be defined in general as the formation of new tissues or organs to replace those lost or damaged due to injury (see Vol. 2, Chapter 4) for a detailed treatment of the subject). Although a response to injury is evoked in most animals, there is a remarkable variety in the degree of morphological and functional recovery, not only between individuals from unrelated groups but also between closely related species and even between organs and parts of the same individual. The regenerative capacity is generally rather limited in vertebrates compared to that of many invertebrates (Goss 1969; Mattson 1976; Tanaka and Reddien 2011). Some vertebrates, including some amphibians and reptiles, are capable of tail, limb, and/or digit replacement, but these properties pale in comparison to the amazing capacity of invertebrates to repair most organs, including the CNS (Goss 1969; Mattson 1976; Tanaka and Reddien 2011)

Among the invertebrates, the Echinodermata, together with the Platyhelminthes (see Vol. 2, Chapters 3 and 4), have a remarkable capacity to regenerate lost or amputated organs (Candia Carnevali and Bonasoro 2001a, b; Candia Carnevali 2006; Candia Carnavali and Burighel 2010). Larval and adult echinoderms from each of the extant classes exhibit natural, rapid regeneration of entire lost parts (Eaves and Palmer 2003; Candia Carnevali 2006). This striking regenerative capacity serves a range of biological purposes (Sköld et al. 1994). Of primary importance is the replacement of tissues following predation and, secondarily, regeneration has developed as part of a process of asexual reproduction where fission results in two (or occasionally more) individuals (Candia Carnevali 2006; Sanchez Alvarado and Tsonis 2006). Many echinoderms regenerate in a seasonal pattern following, for instance, fragmentation of the body for asexual reproduction (Lee et al. 2008). Clearly, these developments have been of substantial adaptive value and are responsible for the ecological success of echinoderms.

Approximately 70 % of the genes known from echinoderms have obvious human homologs (Sodergren et al. 2006). Therefore, the molecular processes involved in echinoderm regeneration are more likely to be shared with mammals than those observed in other classic models, such as cnidarians (e.g., *Hydra*) or planarian flatworms, which are more distantly related to chordates. Moreover, all the regenerative strategies that are currently described in animals are represented in echinoderms; arm regeneration in ophiuroids and crinoids is an epimorphic blastemal process, and in asteroids and echinoids, morphallaxis is the main process involved (Suarez-Castillo et al. 2004; Candia Carnevali 2006). We understand here morphallactic regeneration as that relying on cellular reorganization with only limited production of new cells, while we define epimorphic regeneration as that involving dedifferentiation of adult structures in order to form an undifferentiated mass of cells from which the new structures eventually develop. However, there is clear evidence that regeneration in echinoderms involves contributions from both processes. In fact, some studies have shown that under different experimental conditions, the same individuals employ both epimorphic and morphallactic mechanisms, the use of which depending on the specific needs of the moment (Candia Carnevali and Bonasoro 2001a).

Currently, the best understood processes in echinoderm regeneration are arm regeneration in crinoids, asteroids, and ophiuroids and visceral regeneration in holothurians (and, to a lesser extent, in crinoids). Regeneration of other structures, such the holothurian nervous system, has also attracted much interest over the last few years (Mashanov et al. 2008, 2013). Here, the current knowledge of echinoderm regenerative processes is summarized.

Arm Regeneration

Three classes of echinoderms, namely, crinoids, asteroids, and ophiuroids, are well known for their extraordinary potential to regenerate amputated limbs. This property and the ease with which many species can be handled in the laboratory have been instrumental in the selection of echinoderm species as models for regeneration studies. Many species of asteroids, ophiuroids and holothuroids reproduce asexually by splitting the body into pieces that undergo subsequent regeneration. Moreover, in a few asteroids, a whole animal can be regenerated from just a fragment of the limb, e.g., *Linckia* (Edmondson 1935). The process of arm regeneration has been studied in detail in the crinoid *Antedon mediterranea* (Candia Carnevali and Bonasoro 2001b), the asteroid *Asterias rubens* (Moss et al. 1998; Hernroth et al. 2010; Ben Khadra et al. 2014), and the ophiuroid *Amphiura filiformis* (Bannister et al. 2005; Dupont and Thorndyke 2006; Czarkwiani et al. 2013). While the overall morphological changes have been well documented, the cellular processes involved are still a matter of some debate. However, what is mostly lacking is a good understanding of the molecular processes involved.

In *Antedon mediterranea*, the regeneration of amputated arms has been described as a typical blastemal regeneration in which migratory cells derived from the brachial nerve (amoebocytes) and coelomic epithelium (coelomocytes) are the major contributors to the process. The extensive studies by Candia Carnevali and collaborators have shown that the mitotic activities are located in the blastema and in the coelomic epithelia (reviewed in Candia Carnevali 2006). Moreover, regeneration is under neural control, probably through the modulatory activities of neurotransmitters and growth factors (Thorndyke and Candia Carnevali 2001; Patruno et al. 2003). Interestingly, crinoid arm explants are able to survive and engage in regeneration for several weeks in culture, providing another interesting context for regeneration (Bonasoro et al. 1999).

Asteroid arm regeneration differs from that in crinoids and ophiuroids in that a blastema is not formed. In asteroids the cells contributing to the regrowth of the amputated limb are derived from coelomic epithelium and the pyloric cecum (Holm et al. 2008; Hernroth et al. 2010), most of them originating in locations far from the wound. In asteroids, such as *Antedon*, the regeneration process is dependent on the presence of the nervous system as it has been shown for *Asterina gibbosa* (Huet 1975). Very little is known about the molecular control of asteroid regeneration (Thorndyke and Candia Carnevali 2001). Up to date only a few homeobox genes and a BMP homolog have been identified in regenerating sea star arms (Thorndyke and Candia Carnevali 2001; Ben Khadra et al. 2014). A preliminary report also identified a few enzyme-encoding cDNAs in regenerating larvae (Vickery et al. 2001), but this study was not followed by a more exhaustive characterization of the genes.

Amphiura filiformis is the best-known regenerating model species for the Ophiuroidea (Dupont and Thorndyke 2006; Czarkwiani et al. 2013). However, what is known about the process is still very limited. Few studies have been carried out into the nature of the cells contributing to the growth of new structures, although coelomocytes are thought to be involved (Thorndyke et al. 2001). A few morphological studies have been performed on ophiuroid regeneration (Thorndyke et al. 2003), but these are focused on the ecological adaptive value of regeneration (Sköld and Rosenberg 1996). The only molecular study performed on *A. filiformis* suggests the participation of diverse transcription factors, for instance, several linked to the formation of mesoderm, including *foxb*, *gata, ets, alx*, and also homeobox family members (Czarkwiani et al. 2013; Ben Khadra et al. 2014). Moreover, a TGF growth factor has been identified in the regenerative process (Bannister et al. 2005). However, recent transcriptomic analysis (microarrays) of regenerating *Amphiura* tissues has the potential to open up new fruitful avenues in the study of ophiuroid regeneration (Burns et al. 2012).

Visceral Regeneration

Holothuroids and crinoids are able to regenerate their digestive system after evisceration (autotomy). The best-studied models are the holothuroids

(Mashanov and Garcia-Arraras 2011). Evisceration (discarding of the digestive tract) occurs in response to certain stimuli (e.g., predation) with the rupture of specific breakage planes and detachment from the anchoring mesentery, this porcess being under neural control (Emson and Wilkie 1980; Byrne 2001). Two types of evisceration occur: anterior and posterior. Anterior evisceration occurs in dendrochirotids and results in loss of the gut and anterior associated organs: the tentacles and the pharyngeal bulb. Posterior evisceration occurs in aspidochirotids and results in loss of the gut, from the esophagus to the cloaca, and associated structures such as the respiratory trees.

As in other regenerative processes in echinoderms, regrowth involves an initial phase of wound healing followed by tissue remodeling and growth. The wound is closed during the first few days and involves contraction of body wall muscles. The remaining stump of the digestive tube starts a process of outgrowth and the mesentery also regenerates to provide a path for extension of the new gut. This process involves the mobilization of multiple cells, including the dedifferentiation and transdifferentiation of different cell types. Evisceration necessarily involves a large wave of cell proliferation to replenish missing structures. The tubular rudiments grow along the free edges of the mesentery and eventually fuse to form a whole, continuous, gut. The morphogenetic process, and formation of the final structure, is accompanied by the destruction of some cells via apoptosis (Mashanov et al. 2010).

Visceral regeneration in holothurians is one of the few regenerative processes in echinoderms for which an increasing source of molecular data are available. Conventional cloning (gene candidate approaches) have been used to identify genes involved in the regenerative process, e.g., the homologs of *ependymin*, *wnt6*, and *hox6* (Suarez-Castillo et al. 2004; Sun et al. 2013b), but more recently, transcriptomic tools have also been incorporated to gain an understanding of the changes in global patterns of gene activity (Rojas-Cartagena et al. 2007; Ortiz-Pineda et al. 2009; Sun et al. 2013a). These technologies, and the eventual sequencing of genomes, will prove extremely useful in modeling the molecular events controlling visceral regeneration. However, detailed methods for in situ hybridization and gene knockdown are still lacking.

As mentioned above, crinoids are also able to regenerate the gut after evisceration. The process has been studied in the feather star *A. mediterranea* (Dolmatov et al. 2001; Mozzi et al. 2006). In this case, the wound is sealed through a clotting process, which recruits coelomic and hemal fluids. A process of cell proliferation follows, mostly in the coelomic epithelium. As described for holothurians, the mesenterial tissue is also involved. Moreover, dedifferentiation and transdifferentiation also occur in crinoid regeneration, with the coelomic epithelium being an important source of new cells.

Nervous System Regeneration

Regeneration of the nervous system is an integral part of regeneration of amputated limbs in crinoids, asteroids, and ophiuroids. However, it is from the recent study of holothuroids that new insights have been gained (see Mashanov et al. 2008, 2013). After transection of the radial nerve cord (RNC) in *Eupentacta fraudatrix*, the RNC regenerates and reconnects in about 20 days. This process involves the two components of the nerve cord, the so-called ectoneural and hyponeural cords. Cell proliferation and death (apoptosis) are involved, and radial glial cells are the major source of new cells (neurons and glia). Through a process of dedifferentiation, the radial glia enter into the mitotic cycle and produce the new cells (though some neurons are also seen entering mitosis). While initially dedifferentiation is located at the stump, later on it spreads to other regions of the RNC. Mitotic activity in both halves of the transected nerve cord leads to the growth of the stumps towards each other. During this period, mitotic cells in the areas behind the stump enter into differentiation and restore the normal cytoarchitecture of the nerve cord. The final process is the fusing of the growing tips, which gives rise to a fully functional cord.

Interestingly, it has been shown that in mammals, glial cells are also involved in the regenerative process, as in holothurians (and probably in

all echinoderms), but, while in echinoderms the radial glia are active in the regeneration process (Mashanov et al. 2013), in mammals glial cells become a factor that block the process (Shearer and Fawcett 2001). In early-branching vertebrates, the glial reaction is, instead, permissive of regeneration (Zukor et al. 2011). This reaction may be linked to the fact that early-branching vertebrates also keep, during adulthood, a population of competent radial glial cells. This is not the case with mammals. Overall, it appears that the glial reaction modulates the (limited) regenerative capacity of the nervous system across the vertebrates (Horner and Gage 2000).

Although our knowledge on regenerative processes in different echinoderms has recently improved, we are still missing key information regarding cellular and molecular aspects that control echinoderm regeneration. Gaining knowledge is mostly hampered by the lack of suitable techniques, particularly in the realms of gene knockdown and transgenesis. However, this situation may change over the next few years, given the speed with which new molecular technologies tend to move from the traditional model systems to others.

OUTLOOK

Echinoderms have been used as models in developmental biology for more than a century. Areas ranging from the analysis of early embryogenesis to the study of regeneration mechanisms have been illuminated by the use of echinoderm model systems. Moreover, the well-preserved fossil record of the group provides an excellent reference framework to analyze evolutionary innovations. The recent increase in papers describing genomic and transcriptomic analysis in several species of the phylum and the astounding success of incorporating high-throughput methods to analyze gene regulatory networks suggest that we are entering an era where many fundamental problems in EvoDevo will be tractable in the laboratory, also using echinoderms as model organisms. Challenges in understanding the changes, ranging from cell lineage specification to the evolution of larval forms, or the genesis of adult structures through metamorphosis, will be more amenable to address using experimental approaches.

However, there are still some research areas that will need particular attention. The development of non-echinoid echinoderms has to be further explored, including their molecular control. Our current knowledge of postembryonic development is limited, especially the development of adult structures, which is particularly relevant for modeling the origin of pentameral symmetry. The need of experimental techniques to analyze postembryonic development is urgent. These techniques should prove especially useful in the analysis of adult processes such as regeneration.

The future looks bright for the use of echinoderm models in EvoDevo, although this should not deter us from improving our knowledge on the last-mentioned (and mostly neglected) areas of research.

OPEN QUESTIONS

- The molecular control of echinoderm embryology (other than echinoids)
- The evolution of echinoderm embryogenesis
- The evolution of echinoderm genomes and morphologies (from populations to species and higher taxa)
- The evolution of gene regulatory networks (the mechanistic basis)
- The developmental and genetic basis of echinoderm life history evolution
- Larval morphogenesis and the development of adult echinoderm structures, from molecules to morphologies
- The axial affinities of the adult echinoderm body with the AP axis of other Bilateria
- The molecular control of regeneration

NOTE ADDED IN PROOFS

In the recent paper by Baughman et al. 2014 the authors show that the sea star *Acanthaster planci* has an almost complete HOX cluster, without any major reorganization as it is seen in the genome of the echinoid *Strongylocentrotus purpuratus*.

This would suggest that the HOX cluster was reorganized specifically in the echinoid lineage and that the other echinoderm classes do not share the structure described for *S. purpuratus*. Moreover, this indicates that the ancestral state for the Echinodermata is having an unmodified HOX cluster.

Acknowledgments The authors of this chapter would like to acknowledge the invaluable collaboration of different people that helped us to revise the text and clarify our ideas. All took their time and sent us extensive comments on many aspects of the chapter. We would like to acknowledge, specially, the help offered by Andrew Cameron (CalTech), Chris Mah (Smithsonian, National Museum of Natural History), Valerie Morris (University of Sydney), Rich Mooi (California Academy of Sciences), Claus Nielsen (University Copenhagen), and Samuel Zamora (Universidad Zaragoza).

Also we want to express our gratitude to those that shared with us some of the pictures that are included in this chapter, in particular Koji Akasaka (School of Science, University of Tokyo), Peter Bryant (UC Irvine), Anna Czarkwiani (UC London), Paula Cisternas (University Sydney), David Dylus (UC London), Christian Gache (Observatoire Océanologique de Villefranche-sur-Mer), Veronica Hinman (Carnegie Mellon University), Hisanori Kohtsuka (Misaki Marine Biological Station, University of Tokyo), David McClay (Duke University), Hiroaki Nakano (Shimoda Marine Research Center, University of Tsukuba), Paola Oliveri (UC London), and Mattias Ormestad (SciLifeLab). Our special thanks to Santiago Valero-Medranda for the effort in preparing the many diagrams of larvae that are included in this chapter. Valerie Morris is acknowledged for providing Fig. 1.17.

References

Adams NL, Campanale JP, Foltz KR (2012) Proteomic responses of sea urchin embryos to stressful ultraviolet radiation. Integr Comp Biol 52:665–680

Amemiya S (1989) Electron microscopic studies on primary mesenchyme cell ingression and gastrulation in relation to vegetal pole cell behavior in sea urchin embryos. Exp Cell Res 183:453–462

Andrikou C, Iovene E, Rizzo F, Oliveri P, Arnone MI (2013) Myogenesis in the sea urchin embryo: the molecular fingerprint of the myoblast precursors. Evodevo 4:33

Angerer LM, Yaguchi S, Angerer RC, Burke RD (2011) The evolution of nervous system patterning: insights from sea urchin development. Development 138: 3613–3623

Annunziata R, Arnone MI (2014) A dynamic regulatory network explains *ParaHox* gene control of gut patterning in the sea urchin. Development 141:2462–2472

Annunziata R, Martinez P, Arnone MI (2013) Intact cluster and chordate-like expression of *ParaHox* genes in a sea star. BMC Biol 11:68

Annunziata R, Perillo M, Andrikou C, Cole AG, Martinez P, Arnone MI (2014) Pattern and process during sea urchin gut morphogenesis: the regulatory landscape. Genesis 52:251–268

Appeltans W, Ahyong ST, Anderson G, Angel MV, Artois T, Bailly N, Bamber R, Barber A, Bartsch I, Berta A, Blazewicz-Paszkowycz M, Bock P, Boxshall G, Boyko CB, Brandao SN, Bray RA, Bruce NL, Cairns SD, Chan TY, Cheng LN, Collins AG, Cribb T, Curini-Galletti M, Dahdouh-Guebas F, Davie PJF, Dawson MN, De Clerck O, Decock W, De Grave S, de Voogd NJ, Domning DP, Emig CC, Erseus C, Eschmeyer W, Fauchald K, Fautin DG, Feist SW, Fransen CHJM, Furuya H, Garcia-Alvarez O, Gerken S, Gibson D, Gittenberger A, Gofas S, Gomez-Daglio L, Gordon DP, Guiry MD, Hernandez F, Hoeksema BW, Hopcroft RR, Jaume D, Kirk P, Koedam N, Koenemann S, Kolb JB, Kristensen RM, Kroh A, Lambert G, Lazarus DB, Lemaitre R, Longshaw M, Lowry J, Macpherson E, Madin LP, Mah C, Mapstone G, McLaughlin PA, Mees J, Meland K, Messing CG, Mills CE, Molodtsova TN, Mooi R, Neuhaus B, Ng PKL, Nielsen C, Norenburg J, Opresko DM, Osawa M, Paulay G, Perrin W, Pilger JF, Poore GCB, Pugh P, Read GB, Reimer JD, Rius M, Rocha RM, Saiz-Salinas JI, Scarabino V, Schierwater B, Schmidt-Rhaesa A, Schnabel KE, Schotte M, Schuchert P, Schwabe E, Segers H, Self-Sullivan C, Shenkar N, Siegel V et al (2012) The magnitude of global marine species diversity. Curr Biol 22:2189–2202

Arenas-Mena C, Martinez P, Cameron RA, Davidson EH (1998) Expression of the Hox gene complex in the indirect development of a sea urchin. Proc Natl Acad Sci U S A 95:13062–13067

Arenas-Mena C, Cameron AR, Davidson EH (2000) Spatial expression of Hox cluster genes in the ontogeny of a sea urchin. Development 127:4631–4643

Arenas-Mena C, Cameron RA, Davidson EH (2006) Hindgut specification and cell-adhesion functions of *Sphox11/13b* in the endoderm of the sea urchin embryo. Dev Growth Differ 48:463–472

Arnone MI, Rizzo F, Annunciata R, Cameron RA, Peterson KJ, Martinez P (2006) Genetic organization and embryonic expression of the *ParaHox* genes in the sea urchin *S. purpuratus*: insights into the relationship between clustering and colinearity. Dev Biol 300:63–73

Balser EJ (2002) Phylum echinodermata: crinoidea. In: Young CM, Sewell MA, Rice ME (eds) Atlas of marine invertebrate larvae. Academic, San Diego, pp 463–482

Bannister R, McGonnell IM, Graham A, Thorndyke MC, Beesley PW (2005) *Afuni*, a novel transforming growth factor-beta gene is involved in arm regeneration by the brittle star *Amphiura filiformis*. Dev Genes Evol 215:393–401

Baughman KW, McDougall C, Cummins SF, Hall M, Degnan BM, Satoh N, Shoguchi E (2014) Genomic organization of *Hox* and *ParaHox* clusters in the echinoderm, Acanthaster Planci. Genesis 52(12):952–958

Ben Khadra Y, Said K, Thorndyke M, Martinez P (2014) Homeobox genes expressed during echinoderm arm regeneration. Biochem Genet 52:166–180

Birenheide R, Tamori M, Motokawa T, Ohtani M, Iwakoshi E, Muneoka Y, Fujita T, Minakata H, Nomoto K (1998) Peptides controlling stiffness of connective tissue in sea cucumbers. Biol Bull 194:253–259

Bonasoro F, Candia Carnevali MD, Sala F, Patruno M, Thorndyke MC (1999) Regenerative potential of crinoid arm explants. In: Candia Carnevali MD, Bonasoro F (eds) Echinoderm research 1998. Balkema, Rotterdam, pp 133–138

Boveri T (1902) Uber mehrpolige Mitosen als Mittel zur Analyse des Zellkerns. Verh Phys Med Ges Wurzburg 35:67–90

Burke RD (1989) Echinoderm metamorphosis: comparative aspects of the change in form. In: echinoderm studies, vol 3. Balkema, Rotterdam, pp 81–107

Burke RD, Alvarez CM (1988) Development of the esophageal muscles in embryos of the sea urchin *Strongylocentrotus purpuratus*. Cell Tissue Res 252:411–417

Burke RD, Myers RL, Sexton TL, Jackson C (1991) Cell movements during the initial phase of gastrulation in the sea urchin embryo. Dev Biol 146:542–557

Burke RD, Angerer LM, Elphick MR, Humphrey GW, Yaguchi S, Kiyama T, Liang S, Mu X, Agca C, Klein WH, Brandhorst BP, Rowe M, Wilson K, Churcher AM, Taylor JS, Chen N, Murray G, Wang D, Mellott D, Olinski R, Hallbook F, Thorndyke MC (2006) A genomic view of the sea urchin nervous system. Dev Biol 300:434–460

Burke RD, Moller DJ, Krupke OA, Taylor VJ (2014) Sea urchin neural development and the metazoan paradigm of neurogenesis. Genesis 52:208–221

Burns G, Ortega-Martinez O, Dupont S, Thorndyke MC, Peck LS, Clark MS (2012) Intrinsic gene expression during regeneration in arm explants of *Amphiura filiformis*. J Exp Mar Biol Ecol 413:106–112

Bury H (1895) The metamorphosis of echinoderms. Quart J Microsc Sci (NS) 38:45–135

Bury H (1989) Studies in the embryology of echinoderms. Quart J Microsc Sci (NS) 29:409–449, plates XXXVII–XXXIX

Byrne M (1996) Viviparity and intragonadal cannibalism in the diminutive sea stars *Patiriella vivipara* and *P. parvivipara* (family Asterinidae). Mar Biol 125:551–567

Byrne M (2001) The morphology of autotomy structures in the sea cucumber *Eupentacta quinquesemita* before and during evisceration. J Exp Biol 204:849–863

Byrne M (2006) Life history diversity and evolution in the Asterinidae. Integr Comp Biol 46:243–254

Byrne M, Barker MF (1991) Embryogenesis and larval development of the asteroid *Patiriella regularis* viewed by light and scanning electron-microscopy. Biol Bull 180:332–345

Byrne M, Selvakumaraswamy P (2002) Phylum Echinodermata: ophiuroidea. In: Young CM, Sewell MA, Rice ME (eds) Atlas of marine invertebrate larvae. Academic, San Diego, pp 488–498

Byrne M, Villinski JT, Cisternas P, Siegel RK, Popodi E, Raff RA (1999) Maternal factors and the evolution of developmental mode: evolution of oogenesis in *Heliocidaris erythrogramma*. Dev Genes Evol 209:275–283

Byrne M, Cisternas P, Elia L, Relf B (2005) Engrailed is expressed in larval development and in the radial nervous system of *Patiriella* sea stars. Dev Genes Evol 215:608–617

Byrne M, Nakajima Y, Chee FC, Burke RD (2007) Apical organs in echinoderm larvae: insights into larval evolution in the Ambulacraria. Evol Dev 9:432–445

Cameron RA, Davidson EH (1991) Cell type specification during sea urchin development. Trends Genet 7: 212–218

Cameron RA, Fraser SE, Britten RJ, Davidson EH (1991) Macromere cell fates during sea urchin development. Development 113:1085–1091

Candia Carnavali MD, Burighel P (2010) Regeneration in echinoderms and ascidians. In: eLS. Wiley, Chichester

Candia Carnevali MD (2006) Regeneration in echinoderms: repair, regrowth, cloning. ISJ 3:64–76

Candia Carnevali MD, Bonasoro F (2001a) Introduction to the biology of regeneration in echinoderms. Microsc Res Tech 55:365–368

Candia Carnevali MD, Bonasoro F (2001b) Microscopic overview of crinoid regeneration. Microsc Res Tech 55:403–426

Chia FS (1968) The embryology of the brooding starfish, *Leptasterias hexactis* (Stimpson). Acta Zool 49: 321–354

Chia FS, Burke RD (1978) Echinoderm metamorphosis: fate of larval structures. In: Chia FS, Rice ME (eds) Settlement and metamorphosis of marine invertebrate larvae. Elsevier North Holland Biomedical Press, New York, pp 219–234

Cisternas P, Byrne M (2009) Expression of Hox4 during development of the pentamerous juvenile sea star, *Parvulastra exigua*. Dev Genes Evol 219:613–618

Cobb JLS (1995) The nervous system of echinodermata: recent results and new approaches. In: Breidbach O, Kutsche W (eds) The nervous systems of invertebrates: an evolutionary and comparative approach. Birkhäuser Verlag, Basel

Cole AG, Rizzo F, Martinez P, Fernandez-Serra M, Arnone MI (2009) Two *ParaHox* genes, *SpLox* and *SpCdx*, interact to partition the posterior endoderm in the formation of a functional gut. Development 136:541–549

Croce JC, McClay DR (2010) Dynamics of Delta/Notch signaling on endomesoderm segregation in the sea urchin embryo. Development 137:83–91

Croce J, Lhomond G, Lozano JC, Gache C (2001) *ske-T*, a T-box gene expressed in the skeletogenic mesenchyme lineage of the sea urchin embryo. Mech Dev 107:159–162

Czarkwiani A, Dylus DV, Oliveri P (2013) Expression of skeletogenic genes during arm regeneration in the brittle star *Amphiura filiformis*. Gene Expr Patterns GEP 13:464–472

Dan K (1960) Cyto-embryology of echinoderms and amphibia. Int Rev Cytol 9:321–367

Dan JC, Hagiwara Y (1967) Studies on the acrosome. IX. Course of acrosome reaction in the starfish. J Ultrastruct Res 18:562–579

Dan K, Okazaki K (1956) Cyto-embryological studies of sea urchin. III. Role of the secondary mesenchyme cells in the formation of the primitive gut in the sea urchin larvae. Biol Bull 110:29–42

David B, Mooi R (1998) Major events in the evolution of echinoderms viewed by the light of embryology. In: Mooi R, Telford M (eds) Echinoderms: San Francisco. Balkema, Rotterdam, pp 21–28

David ES, Luke NH, Livingston BT (1999) Characterization of a gene encoding a developmentally regulated winged helix transcription factor of the sea urchin *Strongylocentrotus purpuratus*. Gene 236:97–105

David B, Lefebvre B, Mooi R, Parsley R (2000) Are homalozoans echinoderms? An answer from the extraxial-axial theory. Paleobiology 26:529–555

Davidson EH (1989) Lineage-specific gene expression and the regulative capacities of the sea urchin embryo: a proposed mechanism. Development 105:421–445

Davidson EH (1990) How embryos work: a comparative view of diverse modes of cell fate specification. Development 108:365–389

Davidson EH (2006) The regulatory genome: gene regulatory networks in development and evolution. Academic/Elsevier, San Diego

Davidson EH, Erwin DH (2006) Gene regulatory networks and the evolution of animal body plans. Science 311:796–800

Davidson EH, Cameron RA, Ransick A (1998) Specification of cell fate in the sea urchin embryo: summary and some proposed mechanisms. Development 125:3269–3290

Davidson EH, Rast JP, Oliveri P, Ransick A, Calestani C, Yuh CH, Minokawa T, Amore G, Hinman V, Arenas-Mena C, Otim O, Brown CT, Livi CB, Lee PY, Revilla R, Rust AG, Pan Z, Schilstra MJ, Clarke PJ, Arnone MI, Rowen L, Cameron RA, McClay DR, Hood L, Bolouri H (2002) A genomic regulatory network for development. Science 295:1669–1678

Derbès M (1847) Observations sur le méchanisme et les phénomènes qui accompagnent la formation de l'embryon chez l'oursin comestible. Ann Sci Nat Ill Série Zool 8:80–98

Dolmatov IY, Ferreri P, Bonasoro F, Candia Carnevali MD (2001) Visceral regeneration in the crinoid *Antedon mediterranea*. In: Feral JP, Bruno D (eds) Echinoderm research. A. A. Balkema, Rotterdam

Domazet-Loso T, Tautz D (2010) A phylogenetically based transcriptome age index mirrors ontogenetic divergence patterns. Nature 468:815-U107

Driesch H (1892) The potency of the first two cleavage cells in echinoderm development: experimental production of partial and double formations. In: Willier BH, Oppenheimer JM (eds) Foundations of experimental embryology. Hafner, New York, 1974

Du HX, Bao ZM, Hou R, Wang S, Su HL, Yan JJ, Tian ML, Li Y, Wei W, Lu W, Hu XL, Wang S, Hu JJ (2012) Transcriptome sequencing and characterization for the sea cucumber *Apostichopus japonicus* (Selenka, 1867). PLoS One 7:e33311

Dupont S, Thorndyke MC (2006) Growth or differentiation? Adaptive regeneration in the brittlestar *Amphiura filiformis*. J Exp Biol 209:3873–3881

Eaves AA, Palmer AR (2003) Reproduction: widespread cloning in echinoderm larvae. Nature 425:146

Edmondson CH (1935) Autotomy and regeneration in Hawaiian starfishes. Occas Pap Bernice Pauahi Bishop Mus 11:3–20

Emlet RB (1988) Larval form and metamorphosis of a primitive Sea-urchin, *Eucidaris thouarsii* (Echinodermata, Echinoidea, Cidaroida), with implications for developmental and phylogenetic studies. Biol Bull 174:4–19

Emlet RB (1995) Larval spicules, cilia, and symmetry as remnants of indirect development in the direct developing sea urchin *Heliocidaris erythrogramm*a. Dev Biol 167:405–415

Emlet RB, Joung CM, George SB (2002) Phylum echinodermata: echinoidea. In: Young CM, Sewell MA, Rice ME (eds) Atlas of marine invertebrate larvae. Academic, San Diego, pp 531–551

Emson RH, Wilkie IC (1980) Fission and autotomy in echinoderms. Oceanogr Mar Biol Annu Rev 18:155–250

Elia L, Selvakumaraswamy P, Byrne M (2009) Nervous system development in feeding and nonfeeding Asteroid larvae and the early juvenile. Biol Bull 216:322–334

Elia L, Cisternas P, Byrne M (2010) Characterization and expression of a sea star otx orthologue (ProtxB1/2) in the larva of Paririella regularis. Gene Exp Patterns 216:322–334

Ettensohn CA (1984) Primary invagination of the vegetal plate during sea urchin gastrulation. Am Zool 24:571–588

Ettensohn CA (1985) Gastrulation in the sea urchin embryo is accompanied by the rearrangement of invaginating epithelial cells. Dev Biol 112:383–390

Ettensohn CA, Ingersoll EP (1992) Morphogenesis of the sea urchin embryo. Morphogenesis: an analysis of the development of biological structures. Marcel Dekker, New York, pp 189–262

Ettensohn CA, Ruffins SW (1993) Mesodermal cell interactions in the sea urchin embryo: properties of skeletogenic secondary mesenchyme cells. Development 117:1275–1285

Ferkowicz MJ, Raff RA (2001) *Wnt* gene expression in sea urchin development: heterochronies associated with the evolution of developmental mode. Evol Dev 3:24–33

Fink RD, McClay DR (1985) Three cell recognition changes accompany the ingression of sea urchin primary mesenchyme cells. Dev Biol 107:66–74

Foerder CA, Shapiro BM (1977) Release of ovoperoxidase from sea urchin eggs hardens the fertilization membrane with tyrosine crosslinks. Proc Natl Acad Sci U S A 74:4214–4218

Fol MH (1877) Sur le premier développement d'une Étoile de mer. Comptes Rendus 84:357–360

Foote M (1999) Morphological diversity in the evolutionary radiation of Paleozoic and post-Paleozoic crinoids. Paleobiology 25:1–115

Fortini ME, Artavanis-Tsakonas S (1994) The suppressor of hairless protein participates in notch receptor signaling. Cell 79:273–282

Franco CF, Santos R, Coelho AV (2011a) Exploring the proteome of an echinoderm nervous system: 2-DE of the sea star radial nerve cord and the synaptosomal membranes subproteome. Proteomics 11: 1359–1364

Franco CF, Santos R, Coelho AV (2011b) Proteome characterization of sea star coelomocytes – the innate immune effector cells of echinoderms. Proteomics 11:3587–3592

Franco CF, Soares R, Pires E, Santos R, Coelho AV (2012) Radial nerve cord protein phosphorylation dynamics during starfish arm tip wound healing events. Electrophoresis 33:3764–3778

Franklin LE (1970) Fertilization and the role of the acrosomal region in non-mammals. Biol Reprod 2(Suppl 2):159–176

Fresques T, Zazueta-Novoa V, Reich A, Wessel GM (2014) Selective accumulation of germ-line associated gene products in early development of the sea star and distinct differences from germ-line development in the sea urchin. Dev Dyn 243:568–587

Gan L, Mao CA, Wikramanayake A, Angerer LM, Angerer RC, Klein WH (1995) An orthodenticle-related protein from *Strongylocentrotus purpuratus*. Dev Biol 167:517–528

Gao F, Davidson EH (2008) Transfer of a large gene regulatory apparatus to a new developmental address in echinoid evolution. Proc Natl Acad Sci U S A 105:6091–6096

Gemmill JF (1914) The development and certain points in the adult structure of the starfish *Asterias rubens* L. Philos Trans R Soc Lond B 205:213–294

Ghiglione C, Lhomond G, Lepage T, Gache C (1994) Structure of the sea urchin hatching enzyme gene. Eur J Biochem 219:845–854

Gibson AW, Burke RD (1985) The origin of pigment cells in embryos of the sea urchin *Strongylocentrotus purpuratus*. Dev Biol 107:414–419

Gibson AW, Burke RD (1987) Migratory and invasive behavior of pigment cells in normal and animalized sea urchin embryos. Exp Cell Res 173:546–557

Giusti AF, Hoang KM, Foltz KR (1997) Surface localization of the sea urchin egg receptor for sperm. Dev Biol 184:10–24

Glabe CG, Vacquier VD (1977) Isolation and characterization of the vitelline layer of sea urchin eggs. J Cell Biol 75:410–421

Glabe CG, Vacquier VD (1978) Egg surface glycoprotein receptor for sea urchin sperm bindin. Proc Natl Acad Sci U S A 75:881–885

Gondolf AL (2000) Light and scanning electron microscopic observations on the developmental biology of the common starfish, *Asterias rubens* Linne. Ophelia 52:153–170

Goss RJ (1969) Principles of regeneration. Academic, New York

Gosselin P, Jangoux M (1998) From competent larva to exotrophic juvenile: a morphofunctional study of the perimetamorphic period of *Paracentrotus lividus* (Echinodermata, Echinoida). Zoomorphology 118:31–43

Haag ES (2005) Echinoderm rudiments, rudimentary bilaterians, and the origin of the chordate CNS. Evol Dev 7:280–281

Hall HG (1978) Hardening of the sea urchin fertilization envelope by peroxidase-catalyzed phenolic coupling of tyrosines. Cell 15:343–355

Hara Y, Yamaguchi M, Akasaka K, Nakano H, Nonaka M, Amemiya S (2006) Expression patterns of *Hox* genes in larvae of the sea lily *Metacrinus rotundus*. Dev Genes Evol 216:797–809

Hardin J (1988) The role of secondary mesenchyme cells during sea urchin gastrulation studied by laser ablation. Development 103:317–324

Hardin JD, Cheng LY (1986) The mechanisms and mechanics of archenteron elongation during sea urchin gastrulation. Dev Biol 115:490–501

Hardin J, McClay DR (1990) Target recognition by the archenteron during sea urchin gastrulation. Dev Biol 142:86–102

Hart MW, Johnson SL, Addison JA, Byrne M (2004) Strong character incongruence and character choice in phylogeny of sea stars of the Asterinidae. Invertebr Biol 123:343–356

Heinzeller T, Welsch U (1999) The complex of notochord/neural plate in chordates and the complex hydrocoel/ectoneural cord in echinoderms- analogous or homologous? In: Candia-Carnevali MD, Bonasoro F (eds) Echinoderm research. Balkema, Rotterdam

Heinzeller T, Welsch U (2001) The echinoderm nervous system and its phylogenetic interpretation. In: brain evolution and cognition. Wiley, New York

Hendler G (1991) Echinodermata: Ophiuroidea. In: Giese AC, Pearse JS, Pearse VB (eds) Reproduction of marine invertebrates, echinoderms and lophophorates, vol VI. Boxwood, Pacific Grove, pp 356–479

Hendler G, Byrne M (1987) Fine structure of the dorsal arm plate of Ophiocoma wendtii – evidence for a photoreceptor system (Echinodermata, Ophiuroidea). Zoomorphology 107:261–272

Hernroth B, Farahani F, Brunborg G, Dupont S, Dejmek A, Skold HN (2010) Possibility of mixed progenitor cells in sea star arm regeneration. J Exp Zool B Mol Dev Evol 314:457–468

Hinman VF, Davidson EH (2007) Evolutionary plasticity of developmental gene regulatory network architecture. Proc Natl Acad Sci U S A 104:19404–19409

Hinman VF, Nguyen AT, Cameron RA, Davidson EH (2003a) Developmental gene regulatory network architecture across 500 million years of echinoderm evolution. Proc Natl Acad Sci U S A 100: 13356–13361

Hinman VF, Nguyen AT, Davidson EH (2003b) Expression and function of a starfish Otx ortholog, Am Otx: a conserved role for Otx proteins in endoderm development that predates divergence of the eleutherozoa. Mech Dev 120:1165–1176

Hinman VF, Yankura KA, McCauley BS (2009) Evolution of gene regulatory network architectures: examples of

subcircuit conservation and plasticity between classes of echinoderms. Biochim Biophys Acta Gene Regul Mech 1789:326–332
Hodor PG, Ettensohn CA (1998) The dynamics and regulation of mesenchymal cell fusion in the sea urchin embryo. Dev Biol 199:111–124
Hoekstra LA, Moroz LL, Heyland A (2012) Novel insights into the echinoderm nervous system from histaminergic and FMRFaminergic-like cells in the sea cucumber *Leptosynapta clarki*. PLoS One 7:e44220
Holland ND (1981) Electron microscopic study of development in a sea cucumber, *Stichopus tremulus* (Holothuroidea), from unfertilized egg through hatched blastula. Acta Zool 62:89–111
Holland ND (1991) Echinodermata: Crinoidea. In: Giese AC, Pearse JS, Pearse VB (eds) Reproduction of marine invertebrates, vol VI, Echinoderms and Lophophorates. Boxwood, Pacific Groove
Holm K, Dupont S, Skold H, Stenius A, Thorndyke M, Hernroth B (2008) Induced cell proliferation in putative haematopoietic tissues of the sea star, *Asterias rubens* (L.). J Exp Biol Part B 211:2551–2558
Horner PJ, Gage FH (2000) Regenerating the damaged central nervous system. Nature 407:963–970
Hörstadius SO (1939) The mechanics of sea urchin development studied by operative methods. Biol Rev 14:47
Horstadius SO (1973) Experimental embryology of echinoderms. Clarendon, Oxford
Hotchkiss FHC (1998) A "rays-as-appendages" model for the origin of pentamerism in echinoderms. Paleobiology 24:200–214
Hotchkiss FHC (2012) Growth zones and extraxial-axial skeletal homologies in Asteroidea (Echinodermata). Proc Biol Soc Wash 125:106–121
Howard-Ashby M, Materna SC, Brown CT, Chen L, Cameron RA, Davidson EH (2006) Identification and characterization of homeobox transcription factor genes in *Strongylocentrotus purpuratus*, and their expression in embryonic development. Dev Biol 300:74–89
Huet M (1975) Le róle du système nerveux au cours de la régéneration du bras chez une étoile de mer, *Asterina gibbosa* Penn (Echinoderme, Astéride). J Embryol Exp Morph 33:535–552
Hylander BL, Summers RG (1982) An ultrastructural immunocytochemical localization of hyalin in the sea urchin egg. Dev Biol 93:368–380
Hyman LH (1955) The invertebrates: Echinodermata, vol IV. McGraw-Hill, New York
Imai KS, Stolfi A, Levine M, Satou Y (2009) Gene regulatory networks underlying the compartmentalization of the *Ciona* central nervous system. Development 136:285–293
Ishimoda-Takagi T, Chino I, Sato H (1984) Evidence for the involvement of muscle tropomyosin in the contractile elements of the coelom-esophagus complex in sea urchin embryos. Dev Biol 105:365–376
Jaffe LA (1976) Fast block to polyspermy in sea urchin eggs is electrically mediated. Nature 261:68–71
Janies D (2001) Phylogenetic relationships of extant echinoderm classes. Can J Zool 79:1232–1250
Janies DA, Voight JR, Daly M (2011) Echinoderm phylogeny including *Xyloplax*, a progenetic asteroid. Syst Biol 60:420–438
Jefferies RPS (1968) The subphylum Calcichordata (Jefferies, 1967) primitive fossil chordates with echinoderm affinities. Bull Br Mus Nat Hist (Geol) 16:243–339
Jeffery CH, Emlet RB, Littlewood DTJ (2003) Phylogeny and evolution of developmental mode in temnopleurid echinoids. Mol Phylogenet Evol 28:99–118
Ji C, Wu L, Zhao W, Wang S, Lv J (2012) Echinoderms have bilateral tendencies. PLoS One 7:e28978
Juliano CE, Yajima M, Wessel GM (2010) Nanos functions to maintain the fate of the small micromere lineage in the sea urchin embryo. Dev Biol 337:220–232
Just EE (1919) The fertilization reaction in *Echina rachnius parma* I. Cortical response of egg to insemination. Biol Bull 36:1–10
Kinnander H, Gustafson T (1960) Further studies on the cellular basis of gastrulation in the sea urchin larva. Exp Cell Res 19:278–290
Koga H, Morino Y, Wada H (2014) The echinoderm larval skeleton as a possible model system for experimental evolutionary biology. Genesis 52:186–192
Kohtsuka H, Nakano H (2005) Development and growth of the feather star *Decametra tigrina* (Crinoidea), with emphasis on the morphological differences between adults and juveniles. J Mar Biol Assoc U K 85:1503–1510
Kondo M, Akasaka K (2012) Current status of echinoderm genome analysis – what do we know? Curr Genom 13:134–143
Kroh A, Mooi R (2011) World echinoidea database. Available online at http://www.marinespecies.org/echinoidea. Accessed 11 Apr 2014
Kuraishi R, Osanai K (1992) Cell movements during gastrulation of starfish larvae. Biol Bull 183:258–268
Kurokawa D, Kitajima T, Mitsunaga-Nakatsubo K, Amemiya S, Shimada H, Akasaka K (1999) *HpEts*, an ets-related transcription factor implicated in primary mesenchyme cell differentiation in the sea urchin embryo. Mech Dev 80:41–52
Lane MC, Koehl MA, Wilt F, Keller R (1993) A role for regulated secretion of apical extracellular matrix during epithelial invagination in the sea urchin. Development 117:1049–1060
Lee PY, Davidson EH (2004) Expression of *Spgatae*, the *Strongylocentrotus purpuratus* ortholog of vertebrate GATA4/5/6 factors. Gene Expr Patterns 5:161–165
Lee J, Byrne M, Uthicke S (2008) The influence of population density in fission and growth of Holothuria atra in natural mesocosms. J Exp Mar Biol Ecol 365:126–135
Lepage T, Sardet C, Gache C (1992) Spatial expression of the hatching enzyme gene in the sea urchin embryo. Dev Biol 150:23–32
Levine AE, Walsh KA, Fodor EJ (1978) Evidence of an acrosin-like enzyme in sea urchin sperm. Dev Biol 63:299–306
Lhomond G, McClay DR, Gache C, Croce JC (2012) Frizzled1/2/7 signaling directs beta-catenin nuclearisation and initiates endoderm specification in

macromeres during sea urchin embryogenesis. Development 139:816–825
Li E, Cui M, Peter IS, Davidson EH (2014) Encoding regulatory state boundaries in the pregastrular oral ectoderm of the sea urchin embryo. Proc Natl Acad Sci U S A 111:E906–E913
Littlewood DTJ, Smith AB, Clough KA, Emson RH (1997) The interrelationships of the echinoderm classes: morphological and molecular evidence. Biol J Linn Soc 61:409–438
Lowe CJ, Wray GA (1997) Radical alterations in the roles of homeobox genes during echinoderm evolution. Nature 389:718–721
Lowe CJ, Issel-Tarver L, Wray GA (2002) Gene expression and larval evolution: changing roles of distal-less and orthodenticle in echinoderm larvae. Evol Dev 4:111–123
Luo YJ, Su YH (2012) Opposing nodal and BMP signals regulate left-right asymmetry in the sea urchin larva. PLoS Biol 10:e1001402
MacBride EW (1986) The development of *Asterina gibbosa*. Q J Microsc Sci 38:339–411
Mah CL, Blake DB (2012) Global diversity and phylogeny of the Asteroidea (Echinodermata). PLoS One 7:e35644
Malinda KM, Fisher GW, Ettensohn CA (1995) Four-dimensional microscopic analysis of the filopodial behavior of primary mesenchyme cells during gastrulation in the sea urchin embryo. Dev Biol 172:552–566
Mann K, Wilt FH, Poustka AJ (2010) Proteomic analysis of sea urchin (*Strongylocentrotus purpuratus*) spicule matrix. Proteome Sci 8:33
Martins GG, Summers RG, Morrill JB (1998) Cells are added to the archenteron during and following secondary invagination in the sea urchin *Lytechinus variegatus*. Dev Biol 198:330–342
Mashanov VS, Garcia-Arraras JE (2011) Gut regeneration in holothurians: a snapshot of recent developments. Biol Bull 221:93–109
Mashanov VS, Zueva OR, Heinzeller T (2008) Regeneration of the radial nerve cord in a holothurian: a promising new model system for studying post-traumatic recovery in the adult nervous system. Tissue Cell 40:351–372
Mashanov VS, Zueva OR, Rojas-Catagena C, Garcia-Arraras JE (2010) Visceral regeneration in a sea cucumber involves extensive expression of survivin and mortalin homologs in the mesothelium. BMC Dev Biol 10:117
Mashanov VS, Zueva OR, Garcia-Arraras JE (2013) Radial glial cells play a key role in echinoderm neural regeneration. BMC Biol 11:49
Materna SC, Davidson EH (2012) A comprehensive analysis of delta signaling in pre-gastrular sea urchin embryos. Dev Biol 364:77–87
Materna SC, Nam J, Davidson EH (2010) High accuracy, high-resolution prevalence measurement for the majority of locally expressed regulatory genes in early sea urchin development. Gene Expr Patterns 10:177–184
Mattson P (1976) Regeneration. Bobbs-Merrill, Indianapolis
McCauley BS, Weideman EP, Hinman VF (2010) A conserved gene regulatory network subcircuit drives different developmental fates in the vegetal pole of highly divergent echinoderm embryos. Dev Biol 340:200–208
McCauley BS, Wright EP, Exner C, Kitazawa C, Hinman VF (2012) Development of an embryonic skeletogenic mesenchyme lineage in a sea cucumber reveals the trajectory of change for the evolution of novel structures in echinoderms. EvoDevo 3:17
McClay DR, Gross J, Peterson R, Bradham C (2004) Mechanism of gastrulation in the Sea urchin. In: Stern C (ed) Gastrulation. Cold Spring Harbor Laboratory Press, Cold Spring Harbor, pp 123–138
McEdward LR, Miner BG (2001) Larval and life-cycle patterns in echinoderms. Can J Zool 79:1125–1170
McEdward LR, Jaeckle WB, Komatsu M (2002) Phylum Echinodermata: Asteroidea. In: Young CM, Sewell MA, Rice ME (eds) Atlas of marine invertebrate larvae. Academic, San Diego, pp 419–503
McIntyre DC, Lyons DC, Martik M, McClay DR (2014) Branching out: origins of the sea urchin larval skeleton in development and evolution. Genesis 52:173–185
Minsuk SB, Raff RA (2002) Pattern formation in a pentameral animal: induction of early adult rudiment development in sea urchins. Dev Biol 247:335–350
Minsuk SB, Turner FR, Andrews ME, Raff RA (2009) Axial patterning of the pentaradial adult echinoderm body plan. Dev Genes Evol 219:89–101
Molina MD, de Crozé N, Haillot E, Lepage T (2013) Nodal: master and commander of the dorsal-ventral and left-right axes in the sea urchin embryo. Curr Opin Genet Dev 23:445–453
Mooi R, David B (1997) Skeletal homologies of echinoderms. Paleontol Soc Pap 3:305–335
Mooi R, David B (2000) What a new model of skeletal homologies tells us about asteroid evolution. Am Zool 40:326–339
Mooi R, David B (2008) Radial symmetry, the anterior/posterior axis, and echinoderm *Hox* genes. Ann Rev Ecol Evol Syst 39:43–62
Mooi R, David B, Marchand D (1994) Echinoderm skeletal homologies: classical morphology meets modern phylogenetics. In: David B, Guille A, Feral JP, Roux M (eds) Echinoderms through time. Balkema, Rotterdam, pp 87–95
Mooi R, David B, Wray GA (2005) Arrays in rays: terminal addition in echinoderms and its correlation with gene expression. Evol Dev 7:542–555
Morris VB (1995) Apluteal development of the sea-urchin *Holopneustes purpurescens* Agassiz (Echinodermata, Echinoidea, Euechinoidea). Zool J Linn Soc 114:349–364
Morris VB (2011) Coelomogenesis during the abbreviated development of the echinoid *Heliocidaris erythrogramma* and the developmental origin of the echinoderm pentameral body plan. Evol Dev 13:370–381

Morris VB (2012) Early development of coelomic structures in an echinoderm larva and a similarity with coelomic structures in a chordate embryo. Dev Genes Evol 222:313–323

Morris VB, Byrne M (2005) Involvement of two *Hox* genes and *otx* in echinoderm body-plan morphogenesis in the sea urchin *Holopneustes purpurescens*. J Exp Zool B Mol Dev Evol 304:456–467

Morris VB, Byrne M (2014) Oral-aboral identity displayed in the expression of *HpHox3* and *HpHox11/13* in the adult rudiment of the sea urchin *Holopneustes purpurescens*. Dev Genes Evol 224:1–11

Morris VB, Zhao JT, Shearman DCA, Byrne M, Frommer M (2004) Expression of an *Otx* gene in the adult rudiment and the developing central nervous system in the vestibula larva of the sea urchin *Holopneustes purpurescens*. Int J Dev Biol 48:17–22

Morris VB, Selvakumaraswamy P, Whan R, Byrne M (2009) Development of the five primary podia from the coeloms of a sea star larva: homology with the echinoid echinoderms and other deuterostomes. Proc Roy Soc B 276:1277–1284

Morris VB, Selvakumaraswamy P, Whan R, Byrne M (2011) The coeloms in a late brachiolaria larva of the asterinid sea star *Parvulastra exigua*: deriving an asteroid coelomic model. Acta Zool 92:266–275

Moss C, Hunter AJ, Thorndyke MC (1998) Patterns of bromodeoxyuridine incorporation and neuropeptide immunoreactivity during arm regeneration in the starfish *Asterias rubens*. Philos Trans R Soc Lond B Biol Sci 353:421–436

Mozingo NM, Chandler DE (1991) Evidence for the existence of two assembly domains within the sea urchin fertilization envelope. Dev Biol 146:148–157

Mozzi D, Dolmatov IY, Bonasoro F, Carnevali MDC (2006) Visceral regeneration in the crinoid *Antedon mediterranea*: basic mechanisms, tissues and cells involved in gut regrowth. Centr Eur J Biol 1:609–635

Nakajima Y, Kaneko H, Murray G, Burke RD (2004) Divergent patterns of neural development in larval echinoids and asteroids. Evol Dev 6:95–104

Nakano H, Hibino T, Oji T, Hara Y, Amemiya S (2003) Larval stages of a living sea lily (stalked crinoid echinoderm). Nature 421:158–160

Nakano H, Nakajima Y, Amemiya S (2009) Nervous system development of two crinoid species, the sea lily *Metacrinus rotundus* and the feather star *Oxycomanthus japonicus*. Dev Genes Evol 219:565–576

Nielsen C (2006) Homology of echinoderm radial nerve cords and the chordate neural tube??? Evol Dev 8:1–2

Nielsen C, Martinez P (2003) Patterns of gene expression: homology or homocracy? Dev Genes Evol 213:149–154

Nielsen MG, Popodi E, Minsuk S, Raff RA (2003) Evolutionary convergence in Otx expression in the pentameral adult rudiment in direct-developing sea urchins. Dev Genes Evol 213:73–82

Okazaki K (1975) Spicule formation by isolated micromeres of the sea urchin embryo. Am Zool 15:567–581

Oliveri P, Carrick DM, Davidson EH (2002) A regulatory gene network that directs micromere specification in the sea urchin embryo. Dev Biol 246:209–228

Oliveri P, Walton KD, Davidson EH, McClay DR (2006) Repression of mesodermal fate by *foxa*, a key endoderm regulator of the sea urchin embryo. Development 133:4173–4181

Olson RR, Cameron JL, Young CM (1993) Larval development (with observations on spawning) of the pencil urchin *Phyllacanthus imperialis* – a new intermediate larval form. Biol Bull 185:77–85

Omori A, Akasaka K, Kurokawa D, Amemiya S (2011) Gene expression analysis of *Six3*, *Pax6*, and *Otx* in the early development of the stalked crinoid *Metacrinus rotundus*. Gene Expr Patterns GEP 11:48–56

Ortiz-Pineda PA, Ramirez-Gomez F, Perez-Ortiz J, Gonzalez-Diaz S, Santiago-De Jesus F, Hernandez-Pasos J, Del Valle-Avila C, Rojas-Cartagena C, Suarez-Castillo EC, Tossas K, Mendez-Merced AT, Roig-Lopez JL, Ortiz-Zuazaga H, Garcia-Arraras JE (2009) Gene expression profiling of intestinal regeneration in the sea cucumber. BMC Genomics 10:262

Panganiban G, Irvine SM, Lowe C, Roehl H, Corley LS, Sherbon B, Grenier JK, Fallon JF, Kimble J, Walker M, Wray GA, Swalla BJ, Martindale MQ, Carroll SB (1997) The origin and evolution of animal appendages. Proc Natl Acad Sci U S A 94:5162–5166

Parsley RL (1991) Review of selected North American mitrate stylophorans (Homalozoa, Echinodermata). Bull Am Paleontol 100:5–54

Patruno M, McGonnell I, Graham A, Beesley P, Carnevali MDC, Thorndyke M (2003) *Anbmp2/4* is a new member of the transforming growth factor-beta superfamily isolated from a crinoid and involved in regeneration. Proc Natl Acad Sci U S A 270:1341–1347

Pehrson JR, Cohen LH (1986) The fate of the small micromeres in sea urchin development. Dev Biol 113:522–526

Peter IS, Davidson EH (2010) The endoderm gene regulatory network in sea urchin embryos up to mid-blastula stage. Dev Biol 340:188–199

Peter IS, Davidson EH (2011) A gene regulatory network controlling the embryonic specification of endoderm. Nature 474:635–639

Peterson KJ, Arenas-Mena C, Davidson EH (2000a) The A/P axis in echinoderm ontogeny and evolution: evidence from fossils and molecules. Evol Dev 2: 93–101

Peterson KJ, Cameron RA, Davidson EH (2000b) Bilaterian origins: significance of new experimental observations. Dev Biol 219:1–17

Pisani D, Feuda R, Peterson KJ, Smith AB (2012) Resolving phylogenetic signal from noise when divergence is rapid: a new look at the old problem of echinoderm class relationships. Mol Phylogenet Evol 62:27–34

Poustka AJ, Kuhn A, Groth D, Weise V, Yaguchi S, Burke RD, Herwig R, Lehrach H, Panopoulou G (2007) A global view of gene expression in lithium

and zinc treated sea urchin embryos: new components of gene regulatory networks. Genome Biol 8: R85

Primus AE (2005) Regional specification in the early embryo of the brittle star *Ophiopholis aculeata*. Dev Biol 283:294–309

Raff RA (1992) Direct-developing sea urchins and the evolutionary reorganization of early development. Bioessays 14:211–218

Raff RA, Byrne M (2006) The active evolutionary lives of echinoderm larvae. Heredity 97:244–252

Raff R, Popodi EM (1996) Evolutionary approaches to analyzing development. In: Ferraris JD, Palumbi SR (eds) Molecular zoology: advances, strategies and protocols. Wiley-Liss, New York, pp 245–265

Raff RA, Smith MS (2009) Axis formation and the rapid evolutionary transformation of larval form. Curr Top Dev Biol 86(86):163–190

Ramafofia C, Byrne M, Batteglene S (2003) Reproduction of the commercial sea cucumber *Holothuria scabra* in Solomon Islands. Mar Biol 142:281–288

Ramofafia C, Byrne M, Battaglene S (2001) Reproductive biology of the intertidal sea cucumber *Actinopyga mauritiana* in the Solomon Islands. J Mar Biol Ass UK 81:523–531

Ransick A, Davidson EH (2006) cis-regulatory processing of Notch signaling input to the sea urchin glial cells missing gene during mesoderm specification. Dev Biol 297:587–602

Reynolds SD, Angerer LM, Palis J, Nasir A, Angerer RC (1992) Early mRNAs, spatially restricted along the animal-vegetal axis of sea urchin embryos, include one encoding a protein related to tolloid and BMP-1. Development 114:769–786

Rizzo F, Fernandez-Serra M, Squarzoni P, Archimandritis A, Arnone MI (2006) Identification and developmental expression of the ets gene family in the sea urchin (*Strongylocentrotus purpuratus*). Dev Biol 300: 35–48

Rojas-Cartagena C, Ortiz-Pineda P, Ramirez-Gomez F, Suarez-Castillo EC, Matos-Cruz V, Rodriguez C, Ortiz-Zuazaga H, Garcia-Arraras JE (2007) Distinct profiles of expressed sequence tags during intestinal regeneration in the sea cucumber *Holothuria glaberrima*. Physiol Genomics 31:203–215

Rottinger E, Croce J, Lhomond G, Besnardeau L, Gache C, Lepage T (2006) Nemo-like kinase (NLK) acts downstream of Notch/Delta signalling to downregulate TCF during mesoderm induction in the sea urchin embryo. Development 133:4341–4353

Rouse GW, Jermiin LS, Wilson NG, Eeckhaut I, Lanterbecq D, Oji T, Young CM, Browning T, Cisternas P, Helgen LE, Stuckey M, Messing CG (2013) Fixed, free, and fixed: the fickle phylogeny of extant Crinoidea (Echinodermata) and their permian-triassic origin. Mol Phylogenet Evol 66: 161–181

Ruffins SW, Ettensohn CA (1996) A fate map of the vegetal plate of the sea urchin (*Lytechinus variegatus*) mesenchyme blastula. Development 122:253–263

Ruta M (1999) Brief review of the stylophoran debate. Evol Dev 1:123–135

Sanchez Alvarado A, Tsonis PA (2006) Bridging the regeneration gap: genetic insights from diverse animal models. Nat Rev Gen 7:873–884

Schuel H, Schuel R (1981) A rapid sodium-dependent block to polyspermy in sea urchin eggs. Dev Biol 87:249–258

Scott LB, Lennarz WJ (1989) Structure of a major yolk glycoprotein and its processing pathway by limited proteolysis are conserved in echinoids. Dev Biol 132:91–102

Selvakumaraswamy P, Byrne M (2006) Evolution of larval form in ophiuroids: insights from the metamorphic phenotype of *Ophiothrix* (Echinodermata: Ophiuroidea). Evol Dev 8:183–190

Sewell MA, McEuen FS (2002) Phylum echinodermata: holothuroidea. In: Young CM, Sewell MA, Rice ME (eds) Atlas of marine invertebrate larvae. Academic, San Diego, pp 513–530

Shearer MC, Fawcett JW (2001) The astrocyte/meningeal cell interface – a barrier to successful nerve regeneration? Cell Tissue Res 305:267–273

Sherwood DR, McClay DR (1999) LvNotch signaling mediates secondary mesenchyme specification in the sea urchin embryo. Development 126:1703–1713

Shoguchi E, Harada Y, Numakunai T, Satoh N (2000) Expression of the *Otx* gene in the ciliary bands during sea cucumber embryogenesis. Genesis 27:58–63

Sköld M, Rosenberg R (1996) Arm regeneration frequency in eight species of ophiuroidea (Echinodermata) from European sea areas. J Mar Res 35:353–362

Sköld M, Loo L-O, Rosenberg R (1994) Production, dynamics and demography of an *Amphiura filiformis* population. Mar Ecol Prog Ser 103:81–90

Sly BJ, Hazel JC, Popodi EM, Raff RA (2002) Patterns of gene expression in the developing adult sea urchin central nervous system reveal multiple domains and deep-seated neural pentamery. Evol Dev 4:189–204

Sly BJ, Snoke MS, Raff RA (2003) Who came first-larvae or adults? origins of bilaterian metazoan larvae. Int J Dev Biol 47(7–8):623–32

Smiley S (1986) Metamorphosis of *Stichopus californicus* (Echinodermata, Holothuroidea) and its phylogenetic implications. Biol Bull 171:611–631

Smiley S, McEuen FS, Chafee C, Krishah S (1991) Echinodermata: holothuroidea. In: Giese AC, Pearse JS, Pearse VB (eds) Reproduction of marine invertebrates, echinoderms and lophophorates, vol VI. Boxwood, Pacific Grove, pp 664–750

Smith AB (1984) Classification of the echinodermata. Palaeontology 27:431–459

Smith AB (1997) Echinoderm larvae and phylogeny. Ann Rev Ecol Syst 28:219–241

Smith AB (2005) The pre-radial history of echinoderms. Geol J 40:255–280

Smith AB (2008) Deuterostomes in a twist: the origins of a radical new body plan. Evol Dev 10:493–503

Smith AB, Zamora S (2013) Cambrian spiral-plated echinoderms from Gondwana reveal the earliest pentaradial body plan. Proc Natl Acad Sci U S A 280:1197

Smith J, Kraemer E, Liu H, Theodoris C, Davidson E (2008a) A spatially dynamic cohort of regulatory genes in the endomesodermal gene network of the sea urchin embryo. Dev Biol 313:863–875

Smith MM, Cruz Smith L, Cameron RA, Urry LA (2008b) The larval stages of the sea urchin, *Strongylocentrotus purpuratus*. J Morphol 269:713–733

Smith MS, Collins S, Raff RA (2009) Morphogenetic mechanisms of coelom formation in the direct-developing sea urchin *Heliocidaris erythrogramma*. Dev Genes Evol 219:21–29

Smith AB, Zamora S, Alvaro JJ (2013) The oldest echinoderm faunas from Gondwana show that echinoderm body plan diversification was rapid. Nat Commun 4:1385

Sodergren E, Weinstock GM, Davidson EH, Cameron RA, Gibbs RA, Angerer RC, Angerer LM, Arnone MI, Burgess DR, Burke RD, Coffman JA, Dean M, Elphick MR, Ettensohn CA, Foltz KR, Hamdoun A, Hynes RO, Klein WH, Marzluff W, McClay DR, Morris RL, Mushegian A, Rast JP, Smith LC, Thorndyke MC, Vacquier VD, Wessel GM, Wray G, Zhang L, Elsik CG, Ermolaeva O, Hlavina W, Hofmann G, Kitts P, Landrum MJ, Mackey AJ, Maglott D, Panopoulou G, Poustka AJ, Pruitt K, Sapojnikov V, Song X, Souvorov A, Solovyev V, Wei Z, Whittaker CA, Worley K, Durbin KJ, Shen Y, Fedrigo O, Garfield D, Haygood R, Primus A, Satija R, Severson T, Gonzalez-Garay ML, Jackson AR, Milosavljevic A, Tong M, Killian CE, Livingston BT, Wilt FH, Adams N, Belle R, Carbonneau S, Cheung R, Cormier P, Cosson B, Croce J, Fernandez-Guerra A, Geneviere AM, Goel M, Kelkar H, Morales J, Mulner-Lorillon O, Robertson AJ, Goldstone JV, Cole B, Epel D, Gold B, Hahn ME, Howard-Ashby M, Scally M, Stegeman JJ, Allgood EL, Cool J, Judkins KM, McCafferty SS, Musante AM, Obar RA, Rawson AP, Rossetti BJ, Gibbons IR, Hoffman MP, Leone A, Istrail S, Materna SC, Samanta MP, Stolc V, Tongprasit W et al (2006) The genome of the sea urchin *Strongylocentrotus purpuratus*. Science 314:941–952

Solek CM, Oliveri P, Loza-Coll M, Schrankel CS, Ho EC, Wang G, Rast JP (2013) An ancient role for *Gata-1/2/3* and *Scl* transcription factor homologs in the development of immunocytes. Dev Biol 382:280–292

Stears RL, Lennarz WJ (1997) Mapping sperm binding domains on the sea urchin egg receptor for sperm. Dev Biol 187:200–208

Stohr S, O'Hara TD, Thuy B (2012) Global diversity of brittle stars (Echinodermata: Ophiuroidea). PLoS One 7:e31940

Strathmann RR (1985) Feeding and nonfeeding larval development and life-history evolution in marine-invertebrates. Ann Rev Ecol Syst 16:339–361

Su YH, Li E, Geiss GK, Longabaugh WJR, Kramer A, Davidson EH (2009) A perturbation model of the gene regulatory network for oral and aboral ectoderm specification in the sea urchin embryo. Dev Biol 329:410–421

Suarez-Castillo EC, Medina-Ortiz WE, Roig-Lopez JL, Garcia-Arraras JE (2004) *Ependymin*, a gene involved in regeneration and neuroplasticity in vertebrates, is overexpressed during regeneration in the echinoderm *Holothuria glaberrima*. Gene 334:133–143

Summers RG, Stricker SA, Cameron RA (1993) Applications of confocal microscopy to studies of sea urchin embryogenesis. Methods Cell Biol 38:265–287

Sumrall CD (1996) Late Paleozoic edrioasteroids (Echinodermata) from the North American Midcontinent. J Paleontol 70:969–985

Sumrall CD, Wray GA (2007) Ontogeny in the fossil record: diversification of body plans and the evolution of "aberrant" symmetry in Paleozoic echinoderms. Paleobiology 33:149–163

Sun L, Chen MY, Yang HS, Wang TM, Liu BZ, Shu C, Gardiner DM (2011) Large scale gene expression profiling during intestine and body wall regeneration in the sea cucumber *Apostichopus japonicus*. Comp Biochem Physiol Part D Genomics Proteomics 6:195–205

Sun L, Yang H, Chen M, Ma D, Lin C (2013a) RNA-Seq reveals dynamic changes of gene expression in key stages of intestine regeneration in the sea cucumber *Apostichopus japonicus*. PLoS One 8:e69441

Sun LN, Yang HS, Chen MY, Xu DX (2013b) Cloning and expression analysis of *Wnt6* and *Hox6* during intestinal regeneration in the sea cucumber *Apostichopus japonicus*. Genet Mol Res 12:5321–5334

Sweet HC, Gehring M, Ettensohn CA (2002) LvDelta is a mesoderm-inducing signal in the sea urchin embryo and can endow blastomeres with organizer-like properties. Development 129:1945–1955

Takacs CM, Amore G, Oliveri P, Poustka AJ, Wang D, Burke RD, Peterson KJ (2004) Expression of an NK2 homeodomain gene in the apical ectoderm defines a new territory in the early sea urchin embryo. Dev Biol 269:152–164

Takata H, Kominami T (2004) Behavior of pigment cells closely correlates the manner of gastrulation in sea urchin embryos. Zoolog Sci 21:1025–1035

Tamboline CR, Burke RD (1992) Secondary mesenchyme of the sea urchin embryo: ontogeny of blastocoelar cells. J Exp Zool 262:51–60

Tanaka EM, Reddien PW (2011) The cellular basis for animal regeneration. Dev Cell 21:172–185

Telford MJ, Lowe CJ, Cameron CB, Ortega-Martinez O, Aronowicz J, Oliveri P, Copley RR (2014) Phylogenomic analysis of echinoderm class relationships supports Asterozoa. Proc Biol Sci. doi:10.1098/rspb.2014.0479

Thorndyke MC, Candia Carnevali MD (2001) Regeneration neurohormones and growth factors in echinoderms. Can J Zool 79:1171–1208

Thorndyke MC, Patruno M, Moss C, Beesley PW (2001) Cellular and molecular bases of arm regeneration in brittlestars. In: Barker M (ed) Echinoderms 2000: New Zealand. Balkema, Rotterdam, pp 323–326

Thorndyke MC, Patruno M, Dewael Y, Dupont S, Mallefet J (2003) Regeneration in the ophiuroid *Amphiura filiformis*: cell biology, physiology and bioluminescence.

In: Feral JP, David B (eds) Echinoderm research 2001. Swets and Zeitlinger, Lisse, pp 193–199
Tu Q, Cameron RA, Worley KC, Gibbs RA, Davidson EH (2012) Gene structure in the sea urchin *Strongylocentrotus purpuratus* based on transcriptome analysis. Genome Res 22:2079–2087
Turner RL (1998) The metameric echinoderm. In: Mooi R, Telford M (eds) Echinoderms: San Francisco. Balkema, Rotterdam, p 89
Ubaghs G (1975) Early paleozoic echinoderms. Ann Rev Earth Planet Sci 3:79–98
Ullrich-Luter EM, Dupont S, Arboleda E, Hausen H, Arnone MI (2011) Unique system of photoreceptors in sea urchin tube feet. Proc Natl Acad Sci U S A 108:8367–8372
Uthicke S, Schaffelke B, Byrne M (2009) A boom-bust phylum? Ecological and evolutionary consequences of density variations in echinoderms. Ecol Monogr 79:3–24
Vacquier VD, Moy GW (1977) Isolation of bindin: the protein responsible for adhesion of sperm to sea urchin eggs. Proc Natl Acad Sci U S A 74:2456–2460
Vacquier VD, Tegner MJ, Epel D (1973) Protease released from sea urchin eggs at fertilization alters the vitelline layer and aids in preventing polyspermy. Exp Cell Res 80:111–119
Vaughn R, Garnhart N, Garey JR, Thomas WK, Livingston BT (2012) Sequencing and analysis of the gastrula transcriptome of the brittle star *Ophiocoma wendtii*. EvoDevo 3:19
Vellutini BC, Migotto AE (2010) Embryonic, larval, and juvenile development of the sea biscuit *Clypeaster subdepressus* (Echinodermata: Clypeasteroida). PLoS One 5:e9654
Vickery MC, Vickery MS, McClintock JB, Amsler CD (2001) Utilization of a novel deuterostome model for the study of regeneration genetics: molecular cloning of genes that are differentially expressed during early stages of larval sea star regeneration. Gene 262:73–80
von Ubisch L (1913) Die Entwicklung von *Strongylocentrotus lividus* (*Echinus microtuberculatus, Arbacia pustulosa*). Zeit f wiss Zool 106:409–448
Warner JF, Lyons DC, McClay DR (2012) Left-right asymmetry in the sea urchin embryo: BMP and the asymmetrical origins of the adult. PLoS Biol 10:e1001404
Wei Z, Yaguchi J, Yaguchi S, Angerer RC, Angerer LM (2009) The sea urchin animal pole domain is a Six3-dependent neurogenic patterning center. Development 136:1179–1189
Wessel GM, Brayboy L, Fresques T, Gustafson EA, Oulhen N, Ramos I, Reich A, Swartz SZ, Yajima M, Zazueta V (2013) The biology of the germ line in echinoderms. Mol Reprod Dev. doi:10.1002/mrd.22223
Wilkie IC (1984) Variable tensility in echinoderm collagenous tissues: a review. Mar Behav Physiol 11:1–34
Wilson KA, Andrews ME, Raff RA (2005) Dissociation of expression patterns of homeodomain transcription factors in the evolution of developmental mode in the sea urchins *Heliocidaris tuberculata* and *H. erythrogramma*. Evol Dev 7:401–415
Winchell CJ, Valencia JE, Jacobs DK (2010) Expression of *Distal-less*, *dachshund*, and *optomotor blind* in *Neanthes arenaceodentata* (Annelida, Nereididae) does not support homology of appendage-forming mechanisms across the Bilateria. Dev Genes Evol 220:275–295
Wolpert L, Gustafson T (1961) Studies on the cellular basis of morphogenesis of the sea urchin embryo. The formation of the blastula. Exp Cell Res 25:374–382
Woznica A, Haeussler M, Starobinska E, Jemmett J, Li Y, Mount D, Davidson B (2012) Initial deployment of the cardiogenic gene regulatory network in the basal chordate, *Ciona intestinalis*. Dev Biol 368:127–139
Wray GA (1996) Parallel evolution of nonfeeding larvae in echinoids. Syst Biol 45:308–322
Wygoda JA, Yang Y, Byrne M, Wray GA (2014) Transcriptomic analysis of the highly derived radial body plan of a sea urchin. Genome Biol Evol 6:964–973
Yankura KA, Martik ML, Jennings CK, Hinman VF (2010) Uncoupling of complex regulatory patterning during evolution of larval development in echinoderms. BMC Biol 8:143
Yankura KA, Koechlein CS, Cryan AF, Cheatle A, Hinman VF (2013) Gene regulatory network for neurogenesis in a sea star embryo connects broad neural specification and localized patterning. Proc Natl Acad Sci U S A 110:8591–8596
Yoshimura K, Iketani T, Motokawa T (2012) Do regular sea urchins show preference in which part of the body they orient forward in their walk? Mar Biol 159:959–965
Yuh CH, Brown CT, Livi CB, Rowen L, Clarke PJ, Davidson EH (2002) Patchy interspecific sequence similarities efficiently identify positive cis-regulatory elements in the sea urchin. Dev Biol 246:148–161
Zamora S, Rahman IA, Smith AB (2012) Plated Cambrian bilaterians reveal the earliest stages of echinoderm evolution. PLoS One 7:e38296
Zamora S, Lefebvre B, Alvaro JJ, Clausen S, Elicki O, Fatka O, Jell P, Kouchinsky A, Lin J-P, Nardin E, Parsley R, Rozhnov S, Sprinkle J, Sumrall CD, Vizcaïno D, Smith AB (2013) Chapter 13 Cambrian echinoderm diversity and palaeobiogeography. In: Harper DAT, Servais T (eds) Early Palaeozoic Biogeography and Palaeogeography. Geological Society of London Memoirs, Bath, pp 157–171
Zukor KA, Kent DT, Odelberg SJ (2011) Meningeal cells and glia establish a permissive environment for axon regeneration after spinal cord injury in newts. Neural Dev 6:1

Hemichordata

2

Sabrina Kaul-Strehlow and Eric Röttinger

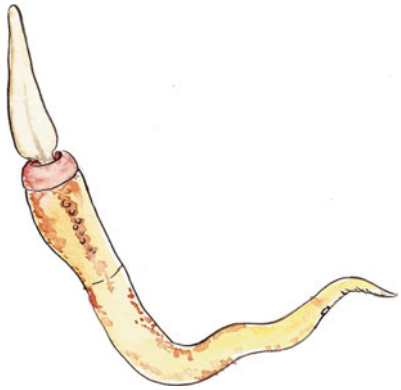

Chapter vignette artwork by Brigitte Baldrian.

S. Kaul-Strehlow (✉)
Department of Integrative Zoology, University of Vienna, Althanstr. 14, Vienna 1090, Austria
e-mail: sabrina.kaul-strehlow@univie.ac.at

E. Röttinger
Institute for Research on Cancer and Aging, Université Nice Sophia Antipolis, IRCAN, UMR 7284, Nice 06107, France

CNRS, IRCAN, UMR 7284, Nice 06107, France

INSERM, IRCAN, U1081, Nice 06107, France

A. Wanninger (ed.), *Evolutionary Developmental Biology of Invertebrates 6: Deuterostomia*
DOI 10.1007/978-3-7091-1856-6_2, © Springer-Verlag Wien 2015

INTRODUCTION

Synopsis

Hemichordata is a group of exclusively marine animals, consisting of two subgroups, the sessile and small colonial pterobranchs and the solitary, vermiform enteropneusts (acorn worms) (Fig. 2.1; van der Horst 1939; Hyman 1959; Benito and Pardos 1997). With about 130 described species, Hemichordata comprises a relatively small taxon of benthic animals (http://www.marinespecies.org/index.php; Cameron 2005). They are distributed worldwide and inhabit shallow coastal areas but are also found in the deep sea. For a long time, pterobranchs have been known only from deep waters, whereas enteropneusts were thought to burrow mainly in shallow waters. However, within the last five decades, about a dozen of different enteropneusts have been documented in the deep sea (Osborn et al. 2012). In contrast, pterobranchs have been found in intertidal zones of tropical waters only recently (Lester 1985) and might have been overlooked previously due to their minute size and superficial similarities in their gross morphology with other tube-dwelling animals, such as polychaetes and ectoprocts.

Enteropneusts as well as pterobranchs exhibit a tripartite body organisation divided into an anterior prosome, a mesosome and a posterior metasomal region (Fig. 2.1). In enteropneusts, the prosome is called "acorn" or "proboscis", while in pterobranchs, it is termed "mouth shield". The middle body region encompasses the anteroventral mouth opening and is referred to as the "collar" or "mesosome", respectively. The mesosome of pterobranchs holds a tentacular crown for filter feeding (van der Horst 1939; Benito and Pardos 1997).

Both hemichordate groups have a characteristic excretory system in the prosoma. It is composed of a contractile pericardium that encloses the heart sinus that anteriorly continues into the glomerulus. The glomerulus is a highly dilated blood plexus lined by podocytes that are capable of mediating ultrafiltration into the protocoel. The accumulated ultrafiltrate then leaves the protocoel via the proboscis pore (Balser and Ruppert 1990). Indeed, such an excretory complex is also present in echinoderms (axial complex), thus representing a synapomorphy for Ambulacraria, yet in hemichordates, the unique stomochord is incorporated into this complex (Dohle 2004). The stomochord is an endodermal protrusion filled with vacuolated cells surrounded by a

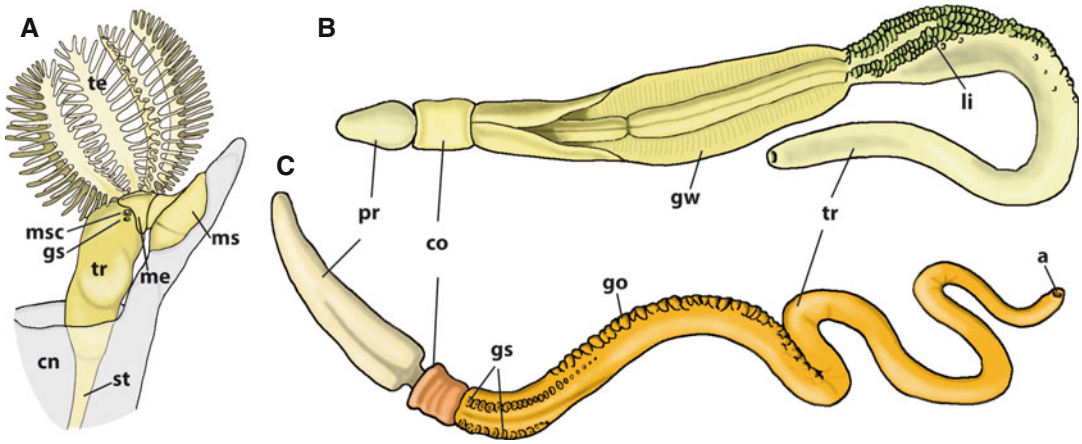

Fig. 2.1 Overview of the general morphology of hemichordates. (**A**) Habitus of an adult pterobranch, *Cephalodiscus* sp (Modified from Lester 1985), 2.5 mm. (**B**) Adult specimen of *Balanoglossus clavigerus* (Ptychoderidae), 25 cm. (C) Adult specimen of *Saccoglossus mereschkowskii* (Harrimaniidae), 4 cm (**B**, **C** modified from Goldschmid 2007). *a* anus, *cn* coenecium, *co* collar, *go* gonads, *gs* gill slit, *gw* genital wing, *li* liver sacs, *me* mesosome, *ms* mouth shield, *msc* mesocoelic pore, *pr* proboscis, *st* stalk, *te* tentacles, *tr* trunk

thickened extracellular matrix that serves as a supportive structure for the pericardium-glomerulus complex (Balser and Ruppert 1990; Mayer and Bartolomaeus 2003; Kaul-Strehlow and Stach 2011; Merker et al. 2013). A possible homology between the stomochord and the notochord of chordates is still debated.

Enteropneusta

Enteropneusta comprises less than 110 described species of worm-shaped animals (Cameron 2005) ranging from 0.5 mm to more than 2 m in size (Hyman 1959; Worsaae et al. 2012). Acorn worms are usually ground dwellers that live in muddy or sandy sediments; only few are known to be associated with the undersides of rocks (Spengel 1893; Hyman 1959; Cameron 2005). The body of acorn worms is vermiform and can be subdivided into three regions, each of which is supported internally by a corresponding coelomic cavity (Spengel 1893; Morgan 1894). The anterior proboscis differs in shape from long and slender (Fig. 2.1C) to conical and short (Fig. 2.1B; van der Horst 1939). Posteriorly, the proboscis connects to the collar region (mesosome) by a robust stalk. The highly muscular proboscis is the main locomotory organ and is used for the search for food and burrowing (van der Horst 1939; Benito and Pardos 1997). The short and barrel-shaped collar region surrounds and overlaps the posterior part of the proboscis including the proboscis stalk (Fig. 2.1B, C). The mouth opening is positioned ventrofrontally between the constriction separating proboscis and collar region (Bateson 1884, 1885; Spengel 1893). The middle collar region is followed by the long trunk region that forms the largest part of the enteropneust body. The trunk is functionally differentiated into the anterior branchio-genital region, the middle hepatic region and the posterior abdominal (intestine) region (Fig. 2.1B, C; Spengel 1893; Hyman 1959). A bilateral row of numerous dorsolateral gill slits accompanies the branchio-genital region. In many large species in particular, the specialised hepatic region is characterised by numerous liver sacs that are projections of the intestine and body wall (Fig. 2.1B). The tubular abdominal region is comparatively long and bears the anus at its terminal end. The nervous system of enteropneusts is developed as a basiepidermal nerve net throughout the body (Silén 1950; Bullock and Horridge 1965). More condensed areas are present in the trunk region, where they constitute a dorsal and a ventral median longitudinal nerve cord, respectively (Bullock 1946; Knight-Jones 1952). Furthermore, the dorsal nerve cord continues anteriorly into the collar region to form the subepidermal, hollow collar cord that is reminiscent of the neural tube present in chordates (Morgan 1894; Kaul and Stach 2010; Miyamoto and Wada 2013). The collar cord links to the basiepidermal plexus at the base of the proboscis, that is, the proboscis stem. Given that enteropneusts mainly consist of soft body parts, they are bad candidates for leaving fossilising remains, explaining their poor fossil record. Nevertheless, a recent finding of a tube-dwelling enteropneust dates their origin back to at least the Cambrian (Caron et al. 2013).

Pterobranchia

Pterobranchia is a small taxon consisting of roughly 25 species, of which all are colonial and semi-sessile animals (Cameron 2005; Nielsen 2011). They are tube dwellers that secrete the so-called coenecium from the anterior mouth shield (Fig. 2.1A). The body size of the individual zooid lies between 1 and 5 mm and an entire colony is built from a single larva that reproduces asexually by budding (Anderson 1907; van der Horst 1939). The mesosome is equipped with tentacles that are used for filter feeding and probably also serve respiratory function. The bulbous trunk region harbours most of the U-shaped digestive tract including the posterior pharynx, stomach and intestine. The anus opens on the dorsal side of the anterior trunk region, just behind the mesosome. The nervous system of pterobranchs constitutes a basiepidermal nerve net. Additionally, a prominent dorsal brain is present at the base of the mesosomal tentacles (Dilly et al. 1975; Rehkämper et al. 1987; Stach et al. 2012). The brain features an anterior neuron-rich area composed of serotonergic and giant neurons as well as a posterior neuropil. Further concentrated parts of the peripheral nervous system are tentacle

nerves, a ventral stalk nerve and a pair of branchial nerves in *Cephalodiscus gracilis* (Stach et al. 2012). Pterobranchs mainly live associated with hard substrates since their secreted tubes build encrusting aggregates on rocks and shells. The majority of described species have been collected in the deep sea and only few species are known from shallow waters. These include *Rhabdopleura normani* and *C. gracilis* that can easily be accessed by snorkelling in shallow waters on the Bermuda Islands (Lester 1985, 1988a, b) or *Rhabdopleura compacta* that lives off the south coasts of England (Sato et al. 2008). Due to their secreted tubes, pterobranchs are associated with the fossil group Graptolithina that are known from the Cambrian through the Carboniferous. Graptolithina composes a quite diverse group of fossils of pelagic tube-dwelling colonies that are supposed to be closely related to the extant genus *Rhabdopleura* (Sato et al. 2008).

Within the last couple of years, Sato and colleagues have begun to develop *Rhabdopleura compacta*, a species that can be found in the south of England, as an emerging model organism that can be used for developmental studies (Sato et al. 2008, 2009; Sato and Holland 2008).

Historical Background

The very first mentioning of an enteropneust can be traced back to the work of Friedrich Eschscholtz in 1825, who described a wormlike animal named *Ptychodera* that he interpreted as a new species of holothuroid echinoderms (Eschscholtz 1825). Only a few years later, and without knowledge of Eschscholtz' description, Stefano Delle Chaje documented a sand-dwelling worm that he named *Balanoglossus clavigerus* (Delle Chaje 1829). However, both reports were only short notes showing sketchy drawings, and it was not before 1866 until the first detailed anatomical description of an enteropneust was published by Alexander Kowalevsky (1866). At that time, phylogenetic relationships of enteropneusts were controversially discussed. Because of a vermiform body, a closer relationship to either nemerteans, annelids or other "worms" was suggested, but also holothurians were considered as relatives. Interestingly, a conspicuous larva, first documented around 1850, played a more important role in resolving this issue than initially thought. In 1849, Johannes Müller found a peculiar larva in the plankton near Marseille, France. He named this larva "tornaria" and placed it in a closer connection to the bipinnaria of sea stars, because of similarities in the arrangement of the ciliary bands (Müller 1850). At the same time, a similar larva was found by August Krohn, but this one had a much more sinuously running ciliary band and he suggested this to be a different species (Krohn 1854). In those days, it was not known that these varying larvae actually display successive developmental stages. Nowadays, this particular larval stage with secondary lobes and saddles of the ciliary feeding band (neotroch) is called "Krohn stage", referring to its original describer. In fact, all of the succeeding larval stages have later on been given specific names, being in connection to the historical background of their discovery. This will be discussed more precisely in the paragraph dealing with late development. Nevertheless, it was Elias Metschnikoff who made a promising finding in 1870, when he collected a larva that showed similarities with the worm of *Balanoglossus* (Metschnikoff 1870), yet his colleagues did not believe in a connection between echinoderm-like tornaria and the wormlike enteropneust. It took three more years until Alexander Agassiz successfully documented the metamorphosis of a tornaria larva into a juvenile *Balanoglossus*, thus finally unravelling the larva's unknown affiliation (Agassiz 1873). In the following years, a number of descriptive studies were added to the existing list. Bateson published a study of direct development of *Saccoglossus kowalevskii* without a tornaria larva and at the same time he was the first who observed early cleavage stages in enteropneusts (Bateson 1884, 1885, 1886). He suggested a close relationship of enteropneusts with chordates, because of shared characters such as gill slits, stomochord and a neurulated collar cord.

Since then, consecutive studies on various aspects of enteropneusts have significantly increased our understanding of the group and were summarised in several classical textbooks and treatises such as Spengel's monograph on enteropneusts (1893), van der Horst's "Enteropneusta" in *Bronn's Klassen und Ordnungen des Tierreichs* (1939) or Hyman's *The Invertebrates* (1959), to name but a few. Strangely, the interest in enteropneust research declined within the last half of the twentieth century and relatively few works were published. Only recently, with upcoming immunocytochemical as well as molecular techniques and the new field of "EvoDevo" research, people have rediscovered the potential and importance of enteropneusts in unravelling evolutionary developmental questions (Tagawa et al. 1998a, b; Lowe et al. 2003, 2006; Röttinger and Martindale 2011; Röttinger and Lowe 2012; and references therein).

Systematics and Phylogenetic Relationships

Morphologically, hemichordates are well supported as deuterostome animals, because the main coelomic cavities originate from the archenteron by enterocoely and the mouth is formed secondarily during development. However, the exact position of Hemichordata within the Deuterostomia and its putative sister group has been controversially discussed within the last decade, due to incongruent morphological as well as molecular data. On the one hand, shared chordate features such as gill slits, stomochord and neurulated collar cord in enteropneusts lead already Bateson (1885) and Barrington (1965) to suggest a closer relationship of Hemichordata and Chordata. Indeed, phylogenetic analyses based on morphological characters strongly support this view (Young 1962; Maisey 1986; Schaeffer 1987; Ax 2001). However, more recent molecular phylogenetic analyses consistently reveal a sister group relationship between Hemichordata and Echinodermata, comprising the Ambulacraria (Fig. 2.2; Bourlat et al. 2006; Cannon et al. 2009; Hejnol et al. 2009; Edgecombe et al. 2011). At present, Ambulacraria seems to be widely accepted and is also morphologically supported by a shared larval type (dipleurula with specialised neotroch ciliary band) as well as similar coelomic systems and excretory organs. Pterobranchs and enteropneusts are classically treated as sister groups, yet molecular phylogenetic analyses strongly support the position of pterobranchs as a sister group to Harrimaniidae (an enteropneust subclade), thus rendering Enteropneusta paraphyletic (Fig. 2.2; Cameron et al. 2000; Cannon et al. 2009; Osborn et al. 2012). The possibility that pterobranchs evolved a sessile and colonial lifestyle secondarily from a solitary, wormlike enteropneust ancestor has further been supported by the recent discovery of a tubicolous enteropneust from the Cambrian (Caron et al. 2013).

There are three main subclades to which the majority of enteropneust species belong to, namely, Ptychoderidae (Spengel 1893), Spengelidae (Willey 1898) and Harrimaniidae (Spengel 1901) (Fig. 2.2). A fourth taxon has recently been described, the Torquaratoridae (Holland et al. 2005), comprising enteropneusts from the deep sea (Osborn et al. 2012). Members of the Torquaratoridae are characterised by lacking a stomochord as adults. Moreover, the proboscis skeleton is either reduced to a small plate or completely absent. The Ptychoderidae includes the first enteropneust species described, *Ptychodera flava*, and is characterised by the presence of gill-slit synapticles and a distinct trunk region featuring liver sacs and genital wings (Figs. 2.1B and 2.2). Members of the Spengelidae do not exhibit genital wings at the trunk region and liver sacs were only described for the genus *Schizocardium* (Spengel 1893; Cameron 2005).

Ptychoderidae and Spengelidae possess a biphasic life cycle and develop indirectly via a pelagic tornaria larva. Harrimaniidae includes the smallest representative of an acorn worm described so far, *Meioglossus psammophilus* (Worsaae et al. 2012), with less than 1 mm in

length. This taxon possesses the simplest anatomy, as their members lack liver sacs as well as genital wings within the dorsal trunk region (Fig. 2.1C). Also, the gill slits in harrimaniids are not supported by synapticles as in other enteropneust subclades (van der Horst 1939; Cameron 2005). Harrimaniid enteropneusts such as *Saccoglossus* develop directly, not passing through an extended pelagic stage. The hatchlings resemble young adults and soon settle in the sediment to grow into a juvenile enteropneust.

Pterobranchs are grouped into two genera, *Cephalodiscus* (M'Intosh 1882) and *Rhabdopleura* (Allman 1869) (Fig. 2.2). A putative third genus is monotypic with *Atubaria heterolopha* (Sato 1936) from deeper Japanese waters, yet the validity of this genus is questionable (Mierzejewski 2004). Many *Cephalodiscus* species live in fingerlike branched coenecia and have individual zooids, although in some species, the zooids are linked to each other by the posterior stalk (Lester 1985). *Cephalodiscus* spp. are characterised by a globular metasomal region, one pair of gill slits, two gonads and mesocoel pores and between five and nine pairs of tentacles on the mesosome (Hyman 1959). A muscular stalk is present at the posterior end of the metasomal region and aids in its withdrawal into the coenecium. Species of the genera *Rhabdopleura*, in contrast, bear only a single pair of tentacles on the mesosome, have only one gonad and lack gill pores altogether (Schepotieff 1907; van der Horst 1939). The zooids of one colony live in tubular coenecia and stay interconnected by the stalk throughout lifetime (Lankester 1884; Hyman 1959).

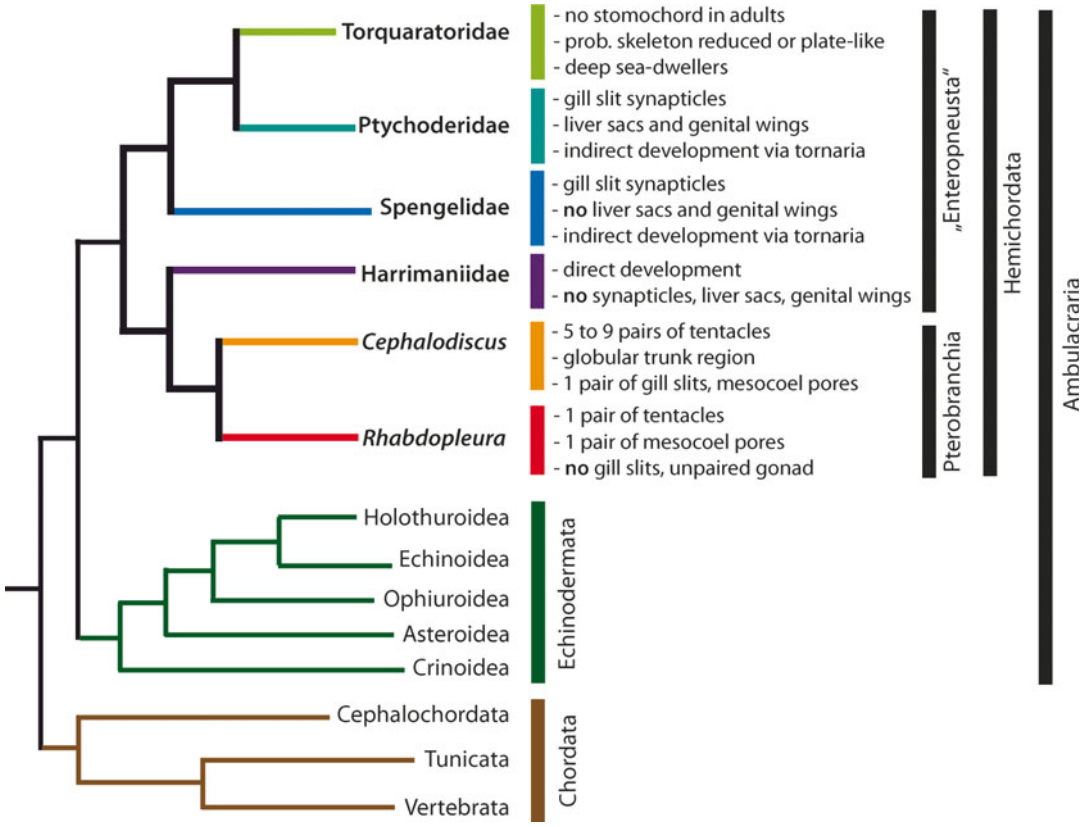

Fig. 2.2 Deuterostome phylogeny. Cladogram compiled from recent phylogenetic analyses (Osborn et al. 2012; Worsaae et al. 2012). The position of Xenacoelomorpha is debated and not shown here (Hejnol et al. 2009; Philippe et al. 2011)

EARLY DEVELOPMENT

Development in Pterobranchs

Pterobranchs are less frequently encountered as enteropneusts, which is why knowledge on the reproduction and development of these minute animals is still fragmentary. So far, it is known from *Rhabdopleura* that the fertilised, yolk-rich egg undergoes holoblastic, radial and equal cleavage, eventually leading to a uniformly ciliated larva (Fig. 2.3A–G; Stebbing 1970; Dilly 1973; Lester 1988a). The larva is of elongated shape with a tapering posterior end (Sato et al. 2008). Its colour is opaque and yellowish. A brown spotty pigmentation is present over the body and the larva exhibits a conspicuous ventral depression (Fig. 2.3F, G). After a short pelagic period, the larva tests the substrate and eventually settles with the ventral side secreting a cocoon. Inside the cocoon, the metamorphosing larva develops the anlagen of the tentacles, the mouth shield and the metasome; thus, the future tripartite body organisation is already established (Fig. 2.3H–K; Lester 1988b). After a few days, the cocoon breaks and the zooid starts to form its coenecium, thereby founding a new colony (Fig. 2.3L). In *Cephalodiscus*, even less is known about development, although a few accounts on single developmental stages are present (Harmer 1905; Anderson 1907; Schepotieff 1907; Dilly 2013). A recent ultrastructural study shows an elongated, three-layered embryonic stage of *C.*

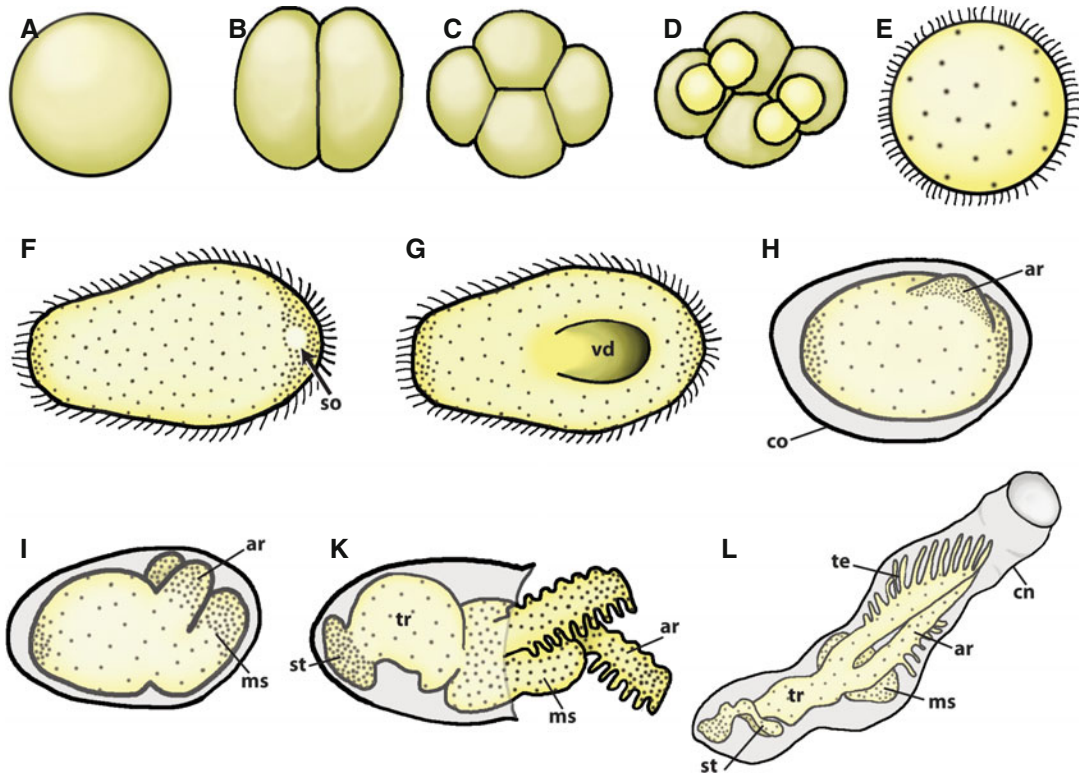

Fig. 2.3 Development and metamorphosis of *Rhabdopleura normani*. (**A**) Zygote. (**B**) Two-cell stage. (**C**) Four-cell stage. (**D**) Eight-cell stage. (**E**) Spherical, ciliated embryo. (**F**) Swimming larva from dorsal. (**G**) Swimming larva from ventral. (**H**) Metamorphosing larva in secreted cocoon, approx. 12 h after settlement. Lateral view. (**I**) Same as in **H**, approx. 33 h after settlement. (**K**) Hatching juvenile, approx. 100 h after settlement. (**L**) Zooid in secreted coenecium. Drawings not to scale (Modified from Lester 1988a, b). *ar* arm holding tentacles, *cn* coenecium, *co* cocoon, *ms* mouth shield, *so* sensory organ, *st* stalk, *te* tentacle, *tr* trunk, *vd* ventral depression

gracilis (Stach 2013). The prospective meso- and metacoels are already separated from the endoderm, whereas the prospective protocoel is still continuous with the endoderm. The one pair of gill pores seems to develop asynchronously, in favour of the left side. The creeping larva lacks any planktonic specialisations and might develop directly into a young zooid without passing through a pelagic stage.

Development in Enteropneusts

Fertilisation is external in all studied enteropneusts and spawning is usually dependent of the species' habitat and correlated with seasons, whereby temperature and light intensity play a major role (Hadfield 1975). As outlined before, two different modes of development have been observed in enteropneusts. Whereas members of Ptychoderidae and Spengelidae develop a pelagic larval stage, the tornaria, harrimaniid enteropneusts develop directly from yolk-rich eggs. Early development including cleavage patterns has been described for several enteropneust species (Bateson 1884; Stiasny 1914a; Burdon-Jones 1952; Colwin and Colwin 1953; Tagawa et al. 1998a; Urata and Yamaguchi 2004). In all studied enteropneusts, cleavage is radial, holoblastic and nearly equal.

Embryology in Direct Developing Enteropneusts

In direct developing enteropneusts such as *Saccoglossus kowalevskii*, a gravid female spawns between 200 and 1.000 oocytes with a diameter of about 300 µm. After fertilisation, a thick vitelline membrane is formed around the zygote. Subsequently, the fertilised egg undergoes radial cleavage of which the two first cleavages are meridional and the third is latitudinal (Bateson 1884; Colwin and Colwin 1953). The fourth cleavage results in a single animal tier of eight cells (Fig. 2.4), whereas the vegetal cells divide latitudinally to yield an upper tier of four larger cells as well as a lower tier of four smaller cells. Cell labelling in *Saccoglossus* showed that the cells of the animal tier give rise to the anterior ectoderm, while the upper tier of vegetal cells will form the middle and posterior ectoderm (Colwin and Colwin 1951; Darras et al. 2011). Only the cells of the lower vegetal tier will differentiate into endo- as well as mesoderm (Fig. 2.4). Continuous cleavages lead to a rounded coeloblastula. Before gastrulation, the blastula becomes cup-shaped by flattening of the animal-vegetal axis, while at the same time, the thickened vegetal pole invaginates circumferentially (Colwin and Colwin 1953). After gastrulation of the prospective endomesoderm, the blastopore closes and the embryo again elongates along the anterior-posterior axis (Fig. 2.5A). At this time of development, the opisthotroch (ciliary band), composed of numerous long compound cilia, is visible demarcating the postanal field. The embryos start to spin around within the vitelline membrane as soon as the cilia start to beat. Only a few hours later, a circumferential groove starts to subdivide the embryo in an anterior proboscis region and a posterior region constituting the future collar and trunk (Fig. 2.5B). At this stage, the anterior part of the invaginated archenteron separates as the first coelomic cavity, thereby forming the future protocoel (Figs. 2.4 and 2.6A). The paired meso- and metacoels are present as separated evaginations from the middle and posterior regions of the archenteron (Figs. 2.6A), yet are still connected to the archenteron. Around 4 days after fertilisation, the embryos are of elongated shape with a perianal field that is bent ventrally (Fig 2.5C). A second circular groove forms the border between the collar and trunk region. By this stage, the meso- and metacoels are pinched off and enclose the endoderm almost completely. A sixth, yet small coelomic cavity is situated at the posterodorsal base of the proboscis and will later differentiate into the pericardium or heart vesicle. In contrast to the pro-, meso- and metacoels that originate from the endoderm by enterocoely, the pericardium develops by schizocoely from the ectoderm in *S. kowalevskii* (Kaul-Strehlow and Stach 2011). Schizocoely is typical for formation of the mesoderm in various protostomes and only rare cases in deuterostomes are known (Technau and Scholz 2003). The endoderm connects to the exterior on the ventral side

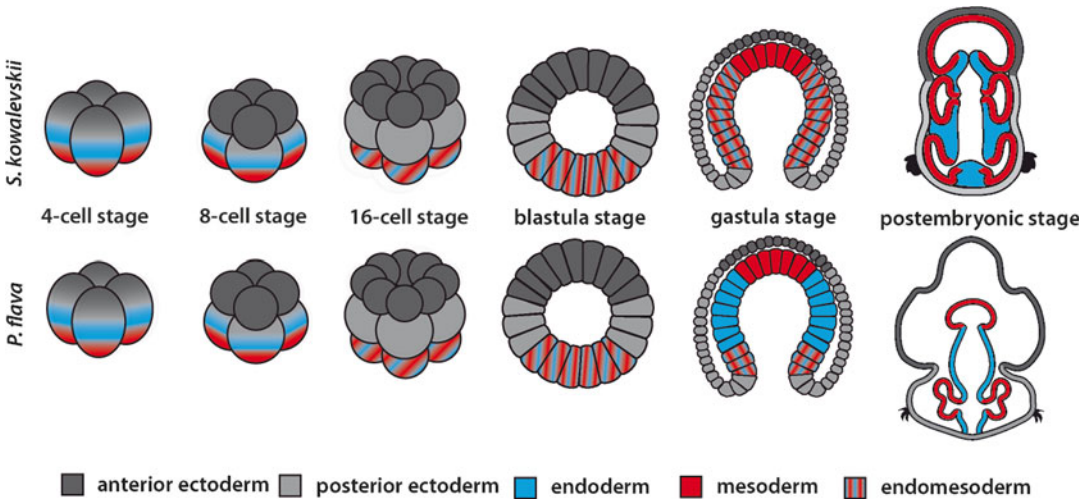

Fig. 2.4 Early embryology of direct and indirect developing enteropneusts. *Upper row*: the direct developing harrimaniid *Saccoglossus kowalevskii*. *Lower row*: the indirect developing ptychoderid *Ptychodera flava*. The exact timing of separation of endo- and mesoderm remains unclear

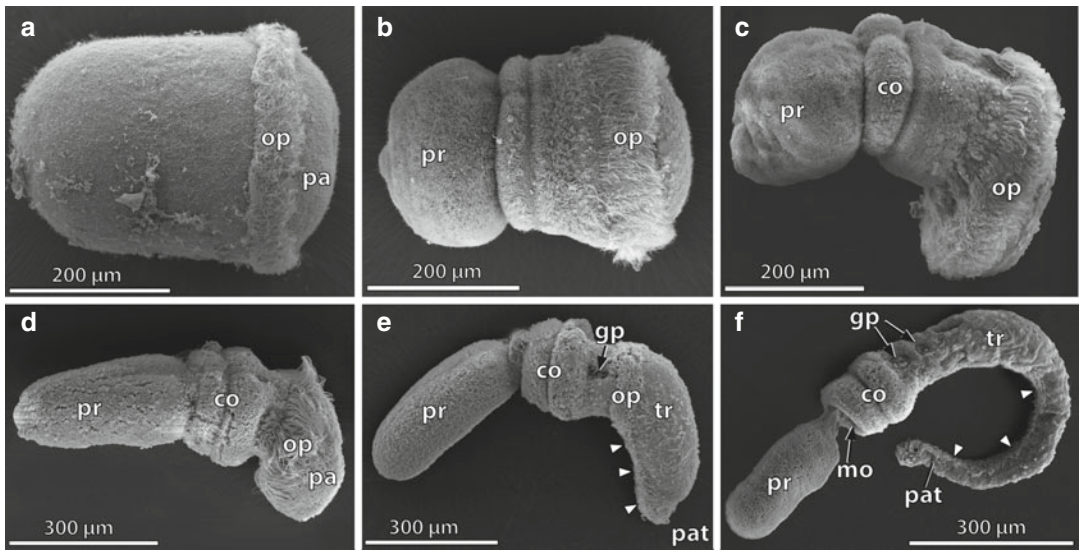

Fig. 2.5 Scanning electron micrographs of developmental stages of *Saccoglossus kowalevskii*. (**A**–**C**) Fertilisation membrane removed. (**A**) Late gastrula. (**B**) Early kink stage. (**C**) Dorsal flexure stage. (**D**) One-gill-slit hatchling. (**E**) Early settling juvenile. Note the ventral creeping sole (*arrowheads*) and the postanal tail. (**F**) Three-gill-slit juvenile with adult-like gross morphology. *co* collar, *gp* gill pore, *mo* mouth opening, *op* opisthotroch, *pa* perianal field, *pat* postanal tail, *pr* proboscis, *tr* trunk (© Sabrina Kaul-Strehlow 2015. All Rights Reserved)

just between the proboscis and collar region, forming the mouth opening, whereas the anus is still closed. The developing stomochord protrudes into the proboscis base as a short, rod-like extension from the anterodorsal roof of the endoderm. Closely behind the posterior margin of the collar region, the endoderm pierces through the metacoel of the trunk region and establishes contact with the ectoderm, thereby forming the anlagen of the first pair of gill pores (Fig 2.6C). Embryogenesis is usually complete at around 5 days after fertilisation in embryos

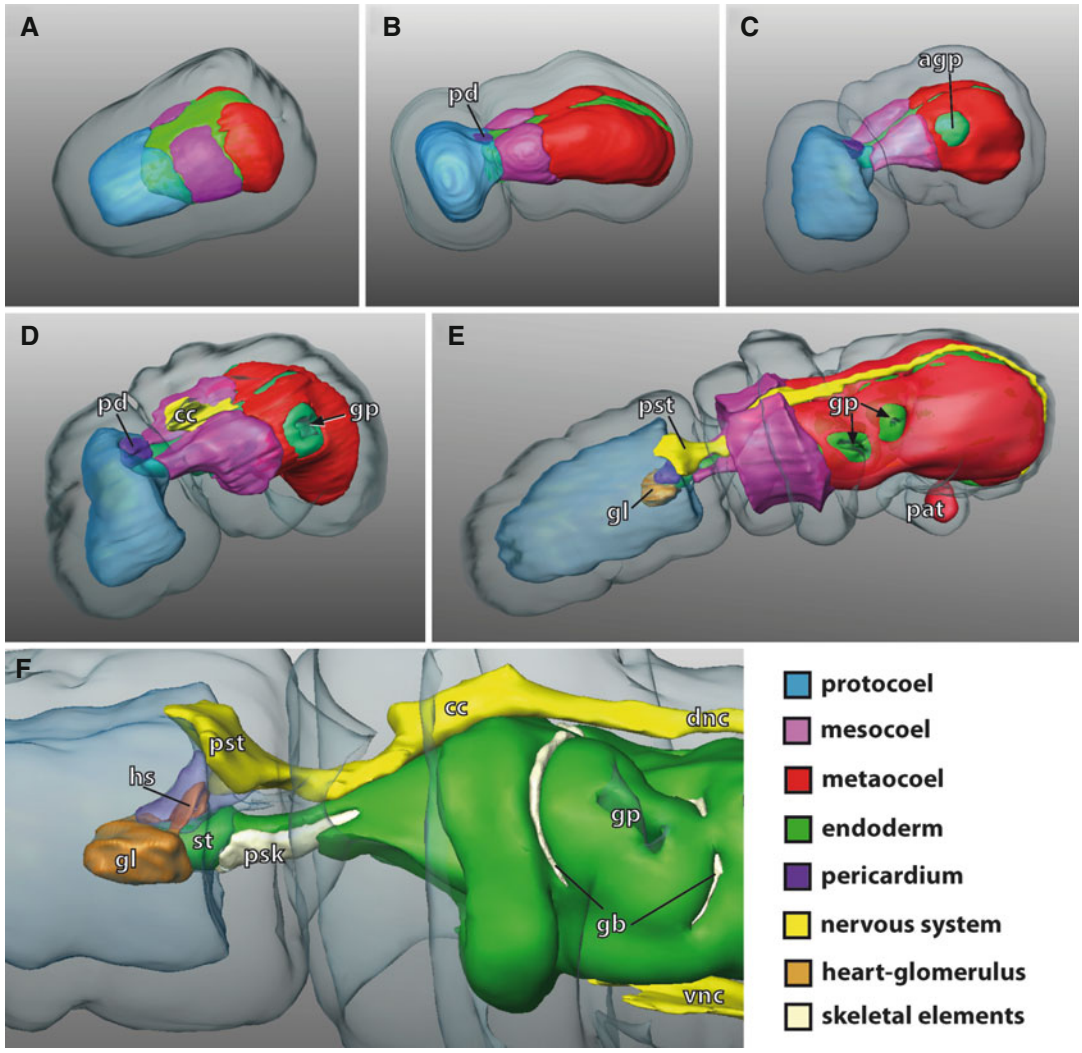

Fig. 2.6 3D reconstructions of major organ systems in different developmental stages of *Saccoglossus kowalevskii* based on complete serial semithin sections. Note, only the centralised parts of the nervous system are reconstructed in (**D**–**F**); the nerve net is not shown. Anterior is (almost) to the left in all images. (**A**) Late gastrula with anlagen of the prospective meso- and metacoels. The anterior protocoel has already pinched off of the endoderm. (**B**) Early kink stage. Meso- and metacoels are separated from endoderm. The pericardium emerges at the dorsal base of the protocoel. (**C**) Dorsal flexure stage showing anlagen of the first pair of gill pores. (**D**) One-gill-slit hatchling with opened pair of gill pores and neurulating collar cord in the mesosome. (**E**) Two-gill-slit juvenile with resembling adult morphology. (**F**) Close-up showing the inner organisation of the proboscis, collar and anterior trunk region in detail. *agp* anlage of gill pore, *cc* collar cord, *dnc* dorsal nerve cord, *gb* gill bar, *gl* glomerulus, *gp* gill pore, *hs* heart sinus, *pat* postanal tail, *pd* pericardium, *psk* proboscis skeleton, *pst* proboscis stem, *st* stomochord, *vnc* ventral nerve cord

cultured at 22 °C and hatch from the fertilisation membrane (Colwin and Colwin 1953; Lowe et al. 2004). At that time, *Saccoglossus* exhibits an elongated body shape measuring ~500 µm in length with a ventrally bent perianal field (Figs. 2.5D and 2.6D). One pair of dorsolateral gill pores is present in the anterior part of the trunk region. After hatching, the animals swim in the water column for a couple of hours and soon start to burrow and feed in the sediment.

Embryology in Indirect Developing Enteropneusts

The ontogeny including metamorphosis of indirect developing enteropneusts has been studied in species of the genera *Balanoglossus* and *Ptychodera* (Morgan 1891; Stiasny 1914a, b; Tagawa et al. 1998a; Urata and Yamaguchi 2004; Nielsen and Hay-Schmidt 2007; Miyamoto et al. 2010). Only recently, the first study of the development of a member of the Spengelidae, *Glandiceps hacksi*, has been investigated (Urata et al. 2014). Although the later development of indirect developers differs considerably from direct developers such as *Saccoglossus*, cleavage patterns and fate maps are identical and moreover show strong resemblance to sea urchins (Henry et al. 2001; see Chapter 1). The 16-cell stage of *Ptychodera flava* comprises an animal tier of eight cells (primordial anterior ectoderm), an upper vegetal tier of four cells (primordial posterior ectoderm) as well as a lower vegetal tier of four cells (primordial endomesoderm) (Fig. 2.4; Tagawa et al. 1998a). Subsequent cleavages give rise to a coeloblastula. Cleavage speed varies greatly between enteropneust species. Whereas in *P. flava* it takes about ~18 h post fertilisation (pf) until gastrulation starts (cultured at 22–24 °C) (Tagawa et al. 1998a), it begins at around ~13 h pf in *Balanoglossus clavigerus* (cultured at 20 °C) (Stiasny 1914a), and in *B. misakiensis*, this stage is already reached within ~9 h pf (cultured at 26 °C) (Urata and Yamaguchi 2004). At the end of gastrulation, the blastopore is closed and the protocoel is pinched off from the anterior region of the archenteron. The protocoel soon attaches to the epidermis of the animal pole and fuses with the dorsal ectoderm to form the hydropore. After ~45 h pf, embryonic development is completed in *P. flava* and the larva hatches from the fertilisation membrane to instantly start swimming (Tagawa et al. 1998a; Nielsen and Hay-Schmidt 2007). The early larva is of more or less spherical shape and soon develops into the typical tornaria larva. The first tornaria stage is called Müller stage and is characterised by a closed mouth as well as anus, open hydropore and a developing neotroch (circumoral ciliary band). The digestive tract is tripartite and composed of pharynx, stomach and intestine. In contrast to *P. flava*, which has a comparably long larval development for enteropneusts, the Japanese species *B. misakiensis* exhibits a shortened larval cycle and its larva hatches already at 24 h pf, thereby skipping the Müller stage (Urata and Yamaguchi 2004). Early hatched larvae of *B. misakiensis* have already developed an opisthotroch that typically characterises the Heider (second) stage of tornaria larvae (Fig. 2.7A). In all enteropneusts studied so far, the hydropore opens only after the protocoel has separated from the endoderm (Spengel 1893; Hyman 1959). However, in the recently studied spengelid *Glandiceps hacksi*, the hydropore forms prior to this event. This "precocious hydropore formation" is so far unique for the enteropneust *G. hacksi*, yet it is known also from various holothuroid echinoderms (Urata et al. 2014 and references therein).

LATE DEVELOPMENT

Late Development in Direct Developing Enteropneusts

When direct developing enteropneusts such as *Saccoglossus kowalevskii* hatch, the first pair of gill pores is open and the animals swim actively by the propelling opisthotroch. As soon as the animals start burrowing in the sand, the opisthotroch is remodelled and extends on the ventral side of the trunk in order to serve as a creeping sole for the juvenile worms (Fig. 2.5E; Burdon-Jones 1952; Stach and Kaul 2012). As the worms grow older, gill pores are added successively and the body size gains considerably in length. The juveniles measure up to a few millimetres at this point and resemble adult worms in many aspects, except for the still present postanal tail and the lower number of gill pores (Figs. 2.5F and 2.6E). The protocoel within the proboscis region is lined by a myoepithelium that forms the body wall musculature, composed of an outer layer of circular muscles and an inner layer of longitudinal muscles. A single proboscis pore is located posterodorsally on the left side and opens to the

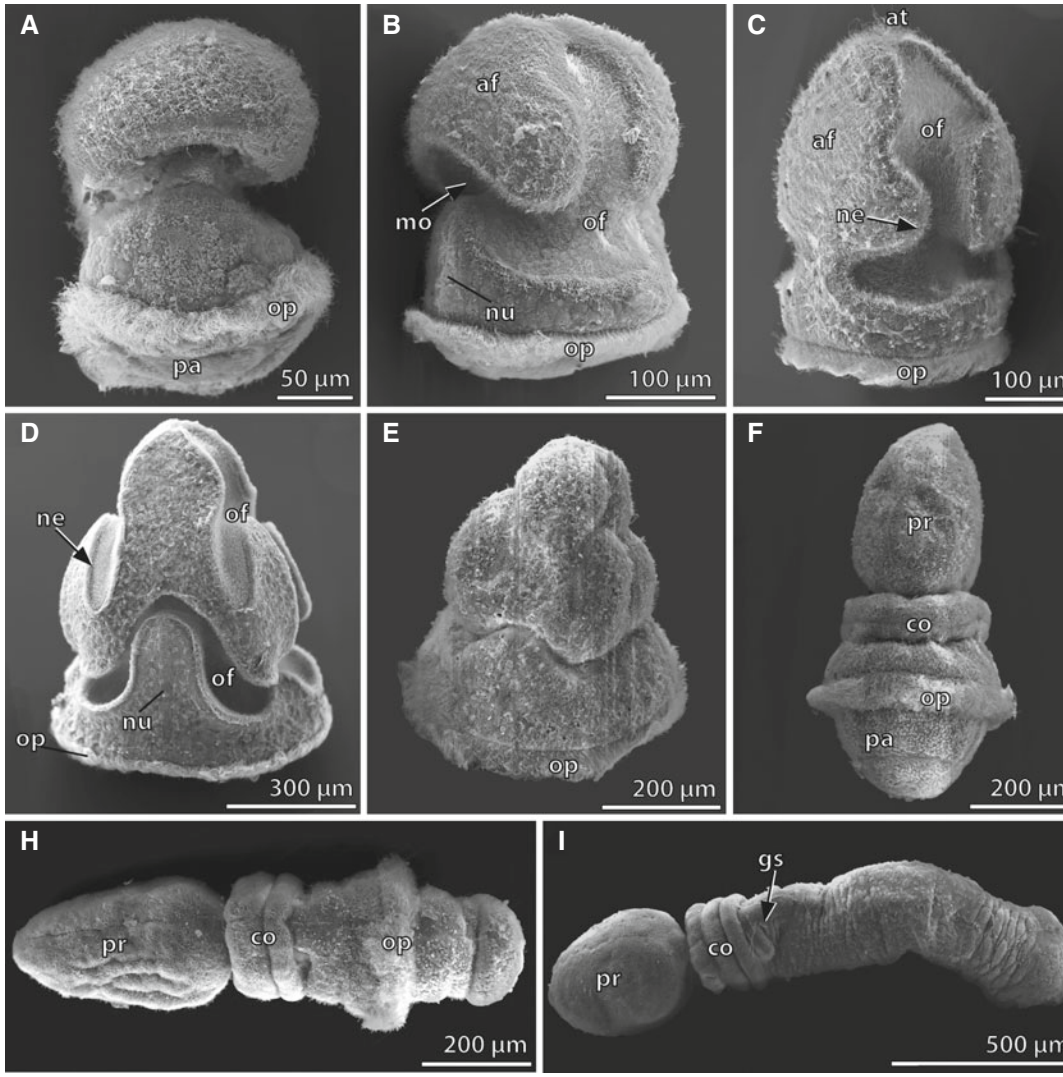

Fig. 2.7 Scanning electron micrographs of developmental stages of *Balanoglossus misakiensis*. (**A**) Early hatched Heider stage larva (30 h pf). (**B**) Tornaria at late Heider stage (48 h pf) with ventral neurotroch and oral field developed. (**C**) Early Metschnikoff stage (120 h pf) showing the beginning of primary lobe formation of the ciliary band of the oral field (neotroch). (**D**) Fully grown tornaria of *B. misakiensis* at late Metschnikoff stage (10 days pf) with deep primary lobes. (**E**) The Spengel stage (13 days pf) designates the beginning of metamorphosis and is characterised by the fusion of the neotroch, eventually obliterating the oral field and reducing the size of the body. (**F**) Agassiz stage tornaria (14 days pf) with acorn-shaped preoral region (future proboscis). This stage is competent to undergo settlement. (**G**) Early settled juvenile (12 h post settlement) with elaborated collar and elongated trunk region. The larval opisthotroch is still present. (**H**) Two-gill-slit juvenile (3 days post settlement) that already resembles a minute adult enteropneust. *af* aboral field, *at* apical tuft, *co* collar, *gs* gill slit, *mo* mouth opening, *ne* neotroch, *nu* neurotroch, *of* oral field, *op* opisthotroch, *pa* perianal field, *pr* proboscis (© Sabrina Kaul-Strehlow 2015. All Rights Reserved)

exterior. The number and position of the proboscis pores in enteropneusts is species dependent. Accordingly, in some species, bilateral pores are present, while in others only a single one is found on the right side. The pericardium is situated posteriorly within the protocoel and is dorsally attached to the stomochord. The pericardium is a small coelomic cavity that is lined ventrally by

epithelial muscle cells overlying the heart sinus, which is in principle an enlarged area within the extracellular matrix (ECM) filled with colourless blood fluid (Balser and Ruppert 1990). By contraction of the pericardial epithelial muscle cells, the blood fluid is forwarded into the anterior glomerulus. The glomerulus is a highly ramified enlargement of the ECM that is lined with podocytes on the protocoelic side. These podocytes have fingerlike extensions and are involved in filtration of the blood fluid. Together with the efferent proboscis pore, the heart-glomerulus complex represents the excretory system of hemichordates. The digestive tract in these juvenile worms is already subdivided into the typical regions, the anterior buccal cavity followed by the pharyngeal region harbouring the dorsolateral gill pores, connected to the stomach by a short and thin tubular esophagus ending in a short hindgut region that opens into the anus. The paired meso- and metacoels are lined by a single layer of epithelial cells that contain basal myofilaments. Within the metacoels, these myofilaments constitute a substantial longitudinal musculature, in particular on the ventral side. The mesocoels send a pair of extensions anteriorly through the proboscis stalk into the base of the proboscis. These mesocoelic protrusions flank the stomochord and contain longitudinal muscle strands that are involved in moving the entire proboscis. The few gill pores situated dorsolaterally at the anterior trunk region are kidney-shaped with the depression facing dorsally (Fig. 2.5F). Only later a dorsal tongue bar grows ventrally to eventually give the gill pores their slitlike U shape. Tongue bars are supported internally by a collagenous bar that forms within the ECM. It is the same material of which the proboscis skeleton is made of. The proboscis skeleton supports the stomochord ventrally and bifurcates within the collar region to flank the buccal cavity on either side. As the juveniles grow, subsequent development primarily involves increase of size, particularly trunk elongation, and addition of gill slits. The number of gill slits in adult *S. kowalevskii* varies greatly as new pairs seem to be added continuously throughout lifetime.

Neurogenesis in Direct Developing Enteropneusts

Neurogenesis in direct developing enteropneusts such as *Saccoglossus* has been studied thoroughly by molecular genetic analyses, yet morphogenetic data are still scarce. At late gastrula stage (Fig. 2.5A), serotonergic neurons form throughout the future proboscis region and project neurites posteriorly (Cunningham and Casey 2014). In stages close to hatching, a considerable basiepidermal nerve net is developed throughout the entire embryo (Kaul and Stach 2010). Before hatching, the collar cord at the dorsal midline of the collar region neurulates gradually from anterior to posterior to finally occupy a subepidermal position underneath the epidermis (Figs. 2.6D–F and 2.8). Just after neurulation, the collar cord comprises a large area of neuronal precursors that surround a central lumen (central canal) and small ventral areas filled with neurites (Fig. 2.8C). In older juvenile worms, a circumferential basiepidermal nerve net is present within the proboscis and collar region. Within the trunk region, the majority of neurites seems to run within the longitudinal nerve cords, i.e., the dorsal and the ventral cord (Kaul and Stach 2010), whereas only scattered neurites are present laterally. The dorsal nerve cord extends posteriorly until the anus and is anteriorly continuous with the collar cord. The ventral nerve cord is usually broader and runs along the midline of the trunk region to end in front of the postanal tail. Within the collar region, the collar cord is differentiated into a dorsal sheath of somata including unipolar giant neurons as well as smaller ependymal cells lining the central canal. About two-thirds of the collar cord are filled with numerous neurites that form a ventral neuropil (Fig. 2.8D). The collar cord continues anteriorly into the proboscis stem, a thickened area of neurites located at the dorsal base of the proboscis (Fig. 2.6E, F).

Late Development in Indirect Developing Enteropneusts

After hatching, the larvae of the indirect developer *Balanoglossus misakiensis* are of slightly

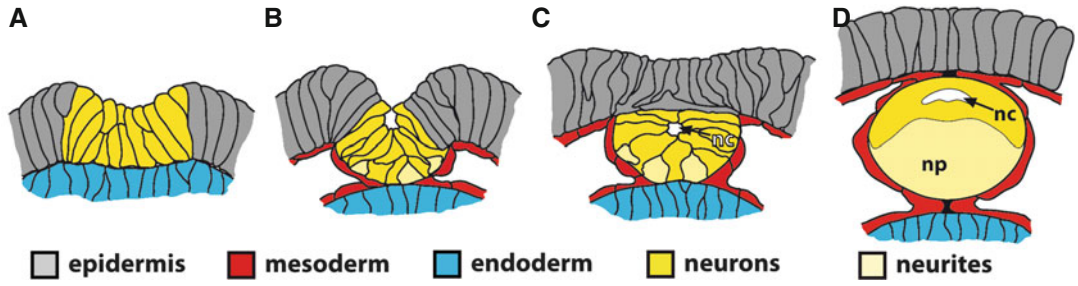

Fig. 2.8 Semi-schematic illustration of the neurulation process in *Saccoglossus kowalevskii* as revealed by transmission electron microscopy. (**A**) Early stage showing dorsal neural plate. (**B**) the neural plate invaginats ventrally. (**C**) The neural plate has formed a subepidermal tubular nerve cord. (**D**) The collar cord comprises a dorsal sheath of soma and a ventral neuropil. (Modified from Kaul and Stach 2010). *nc* neural canal, *np* neuropil

elongated shape and feature an apical hood below which the mouth opening will soon break through on the ventral side. A less pronounced perianal ciliary ring and the opisthotroch are present near the posterior end of the larvae (Heider stage) (Fig. 2.7A). Approximately 1 day after hatching, a simple neotroch is developed, separating the aboral field from the oral field that is used for food collection and transport (Fig. 2.7B). On the ventral side, another longitudinal yet short ciliary band is present, the neurotroch. The larvae swim actively in the water column and feed on phytoplankton as soon as the mouth and anus have opened. A few days later, the tornaria has increased in size and the neotroch develops a more complex pattern of ciliary bands on the anterior half of the larva by forming primary lobes (Fig. 2.7C). The beginning of primary lobe formation is characteristic for the early Metschnikoff stage. At the anterior tip, a pair of dark eye spots is visible alongside the central ciliary tuft. During subsequent development, the tornaria of *B. misakiensis* grows to a remarkable size of 1.5 mm and the primary lobes of the neotroch form deep protrusions to enlarge the oral field considerably (Fig. 2.7D). At the Metschnikoff stage, adult structures such as the proboscis vesicle (pericardium) and the meso- and metacoels become apparent. The proboscis vesicle forms a small coelomic cavity close to the hydropore on the right side (Fig. 2.9A). Its origin seems to be species dependent and has been reported from the ectoderm (Spengel 1893; Stiasny 1914b) or mesoderm by pinching off of the protocoel (Dawydoff 1907; Morgan 1894; Ruppert and Balser 1986). The meso- and metacoels in *B. misakiensis* form as a lateral pair of protrusions from the intestine region (Figs. 2.4 and 2.9A). They elongate anteriorly to subsequently constrict in the middle to subdivide into the anterior mesocoel and posterior metacoel. This mode of development has also been reported from *B. clavigerus* (Bourne 1889; Spengel 1893; Stiasny 1914a) and *Glandiceps* sp. (Rao 1953). In tentaculated tornaria of, e.g., *Ptychodera*, however, the meso- and metacoels form from multiple clusters of mesenchymatic cells within the blastocoel (Morgan 1894). After the Metschnikoff stage, indirect developers typically enter the so-called Krohn stage by developing secondary lobes and saddles on the neotroch without obvious changes of their internal anatomy. In this stage, the tornaria exhibits a more compact shape with a nearly planar perianal field. The Krohn stage larva may differ morphologically between species and exhibit species-specific characters. For instance, the Krohn tornaria of *Ptychodera flava* develops a highly sinuous neotroch eventually resulting in small tentacles (Hadfield 1975; Nielsen and Hay-Schmidt 2007). In contrast, the neotroch in *B. clavigerus* never develops tentacles on the secondary lobes, and in *B. misakiensis*, the Krohn stage is skipped completely by proceeding directly into the Spengel stage (Figs. 2.7E and 2.9B). An elaborated neotroch with tentacles as found in *P. flava* is likely to result in a more efficient food uptake and correlates with the extended pelagic period of up to 5 months in this species.

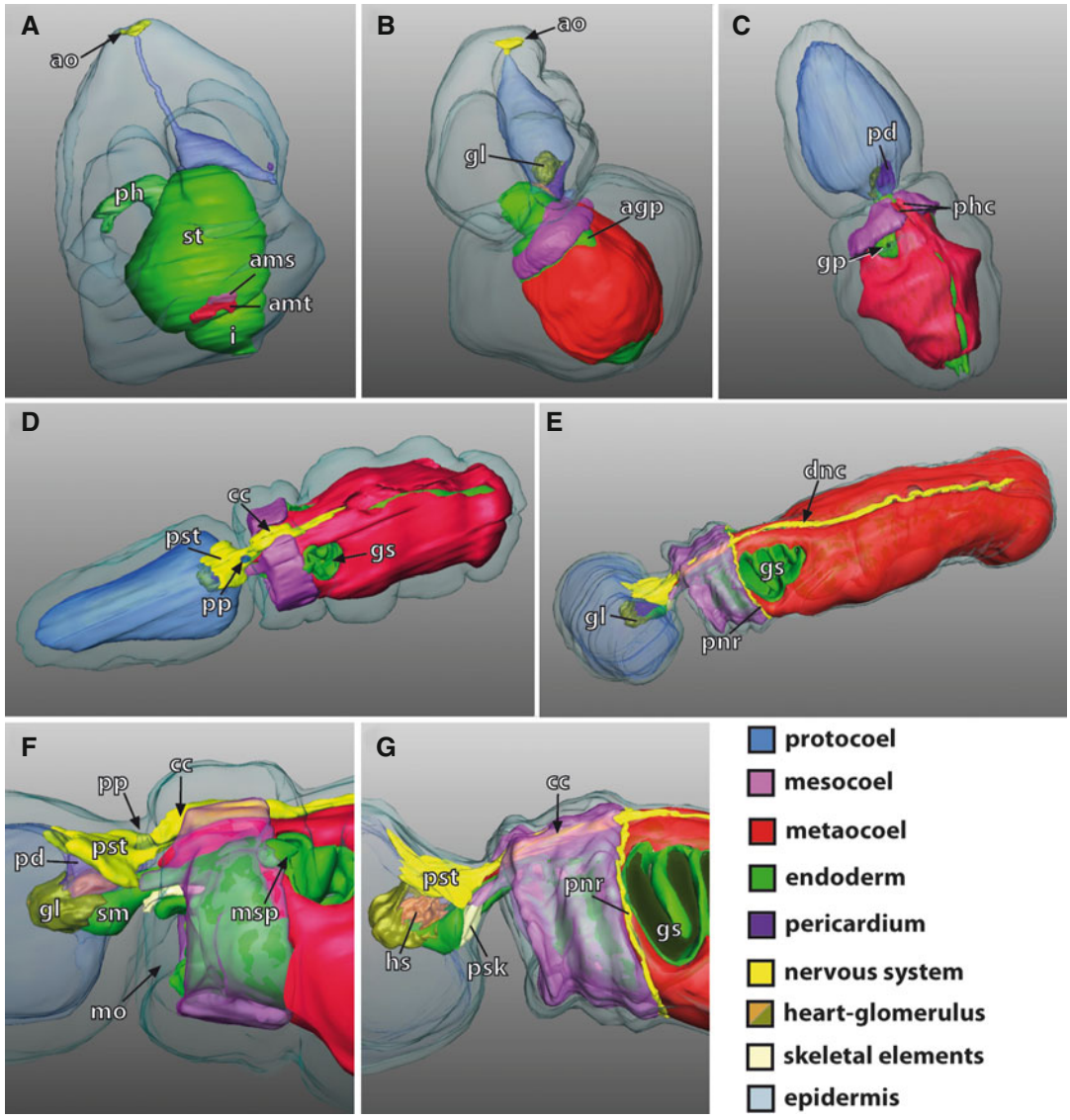

Fig. 2.9 3D reconstructions of major organ systems in different developmental stages of *Balanoglossus misakiensis* revealed from complete serial semithin sections. Opisthotroch and ciliary bands are omitted. Anterior to the top in (**A**–**C**) and to the left in (**D**–**G**). (**A**) Overview of the inner anatomy of a typical tornaria at the Metschnikoff stage. (**B**) Spengel stage. All coelomic cavities have enlarged considerably. The digestive tract is pulled backwards. Anlagen of the first gill pores are visible. (**C**) Agassiz stage with first pair of gill pores opened. (**D**) Early settled juvenile. The gill slit is U-shaped, because of a dorsal tongue bar. The central nervous system forms at this stage. (**E**) Two-gill-slit juvenile (3 days post settlement). (**F**) Close-up of D showing the inner organisation of the proboscis, collar and anterior trunk region in detail. (**G**) Close-up of E showing the inner organisation of the proboscis, collar and anterior trunk region in detail. *agp* anlage of the gill pore, *ams* anlage of the mesocoel, *amt* anlage of the metacoel, *ao* apical organ, *cc* collar cord, *dnc* dorsal nerve cord, *gl* glomerulus, *gp* gill pore, *gs* gill slit, *hs* heart sinus, *i* intestine, *mo* mouth opening, *msp* mesocoelic pore, *pd* pericardium, *ph* pharynx, *phc* perihaemal cavity, *pnr* peribranchial nerve ring, *pp* proboscis pore, *psk* proboscis skeleton, *pst* proboscis stem, *sm* stomochord, *st* stomach

All the preceding larval stages (Müller, Heider, Metschnikoff, Krohn) comprise the so-called progressive larval development where the larvae increase in size. The following Spengel stage marks the beginning of the regressive larval development and is characterised by a decrease in size of the larva and remodelling of the preoral part by fusion of the ciliary bands of the neotroch (Stiasny 1914b; Agassiz 1873; Nielsen and Hay-Schmidt 2007). As a result, the future proboscis gets a more and more smooth surface and the position of the neotroch is indicated by grooves. At the same time, a number of internal modifications occur. The protocoel enlarges significantly and begins to fill up the preoral part of the larva, thereby subsequently reducing the blastocoel (Fig. 2.9B). The proboscis vesicle has increased in size and is now situated dorsally onto the developing stomochord. The mouth opening and pharynx have shifted backwards and the anlagen of the gill pores are visible as paired, lateral evaginations from the posterior pharyngeal region (Fig. 2.9B). The meso- and metacoels have extended anteriorly as well as medially and surround the digestive tract almost completely. The Spengel stage in *Balanoglossus misakiensis* lasts only for a couple of hours and marks the transition from the fully grown tornaria into the competent Agassiz stage. The Agassiz stage is the last stage before the animals settle and grow into a juvenile acorn worm. This stage is characterised by the complete absence of the neotroch and potential tentacles. The larvae of *B. misakiensis* are of elongated shape and the future three body regions can be distinguished (Figs. 2.7F and 2.9C). The anterior proboscis region is conical and separated from the posterior part by a deep constriction where the mouth opens into on the ventral side. The collar region is short and subdivided from the posterior trunk region by a shallow circular depression. The former planar perianal field is now highly convex as it has started to grow out posteriorly. The opisthotroch is still well developed and continues to propel the larva through the water. The protocoel has completely extended and opens to the exterior through the proboscis pore on the left side of the dorsal base of the proboscis (Fig. 2.9C). The glomerulus spans the anterior tip of the protruding stomochord and is posterodorsally adjoined by the pericardium. In *B. misakiensis*, one pair of dorsolateral gill pores is present at this stage at the anterior margin of the trunk region (Fig. 2.9C). Time and number of formation of gill pores is species specific, since reports from other enteropneust species show competent Agassiz larvae with several pairs of gill pore anlagen (Agassiz 1873; Morgan 1894). The meso- and metacoels progressively reduce the blastocoel to the dorsal and ventral midline by which the haemal system is formed. The paired metacoel sends anterodorsal projections into the base of the proboscis, that is, the perihaemal cavities. Larvae at the Agassiz stage usually stop swimming in the upper water column and instead begin to visit the bottom more frequently. The pair of apical eye spots degenerates at this stage and the larvae are now competent for settlement. After settlement, the larva grows into a young juvenile worm mainly by elongation of the trunk region. In settled juveniles of *B. misakiensis* approximately 12 h post fertilisation, the opisthotroch is still present in the middle of the trunk region in the majority of specimens (Fig. 2.7G). The overall morphology shows only minor changes compared to the competent Agassiz stage which concern the collar region, shape of the gill pores and the coelomic cavities. The collar region is subdivided into an anterior and a posterior part by a circular constriction. A dorsal tongue bar grows ventrally and gives the gill slit its final U shape. Moreover, paired mesocoel ducts open into the first gill slit on both sides and connect the mesocoel to the exterior (Fig. 2.9F). Within the posterior part of the protocoel, the stomochord-heart-glomerulus complex is almost completely developed. The coelomic system gets more and more intricate as the animals grow and aside from the perihaemal cavities, that are extensions from the trunk coelom (metacoel), the collar coelom (mesocoel) also sends bilateral projections anteriorly into the base of the proboscis, thereby flanking the stomochord (Fig. 2.9G). At ~3 days post settlement, the juvenile worms of *B. misakiensis* have completely lost the opisthotroch (Fig. 2.7H). The proboscis is short and conical and the collar region

exhibits a three-lobed shape (Figs. 2.7H and 2.9E, G). The proboscis skeleton is present and supports the fragile neck region by underlying the stomochord (Fig. 2.9G).

Approximately 1 week after settlement, formation of a premature juvenile featuring a distinct hepatic region and three pairs of gill slits is completed in *Balanoglossus misakiensis* (Urata and Yamaguchi 2004).

Neurogenesis in Indirect Developing Enteropneusts

In particular, the broad usage of antibody stainings to visualise specific parts of the nervous system has contributed significantly to our knowledge of neurogenesis in indirect developing enteropneusts. Several papers are available that describe the nervous system in single tornaria stages, yet only two detailed studies documenting a complete developmental series have been published so far (Nielsen and Hay-Schmidt 2007; Miyamoto et al. 2010). In particular, the exact mode of neural remodelling from metamorphosis through juvenile stages is still unclear.

The nervous system in tornaria larvae develops gradually from anterior to posterior. In early hatched larvae, the nervous system comprises a small apical organ of few synaptotagmin-like immunoreactive (LIR) as well as serotonin-LIR cells with neurites projecting posteriorly (Fig. 2.10A, B) (Nielsen and Hay-Schmidt 2007; Miyamoto et al. 2010). As the neotroch develops neurite bundles, neurons form along the ciliary band. In addition, the pan-neuronal marker synaptotagmin reveals a nerve net throughout the oral field of the larvae (Miyamoto et al. 2010). In older larvae, the apical organ usually consists of numerous serotonin- as well as FMRFamide-LIR neurons and a pair of eye spots situated laterally within the apical organ (Fig. 2.10C, D) (Nezlin and Yushin 2004). The exact ultrastructure of the eyes has not been investigated in detail. The scarce data available describe a mixed photoreceptor cell with a rhabdomere as well as a modified cilium (Brandenburger et al. 1973). If true, tornaria larvae would feature a photoreceptor cell type that is unique in the animal kingdom, i.e., a combined rhabdomeric and ciliary photoreceptor. However, further studies including serial sections for TEM and characterisation of the molecular signature of the eyes in tornaria larvae are necessary in order to substantiate or reject this postulation. For instance, the composition of the sea urchin eye was also discovered only recently (Ullrich-Lüter et al. 2011) and revealed a solely rhabdomeric photoreceptor.

In older tornaria larvae, serotonin-LIR as well as FMRFamide-LIR neurons of the apical organ are arranged in two clusters of cells, one situated in the preoral part of the neotroch and the other in the postoral part of the neotroch (Fig. 2.10C, D). Both clusters of neurons are interconnected by a comprehensive central neuropil (Nezlin and Yushin 2004). The opisthotroch nerve ring contains synaptotagmin and tyrosine hydroxylase in early stages and later also serotonin (Nielsen and Hay-Schmidt 2007; Miyamoto et al. 2010). The neural arrangement in the tornaria shows strong congruence to that in echinoderm larvae, further supporting the assumption that both larval types are homologous and evolved from a common ambulacrarian ancestor (Byrne et al. 2007). At the time of metamorphosis when tornariae reach the Agassiz stage, the larval nervous system degrades and the adult nervous system starts to develop (Miyamoto et al. 2010). It could be shown that the majority of nervous cells of the ciliary band degrade and contribute little to the adult nervous system. During settlement, a basiepidermal nerve net within the proboscis and collar region becomes apparent and the nerve cords develop along the ventral and dorsal midline of the trunk region. The collar cord within the collar region neurulates in a similar way as in *Saccoglossus kowalevskii* (Fig. 2.8) and eventually becomes situated subepidermally (Morgan 1894; Miyamoto and Wada 2013). From approx. 3 days post settlement in *Balanoglossus misakiensis*, all main parts of the centralised nervous system are present (Fig. 2.9E, F), that is, anterior proboscis stem, neurulated collar cord, circumferential peribranchial nerve ring and a dorsal as well as a ventral longitudinal nerve cord within the trunk region. Unfortunately, almost nothing is known about the formation and distribution of specific neurotransmitters such as serotonin or

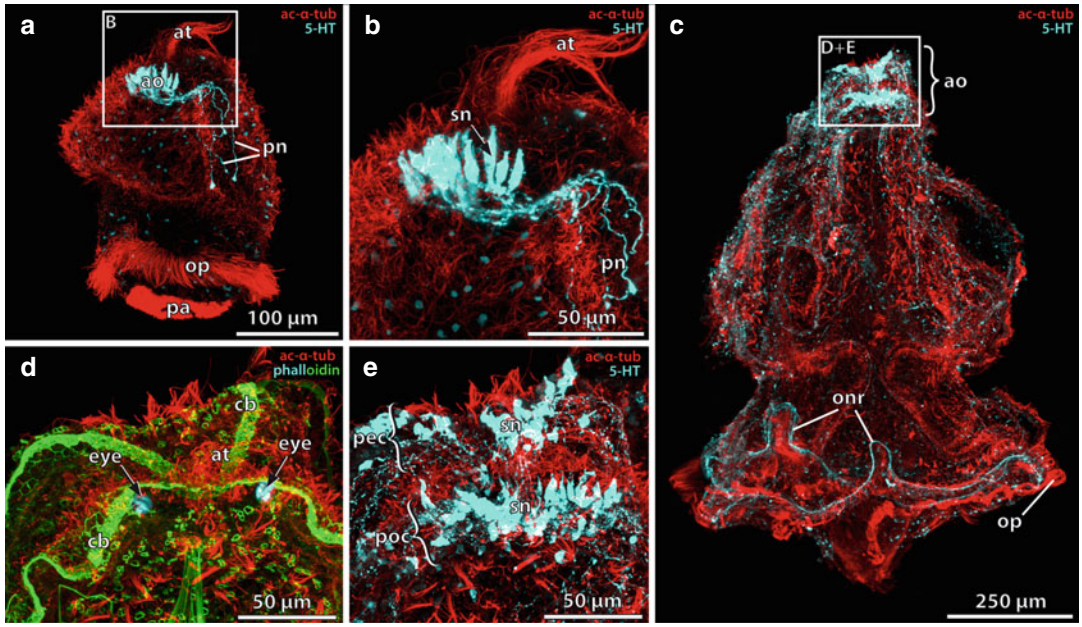

Fig. 2.10 Antibody stainings of the developing nervous system in *Balanoglossus misakiensis*. (**A**) Early tornaria (Heider stage). (**B**) Same stage as in (**A**). The apical organ consists of about 18 serotonin-LIR (5-HT) sensory cells. (**C**) Fully grown tornaria (late Metschnikoff). Dorsal view. (**D**) Close-up of the apical region of fully grown tornaria showing the lateral pair of eye spots and the course of the ciliary bands. (**E**) Same region as in (**D**). The apical organ consists of numerous sensory cells (5-HT), subdivided into a ventral and a dorsal cluster. *ao* apical organ, *at* apical tuft, *cb* ciliary band, *eye* eye spot, *onr* opisthotroch nerve ring, *op* opisthotroch, *pa* perianal field, *pec* preoral cluster, *poc* postoral cluster, *pn* posteriorly neurites, *sn* sensory cell

FMRFamide in juvenile enteropneusts. One sole immunocytochemical study has been published on the nervous system of the miniaturised species *Meioglossus psammophilus* (Worsaae et al. 2012). The adult nervous system of *M. psammophilus* comprises several serotonergic sensory neurons within the anterior and middle part of the proboscis. A basiepidermal nerve net extends throughout the proboscis and is most prominent at the dorsal base (proboscis stem). Posterior to the proboscis stem, individual serotonergic neurites pass through the collar cord. A circumferential ring of serotonergic neurons is present in the collar region. These sensory neurons project with a single neurite at first posteriorly, until the end of the collar region, and then ventrally into a median nerve cord. Serotonin-LIR reveals a comparably short ventral nerve cord that bifurcates at the level of the midgut into a pair of ventrolateral neurite bundles that further extend posteriorly until the end of the trunk region. Individual serotonergic neurons are scattered throughout the trunk epidermis and project into one of the two ventral nerve cords.

Taken together, the few available data on neurogenesis of the adult nervous system in enteropneusts make it considerably difficult to compare it to other deuterostomes and accordingly render testing of homology hypotheses difficult.

Comparative Aspects of Hemichordate Development

Hemichordates and particularly enteropneusts seem to have retained a number of ancestral deuterostome traits, such as radial cleavage, enterocoely and bilateral symmetry. Early development including cleavage and cell fates is highly conserved among hemichordates (Colwin and Colwin 1951, 1953; Tagawa et al. 1998a). The radial, equal and holoblastic cleavage leads to a

coeloblastula that subsequently undergoes gastrulation. Hemichordates share this cleavage pattern with echinoderms (Henry et al. 2001; McClay 2011; Chapter 1) and, depending on the yolk content, also with chordates (Bertrand and Escriva 2011; Lemaire 2011; Chapters 3 and 4). Radial cleavage is a plesiomorphic feature for Ambulacraria and Chordata and was most likely inherited from an early ancestor (Ax 2001; Nielsen 2011).

The five main coelomic cavities (single protocoel, paired meso- and metacoels) in hemichordates originate from the endoderm by enterocoely. While the protocoel derives from the anterior end of the archenteron in all species studied, the formation of the meso- and metacoels varies considerably. For instance, the meso- and metacoels in *Saccoglossus kowalevskii* and *Glandiceps hacksi* (Urata et al. 2014) develop from separate evaginations of the middle and posterior endodermal region (Bateson 1884; Kaul-Strehlow and Stach 2013), whereas in *Balanoglossus clavigerus* and *B. misakiensis*, they emerge from a single pair of evaginations that eventually subdivide into the more anterior mesocoels and posterior metacoels (Stiasny 1914b; Spengel 1893; Urata and Yamaguchi 2004). A closer look at other enteropneust species and echinoderms reveals enormous intraphyletic variation of coelom formation (for review, see Nielsen 2011). Although an ancestral deuterostome pattern may be hard to reconstruct, it seems that at least in all cases, the mesoderm is formed from the endoderm. Moreover, in echinoderms as well as hemichordates, the mesoderm forms as three successive pairs of coelomic cavities (proto-, meso- and metacoels) (Chapter 1). During the development of the cephalochordate amphioxus, the larva passes a similar tricoelomate stage, before additional coelomic pouches are added (Stach 2002) (Chapter 3). The fact that three pairs of coelomic cavities are present in members of all main deuterostome groups, at least at a certain developmental stage, leads to the conclusion that this is an ancestral condition for deuterostomes. As mentioned before, the development of the protocoel seems to be rather conserved among ambulacrarians in being always the first coelomic cavity that pinches off very early from the anterior end of the endoderm. In this aspect, the precocious hydropore formation documented in some holothurians and the spengelid enteropneust *G. hacksi* (Urata et al. 2014) is very interesting. The mode of development is so strikingly similar that an independent evolution can hardly be assumed. It shows that irrespective of the derived phylogenetic position of holothurians within Echinodermata, they nevertheless may have retained more ancestral traits than previously thought. It should be repeated here that it was already Eschscholtz (1825) who compared and related the first described enteropneust *Ptychodera flava* to holothurians.

The sixth coelomic cavity, the pericardium, is part of the heart-glomerulus complex and thus indirectly involved in excretory function. Homology of this heart-glomerulus complex of hemichordates with the axial complex of echinoderms is widely accepted, because of a number of functional and structural similarities (Balser and Ruppert 1990; Mayer and Bartolomaeus 2003; Kaul-Strehlow and Stach 2011; Nielsen 2011; Merker et al. 2013). These include a contractile pericardium (pulsatile vesicle in echinoderms), filtrating podocytes on the protocoelic (axocoelic) side, an excretory hydropore and a glomerulus. However, despite the unquestioned homology of the differentiated structures, the ontogenetic origin shows considerable variations between enteropneust species as well as echinoderm species. For instance, the pericardium in *Saccoglossus kowalevskii* develops from the ectoderm by schizocoely (Kaul-Strehlow and Stach 2011), a mode of development that is usually associated with protostomes (Technau and Scholz 2003). On the other hand, a mesenchymatic (Morgan 1891; Rao 1953) and further enterocoelic origin (Dawydoff 1907) of the pericardium has been reported from other enteropneust species. The same holds true for echinoderms (for review, see Hyman 1955) and demonstrates that homologous structures indeed may have different ontogenetic origins. However, a general or even ancestral mode of pericardial formation for Ambulacraria is thus hard to infer. The situation is even more complicated by the fact that corresponding counterparts of the nephridial com-

plex of ambulacrarians may be present in chordates. In particular, homology of the pericardium with Hatschek's left diverticulum or Hatschek's pit in cephalochordates (Goodrich 1917; Franz 1927; Nielsen 2011) or with Hatschek's nephridium in cephalochordates (Stach 2002) has been suggested earlier. In any case, if homologous structures are present in chordates, then the nephridial complex of Ambulacraria may represent a plesiomorphic character within deuterostomes rather than constituting a synapomorphy of Echinodermata and Hemichordata.

The nervous system of the tornaria larva consists of an apical organ comprising different types of neurons and nerves along the ciliary bands (Hay-Schmidt 2000; Nezlin and Yushin 2004; Miyamoto et al. 2010). Serotonin-LIR cells in the apical organ are arranged in bilateral clusters interconnected by a median neuropil (Nezlin and Yushin 2004). During ontogeny, the nervous system develops gradually from anterior to posterior, and at metamorphosis, the larval nervous system degrades and the adult nervous system is formed (Miyamoto et al. 2010). The nervous system of the different echinoderm larvae develops likewise and features in principle the same components. Of course, taxon-specific traits are present, but the general neural body plan of an apical organ with sensory cells resting in the apical ciliary band and nerves along the neotroch is present (Hay-Schmidt 2000; Burke et al. 2006; Byrne et al. 2007). As in hemichordate tornariae, the echinoderm larval nervous system contributes little if anything to the pentameral nervous system of the juveniles (Byrne and Cisternas 2002; Cisternas and Byrne 2003; Nakano et al. 2006). Because of numerous resemblances between the morphology of hemichordate tornariae and echinoderm larvae, they have been grouped together under the term dipleurula-type larvae (Metschnikoff 1881). However, since the sister group of Ambulacraria, that is, Chordata, do not have primary larvae, it remains uncertain if a dipleurula larva was already present in the last common ancestor of Deuterostomia. Thus, the dipleurula larva with its specific neotroch is likely to be a synapomorphy uniting Hemichordata and Echinodermata (Nielsen 2011).

GENE EXPRESSION

The pivotal phylogenetic position of hemichordates, the shared fate map during ambulacrarian embryonic development (Colwin and Colwin 1951; Cameron et al. 1987, 1989; Cameron and Davidson 1991; Henry et al. 2001) and the above-mentioned classical and modern morphological descriptions have suggested homologies between various hemichordate, echinoderm and chordate features. Hence, hemichordates are particularly appealing to investigate the evolution of deuterostome developmental mechanisms, and in the past decades, the growing community working on hemichordates has developed a basic toolset to gain insight into the molecular mechanisms that drive embryonic development, the patterning of the larval and adult body plan as well as the molecular signature of particular structures, i.e., gill slits (Rychel and Swalla 2007; Gonzalez and Cameron 2009; Gillis et al. 2011).

As for most "non-model" organisms, classical degenerative PCR approaches (Tagawa et al. 1998b) or, more recently, the analysis of transcriptomic data sets were used to identify genes and characterise their expression in hemichordates (Lowe et al. 2003; Röttinger and Martindale 2011; Chen et al. 2014). Lately, the genomes of *Ptychodera flava* and *Saccoglossus kowalevskii* have been sequenced and used for genome comparisons between these two species (Freeman et al. 2012). This will provide an important resource to identify the genetic toolkit and regulatory elements of acorn worms. Protocols have been developed and optimised for whole mount or section in situ hybridisation or immunocytochemistry and are now routinely applied on several hemichordate species (Tagawa et al. 1998b; Okai et al. 2000; Lowe et al. 2003; Smith et al. 2003; Sato et al. 2009; Miyamoto et al. 2010; Miyamoto and Wada 2013). In order to determine relative spatial gene expression for a set of genes, double fluorescent in situ hybridisation has been developed in *S. kowalevskii* (Pani et al. 2012).

During the reproductive season, controlled spawning and fertilisation produce large numbers of synchronously developing embryos and larvae

that are amenable for pharmacological drug or recombinant protein treatments to analyse the effects of perturbing signalling pathways on the developmental process (Lowe et al. 2006; Darras et al. 2011; Röttinger and Martindale 2011; Pani et al. 2012; Green et al. 2013). However, specific gene knockdown experiments using siRNA and mRNA that are microinjected into fertilised oocytes have so far been reported only from *Saccoglossus kowalevskii* (Lowe et al. 2006; Darras et al. 2011; Pani et al. 2012; Cunningham and Casey 2014; Green et al. 2013). *S. kowalevskii* appears also to be the most suitable acorn worm species for classical embryological experiments (Colwin and Colwin 1950) that have recently inspired researchers to combine blastomere isolation and grafting experiments with molecular analysis to investigate the inductive capacities of individual blastomeres or animal-vegetal explants (Darras et al. 2011; Green et al. 2013).

Endomesoderm Formation and the Posterior Organiser

In metazoans, canonical ß-catenin/Wnt (cWnt) signalling plays crucial roles during various aspects of embryonic development such as embryonic polarity, germ layer specification, posterior growth and anterior-posterior axis patterning (Croce and McClay 2006; Lee et al. 2006; Martin and Kimelman 2009; Cho et al. 2010; Niehrs 2010). A recent study in *Saccoglossus kowalevskii* has dissected the role of cWnt signalling during enteropneust development (Darras et al. 2011). Combining classical embryology, gene-specific knockdown experiments and gene expression analysis, the authors showed that ß-catenin is accumulated at the vegetal pole, the future site of gastrulation, which is required for endomesoderm specification. In addition, the endomesoderm secretes yet undefined signals that determine the posterior fate of the adjacent ectoderm, as the ectoderm will adopt default anterior fates when the endomesoderm is removed (Darras et al. 2011). This mechanism is very similar to the one observed in echinoderms (Angerer et al. 2011) and vertebrates (Niehrs 2010), suggesting a conserved function of cWnt signalling at the base of deuterostomes in germ layer specification and the formation of a posterior organiser (Darras et al. 2011).

In hemichordates, mesoderm forms by enterocoely (Bateson 1884), a process that is shared with echinoderms and basal chordates such as amphioxus and ascidians. The FGF signalling pathway plays a crucial role in mesoderm induction in vertebrates and basal chordates (Slack et al. 1989; Kim et al. 2000; Imai et al. 2002; Fletcher et al. 2006; Kimelman 2006; Bertrand et al. 2011; Chapters 3 and 4). In order to investigate the evolution of mesoderm formation, a recent study has examined the role of FGF signalling during mesoderm formation in *Saccoglossus kowalevskii* (Green et al. 2013). Expression of the FGF ligand *fgf8/17/18* is restricted to ectodermal regions overlying sites of mesoderm specification within the archenteron, while the regions that will form mesoderm express the receptor *fgfr-B*. The resulting suggestion that mesoderm induction in the archenteron requires contact with the ectoderm to allow FGF/FGFR signalling is confirmed by embryological experiments that are combined with gene expression analysis of the downstream target *snail*. Gene-specific knockdown and gain-of-function experiments show that FGF8/17/18 is required and sufficient for mesoderm induction in *S. kowalevskii* and support the idea that FGF signalling played an ancestral role in deuterostome mesoderm formation (Green et al. 2013).

Dorsoventral Patterning

BMP, a ligand of the TGFß family, and its antagonist Chordin play a central role in establishing the dorsoventral axis and the specification of the central nervous system (CNS) in bilaterian animals (Arendt and Nübler-Jung 1996; De Robertis and Sasai 1996; Holley and Ferguson 1997; De Robertis et al. 2000; De Robertis and Kuroda 2004). Gene expression analysis in *Saccoglossus kowalevskii* and *Ptychodera flava* has shown expression of *bmp2/4* and its potential downstream target *dlx* in dorsal territories (Fig. 2.11D,

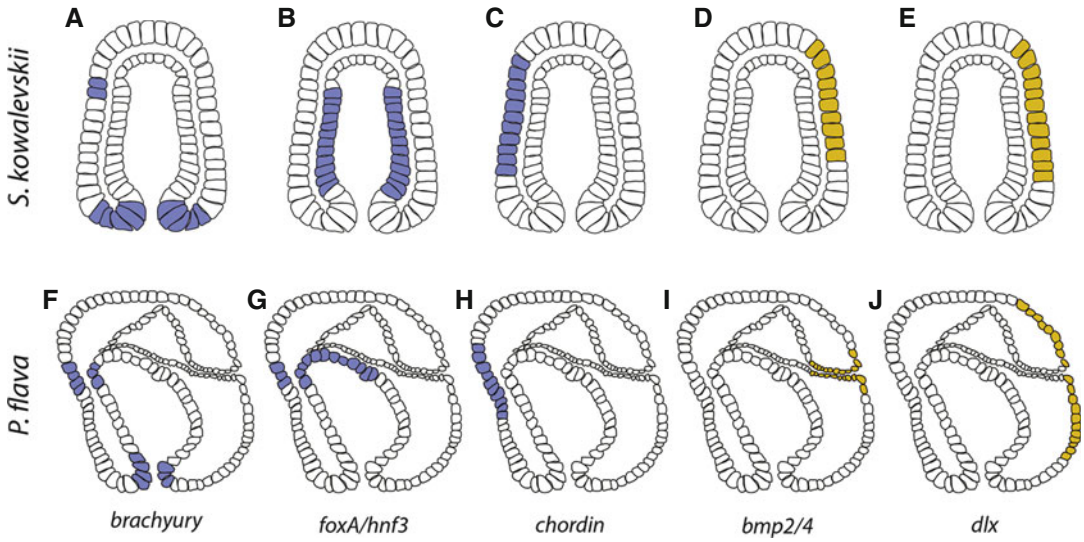

Fig. 2.11 Comparison of dorsoventral gene expression patterns in hemichordates. Illustrations of ventral (*purple*) and dorsal (*yellow*) gene expression patterns in late gastrulae of *Saccoglossus kowalevskii* (**A**–**E**) and *Ptychodera flava* (**F**–**J**). All illustrations are based on published data: **A**, **B and E**, Lowe et al. (2006); **C**, Röttinger and Lowe (2012); **D**, Darras et al. (2011); and **F**–**J,** Röttinger and Martindale (2011)

E, I, J), while *chordin* transcripts (Fig. 2.11C, H) are localised in the ventral ectoderm, suggesting that these proteins are also involved in dorsoventral patterning in hemichordates (Harada et al. 2001, 2002; Lowe et al. 2006; Röttinger and Martindale 2011). Functional studies in *S. kowalevskii* demonstrate the implication of BMP signalling in this process, as overexpression and knockdown of BMP2/4 result in dorsalised or ventralised embryos, respectively (Lowe et al. 2006). Based on functional studies in other bilaterian animals, the prediction would be that overactivating BMP signalling represses neural fates (De Robertis and Kuroda 2004). However, this is not the case in *S. kowalevskii* embryos treated with recombinant BMP4 protein, suggesting that BMP signalling in hemichordates is involved in dorsoventral patterning but not in neurogenesis (Lowe et al. 2006).

The molecular mechanisms underlying dorsoventral patterning have been extensively studied in echinoderms (Angerer et al. 2000; Duboc et al. 2004; Su and Davidson 2009; Saudemont et al. 2010) and are represented in a simplified version in Fig. 2.12A (for a more comprehensive version, see Chapter 1). To date, the only functional molecular studies that have been performed in harrimaniid (*Saccoglossus kowalevskii*) and also in ptychoderid (*Ptychodera flava*) enteropneusts aim to describe the dorsoventral patterning event in hemichordates (Lowe et al. 2006; Röttinger and Martindale 2011). This enables comparing the molecular mechanism controlling dorsoventral patterning within ambulacrarians (Fig. 2.12).

While *bmp2/4* expression in enteropneusts is restricted to dorsal structures (Fig. 2.11D, I; Harada et al. 2002; Lowe et al. 2006; Röttinger and Martindale 2011), *bmp2/4* expression in echinoderms is localised on the opposite site in the ventral ectoderm (Angerer et al. 2000; Duboc et al. 2004). Interestingly, functional studies in *Saccoglossus kowalevskii* and echinoderms have shown that regardless the expression domain of the diffusible ligand *bmp2/4*, its activity is always confined to the dorsal ectoderm (Duboc et al. 2004; Lowe et al. 2006). In *S. kowalevskii* and *Paracentrotus lividus* (echinoderm), *dlx* is an indirect downstream target of BMP signalling (Lowe et al. 2006; Saudemont et al. 2010). In *Ptychodera flava*, *dlx* transcripts are detected in the dorsal ectoderm (Harada et al. 2001; Röttinger and Martindale

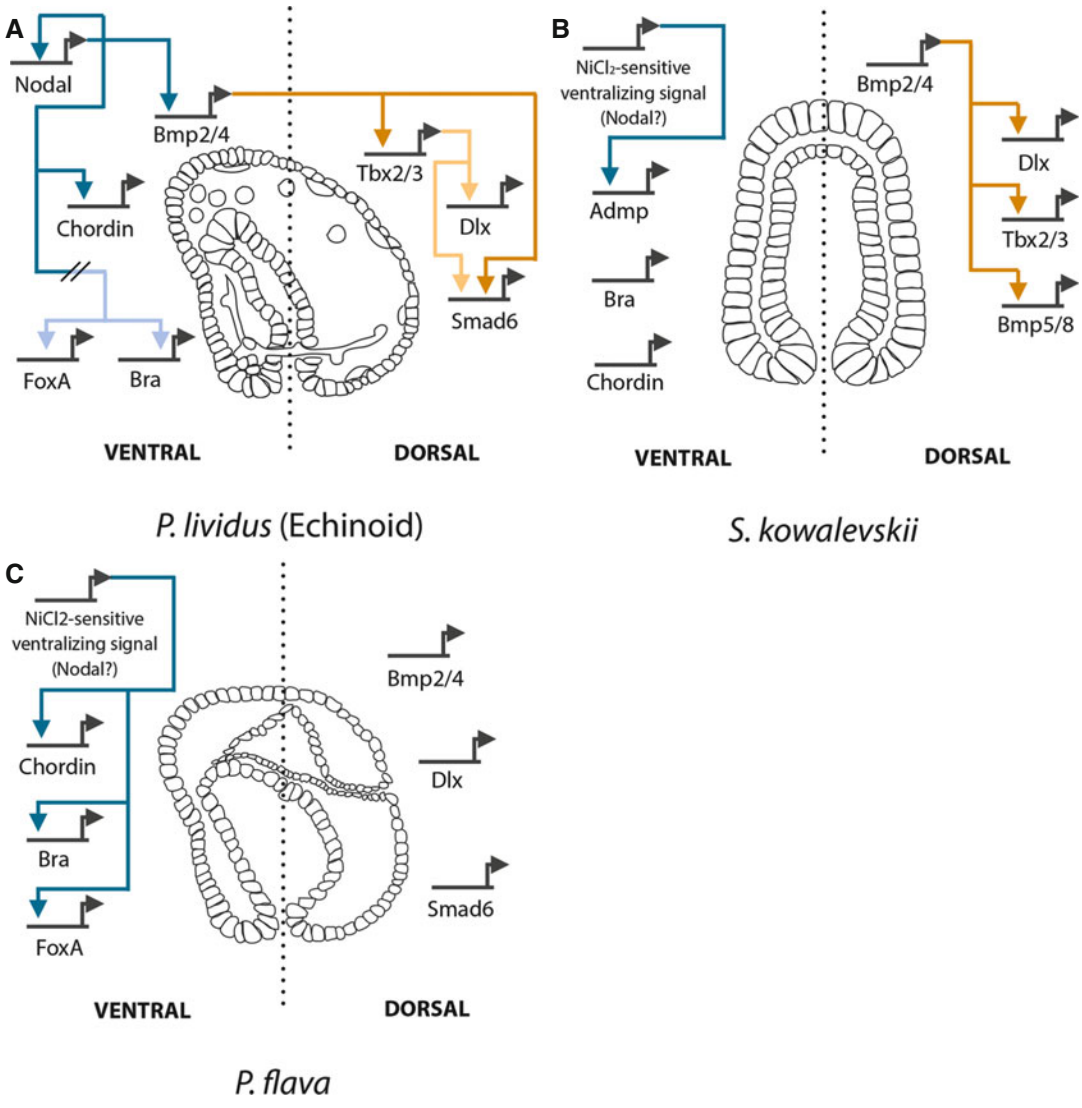

Fig. 2.12 Comparison of dorsoventral patterning mechanisms in ambulacrarians. In echinoderms (**A**), Nodal signalling is essential to determine ventral fates and induce expression of *bmp2/4* that acts on the dorsal side to specify dorsal ectoderm. In *Saccoglossus kowalevskii* (**B**), BMP signalling is crucial for specifying the dorsal ectoderm as well, which might potentially also be the case for *Ptychodera flava* (**C**). While a $NiCl_2$-sensitive signal is involved in specifying ventral fates in enteropneusts (**B**, **C**), the relation to Nodal signalling remains unknown. (**A**) *Paracentrotus lividus* (echinoderm), simplified diagram based on data from Saudemont et al. (2010). (**B**) *Saccoglossus kowalevskii* (harrimanid enteropneust), diagram based on data from Lowe et al. (2006), Saudemont et al. (2010) and Röttinger and Martindale (2011). (**C**) *Ptychodera flava* (ptychoderid enteropneust), diagram based on data from Tagawa et al. (1998b), Taguchi et al. (2000), Harada et al. (2001, 2002) and Röttinger and Martindale (2011)

2011), suggesting that BMP signalling is active in this territory as well. However, additional experiments are required to confirm this hypothesis.

The Nodal signalling pathway plays crucial roles in various deuterostome developmental processes such as endo- and mesoderm formation and axial patterning events along the anterior-posterior, dorsoventral and left-right axis (Whitman 2001; Hamada et al. 2002; Morokuma et al. 2002; Stainier 2002; Yu et al.

2002; Chapters 1, 3, and 4). In echinoderms, Nodal signalling is not only crucial for establishing left-right asymmetries in the larva (Duboc et al. 2005) but plays also an essential role in the establishment of the dorsoventral axis during embryonic development (Duboc et al. 2004). In fact, *nodal* expression in the ventral ectoderm induces ventral expression of *bmp2/4* which in turn diffuses to the dorsal ectoderm to induce expression of its downstream targets (Fig. 2.12A; Duboc et al. 2004; Lapraz et al. 2009; Su and Davidson 2009; Saudemont et al. 2010). Among the downstream targets of Nodal signalling in echinoderms are the ventrally expressed genes *chordin*, *foxA* and *bra* (Saudemont et al. 2010; Chapter 1). With the exception of the strictly endodermal expression of *foxA* in *Saccoglossus kowalevskii* (Darras et al. 2011; Fritzenwanker et al. 2014), *bra* and *chordin* transcripts are also detected in ventral domains in *S. kowalevskii* and *Ptychodera flava* (Fig. 2.11; Tagawa et al. 1998b; Röttinger and Lowe 2012), suggesting that a Nodal-dependent mechanism may be required to define ventral domains in hemichordates.

$NiCl_2$ treatments in echinoderms ventralise the embryos and induce radialised expression of *nodal* (Duboc et al. 2004). Interestingly, $NiCl_2$ treatments in *Saccoglossus kowalevskii* and *Ptychodera flava* also ventralise the embryos and radialise expression of *bra* and *foxA* in *P. flava* (Röttinger and Martindale 2011), further strengthening the idea that a $NiCl_2$-sensitive and potentially Nodal-dependent mechanism is involved in dorsoventral patterning in hemichordates. However, the potential molecular link between $NiCl_2$ and Nodal and the molecular connection between the ventralising $NiCl_2$-sensitive signal and dorsalising BMP effects in hemichordates remain unclear, and additional work is required to understand the degree of conservation to the mechanism of dorsoventral patterning in echinoderms.

Anterior-Posterior Patterning

The bulk of molecular studies in hemichordates have been carried out in the direct developing species *Saccoglossus kowalevskii*, the indirect developer *Ptychodera flava* and, more recently, in another ptychoderid hemichordate species, *Balanoglossus simodensis*. The recent sequencing and comparison of the *S. kowalevskii* and *P. flava* genomes has revealed the identical genomic organisation of their 12-gene Hox clusters (Freeman et al. 2012), which is reminiscent of the Hox cluster organisation of *B. simodensis* (Ikuta et al. 2009). With the exception of differences at the posterior end of these clusters, the hemichordate organisation is strikingly similar to that of chordates, supporting the idea that the ambulacrarian ancestor possessed minimally a 12-gene Hox cluster with at least nine genes organised and oriented the same as their chordate orthologs (Freeman et al. 2012).

In vertebrates, expression of Hox genes as well as other transcription factors such as *barH*, *engrailed*, *pax2/5/8*, *six3*, etc., is restricted to the central nervous system (CNS). To gain insight into the origin of the chordate CNS, previous studies in *Saccoglossus kowalevskii* have analysed the expression patterns of these genes and showed their circumferential epidermal expression during early development that potentially reflects the broad and diffuse distribution of neurons in these stages (Lowe et al. 2003; Aronowicz and Lowe 2006; Lemons et al. 2010; Pani et al. 2012). In adult tissue, however, gene expression analysis of neuronal markers such as *Elav*, *synaptotagmin*, *VAChT*, *serotonin*, *Hb9*, *Drg11* and *GABA* has shown the existence of a centralised ventral as well as dorsal nerve cord that is internalised at the level of the enteropneust worm's collar into the collar cord (Nomaksteinsky et al. 2009). Intriguingly, the observed centralisation of the enteropneust nervous system was in contrast to previous studies that described the presence of a diffuse nerve net in hemichordates (Lowe et al. 2003). One idea to explain these fundamental differences was that the developing ectoderm may represent a transient diffuse nerve net unrelated to that of the adult (Nomaksteinsky et al. 2009). In order to gain a better understanding of the relation between the embryonic and adult nervous systems, a recent study has analysed a broad range of genes associated with neurogenesis during early *S. kowalevskii* development (Cunningham and Casey 2014).

This analysis has revealed that already during embryonic development, expression of most of the analysed genes transitions from a circumferential to a dorsal and ventral midline localisation. Hence, this observation suggests that developmental centralisation of the nervous system in hemichordates occurs earlier than initially anticipated (prior to hatching) (Cunningham and Casey 2014).

Perturbation of BMP signalling in *Saccoglossus kowalevskii* affects dorsoventral patterning but not the distribution of neurons in the analysed embryos (Lowe et al. 2006). This observation has led to the idea that nervous system formation in hemichordates may be insensitive to a BMP/Chordin gradient that is crucial for the formation of the CNS in protostomes and vertebrates. However, this analysis was carried out on embryos that presented a diffuse expression pattern of neuronal markers (Lowe et al. 2006). With the recent observations of a ventral and dorsal CNS in hemichordates (Nomaksteinsky et al. 2009; Cunningham and Casey 2014), it would be crucial to re-analyse the effects of perturbing BMP signalling on the centralisation of the nervous system at adequate embryonic stages.

Taken together, the studies described above do not contradict the classical idea that portions of the hemichordate central nervous system may be homologous to the chordate CNS (Knight-Jones 1952; Lowe et al. 2003; Nomaksteinsky et al. 2009). However, the current data make it impossible to unequivocally settle this issue at present (Holland et al. 2013).

The tubular organisation of the collar cord of enteropneusts has been proposed to be homologous to the chordate neural tube (Morgan 1894; Bateson 1886; Ruppert 2005; Kaul and Stach 2010; Luttrell et al. 2012). However, gene expression data of *bmp* and *chordin* (see above) support the theory of dorsoventral inversion of body axes at the base of chordates (Lowe et al. 2006). According to this, the chordate neural tube would be homologous to the ventral nerve cord of enteropneusts, yet it is the dorsal collar cord that neurulates in enteropneusts. Moreover, genes such as *pax6*, *nkx 2.2* and *msx* that have similar domains in the chordate neural tube and the protostome nerve cord (Denes et al. 2007) do not at all have resembling domains in *Saccoglossus kowalevskii* (Lowe et al. 2006). Hence, because of the lack of clear molecular data, its homology remains controversial (Ruppert 2005; Nomaksteinsky et al. 2009; Kaul and Stach 2010; Holland et al. 2013).

Recent work in the ptychoderid enteropneust *Balanoglossus simodensis* has analysed the expression of genes known to be crucial of formation and patterning of the chordate neural tube (Miyamoto and Wada 2013). This study reports expression of *bmp2/4*, *dlx*, *pax3/7* and *soxE* in dorsal regions of the collar cord but failed to observe expression of a potential ventral marker, *pax6*, thus suggesting a partially conserved patterning mechanism between the hemichordate collar cord and the chordate neural tube (Miyamoto and Wada 2013). In chordates, Hedgehog (hh) signalling emitted from the notochord and received by the neural plate (via the Hedgehog receptor patched (ptc)) is essential for patterning the neural tube along the dorsoventral axis (Echelard et al. 1992). In *B. simodensis*, expression of *hh* appears restricted to the stomochord and the anterior endoderm, which lies beneath the collar cord, during metamorphosis. In contrast, *ptc* is expressed in the mesoderm surrounding *hh*-expressing endoderm as well as the midline of the neural plate (Miyamoto and Wada 2013). These results suggest that Hedgehog signalling from the underlying endoderm may be received by the collar cord. However, gene-specific functional assays are required to determine if Hedgehog signalling is required for dorsoventral patterning of the neural tube in hemichordates.

In summary, the molecular studies currently available show striking similarities between vertebrates and enteropneusts in regard to the spatial deployment of transcription factors (Fig. 2.13) and signalling centres involved in neuronal anterior-posterior and dorsoventral patterning of the neural tube. The implications of these observations in establishing potential homologies between enteropneust and vertebrate body plans and on the evolution of the chordate CNS are currently highly debated (Holland et al. 2013) and additional work is required on hemichordates as well as invertebrate chordates (ascidians and amphioxus) to gain more insights into this long-lasting question (see Chapters 3 and 4).

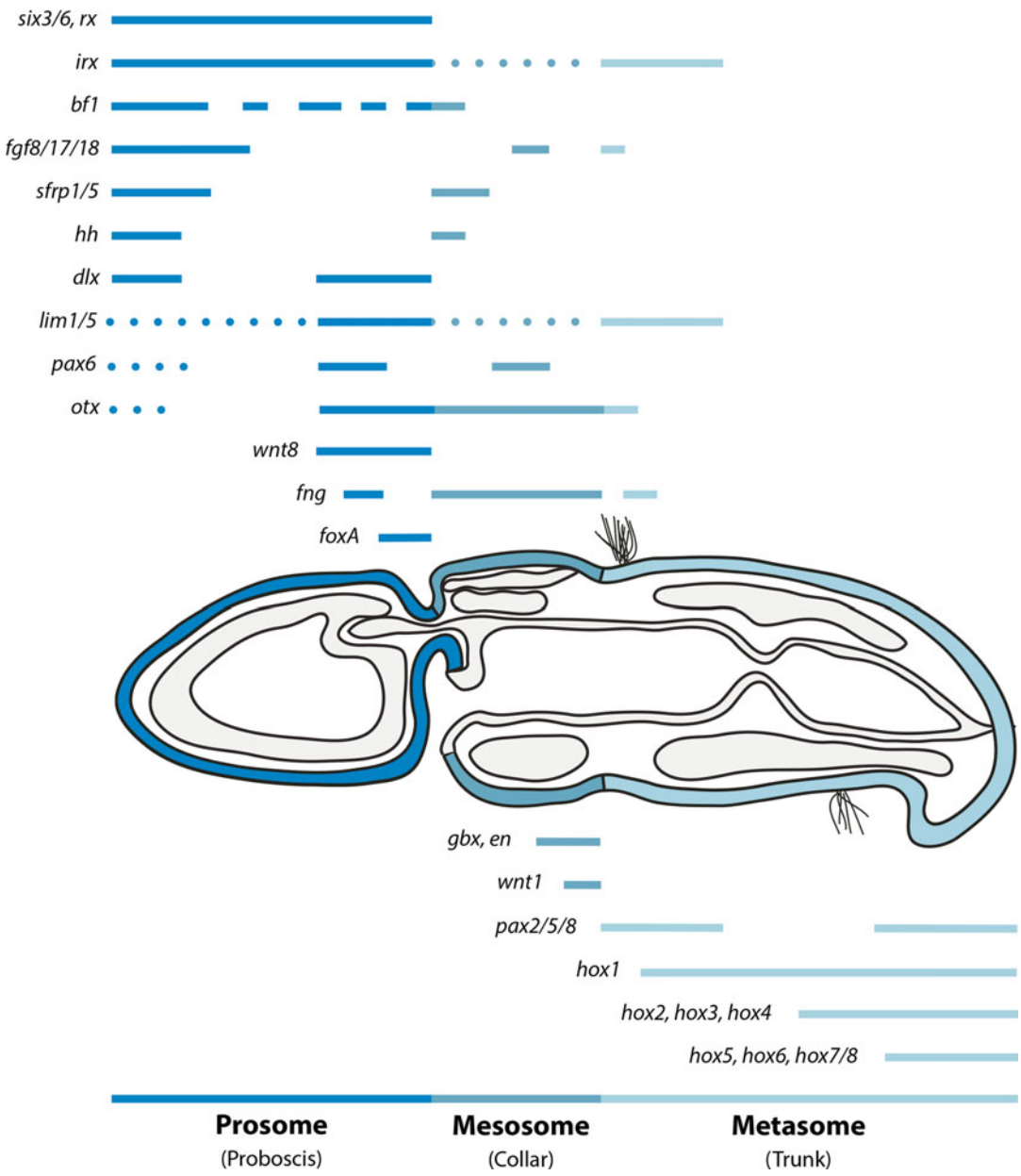

Fig. 2.13 Ectodermal anterior-posterior gene expression in hemichordates. Diagram summarising anterior-posterior regionalisation of gene expression domains in the ectoderm of the harrimanid enteropneust hemichordate *Saccoglossus kowalevskii* (Represented gene expression patterns based on data from Lowe et al. (2003), Aronowicz and Lowe (2006), Pani et al. (2012))

OPEN QUESTIONS

- Neurogenesis of the adult nervous system
- Function of the gill slits
- Investigations and characterisation of the light sense organs in tornaria larvae and adult enteropneusts
- Development of the muscular system in direct and indirect developing enteropneusts
- Roles of canonical Wnt and FGF signalling in ptychoderids and of Nodal signalling in direct and indirect developing enteropneusts
- All aspects of pterobranch embryogenesis and development

References

Agassiz A (1873) The history of *Balanoglossus* and Tornaria. Mem Am Acad Arts Sci 9:421–436

Al C, Colwin LH (1950) The developmental capacities of separated early blastomeres of an enteropneust, *Saccoglossus kowalevskii*. J Exp Zool 115:263–295

Allman GJ (1869) Rhabdopleura normani, Allman, nov. gen. et sp. Report of the British Association for the Advancement of Science 311–312

Anderson K (1907) Die Pterobranchier der schwedischen Südpolar-Expedition 1901–1903. Wiss Ergebn Schwedischen Südpolar 5:1–122

Angerer LM, Oleksyn DW, Logan CY, McClay DR, Dale L, Angerer RC (2000) A BMP pathway regulates cell fate allocation along the sea urchin animal-vegetal embryonic axis. Development (Cambridge, England) 127:1105–1114

Angerer LM, Yaguchi S, Angerer RC, Burke RD (2011) The evolution of nervous system patterning: insights from sea urchin development. Development (Cambridge, England) 138:3613–3623

Arendt D, Nübler-Jung K (1996) Common ground plans in early brain development in mice and flies. Bioessays 18:255–259

Aronowicz J, Lowe CJ (2006) Hox gene expression in the hemichordate *Saccoglossus kowalevskii* and the evolution of deuterostome nervous systems. Integr Comp Biol 46:890–901

Ax P (2001) Das System der Metazoa III. Ein Lehrbuch der phylogenetischen Systematik. Spektrum Akademischer Verlag, Heidelberg

Balser EJ, Ruppert EE (1990) Structure, ultrastructure and function of the preoral heart-kidney in *Saccoglossus kowalevskii* (Hemichordata, Enteropneusta) including new data on the stomochord. Acta Zool 71:235–249

Barrington EJ (1965) The biology of Hemichordata and Protochordata. WH Freeman, San Francisco

Bateson W (1884) The early stages of the development of *Balanoglossus* (sp. incert.). Q J Microsc Sci NS 24:208–236, pls 18–21

Bateson W (1885) The later stages in the development of *Balanoglossus kowalevskii*, with a suggestion on the affinities of the Enteropneusta. Q J Microsc Sci 25:81–128

Bateson W (1886) Continued account of the later stages in the development of *Balanoglossus kowalevskii*, and the morphology of the Enteropneusta. Q J Microsc Sci 26:511–533

Benito J, Pardos F (1997) Hemichordata. In: Harrison FW, Ruppert EE (eds) Microscopic anatomy of invertebrates, vol 15. Wiley-Liss, New York, pp 15–101

Bertrand S, Escriva H (2011) Evolutionary crossroads in developmental biology: amphioxus. Development 138:4819–4830

Bertrand S, Camasses A, Somorjai I, Belgacem MR, Chabrol O, Escande M, Pontarotti P, Escriva H (2011) Amphioxus FGF signaling predicts the acquisition of vertebrate morphological traits. Proc Natl Acad Sci 108:9160–9165

Bourlat SJ, Juliusdottir T, Lowe CJ, Freeman R, Aronowicz J, Kirschner M, Lander ES, Thorndyke M, Nakano H, Kohn AB, Heyland A, Moroz LL, Copley RR, Telford MJ (2006) Deuterostome phylogeny reveals monophyletic chordates and the new phylum Xenoturbellida. Nature 444:85–88

Bourne GC (1889) On a Tornaria found in British seas. J Mar Biol Assoc 1:63–68, pls 7–8

Brandenburger JL, Woollacott RM, Eakin RE (1973) Fine structure of the eyespots in tornaria larvae. Z Zellforsch 142:605–613

Bullock TH (1946) The anatomical organization of the nervous system of enteropneusts. Q J Microsc Sci 86:55–111, pls2–8

Bullock TH (1965) The nervous system of hemichordates. In: Bullock TH and Horridge GA (eds.) Structure and Function in the Nervous Systems of Invertebrates. WH Freeman and Co, San Francisco

Burdon-Jones C (1952) Development and biology of the larva of *Saccoglossus horsti* (Enteropneusta). Phil Trans R Soc B 236:553–590

Burke RD, Angerer LM, Elphick MR, Humphrey GW, Yaguchi SS, Kiyama T, Liang S, Mu X, Agca C, Klein WH, Brandhorst BP, Rowe M, Wilson K, Churcher AM, Taylor JS, Chen N, Murray G, Wang DY, Mellott D, Hallbook F, Olinski R, Thorndyke MC (2006) A genomic view of the sea urchin nervous system. Dev Biol 300:434–460

Byrne M, Cisternas P (2002) Development and distribution of the peptidergic system in larval and adult *Patiriella*: comparison of sea star bilateral and radial nervous systems. J Comp Neurol 451:101–114

Byrne M, Nakajima Y, Chee FC, Burke RD (2007) Apical organs in echinoderm larvae: insights into larval evolution in the Ambulacraria. Evol Dev 9:432–445

Cameron CB (2005) A phylogeny of the hemichordates based on morphological characters. Can J Zool 83:196–215

Cameron RA, Davidson EH (1991) Cell type specification during sea urchin development. Trends Genet 7:212–218

Cameron RA, Hough-Evans BR, Britten RJ, Davidson EH (1987) Lineage and fate of each blastomere of the eight-cell sea urchin embryo. Genes Dev 1:75–85

Cameron RA, Fraser SE, Britten RJ, Davidson EH (1989) The oral-aboral axis of a sea urchin embryo is specified by first cleavage. Development (Cambridge, England) 106:641–647

Cameron CB, Garey JR, Swalla BJ (2000) Evolution of the chordate body plan: new insights from phylogenetic analyses of deuterostome phyla. Proc Natl Acad Sci U S A 97:4469–4474

Cannon JT, Rychel AL, Eccleston H, Halanych KM (2009) Molecular phylogeny of hemichordata, with updated status of deep-sea enteropneusts. Mol Phylogenet Evol 52:17–24

Caron J-B, Morris SC, Cameron CB (2013) Tubicolous enteropneusts from the Cambrian period. Nature 495:503–506

Chen SH, Li KL, Lu IH, Wang YB, Tung CH, Ting HC, Lin CY, Lin CY, Su YH, Yu JK (2014) Sequencing and analysis of the transcriptome of the acorn worm *Ptychodera flava*, an indirect developing hemichordate. Mar Genomics 15:35–43

Cho S-J, Vallès Y, Giani VC, Seaver EC, Weisblat DA (2010) Evolutionary dynamics of the wnt gene family: a lophotrochozoan perspective. Mol Biol Evol 27:1645–1658

Cisternas P, Byrne M (2003) Peptidergic and serotonergic immunoreactivity in the metamorphosing ophiopluteus of *Ophiactis resiliens* (Echinodermata, Ophiuroidea). Invertebr Biol 122:177–185

Colwin AL, Colwin LH (1951) Relationships between the egg and larva of *Saccoglossus kowalevskii* (Enteropneusta): axes and planes: general prospective significance of the early blastomeres. J Exp Zool 117:111–137

Colwin AL, Colwin LH (1953) The normal embryology of *Saccoglossus kowalevskii*. J Morphol 92:401–453

Croce J, McClay D (2006) The canonical Wnt pathway in embryonic axis polarity. Semin Cell Dev Biol 17:168–174

Cunningham D, Casey ES (2014) Spatiotemporal development of the embryonic nervous system of *Saccoglossus kowalevskii*. Dev Biol 386:252–263

Darras S, Gerhart J, Terasaki M, Kirschner M, Lowe CJ (2011) Beta-catenin specifies the endomesoderm and defines the posterior organizer of the hemichordate *Saccoglossus kowalevskii*. Development 138:959–970

Dawydoff C (1907) Sur la morphologie des formations cardiope 'ricardique des Enteropneusts. Zool Anz 31:352–362

De Robertis EM, Kuroda H (2004) Dorsal-ventral patterning and neural induction in *Xenopus* embryos. Annu Rev Cell Dev Biol 20:285–308

De Robertis EM, Sasai Y (1996) A common plan for dorsoventral patterning in Bilateria. Nature 380:37–40

De Robertis EM, Larraín J, Oelgeschläger M, Wessely O (2000) The establishment of Spemann's organizer and patterning of the vertebrate embryo. Nat Rev Genet 1:171–181

Delle Chiaje S (1829) Memorie sulla storia e notomia degli animali senza vertebre del Regno di Napoli. Napoli 4:117–120

Denes AS, Jékely G, Steinmetz PRH, Raible F, Snyman H, Prud'homme B, Ferrier DEK, Balavoine G, Arendt D (2007) Molecular architecture of annelid nerve cord supports common origin of nervous system centralization in Bilateria. Cell 129:277–288

Dilly PN (1973) The larva of *Rhabdopleura compacta* (Hemichordata). Mar Biol (Berlin) 18:69–86

Dilly PN (1975) The pterobranch *Rhabdopleura compacta*: its nervous system and phylogenetic position. Symp Zool Soc Lond 36:1–16

Dilly PN (2013) *Cephalodiscus* reproductive biology (Pterobranchia, Hemichordata). Acta Zool. doi:10.1111/azo.12015

Dohle W (2004) Die Verwandtschaftsbeziehungen der Großgruppen der Deuterostomier: alternative Hypothesen und ihre Begründungen. Sber Ges Naturf Freunde Berlin 43:123–162

Duboc V, Röttinger E, Besnardeau L, Lepage T (2004) Nodal and BMP2/4 signaling organizes the oral-aboral axis of the sea urchin embryo. Dev Cell 6:397–410

Duboc V, Röttinger E, Lapraz F, Besnardeau L, Lepage T (2005) Left-right asymmetry in the sea urchin embryo regulated by nodal signaling on the right side. Dev Cell 9:147–158

Echelard Y, Epstein DJ, St-Jacques B, Shen L, Mohler J, McMahon JA, McMahon AP (1992) Sonic hedgehog, a member of a family of putative signaling molecules, is implicated in the regulation of CNS polarity. Cell 75:1417–1430

Edgecombe G, Giribet G, Dunn C, Hejnol A, Kristensen R, Neves R, Rouse G, Worsaae K, Sørensen M (2011) Higher-level metazoan relationships: recent progress and remaining questions. Org Divers Evol 11:151–172

Eschscholtz F (1825) Bericht über die zoologische Ausbeute der Reise von Kronstadt bis St.-Peter und Paul. Oken's Isis. pp 734–747

Fletcher RB, Baker JC, Harland RM (2006) FGF8 splice forms mediate early mesoderm and posterior neural tissue formation in *Xenopus*. Development 133:1703–1714

Franz V (1927) Morphologie der Akranier. Z Anat 27:464–692

Freeman R, Ikuta T, Wu M, Koyanagi R, Kawashima T, Tagawa K, Humphreys T, Fang G-C, Fujiyama A et al (2012) Identical genomic organization of two hemichordate Hox clusters. Curr Biol 22:2053–2058, 1–6

Fritzenwanker JH, Gerhart J, Freeman RM, Lowe CJ (2014) The Fox/Forkhead transcription factor family of the hemichordate *Saccoglossus kowalevskii*. EvoDevo 5:17

Gillis JA, Fritzenwanker JH, Lowe CJ (2011) A stem-deuterostome origin of the vertebrate pharyngeal transcriptional network. Proc R Soc B Biol Sci 279:237–246

Goldschmid A (2007) Hemichordata. In: Westheide W, Rieger R (eds) Spezielle Zoologie, vol 1, 2nd edn, Einzeller und wirbellose Tiere. Elsevier GmbH, Spektrum Akademischer Verlag, Heidelberg

Gonzalez P, Cameron CB (2009) The gill slits and preoral ciliary organ of *Protoglossus* (Hemichordata: Enteropneusta) are filter-feeding structures. Biol J Linn Soc Lond 98:898–906

Goodrich ES (1917) 'Proboscis pores' in craniate vertebrates, a suggestion concerning the premandibular somites and hypophysis. Q J Microsc Sci 62: 539–553

Green SA, Norris RP, Terasaki M, Lowe CJ (2013) FGF signaling induces mesoderm in the hemichordate *Saccoglossus kowalevskii*. Development (Cambridge, England) 140:1024–1033

Hadfield M (1975) Hemichordata. In: Giese AC, Pearse JS (eds) Reproduction of marine invertebrates. Academic, New York, pp 185–240

Hamada H, Meno C, Watanabe D, Saijoh Y (2002) Establishment of vertebrate left-right asymmetry. Nat Rev Genet 3:103–113

Harada Okai N, Taguchi S, Shoguchi E, Tagawa K (2001) Embryonic expression of a hemichordate distal-less gene. repository.kulib.kyoto-u.ac.jp

Harada Y, Shoguchi E, Taguchi S, Okai N, Humphreys T, Tagawa K, Satoh N (2002) Conserved expression pattern of BMP-2/4 in hemichordate acorn worm and echinoderm sea cucumber embryos. Zool Sci 19:1113–1121

Harmer SF (1905) The Pterobranchia of the Siboga Expedition with an account of other species. In: Weber M (ed) Siboga-Expeditie: uitkomsten op zoölogisch, botanisch, oceanographisch en geologisch gebied verzameld in Nederlandsch Oost-Indië 1899–1900 aan boord HM Siboga onder commando van Luitenant ter Zee 1e kl GF Tydeman. E. J Brill, Leyden, p 132

Hay-Schmidt A (2000) The evolution of the serotonergic nervous system. Phil Trans R Soc Lon B 267: 1071–1079

Hejnol A, Obst M, Stamatakis A, Ott M, Rouse GW, Edgecombe GD, Martinez P, Baguñà J, Bailly X, Jondelius U, Wiens M, Müller WE, Seaver E, Wheeler WC, Martindale MQ, Giribet G, Dunn CW (2009) Assessing the root of bilaterian animals with scalable phylogenomic methods. Proc R Soc Lond B 276:4261–4270

Henry JQ, Tagawa K, Martindale M (2001) Deuterostome evolution: early development in the enteropneust hemichordate, *Ptychodera flava*. Evol Dev 3:375–390

Holland LZ, Carvalho JE, Escriva H, Laudet V, Schubert M, Shimeld SM, Yu J-K (2013) Evolution of bilaterian central nervous systems: a single origin? EvoDevo 4:27

Holland ND, Clague DA, Gordon DP, Gebruk A, Pawson DL, Vecchione M (2005) 'Lophenteropneust' hypothesis refuted by collection and photos of new deep-sea hemichordates. Nature 434:374–376

Holley SA, Ferguson EL (1997) Fish are like flies are like frogs: conservation of dorsal-ventral patterning mechanisms. Bioessays 19:281–284

Hyman LH (1955) The Invertebrates, vol 4, Echinodermata. McGraw-Hill, New York

Hyman LH (1959) The invertebrates, vol 5, Smaller coelomate groups. McGraw-Hill Book Company, New York

Ikuta T, Miyamoto N, Saito Y, Wada H, Satoh N, Saiga H (2009) Ambulacrarian prototypical Hox and ParaHox gene complements of the indirect-developing hemichordate *Balanoglossus simodensis*. Dev Genes Evol 219(7):383–389

Imai KS, Satoh N, Satou Y (2002) Early embryonic expression of FGF4/6/9 gene and its role in the induction of mesenchyme and notochord in *Ciona savignyi* embryos. Development 129:1729–1738

Kaul S, Stach T (2010) Ontogeny of the collar cord: neurulation in the hemichordate *Saccoglossus kowalevskii*. J Morphol 271:1240–1259

Kaul-Strehlow S, Stach T (2011) The pericardium in the deuterostome *Saccoglossus kowalevskii* (Enteropneusta) develops from the ectoderm via schizocoely. Zoomorphology 130:107–120

Kaul-Strehlow S, Stach T (2013) A detailed description of the development of the hemichordate Saccoglossus kowalevskii using SEM, TEM, Histology and 3D-reconstructions. Frontiers in Zoology 10:53

Kim GJ, Yamada A, Nishida H (2000) An FGF signal from endoderm and localized factors in the posterior-vegetal egg cytoplasm pattern the mesodermal tissues in the ascidian embryo. Development 127: 2853–2862

Kimelman D (2006) Mesoderm induction: from caps to chips. Nat Rev Genet 7:360–372

Knight-Jones EW (1952) On the nervous system of *Saccoglossus cambrensis* (Enteropneusta). Philos Trans R Soc Lond B 236:315–354

Kowalevsky A (1866) Anatomie des Balanoglossus Delle Chiaje. Mem Acad Imp Sc St Petersbourg 7:1–18

Krohn A (1854) Beobachtungen über Echinodermenlarven. Arch Anat Physiol wiss Med 208–213

Lankester ER (1884) A Contribution of the knowledge of *Rhabdopleura*. Q J Microsc Sci 96:622–647

Lapraz F, Besnardeau L, Lepage T (2009) Patterning of the dorsal-ventral axis in echinoderms: insights into the evolution of the BMP-chordin signaling network. PLoS Biol 7:e1000248

Lee PN, Pang K, Matus DQ, Martindale MQ (2006) A WNT of things to come: evolution of Wnt signaling and polarity in cnidarians. Semin Cell Dev Biol 17:157–167

Lemaire P (2011) Evolutionary crossroads in developmental biology: the tunicates. Development 138:2143–2152

Lemons D, Fritzenwanker JH, Gerhart J, Lowe CJ, Mcginnis W (2010) Co-option of an anteroposterior head axis patterning system for proximodistal patterning of appendages in early bilaterian evolution. Dev Biol 344:358–362

Lester SM (1985) *Cephalodiscus* sp. (Hemichordata: Pterobranchia): observations of functional morphology, behavior and occurrence in shallow water around Bermuda. Mar Biol 85:263–268

Lester SM (1988a) Ultrastructure of adult gonads and development and structure of the larva of *Rhabdopleura normani* (Hemichordata: Pterobranchia). Acta Zool 69:95–109

Lester SM (1988b) Settlement and Metamorphosis of *Rhabdopleura normani* (Hemichordata: Pterobranchia). Acta Zool 69:111–120

Lowe CJ, Wu M, Salic A, Evans L, Lander E, Stange-ThomannN GCE, Gerhart J, Kirschner M (2003) Anteroposterior patterning in hemichordates and the origin of the chordate nervous system. Cell 113:853–865

Lowe CJ, Tagawa K, Humphreys T, Kirschner M, Gerhart J (2004) Hemichordate embryos: procurement, culture, and basic methods. Methods Cell Biol 74:171–194

Lowe CJ, Terasaki M, Wu M, Freeman RM, Runft L, Kwan K, Haigo S, Aronowicz J, Lander E, Gruber C, Smith M, Kirschner M, Gerhart J (2006) Dorsoventral patterning in hemichordates: insights into early chordate evolution. PLoS Biol 4:e291

Luttrell S, Konikoff C, Byrne A, Bengtsson B, Swalla BJ (2012) Ptychoderid hemichordate neurulation without a notochord. Integr Comp Biol 52:829–834

Maisey JG (1986) Heads and tails: a chordate phylogeny. Cladistics 2:201–256

Martin BL, Kimelman D (2009) Wnt signaling and the evolution of embryonic posterior development. Curr Biol 19:R215–R219

Mayer G, Bartolomaeus T (2003) Ultrastructure of the stomochord and the heart-glomerulus complex in *Rhabdopleura compacta* (Pterobranchia): phylogenetic implications. Zoomorphology 122:125–133

McClay DR (2011) Evolutionary crossroads in developmental biology: sea urchins. Development 138: 2639–2648

Merker S, Gruhl A, Stach T (2013) Comparative anatomy of the heart – glomerulus complex of *Cephalodiscus gracilis* (Pterobranchia): structure, function, and phylogenetic implications. Zoomorphology 133:83–98

Metschnikoff E (1870) Untersuchungen über die Metamorphose einiger Seethiere. Z Wiss Zool 20:131–144

Metschnikoff E (1881) Über die systematische Stellung von *Balanoglossus*. Zool Anz 4:139–157

Mierzejewski P (2004) Classification of the cephalodiscoidea. iNet: Graptolite Net: http://pterobranchia.graptolite.net/Cephalodiscoidea.html

M'Intosh WC (1882) Preliminary notice of Cephalodiscus, a new type allied to Prof. Allman's Rhabdopleura, dredged in H. M. S. 'Challenger'. Ann Mag Nat Hist Ser 5:337–348

Miyamoto N, Wada H (2013) Hemichordate neurulation and the origin of the neural tube. Nat Commun 4:2713

Miyamoto N, Nakajima Y, Wada H, Saito Y (2010) Development of the nervous system in the acorn worm *Balanoglossus simodensis*: insights into nervous system evolution. Evol Dev 12:416–424

Morgan TH (1891) The growth and metamorphosis of Tornaria. J Morphol 5:407–458

Morgan TH (1894) The development of *Balanoglossus*. J Morphol 9:1–86

Morokuma J, Ueno M, Kawanishi H, Saiga H, Nishida H (2002) *HrNodal*, the ascidian nodal -related gene, is expressed in the left side of the epidermis, and lies upstream of *HrPitx*. Dev Genes Evol 212:439–446

Müller J (1850) Ueber die Larve und die Metamorphose der Echinodermen. Akad Wiss Berlin 2:75–109

Nakano H, Murabe N, Amemiya S, Nakajima Y (2006) Nervous system development in the sea cucumber *Stichopus japonicus*. Dev Biol 292:205–212

Nezlin LP, Yushin VV (2004) Structure of the nervous system in the tornaria larva of *Balanoglossus proterogonius* (Hemichordata: Enteropneusta) and its phylogenetic implications. Zoomorphology 123:1–13

Niehrs C (2010) On growth and form: a Cartesian coordinate system of Wnt and BMP signaling specifies bilaterian body axes. Development (Cambridge, England) 137:845–857

Nielsen C (2011) Animal evolution. Interrelationships of the living phyla, 2nd edn. Oxford University Press, New York

Nielsen C, Hay-Schmidt A (2007) Development of the enteropneust *Ptychodera flava*: ciliary bands and nervous system. J Morphol 268:551–570

Nomaksteinsky M, Röttinger E, Dufour H, Chettouh Z, Lowe C, Martindale M, Brunet J (2009) Centralization of the deuterostome nervous system predates chordates. Curr Biol 19:1264–1269

Okai N, Tagawa K, Humphreys T, Satoh N, Ogasawara M (2000) Characterization of gill-specific genes of the acorn worm Ptychodera flava. Dev Dyn 217:309–319

Osborn KJ, Kuhnz LA, Priede IG, Urata M, Gebruk AV, Holland ND (2012) Diversification of acorn worms (Hemichordata, Enteropneusta) revealed in the deep sea. Proc R Soc B 279:1646–1654

Pani AM, Mullarkey EE, Aronowicz J, Assimacopoulos S, Grove EA, Lowe CJ (2012) Ancient deuterostome origins of vertebrate brain signalling centres. Nature 483:289–294

Philippe H, Brinkmann H, Copley RR, Moroz LL, Nakano H, Poustka AJ, Wallberg A, Peterson KJ, Telford MJ (2011) Acoelomorph flatworms are deuterostomes related to *Xenoturbella*. Nature 470:255–258

Rao KP (1953) The development of *Glandiceps* (Enteropneusta; Spengelidae). J Morphol 93:1–17

Rehkämper G, Welsch U, Dilly PN (1987) Fine structure of the ganglion of Cephalodiscus gracilis (pterobranchia, hemichordata). J Comp Neurol 259:308–315

Röttinger E, Lowe CJ (2012) Evolutionary crossroads in developmental biology: hemichordates. Development 139:2463–2475

Röttinger E, Martindale M (2011) Ventralization of an indirect developing hemichordate by NiCl suggests a conserved mechanism of dorsoventral (D/V) patterning in Ambulacraria (hemichordates and echinoderms). Dev Biol 354:173–190

Ruppert EE (2005) Key characters uniting hemichordates and chordates: homologies or homoplasies? Can J Zool 83:8–23

Ruppert EE, Balser EJ (1986) Nephridia in the larvae of hemichordates and echinoderms. Biol Bull 171: 188–196

Rychel AL, Swalla BJ (2007) Development and evolution of chordate cartilage. J Exp Zool 308:325–335

Sato T (1936) Vorläufige Mitteilung über *Atubaria heterolopha* gen. nov. sp. nov., einen in freiem Zustand aufgefundenen Pterobranchier aus dem Stilen Ozean. Zool Anz 115:97–106

Sato A, Holland PW (2008) Asymmetry in a pterobranch hemichordate and the evolution of left-right patterning. Dev Dyn 237:3634–3639

Sato A, Bishop JDD, Holland PWH (2008) Developmental biology of pterobranch hemichordates: history and perspectives. Genesis 46:587–591

Sato A, White-Cooper H, Doggett K, Holland PW (2009) Degenerate evolution of the hedgehog gene in a hemichordate lineage. Proc Natl Acad Sci U S A 106: 7491–7494

Saudemont A, Haillot E, Mekpoh F, Bessodes N, Quirin M, Lapraz F, Duboc V, Röttinger E, Range R, Oisel A et al (2010) Ancestral regulatory circuits governing ectoderm patterning downstream of Nodal and

BMP2/4 revealed by gene regulatory network analysis in an echinoderm. PLoS Genet 6:e1001259
Schaeffer B (1987) Deuterostome monophyly and phylogeny. Evol Biol 21:179–235
Schepotieff A (1907) Die Pterobranchier. Anatomische und histologische Untersuchungen über *Rhabdopleura normani* Allman und *Cephalodiscus dodecalophus* M'int. 1. Teil. *Rhabdopleura normani*. 1. Abschnitt. Die Anatomie von *Rhabdopleura*. Zool Jahrb Anat 23:463–534
Silén L (1950) On the nervous system of *Glossobalanus marginatus* Meek (Enteropneusta). Acta Zool 31:149–175
Slack JM, Darlington BG, Gillespie LL, Godsave SF, Isaacs HV, Paterno GD (1989) The role of fibroblast growth factor in early *Xenopus* development. Development 107(Suppl):141–148
Smith S, Douglas R, da Silva K, Swalla B (2003) Morphological and molecular identification of *Saccoglossus* species (Hemichordata: Harrimaniidae) in the Pacific Northwest. Can J Zool 81:133–141
Spengel JW (1893) Die Enteropneusten des Golfes von Neapel und der angrenzenden Meeres-Abschnitte. Fauna und Flora des Golfes von Neapel, vol 18. Engelmann, Leipzig
Spengel JW (1901) Die Benennung der Enteropneusten–Gattungen. Zool Jahrb Abt Syst 15:209–218
Stach T (2002) Minireview: on the homology of the protocoel in Cephalochordata and 'lower' Deuterostomia. Acta Zool 83:25–31
Stach T (2013) Larval anatomy of the pterobranch *Cephalodiscus gracilis* supports secondarily derived sessility concordant with molecular phylogenies. Naturwiss. doi:10.1007/s00114-013-1117-3
Stach T, Kaul S (2012) The postanal tail of the enteropneust *Saccoglossus kowalevskii* is a ciliary creeping organ without distinct similarities to the chordate tail. Acta Zool 92:150–160
Stach T, Gruhl A, Kaul-Strehlow S (2012) The central and peripheral nervous system of *Cephalodiscus gracilis* (Pterobranchia, Deuterostomia). Zoomorphology 131:11–24
Stainier DYR (2002) A glimpse into the molecular entrails of endoderm formation. Genes Dev 16:893–907
Stebbing ARD (1970) Aspects of the reproduction and life cycle of *Rhabdopleura compacta* (Hemichordata). Mar Biol (Berlin) 5:205–212
Stiasny G (1914a) Studium über die Entwicklung des *Balanoglossus clavigerus* Delle Chiaje. I. Die Entwicklung der Tornaria. Mitt Zool Stat Neapel 22:36–75
Stiasny G (1914b) Studium über die Entwicklung des *Balanoglossus clavigerus* Delle Chiaje. II. Darstellung der weiteren Entwicklung bis zur Metamorphose. Mitt Zool Stat Neapel 22:255–290
Su Y-H, Davidson EH (2009) A perturbation model of the gene regulatory network for oral and aboral ectoderm specification in the sea urchin embryo. Dev Biol 329:410–421
Tagawa K, Nishino A, Humphreys T, Satoh N (1998a) The spawning and early development of the Hawaiian acorn worm (hemichordate), *Ptychodera flava*. Zool Sci 15:85–91
Tagawa K, Humphreys T, Satoh N (1998b) Novel pattern of Brachyury gene expression in hemichordate embryos. Mech Dev 75:139–143
Taguchi S, Tagawa K, Humphreys T, Nishino A, Satoh N, Harada Y (2000) Characterization of a hemichordate fork head/HNF-3 gene expression. Dev Genes Evol 210:11–17
Technau U, Scholz CB (2003) Origin and evolution of endoderm and mesoderm. Int J Dev Biol 47:531–539
Ullrich-Lüter EM, Dupont S, Arboleda E, Hausen H, Arnone MI (2011) Unique system of photoreceptors in sea urchin tube feet. Proc Natl Acad Sci 108:8367–8372
Urata M, Yamaguchi M (2004) The development of the enteropneust hemichordate *Balanoglossus misakiensis* Kuwano. Zool Sci 21:533–540
Urata M, Iwasaki S, Ohtsuka S, Yamaguchi M (2014) Development of the swimming acorn worm *Glandiceps hacksi*: similarity to holothuroids. Evol Dev 16:149–154
van der Horst CJ (1939) In: Bronn HG (ed) Hemichordata. Akademische Verlagsgesellschaft mbH, Leipzig, 737 p
Whitman M (2001) Nodal signaling in early vertebrate embryos themes and variations. Dev Cell 1:605–617
Willey A (1898) Spengelia, a new genus of Enteropneusta. Q.J Microsc Sci 40:623–630
Worsaae K, Sterrer W, Kaul-Strehlow S, Hay-Schmidt A, Giribet G (2012) An anatomical description of a miniaturized acorn worm (hemichordata, enteropneusta) with asexual reproduction by paratomy. PLoS One 7(11):e48529. doi:10.1371/journal.pone.0048529
Young JZ (1962) The life of vertebrates, 2nd edn. Oxford University Press, Oxford
Yu J-K, Holland LZ, Holland ND (2002) An amphioxus nodal gene (*AmphiNodal*) with early symmetrical expression in the organizer and mesoderm and later asymmetrical expression associated with left-right axis formation. Evol Dev 4:418–425

Cephalochordata

3

Linda Z. Holland

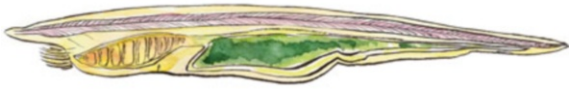

Chapter vignette artwork by Brigitte Baldrian.

L.Z. Holland
Marine Biology Research Division, Scripps
Institution of Oceanography, University of California
San Diego, La Jolla, CA 92093-0202, USA
e-mail: lzholland@ucsd.edu

A. Wanninger (ed.), *Evolutionary Developmental Biology of Invertebrates 6: Deuterostomia*
DOI 10.1007/978-3-7091-1856-6_3, © Springer-Verlag Wien 2015

INTRODUCTION

Cephalochordates, which together with vertebrates and tunicates constitute the Chordata, were initially thought to be mollusks by Pallas (1774), who described *Limax lanceolatus*. The name was revised to *Branchiostoma lubricum* by Costa (1834), who recognized its affinity to fishes, and to *Amphioxus lanceolatus* by Yarrell, who considered it most closely allied to the agnathans among the vertebrates (Yarrell 1836). Due to precedence of the name *Branchiostoma*, the European species came to be classified as *Branchiostoma lanceolatum*, and the term "amphioxus" has become a common name for cephalochordates, which are also called lancelets. The name "*Branchiostoma*" means "gill mouth" and is an apparent reference to the motile sensory cirri around the mouth which keep too large particles from being eaten. The terms "lanceolatum" and "amphioxus" refer to the elongated shape of the animal, which reaches a maximum length of about 6 cm and is pointed at both ends. Today, about 25 species of *Branchiostoma* are recognized. There are two additional genera, *Asymmetron* and *Epigonichthys*, which are similar to *Branchiostoma*, but have a series of gonads only on the right side compared to both sides in *Branchiostoma* (Fig. 3.1B). A single species of *Epigonichthys* (*E. maldivensis*) and two of *Asymmetron* (*A. lucayanum* and *A. interferum*) have been described; however, there may be additional cryptic species of *Asymmetron* (Kon et al. 2007). In phylogenetic analysis with whole mitochondrial genome sequences, *Asymmetron* is basal in the cephalochordates with a divergence time of about 162 my from the *Branchiostoma* and *Epigonichthys* clade (Fig. 3.1A; Kon et al. 2007; Nohara et al. 2005). Although virtually nothing is known about any

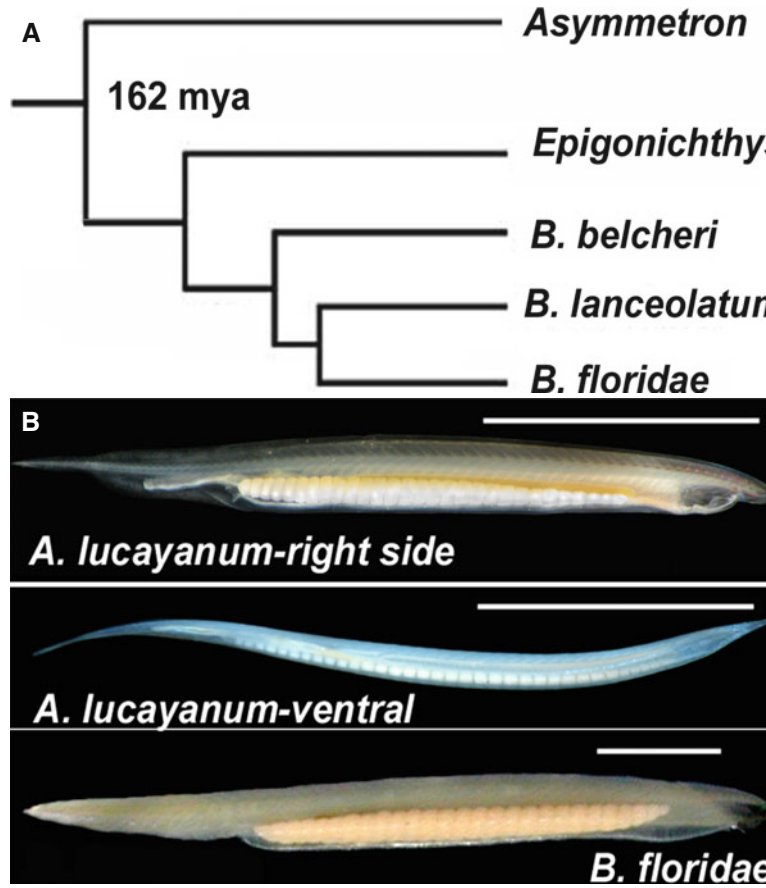

Fig. 3.1 (**A**) Phylogenetic tree of cephalochordates based on mitochondrial DNA sequences. *Asymmetron lucayanum* diverged from the *Branchiostoma* + *Epigonichthys* clade about 162 mya. Nonparametric smoothing method. Cephalochordates are basal to the tunicate + vertebrate clade. After (Nohara et al. 2005; Kon et al. 2007). (**B**) Living adult amphioxus. *Top Asymmetron lucayanum*, *right side. Center*, *Asymmetron lucayanum*, ventral view showing gonads only on the right side. *Bottom. Branchiostoma floridae*. Female. *B. floridae* has gonads on both right and left sides. Scale bars = 0.5 cm

aspect of the biology of *Epigonichthys*, much more is known about *Asymmetron lucayanum*, which was first described from Bimini, Bahamas, by Andrews (1893). He obtained a few embryos, which developed to the gastrula stage when they "were destroyed by an accident." It was over 100 years before more embryos of *A. lucayanum* were obtained and the embryology described (Holland and Holland 2010). It was discovered that animals spawn a few days before the new moon (Holland 2011), but to date, there are no studies of developmental genes.

Cephalochordates have long been thought to give clues to evolution of the vertebrates. They share with vertebrates and tunicates the defining chordate characters of a dorsal hollow nerve cord, notochord, and pharyngeal gill slits. In the nineteenth century, there were several ideas concerning the relation between these three groups. Haeckel (1876) regarded amphioxus as the simplest vertebrate and therefore key to understanding evolution of the vertebrates. Alternatively, amphioxus was considered a degenerate form of the earliest vertebrate ancestor (Dohrn 1875; Lankester 1875). Willey (1894) regarded the proximate ancestor of the vertebrates to be free-swimming and intermediate between an ascidian tadpole and amphioxus, while MacBride (1898) considered amphioxus to be a "more primitive offshoot from the vertebrate stem than ascidians." Although amphioxus had been considered a vertebrate, its affinities with tunicates were ultimately recognized, and in 1906, amphioxus was moved from the fishes section of the Zoological Record to the protochordate section. Subsequently, phylogenetic analyses based on morphological characters or on rDNA sequences placed cephalochordates as sister group of vertebrates within the chordates, with tunicates basal in the phylum (Winchell et al. 2002; Mallatt and Winchell 2007). However, more recent reanalysis with large sets of concatenated nuclear genes has reversed the positions of tunicates, with cephalochordates as basal to a clade of tunicates plus vertebrates (Blair and Hedges 2005; Delsuc et al. 2006, 2008). Comparisons of the genome sequences of the Florida amphioxus, *Branchiostoma floridae*, the tunicates *Ciona intestinalis* and *Oikopleura dioica*, and several vertebrates have shown that 18S rDNA sequences erroneously placed tunicates basal in the chordates because tunicates are evolving particularly rapidly, while amphioxus and vertebrates are evolving much more slowly. Moreover, the genomes of amphioxus (~520 mb) and vertebrates (~1,500–3,000 mb) share considerable synteny, whereas the very small tunicate genomes (~170 and ~70 mb for *C. intestinalis* and *O. dioica*, respectively) share virtually no synteny with other chordate genomes (Denoeud et al. 2010).

Amphioxus species occur worldwide, chiefly from the tropics to the temperate zones, except for high latitude populations of *Branchiostoma lanceolatum*. All species of amphioxus but one live in shallow coastal waters with sandy substrata, protected from wave action. The exception is *Asymmetron interferum* which was found at 229 m adjacent to the bones of a decomposing whale carcass off Cape Nomamisaki, Japan (Kon et al. 2007). All amphioxus species burrow in the sand with the anterior tip approximately flush with the ocean bottom for filter feeding. Sexes are separate. Individuals of warm water species like *B. floridae* will spawn every 9–14 days throughout the summer (Stokes and Holland 1996). Populations of cold water species like *B. lanceolatum* may spawn only twice during the summer (Fuentes et al. 2004, 2007). Female gametes are stored in the ovary as primary oocytes, attached to follicle cells at the animal pole. On the day of spawning, oocytes undergo meiotic maturation. They produce one polar body, arresting at second meiotic metaphase, and are ovulated in the early afternoon. At the same time, sperm, which are in a syncytium, become individualized and gain the capacity to become mobile on exposure to seawater. Spawning of ovulated eggs is induced by falling light levels after dusk. On spawning days, males and females emerge from the sand about half an hour after sunset, swim in the water column, and spawn (Mizuta and Kubokawa 2004). Fertilization is external. Spawning in species of *Branchiostoma* is influenced by changes in water temperature. Hatschek (1893) noted for the population in Sicily that amphioxus (*B. lanceolatum*) begins to spawn in the "first warm days of spring" and that

spawning throughout the summer tends to occur after 2 or 3 warm days following a long period of cold weather. It is, therefore, not surprising that for *B. lanceolatum*, a 4–5 °C shift in temperature can induce meiotic maturation a day later followed by spawning in response to darkness (Fuentes et al. 2004, 2007; Benito-Gutiérrez et al. 2013). Spawning of gametes that have matured can also be induced in at least *Branchiostoma floridae* by a brief pulse of 50V DC (Holland and Yu 2004). However, this method may not be effective with other species (Yasui et al. 2007). In *Branchiostoma floridae* there is no clear relationship between days of spawning and the tides or phases of the moon (Stokes and Holland 1996). We have achieved year around spawning in the laboratory by keeping ripe adults at 16–17 °C for several weeks and then bringing them up to 24 °C. Under these conditions 10 % or more of the animals typically spawn 24–48 h after the temperature shift. The Asian species *B. belcheri* and *B. japonicum* have also been cultured in the laboratory (Wu et al. 2000a, b; Yasui et al. 2013). In contrast, *Asymmetron lucayanum* spawns monthly approximately 1–2 days before the new moon each month (Holland 2011).

Adults of *Branchiostoma* are morphologically very much the same from species to species. They differ chiefly in the maximum length (6 cm in *B. belcheri* and *B. lanceolatum* (Yamaguchi and Henmi 2003; Desdevises et al. 2011) and 5 cm in *B. floridae* (Stokes and Holland 1996)), in the number of myotomes, and in the presence or absence of pigment in the larval tail fin (Fig. 3.1; Flood 1975a; Holland and Holland 2010). The larval tail fin is pigmented in *B. lanceolatum*, *B. belcheri*, and *B. japonicum*, but not in *B. floridae*. Species of *Asymmetron* are much smaller than *Branchiostoma. Asymmetron lucayanum* reaches a maximum length of only 2.5–2.8 cm, while some species of *Epigonichthys* attain a length of ~4 cm. The larval tail fin is also pigmented in *A. lucayanum*, suggesting that this was an ancestral characteristic that was lost in *B. floridae*. The major difference between *Branchiostoma* and other genera is that it has a series of gonads on both sides of the body, while *Asymmetron* and *Epigonichthys* have gonads only on the right. The sexes are separate, although hermaphrodites of *Branchiostoma* species have very occasionally been found (Yamaguchi and Henmi 2003). Other differences between the genera include the larval gill slits located more ventrally in *A. lucayanum* than in *Branchiostoma* and the anterior coeloms of *A. lucayanum* being formed schizocoelically in *A. lucayanum* and enterocoelically in *Branchiostoma* (Holland and Holland 2010).

EARLY DEVELOPMENT

There are three main eras of amphioxus embryology – the era of classical morphology from the 1860s to the early 1960s, the era of fine structural studies from about 1960–1985, and the EvoDevo era since the late 1980s. The techniques of the classical era were limited to histology including examination of whole mounts and paraffin sections as well as to experiments determining the fates of isolated blastomeres or tiers of blastomeres. It is, therefore, not altogether surprising that given the small size of the eggs (~140 μm in diameter; Fig. 3.2), embryos, and larvae (~4–5 mm at metamorphosis; Fig. 3.3) and the desire of many researchers to see parallels between amphioxus embryos and those of other organisms, there was considerable controversy and many misconceptions over early embryology of amphioxus. The electron microscopic studies reexamined controversies about embryonic and adult morphology remaining from classical studies, while the EvoDevo era began with the use of gene expression to infer homologies between amphioxus and vertebrates and is now transitioning to gene knockdown and overexpression for dissecting gene networks and with the goal of reconstructing the ancestral chordate and shedding light on the course of chordate evolution.

The embryology of amphioxus was first described by Kowalevsky (1867), who raised embryos of *Branchiostoma lanceolatum* obtained in Naples, Italy, to the two-gill-slit stage and obtained later ones from plankton tows. Subsequently a large population of *B. lanceolatum* was found in the pontano at Lago di Faro, Sicily. A number of studies were done on the embryology of this population of *B. lanceolatum* until it was eliminated by an eruption of Mt. Etna

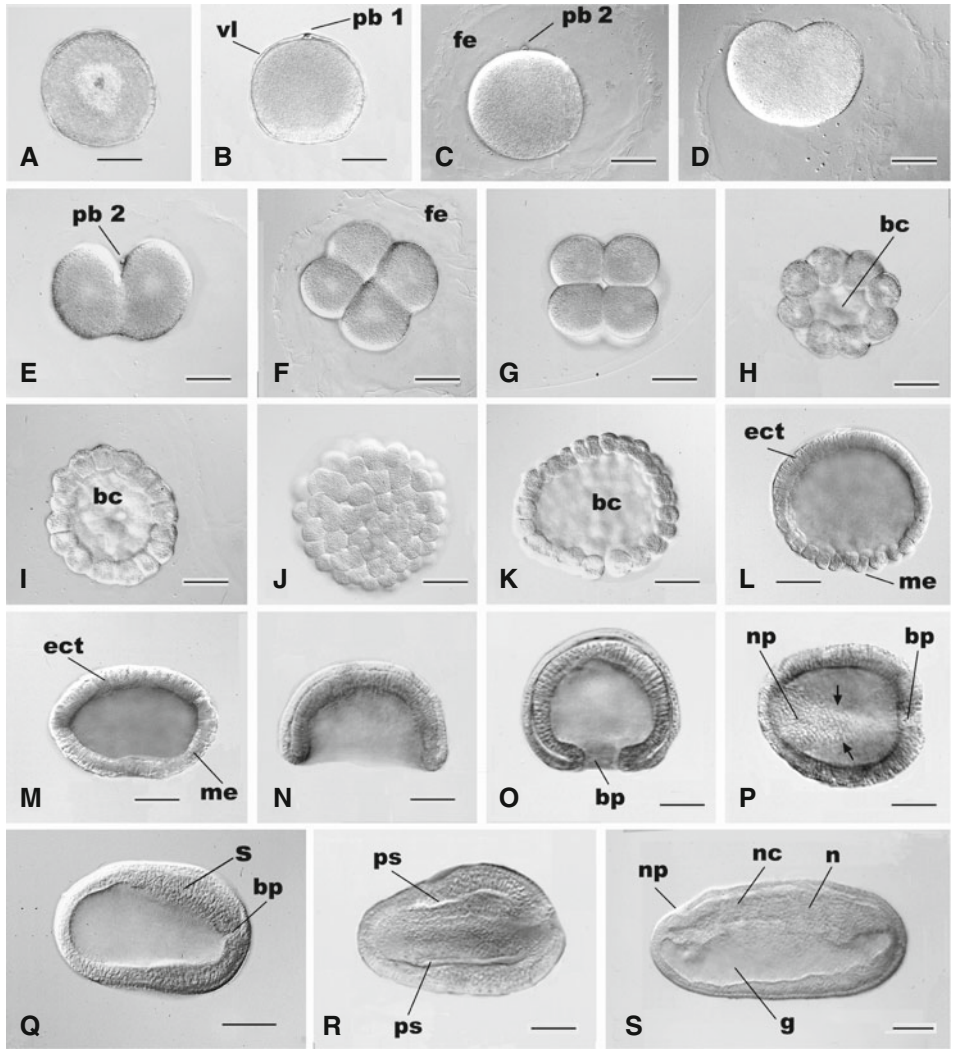

Fig. 3.2 Light micrographs of embryos of *Branchiostoma floridae*. (**A**) Primary oocyte with central nucleus and nucleus. The vitelline layer is not visible. (**B**) Spawned egg arrested at second meiotic metaphase. The vitelline layer (*vl*) is slightly elevated from the egg surface over the first polar body (*pb1*). (**C**) Zygote 20 min after insemination. The second polar body (*pb2*) is at the animal pole. The fertilization envelope (*fe*) has completely elevated, but collapsed in this fixed specimen. (**D**) An embryo at the onset of first cleavage, which begins at the animal pole. (**E**) Two-cell stage. Nuclei have divided, but the cells have not separated. (**F**) Two-cell stage viewed from the animal pole. *Fe* fertilization envelope. (**G**) Eight-cell stage viewed from the animal pole. (**H**) Early blastula. *bc* blastocoel. (**I**) Mid-blastula. All the blastomeres are approximately the same size. *bc* blastocoel. (**J**) Surface view of late blastula. (**K**) Optical section through late blastula. The cells at the vegetal pole are slightly larger and more loosely adherent than elsewhere. *bc* blastocoel. (**L**) Optical section through very late blastula. The future ectoderm (*ect*) is distinguished from the future mesendoderm (*me*) by tighter packing of the cells. (**M**) Early gastrula. The blastula has slightly flattened at the equator, which is the future blastoporal lip. The mesendoderm (*me*) has begun to invaginate. *ect* ectoderm. (**N**) Mid-gastrula. Invagination is complete and the blastopore is wide open. (**O**) Late gastrula. The blastopore (*bp*) has nearly closed. (**P**) Dorsal view of early neurula. Anterior is at left. The blastopore (*bp*) marking the posterior of the embryo is at the right. In amphioxus, the non-neural ectoderm (*arrows*) detaches from the edges of the neural plate (*np*) and migrates over it to fuse in the dorsal midline. Then the neural plate rounds up. (**Q**) Side view of early neurula. The blastopore (*bp*) is posterior and is covered by the non-neural ectoderm that has migrated over it. (**R**) Dorsal view of early neurula. Optical section through the forming somites. The anterior-most somites pinch off from presomitic grooves (*ps*) in the dorsolateral edges of the archenteron. Anterior at left. (**S**) Side view of neurula. Anterior at left. The neuropore (*np*) is open at the anterior end of the nerve cord (*nc*). The notochord (*n*) has pinched off from the dorsal medial mesoderm. *g* gut. All scale bars = 50 μm (Reprinted from Holland and Yu (2004) with permission from Elsevier publishers)

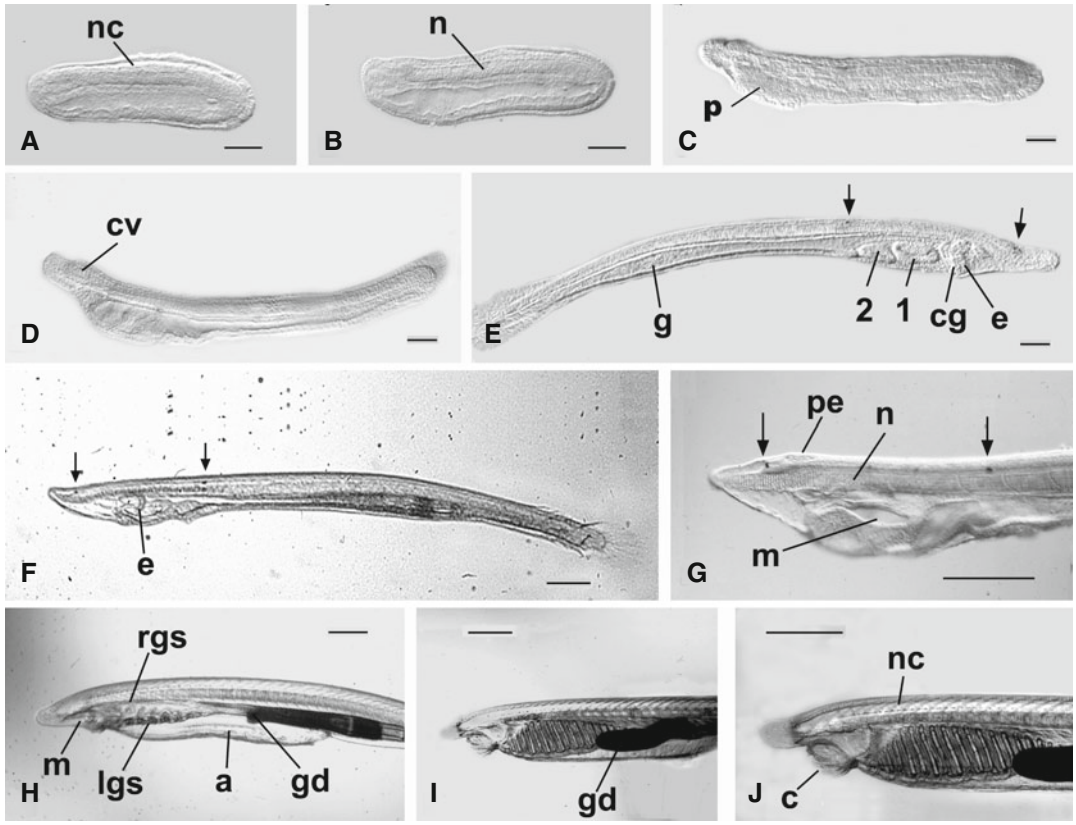

Fig. 3.3 Development of neurulae and larvae of amphioxus at 24 °C. Side views. Anterior at left in (**A**–**D**, **F**–**J**). anterior at right in (**E**). (**A**) Mid-neurula [18 h]. Nerve cord (*nc*). (**B**) Mid-neurula [20 h]. Muscular movements begin at this stage. *n* notochord. (**C**) Late neurula [24 h]. *p* pharynx. (**D**) Early larva [36 h]. The cerebral vesicle (*cv*) is visible at the anterior end of the nerve cord. The mouth has opened on the left side of the pharynx (not visible). (**E**) Six-day larva viewed from the right side. The first two gill slits (*1*, *2*) have penetrated on the right behind the club-shaped gland (*cg*), an enigmatic structure, which is just behind the endostyle (*e*), the thyroid homolog. *Arrows* show the first two pigment spots associated with photoreceptors in the nerve cord. The first of these, the more posterior one, first appears at the mid-neurula stage [15 h]. The anterior-most one, associated with the frontal eye, appears at 2.5 d. *g* gut. (**F**) Photograph of a live, 10-day larva with three gill slits. *E* endostyle visible through the transparent pharynx. *Arrows* show the first two pigment spots in the nerve cord. The dark material in the gut is food. The gut cells turn the color of the algal pigments. (**G**) Anterior end of a 10-day larva. *Arrows* show the first two pigment spots in the nerve cord. *N* notochord. In this fixed specimen, the pineal eye (*pe*), also called the lamellar body, is dorsal in the cerebral vesicle. *m* mouth, which in larvae is on the left side. (**H**) Side view of a living larva at the onset of metamorphosis (about 3 weeks). At the five to nine-gill-slit stage, the row of gill slits on the right migrates around the ventral side of the larva to become the left gill slits (*lgs*). Then a new row of gill slits (*rgs*) forms above them on the right. The mouth is still on the left, but has begun to migrate anteriorly. Atrial folds grow out and downward from above the gill slits to fuse in the ventral midline, forming the atrium (*a*). A diverticulum (*gd*) has begun to grow anteriorly from the gut. (**I**) A newly metamorphosed adult. The gut diverticulum (*gd*) extends anteriorly. (**J**) Higher magnification of the newly metamorphosed adult in I. Numerous pigment spots associated with photoreceptor cells (the organs of Hesse) have formed in the nerve cord (*nc*). The mouth has moved anteriorly, and the buccal cirri (*c*) have formed. These keep particles that are too large to pass through the digestive tract from entering the mouth. Each of the gill slits has become divided into two by downward growth of a medial bar. Additional gill slits form as the animal grows larger. Scale bars (**A**–**E**) = 50 μm. (**F**, **G**) = 100 μm. (**H**–**J**) = 500 μm (Reprinted from Holland and Yu (2004) with permission from Elsevier publishers)

in 1910 (Lankester and Willey 1890; Willey 1891; Hatschek 1893; Wilson 1893; Sobotta 1895, 1897a, b; Van der Stricht 1896; MacBride 1898; Cerfontaine 1906). At present, the pontano is used mainly for bivalve aquaculture (Giacobbe 2012) and *B. lanceolatum* is evidently still absent. A major difficulty for studies of early development was that researchers had to rely on natural spawnings

of the animals. Only rarely could they obtain eggs and sperm separately and thereby control fertilization to obtain synchronous cultures. An additional difficulty arose with the recognition that tunicates and amphioxus are closely related. Consequently, with the publication of a thorough study of ascidian tunicate development (Conklin 1905b), interpretations of amphioxus development, particularly those of Conklin himself (Conklin 1905a, 1926, 1932, 1933), were strongly influenced by the idea that amphioxus and tunicate development should be much the same (see Chapter 4). Although amphioxus and tunicates are closely related, this prejudice is quite surprising, as experiments done in the nineteenth century by Chabry (1887) and Wilson (1893) showed that ascidian development is mosaic while that of amphioxus is regulative (Chapter 4).

Given the small size of the embryos (eggs of all *Branchiostoma* species are about 140 μm in diameter), the difficulty of obtaining embryos, and the limitations of light microscopy together with the notion that ascidian and amphioxus development should be fundamentally the same, many misconceptions arose concerning amphioxus development. These were ultimately corrected by our electron microscopic studies, which began in the late 1980s when we rediscovered a population of amphioxus in Old Tampa Bay, Florida, first described by Wright (1890) and found that animals could be induced to spawn in the laboratory on the same days that they would normally spawn in the field. This meant that for the first time, amphioxus eggs and sperm could be obtained separately, allowing the events surrounding fertilization and very early development to be studied in detail (Holland and Holland 1989, 1990, 1991a, 1992, 1993a, b).

Fertilization

The second meiotic division of oocytes is completed about 10 min after fertilization (Fig. 3.2B). A second polar body is produced and groups of maternal chromosomes migrate to one side of the animal pole until the sperm nucleus migrates to them and a zygote nucleus is formed. The sperm has a flagellum, a round head, a single mitochondrion, and an acrosomal granule (Baccetti et al. 1972) that undergoes exocytosis, producing a long acrosomal tubule (Morisawa et al. 2004) that fuses with the egg (Holland and Holland 1992). Sperm/egg fusion follows the model of most other invertebrates having sperm with an acrosomal granule (Holland and Holland 1992).

There was considerable disagreement concerning the sperm entry point. The problem is that in light microscopy, the fertilizing sperm nucleus is first visible in the vegetal cytoplasm of the egg about 3 min after insemination. Therefore, although Sobotta (1895, 1897b) thought that the sperm might enter anywhere on the egg surface but preferentially entered the vegetal pole, Conklin and others were convinced that the sperm entered only near the vegetal pole (Cerfontaine 1906; Conklin 1932; Hatschek 1893). However, serial transmission electron microscopy (TEM) of eggs fixed at intervals of a few seconds after fertilization demonstrated that the sperm can enter in the animal half but, regardless of where it enters, migrates to the vegetal pole, arriving in the vegetal cytoplasm about 45 s after insemination where it decondenses (Fig. 3.4A; Holland and Holland 1992). Then, accompanied by a cloud of mitochondria, which appear to migrate along the astral rays of the sperm centrosome, the sperm nucleus migrates towards the animal half, meeting the maternal chromosomes to one side of the animal pole (Holland and Holland 1992). Although Conklin thought the path of sperm migration at the vegetal pole marked the future posterior pole of the embryo and larva, subsequent work showed that the lips of the blastopore, which forms around the equator of the blastula, constitute the posterior end of the embryo (Zhang et al. 1997).

As the sperm nucleus migrates to the vegetal pole, the egg undergoes cortical granule exocytosis (Fig. 3.2B). Cortical granules were first seen by Van der Stricht (1896) who mistakenly thought these were yolk granules that migrated into the interior of the egg after fertilization. This error was corrected by Sobotta (1895) and (Cerfontaine 1906), who noted the disappearance of the cortical granules at fertilization and the simultaneous appearance of a "second membrane" at the periphery of the oocyte. In contrast, Conklin, who had noticed that eggs of ascidian tunicates had no such cortical granules (Conklin 1905b) and believing that development in amphioxus must be essentially the same, mistook the cortical

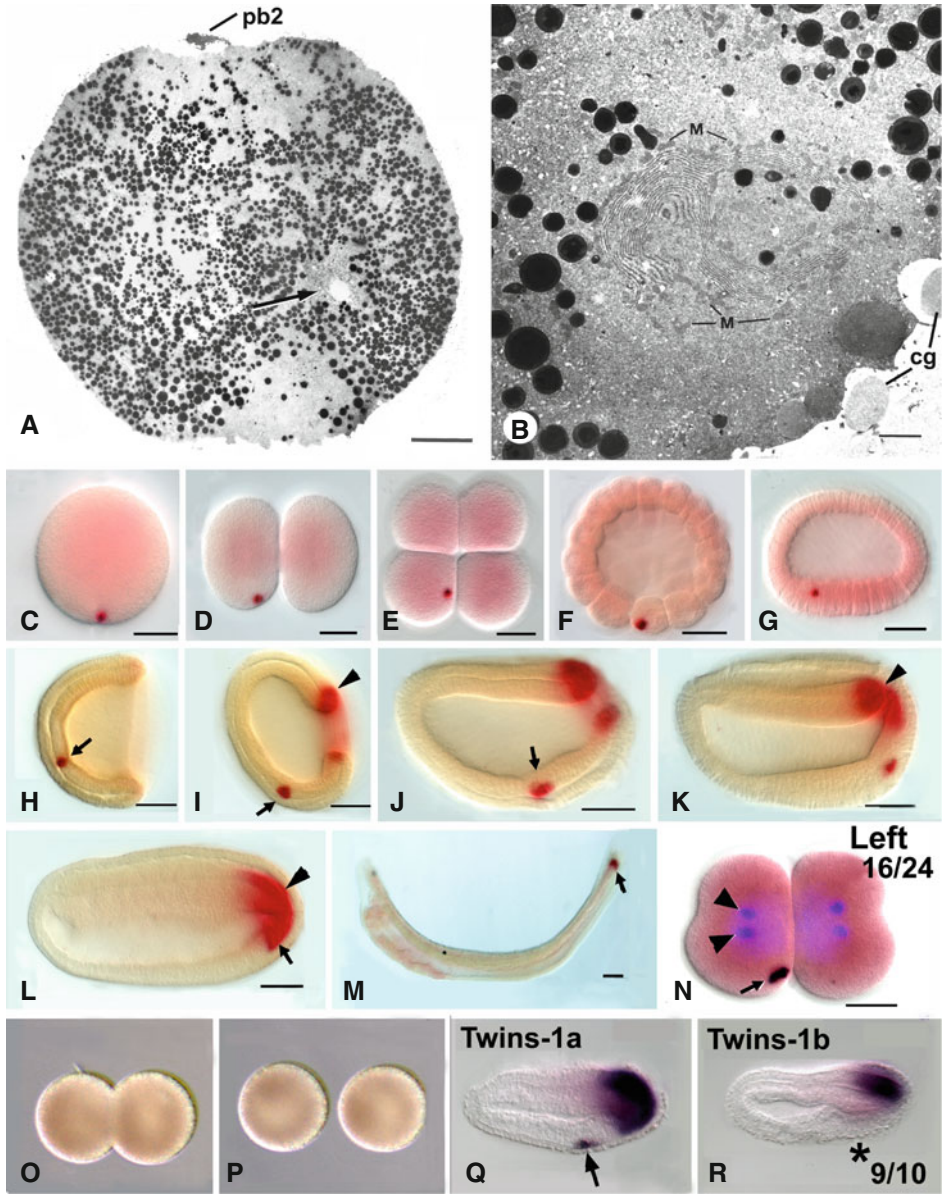

Fig. 3.4 Germ cells of *Branchiostoma floridae* are specified by pole plasm. (**A**) At 10-min post insemination, the pole plasm has coalesced at the vegetal pole of the egg. Second polar body (*pb2*) has formed and the sperm nucleus 9 (*arrow*) with an associated cloud of mitochondria is migrating into the animal half of the egg where it will join the female chromosomes. Scale = 20 μm. (**B**) Enlargement of the pole plasm showing whorls of endoplasmic reticulum surrounded by mitochondria (*M*). Scale = 1 μm. *cg* contents of cortical granules that have undergone exocytosis, but not yet dispersed. (**C**–**M**) Expression of the germ cell marker *Nanos* in embryos and larvae. Scale = 50 μm. C. *Nanos* mRNA is localized to the pole plasm in the fertilized egg and is segregated into a single cell until the mid-gastrula (H), when the *Nanos-containing* cell divides into a small group of cells (*arrows*, **I**–**M**). At the late gastrula stage, zygotic *Nanos* (*arrowhead*) is expressed around the blastopore (future tail bud). (**L**) By the mid-neurula, germ cells have reached the tail bud. (**M**) At the late neurula and larval stages, germ cells associate with each somite as it buds from the tail bud (Wu et al. 2011). (**N**) Onset of second cleavage. Out of 24 embryos labeled for another germ cell marker *Vasa*, 16 localized the germplasm to the left, vegetal blastomere, and 8 to the right, vegetal blastomere. (**O**–**R**) If the first two blastomeres are separated (**P**) and allowed to develop apart, germplasm (labeled for *Vasa*) is segregated into only one blastomere (**Q**, *arrow*). The other blastomere does not inherit any germplasm (**R**, *asterisk*) ((**A**, **B**) Reprinted from Holland and Holland (1992), (**C**–**R**) From Wu et al. (2011))

granules for mitochondria (Conklin 1905a). He argued that, as in ascidians, this mitochondrion-containing layer migrated vegetally after fertilization, finally accumulating over the astral rays at the posterior-vegetal end of the embryo where it constituted a "mesodermal crescent" destined to form much of the axial musculature (Conklin 1932). Other early studies failed to find this mesodermal crescent for the simple reason that it does not exist (Hatschek 1893; Van der Stricht 1896; Sobotta 1897b; Cerfontaine 1906).

Pole Plasm

In the vegetal cortex of the unfertilized egg are sheets of endoplasmic reticulum and associated RNA (Fig. 3.4A, B; Holland and Holland 1992). Shortly after fertilization, these sheets round up into whorls, excluding yolk granules from this region. Some of the early researchers mistook the pole plasm for the fertilizing sperm (Sobotta 1897b; Cerfontaine 1906). Alternatively, Conklin (1932) erroneously equated this relatively yolk-free zone with a mesodermal crescent destined to form myoplasm as in ascidian embryos (Conklin 1905b). During cleavage in *Branchiostoma floridae*, the pole plasm is segregated into a single cell. More recently, analysis of gene expression confirmed that the pole plasm expresses the characteristic germ cell markers *Vasa* and *Nanos*, which are also expressed in germ cells in the adult gonad, and thus constitutes the germplasm (Wu et al. 2011; Zhang et al. 2013). There are minor species differences in the development of the germ cells among species of *Branchiostoma*. In *B. belcheri*, the pole plasm is segregated into two cells during the fairly early blastula stage.

Cleavage and Gastrulation

First cleavage starts at the animal pole as depicted by Cerfontaine (1906) (Fig. 3.2D). Cleavage is equal (Fig. 3.2E–G). Second cleavage is at right angles, and third cleavage divides the embryo into an animal half and a vegetal half. Blastomeres are roughly equal in size, although sometimes vegetal blastomeres are slightly larger than animal ones (Fig. 3.2H–L). The blastomeres are not tightly adherent until the mid-late blastula. As a result, twins and even quadruplets are common in some egg batches.

There was little disagreement about cleavage and formation of the blastula. However, misinterpretations concerning the late blastula and gastrulation were rampant, chiefly because most researchers felt that in amphioxus, as in vertebrates, gastrulation in amphioxus had to involve some sort of involution. According to Lwoff (1892), the blastopore is posterior. He argued for considerable inrolling of tissue over its lips. Hatschek (1893) argued that the blastopore was dorsal and closed from front to back. Hatschek also felt that there were two particularly large cells, evidently mesodermal, similar to those in some annelids, that marked the posterior pole of the embryo. These cells were subsequently found not to exist. Cerfontaine (1906), in agreement with Lwoff, found that at the onset of gastrulation, at one side of the flattening vegetal plate, the cells were rounded and rather loose (Fig. 3.2L). He went on to describe preferential involution over the dorsal blastopore lip. However, Wilson (1893) correctly found that invagination was radially symmetrical. Morgan and Hazen (1900) disagreed, arguing that the dorsal side was less rounded than the ventral side. They also felt erroneously that cells dorsally were lighter and had fewer yolk granules than those ventrally. Conklin (1932) further clouded the picture. First, he thought that the cells of the (nonexistent) mesodermal crescent preferentially divided near the vegetal pole of the late blastula and early gastrula. Second, he believed that as invagination progressed, mesodermal pouches formed just inside of the ventral lip of the blastopore. They do not. He did correctly observe that as the blastopore began to close, the ventral side of the embryo elongates more than the dorsal side, but concluded that the mesodermal crescent grows dorsally so that it extends to the dorsolateral blastopore lip; then the arms of the crescent move anteriorly, giving rise to the mesodermal grooves, which subsequently form the somites. He argued that, as the mesodermal crescent extended dorsolaterally, the future notochord folds in under the

neural plate. Not only is there no mesodermal crescent, none of these movements of tissue around the blastopore occur.

Subsequent work has shown that gastrulation is far simpler than most of these earlier authors believed. Spotting of the fluorescent dye DiI on the blastopore lip at the beginning of gastrulation and following the dye as the blastopore closed demonstrated that the hollow blastula gastrulates by simple invagination with only a slight movement of cells over the lips of the gastrula (Fig. 3.5; Zhang et al. 1997). The "petite cells" that migrate into the interior of the archenteron and the epiboly described by Cerfontaine (1906) do not exist. The blastopore constricts with the tissue at the ventral side elongating more than the dorsal side. Importantly, Hirakow and Kajita (1991) found by scanning electron microscopy (SEM) that the cells around the blastopore of *Branchiostoma belcheri* were all about the same size, in contrast to some authors who claimed that the cells were smaller dorsally (Fig. 3.2M–O; Morgan and Hazen 1900; Cerfontaine 1906). At the late gastrula, each ectodermal cell develops a cilium, and the gastrula begins to rotate within the fertilization layer. About the same time, the gastrula begins to secrete a hatching enzyme which is thought to be a metalloproteinase (Denuce 1996).

The dorsal and dorsolateral cells of the inner layer of the gastrula (the hypoblast) comprise the future mesoderm. The remainder of the inner layer of the gastrula is endoderm (for fate maps at the four cell stage, see Fig. 3.6 and below). During the late gastrula, the notochord begins to form as a fold in the dorsal midline of the inner layer of the gastrula and presomitic grooves form on either side of the nascent notochord (Fig. 3.2R). Starting at the anterior end of the embryo, somites pinch off from the two dorsolateral grooves. At hatching, there are about three somites (Fig. 3.3). Simultaneously, the neural plate begins to flatten. The ectoderm on either side of the neural plate detaches from the neural plate and "walks" over it via lamellipodia (Fig. 3.7L) to fuse in the dorsal midline (Holland et al. 1996). Then the neural plate curls up to form the neural tube. In spite of

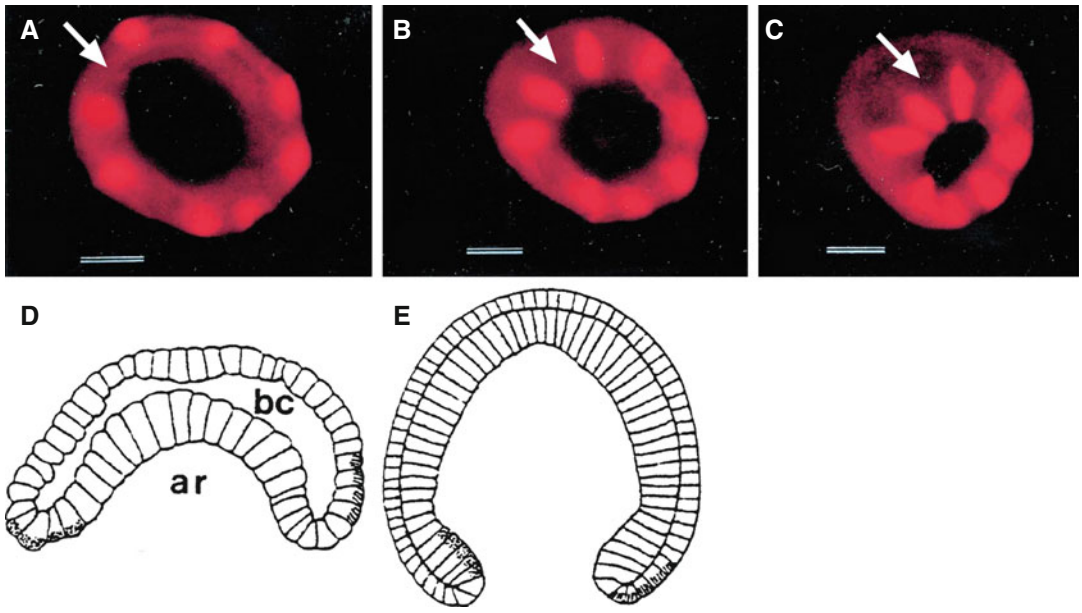

Fig. 3.5 DiI spotted around the amphioxus blastopore at the wide-open gastrula stage (**A**) and followed as the blastopore closes (**B**, **C**) shows that gastrulation occurs by invagination without involution. (**D**, **E**) Schematic diagram of the fate of DiI spotted on the lips of an early gastrula. A spot of dye on the edge of the blastopore (**D**) is barely internalized (**E**) by the late gastrula. A spot of dye just back of the blastopore edge (**D**) remains on the ectoderm as the blastopore closes (**E**). *Arrows* in (**A**–**C**) show the dorsal lip of the blastopore. *ar* archenteron, *bc* blastocoel (Reprinted from Zhang et al. (1997) with permission from Springer Verlag)

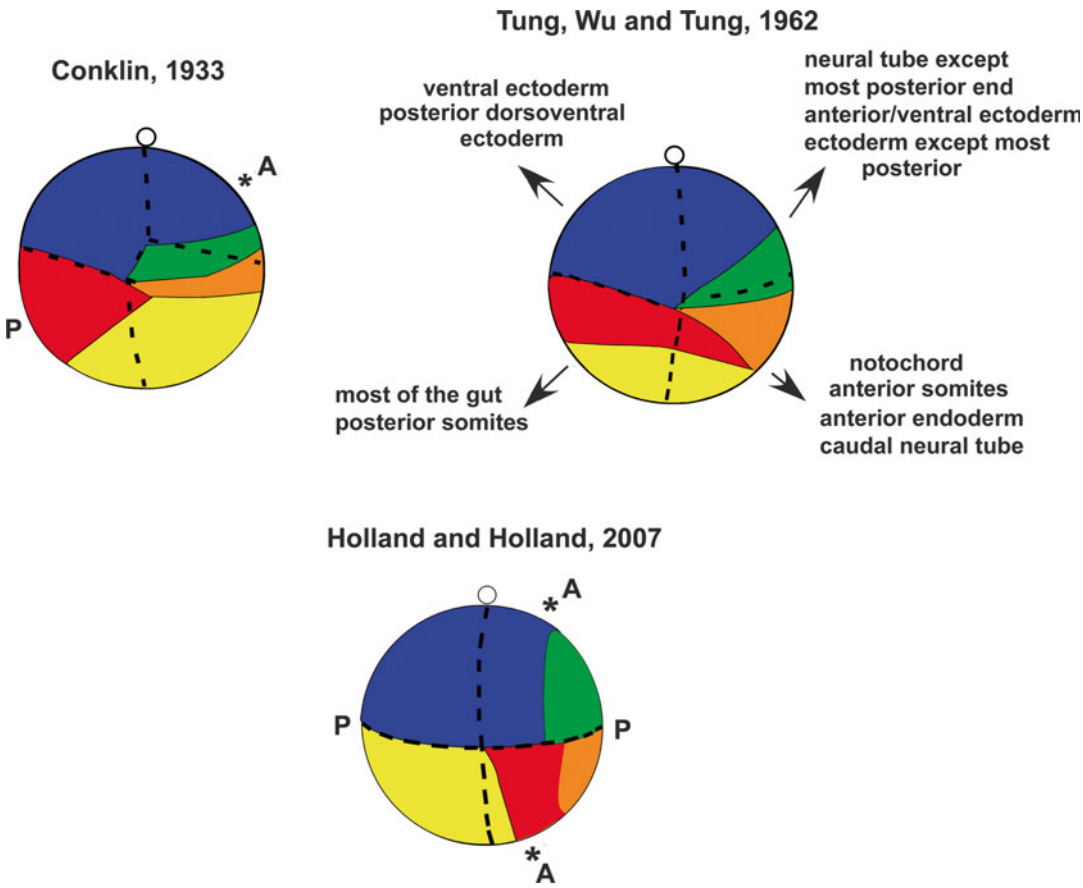

Fig. 3.6 Fate maps of amphioxus embryos at the 4-cell stage according to Conklin (1933), Tung et al. (1962b), and Holland and Holland (2007). The first two of these maps assumed that there was involution over the blastopore lips during gastrulation. The map of Holland and Holland takes into consideration the study of (Zhang et al. 1997), which showed that there is not involution over the blastopore lips as well as expression of developmental genes marking particular structures such as the future neural plate and non-neural ectoderm at the early gastrula stage (e.g., (Holland et al. 1996, 2000). A* anterior pole, P posterior pole. *Arrows* indicate the presumed fate of the adjacent portions of the embryo. *Dotted lines* indicate cell boundaries. The second polar body is at the animal pole. *Blue* non-neural ectoderm, *green* neural plate, *yellow* endoderm, *orange* somites, *red* notochord (Reprinted from Holland and Holland (2007) with permission from Oxford University Press)

misconceptions chiefly due to Conklin's "mesodermal crescent," there is no mesoderm ventrally until the neurula stage, when it forms as outgrowths from the somites (Kozmik et al. 2001).

Fate Map

Conklin was extremely influential. In 1905, he published a monograph on ascidian tunicate development (Conklin 1905b) and in the same year put forth the idea that amphioxus development was probably very like that in ascidians (Conklin 1905a). This is surprising since Chabry (1887) and Wilson (1893) working, respectively, on ascidians and amphioxus had already shown that development in ascidians is determinant or mosaic and that in amphioxus is indeterminant or regulative. Thus, Chabry (1887) found that if one of the first two blastomeres of an ascidian embryo was killed, the other could only develop into what it normally would have formed in the intact embryo; cell fates are largely fixed before first cleavage. In contrast, Wilson (1893) separated

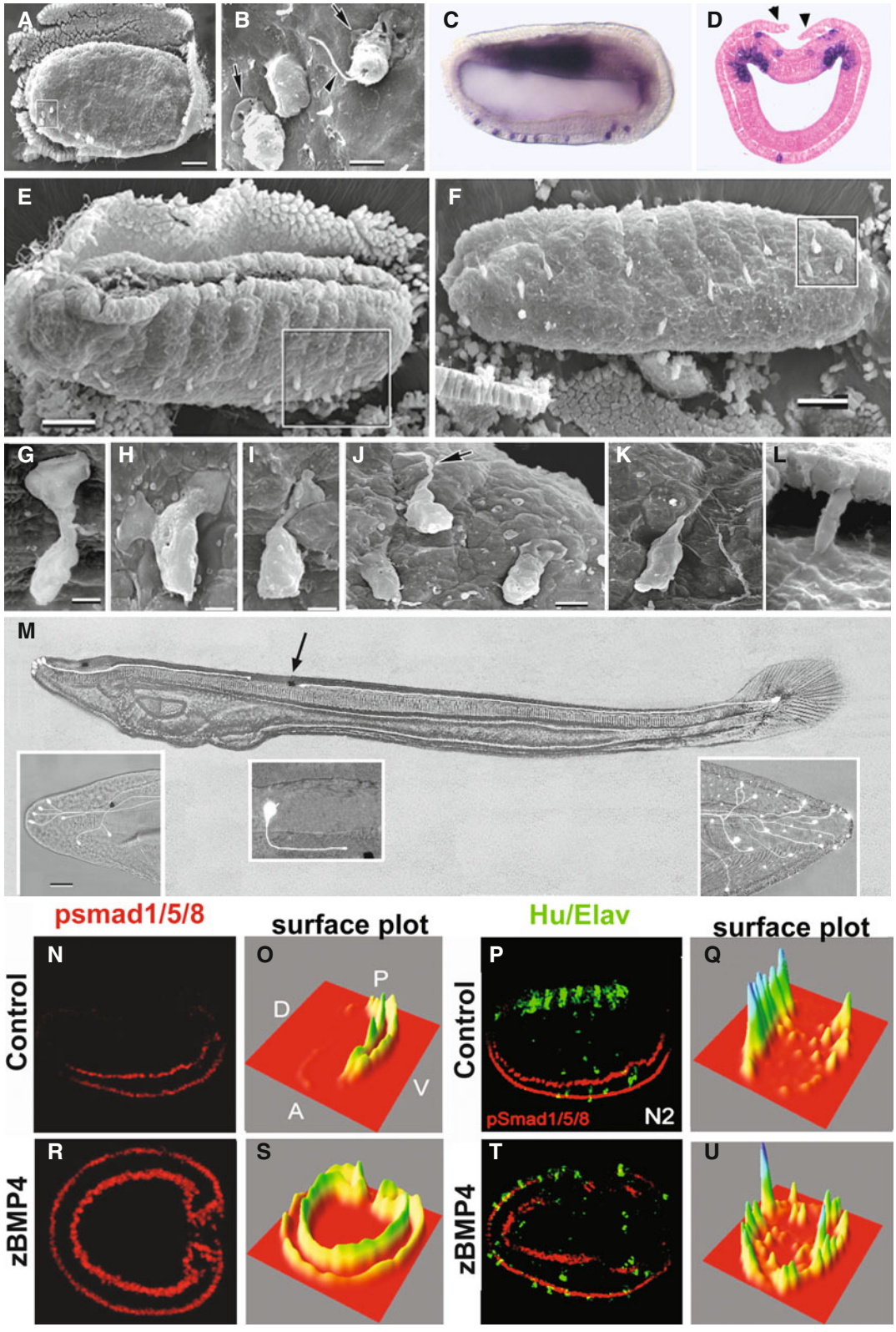
A
B
C
D
E
F
G
H
I
J
K
L
M
psmad1/5/8
surface plot
Hu/Elav
surface plot
N
O
P
Q
Control
D
P
V
A
pSmad1/5/8
N2
Control
R
S
T
U
zBMP4
zBMP4

blastomeres of amphioxus embryos and showed that the first two cells could each develop into a half-sized larva. Even the first four cells could develop into larvae, albeit incomplete ones. This is a major difference in development of the two species.

Even so, Conklin remained convinced that development in amphioxus and ascidians was fundamentally the same, stating "In preparation for the study of the development of wholly or partially separated blastomeres of Amphioxus, I have made a careful study of the typical development of that animal and find that it is more strikingly like that of ascidians than has been recognized hitherto" (Conklin 1933). Therefore, even though he repeated the experiments of Wilson on amphioxus and Chabry on ascidian tunicates and obtained essentially the same results as these previous authors, he presented a fate map of amphioxus embryos which is very like the fate map for ascidians (Fig. 3.6; Conklin 1933) and which later work showed is largely wrong (reviewed in Holland and Holland (2007); Chapter 4).

Thus, Conklin (1933) argued that the relatively yolk-free zone containing the pole plasm located near the vegetal pole of amphioxus zygotes (Fig. 3.4) constituted a myoplasm such as that which exists in ascidian eggs. He also hoped to find parallels between amphioxus and frog development. Although he could not find anything in amphioxus eggs like the gray crescent of frog's eggs, he was convinced it must exist and that small round cells at the dorsal lip of the blastopore constituted a crescent of mesodermal cells. In reality, there is no myoplasm and no gray crescent in amphioxus. However, in spite of the experiments of Chabry and Wilson and the failure of any other researcher to find a mesodermal crescent or gray crescent, Conklin's fate map (Fig. 3.6) became incorporated into a wide range of textbooks and publications. For example, Drach (1948) maintained that the only real difference in early development of amphioxus and tunicates was that determination of cell fates occurred earlier in tunicates than in amphioxus, while Balinsky (1981) elaborated upon the idea that mesoderm ventrally around the blastopore flowed dorsally

Fig. 3.7 Ectodermal sensory cells are "born" in the ventral midline of amphioxus embryos and migrate dorsally. Levels of BMP signaling control their number and position. For all whole mounts, anterior is to the left. (**A**–**B**, **E**–**L**) Scanning electron micrographs. (**A**) Side view of early neurula (14 h) with ectoderm removed, showing earliest ectodermal sensory neurons on the ventral side. Scale = 20 μm. (**B**) Enlargement of box in (**A**). Lamellate pseudopodia (*arrows*) extend from the cell bases. One cell has not yet lost its cilium (*arrowhead*). Scale = 3 μm. (**C**) Early mid-neurula. In situ hybridization showing *Delta* expression in ectodermal sensory cells ventrally. *Delta* is also expressed in the nascent somites and in scattered cells in the CNS. (**D**) Cross section through early neurula. In situ hybridization for *Delta*. One nascent ectodermal sensory cell ventrally expresses *Delta*. *Arrowheads* show the ectoderm adjacent the neural plate which has moved laterally over the neural plate but has not yet fused in the midline. *Delta* is also expressed in the nascent somites and scattered cells in the CNS. (**E**) Side view of late mid-neurula (16 h) with ectoderm removed. Ectodermal sensory cells are moving up the sides of the embryo. Scale = 20 μm. (**F**) Side view of late (18 h) neurula with ectodermal sensory cells having migrated dorsolaterally. Scale = 20 μm (**F**). (**G**–**I**) Enlargements of the ectodermal sensory cells within the box in (**E**). Each has one or two pseudopodia and has lost the cilium. Scale = 2 μm. (**J**) Enlargement of the box in (**F**). The ectodermal sensory cell at the top has reached its final position and is extending an axon (*arrow*), which will enter the CNS. Scale = 3 μm. (**K**) Ectodermal sensory cell beginning to extend an axon. Scale as in (**J**). (**L**) Ectodermal sensory cell with axon which has reinserted the apex into the ectoderm. It will soon regrow a cilium. (**M**) Larvae soaked in a DiI solution. The dye is preferentially taken up by the ectodermal sensory neurons. The whole larva is 4 days old; anterior to the left. Neurons in the anterior and posterior tips of the larva are sending axons towards the first photoreceptor to form (*arrow*). Inserts; show head, first photoreceptor, and tail of 30-day larvae. By 30 days, metamorphosis is in progress and the tail fin has been remodeled. (**N**–**U**) Zebrafish BMP4 (250 ng/ml) added to amphioxus embryos during the gastrula stage increases the number of ectodermal sensory cells and radializes their location. Concomitantly, the dorsal ectoderm is not specified as neural plate. (**N**, **R**) and (**P**, **T**) indicate double labeling for *pSmad1/5/8* (*red*) and *Hu/Elav* (*green*) at the late gastrula/early neurula stage. (**O**, **Q**, **S**) and (**U**) are quantitative surface plots of the fluorescence in (**N**, **P**, **R**) and (**T**), respectively. Controls (**L**–**O**) and zBMP4 treated (**P**–**S**). (**A**, **B**, **E**, **F**–**L** reprinted from Kaltenbach et al. (2009) and (**M**) reprinted from Holland and Yu (2002) with permission from John Wiley and Sons. (**N**, **R**) and (**P**, **T**) reprinted from Wu et al. (2011))

and extended anteriorly to form the somites, while the notochord cells involuted posteriorly. Other authors have copied Conklin's fate map (Browder et al. 1991; Khanna 2004; Bhatnagar and Bansal 2008) (e.g., while some have made minor variations (Gerhart and Kirschner 1997; Chea et al. 2005). Conklin's erroneous fate map also appears prominently on the web (http://www.biozoomer.com/2011/01/amphioxus-reproduction-post.html, http://www.preservearticles.com/201104085120/brief-note-on-the-fate-map-and-process-of-gastrulation-in-amphioxus.html, and http://darwin.wcupa.edu/beneski/devo2/pdf/07-Devo-amphioxus-HO.pdf).

One reason Conklin's fate map became the last word was that by the mid-twentieth century amphioxus populations in Sicily and Naples, Italy, had declined and embryos could not be obtained. The first attempt to reexamine the amphioxus fate map came in the late 1950s. T. C. Tung and colleagues working on the Chinese species of amphioxus, *Branchiostoma belcheri*, repeated several of these classic experiments (Tung et al. 1958; Tung et al. 1960, 1962a, b). They followed the fates of isolated blastomeres and tiers of blastomeres of *B. belcheri* embryos and performed dye labeling in order to reexamine the fate map (Fig. 3.6). They found that their data were not in agreement with those of Conklin (1933) (Fig. 3.6). For example, they argued that only the posterior portion of the neural plate derived from the vegetal cytoplasm, although Conklin (1933) had placed much of the future neural plate in the vegetal half of the early embryo. However, evidently influenced to some extent by Conklin's drawing, they depicted the future mesoderm in a band around the entire embryo just vegetal to the equator of the blastula (Fig. 3.6; Tung et al. 1962b). Finally they concluded that the amphioxus fate map was more like that of amphibian eggs than ascidian eggs. This modified fate map was accepted by some (e.g., (Browder et al. 1991; Gerhart and Kirschner 1997), but was, unfortunately, far from correct.

EvoDevo studies finally resulted in a thoroughly revised fate map (Holland and Holland 2007; Fig. 3.6). Most importantly, the demonstration by spotting DiI on the lip of the wide-open blastopore of *Branchiostoma floridae* showed conclusively that there is only a slight involution over the blastopore lip (Fig. 3.5; Zhang et al. 1997). Therefore, the vegetal half of the egg and blastula is destined to become mesendoderm and the animal half ectoderm. The equator of the blastula is the future blastoporal lip. Secondly, expression of the ventral mesoderm marker, *AmphiVent*, demonstrated that at the early neurula stage, ventral mesoderm arises from ventral outgrowths of the somites (Kozmik et al. 2001). These outgrowths fuse laterally and migrate between the ectoderm and endoderm as sheets of mesoderm. The left and right sheets of mesoderm fuse in the ventral midline. Therefore, at the blastula stage, the presumptive mesoderm is all located dorsally (Fig. 3.6; Holland and Holland 2007). At the early gastrula stage, the future neural plate becomes visible by in situ hybridization when the mesendoderm invaginates and first comes into contact with the ectoderm. As soon as this happens, *Distalless* which was expressed throughout the ectoderm at the onset of gastrulation becomes downregulated in the future neural plate (Holland et al. 1996), while one of the two *SoxB* genes turns on there (Holland et al. 2000).

Transmission electron microscopy also helped clarify misconceptions made on the basis of light microscopy that cells at the dorsal lip of the blastopore were substantially different from those at the ventral lip. S.C. Wu, who had published with the Tungs and been unable to work during the cultural revolution in China, returned to Qingdao and began to publish on early development of *Branchiostoma belcheri* (Wu 1986), while Hirakow and Kajita, who also obtained material in Qingdao, China, described early development of the fertilized egg through the early larva with TEM and scanning electron microscopy (SEM) (Hirakow and Kajita 1990, 1991, 1994). They found that at the mid-gastrula stage, one surface of the blastopore lip was "smoother" than the others. This might be because at the mid-gastrula, cell division decreases in the ectoderm and increases in the endoderm; however, some ectodermal cells around the blastopore continue to divide – more at the dorsal lip than at the ventral lip (Holland and Holland 2006). As cells divide

they round up, which would give a transient rougher appearance in SEM. Later during gastrulation, Hirakow and Kajita (1991) could detect no difference between cells at the dorsal and ventral lips of the gastrula.

Spemann's Organizer

The first experiments to determine if amphioxus has an equivalent of Spemann's organizer were by Tung et al. (1962a). Because it is impossible to distinguish dorsal from ventral or lateral in early amphioxus gastrulae, they cut out pieces of the blastopore lip at random and inserted them into the blastocoel of a host embryo. As the embryos are very small – no more than 300 μm in diameter – it is impossible to know just how much tissue was transplanted. Even so (Tung et al. 1962a) found that in about 25 % of the embryos with transplants, a partial secondary axis was obtained. Therefore, they concluded that amphioxus has a homolog of Spemann's organizer. However, these results are difficult to interpret because, first, it is not possible to determine which part of the blastoporal lip was transplanted; second, the small size of the gastrula makes it difficult to dissect a small portion of tissue; and, third, it is not possible to distinguish host from donor tissue. In the absence of photographs (the authors made line drawings of their results) and without the experiments being independently verified (they have never been repeated), it is uncertain whether the results reflected a true induction of a secondary axis.

Even so, comparisons of gene expression patterns and functions between amphioxus and vertebrates have provided convincing evidence that amphioxus has an equivalent of Spemann's organizer or the node in vertebrates. The key technical breakthrough was the construction of 5 gridded cDNA libraries of unfertilized eggs, embryonic stages, and adults of *Branchiostoma floridae* and the end sequencing (EST) of 210,000 clones (Yu et al. 2008b). This allowed the rapid determination of expression patterns of a large number of amphioxus homologs of genes expressed in Spemann's organizer in vertebrates (Yu et al. 2007, 2008b). These studies showed that the dorsal lip of the blastopore of the amphioxus gastrula expresses *Nodal*, its antagonist *Lefty*, *Fgf8/17/18*, and homologs of other genes expressed in Spemann's organizer of vertebrates. Bone morphogenic proteins (*BMPs*) and their antagonists are also expressed in patterns in amphioxus similar to those of their homologs in vertebrates. Moreover, addition of vertebrate BMP4 protein to early amphioxus embryos caused the loss of all dorsal and anterior structures; the notochord and nerve cord were absent, but the larvae had a tail fin. Conversely, upregulation of the Nodal signaling pathway anteriorized embryos and converted all the ectoderm to neuroectoderm (Onai et al. 2010). Moreover, inhibition of Fgf signaling during early cleavage inhibited gastrulation; treatment at the early neurula inhibited formation of the anterior-most somites (Bertrand et al. 2011). These results demonstrated that amphioxus has a homolog of Spemann's organizer and that such an organizer was probably present in the ancestral chordate.

Expression and functional studies of additional genes indicated that anterior-posterior (AP) patterning during the gastrula stage involves signaling by both Wnt/β-catenin and retinoic acid (RA). Wnt/β-catenin signaling around the blastopore specifies posterior identity. Anteriorly, Wnt/β-catenin signaling is suppressed by a number of antagonists (Onai et al. 2009, 2012). Several Wnts are expressed around the blastopore. *Wnt1* is noteworthy as it is expressed around the single gut opening of cnidarians and the posterior gut opening of most bilaterians. This is very like the situation in sea urchin embryos (Emily-Fenouil et al. 1998; Angerer and Angerer 2000; Bandhorst and Klein 2002), indicating that the ancestral chordate probably used posterior Wnt/β-catenin signaling and its anterior suppression to mediate AP patterning (Yu et al. 2007; Holland 2002). Subsequent to genome duplications in vertebrates, expression of *Wnt1* around the blastopore was lost; presumably its function has been taken over by other Wnts such as *Wnt3*, which preferentially signal via β-catenin. Functional studies have demonstrated that Wnt/β-catenin signaling in tissue around the amphioxus blastopore specifies

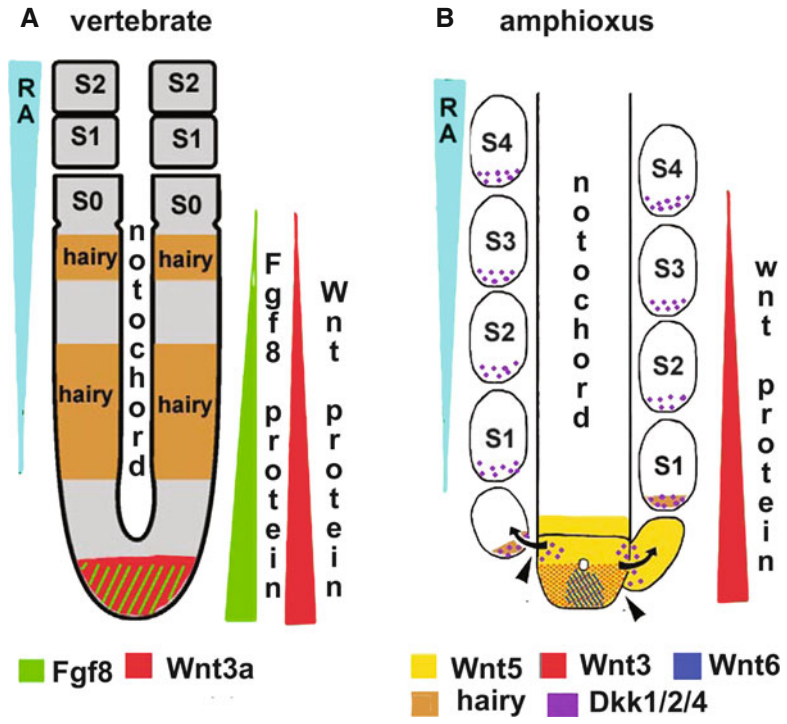

Fig. 3.8 Somite segmentation from the tail bud in vertebrates (**A**) and amphioxus (**B**) is similar except that in amphioxus, somites bud off directly from the tail bud and not from bands of presomitic mesoderm as in vertebrates. In both Wnt/β-catenin signaling from the tail bud is opposed by an anterior gradient of retinoic acid (*RA*) signaling. Expression of the Notch pathway member *hairy* is involved in specification of segment boundaries. At least in amphioxus and probably also in vertebrates, Wnt/β-catenin signaling is suppressed in the posterior portion of each somite – in at least amphioxus (T. Onai and L.Z. Holland, unpublished data) and probably vertebrates as well – by the Wnt antagonist, Dkk1/2/4 (Zhang and Mao 2010; Pedersen et al. 2011)

posterior identity, but does not specify position along the AP axis (Onai et al. 2009).

During the gastrula stage, position along the AP axis is specified by retinoic acid (RA) signaling. RA, a natural morphogen synthesized from vitamin A, binds to heterodimers of the retinoic acid receptor (RAR) and retinoid X receptor (RXR), which then act as transcription factors to activate direct targets. The expression of RAR is taken to reflect the level of RA signaling. RAR is expressed throughout the mesendoderm of the amphioxus gastrula (Escriva-Garcia et al. 2002). Of 40 genes with spatially restricted expression in the amphioxus gastrula, only *HNF3-1*, *Hox1*, and *Hox3* are direct targets of RA (Koop et al. 2010). *HNF3-1* is expressed in the dorsal/posterior mesendoderm and ventral/anterior mesendoderm, while the two Hox genes are expressed in both germ layers around the blastopore with Hox3 more strongly expressed dorsally (Koop et al. 2010). These three genes are all upregulated by exogenous RA and their expression patterns expanded. RA-treated embryos fixed at the neurula and larval stages show that the heads have been respecified as more posterior tissues.

It is highly likely that the patterning of the amphioxus gastrula reflects the mechanism that was present in the ancestral chordate with RA directly regulating Hox and *HNF3* genes during the gastrula stage. For vertebrates, because of extensive tissue movements during gastrulation, experiments to investigate direct targets are difficult to interpret. Even so, manipulation of RA, BMP, Fgf, and Wnt signaling during the gastrula stage of vertebrate embryos results in defects in anterior-posterior and dorsoventral patterning at the late gastrula/neurula stages similar to those

that result from comparable experiments in amphioxus (Chapman et al. 2002; Hashiguchi and Mullins 2013).

The Neurula

At the late gastrula, all the ectodermal cells develop cilia, and the gastrula begins to rotate within the fertilization envelope. Before hatching, the anterior somites begin to pinch off from the presomitic grooves starting at the anterior end of the late gastrula. As the neurula elongates, somites continue to pinch off from the presomitic grooves. By the late neurula stage, when there are 8–12 somites, somites begin to pinch off one at a time from the tail bud – for a total of about 57–60 on each side in *Branchiostoma floridae* (Boschung and Gunter 1962) and 62–66 in *B. belcheri* (Henmi and Yamaguchi 2003). Thus, the anterior somites are formed enterocoelically and the remainder by schizocoely. Formation of the somites from the tail bud is essentially like that in vertebrates with many of the same genes expressed (Fig. 3.8). However, in vertebrates, bands of presomitic mesoderm intervene between the tail bud and the budding somites.

The dorsal side of the late gastrula flattens to form the neural plate. Once the neural plate forms, the non-neural ectoderm moves over the neural plate (Fig. 3.7D; 3.9D). There was considerable controversy as how this is done. The majority opinion, which is incorrect, was that the ectoderm moved anterior from the posterior end of the embryo to cover the neural plate (Kowalevsky 1867; Hatschek 1893; Cerfontaine 1906; Conklin 1932). Samassa (1898) was closer to the truth. He thought that ectoderm lateral to the neural plate extended over the neural plate to fuse in the center, with fusion extending anteriorly and posteriorly over the blastopore (Samassa 1898). Scanning and transmission electron microscopy ultimately showed that Samassa (1898) was nearly correct – after the neural plate flattens, sheets of ectoderm adjacent the neural plate detach from it and migrate from the sides over the neural plate to fuse in the dorsal midline starting at the anterior end of the embryo (Hirakow and Kajita 1994; Holland et al. 1996). In *Branchiostoma floridae* at room temperature, the whole process requires about 15 min. After the ectoderm covers the neural plate, the neural plate rounds up into a tube. A neuropore remains open at the anterior end of the embryo and the lumen of the CNS remains continuous with the lumen of the gut via the neurenteric canal.

LATE DEVELOPMENT

Larvae and Metamorphosis

Amphioxus is considered a direct developer. That is, metamorphosis reorients the mouth, gill slits, and endostyle, but many larval structures persist into the adult (Fig. 3.3). This is important because the results of many electron microscopic studies starting in the 1960s, which were chiefly on adults, are mostly applicable to larvae as well (e.g., Flood (1966, 1975b), Welsch (1968)). By definition, the larval stage begins when the mouth, thought to be a modified gill slit, opens on the left. In *Branchiostoma floridae* this is about 30 h after fertilization at 24 °C. At this time, there is one gill slit, and the major organs are developing. The larval kidney (Hatschek's nephridium) is on the left, between the ectoderm and the anterior-most somite (Hatschek 1884, 1893, Van Wijhe 1893; Legros 1910; Goodrich 1933; Ruppert 1996). It has been quite controversial as to whether amphioxus has a heart (reviewed in Holland et al. 2003). For example, Franz (1933) argued that amphioxus had no heart (Franz 1933), while Paxual-Anaya et al. (2013) maintain that amphioxus lacks a "proper heart." There is a subenteric contractile vessel capable of smooth-muscle-driven peristalsis (Rahr 1981). The direction periodically reverses at least in some species of *Branchiostoma*. However, gene expression, especially for *tinman* (*Nkx2.5*), considerably strengthened the idea that the contractile vessel, even if not a "proper heart," is homologous to other chordate hearts (Holland et al. 2003).

The endostyle, a homolog of the vertebrate thyroid gland, develops on the right side of the

larva (Van Wijhe 1907; Conklin 1932; Olsson 1983), and behind it the club-shaped gland forms (Fig. 3.3E, F). The developing endostyle expresses genes including *Pax2/5/8* characteristic of the developing vertebrate thyroid (Kozmik et al. 1999, 2007). At metamorphosis, the endostyle migrates to the floor of the pharynx. It secretes proteins, at least some of which are iodoproteins, used in feeding (Kobayashi and Tsuneki 1983; Fredriksson et al. 1984, 1985). The function of the club-shaped gland was controversial, but the consensus is that it is secretory, perhaps involved in larval feeding (Legros 1898; Conklin 1932; Olsson 1983; Gilmour 1996; Lacalli 2008b; Holland et al. 2009). Histochemistry showed that it secretes mucoproteins (Holland et al. 2009). At metamorphosis, the club-shaped gland undergoes apoptosis and disappears (Holland et al. 2009).

The ciliated pit, open to the environment on the left side of the larva, fuses with the left anterior diverticulum of the gut (Hatschek's diverticulum). At metamorphosis, it becomes Hatschek's pit (Hatschek 1884), which is considered homologous to the vertebrate adenohypophysis (Van Wijhe 1907). During development, genes such as *Pax6*, which are characteristically expressed in the developing adenohypophysis of vertebrates, are also expressed in either the ciliated pit and/or Hatschek's diverticulum in amphioxus (Glardon et al. 1998). Two gill slits form within the first 2 days of development. By 36 h, the anus is open (Stokes 1996). In the wild, the larvae grow faster in summer, presumably because the temperature is higher in summer and the food more abundant. As the larvae grow, they add gill slits. About the eight-gill-slit stage, which in *Branchiostoma floridae* occurs about 3 weeks after fertilization at 30 °C, a gradual metamorphosis begins.

Metamorphosis, which can be triggered by T3 thyroid hormone (Paris et al. 2008), consists first of the outgrowth of folds of the body wall over the gill slits which fuse in the ventral midline to form the atrial cavity. The current of water that enters the mouth exits the gill slits and reaches the exterior via the atrial pore at the posterior end of the atrial cavity. Apoptosis of the club-shaped gland begins upon the addition of T3 thyroid hormone (Holland et al. 2009). Next, a second row of gill slits appears on the right above the first, and the first row begins to migrate to the left side. A bar grows from dorsal to ventral and divides each gill slit into two (Fig. 3.3H–J). The mouth migrates to the anterior end of the larva and cirri grow from the edges of the mouth (Fig. 3.3J). These cirri are studded with mechanosensory cells. They are capable of regeneration (Kaneto and Wada 2011) and function to keep large particles out of the mouth and pharynx. The larval tailfin, the rays of which are composed of ciliary rootlets, is remodeled (Fig. 3.7M; Flood 1975a; Mansfield and Holland 2015). Finally, the anus then moves from the right side to the left (Stokes and Holland 1995b) and the endostyle migrates to the ventral midline of the pharynx. Interestingly, if the anterior or posterior tips of adults are cut off, they can regenerate (Somorjai et al. 2012).

Photoreceptors

Amphioxus lacks image-forming eyes, but has several types of photoreceptors. At the midneurula stage, the first photoreceptor develops in the ventral midline of the nerve cord at the level of somite 4 (Fig. 3.7M). This is the first "organ of Hesse" and consists of two neurons (microvillar photoreceptors) and one pigment cup cell. The neurulae are positively phototropic, swimming up and towards the light. Later during the larval stage, additional organs of Hesse consisting of a single neuron and a single pigment cup cell develop along the neural tube from the posterior portion of the cerebral vesicle (forebrain + small midbrain) to the posterior tip of the animal (Hesse 1898; Eakin and Westfall 1962; Nakao 1964). These photoreceptors contain melanopsin and are maximally sensitive to blue light (del Pilar Gomez et al. 2009; del Pilar Gomez and Nasi 2010; Pulido et al. 2012). There are three other kinds of photoreceptors in the CNS. The Joseph cells are also microvillar but lack associated pigment cells, while two (the frontal eye and the lamellar body) are ciliary (Figs. 3.7M

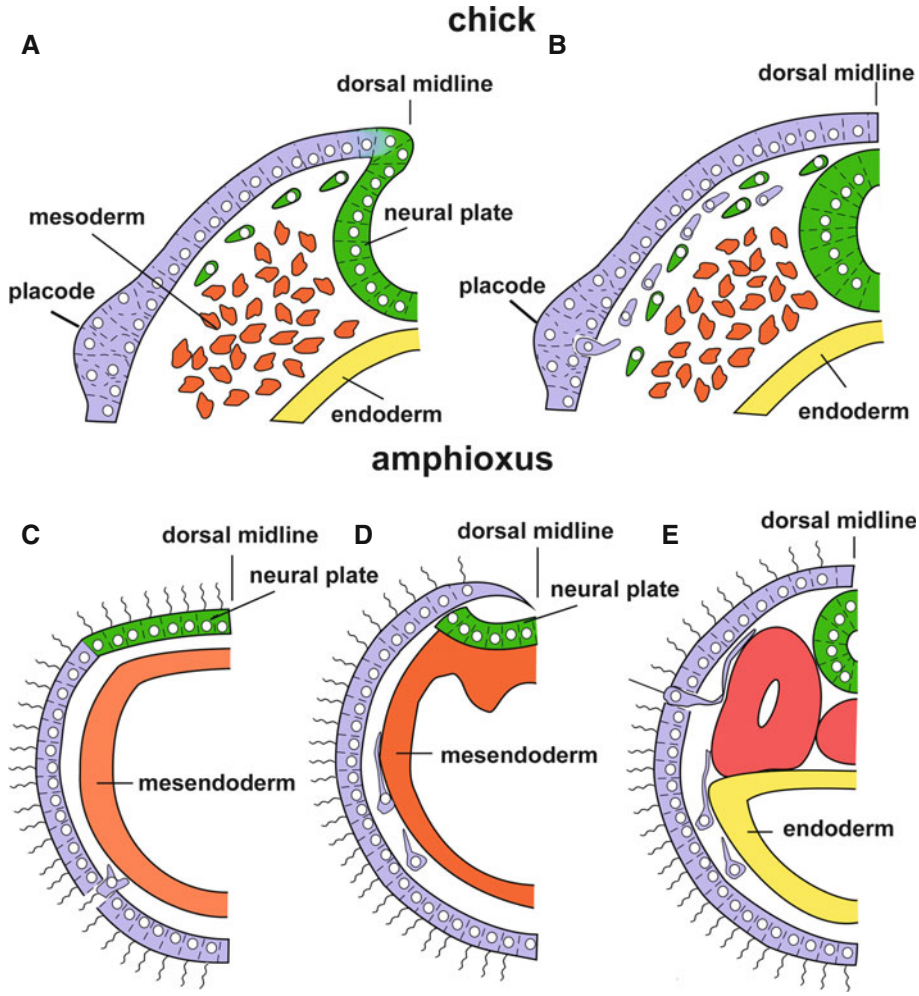

Fig. 3.9 Migration of neuroblasts from neurogenic placodes in the chick (**A**, **B**) is similar to migration of ectodermal sensory cells in amphioxus (**C**–**E**). In the chick, neuroblasts migrate from the neurogenic placodes (**A**) and contribute to cranial ganglia (**B**), while neural crest cells (*green*) migrate from the neural folds in the opposite direction. (**C**–**E**) In amphioxus, ectodermal sensory cells are generated in the ventral ectoderm; lose their cilia and migrate dorsally (**C**); generate axons (**D**), which grow into the CNS; develop a specialized cilium; and reinsert into the ectoderm (**E**) (After Holland (2009))

and 3.10; Lacalli et al. 1994). The Joseph cells are located dorsally in the posterior portion of the cerebral vesicle (Boveri 1904; Joseph 1904; Nakao 1964). They also contain melanopsin and have electrical properties similar to those of the organs of Hesse (Eakin and Westfall 1962; Koyanagi et al. 2005; Pulido et al. 2012). At the early larval stage, the frontal eye, which consists of pigment cells and several photoreceptor cells, forms, and the larvae orient to the light as they hang in the water column and filter feed (Fig. 3.10; Stokes and Holland 1995a). During the larval stage, the cilia of the frontal eye extend out through the neuropore. The lamellar body, which is a ciliary photoreceptor, is located dorsally in the cerebral vesicle of the larva in the equivalent of the forebrain (Fig. 3.10; Lacalli et al. 1994). It is not associated with pigment cells. Morphologically, it is very much like the pineal in the larval lamprey (Cole and Youson 1982) and has been suggested to be involved in circadian rhythms (Wicht and Lacalli 2005).

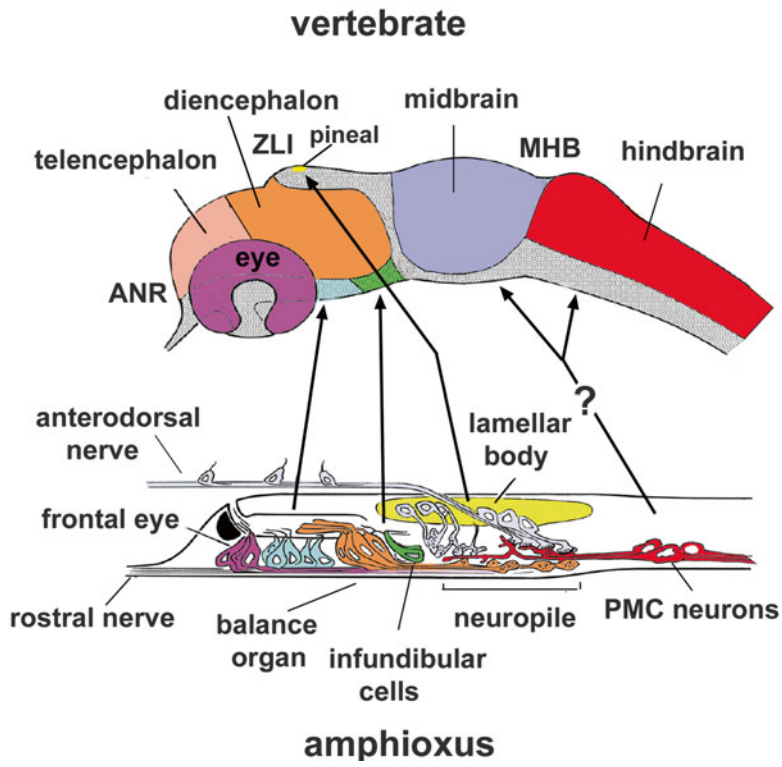

Fig. 3.10 Comparison of neuroanatomy between the vertebrate and amphioxus CNS. Amphioxus lacks a telencephalon. The frontal eye has been homologized with the vertebrate paired eyes. In both vertebrates and amphioxus, neuronal processes extend posteriorly to the midbrain. Infundibular cells, which secrete an extracellular fiber that extends in the neural canal, are characteristic of the diencephalon. The pineal eye of vertebrates is homologous to the lamellar body of amphioxus. Motor neurons are characteristic of the midbrain and hindbrain in both vertebrates and amphioxus. In vertebrates *ANR*, *ZLI*, and *MHB* function as organizers. Amphioxus has homologs of these regions, but they may not function as organizers (After Lacalli (2008a) with permission from Elsevier publishers)

Development of the Central Nervous System (CNS)

Gene Expression During Neurogenesis

The first question addressed by studies of genes and development in amphioxus concerned evolution of the vertebrate brain. Before the EvoDevo era, there were several competing theories concerning homology of the amphioxus CNS and the vertebrate brain. Gans and Northcutt (1983) postulated that the portion of the vertebrate head anterior to the posterior hindbrain was a vertebrate invention. They based this argument on the fact that somites in vertebrates only extends as far anteriorly as the posterior part of the vertebrate hindbrain, whereas in amphioxus somites extend to the anterior tip of the animal. This is essentially a partial-brain theory as also advocated by Langille and Hall (1989). In contrast, others argued that the cerebral vesicle is equivalent to the entire vertebrate brain or to at least the vertebrate brain minus the telencephalon (the big-brain theory) (Stieda 1873; Huxley 1875; Ayers 1890, 1907; Guthrie 1975). Other theories were the no-brain theory (amphioxus is essentially brainless; the vertebrate brain is an entirely new structure) (Berrill 1955; Garstang 1960) and the small brain theory (amphioxus has a tiny, rudimentary brain, which expanded in the vertebrate lineage) (Balfour 1885; Delsman 1922).

EvoDevo of amphioxus strengthened the idea that amphioxus has a brain and showed that

regional patterning of the amphioxus brain is very like that of vertebrate brains. In the early 1990s, N.D. Holland, L.Z. Holland, and P.W.H. Holland' inspired by the finding of conserved collinear expression of Hox genes along the body axis of flies and in the CNS of the mouse (reviewed in De Robertis et al. 1990), decided to address the question of how the vertebrate brain evolved by examining expression of Hox genes in the CNS of amphioxus. Our first paper on genes and development in amphioxus showed that *Hox3* is expressed in the amphioxus CNS with an anterior limit at the level of the boundary between somites 4 and 5 – just anterior to the first photoreceptor to form (Fig. 3.11; Holland et al. 1992). This is similar to expression of *Hoxb3* in vertebrate brains with an anterior limit at the boundary between rhombomeres 4 and 5 in the hindbrain (Manzanares et al. 2001). This comparison indicated that amphioxus has a homolog of the vertebrate hindbrain and, since there is a considerable amount of nerve cord anterior to the *Hox3*-expressing zone, the data suggested that there is also a forebrain and/or midbrain. This study was accompanied by sequencing of the amphioxus Hox cluster. Although it was initially claimed that amphioxus has two Hox clusters (Pendleton et al. 1993), it was since shown that amphioxus has a single cluster of 15 colinear Hox genes, which, with the possible exception of *Hox14* and *Hox15*, likely represents the Hox cluster in the ancestral chordate (Garcia-Fernandez and Holland 1994; Ferrier et al. 2000; Holland et al. 2008a). This is important as it is good evidence that the four clusters of Hox genes in vertebrates probably evolved from two rounds of whole-genome duplications as proposed by Ohno (1970). Even stronger evidence was obtained from sequencing the entire genome of *Branchiostoma floridae*, which not only confirmed that amphioxus had not undergone any whole-genome duplications but also showed that the amphioxus genome shared remarkable synteny with vertebrate genomes (Putnam et al. 2008). This result allowed reconstruction of 17 ancestral chordate linkage groups (chromosomes) and supported the validity of using amphioxus as a proxy for the ancestral chordate in studies of how the vertebrates evolved from their invertebrate ancestors.

Subsequent studies of developmental gene expression complemented with transmission electron microscopy (TEM) of serial fine sections have elaborated upon this result. Fairly extensive gene maps of the CNS of neurulae and larvae compared to those of vertebrates have shown that not only does amphioxus have a hindbrain, but it also has a diencephalic forebrain, a small midbrain, and a spinal cord (Figs. 3.10 and 3.11). For example, at the neurula stage the cerebral vesicle expresses a suite of homologs of genes expressed in similar patterns in the developing vertebrate forebrain (Sánchez-Arrones et al. 2009). These genes include *Otx*, *Pax6*, and *Fgf8/17/18* (Williams and Holland 1996; Glardon et al. 1997; Bertrand et al. 2011) expressed throughout the amphioxus cerebral vesicle and *Six3/6*, *FoxG1*(*BF1*), and *Dlx* (Holland et al. 1996; Toresson et al. 1998; Kozmik et al. 2007) expressed at its tip. *FoxG1* is a telencephalon marker in vertebrates, but it is also expressed in the developing retina, a diencephalic derivative (Shimamura and Rubenstein 1997). Taken together with evidence from serial TEM (Lacalli 1996a, b), it is likely that expression of *FoxG1* (*BF1*) at the tip of the cerebral vesicle in amphioxus is indicative of homology with the diencephalon.

The Organizing Centers in the CNS

Comparison of gene expression between amphioxus and vertebrates indicates that the amphioxus CNS has in place parts of the genetic mechanisms specifying the three organizing centers of the vertebrate CNS: anterior neural ridge (ANR), zona limitans intrathalamica (ZLI), and midbrain-hindbrain boundary (MHB) (Fig. 3.11). In vertebrates, the ANR is at the tip of the developing CNS, the ZLI is about the midpoint of the diencephalon, and the MHB, as the name implies, is between the hindbrain and midbrain. The ZLI and MHB separate lineage-restricted compartments in the CNS. In addition, transplantation experiments showed that all three regions of the vertebrate brain function as organizers (Eagleson and Dempewolf 2002).

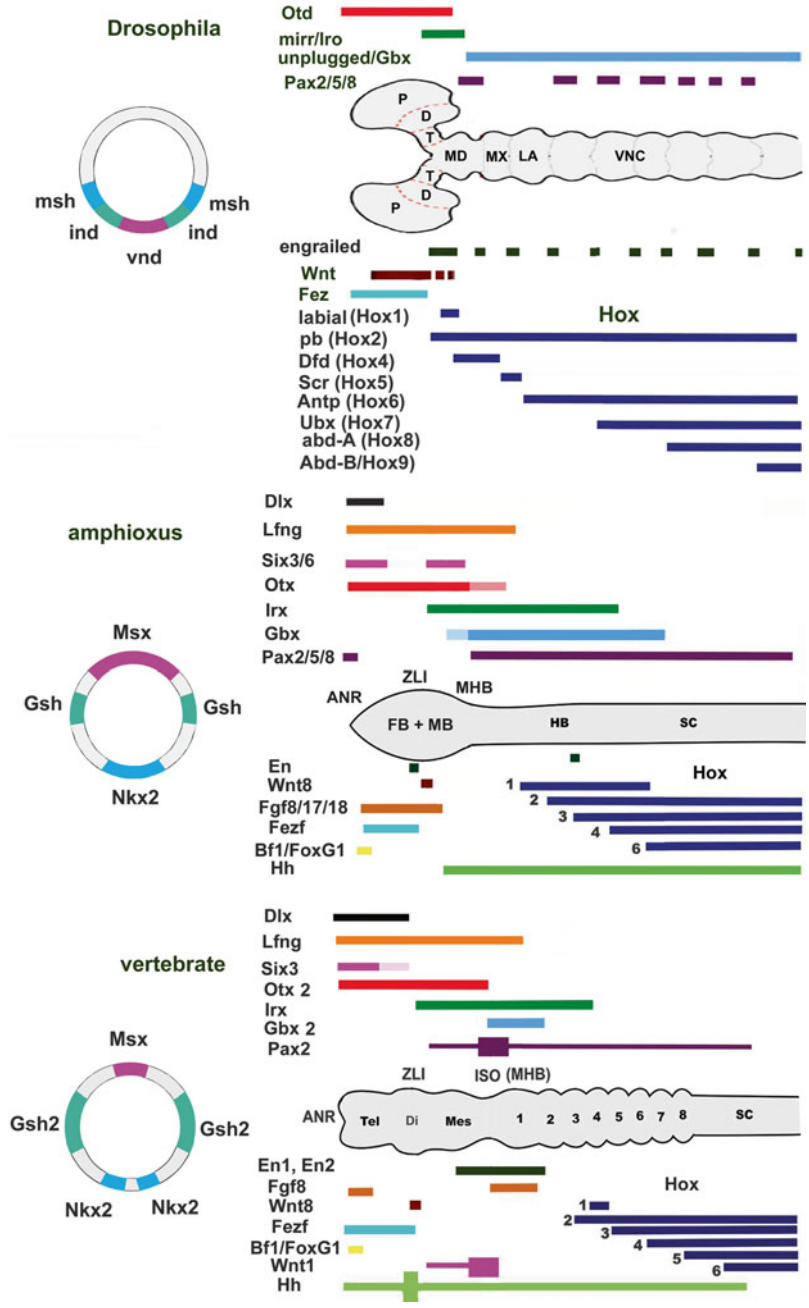

Fig. 3.11 Expression of both dorsoventral and anterior-posterior patterning genes is conserved in the central nervous systems of *Drosophila* (*top*), amphioxus (*middle*), and vertebrate (*bottom*). *Left*: expression of dorsoventral patterning genes in the *Drosophila* neuroectoderm, amphioxus, and vertebrate nerve cords. For *Drosophila*, the entire circumference of the embryo is shown with *msh*, *ind*, and *vnd*, respectively, expressed in lateral, intermediate, and medial columns of neuroblasts in the ventral ectoderm. For amphioxus and vertebrates, only the neural tube is shown. *Msx* is homologous to *msh*, *Gsh* to *ind*, and *Nkx2* to *vnd*. *Right*: expression of anterior-posterior patterning genes. The chordate equivalents of the *Drosophila* Hox genes are indicated in parentheses. Boundaries in the CNSs of the amphioxus and vertebrate brains are the anterior neural ridge (*ANR*), zona limitans intrathalamica (*ZLI*), and the midbrain-hindbrain boundary (*MHB*). In vertebrates, but perhaps not in amphioxus, these regions have organizer function. Hence, the vertebrate MHB is also called the isthmic organizer (*ISO*). *P* protocerebrum, *D* deuterocerebrum, *T* tritocerebrum, *MD* mandibular head segment, *MX* maxillary head segment, *LA* labial head segment, *VNC* ventral nerve cord, *FB* forebrain, *MB* midbrain, *HB* hindbrain, *SC* spinal cord, *Tel* telencephalon, *DI* diencephalon, *Mes* mesencephalon (After Holland et al (2013))

The vertebrate ANR is characterized by expression of *Dlx5*, *FoxG1*, and *Fgf8* (Yang et al. 1998). *FoxG1* directly represses Wnt signaling in the anterior CNS (Danesin et al. 2009). Homologs of these three genes are also expressed at the anterior tip of the amphioxus CNS. *Fgf8/17/18* is expressed in the entire forebrain of amphioxus, while *Bf-1* (*FoxG1*), *Pax2/5/8*, and *Six3/6* and the Wnt antagonist *sFRP1/2/5* are expressed in the anterior-most neuroectoderm (Toresson et al. 1998; Kozmik et al. 2007; Yu et al. 2007). Upregulation of Wnt/β-catenin signaling suppresses *Otx* and eliminates expression of the anterior marker *FoxQ2* (Onai et al. 2009) indicating that suppression of Wnt/β-catenin is necessary for forebrain development in amphioxus. *Dlx* is expressed both in the ectoderm adjacent the anterior tip of the amphioxus neural plate and in the neural plate itself as is vertebrate *Dlx5* (Holland et al. 1996). *Otx* and *Pax6* are expressed in comparable patterns with strong expression in the anterior forebrain (Glardon et al. 1998; Castro et al. 2006). Moreover, as in vertebrates, *Hedgehog* is expressed in the floor plate and in the underlying notochord (Shimamura and Rubenstein 1997; Shimeld 1999). These expression patterns indicate that amphioxus has in place many of the components that pattern the vertebrate ANR. Whether or not this region (or any region of the amphioxus CNS) acts as an organizer cannot be determined by classical transplantation studies as the embryos at the neurula stage are only ~300 μm long and ~50 μm wide and uniformly ciliated. No one has succeeded in immobilizing these embryos and having them develop normally. Consequently, even experiments juxtaposing secreted-protein-soaked beads would not be feasible.

In vertebrates, the zona limitans intrathalamica (ZLI) functions as an organizer of diencephalic development. Organizer properties were demonstrated by transplantation experiments (reviewed in Martinez-Ferre and Martinez 2012). The vertebrate ZLI is positioned by anterior expression of *Otx* and *Fezf* abutting a posterior domain of *Irx* (Jeong et al. 2007; Scholpp et al. 2007). Organizer properties are conferred by Hh which is regulated by *Wnt8b* (Martinez-Ferre et al. 2013). *Wnt8b* expression is adjacent to a zone of *L-fng*. Knockdown of *Fezf2* eliminates the prethalamus and mis-specifies the ZLI, while knockdown of *Otx* inhibits expression of *Shh* at the ZLI and reduces expression of *Ptc1* and *Wnt8b* (Scholpp et al. 2007). Patterns of gene expression indicate that amphioxus probably has much of the genetic mechanism in place for specification of the ZLI. Anterior expression of *Fezf* abuts posterior expression of *IrxB* about the midpoint of the amphioxus forebrain (Irimia et al. 2010) – approximately where *Wnt8* is expressed and where there is a zone of reduced *Otx* expression (Schubert et al. 2000). Moreover, the *Wnt8* and *Fng* domains are in close proximity to one another and may abut (Schubert et al. 2000; Mazet and Shimeld 2003). *Dlx*, *Nkx2-2*, and *Gli*, which mediates *Hh* signaling, are also expressed in this region and, as noted above, *Fgf8/17/18* is expressed throughout the forebrain (Holland et al. 1996, 1998; Shimeld et al. 2007). As in vertebrates *Hh* is expressed in the floor plate at the neurula stage; however, it is unclear whether or not it is co-expressed together with *Engrailed* and *Wnt8*. Later expression is restricted posterior to the forebrain (Shimeld 1999). Experiments to knock down *Fezf* function in amphioxus are feasible and would help show whether *Fezf* has the same role in the forebrains of amphioxus and vertebrates.

The vertebrate MHB is positioned by opposition between *Otx2* expressed in the forebrain and midbrain and *Gbx2* expressed in the hindbrain (Sunmonu et al. 2011; Hidalgo-Sánchez et al. 2005). Cells in this region function as an organizer, since if ectopically transplanted, they will change the fate of neighboring cells (Wassef and Joyner 1997). Organizer properties are conferred on the vertebrate MHB by the secreted signaling factors *Fgf8* and *Wnt1* together with expression of the transcription factors *Pax2/5/8* and *En1/2*. Continued expression of these genes is necessary for maintaining the MHB (Dworkin and Jane 2013). *Xiro* (*Iroquois/Irx*) is co-expressed with *Otx2* and *Gbx2*. It activates the latter gene and is vital for induction of *FGF8* (Glavic et al. 2002). In addition, genes in the Notch/Delta signaling pathway are upstream of *Fgf8* at the MHB

(Tossell et al. 2011). In addition, in vertebrates, *En1*, *En2*, *Wnt1*, and *Pax2/5/8* are expressed at the MHB.

In amphioxus, all these genes except for *Wnt1* are expressed in the CNS, and all but *Engrailed*, *Fgf8/17/18*, and *Pax2/5/8* are expressed in patterns entirely comparable to those in vertebrates. For example, as in vertebrates, *Otx* is expressed in the cerebral vesicle with a posterior limit at the boundary between the cerebral vesicle and hindbrain (Williams and Holland 1996), while *Gbx* is expressed in the CNS with an anterior limit abutting that of *Otx* (Castro et al. 2006; Holland and Short 2008). *Otx* is largely co-expressed with *Fgf8/17/18* at the early neurula stage (Bertrand et al. 2011). In contrast, in vertebrates, *Fgf8* is expressed in a ring of cells just posterior to the MHB. It negatively regulates *Otx2* and is vital for maintenance of the MHB (Sunmonu et al. 2011). These data indicate that amphioxus probably has a homolog of the vertebrate MHB, but it may not function as an organizer.

Taken together, these studies on amphioxus strongly support the idea that the common ancestor of amphioxus and the vertebrates had a CNS divided into a forebrain plus small midbrain, hindbrain, and spinal cord that was rostrally/caudally patterned with *Dlx*, *FoxG*, *Six3/6*, and *Wnt* suppressors demarcating the anterior tip of the CNS, abutting *Fezf* and *Irx* demarking the midpoint of the diencephalon, and abutting *Otx* and *Gbx* delimiting the boundary between midbrain and hindbrain, with nested expression of Hox genes marking positions in the hindbrain. The amphioxus homologs of the ZLI and MHB may not function as organizers, but they probably demarcate compartment boundaries, while the ANR forms the boundary between the neural plate and the adjacent ectoderm. It may be that in evolution, the chordate CNS was first compartmentalized and subsequently, as the brain grew much larger, tissue at these compartment boundaries acquired the ability to influence the fate of neighboring tissues.

Interpretations of data from gene expression studies can be reinforced by morphological data. For evolution of the CNS, Lacalli's serial TEM studies (Fig. 3.10) have complemented gene expression. Starting at the anterior tip of a midlarva of amphioxus, he serially sectioned the CNS and made 3D reconstructions, mapping each cell and its connections. He could do this because it is estimated that amphioxus adults have only about 20.000 neurons (Nicol and Meinertzhagen 1991; Lacalli et al. 1994; Lacalli 1996a, b, 2002a, b, 2003; Lacalli and Kelly 1999, 2000, 2002, 2003; Wicht and Lacalli 2005). His studies provided evidence that the frontal eye of amphioxus is homologous to the paired eyes of vertebrates, that the lamellar body is homologous to the pineal, and that the infundibulum, which secretes an extracellular fiber that extends posteriorly in the neural canal is homologous to the vertebrate infundibulum. All three of these characters are indicative of a diencephalon (Fig. 3.10). A region at the posterior end of the cerebral vesicle receives input from neurons of the frontal eye and was suggested as a possible homolog of the midbrain (Lacalli 1996a). Motor neurons extend from this region into the hindbrain. TEM revealed similarities between the Retzius bipolar cells of amphioxus and the Rohon-Beard cells of vertebrates, while midbrain-level dopaminergic and serotonergic neurons were found to be in roughly comparable places in the vertebrate CNS (reviewed in Wicht and Lacalli (2005)). Moreover, there are bilateral clusters of serotonergic neurons at the posterior end of the amphioxus cerebral vesicle (Holland and Holland 1993b), while in lamprey there are two large bilateral clusters, one anterior and one posterior near the MHB. The latter clusters are probably homologous to the ones in amphioxus. In addition, lampreys have a smaller cluster of serotonergic neurons in the hindbrain (Antri et al. 2006). Taken together, these results indicate that the vertebrate brain probably evolved by amplification and elaboration of the brain of an amphioxus-like ancestral chordate.

Dorsoventral Patterning of the CNS

Genes that mediate dorsoventral patterning of the CNS are also expressed in comparable patterns in amphioxus and the vertebrates. *Nkx2* genes are expressed ventrally, *Gsh* in an intermediate position, and *Msx* dorsally in both vertebrates

and amphioxus (Fig. 3.11; Holland et al. 1998; Sharman et al. 1999; Reichert and Simeone 2001; Osborne et al. 2009). Moreover, in both, *Shh* is expressed in the floor plate and underlying notochord (Shimeld 1999) and *Pax3/7* genes are expressed in the roof plate (Holland et al. 1999; Lee and Jessell 1999). The dorsoventral arrangement of cells types is also conserved between the amphioxus and vertebrate CNS. Lacalli (2002a) identified two columns of dorsal compartment motor neurons that extend from just anterior to the MHB and into the hindbrain (Fig. 3.10). These neurons are arranged on either side of the ventral midline of the neural plate roughly in line with the somites. This arrangement is similar to that of motor neurons in such diverse organisms as flies and vertebrates. However, in amphioxus these motor neurons, which appear to control slow, undulatory swimming, synapse directly with muscle tails that extend from the axial muscles to the nerve cord (Flood 1966; Lacalli 2002a). This arrangement appears to be unique to amphioxus among the chordates. Also unique to amphioxus is a muscular notochord, which also synapses directly with the nerve cord (Flood 1970, 1975b). During development, the two columns of dorsal compartment motor neurons express a suite of genes characteristic of developing motor neurons in other organisms. These genes include *Islet* (Jackman et al. 2000), *Mnx* (Ferrier et al. 2001; Seredick et al. 2012), *Err* (Bardet et al. 2005), and *Hox1* (Schubert et al. 2006). In late larvae, there is a second set of motor neurons, the ventral compartment motor neurons (Lacalli and Kelly 1999). These motor neurons, which are thought to innervate the deep fibers involved in burst swimming, lack the regular arrangement of the dorsal compartment motor neurons (Lacalli and Kelly 2003).

Organization of Neurons in the Amphioxus and Vertebrate CNSs

Expression of neuropeptides and microRNAs has shown considerable conservation of other neuronal subtypes between amphioxus and vertebrates. The arrangement of glycinergic neurons in the amphioxus CNS is very much like that in vertebrates (Candiani et al. 2012). *VGlut* is expressed in cells of the frontal eye complex, supporting proposed homologies to the vertebrate retina, and is also expressed in dorsolateral cells in the posterior forebrain which have been suggested to be homologous to Rohon-Beard sensory neurons (Jackman et al. 2000; Lacalli and Kelly 2003; Candiani et al. 2012). The distribution of glycinergic neurons is also similar in amphioxus and vertebrates (Candiani et al. 2012). As already mentioned, clusters of serotonergic neurons are also similarly located in amphioxus and vertebrates. Expression of several microRNAs has also been studied in amphioxus, although it is often difficult to correlate expression of particular miRNAs with particular cell types. Mir-7 is expressed in the frontal eye in amphioxus and in photoreceptors in both *Drosophila* and vertebrates. It is also expressed in the ciliated pit in amphioxus, which will develop into a homolog of the anterior pituitary, as well as in the pituitary in mammals (Candiani et al. 2011). Altogether, the data from gene expression and anatomy strongly suggest that the ancestral chordate had a CNS that was regionalized along the anterior-posterior and dorsoventral axes into a diencephalic forebrain, small midbrain, hindbrain, and spinal cord with a floor plate and a roof plate.

In addition to neurons identified with gene markers, Lacalli and colleagues used TEM to identify numerous homologies of specific neurons in the amphioxus and vertebrate nerve cords. For example, the infundibulum of the amphioxus and vertebrate CNS makes a similar extracellular fiber (Reissner's fiber), the Retzius bipolar cells of amphioxus may be homologous to the Rohon-Beard cells of vertebrates, and the Rhode cells of amphioxus may be homologous to some of the reticulospinal giant cells in vertebrates (reviewed in Wicht and Lacalli 2005). Even so, most dorsal structures of the vertebrate CNS except for the pineal eye do not have an obvious counterpart in amphioxus (Wicht and Lacalli 2005).

Homology of Chordate and Protostome Nerve Cords

Arguments based on both gene expression and anatomy have also been made for homology of the arthropod and annelid nerve cords with chordate

nerve cords, implying that the ancestral bilaterian had a longitudinal CNS (Lichtneckert and Reichert 2005; Urbach and Technau 2008; Strausfeld 2010; Tomer et al. 2010; Strausfeld and Hirth 2013; Tosches and Arendt 2013; Fig. 3.11). Expression of anterior-posterior patterning genes (including *Otx*, *Gbx*, *Fezf*, *Irx*, and Hox) is highly conserved between amphioxus, vertebrates, and arthropods (Fig. 3.11). However, many of these genes, including Hox genes, are also colinearly expressed in ectodermal tissues outside of the CNS, and, therefore, while they indicate homologous anterior-posterior patterning mechanisms, they do not necessarily indicate homology of the CNSs (reviewed in Holland et al. 2013).

Dorsoventral patterning genes are also conserved between the *Drosophila* and chordate nerve cords. *Msh*, *ind*, and *vnd* are the *Drosophila* homologs of vertebrate and amphioxus *Msx*, *Gsh*, and *Nkx2*, respectively. These genes are expressed in the developing *Drosophila* CNS in the same order as in the amphioxus and vertebrate nerve cords. The developing *Drosophila* CNS has three anterior-posterior columns of neuroblasts. The lateral one expresses *Msh*, the intermediate one *ind*, and the medial one *vnd* (Kim et al. 2005). This is precisely the same order as in amphioxus and vertebrates if one takes into consideration that the *Drosophila* CNS is ventral and inverted compared to chordate CNS (Fig. 3.11). As these genes are not comparably expressed in ectoderm outside the CNS, their expression strongly argues for a single origin of the CNS in the ancestral bilaterian.

Neural Crest and Placodes

Amphioxus development has shed considerable light on the evolution of vertebrate neural crest and placodes. The first insight into the evolution of neural crest was that the leading edges of the ectoderm that "walks" over the neural plate express *Distalless* (Holland et al. 1996). This indicated that in amphioxus, ectoderm comparable to that giving rise to neural crest in vertebrates is capable of migration, although as sheets and not as individual cells. In vertebrates, several of the up to seven *Dlx* genes, depending on the species, are expressed at the neural plate border and/or preplacodal region (McLarren et al. 2003; Reichert et al. 2013). In the chick, *Dlx5* is involved in specification of the neural plate border; it suppresses neural identity and promotes neural plate border/preplacodal identity (McLarren et al. 2003), while in zebrafish *Dlx3b* and *Dlx4b* are expressed in the preplacodal ectoderm and mediate repression of BMPs (Reichert et al. 2013). Expression of other genes (e.g., *Pax3*/7) (Holland et al. 1999) at the neural plate border is also conserved between amphioxus and vertebrates as is expression of the genes that specify the neural plate such as *SoxB* (Holland et al. 2000; Meulemans and Bronner-Fraser 2004).

Importantly, however, genes that are involved in neural crest migration and differentiation are not similarly expressed in amphioxus and vertebrates. One such gene is *FoxD*. The single amphioxus *FoxD* gene is expressed in mesoderm and in a few cells in the forebrain like several of the five vertebrate homologs resulting from whole-genome duplications, but it is not expressed at the edges of the neural plate like vertebrate *FoxD3* (Yu et al. 2002). A tissue-specific enhancer of amphioxus *FoxD* that directs expression to all the domains normally expressing the gene (i.e., notochord, forebrain, and paraxial muscles) (Yu et al. 2004) also directs expression to comparable domains in the chick, but not to neural crest (Yu et al. 2008a), indicating that after genome duplication in vertebrates, *FoxD3* acquired new regulatory elements directing expression to neural crest. In addition, the FoxD3 protein evolved a new motif in the N-terminus that is necessary for inducing differentiation of neural crest cells (Ono et al. 2014). Neither amphioxus FoxD nor other vertebrate FoxD proteins had this capability, but a chimeric protein with a 39 amino acid portion of zebrafish FoxD3 substituted for the N-terminal sequence of amphioxus FoxD was able to induce neural crest differentiation (Ono et al. 2014). These experiments demonstrated that evolution of neural crest in vertebrates not only required the recruitment of new genes into the gene network at the border of the neural plate but also required the evolution of new protein sequences. It had been theorized that gene duplicates that

arose due to whole-genome duplications at the base of the vertebrates made possible the acquisition of new characters such as neural crest (Holland et al. 1994; Holland and Short 2008). These experiments have shown that this is at least one way that new characters evolve.

Comparisons of the development of ectodermal sensory cells in amphioxus with cells in vertebrate placodes leaves little doubt that placodes evolved from the ectodermal sensory cells in an amphioxus-like ancestor. In vertebrates, the pan-placodal region is a 100–200 μm wide strip of ectoderm immediately adjacent the neural plate. In amphioxus, the embryos are so small that the dorsoventral extent of the entire ectoderm outside the neural plate is only about 200 μm – about the same extent as the width of the pan-placodal region in vertebrates. At the early neurula stage in amphioxus, ectodermal sensory cells expressing *Hu*/*Elav*, *Coe*, and *Delta* differentiate in the ventral midline of the ectoderm (Fig. 3.7A, C; Satoh et al. 2001; Mazet et al. 2004; Rasmussen et al. 2007). They lose their cilia, withdraw from the ectoderm, and migrate dorsally underneath the ectoderm. Arriving at positions along the flanks of the mid-neurula, the cells regrow a cilium, reinsert into the ectoderm, and then grow an axon, which extends into the central nervous system (CNS) (Fig. 3.7A–L; Mazet et al. 2004; Rasmussen et al. 2007). The position and number of these cells is determined by levels of BMP signaling (Fig. 3.7N–U; Lu et al. 2012). Addition of exogenous BMP protein increases the number of ectodermal sensory cells and shifts their positions dorsally, essentially converting the neuroectoderm to sensory/cell containing ectoderm.

The migratory pattern and role of BMP in regulating the migratory behavior of these sensory cell precursors in amphioxus are very like those of cells migrating from neurogenic placodes to the cranial ganglia of vertebrate (Fig. 3.9 Blentic et al. 2011; Freter et al. 2013) and strongly suggest a common evolutionary origin. Thus, the entire amphioxus ectoderm would be the equivalent of the pan-placodal ectoderm of vertebrates. Even so, there are major differences between the ectodermal sensory cells in amphioxus and cells from neurogenic placodes in vertebrates indicating that considerable evolution has taken place in the two lineages. For example, with few exceptions, most amphioxus ectodermal sensory cells are primary neurons, sending their axonal processes all the way into the CNS (Fig. 3.7M; Lacalli and Hou 1999; Holland and Yu 2002; Lacalli 2004). In contrast, in vertebrates, except for neurons of the olfactory placode, placodal neurons are typically secondary neurons, which synapse with interneurons. Moreover, amphioxus lacks cranial ganglia, and the ectodermal sensory cells in amphioxus are not organized into neuromasts as in many vertebrate placodes (reviewed in Holland and Holland 2001; Holland 2009; Patthey et al. 2014; Schlosser et al. 2014).

It has also been proposed that amphioxus has homologs of the adenohypophyseal and olfactory placodes (Glardon et al. 1998). *Pax6*, *Pitx2*, and *Islet* genes are expressed in the hypophyseal placode in the chick (Sjödal and Gunhaga 2008). Similarly, in amphioxus, *Pax6* is expressed together with *Islet* in Hatschek's anterior left diverticulum of the gut, which fuses with the ciliated pit, which expresses *Pitx* (Glardon et al. 1998; Jackman et al. 2000; Yasui et al. 2000). At metamorphosis, this fused structure becomes Hatschek's pit by migrating dorsal and anterior to the mouth. Hatschek's pit immunostains with antibodies to LH-like gonadotropins and is considered homologous to the adenohypophysis of the vertebrate pituitary (Van Wijhe 1907; Gorbman 1999; Gorbman et al. 1999).

As in the vertebrate olfactory placode (Purcell et al. 2005), *Pax6* and *Six3/6* are expressed in the anterior-most ectoderm of the amphioxus neurula (Glardon et al. 1998; Holland and Holland 2001; Kozmik et al. 2007), while *Msx* is expressed in two patches of anterior ectoderm of the early larva (Sharman et al. 1999). Homologs of *Pax6* and *Six3/6* are also expressed in the olfactory placode in vertebrates. Amphioxus has several types of rostral sensory cells, most of which are primary neurons as are the neurons deriving from the olfactory placode in vertebrates (Holland and Yu 2002). It is, therefore, likely that the vertebrate olfactory and adenohypophyseal placodes, as well as the neurogenic placodes, originated from the anterior-most ectoderm in an ancestral chordate.

Segmentation

Amphioxus has figured prominently in two related questions concerning the evolution of segmentation: (1) was the ancestral bilaterian segmented along the anterior-posterior axis and (2) are the segmental "head cavities" of agnathans and sharks evolutionarily related to one another and to the anterior segments in amphioxus? In amphioxus, the somites extend to the anterior tip of the animal. The anterior-most 8–12 somites segment from grooves in the dorsolateral mesendoderm, and the remainder segment from the tail bud. All of these somites give rise to paraxial muscles. In vertebrates, all of the somites ultimately derive from the tail bud. Bilateral bands of presomitic mesoderm extend anteriorly from the tail bud, and somites bud off from their tips. Vertebrate somites extend only as far as the posterior hindbrain. Lampreys are a minor exception in that the anterior-most somites have anterior extensions that give rise to the supraoptic and infraoptic muscles (Kusakabe et al. 2004). The anterior limit of somites is at the level of rhombomere 7 in the hindbrain.

The major difference between amphioxus and vertebrates in segmentation of somites from the tail bud is that in amphioxus, the somites segment directly from the tail bud and not at the anterior end bands of presomitic mesoderm (Fig. 3.8). Even so, the genetic mechanisms for segmentation of somites from the tail bud are quite conserved between amphioxus and vertebrates, indicating that the ancestral chordate probably segmented somites from a tail bud (Beaster-Jones et al. 2008).

A Segmented Bilaterian Ancestor?

The chief early proponent of the idea that the ancestor of chordates was segmented, the so-called annelid theory, was Anton Dohrn, who, however, believed that amphioxus was a degenerate vertebrate (Dohrn 1875). Hatschek agreed that vertebrates arose from an annelid-like ancestor (Hatschek 1878), while in a variation on the theme, Delsman (1922) argued that annelids gave rise to an amphioxus-like animal, which in turn gave rise to vertebrates. Others, such as Bateson (1886) viewed segmentation in annelids and vertebrates as independently evolved and proposed the theory that vertebrates evolved from an unsegmented enteropneust hemichordate. These ideas were largely superseded by the neoteny theory of Walter Garstang (Garstang and Garstang 1926; Garstang 1928), who proposed that the ancestor of the vertebrates was a sessile ascidian tunicate and vertebrates and amphioxus evolved from the larva of this animal by paedomorphosis. Since tunicate larval tails are not segmented, this idea, which was widely accepted in the twentieth century, implied that segmentation in amphioxus and vertebrates had evolved independently of that in protostomes (Romer 1962; Alexander 1981; Berrill 1987). However, EvoDevo studies starting in the late 1980s indicating conserved molecular mechanisms for segmentation in protostomes and deuterostomes revived the idea that the ancestral bilaterian was segmented (Balavoine and Adoutte 2003; De Robertis 2008a, b; Couso 2009). Even so, this idea has been countered by the idea that homologous gene networks were independently co-opted for segmentation in both groups (Chipman 2010). The first evidence from EvoDevo for a segmented bilaterian ancestor was the colinear expression of Hox genes along the body axis of protostomes, amphioxus, and vertebrates (reviewed in De Robertis et al. (1990)). The idea gained considerable momentum with the finding that *engrailed* is expressed in stripes in the posterior portion of each of the anterior-most somites of amphioxus as well as in the posterior portion of arthropod segments (Kornberg 1981; Fjose et al. 1985; Holland et al. 1993, 1997, 2008b). More recently, additional parts of the gene networks controlling segmentation in arthropods and chordates have been shown to be conserved between amphioxus and arthropods including Wnt signaling and its segmental repression and Notch/Delta signaling (Holland et al. 2001; Minguillon et al. 2003; Damen 2007; Rasmussen et al. 2007; Yu et al. 2007; Beaster-Jones et al. 2008; Lynch et al. 2012; Eriksson et al. 2013). In addition, *engrailed* and *Wnt* genes are segmentally expressed during development of the polychaete annelid *Platynereis* as they are in flies, amphioxus, and

vertebrates (Proud'homme et al. 2003). However, not all polychaetes are the same. *engrailed* is not similarly expressed in the polychaete *Chaetopterus* (Seaver et al. 2001). Taken together, these results have in the main supported the idea of a segmented bilaterian ancestor, but have far from settled the question (Minelli and Fusco 2004). Some have argued strongly that the same gene network was independently co-opted for segmentation in protostomes and chordates (Chipman 2010) or even among the insects (Peel 2008). The question of how much of the segmentation network must be evolutionarily conserved in protostomes and deuterostomes to be sure that there was a common segmented ancestor is still being debated (Sanetra et al. 2005) and may never be answered to everyone's satisfaction.

The molecular model explaining the mechanism of somitogenesis in vertebrates has been termed the "clock and wavefront" model. For amphioxus, in the absence of bands of presomitic mesoderm, there is a clock without a wavefront (Fig. 3.8; Beaster-Jones et al. 2008). As the clock and wavefront operate simultaneously in vertebrates, it has been difficult to determine exactly how the clock works. The presence of only a clock could make amphioxus a favorable model for understanding the fundamentals of somitogenesis in chordates.

Evolution of Head Segmentation in Chordates

In lampreys and sharks, anterior to the unequivocal somites are head cavities with muscular walls. The lamprey head cavities, like the anterior somites of amphioxus, form by enterocoely (Damas 1944), although the shark head cavities form by schizocoely (Adachi and Kuratani 2012). Even so, it has been proposed that the head cavities of both lampreys and sharks evolved from the anterior somites of an amphioxus-like ancestor (Fig. 3.12; reviewed in Holland et al. 2008b). Bony vertebrates do not have head cavities, but their extraocular and jaw muscles derive from head mesoderm, which is thought to be evolutionarily related to the mesoderm giving rise to the head cavities of the shark (reviewed in Holland et al. 2008b). In fact, it has been proposed that the extraocular and jaw muscles of vertebrates evolved from the walls of the first three myotomes of an amphioxus-like ancestor (Neal 1918). This idea has been hotly contested. One school of thought (Kuratani et al. 1998, 2004; Kusakabe et al. 2004, 2011; Kusakabe and Kuratani 2005, 2007; Kuratani 2008; Adachi et al. 2012) is that although the lamprey head cavities and the anterior somites of amphioxus evolved from a common ancestor, the head cavities of the shark and the head mesoderm of other gnathostomes are vertebrate innovations (Kusakabe and Kuratani 2007; Adachi et al. 2012). This argument has the problem that there are similar patterns of gene expression in the anterior somites of amphioxus, head cavities of lampreys and sharks, and the head muscles of bony gnathostomes. For example, *Engrailed* is expressed in the posterior wall of the anterior somites in amphioxus embryos; in the velar and upper lip muscles of the lamprey, which develop from the mandibular head cavity; in the mandibular arch in the shark; and in the jaw muscles of gnathostomes (Fig. 3.12; Hatta et al. 1990; Holland et al. 1993; Matsuura et al. 2008; Adachi et al. 2012; reviewed in Holland et al. 2008b; Sambasivan et al. 2011). Moreover, one of the four lamprey *Engrailed* genes is expressed in the ectoderm of the pharyngeal arches (Matsuura et al. 2008), similar to expression of amphioxus *Engrailed* in a stripe in the ectoderm ventral to the first somite (Holland et al. 1997).

The anterior somites of amphioxus and their ventral extensions into the pharynx also express *Tbx1/10*, as do the pharyngeal arches and the upper and lower lip muscles of the lamprey, the head mesoderm and mesoderm of the pharyngeal arches of the shark and the extraocular muscles of bony vertebrates (Fig. 3.12; Holland et al. 2008b; Adachi et al. 2012). In amphioxus, *Pitx* is expressed in mesoderm and endoderm extending ventrally into the pharynx anterior to the *Tbx1* domain (Yasui et al. 2000). Expression in the lamprey is similar (Boorman and Shimeld 2002) while in the shark, *Pitx* is expressed in the hyoid head cavity (the second

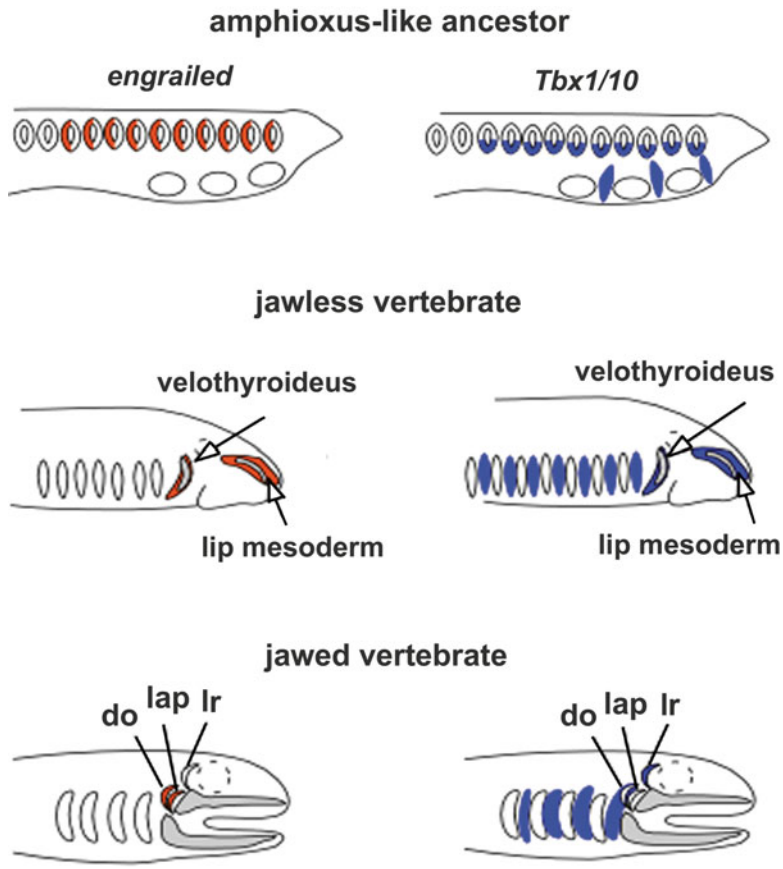

Fig. 3.12 The evolution of head segmentation. In an amphioxus-like ancestral chordate, somites extend to the anterior tip of the larva. *Engrailed* is expressed in the posterior portion of each of the anterior-most 8–12 somites. *Tbx1/10* is expressed in the ventral portions of the anterior-most somites and in stripes in the ventral extensions of the somites that grow ventrally into the pharyngeal arches. In jawless vertebrates, the anterior-most somites of the ancestral chordate have evolved into the three head cavities (premandibular, mandibular, and hyoid). The walls of these head cavities gave rise to the velothyroideus muscles and mesoderm of the lips, which express *Engrailed. Tbx1/10* is expressed in the pharyngeal arches, in the velothyroideus muscles, and in the lip mesoderm. In jawed vertebrates, the mandibular arch has evolved into the jaw bones. *Engrailed* in expressed in several head muscles, namely, the dorsal oblique (*do*) and the levator arcus palatini (*lap*); *lr* lateral rectus muscle. *Tbx1/10* genes are expressed in the pharyngeal arches and in the lateral rectus muscle

of three) and mandibular arch (Adachi et al. 2012). However, Kuratani et al. (2004) and Kusakabe and Kuratani (2007) have argued that similar patterns of gene expression may not indicate morphological homology especially in light of the enterocoelic formation of head cavities in lampreys and their schizocoelic formation in sharks (Neal 1918). Although parts of gene networks can be co-opted for making nonhomologous structures (e.g., *Distalless* genes expressed in the tips of insect and vertebrate appendages), differences in the mode of formation (schizocoely vs. enterocoely) of similar structures do not disprove a common ancestry. For example, the anterior (enterocoelic) and posterior (schizocoelic) somites of amphioxus have always been considered serially homologous as they form identical structures. Therefore, the scenario outlined in Fig. 3.12, in which the anterior, *Engrailed-expressing* somites of amphioxus gave rise to the head cavities of agnathans and in turn to the jaw muscles of vertebrates, seems most likely (Holland et al. 2008b).

The Future of Amphioxus EvoDevo

EvoDevo studies of amphioxus have shown that amphioxus is an excellent stand-in for the ancestral chordate in studies of how vertebrates evolved from their invertebrate ancestors. This is largely because amphioxus is basal in the chordates and evolving relatively slowly as are vertebrates. In addition, amphioxus has a very vertebrate-like body plan, but it is much simpler due, at least in part, to its absence of whole-genome duplications. Although vertebrates lost most duplicate genes after the whole-genome duplications, they preferentially retained those in signaling pathways and developmental genes (Putnam et al. 2008). As has been shown for the *FoxD* genes, for which one of the five duplicates in vertebrates acquired a new role in neural crest, the whole-genome duplications in vertebrates have allowed some duplicates to gain new regulatory elements as well as modify the protein structure in order to enable new functions and the evolution of new structures. It is highly likely that other examples of duplicate genes acquiring new functions and structures will come to light.

Amphioxus EvoDevo has also benefitted from detailed anatomical studies – particularly the detailed fine structural studies of Lacalli and colleagues that reconstructed the wiring diagram of all neurons in the anterior CNS of the larva. When anatomy and gene expression patterns agree concerning homologies, the inferences of homologous structures are strengthened. It is when anatomy differs, even only a moderate amount as in the case of head cavities of lampreys and sharks, that inferring homologies and reconstructing evolutionary history can become quite contentious.

The most common definition of homology used today is "inheritance from a common ancestor." That is, even if morphology has changed during evolution, as long as two structures evolved from a particular ancestral structure, they are homologous (Wagner 2007). Although a number of people have considered the extent to which conservation of gene networks can indicate homologies, a major question is how much of a gene network must be conserved to be reasonably interpreted as a result of common ancestry regardless of whether it directs development of anatomically diverse or even anatomically similar structures (Holland and Holland 1999). For example, it is generally agreed that the ancestral insect was segmented, but it is controversial whether the ancestral bilaterian or even the ancestral protostome was segmented. In *Drosophila*, segmentation is mediated by pair rule genes (e.g., *hairy*, *even skipped*, *paired*, *runt*, *fushi tarazu*), gap genes (e.g., *Knirps*, *Krüppel*, hunchback), and segment-polarity genes (e.g., *Wnt*, *hedgehog*, *engrailed*, *gooseberry*). However, some of these pair rule genes such as *even skipped* and *fushi tarazu* have different functions in grasshoppers *Schistocerca sp*. (Patel et al. 1992; Dawes et al. 1994). Complicating the picture even more, in an onychophoran, *even skipped* (*eve*) is involved in segmentation, but most of the other pair rule genes are not (Janssen and Budd 2013). In contrast, expression of most of the segment-polarity genes including *hedgehog*, *Wnt*, and *Engrailed* is conserved in an onychophoran and other arthropods (Janssen and Budd 2013). Presumably this means that some parts of gene networks are more informative than others for inferring homology. Complicating the picture, in some polychaete annelids, expression of segment-polarity genes including *Wnt* and *engrailed* is conserved with arthropods (Prud'homme et al. 2003), leading to the suggestion that the ancestral protostome was segmented and used these genes in segmentation. However, in two other polychaetes, neither *Wnt* nor *hedgehog* nor *engrailed* is expressed so as to suggest roles in segmentation (Seaver and Kaneshige 2006; Seaver et al. 2012), implying that mechanisms of segmentation in annelids and arthropods evolved independently (Chipman 2010). A further problem is that *Engrailed*, the *hedgehog* mediator *Gli* and *Wnts* and *Wnt* antagonists are expressed in patterns suggesting roles in segmentation in amphioxus (Holland et al. 1997; Shimeld et al. 2007; Yu et al. 2007). This has reinforced ideas that the urbilaterian was segmented (De Robertis 2008a), but has not convinced the doubters (Chipman 2010).

Hinman and Davidson (2007) used the term "kernel" to refer to the most conserved parts of gene regulatory networks and pointed out that only the core part of the gene regulatory network is conserved in endoderm specification in sea urchins and starfish – upstream and downstream parts of the network have diverged. By definition "'kernels' are dedicated to given developmental functions and are not used elsewhere in development of the organism" (Davidson and Erwin 2006). The question is whether conservation of this core is enough to infer homology among different organisms. It may be enough when animals are fairly closely related such as starfish and sea urchins, but whether it suffices over larger phylogenetic distances is problematic. It is well known that conserved parts of gene networks can be co-opted for patterning nonhomologous structures. For example, the gene networks involved in formation of vertebrate limbs such as *Fgf8* and *Shh* are also involved in patterning the CNS (Capdevila and Belmonte 2001). Another example is that while *Engrailed*, hedgehog, and Wnt signaling sometimes go together, they don't always do so. For example, while Wnt and hedgehog signaling cooperate in establishing boundaries in the vertebrate brain such as the zona limitans intrathalamica, all three genes interact in dorsal/ventral patterning of the chick limb (Logan et al. 1997). It would require a very large amount of dissection of gene networks to determine if there are truly any "kernels" that are restricted to homologous structures in distantly related animals and even then, if two structures didn't express the entire "kernel," one couldn't be certain that they are nonhomologous.

Amphioxus would be a good organism to start piecing together entire gene networks in order to ask questions about chordate evolution. Since amphioxus is similar to vertebrates but has relatively few gene duplications, gene networks should be comparatively easy to elucidate. Species of amphioxus are maintained in laboratory breeding cultures and have been raised through several generations. There are techniques for knockdown and overexpression of genes. Genomes of several species of *Branchiostoma* have been sequenced and there is an EST analysis for *Branchiostoma floridae*. The only technique yet to be developed is the production of germ line transgenics. However, given sufficient resources and a generation time of about 3 months, it is probably only a matter of time before these resources are developed. Even so, as the studies on the sea urchin endomesoderm gene network have shown, dissecting gene networks requires resources that few labs possess.

OPEN QUESTIONS

- Was the ancestral bilaterian segmented or did segmentation evolve independently in protostomes and deuterostomes?
- Did the ancestral bilaterian have a central nervous system or a nerve net or some combination of both?
- Virtually all aspects of organogenesis and gene expression in *Asymmetron.*

Since *Asymmetron* differs from *Branchiostoma* in several respects, particularly in left/right asymmetry, EvoDevo studies may well provide answers for questions concerning:

- The role of noncoding DNA in evolution of new genes and new functions for old genes
- How germ cells migrate to both sides in *Branchiostoma* but end up only on one side in *Asymmetron*
- The genetic mechanisms controlling the position of gill slits and other asymmetrically arrayed structures in cephalochordates

Acknowledgments I thank N.D. Holland for his critical reading of the manuscript and Greg Rouse for the photographs of *Asymmetron lucayanum* in Fig. 3.1.

References

Adachi N, Kuratani S (2012) Development of head and trunk mesoderm in the dogfish, *Scyliorhinus torazame*: I. Embryology and morphology of the head cavities and related structures. Evol Dev 14(3):234–256. doi:10.1111/j.1525-142X.2012.00542.x

Adachi N, Takechi M, Hirai T, Kuratani S (2012) Development of the head and trunk mesoderm in the dogfish, *Scyliorhinus torazame*: II. Comparison of gene expression between the head mesoderm and somites with reference to the origin of the vertebrate head. Evol Dev 14(3):257–276. doi:10.1111/j.1525-142X.2012.00543.x

Alexander RM (1981) The chordates. Cambridge University Press, Cambridge

Andrews EA (1893) An undescribed acraniate: *Asymmetron lucayanum*. Stud Biol Lab Johns Hopkins Univ 5:213–247 + pl. XII–XIV

Angerer LM, Angerer RC (2000) Animal – vegetal axis patterning mechanisms in the early sea urchin embryo. Dev Biol 218(1):1–12. doi:http://dx.doi.org/10.1006/dbio.1999.9553

Antri M, Cyr A, Auclair F, Dubuc R (2006) Ontogeny of 5-HT neurons in the brainstem of the lamprey, *Petromyzon marinus*. J Comp Neurol 495(6):788–800. doi:10.1002/cne.20910

Ayers H (1890) Contribution to the morphology of the vertebrate head. Zool Anz 13:504–507

Ayers H (1907) Vertebrate cephalogenesis. III. Amphioxus and *Bdellostoma*. University of Cincinnati, pp 1–40

Baccetti B, Burrini AG, Dallai R (1972) The spermatozoon of *Branchiostoma lanceolatum* L. J Morphol 136:211–226

Balavoine G, Adoutte A (2003) The segmented urbilateria: a testable scenario. Integr Comp Biol 43(1):137–147. doi:10.1093/icb/43.1.137

Balfour FM (1885) A treatise on comparative embryology, vol 2, 2nd edn. MacMillan, London

Balinsky BI (1981) An introduction to embryology, 5th edn. Saunders College Publishing, Philadelphia

Bardet PL, Schubert M, Horard B, Holland LZ, Laudet V, Holland ND, Vanacker JM (2005) Expression of estrogen-receptor related receptors in amphioxus and zebrafish: implications for the evolution of posterior brain segmentation at the invertebrate-to-vertebrate transition. Evol Dev 7:223–233

Bateson W (1886) The ancestry of the Chordata. Q J Microsc Sci 26:535–571

Beaster-Jones L, Kaltenbach SL, Koob TJ, Yuan SC, Chastain R, Holland LZ (2008) Expression of somite segmentation genes in amphioxus: a clock without a wavefront? Dev Genes Evol 218:599–611

Benito-Gutiérrez È, Weber H, Bryant DV, Arendt D (2013) Methods for generating year-round access to amphioxus in the laboratory. PLoS One 8(8):e71599. doi:10.1371/journal.pone.0071599

Berrill NJ (1955) The origin of vertebrates. Clarendon Press, Oxford

Berrill NJ (1987) Early chordate evolution. Part 1. Amphioxus, the riddle of the sands. Int J Invertebr Reprod Dev 11:1–14

Bertrand S, Camasses A, Somorjai I, Belgacem MR, Chabrol O, Escande M-L, Pontarotti P, Escriva H (2011) Amphioxus FGF signaling predicts the acquisition of vertebrate morphological traits. Proc Natl Acad Sci U S A 108(22):9160–9165. doi:10.1073/pnas.1014235108

Bhatnagar MC, Bansal G (2008) Developmental biology. Krishna Prakashan Media Ltd., Meerut

Blair JE, Hedges SB (2005) Molecular phylogeny and divergence times of deuterostome animals. Mol Biol Evol 19:2275–2284

Blentic A, Chambers D, Skinner A, Begbie J, Graham A (2011) The formation of the cranial ganglia by placodally-derived sensory neuronal precursors. Mol Cell Neurosci 46(2):452–459. doi:http://dx.doi.org/10.1016/j.mcn.2010.11.010

Boorman C, Shimeld S (2002) Cloning and expression of a Pitx homeobox gene from the lamprey, a jawless vertebrate. Dev Genes Evol 212(7):349–353

Boschung HV, Gunter G (1962) Distribution and variation of *Branchiostoma caribaeum* in Mississippi Sound. Tulane Stud Zool 9:245–257

Boveri T (1904) Ueber die phylogenetische Bedeutung der Sehorgane des Amphioxus. Zool Jahrb 7(suppl):409–428

Brandhorst BP, Klein WH (2002) Molecular patterning along the sea urchin animal-vegetal axis. In: Kwang WJ (ed) Int rev cytol, vol 213. Acad Press, San Diego. pp 183–232. doi:http://dx.doi.org/10.1016/S0074-7696(02)13015-4

Browder LS, Erickson CA, Jeffery WR (1991) Developmental biology. Saunders College Publishing, Philadelphia

Candiani S, Moronti L, De Pietri Tonelli D, Garbarino G, Pestarino M (2011) A study of neural-related microRNAs in the developing amphioxus. EvoDevo 2:15

Candiani S, Moronti L, Ramoino P, Schubert M, Pestarino M (2012) A neurochemical map of the developing amphioxus nervous system. BMC Neurosci 13:59. doi:10.1186/1471-2202-13-59

Capdevila J, Belmonte JCI (2001) Patterning mechanisms controlling vertebrate limb development. Annu Rev Cell Dev Biol 17:87–132

Castro LFC, Rasmussen SLK, Holland PWH, Holland ND, Holland LZ (2006) A *Gbx* homeobox gene in amphioxus: insights into ancestry of the ANTP class and evolution of the midbrain/hindbrain boundary. Dev Biol 295(1):40–51. doi:10.1016/j.ydbio.2006.03.003

Cerfontaine P (1906) Recherches sur le développement de l'amphioxus. Arch Biol Liege 22:229–418 + pl. XII–XXII

Chabry L (1887) Contribution à embryologie normale et tératologique des Ascidie. J Anat Physiol 23: 167–319

Chapman SC, Schubert FR, Schoenwolf GC, Lumsden A (2002) Analysis of spatial and temporal gene expression patterns in blastula and gastrula stage chick embryos. Dev Biol 245(1):187–199. doi:http://dx.doi.org/10.1006/dbio.2002.0641

Chea HK, Wright CV, Swalla BJ (2005) Nodal signaling and the evolution of deuterostome gastrulation. Dev Dyn 234(2):269–278. doi:10.1002/dvdy.20549

Chipman AD (2010) Parallel evolution of segmentation by co-option of ancestral gene regulatory networks. Bioessays 32(1):60–70. doi:10.1002/bies.200900130

Cole WC, Youson JH (1982) Morphology of the pineal complex of the anadromous sea lamprey, *Petromyzon*

marinus L. Am J Anat 165(2):131–163. doi:10.1002/aja.1001650205
Conklin EG (1905a) The early development of chordates in the light of the embryology of ascidians. Science 21:264–265
Conklin EG (1905b) The organization and cell-lineage of the ascidian egg. J Acad Nat Sci Phila 13(Ser 2):1–119, pl.I-XI
Conklin EG (1926) The embryology of amphioxus and the equipotential theory of development. Science 64:508–509
Conklin EG (1932) The embryology of amphioxus. J Morphol 54:69–141
Conklin EG (1933) The development of isolated and partially separated blastomeres of amphioxus. J Exp Zool 64:303–375
Costa OG (1834) Cenni Zoologici ossia descrizione sommaria delle specie nuove di animali discoperti in diverse contrade del regno nell'anno 1834. Azzolino, Napoli
Couso JP (2009) Segmentation, metamerism and the Cambrian explosion. Int J Dev Biol 53:1305–1316
Damas H (1944) Recherches sur le developpement de *Lampetra fluviatilis* L. Contribution à l'étude de la céphalogenèse des vertébrés. Arch Biol 55:1–248 + pl. I–III
Damen WGM (2007) Evolutionary conservation and divergence of the segmentation process in arthropods. Dev Dyn 236(6):1379–1391. doi:10.1002/dvdy.21157
Danesin C, Peres JN, Johansson M, Snowden V, Cording A, Papalopulu N, Houart C (2009) Integration of telencephalic Wnt and Hedgehog signaling center activities by *Foxg1*. Dev Cell 16(4):576–587. doi:http://dx.doi.org/10.1016/j.devcel.2009.03.007
Davidson EH, Erwin DH (2006) Gene regulatory networks and the evolution of animal body plans. Science 311(5762):796–800. doi:10.1126/science.1113832
Dawes R, Dawson I, Falciani F, Tear G, Akam M (1994) Dax, a locust Hox gene related to *fushi-tarazu* but showing no pair-rule expression. Development 120(6):1561–1572
De Robertis EM (2008a) Evo-devo: variations on ancestral themes. Cell 132(2):185–195. doi:http://dx.doi.org/10.1016/j.cell.2008.01.003
De Robertis EM (2008b) The molecular ancestry of segmentation mechanisms. Proc Natl Acad Sci U S A 105:16411–16412
De Robertis EM, Oliver G, Wright CV (1990) Homeobox genes and the vertebrate body plan. Sci Am 263:46–52
del Pilar Gomez M, Nasi E (2010) On the transduction gain of melanopsin-mediated light signaling in amphioxus: single-photon, unitary, and early receptor currents. J Gen Physiol 136:6A
del Pilar Gomez M, Angueyra JM, Nasi E (2009) Light-transduction in melanopsin-expressing photoreceptors of amphioxus. Proc Natl Acad Sci 106:9081–9086
Delsman HC (1922) The ancestry of vertebrates. Valkoff, Amersfoort
Delsuc F, Brinkmann H, Chourrout D, Philippe H (2006) Tunicates and not cephalochordates are the closest living relatives of the vertebrates. Nature 439:965–968
Delsuc F, Tsagkogeorga G, Lartillot N, Philippe H (2008) Additional molecular support for the new chordate phylogeny. Genesis 46:592–604
Denoeud F, Henriet S, Mungpakdee S, Aury J-M, Da Silva C, Brinkmann H, Mikhaleva J, Olsen LC, Jubin C, Cañestro C, Bouquet J-M, Danks G, Poulain J, Campsteijn C, Adamski M, Cross I, Yadetie F, Muffato M, Louis A, Butcher S, Tsagkogeorga G, Konrad A, Singh S, Jensen MF, Cong EH, Eikeseth-Otteraa H, Noel B, Anthouard V, Porcel BM, Kachouri-Lafond R, Nishino A, Ugolini M, Chourrout P, Nishida H, Aasland R, Huzurbazar S, Westhof E, Delsuc F, Lehrach H, Reinhardt R, Weissenbach J, Roy SW, Artiguenave F, Postlethwait JH, Manak JR, Thompson EM, Jaillon O, Du Pasquier L, Boudinot P, Liberles DA, Volff J-N, Philippe H, Lenhard B, Crollius HR, Wincker P, Chourrout D (2010) Plasticity of animal genome architecture unmasked by rapid evolution of a pelagic tunicate. Science 330(6009):1381–1385. doi:10.1126/science.1194167
Denuce JM (1996) Enzymatischer Abbau der Embryonalhüllen des Lanzettfischens, *Branchiostoma lanceolatum*, während des Schlupfens. Z Naturforsch C 51:113–118
Desdevises Y, Maillet V, Fuentes M, Escriva H (2011) A snapshot of the population structure of *Branchiostoma lanceolatum* in the Racou Beach, France, during its spawning season. PLoS One 6(4):e18520. doi:10.1371/journal.pone.0018520
Dohrn A (1875) Der Ursprung der Wirbelthiere und das Princip des Functionswechsels. Genealogische Skizzen, 4th edn. Wilhelm Engelmann, Leipzig
Drach P (1948) La notion de procordé dt les embranchements de cordés. In: Grasse PP (ed) Traité de Zoologie: Anatomie, Systematique, Biologie: Echinodermes, Stomocordes, Procordes, vol XI. Masson et Cie, Paris, pp 545–551
Dworkin S, Jane S (2013) Novel mechanisms that pattern and shape the midbrain-hindbrain boundary. Cell Mol Life Sci 70(18):3365–3374. doi:10.1007/s00018-012-1240-x
Eagleson GW, Dempewolf RD (2002) The role of the anterior neural ridge and *Fgf-8* in early forebrain patterning and regionalization in *Xenopus laevis*. Comp Biochem Physiol B Biochem Mol Biol 132(1):179–189. doi:10.1016/s1096-4959(01)00521-8
Eakin RM, Westfall JA (1962) Fine structure of photoreceptors in amphioxus. J Ultrastruct Res 6:531–539
Emily-Fenouil F, Ghiglione C, Lhomond G, Lepage T, Gache C (1998) GSK3beta/shaggy mediates patterning along the animal-vegetal axis of the sea urchin embryo. Development 125(13):2489–2498
Eriksson BJ, Ungerer P, Stollewerk A (2013) The function of Notch signalling in segment formation in the crustacean *Daphnia magna* (Branchiopoda). Dev Biol 383(2):321–330. doi:http://dx.doi.org/10.1016/j.ydbio.2013.09.021

Escriva H, Holland ND, Groenmeyer H, Laudet V, Holland LZ (2002) The retinoic acid signaling pathway regulates anterior/posterior patterning in the nerve cord and pharynx of amphioxus, a chordate lacking neural crest. Development 129:2905–2916

Ferrier DEK, Minguillon C, Holland PWH, Garcia-Fernàndez J (2000) The amphioxus Hox cluster: deuterostome posterior flexibility and *Hox 14*. Evol Dev 2:284–293

Ferrier DEK, Brooke NM, Panopoulou G, Holland PWH (2001) The Mnx homeobox gene class defined by *HB9*, *MNR2* and amphioxus *AmphiMnx*. Dev Genes Evol 211:103–107

Fjose A, McGinnis WJ, Gehring WJ (1985) Isolation of a homoeo box-containing gene from the engrailed region of Drosophila and the spatial distribution of its transcripts. Nature 313(6000):284–289

Flood PR (1966) A peculiar mode of muscular innervation in amphioxus. Light and electron microscopic studies of the so-called ventral roots. J Comp Neurol 126:181–218

Flood PR (1970) The connection between spinal cord and notochord in amphioxus (*Branchiostoma lanceolatum*). Z Zellforsch Mikrosk Anat 103:115–128

Flood PR (1975a) Ciliary rootlet-fibres as tail fin-rays in larval amphioxus (*Branchiostoma lanceolatum*, Pallas). J Ultrastruct Res 51:218–225

Flood PR (1975b) Fine structure of the notochord of amphioxus. Symp Zool Soc Lond 36:81–104

Franz V (1933) Das Gefasssystem der Akranier. Handb Verg Anat Wirbeltiere 6:451–466

Fredriksson G, Ericson LE, Olsson R (1984) Iodine binding in the endostyle of larval *Branchiostoma lanceolatum* (Cephalochordata). Gen Comp Endocrinol 56:177–184

Fredriksson G, Ofverholm T, Ericson LE (1985) Electron-microscopic studies of iodine-binding and peroxidase activity in the endostyle of the larval amphioxus (*Branchiostoma lanceolatum*). Cell Tissue Res 241:257–266

Freter S, Fleenor SJ, Freter R, Liu KJ, Begbie J (2013) Cranial neural crest cells form corridors prefiguring sensory neuroblast migration. Development 140(17):3595–3600. doi:10.1242/dev.091033

Fuentes M, Schubert M, Dalfo D, Candiani S, Benito E, Gardenyes J, Godoy L, Moret F, Illas M, Patten I, Permanyer J, Oliveri D, Boeuf G, Falcon J, Pestarino M, Garcia Fernandez J, Albalat R, Laudet V, Vernier P, Escriva H (2004) Preliminary observations on the spawning conditions of the European amphioxus (*Branchiostoma lanceolatum*) in captivity. J Exp Zool 302B:384–391

Fuentes M, Benito E, Bertrand S, Paris M, Mignardot A, Godoy L, Jimenez-Delgado S, Oliveri D, Candiani S, Hirsinger E, D'Aniello S, Pascual-Anaya J, Maeso I, Pestarino M, Vernier P, Nicolas J-F, Schubert M, Laudet V, Geneviere AM, Albalat R, Garcia Fernandez J, Holland ND, Escriva H (2007) Insights into spawning behavior and development of the European amphioxus (*Branchiostoma lanceolatum*). J Exp Zool 308B:484–493

Gans C, Northcutt RG (1983) Neural crest and the origin of vertebrates: a new head. Science 220:268–274

Garcia-Fernàndez J, Holland PWH (1994) Archetypal organization of the amphioxus Hox gene cluster. Nature 370:563–566

Garstang W (1928) The morphology of the Tunicata, and its bearings on the phylogeny of the Chordata. QJMS 72(na):51–187

Garstang W (1960) Amphioxus. In: Yust W (ed) Encyclopaedia Britannica, vol 1, 14th edn. Encyclopaedia Britannica, Chicago, pp 843–846

Garstang SL, Garstang W (1926) On the development of *Botrylloides* and the ancestry of vertebrates. Proc Leeds Phil Lit Soc 1:81–86

Gerhart J, Kirschner M (1997) Cells, embryos, and evolution. Blackwell, Malden

Giacobbe S (2012) Biodiversity loss in Sicilian transitional waters: the molluscs of Faro lake. Biodivers J 3:501–510

Gilmour THJ (1996) Feeding methods of cephalochordate larvae. Isr J Zool 42(Supplement):87–95

Glardon S, Callaerts P, Halder G, Gehring WJ (1997) Conservation of Pax-6 in a lower chordate, the ascidian *Phallusia mammillata*. Development 124:817–825

Glardon S, Holland LZ, Gehring WJ, Holland ND (1998) Isolation and developmental expression of the amphioxus Pax-6 gene (*AmphiPax-6*): insights into eye and photoreceptor evolution. Development 125(14):2701–2710

Glavic A, Gómez-Skarmeta JL, Mayor R (2002) The homeoprotein *Xiro1* is required for midbrain-hindbrain boundary formation. Development 129(7):1609–1621

Goodrich ES (1933) The nephridia of *Asymmetron* and *Branchiostoma* compared. Q J Microsc Sci 75:723–734

Gorbman A (1999) Brain-Hatschek's pit relationships in amphioxus species. Acta Zool Stockh 80:301–305

Gorbman A, Nozaki M, Kubokawa K (1999) A brain-Hatschek's pit connection in amphioxus. Gen Comp Endocrinol 113:251–254

Guthrie DM (1975) The physiology and structure of the nervous system of amphioxus (the lancelet), *Branchiostoma lanceolatum* Pallas. Symp Zool Soc Lond 36:43–80

Haeckel E (1876) The evolution of man: a popular exposition of the principal points of human ontogeny and phylogeny (Anyhropogenie oder Entwicklungseschichte des Menschen). Kegen Paul, London, (Translated from the German) Wilhelm Engelmann, Leipzig

Hashiguchi M, Mullins MC (2013) Anteroposterior and dorsoventral patterning are coordinated by an identical patterning clock. Development 140(9):1970–1980. doi:10.1242/dev.088104

Hatschek B (1878) Studien über Entwicklungsgeschichte der Anneliden. Ein Beitrag zur Morphologie der Bilaterien. Arb Zool Inst Wien 11:1–128

Hatschek B (1884) Mittheilungen uber Amphioxus. Zool Anz 7:517–520

Hatschek B (1893) The amphioxus and its development (translated by Tuckey J). Swan Sonnenschein, London

Hatta K, Schilling TF, BreMiller RA, Kimmel CB (1990) Specification of jaw muscle identity in zebrafish: correlation with engrailed-homeoprotein expression. Science 250:802–805

Henmi Y, Yamaguchi T (2003) Biology of the amphioxus, *Branchiostoma belcheri* in the Ariake Sea, Japan. I. Population structure and growth. Zoolog Sci 20:897–906

Hesse R (1898) Die Sehorgane des Amphioxus. Jahareshefte des Vereins fur vaterlandische. Naturkunde Wurttemberg 54:lxxxiii–lxxxiv

Hidalgo-Sánchez M, Millet S, Bloch-Gallego E, Alvarado-Mallart R-M (2005) Specification of the meso-isthmo-cerebellar region: the *Otx2*/*Gbx2* boundary. Brain Res Rev 49(2):134–149. doi:10.1016/j.brainresrev.2005.01.010

Hinman VF, Davidson EH (2007) Evolutionary plasticity of developmental gene regulatory network architecture. Proc Natl Acad Sci 104(49):19404–19409. doi:10.1073/pnas.0709994104

Hirakow R, Kajita N (1990) An electron microscopic study of the development of amphioxus, *Branchiostoma belcheri tsingtauense*: cleavage. J Morphol 203:331–334

Hirakow R, Kajita N (1991) Electron microscopic study of the development of amphioxus *Branchiostoma belcheri tsingtauense*: the gastrula. J Morphol 207:37–52

Hirakow R, Kajita N (1994) Electron microscopic study of the development of amphioxus, *Branchiostoma belcheri tsingtauense*: the neurula and larva. Acta Anat Nippon 69:1–13

Holland PWH (2002) Heads or tails? Amphioxus and the evolution of anterior-posterior patterning in deuterostomes. Dev Biol 241:209–228

Holland LZ (2009) Chordate roots of the vertebrate nervous system: expanding the molecular toolkit. Nat Rev Neurosci 10:736–746

Holland ND (2011) Spawning periodicity of the lancelet, *Asymmetron lucayanum* (Cephalochordata), in Bimini, Bahamas. Ital J Zool 78:478–486. doi:10.1080/11250003.2011.594097

Holland ND, Holland LZ (1989) Fine structural study of the cortical reaction and formation of the egg coats in a lancelet (= amphioxus), *Branchiostoma floridae* (phylum Chordata: subphylum Cephalochordata = Acrania). Biol Bull 176:111–122

Holland ND, Holland LZ (1990) Fine structure of the mesothelia and extracellular materials in the coelomic fluid of the fin boxes, myocoels and sclerocoels of a lancelet, *Branchiostoma floridae* (Cephalochordata = Acrania). Acta Zool (Stockh) 71:225–234

Holland ND, Holland LZ (1991a) The fine structure of the growth stage oocytes of a lancelet (= amphioxus), *Branchiostoma lanceolatum*. Invertebr Reprod Dev 19:107–122

Holland ND, Holland LZ (1991b) The histochemistry and fine structure of the nutritional reserves in the fin rays of a lancelet, *Branchiostoma lanceolatum* (Cephalochordata = Acrania). Acta Zool (Stockh) 72:203–207

Holland LZ, Holland ND (1992) Early development in the lancelet (= amphioxus) *Branchiostoma floridae* from sperm entry through pronuclear fusion: presence of vegetal pole plasm and lack of conspicuous ooplasmic segregation. Biol Bull 182:77–96

Holland ND, Holland LZ (1993a) Embryos and larvae of invertebrate deuterostomes. In: Stern CD, Holland PWH (eds) Essential developmental biology, a practical approach. IRL Press, Oxford, pp 21–33

Holland ND, Holland LZ (1993b) Serotonin-containing cells in the nervous system and other tissues during ontogeny of a lancelet, *Branchiostoma floridae*. Acta Zool (Stockh) 74:195–204

Holland ND, Holland LZ (1999) Amphioxus and the utility of molecular genetic data for hypothesizing body part homologies between distantly related animals. Am Zool 39:630–640

Holland LZ, Holland ND (2001) Evolution of neural crest and placodes: amphioxus as a model for the ancestral vertebrate? J Anat 199(1–2):85–98. doi:10.1046/j.1469-7580.199.parts1-2.8.x

Holland ND, Holland LZ (2006) Stage- and tissue-specific patterns of cell division in embryonic and larval tissues of amphioxus during normal development. Evol Dev 8:142–149

Holland LZ, Holland ND (2007) A revised fate map for amphioxus and the evolution of axial patterning in chordates. Integr Comp Biol 47:360–372

Holland ND, Holland LZ (2010) Laboratory spawning and development of the Bahama lancelet, *Asymmetron lucayanum* (Cephalochordata): fertilization through feeding larvae. Biol Bull 219:132–141

Holland LZ, Short S (2008) Gene duplication, co-option and recruitment during the origin of the vertebrate brain from the invertebrate chordate brain. Brain Behav Evol 72:91–105

Holland ND, Yu JK (2002) Epidermal receptor development and sensory pathways in vitally stained amphioxus (*Branchiostoma floridae*). Acta Zool Stockh 83:309–319

Holland LZ, Yu JK (2004) Cephalochordate (amphioxus) embryos: procurement, culture, basic methods. Methods Cell Biol 74:195–215

Holland PWH, Holland LZ, Williams NA, Holland ND (1992) An amphioxus homeobox gene: sequence conservation, spatial expression during development and insights into vertebrate evolution. Development 116:653–661

Holland ND, Holland LZ, Honma Y, Fujii T (1993) *Engrailed* expression during development of a lamprey, *Lampetra japonica*: a possible clue to homologies between agnathan and gnathostome muscles of the mandibular arch. Dev Growth Differ 35(2):153–160. doi:10.1111/j.1440-169X.1993.00153.x

Holland PWH, Garcia-Fernandez J, Williams NA, Sidow A (1994) Gene duplications and the origins of vertebrate development. Development 1994(supplement):125–133

Holland ND, Panganiban G, Henyey EL, Holland LZ (1996) Sequence and developmental expression of *AmphiDll*, an amphioxus Distal-less gene transcribed

in the ectoderm, epidermis and nervous system: insights into evolution of craniate forebrain and neural crest. Development 122:2911–2920

Holland LZ, Kene M, Williams NA, Holland ND (1997) Sequence and embryonic expression of the amphioxus engrailed gene (*AmphiEn*): the metameric pattern of transcription resembles that of its segment-polarity homolog in *Drosophila*. Development 124(9): 1723–1732

Holland LZ, Venkatesh TV, Gorlin A, Bodmer R, Holland ND (1998) Characterization and developmental expression of *AmphiNk2-2*, an NK2 class homeobox gene from amphioxus (Phylum Chordata; Subphylum Cephalochordata). Dev Genes Evol 208(2):100–105. doi:10.1007/s004270050159

Holland LZ, Schubert M, Kozmik Z, Holland ND (1999) Characterization of *AmphiPax3/7*, an amphioxus paired box gene: insights into chordate myogenesis, neurogenesis, and the possible evolutionary precursor of definitive vertebrate neural crest. Evol Dev 1:153–165

Holland LZ, Schubert M, Holland ND, Neuman T (2000) Evolutionary conservation of the presumptive neural plate markers *AmphiSox1/2/3* and *AmphiNeurogenin* in the invertebrate chordate amphioxus. Dev Biol 226:18–33

Holland LZ, Rached LA, Tamme R, Holland ND, Inoko H, Shiina T, Burgtorf C, Lardelli M (2001) Characterization and developmental expression of the amphioxus homolog of *Notch* (*AmphiNotch*): evolutionary conservation of multiple expression domains in amphioxus and vertebrates. Dev Biol 232(2):493–507. doi:http://dx.doi.org/10.1006/dbio.2001.0160

Holland ND, Venkatesh TV, Holland LZ, Jacobs DK, Bodmer R (2003) *AmphiNk2-tin*, an amphioxus homeobox gene expressed in myocardial progenitors: insights into evolution of the vertebrate heart. Dev Biol 255:128–137

Holland LZ, Albalat R, Azumi K, Benito-Gutiérrez E, Blow MJ, Bronner-Fraser M, Brunet F, Butts T, Candiani S, Dishaw LJ, Ferrier DE, Garcia-Fernàndez J, Gibson-Brown JJ, Gissi C, Godzik A, Hallböök F, Hirose D, Hosomichi K, Ikuta T, Inoko H, Kasahara M, Kasamatsu J, Kawashima T, Kimura A, Kobayashi M, Kozmik Z, Kubokawa K, Laudet V, Litman GW, McHardy AC, Meulemans D, Nonaka M, Olinski RP, Pancer Z, Pennacchio LA, Pestarino M, Rast JP, Rigoutsos I, Robinson-Rechavi M, Roch G, Saiga H, Sasakura Y, Satake M, Satou Y, Schubert M, Sherwood N, Shiina T, Takatori N, Tello J, Vopalensky P, Wada S, Xu A, Ye Y, Yoshida K, Yoshizaki F, Yu JK, Zhang Q, Zmasek CM, de Jong PJ, Osoegawa K, Putnam NH, Rokhsar DS, Satoh N, Holland PW (2008a) The amphioxus genome illuminates vertebrate origins and cephalochordate biology. Genome Res 18:1100–1111. doi:10.1101/gr.073676.107

Holland LZ, Holland ND, Gilland E (2008b) Amphioxus and the evolution of head segmentation. Integr Comp Biol 48:630–646

Holland ND, Paris M, Koop D (2009) The club-shaped gland of amphioxus: export of secretion to the pharynx in pre-metamorphic larvae and apoptosis during metamorphosis. Acta Zool 90(4):372–379. doi:10.1111/j.1463-6395.2008.00379.x

Holland LZ, Carvalho JE, Escriva H, Laudet V, Schubert M, Shimeld SM, Yu JK (2013) Evolution of bilaterian central nervous systems: a single origin? EvoDevo 4(1):27. doi:10.1186/2041-9139-4-27

Huxley TH (1875) Preliminary note upon the brain and skull of *Amphioxus lanceolatus*. Proc R Soc Lond 23:127–132

Irimia M, Piñeiro C, Maeso I, Gómez-Skarmeta JL, Casares F, Garcia-Fernàndez J (2010) Conserved developmental expression of *Fezf* in chordates and *Drosophila* and the origin of the Zona Limitans Intrathalamica (ZLI) brain organizer. EvoDevo 1(1):7

Jackman WR, Langeland JA, Kimmel CB (2000) *Islet* reveals segmentation in the amphioxus hindbrain homolog. Dev Biol 230:16–26

Janssen R, Budd GE (2013) Deciphering the onychophoran 'segmentation gene cascade': gene expression reveals limited involvement of pair rule gene orthologs in segmentation, but a highly conserved segment polarity gene network. Dev Biol 382(1):224–234. doi:http://dx.doi.org/10.1016/j.ydbio.2013.07.010

Jeong J-Y, Einhorn Z, Mathur P, Chen L, Lee S, Kawakami K, Guo S (2007) Patterning the zebrafish diencephalon by the conserved zinc-finger protein Fezl. Development 134(1):127–136. doi:10.1242/dev.02705

Joseph H (1904) Ueber eigentumliche Zellstrukturen im Zentralnervensystem von Amphioxus. Verh Anat Ges 18:16–26

Kaltenbach SL, Yu JK, Holland ND (2009) The origin and migration of the earliest-developing sensory neurons in the peripheral nervous system of amphioxus. Evol Dev 11:142–151

Kaneto S, Wada H (2011) Regeneration of amphioxus oral cirri and its skeletal rods: implications for the origin of the vertebrate skeleton. J Exp Zool 316B:409–417

Khanna R (2004) Textbook of embryology. Discovery Publishing Pvt. Ltd, New Delhi

Kim IOK, Kim IC, Kim S, Kwon YK, Han P-L, Jeon S-H, Kim SH (2005) CNS midline cells contribute to maintenance of the initial dorsoventral patterning of the *Drosophila* ventral neuroectoderm. J Neurobiol 62(4):397–405. doi:10.1002/neu.20104

Kobayashi H, Tsuneki K (1983) Histochemical distribution of peroxidase in ascidians with special reference to the endostyle and the branchial sac. Gen Comp Endocrinol 50:172–187

Kon T, Nohara M, Yamanoue Y, Fujiwara Y, Nishida M, Nishikawa T (2007) Phylogenetic position of a whale-fall lancelet (Cephalochordata) inferred from whole mitochondrial genome sequences. BMC Evol Biol 7(127):1–12

Koop D, Holland ND, Semon M, Alvarez S, Rodriquez de Lera A, Laudet V, Holland LZ, Schubert M (2010) Retinoic acid signaling targets Hox genes during the amphioxus gastrula stage: insights into early anterior-posterior patterning of the chordate body plan. Dev Biol 338:98–106

Kornberg T (1981) *Engrailed*: a gene controlling compartment and segment formation in *Drosophila*. Proc Natl Acad Sci U S A 78:1095–1099

Kowalevsky AO (1867) Die Entwickelungsgeschichte des *Amphioxus lanceolatus*. Mem Acad Imp Sci St Petersb (Ser VII) 11(4):1–17 + pl. I–III

Koyanagi M et al (2005) Cephalochordate melanopsin: evolutionary linkage between invertebrate visual cells and vertebrate photosensitive retinal ganglion cells. Curr Biol 15:1065–1069

Kozmik Z, Holland ND, Kalousova A, Paces J, Schubert M, Holland LZ (1999) Characterization of an amphioxus paired box gene, *AmphiPax2/5/8*: developmental expression patterns in optic support cells, nephidium, thyroid-like structures and pharyngeal gill slits, but not in the midbrain-hindbrain boundary region. Development 126:1295–1304

Kozmik Z, Holland LZ, Schubert M, Lacalli TC, Kreslova J, Vlcek C, Holland ND (2001) Characterization of amphioxus *AmphiVent*, an evolutionarily conserved marker for chordate ventral mesoderm. Genesis 29:172–179

Kozmik Z, Holland ND, Kreslova J, Oliveri D, Schubert M, Jonasova K, Holland LZ, Pestarino M, Benes V, Candiani S (2007) Pax–Six–Eya–Dach network during amphioxus development: conservation in vitro but context specificity in vivo. Dev Biol 306(1):143–159. doi:10.1016/j.ydbio.2007.03.009

Kuratani S (2008) Is the vertebrate head segmented?—evolutionary and developmental considerations. Integr Comp Biol 48(5):647–657. doi:10.1093/icb/icn015

Kuratani S, Ueki T, Hirano S, Aizawa S (1998) Rostral truncation of a cyclostome, *Lampetra japonica*, induced by all-trans retinoic acid defines the head/trunk interface of the vertebrate body. Dev Dyn 211:35–51

Kuratani S, Murakami Y, Nobusada Y, Kusakabe R, Hirano S (2004) Developmental fate of the mandibular mesoderm in the lamprey, *Lethenteron japonicum*: comparative morphology and development of the gnathostome jaw with special reference to the nature of the trabecula cranii. J Exp Zool 302B(5):458–468. doi:10.1002/jez.b.21011

Kusakabe R, Kuratani S (2005) Evolution and developmental patterning of the vertebrate skeletal muscles: perspectives from the lamprey. Dev Dyn 234(4):824–834. doi:10.1002/dvdy.20587

Kusakabe R, Kuratani S (2007) Evolutionary perspectives from development of mesodermal components in the lamprey. Dev Dyn 236(9):2410–2420. doi:10.1002/dvdy.21177

Kusakabe R, Takechi M, Tochinai S, Kuratani S (2004) Lamprey contractile protein genes mark different populations of skeletal muscles during development. J Exp Zool 302B(2):121–133. doi:10.1002/jez.b.20009

Kusakabe R, Kuraku S, Kuratani S (2011) Expression and interaction of muscle-related genes in the lamprey imply the evolutionary scenario for vertebrate skeletal muscle, in association with the acquisition of the neck and fins. Dev Biol 350(1):217–227. doi:http://dx.doi.org/10.1016/j.ydbio.2010.10.029

Lacalli TC (1996a) Frontal eye circuitry, rostral sensory pathways, and brain organization in amphioxus larvae: evidence from 3D reconstructions. Phil Trans R Soc B 351:243–263

Lacalli TC (1996b) Landmarks and subdomains in the larval brain of *Branchiostoma*: vertebrate homologs and invertebrate antecedents. Isr J Zool 42(Supplement):131–146

Lacalli TC (2002a) The dorsal compartment locomotory control system in amphioxus larvae. J Morphol 252:227–237

Lacalli TC (2002b) Sensory pathways in amphioxus larvae 1. Constituent fibre of the rostral and anterodorsal nerves, their targets and evolutionary significance. Acta Zool Stockh 83:149–166

Lacalli TC (2003) Ventral neurons in the anterior nerve cord of amphioxus larvae. II. Further data on the pacemaker circuit. J Morphol 257:212–218

Lacalli TC (2004) Sensory systems in amphioxus: a window on the ancestral chordate condition. Brain Behav Evol 64(3):148–162

Lacalli TC (2008a) Basic features of the ancestral chordate brain: a protochordate perspective. Brain Res Bull 75:319–323

Lacalli TC (2008b) Mucus secretion and transport in amphioxus larvae: organization and ultrastructure of the food trapping system, and implications for head evolution. Acta Zool (Stockh) 89:219–230

Lacalli TC, Hou SF (1999) A reexamination of the epithelial sensory cells of amphioxus (*Branchiostoma*). Acta Zool Stockh 80:125–134

Lacalli TC, Kelly SJ (1999) Somatic motoneurones in amphioxus larvae: cell types, cell position and innervation patterns. Acta Zool Stockh 80:113–124

Lacalli TC, Kelly SJ (2000) The infundibular balance organ in amphioxus larvae and related aspects of cerebral vesicle organization. Acta Zool Stockh 81:37–47

Lacalli TC, Kelly SJ (2002) Floor plate, glia and other support cells in the anterior nerve cord of amphioxus larvae. Acta Zool Stockh 83:87–98

Lacalli TC, Kelly SJ (2003) Ventral neurons in the anterior nerve cord of amphioxus larvae I. An inventory of cell types and synaptic patterns. J Morphol 257:190–211

Lacalli TC, Holland ND, West JE (1994) Landmarks in the anterior central nervous system of amphioxus larvae. Phil Trans R Soc B 344:165–185

Langille RM, Hall BK (1989) Developmental processes, developmental sequences and early vertebrate phylogeny. Biol Rev 64:73–91

Lankester ER (1875) On some new points in the structure of amphioxus, and their bearing on the morphology of Vertebrata. Q J Microsc Sci (NS) 15:257–267

Lankester ER, Willey A (1890) The development of the atrial chamber of *Amphioxus*. Q J Microsc Sci 31:445–466 + pl. XXIX–XXXII

Lee KJ, Jessell TM (1999) The specification of dorsal cell fates in the vertebrate central nervous system. Ann Rev Neurosci 22(1):261–294. doi:10.1146/annurev.neuro.22.1.261

Legros R (1898) Développement de la cavité buccale du *l'Amphioxus lanceolatus*: contribution a l'étude de la morphologie de la tête. Arch Anat Microsc 1:497–542 + pl. XXI–XXIII

Legros R (1910) Sur quelques points de l'anatomie et du développement de l'*Amphioxus*, I. Sur le nephridium de Hatschek. Anat Anz 35:561–587

Lichtneckert R, Reichert H (2005) Insights into the urbilaterian brain: conserved genetic patterning mechanisms in insect and vertebrate brain development. Heredity (Nature) 94:465–477

Logan C, Hornbruch A, Campbell I, Lumsden A (1997) The role of *Engrailed* in establishing the dorsoventral axis of the chick limb. Development 124(12):2317–2324

Lu T-M, Luo Y-J, Yu J-K (2012) BMP and Delta/Notch signaling control the development of amphioxus epidermal sensory neurons: insights into the evolution of the peripheral sensory system. Development 139(11):2020–2030. doi:10.1242/dev.073833

Lwoff B (1892) Ueber einige wichtige Punkte in der Entwicklung des *Amphioxus*. Biol Centralbl 12:729–744

Lynch JA, El-Sherif E, Brown SJ (2012) Comparisons of the embryonic development of *Drosophila*, *Nasonia*, and *Tribolium*. Wiley Interdiscip Rev Dev Biol 1(1):16–39. doi:10.1002/wdev.3

MacBride EW (1898) The early development of amphioxus. Q J Microsc Sci 40:589–612

Mallatt J, Winchell CJ (2007) Ribosomal RNA genes and deuterostome phylogeny revisited: more cyclostomes, elasmobranchs, reptiles, and a brittle star. Mol Phylogenet Evol 43:1005–1022

Mansfield JH, Holland ND (2015) Amphioxus tails: source and fate of larval fin rays and the metamorphic transition from anectodermal to a predominantly mesodermal tail. Acta Zool 96:117–125

Manzanares M, Bel-Vialar S, Ariza-McNaughton L, Ferretti E, Marshall H, Maconochie MM, Blasi F, Krumlauf R (2001) Independent regulation of initiation and maintenance phases of *Hoxa3* expression in the vertebrate hindbrain involve auto- and cross-regulatory mechanisms. Development 128(18):3595–3607

Martinez-Ferre A, Martinez S (2012) Molecular regionalization of the diencephalon. Front Neurosci 6:73. doi:10.3389/fnins.2012.00073

Martinez-Ferre A, Navarro-Garberi M, Bueno C, Martinez S (2013) Wnt signal specifies the intrathalamic limit and its organizer properties by regulating Shh induction in the alar plate. J Neurosci 33(9):3967–3980

Matsuura M, Nishihara H, Onimaru K, Kokubo N, Kuraku S, Kusakabe R, Okada N, Kuratani S, Tanaka M (2008) Identification of four *Engrailed* genes in the Japanese lamprey, *Lethenteron japonicum*. Dev Dyn 237(6):1581–1589. doi:10.1002/dvdy.21552

Mazet F, Shimeld S (2003) Characterisation of an amphioxus *Fringe* gene and the evolution of the vertebrate segmentation clock. Dev Genes Evol 213(10):505–509. doi:10.1007/s00427-003-0351-7

Mazet F, Masood S, Luke GN, Holland ND, Shimeld SM (2004) Expression of *AmphiCoe*, an amphioxus COE/EFB gene, in the developing central nervous system and epidermal sensory neurons. Genesis 38:58–65

McLarren KW, Litsiou A, Streit A (2003) *DLX5* positions the neural crest and preplacode region at the border of the neural plate. Dev Biol 259(1):34–47. doi:http://dx.doi.org/10.1016/S0012-1606(03)00177-5

Meulemans D, Bronner-Fraser M (2004) Gene-regulatory interactions in neural crest evolution and development. Dev Cell 7:291–299

Minelli A, Fusco G (2004) Evo-devo perspectives on segmentation: model organisms, and beyond. Trends Ecol Evol 19(8):423–429. doi:http://dx.doi.org/10.1016/j.tree.2004.06.007

Minguillon C, Jimenez-Delgado S, Panopoulou G, Garcia-Fernàndez J (2003) The amphioxus Hairy family: differential fate after duplication. Development 130:5903–5913

Mizuta T, Kubokawa K (2004) Non-synchronous spawning behavior in the laboratory rearing amphioxus, *Branchiostoma belcheri*. J Exp Mar Biol Ecol 309:239–251

Morgan TH, Hazen AP (1900) The gastrulation of amphioxus. J Morphol 16:569–600 + pl. XXXIII–XXXIV

Morisawa S, Mizuta T, Kubokawa K, Tanaka H, Morisawa M (2004) Acrosome reaction in spermatozoa from the amphioxus *Branchiostoma belcheri* (Cephalochordata, Chordata). Zoolog Sci 11:1079–1084

Nakao T (1964) On the fine structure of the amphioxus photoreceptor. Tohoku J Exp Med 82:349–369

Neal HV (1918) The history of the eye muscles. J Morphol 30:433–453

Nicol D, Meinertzhagen IA (1991) Cell counts and maps in the larval central nervous system of the ascidian *Ciona intestinalis* (L.). J Comp Neurol 309:415–429

Nohara M, Nishida H, Miya M, Nishikawa T (2005) Evolution of the mitochondrial genome in Cephalochordata as inferred from complete nucleotide sequences from two *Epigonichthys* species. J Mol Evol 60:526–537

Ohno S (1970) Evolution by gene duplication. Springer, New York

Olsson R (1983) Club-shaped gland and endostyle in larval *Branchiostoma lanceolatum* (Cephalochordata). Zoomorphology 103:1–13

Onai T, Lin H-C, Schubert M, Koop D, Osborne PW, Alvarez S, Alvarez R, Holland ND, Holland LZ (2009) Retinoic acid and Wnt/β-catenin have complementary roles in anterior/posterior patterning embryos of the basal chordate amphioxus. Dev Biol 332(2):223–233. doi:http://dx.doi.org/10.1016/j.ydbio.2009.05.571

Onai T, Yu JK, Blitz IL, Cho KWY, Holland LZ (2010) Opposing Nodal/Vg1 and BMP signals mediate axial patterning in embryos of the basal chordate amphioxus. Dev Biol 344:377–389

Onai T, Akira T, Setiamarga DHE, Holland LZ (2012) Essential role of Dkk3 for head formation by inhibiting Wnt/β-catenin and Nodal/Vg1 signaling pathways in the basal chordate amphioxus. Evol Dev 14(4):338–350. doi:10.1111/j.1525-142X.2012.00552.x

Ono H, Kozmik Z, Yu J-K, Wada H (2014) A novel N-terminal motif is responsible for the evolution of neural crest-specific gene-regulatory activity in vertebrate *FoxD3*. Dev Biol 385(2):396–404. doi:http://dx.doi.org/10.1016/j.ydbio.2013.11.010

Osborne PW, Benoit G, Laudet V, Schubert M, Ferrier DE (2009) Differential regulation of ParaHox genes by retinoic acid in the invertebrate chordate amphioxus (*Branchiostoma floridae*). Dev Biol 327:252–262

Pallas PS (1774) Spicilegia Zoologica, vol 1. Fascicle 10, vol 1. G. A. Lange, Berlin

Paris M, Escriva H, Schubert M, Brunet F, Brtko J, Ciesielski F, Roecklin D, Vivat-Hannah V, Jamin EL, Cravedi JP, Scanlan TS, Renaud JP, Holland ND, Laudet V (2008) Amphioxus postembryonic development reveals the homology of chordate metamorphosis. Curr Biol 18:825–830

Pascual-Anaya J, Albuixech-Crespo B, Somorjai IML, Carmona R, Oisi Y, Álvarez S, Kuratani S, Muñoz-Chápuli R, Garcia-Fernàndez J (2013) The evolutionary origins of chordate hematopoiesis and vertebrate endothelia. Dev Biol 375(2):182–192. doi:http://dx.doi.org/10.1016/j.ydbio.2012.11.015

Patel NH, Ball EE, Goodman CS (1992) Changing role of even-skipped during the evolution of insect pattern formation. Nature 357(6376):339–342

Patthey C, Schlosser G, Shimeld SM (2014) The evolutionary history of vertebrate cranial placodes – I: cell type evolution. Dev Biol 389:82–97. doi:http://dx.doi.org/10.1016/j.ydbio.2014.01.017

Pedersen L, Jensen MH, Krishna S (2011) Dickkopf1–a new player in modelling the Wnt pathway. PLoS One 6:e25550. doi:10.1371/journal.pone.0025550

Peel AD (2008) The evolution of developmental gene networks: lessons from comparative studies on holometabolous insects. Phil Trans R Soc B Biol Sci 363(1496):1539–1547. doi:10.1098/rstb.2007.2244

Pendleton JW, Nagai BK, Murtha MT, Ruddle FH (1993) Expansion of the Hox gene family and the evolution of chordates. Proc Natl Acad Sci U S A 90(13):6300–6304

Prud'homme B, de Rosa R, Arendt D, Julien J-F, Pajaziti R, Dorresteijn AWC, Adoutte A, Wittbrodt J, Balavoine G (2003) Arthropod-like expression patterns of *engrailed* and *wingless* in the annelid *Platynereis dumerilii* suggest a role in segment formation. Curr Biol 13(21):1876–1881. doi:http://dx.doi.org/10.1016/j.cub.2003.10.006

Pulido C, Malagón G, Ferrer C, Chen JK, Angueyra JM, Nasi E, Gomez MP (2012) The light-sensitive conductance of melanopsin-expressing Joseph and Hesse cells in amphioxus. J Gen Physiol 139(1):19–30. doi:10.1085/jgp.201110717

Purcell P, Oliver G, Mardon G, Donner AL, Maas RL (2005) *Pax6*-dependence of *Six3*, *Eya1* and *Dach1* expression during lens and nasal placode induction. Gene Expr Patterns 6(1):110–118. doi:http://dx.doi.org/10.1016/j.modgep.2005.04.010

Putnam NH, Butts T, Ferrier DEK, Furlong RF, Hellsten U, Kawashima T, Robinson-Rechavi M, Shoguchi E, Terry A, Yu J-K, Benito-Gutierrez E, Dubchak I, Garcia-Fernandez J, Gibson-Brown JJ, Grigoriev IV, Horton AC, de Jong PJ, Jurka J, Kapitonov VV, Kohara Y, Kuroki Y, Lindquist E, Lucas S, Osoegawa K, Pennacchio LA, Salamov AA, Satou Y, Sauka-Spengler T, Schmutz J, Shin-I T, Toyoda A, Bronner-Fraser M, Fujiyama A, Holland LZ, Holland PWH, Satoh N, Rokhsar DS (2008) The amphioxus genome and the evolution of the chordate karyotype. Nature 453(7198):1064–1071. doi:http://www.nature.com/nature/journal/v453/n7198/suppinfo/nature06967_S1.html

Rahr H (1981) The ultrastructure of the blood vessels of *Branchiostoma lanceolatum* (Pallas) (Cephalochordata. I. Relations between blood vessels, epithelia, basal laminae, and "connective tissue". Zoomorphology 97:53–74

Rasmussen SLK, Holland LZ, Schubert M, Beaster-Jones L, Holland ND (2007) Amphioxus *AmphiDelta*: evolution of delta protein structure, segmentation, and neurogenesis. Genesis 45(3):113–122. doi:10.1002/dvg.20278

Reichert H, Simeone A (2001) Developmental genetic evidence for a monophyletic origin of the bilaterian brain. Phil Trans R Soc B Biol Sci 356(1414):1533–1544. doi:10.1098/rstb.2001.0972

Reichert S, Randall RA, Hill CS (2013) A BMP regulatory network controls ectodermal cell fate decisions at the neural plate border. Development 140(21):4435–4444. doi:10.1242/dev.098707

Romer AS (1962) The vertebrate body, 3rd edn. W. B Saunders, Philadelphia

Ruppert EE (1996) Morphology of Hatschek's nephridium in larval and juvenile stages of *Branchiostoma virginiae* (Cephalochordata). Isr J Zool 42(Suppl):161–182

Samassa P (1898) Studien über den Einfluss des Dotters auf die Gastrulation und die Bildung der primären Keimblätter der Wirbelthiere. IV. Amphioxus. Arch Entwicklungsmech 7:1–33 + pl. I–III

Sambasivan R, Kuratani S, Tajbakhsh S (2011) An eye on the head: the development and evolution of craniofacial muscles. Development 138(12):2401–2415. doi:10.1242/dev.040972

Sánchez-Arrones L, Ferrán JL, Rodríguez-Gallardo L, Puelles L (2009) Incipient forebrain boundaries traced by differential gene expression and fate mapping in the chick neural plate. Dev Biol 335(1):43–65. doi:http://dx.doi.org/10.1016/j.ydbio.2009.08.012

Sanetra M, Begemann G, Becker MB, Meyer A (2005) Conservation and co-option in developmental programmes: the importance of homology relationships. Front Zool 10(2):15

Satoh G, Wang Y, Zhang PJ, Satoh N (2001) Early development of amphioxus nervous system with special reference to segmental cell organization and putative sensory cell precursors: a study based on the expression of pan-neuronal marker gene *Hu/elav*. J Exp Zool 291:354–364

Schlosser G, Patthey C, Shimeld SM (2014) The evolutionary history of vertebrate cranial placodes II. Evolution of ectodermal patterning. Dev Biol 389:98–119. piis0012-1606(14) 00047-5. doi:http://dx.doi.org/10.1016/j.ydbio.2014.01.019

Scholpp S, Foucher I, Staudt N, Peukert D, Lumsden A, Houart C (2007) *Otx1*, *Otx2* and *Irx1b* establish and position the ZLI in the diencephalon. Development 134(17):3167–3176. doi:10.1242/dev.001461

Schubert M, Holland LZ, Panopoulou GD, Lehrach H, Holland ND (2000) Characterization of amphioxus AmphiWnt8: insights into the evolution of patterning of the embryonic dorsoventral axis. Evol Dev 2(2):85–92. doi:10.1046/j.1525-142x.2000.00047.x

Schubert M, Holland ND, Laudet V, Holland LZ (2006) A retinoic acid-Hox hierarchy controls both anterior/posterior patterning and neuronal specification in the developing central nervous system of the cephalochordate amphioxus. Dev Biol 296:190–202

Seaver EC, Kaneshige LM (2006) Expression of 'segmentation' genes during larval and juvenile development in the polychaetes *Capitella* sp. I and *H. elegans*. Dev Biol 289(1):179–194. doi:http://dx.doi.org/10.1016/j.ydbio.2005.10.025

Seaver EC, Paulson DA, Irvine SQ, Martindale MQ (2001) The spatial and temporal expression of *Ch-en*, the *engrailed* gene in the polychaete *Chaetopterus*, does not support a role in body axis segmentation. Dev Biol 236(1):195–209. doi:http://dx.doi.org/10.1006/dbio.2001.0309

Seaver EC, Yamaguchi E, Richards GS, Meyer NP (2012) Expression of the pair-rule gene homologs *runt*, *Pax3/7*, *even-skipped-1* and *even-skipped-2* during larval and juvenile development of the polychaete annelid *Capitella teleta* does not support a role in segmentation. EvoDevo 3:8. doi:10.1186/2041-9139-3-8

Seredick SD, Ryswyk L, Hutchinson SA, Eisen JS (2012) Zebrafish Mnx proteins specify one motoneuron subtype and suppress acquisition of interneuron characteristics. Neural Dev 7:35

Sharman AC, Shimeld SM, Holland PWH (1999) An amphioxus *Msx* gene expressed predominantly in the dorsal neural tube. Dev Genes Evol 209:260–263

Shimamura K, Rubenstein JL (1997) Inductive interactions direct early regionalization of the mouse forebrain. Development 124(14):2709–2718

Shimeld SM (1999) The evolution of the hedgehog gene family in chordates: insights from amphioxus hedgehog. Dev Genes Evol 209(1):40–47. doi:10.1007/s004270050225

Shimeld SM, van den Heuvel M, Dawber R, Briscoe J (2007) An amphioxus *Gli* gene reveals conservation of midline patterning and the evolution of hedgehog signalling diversity in chordates. PLoS One 2(9):e864. doi:10.1371/journal.pone.0000864

Sjödal M, Gunhaga L (2008) Expression patterns of *Shh*, *Ptc2*, *Raldh3*, *Pitx2*, *Isl1*, *Lim3* and *Pax6* in the developing chick hypophyseal placode and Rathke's pouch. Gene Expr Patterns 8(7–8):481–485. doi:http://dx.doi.org/10.1016/j.gep.2008.06.007

Sobotta J (1895) Die Befruchtung des Eies von *Amphioxus lanceolatus*; vorlaufige Mitteilung. Anat Anz 11: 129–137

Sobotta J (1897a) Beobachtungen über den Gastrulationsvorgang beim Amphioxus. Verh Phys Med Ges Wurzburg 31:101–121 + pl. 101

Sobotta J (1897b) Die Reifung und Befruchtung des Eies von *Amphioxus lanceolatus*. Arch Mikrosk Anat 50:15–71 + pl. II–V

Somorjai IML, Somorjai RL, Garcia-Fernàndez J, Escrivà H (2012) Vertebrate-like regeneration in the invertebrate chordate amphioxus. Proc Natl Acad Sci 109(2):517–522. doi:10.1073/pnas.1100045109

Stieda L (1873) Studien über den *Amphioxus lanceolatus*. Mem Acad Imp Sci St Petersbourg (ser VII) 19(7):1–70 + pl.I–IV

Stokes MD (1996) Larval settlement, post-settlement growth and secondary production of the Florida lancelet (=amphioxus), *Branchiostoma floridae*. Mar Ecol Prog Ser 130:71–84

Stokes MD, Holland ND (1995a) Ciliary hovering in larval lancelets (= amphioxus). Biol Bull 188:231–233

Stokes MD, Holland ND (1995b) Embryos and larvae of a lancelet, *Branchiostoma floridae*, from hatching through metamorphosis–growth in the laboratory and external morphology. Acta Zool Stockh 76:105–120

Stokes MD, Holland ND (1996) Reproduction of the Florida lancelet (*Branchiostoma floridae*): spawning patterns and fluctuations in gonad indexes and nutritional reserves. Invertebr Biol 115:349–359

Strausfeld NJ (2010) Brain homology: dohrn of a new era. Brain Behav Evol 76:165–167

Strausfeld NJ, Hirth F (2013) Deep homology of arthropod central complex and vertebrate basal ganglia. Science 340(6129):157–161. doi:10.1126/science.1231828

Stricht O van der (1896) La maturation et la fécondation de l'oeuf d'*Amphioxus lanceolatus*. Arch Biol 14:469–495 + pl. XX–XXI

Sunmonu NA, Li K, Guo Q, Li JYH (2011) *Gbx2* and *Fgf8* are sequentially required for formation of the midbrain-hindbrain compartment boundary. Development 138(4):725–734. doi:10.1242/dev.055665

Tomer R, Denes AS, Tessmar-Raible K, Arendt D (2010) Profiling by image registration reveals common origin of annelid mushroom bodies and vertebrate pallium.

Cell 142(5):800–809. doi:http://dx.doi.org/10.1016/j.cell.2010.07.043
Toresson H, Martinez-Barbera JP, Bardsley A, Caubit X, Krauss S (1998) Conservation of *BF-1* expression in amphioxus and zebrafish suggests evolutionary ancestry of anterior cell types that contribute to the vertebrate telencephalon. Dev Genes Evol 208(8):431–439. doi:10.1007/s004270050200
Tosches MA, Arendt D (2013) The bilaterian forebrain: an evolutionary chimaera. Curr Opin Neurobiol 23(6):1080–1089. doi:http://dx.doi.org/10.1016/j.conb.2013.09.005
Tossell K, Kiecker C, Wizenmann A, Lang E, Irving C (2011) Notch signalling stabilises boundary formation at the midbrain-hindbrain organiser. Development 138(17):3745–3757. doi:10.1242/dev.070318
Tung TC, Wu SC, Tung YFY (1958) The development of isolated blastomeres of amphioxus. Sci Sin 7:1280–1320
Tung TC, Wu SC, Tung YYF (1960) The developmental potencies of the blastomere layers in Amphioxus egg at the 32-cell stage. Sci Sin 9:119–141
Tung TC, Wu SC, Tung YYF (1962a) Experimental studies on the neural induction in amphioxus. Sci Sin 11:805–820
Tung TC, Wu SC, Tung YYF (1962b) The presumptive areas of the egg of amphioxus. Sci Sin 11:629–644
Urbach R, Technau G (2008) Dorsoventral patterning of the brain: a comparative approach. In: Technau G (ed) Brain development in *Drosophila melanogaster*, vol 628, Advances in Experimental Medicine and Biology. Springer, New York, pp 42–56. doi:10.1007/978-0-387-78261-4_3
Wagner GP (2007) The developmental genetics of homology. Nat Rev Genet 8(6):473–479
Wassef M, Joyner AL (1997) Early mesencephalon/metencephalon patterning and development of the cerebellum. Perspect Dev Neurobiol 5(1):3–16
Welsch U (1968) Die Feinstruktur der Josephschen Zellen im Gehirn von Amphioxus. Z Zellsorsch 86:252–261
Welsch U (1975) The fine structure of the pharynx, cyrtopodocytes and digestive caecum of amphioxus (*Branchiostoma lanceolatum*). Symp Zool Soc Lond 36:17–41
Wicht H, Lacalli TC (2005) The nervous system of amphioxus: structure, development, and evolutionary significance. Can J Zool 83:122–150
Wijhe WJ van (1893) Ueber Amphioxus. Anatom Anz 8:152–172
Wijhe WJ van (1907) Beiträge zur Anatomie der Kopfregion des Amphioxus lanceolatus. Petrus Camper Anatomische Beiträge hrsg. von L. Bolk und C. Winkler, 1:109–194 + pl. VIII–XI
Willey A (1891) On the development of the atrial chamber in amphioxus. Proc R Soc 48:80–89
Willey A (1894) Amphioxus and the ancestry of the vertebrates. MacMillan, New York
Williams NA, Holland PWH (1996) Old head on young shoulders. Nature 383:490, only
Wilson EB (1893) Amphioxus, and the mosaic theory of development. J Morphol 8:579–639 + pl. XXIX–XXXVIII
Winchell CJ, Sillivan J, Cameron CB, Swalla BJ, Mallatt J (2002) Evaluating hypotheses of deuterostome phylogeny and chordate evolution with new LSU and SSU ribosomal DNA data. Mol Biol Evol 19: 762–776
Wright AA (1890) Amphioxus in Tampa Bay. Am Nat 24:1085
Wu SC (1986) The early development of *Amphioxus*. In: Ganguan Z (ed) Advances in science of China, vol I, Biology. Wiley, New York, pp 231–266
Wu XH, Zhang BL, Guo ZY, Qu YM (2000a) Laboratory culture of the amphioxus (Branchiostoma belcheri tsingtauense)–effects of food and sand on larvae survival. Chinese J Oceanol Limnol 18:134–136
Wu XH, Zhang BL, Guo ZY, Qu YM (2000b) Artificial culture of amphioxus (*Branchiostoma belcheri tsingtauense*). Chinese J Oceanol Limnol 18:334–337
Wu HR, Wu HR, Chen YT, Su YH, Luo YJ, Holland LZ, Yu JK (2011) Asymmetric localization of germline markers Vasa and Nanos during early development in the amphioxus *Branchiostoma floridae*. Dev Biol 353:147–159
Yamaguchi T, Henmi Y (2003) Biology of the amphioxus, *Branchiostoma belcheri* in the Ariake Sea, Japan. II. Reproduction. Zoolog Sci 20:907–918
Yang L, Zhang H, Hu G, Wang H, Abate-Shen C, Shen MM (1998) An early phase of embryonic *Dlx5* expression defines the rostral boundary of the neural plate. J Neurosci 18(20):8322–8330
Yarrell W (1836) A history of British fishes (Edition I), Volume 1, vol II. J. Van Voorst, London
Yasui K, Zhang SC, Uemura M, Saiga H (2000) Left-right asymmetric expression of *BbPtx*, a Ptx-related gene, in a lancelet species and the developmental left-sidedness of deuterostomes. Development 127:187–195
Yasui K, Urata M, Yamaguchi M, Ueda H, Henmi Y (2007) Laboratory culture of the oriental lancelet *Branchiostoma belcheri*. Zoolog Sci 24:514–520
Yasui K, Igawa T, Kaji T, Henmi Y (2013) Stable aquaculture of the Japanese lancelet *Branchiostoma japonicum* for 7 years. J Exp Zool 320B(8):538–547. doi:10.1002/jez.b.22540
Yu JK, Holland ND, Holland LZ (2002) An amphioxus winged helix/forkhead gene, *AmphiFoxD*: insights into vertebrate neural crest evolution. Dev Dyn 225:289–297
Yu JK, Holland ND, Holland LZ (2004) Tissue-specific expression of *FoxD* reporter constructs in amphioxus embryos. Dev Biol 274:452–461
Yu J-K, Satou Y, Holland ND, Shin-I T, Kohara Y, Satoh N, Bronner-Fraser M, Holland LZ (2007) Axial patterning in cephalochordates and the evolution of the organizer. Nature 445(7128):613–617. doi:http://www.nature.com/nature/journal/v445/n7128/suppinfo/nature05472_S1.html
Yu J-K, Meulemans D, McKeown SJ, Bronner-Fraser M (2008a) Insights from the amphioxus genome on the

origin of vertebrate neural crest. Genome Res 18(7):1127–1132. doi:10.1101/gr.076208.108

Yu JK, Wang MC, Shin-I T, Kohara Y, Holland LZ, Satoh N, Satou Y (2008b) A cDNA resource for the cephalochordate amphioxus *Branchiostoma floridae*. Dev Genes Evol 218:723–727

Zhang Y, Mao B (2010) Embryonic expression and evolutionary analysis of the amphioxus *Dickkopf* and *Kremen* family genes. J Genet Genom 37(9):637–645. doi:http://dx.doi.org/10.1016/S1673-8527(09)60082-5

Zhang SC, Holland ND, Holland LZ (1997) Topographic changes in nascent and early mesoderm in amphioxus embryos studied by DiI labeling and by in situ hybridization for a *Brachyury* gene. Dev Genes Evol 206:532–535

Zhang QJ, Luo YJ, Wu HR, Chen YT, Yu JK (2013) Expression of germline markers in three species of amphioxus supports a preformation mechanism of germ cell development in cephalochordates. EvoDevo 4:17

Tunicata

4

Alberto Stolfi and Federico D. Brown

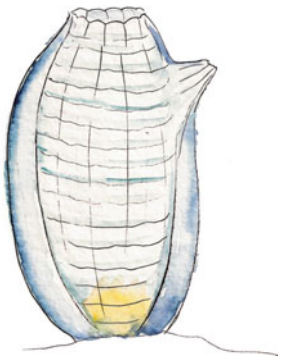

Chapter vignette artwork by Brigitte Baldrian.

A. Stolfi
Department of Biology, Center for Developmental Genetics, New York University, New York, NY, USA

F.D. Brown (✉)
EvoDevo Laboratory, Departamento de Zoologia, Instituto de Biociências, Universidade de São Paulo, São Paulo, SP, Brazil

Evolutionary Developmental Biology Laboratory, Department of Biological Sciences, Universidad de los Andes, Bogotá, Colombia

Centro Nacional de Acuicultura e Investigaciones Marinas (CENAIM), Escuela Superior Politécnica del Litoral (ESPOL), San Pedro, Santa Elena, Ecuador
e-mail: fdbrown@usp.br

A. Wanninger (ed.), *Evolutionary Developmental Biology of Invertebrates 6: Deuterostomia*
DOI 10.1007/978-3-7091-1856-6_4, © Springer-Verlag Wien 2015

Above all, perhaps, I am indebted to a decidedly vegetative, often beautiful, and generally obscure group of marine animals, both for their intrinsic interest and for the enjoyment I have had in searching for them. N. J. Berrill (1955)

INTRODUCTION

Tunicates are a group of marine filter-feeding animals[1] that have been traditionally divided into three classes: (1) Appendicularia, also known as larvaceans because their free-swimming and pelagic adult stage resembles a larva; (2) Thaliacea, which includes three orders of free-swimming and pelagic adult forms with complex life cycles (Salpida, Pyrosomida, and Doliolida); and (3) Ascidiacea, colloquially referred to as sea squirts,[2] which is comprised of diverse sessile solitary and colonial species and includes some of the most extensively studied tunicates. It was mainly the ascidians that served as the inspiration for seminal studies in developmental biology and evolution conducted last century by British zoologist and prolific writer N. J. Berrill, whose quote appears above.

Evolutionary Relationships

Although Tunicata is well established as a monophyletic group and united by their indisputably synapomorphic ability to synthesize cellulose, the phylogenetic relationships between the three classes and many orders and families have yet to be satisfactorily settled. Appendicularia, Thaliacea, and Ascidiacea remain broadly used in textbooks and scientific literature as the three classes of tunicates; however, recent molecular phylogenies have provided support for the monophyly of only Appendicularia and Thaliacea, but not of Ascidiacea (Swalla et al. 2000; Tsagkogeorga et al. 2009; Wada 1998). A paraphyletic Ascidiacea calls for a reevaluation of tunicate relationships. The most up-to-date phylogeny with a comprehensive taxonomic sampling of tunicates using 18S rRNA supports three clades for the Tunicata (Fig. 4.1; Tsagkogeorga et al. 2009): (1) Appendicularia, (2) Stolidobranch ascidians, and (3) Aplousobranch ascidians+Phlebobranch ascidians+Thaliacea. All three groups of the latter clade show resemblance in association of the gonads to the gut in concordance with the Enterogona classification (Perrier 1898). However, the precise position of the Appendicularia and the Thaliacea remains unresolved. Appendicularia has traditionally been considered to be at the base of the Tunicata (Wada 1998; Swalla et al. 2000), but recent molecular phylogenies place them as sister group to Stolidobranchia (Zeng et al. 2006; Tsagkogeorga et al. 2009). On the other hand, Thaliacea generally groups closer to Phlebobranchia than to Aplousobranchia using ribosomal molecular phylogenies (Zeng et al. 2006; Tsagkogeorga et al. 2009), but the low taxonomic sampling and a high 18S evolutionary rate of thaliaceans and aplousobranchs bring some uncertainty to this grouping. In an attempt to provide an evolutionary framework of the developmental mechanisms in Tunicata, developmental studies of several species of tunicates are reviewed here in a comparative manner with respect to our understanding of tunicate relationships.

Relationships to Other Chordates

For several centuries after Linnaeus first established the classification system for living organisms, ascidians were grouped together based on adult morphological features. This group contained a stereotypical adult body plan including

[1] Actually, there are specialized predatory ascidians in the Molgulidae and Octacnemidae families that do not filter feed but rather swallow whole crustaceans and other invertebrates (Tatián et al. 2011).

[2] The term "sea squirt" has been adopted for these animals, as seawater can be strongly propelled through the oral siphon upon physical perturbation. Other colloquial terms apply to certain species or genera ("sea peach" for *Halocynthia aurantium*, "sea grape" for *Molgula* spp.). The literate translation for "sea squirt" is used in Spanish (*chorro de mar*), Finnish (*meritupet*), Swedish (*Sjöpungar*), or Polish (*Żachwy*); more externally descriptive terms are also used, such as "sea bag" (*Sekkedyr* in Norwegian or *Søpunge* in Danish), "sack pipe" (*Zakpijpen* in Dutch), or "sea sheath" or "sea vagina" (*Seescheide* in German). Humorous, if crude, terms abound especially in Portuguese, like *mija-mija* ("piss-piss"), *Maria Mijona* ("Pissing Mary"), or *mijão* ("big pisser").

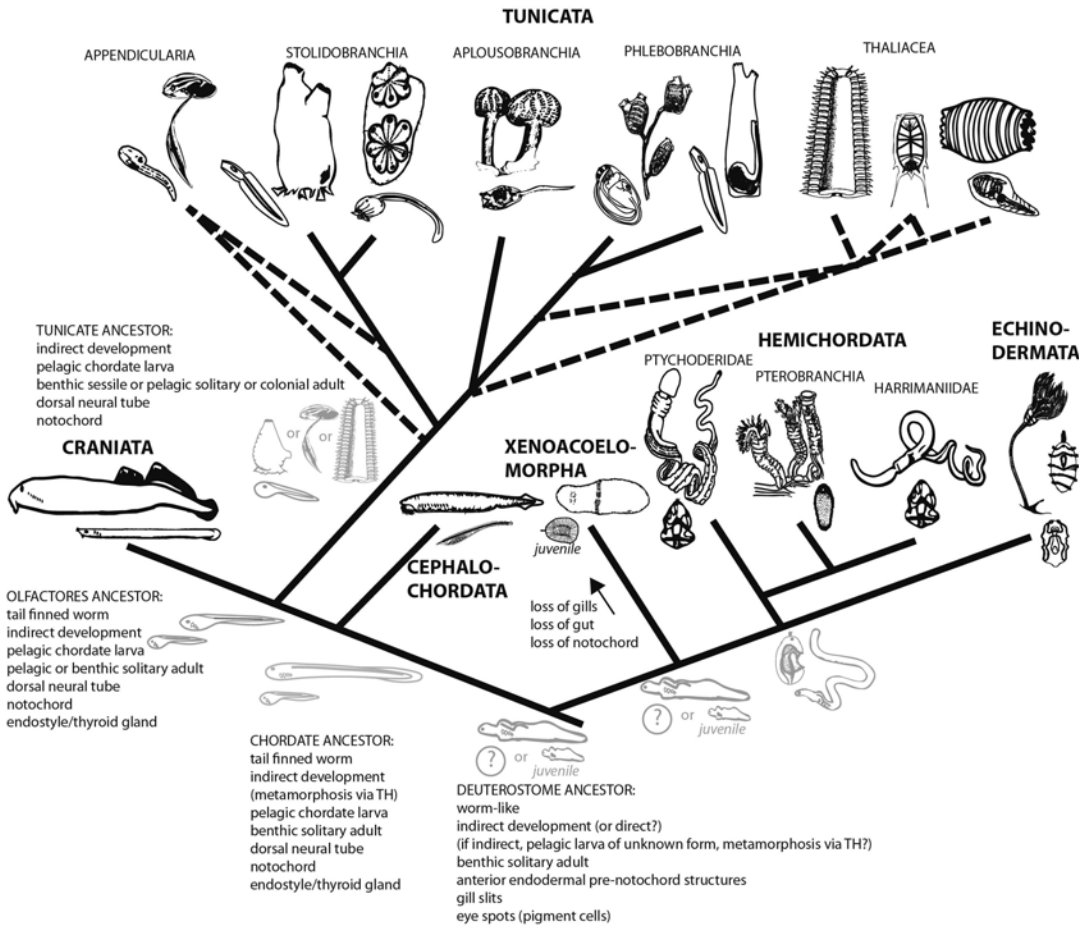

Fig. 4.1 Current understanding of tunicate relationships within the deuterostomes. *Dashed lines* represent possible relationships in uncertain branches (see text for details). Larval (*below*) and adult (*above*) forms have been included at each node to facilitate understanding of distinct arguments discussed in the text of the major evolutionary transitions of extant clades and their ancestors (in *gray*). Descriptions of the most parsimonious ancestral characteristics are shown at every node representing possible tunicate ancestors. Cases of multiple larval or adult ancestral forms are separated by "or", direct development (no larva) is shown by "juvenile," and unknown forms are presented as a question mark (?) in a *circle*

(1) a U-shaped gut delimited by an incurrent and an excurrent siphon, (2) a large branchial cavity for filter feeding, and (3) the tunic, a characteristic mantle later discovered to be made of animal cellulose. Already by the turn of the nineteenth century, Jean-Baptiste de Lamarck realized that ascidians and thaliaceans could be grouped as Tunicata (Lamarck 1816). However, based strictly on the adult morphological features of solitary or colonial forms, these animals remained difficult to place in broader evolutionary animal groups; for example, in the mid-nineteenth century, tunicates were grouped together with ectoprocts and brachiopods within the mollusks (Fig. 4.2A) (Milne-Edwards 1843; Haeckel 1866). A unified Tunicata as we consider them today was first proposed by Huxley (1851), who included Appendicularia in the Tunicata proposed by Lamarck.

Only after Kowalevsky had described the tailed larval form of ascidians (Kowalewski 1866), containing a dorsal neural tube, a typical chordate notochord, and lateral muscle cells, did zoologists begin to realize that tunicates should be

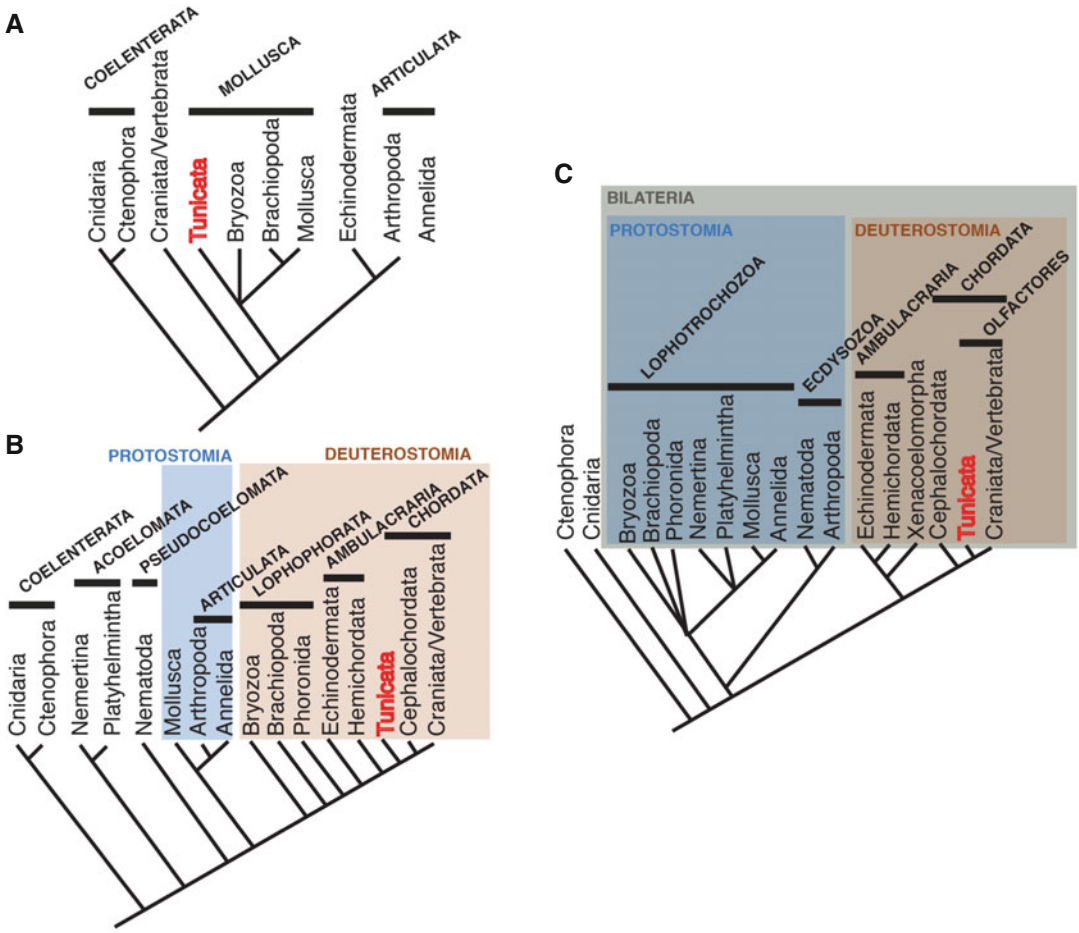

Fig. 4.2 Historic overview of the position of Tunicata within the Metazoa. (**A**) View of animals relationships through the nineteenth century (Milne-Edwards 1843; Haeckel 1866), highlighting the position of the Tunicata as a chordate due to the presence of the notochord (in *red*). (**B**) Popular view of animal relationships throughout the twentieth century with the lophophorates (Hyman 1959; Zimmer and Larwood 1973; Nielsen 2002) basal to the tunicates. (**C**) Current view using molecular phylogenies (Field et al. 1988; Cameron et al. 2000; Swalla et al. 2000; Winchell et al. 2002)

placed within the chordates. In the late nineteenth century, zoologists such as Haeckel (1874), Bateson (1884, 1886), Brooks (1893), Willey (1894), and Garstang (1894) supported Chordata and Hemichordata as sister phyla based on notochord-like structures as the main synapomorphy. Within Chordata three subphyla were recognized, Vertebrata, Cephalochordata, and Tunicata, which Lankester (1877) attempted to rename as Urochordata, to highlight the evolutionary importance of this character within the phylum. Because cephalochordates shared more morphological features with the vertebrates, including a metameric muscle segmentation pattern, the tunicates were placed at the base of Chordata. Because of the unique body plan of adult tunicates, it was even proposed that they be raised to phylum status (Kozloff 1990; Cameron et al. 2000; Zeng and Swalla 2005).

At the turn of the twentieth century, zoologists realized that chordates, hemichordates, and echinoderms share a common embryological trait: the blastopore, the first opening that forms in the gastrulating embryo, developed into the anus of the adult. Thus, they were classified within the superphylum Deuterostomia (Grobben 1908), opposite to Protostomia, or animals whose blastopores developed into the mouth instead. A morphological

feature that generated confusion for almost the entire twentieth century but that was relevant to the general debate of early deuterostome evolution was the lophophore of brachiopods, ectoprocts, and phoronids (see Vol. 2, Chapters 10, 11, and 12), a crown-like feeding apparatus composed of numerous tentacles. In spite of convincing arguments for nearly half a century that supported a monophyletic Lophophorata (those animals bearing a lophophore) as being part of or closely related to Deuterostomia (Fig. 4.2B; Hyman 1959; Zimmer and Larwood 1973; Nielsen 2002), molecular phylogenetic work contested their deuterostome affinities and instead grouped them together with annelids, mollusks, and other diverse phyla in Lophotrochozoa (Halanych 2004; Helmkampf et al. 2008).

Conserved gene sequences, such as large and small subunit ribosomal rDNAs, were the first molecular characters used for testing phylogenies of deuterostomes and other phyla (Field et al. 1988; Cameron et al. 2000; Swalla et al. 2000; Winchell et al. 2002). Additional protein-coding gene sequences (both mitochondrial and nuclear), intron-exon boundaries, miRNAs, and other empirical evidence rendered additional support for the monophyly of Deuterostomia and Ambulacraria (Echinodermata + Hemichordata) and also resulted in new and previously unexplored hypothetical relationships such as the placement of *Xenoturbella* together with acoel worms as the sister group to the Ambulacraria (see Vol. 1, Chapter 9 for discussion) or the inversion of Tunicata and Cephalochordata positions within Chordata (Delsuc et al. 2006; Telford and Copley 2011). The latter proposed relationship for Chordata suggests that Tunicata is the sister group to Craniata/Vertebrata within a group named Olfactores (reviewed in Delsuc et al. 2006), to the exclusion of Cephalochordata (Fig. 4.2C). Some of the implications of this new rearrangement for our understanding of chordate evolution will be discussed in the following.

Tunicate and Chordate Origins

For nearly 200 years, zoologists have wondered about the origins of our own phylum, and the literature is rife with heated debates on the origins of chordates (Fig. 4.3). In this section the main hypotheses that have been proposed and how more recent views of deuterostome relationships have affected our understanding of the chordate ancestor are reviewed.

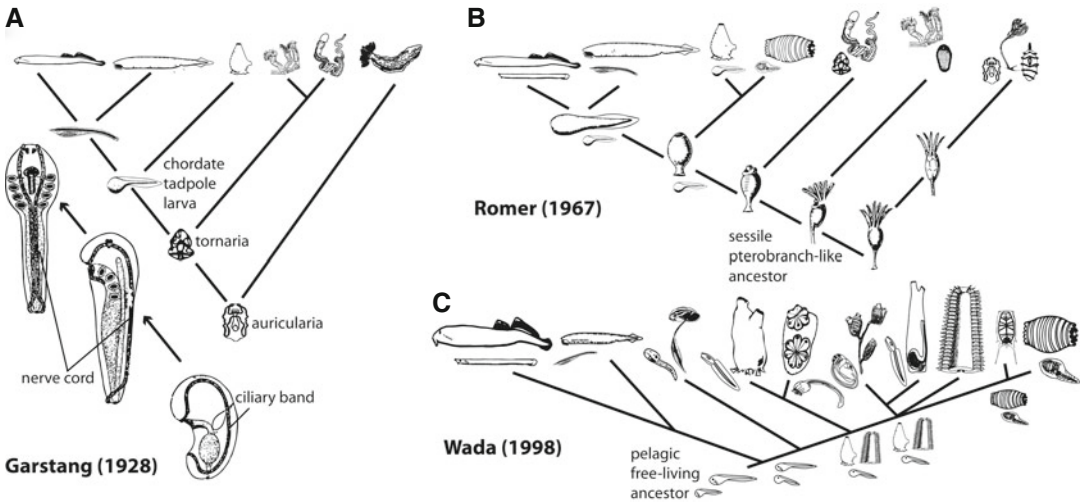

Fig. 4.3 Chordate origins hypotheses. (**A**) Garstang's hypothesis suggested that chordates evolved from larval pelagic forms; a scenario representing the evolutionary transition from a dipleurula-like ancestor that modified the ciliary band into the nerve cord of the chordate larva is shown. (**B**) Romer hypothesized the evolution of chordates from a colonial pterobranch-like ancestor; the ancestor eventually transitioned to a free-living life history and modified the tentacles into gills. (**C**) Wada's hypothesis was formulated according to the phylogenetic understanding of chordate relationships by the turn of the century; the basal position of the larvaceans among the tunicates and the paraphyly of ascidians suggested an ancestor with both a pelagic larva and adult

Garstang Hypothesis (1928): Walter Garstang proposed that chordates evolved through a series of modifications to the ancestral larva, independently from changes in the adult form (Fig. 4.3A), and therefore retraced the evolutionary steps back in time starting from (1) a permanently free-swimming chordate larva to (2) a protochordate-like larva (i.e., cephalochordate or ascidian), to (3) a tornaria-like larva (i.e., hemichordate), to (4) an auricularia-like larva (i.e., echinoderm). From this ancestral reconstruction, it may be extrapolated that the free-swimming larval and adult stages of Craniata/Vertebrata as well as Cephalochordata evolved from an ascidian-like ancestor that suppressed metamorphosis. The latter, in turn, evolved from plankton-feeding benthic organisms (similar to extant hemichordates and echinoderms) with external ciliated tentacles and food groves that contained pelagic larvae (tornaria and auricularia, respectively) (reviewed in Berrill 1955; Brown et al. 2008). Garstang also observed similarities between the development of the neural tube and endostyle (i.e., the thyroid gland precursor; see Metamorphosis section below for more details) of chordate larvae and the formation of the circumoral and adoral ciliary bands of echinoderm larvae. He assumed these processes were homologous, which would support his hypothesis. However, expression patterns of several key developmental genes in the echinoderm larva do not resemble the expected expression patterns of either invertebrate or vertebrate embryos and generally show echinoderm-specific patterns. These results have caused some difficulties in inferring homologies between chordate and echinoderm larvae and have been used to support the view of a secondarily acquired indirect-developing larva in the Ambulacraria (Echinodermata + Hemichordata) (reviewed in Swalla 2006; Brown et al. 2008).

Garstang was highly influenced at the time by work and ideas previously developed by Arthur Willey (1894). Willey had already noted that larval forms could recapitulate ancestral forms since the discovery of the chordate nature of the ascidian larva (Kowalewski 1866) and had also proposed the close relationship of the hemichordates and echinoderms due to the similarities of the tornaria and auricularia larvae. Ideas of recapitulation prevailed in the nineteenth century (Haeckel 1869) and set the stage for twentieth century ideas of heterochrony in development as an important factor in the evolution of animals.

Romer Hypothesis (1967): Alfred Romer was a vertebrate paleontologist and comparative morphologist who came to address the question of chordate evolution from a vertebrate point of view (Fig. 4.3B). In his hypothesis, two major evolutionary novelties were necessary for the evolution of the chordate body plan: (1) the evolution of pharyngeal slits from feeding tentacles (lophophores) and (2) the evolution of a free-living stage in the life cycle of an ancestral sessile, filter-feeding organism. As Romer explained in his departing American Association for the Advancement of Science (AAAS) presidential address published in Science (1967): "Instead of passively waiting for food to come to it, the animal could go in search of food and could explore new areas or new habitats in which it might exist," thus leading to the evolution of the cephalochordates and the vertebrates. A recurrent idea previously postulated by Garstang was that of a pedomorphic event in an ancestral ascidian-like larva that evolved into a free-living form in the cephalochordate and craniate/vertebrate ancestor.

The Romer hypothesis of chordate evolution became popular in the twentieth century and prevailed in many Zoology textbooks. Phylogenies at the time supported the pterobranchs and crinoids at the base of Deuterostomia, with the lophophorates as the sister group to the deuterostomes. However, phylogenetic data no longer support this hypothesis (Fig. 4.3B), and the sessile pterobranchs are likely derived from a free-living wormlike ancestor within the hemichordates (Fig. 4.1; Brown et al. 2008).

Wada Hypothesis (Wada 1998): Based on phylogenetic understanding of Tunicata relationships using 18S rDNA, Hiroshi Wada proposed a pelagic free-living ancestor of the chordates. The relationship generally accepted at the time was as follows: Cephalochordates were the sister taxon to the Craniata/Vertebrata; larvaceans were at the

base of the tunicates; ascidians were shown to be paraphyletic (Fig. 4.3C). Therefore, the most parsimonious reconstruction scenario of the chordate ancestor was that of a pelagic noncolonial and indirect-developing free-swimming form resembling the life cycles of lampreys, cephalochordates, and larvaceans that were placed at the base of the Tunicata. Since then, phylogenetic relationships of the chordates have gained from new analysis methods, additional gene sequences, and new genomes and transcriptomes that have substantially changed our view of tunicate relationships. In particular, a new placement of Tunicata as sister group of the Craniata/Vertebrata and genome-wide sequence analyses and developmental studies in larvaceans have begun to change our views of chordate ancestry. These will be discussed next.

The Wormlike or Vermiform Deuterostome Ancestor Hypothesis: Although references to a wormlike ancestor of the chordates date back to A. Willey (1894),[3] later work by morphologists focused mostly on macroevolutionary reconstructions based solely on ancestral pelagic larval forms (Garstang 1928; Nielsen 1995). Only recently has this hypothesis been revisited, thanks to recent developmental studies and a new understanding of deuterostome relationships. More specifically, gene expression patterns have emerged as new characters that can be evaluated as shared novelties (synapomorphies) among the various groups within the deuterostomes (Nielsen 1995; Cameron et al. 2000; Wicht and Lacalli 2005; Gudo and Syed 2008).

The vermiform ancestor hypothesis postulates that chordates and deuterostomes evolved from a solitary, sexually reproducing, free-living wormlike ancestor with pharyngeal slits, i.e., similar to an enteropneust worm (Fig. 4.1; Cameron et al. 2000; Gerhart et al. 2005; Brown et al. 2008). Initially, a benthic vermiform deuterostome ancestor with a pelagic dipleurula-like larva, termed the "notoneuron," was discussed by Nielsen (1995) in his Trochaea hypothesis. However, the evolutionary sequence that gave rise to the notoneuron assumed the existence of ancestral holopelagic forms, which very much resembles the recapitulation hypothesis of the nineteenth century (Fig. 4.3A; Haeckel 1869; reviewed in Garstang 1928; Collins and Valentine 2001).

In contrast to the previous hypotheses, the most complete and parsimonious scenario based on current phylogenetic evidence (Fig. 4.1) is presented here. Within the Chordata, three hypothetical ancestors are discussed: chordate, olfactorean (tunicate + vertebrate), and tunicate.

The chordate and olfactorean ancestors may be assumed as being very similar in development and form: indirect-developing vermiform organisms with gill slits, dorsal neural tube, notochord, and a pigmented sensory organ throughout all stages of their life cycle (Fig. 4.1). Whether the adult of the olfactorean ancestor was pelagic or benthic is difficult to predict with confidence, but the chordate ancestor was very likely benthic, with a lifestyle resembling that of the cephalochordate adult. This view can be supported as cephalochordates are now placed basal to Olfactores. The parsimonious conclusion is that the olfactorean ancestor was also benthic.

The tunicate ancestor was likely an indirect developer that had a pelagic free-swimming larva with a notochord, a dorsal neural tube, and asymmetric pigmented sensory organs, traits that are found in most tunicate clades (Fig. 4.1). This ancestral larva probably did not have any gills, as most larvae in extant tunicates do not develop or utilize their gills until after metamorphosis. Due to the unresolved phylogenetic positions of Appendicularia, Thaliacea, and several species of phlebobranch and aplousobranch ascidians, there are few confident predictions we can make on the adult form of the tunicate ancestor, other than to say it was likely a filter feeder. While the first tunicate ancestor was likely very similar to its vermiform olfactorean forebear, we cannot rule out a scenario in which the transition to sessility occurred in the stem leading to the last common ancestor of all extant tunicates.

[3] A. Willey wrote in his treaty on "Amphioxus and the Ancestry of the Vertebrates" (1894): "The ultimate or primordial ancestor of the vertebrates would, on the contrary, be a wormlike animal whose organization was approximately on a level with that of the bilateral ancestors of the Echinoderms."

Historical Milestones of Tunicate Developmental Biology

The chordate nature of ascidians was first recognized by Russian zoologist Alexander Kowalevsky (1866). He generated detailed descriptions of embryogenesis and the anatomy and general organization of the chordate larva in two species of ascidians, *Phallusia mammillata* and *Ciona intestinalis*. As mentioned above, his original descriptions suggested that these animals were closer to the vertebrates rather than to their previous classification as mollusks. His discovery set the stage for renewed discussions of the centuries-old questions about the evolution of animal form (Raff and Love 2004).

Kowalevsky's careful anatomical descriptions of the ascidian embryo and larva served as one of the inspirations for an attempt to unravel the evolutionary history of animals by analyzing the features that appeared transiently during particular developmental stages. The ascidian embryo was thus held up in support of a recapitulatory view of evolution. Although such views have been largely superseded, it is imperative to contextualize them. At that time, these studies were among the first to suggest that the development of an organism could reveal information about its evolutionary origins. A modern-day analogy would be the "hidden" evolutionary history that is stored in morphogenesis as well as the genes and genomes of organisms, which has revolutionized our understanding of phylogeny and evolution in the last decades.

Near the end of the nineteenth century, the French embryologist Laurent Chabry, working on *Ascidiella aspersa*, performed the first experiments on animal embryos at the single-cell level, manipulating individual blastomeres with the micromanipulator he had invented and built himself (Fig. 4.4A; Chabry 1887; reviewed in Fischer 1992; Sander and Fischer 1992). This was a radically new approach at the time and generated much discussion in those days of wildly differing theories

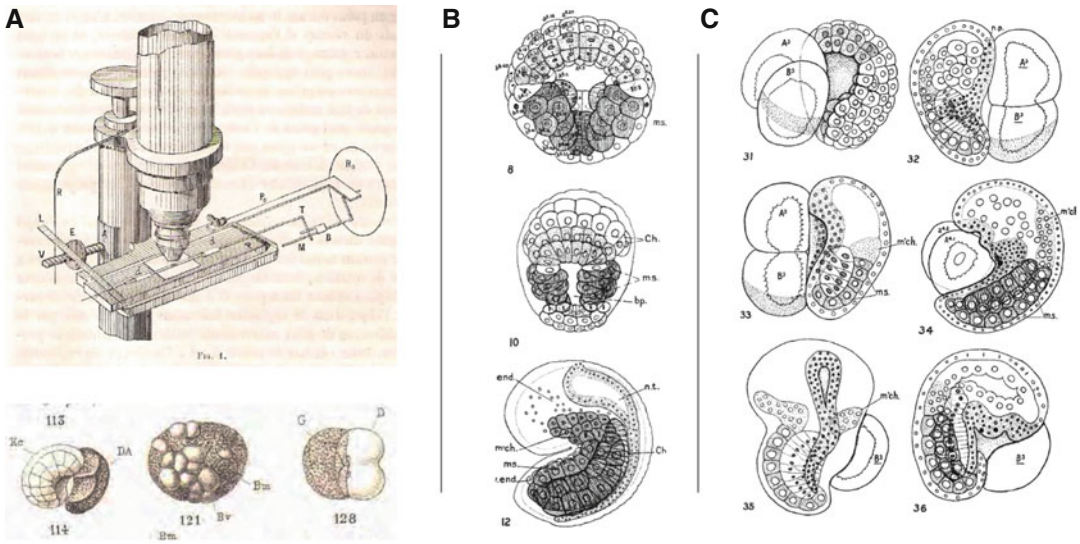

Fig. 4.4 Classic works of ascidian embryology. (**A**) *Top*: Laurent Chabry's micromanipulator, of his own invention and construction. *Bottom row*: some of the "monsters" (damaged or naturally defective embryos) whose abnormal development he characterized. The illustrations are from his thesis (Chabry 1887). (**B**) Illustrations by Conklin of a *Styela canopus* embryo, showcasing two of his greatest discoveries: the posterior vegetal myoplasm, or "organ-forming substance" (Conklin 1905a), and the invariant cell lineages of the early embryo (Conklin 1905b). (**C**) Conklin's illustrations of the embryos whose blastomeres he managed to damage through swirling or suction. His documentation of these half or quarter embryos helped establish a role for mosaic, as opposed to regulative, mechanisms of cell fate specification (Conklin 1905c)

on the very essence of embryogenesis. Chabry's work was eagerly followed up by other luminaries of those early days of experimental embryology, such as Roux, Driesch, Spemann, and Mangold.

In the history of ascidian embryology, we skip some 20 years forward to describe the work of American embryologist Edwin G. Conklin, who conducted both detailed descriptive and ingenious experimental research on the ascidian embryo. At the Marine Biological Laboratories at Woods Hole, Conklin used a local species, *Styela canopus*,[4] to ask basic questions about cell fates during embryonic development. This species was particularly suited for this line of inquiry because its eggs contained a naturally occurring yellow-orange pigment in the cytoplasm that became progressively restricted after each round of cell division until it was ultimately inherited by the larval muscles (Fig. 4.4B). Conklin therefore hypothesized, correctly, that this cytoplasm contained an "organ-forming substance" that was sufficient and necessary for larval muscle specification and differentiation (Conklin 1905a).

The cellular simplicity of the ascidian embryo also allowed Conklin to follow embryonic cells during development up to their final fate. The cell lineages he described for *Styela* became the most complete embryonic lineage mapping ever done for any animal at the time (Conklin 1905b). Moreover, he could manipulate early embryos en masse by spurting and shaking and assess the results of injuring particular blastomeres in this way (Conklin 1905c). This allowed him to demonstrate the highly deterministic mode of development of ascidians, which contrasted abruptly with the highly regulative mode of development that was discovered in sea urchins around the same time (Fig. 4.4C). He called this highly deterministic mode of development in ascidians "mosaic." He and others also noted similar patterns of embryogenesis and highly stereotypical cell numbers and lineages in embryos of other species of solitary ascidians. This was followed by several decades of comparative works describing the diversity and evolution of developmental modes found in ascidians and tunicates, most notably by Berrill (1930, 1931, 1932, 1935a, b, 1936, 1947a, b, c, 1948a, b, c, d, e, 1950a, b, 1951).

As the broader field of developmental genetics matured and incorporated the techniques and approaches of molecular biology and genomics, ascidian embryogenesis quickly came to be understood and interpreted in the light of gene expression and function. Gone were the sectarian squabbles of regulative vs. mosaic development: conserved intercellular signaling pathways were found to regulate the induction of the majority of cell fates in the ascidian embryo. A new picture emerged, in which mechanisms of "mosaic" development (e.g., localized maternal determinants) critically set the stage for the intricate and invariant unfolding of events that nonetheless require the constant instructions and affirmations of cell-cell communication, until all progenitors are specified and their derivatives fully differentiated.

Many of the first discoveries in this new molecular age of ascidian biology were achieved by researchers working on *Halocynthia roretzi*, but *Ciona intestinalis* quickly rose to prominence[5] when its genome was sequenced in 2002 (Dehal et al. 2002). Researchers working on ascidians were privileged to be among the first to lay eyes on the genomic underpinnings of animal development, as *C. intestinalis* was only the seventh animal to have its genome sequenced at the time. The adaptation of an electroporation-based high-throughput transgenesis protocol also boosted the popularity of *C. intestinalis* among developmental biologists (Corbo et al. 1997).

[4] There appears to be some confusion as to which species was originally used in Conklin's experiments. Although in his original studies the species was named as *Cynthia* (*Styela*) *partita*, this name is no longer valid, having been synonymized with *Styela canopus*. However, the ecologically dominant *Styela* species around Woods Hole nowadays is the invasive *S. clava*.

[5] There are approximately 70 laboratories in the world currently using *Ciona* as a model species; for further information on *Ciona* and other ascidian online resources, visit http://www.aniseed.cnrs.fr/aniseed/.

Tunicata: Experimental Models for EvoDevo Research

There has been a variety of work on many different species representing all orders in the Tunicata, and it is with some injustice that the four species below have been highlighted above all the others, solely based on the relative importance attached to them by a handful of bipedal terrestrial olfactoreans. However, they represent a good sampling of different traits, historical backgrounds, and other points of interest to the experimentalist.

Ciona intestinalis (*Linnaeus*, *1767*), like its close relative *C. savignyi*, is a rather unspecialized solitary phlebobranch ascidian. A common invasive species in temperate waters around the globe, it is easily obtainable from the wild. In fact, this was the major reason *C. intestinalis* gained traction with developmental biologists (culminating in the sequencing of its genome in 2002): researchers in Japan, North America, and Northern and Southern Europe could work on the same species… or so they thought! It is now understood that the same name has been used for two closely related but genetically distinct and reproductively isolated species, currently referred to as "Type A" and "Type B." The *Ciona* community awaits official publication of the bombshell revelation (Lucia Manni, personal communication) that the specimen originally described by Linnaeus, and thus the specific epithet *intestinalis*, most likely belonged to the "Type B" species of Northern Europe. This would mean that the "Type A," studied by the majority of labs around the world, actually corresponds to *Ciona robusta*, currently a junior synonym that nonetheless describes the type specimen for "Type A."

Halocynthia roretzi (*Drasche*, *1884*), also known as the sea pineapple, is a prized culinary delicacy in parts of Japan and Korea. A large solitary stolidobranch ascidian, its eggs and larvae are roughly twice as large as those of *Ciona* spp., but develop according to the same cell lineages, with roughly the same number of cells as *Ciona* and other smaller solitary species. Many of the modern-day classics in ascidian developmental biology were performed on *H. roretzi* by Hiroki Nishida in Japan. However, its limited distribution has prevented its adoption as a model organism by researchers outside East Asia. Other obstacles to widespread use as a model organism include its inaptitude for the electroporation protocol so useful for transient transfections in *Ciona*, and deadly outbreaks of the insidious soft tunic syndrome disease (caused by a species of kinetoplastid flagellate) among sea pineapples under intense cultivation. However, important insights into developmental biology continue to be regularly generated by work on this venerable model, and the community eagerly awaits the results of the ongoing efforts to sequence and annotate its genome and that of its North American close relative, the sea peach *Halocynthia aurantium*.

Botryllus schlosseri (*Pallas*, *1766*) is the leading model colonial species. Research in *Botryllus schlosseri* has focused mainly in the study of budding, i.e., blastogenesis, and in studies of self- and nonself recognition of adult colonies. Also known as the star tunicate due to the star-shaped arrangement of individual zooids within the colony, *B. schlosseri* develops synchronously and undergoes weekly developmental cycles that generate new zooids at the same time as old zooids regress. A relatively fast turnover of zooids and simplicity in the maintenance of colonies in the laboratory have made this species a suitable model organism for studies on stem cells, differentiation, apoptosis, and sexual vs. asexual development. Stages of blastogenic development were described by Sabbadin as well as Watanabe, and its complete genome was finally published in 2013. Upon contact of two adult colonies, an allorecognition reaction occurs, which results in either fusion of the colonies forming a larger chimeric colony (parabiont) or

rejection of the two colonies, revealing a histocompatibility locus with important evolutionary implications for the evolution of adaptive immunity of vertebrates.

Oikopleura dioica (*Fol*, *1872*) is an emerging model organism for larvacean biology. Their small size and rapid generation cycle mean they have to be cultured in suspensions of large numbers of individuals. Nonetheless, this allows for inland culturing of different strains, enabling classical genetic analyses. Furthermore, the female germ line and ovary develop as a single, multinucleated syncytium called a coenocyst, allowing for targeted genetic manipulations in ovo by injecting the coenocyst. Larvaceans hold many of the keys to understanding the evolution of tunicates and chordates, and work on *O. dioica* will figure heavily into understanding the biology of these amazing creatures.

Soon thereafter the genome of the related *Ciona savignyi* was sequenced (Vinson et al. 2005; Small et al. 2007). This was followed by the genome sequence of the larvacean *Oikopleura dioica* (Denoeud et al. 2010) and the colonial stolidobranch ascidian *Botryllus schlosseri* (Voskoboynik et al. 2013), which was already the established colonial tunicate model for studies on blastogenesis and histocompatibility. Other tunicate genomes currently in the sequencing pipeline include those of the phlebobranch ascidians *Phallusia mammillata*, *Phallusia fumigata* (Tassy et al. 2010; Roure et al. 2014), and *Didemnum vexillum* (Abbott et al. 2011; Stefaniak et al. 2012), as well as the stolidobranch ascidians *Halocynthia roretzi*, *Halocynthia aurantium* (Tassy et al. 2010), *Molgula occulta*, *Molgula oculata*, and *Molgula occidentalis* (Stolfi et al. 2014).

Tunicate genomes are rapidly evolving (Denoeud et al. 2010; Tsagkogeorga et al. 2012) and quite compact relative to the genomes of their sister taxa, the vertebrates. The *Ciona* genomes are approx. 150–170 Mb in length, while the *Oikopleura dioica* genome is the smallest chordate genome sequenced to date, at 70 Mb. The *Botryllus schlosseri* genome is the largest tunicate genome sequenced thus far, at an estimated 580 Mb. The sizes of the tunicate genomes currently being sequenced appear to fall somewhere in the range of those already sequenced. Protein-coding genes are estimated to number between 15.000 in *Ciona* and 27.000 in *Botryllus*.

Thanks to the *Ciona intestinalis* sequencing efforts, a large amount of gene expression data has been generated for this species, including spatiotemporal expression pattern profiles for the vast majority of the approx. 700 transcriptional regulators (i.e., sequence-specific transcription factors and major cell signaling molecules) during embryonic development (Satou et al. 2001, 2002, 2003; Kusakabe et al. 2002; Mochizuki et al. 2003; Imai et al. 2004). Concurrent to the genomic revolution, the adaptation and refinement of techniques for molecular manipulation of ascidian embryos (Corbo et al. 1997; reviewed in Stolfi and Christiaen 2012; Treen et al. 2014) have allowed researchers to characterize the functions of many developmentally important genes in ascidians in quite some detail. The ease of manipulation of great numbers of synchronized embryos allows for large-scale analyses of gene function, a prime example of which was the construction of a provisional "blueprint" of regulatory networks at single-cell resolution for every cell of the *C. intestinalis* early embryo and larval nervous system (Fig. 4.5; Imai et al. 2006, 2009).

EARLY DEVELOPMENT

Tunicate development is marked by the contrast between the simple and the complex and between the conservative and the innovative. We use the ascidian embryo as a starting point for understanding the development of tunicates as a group,

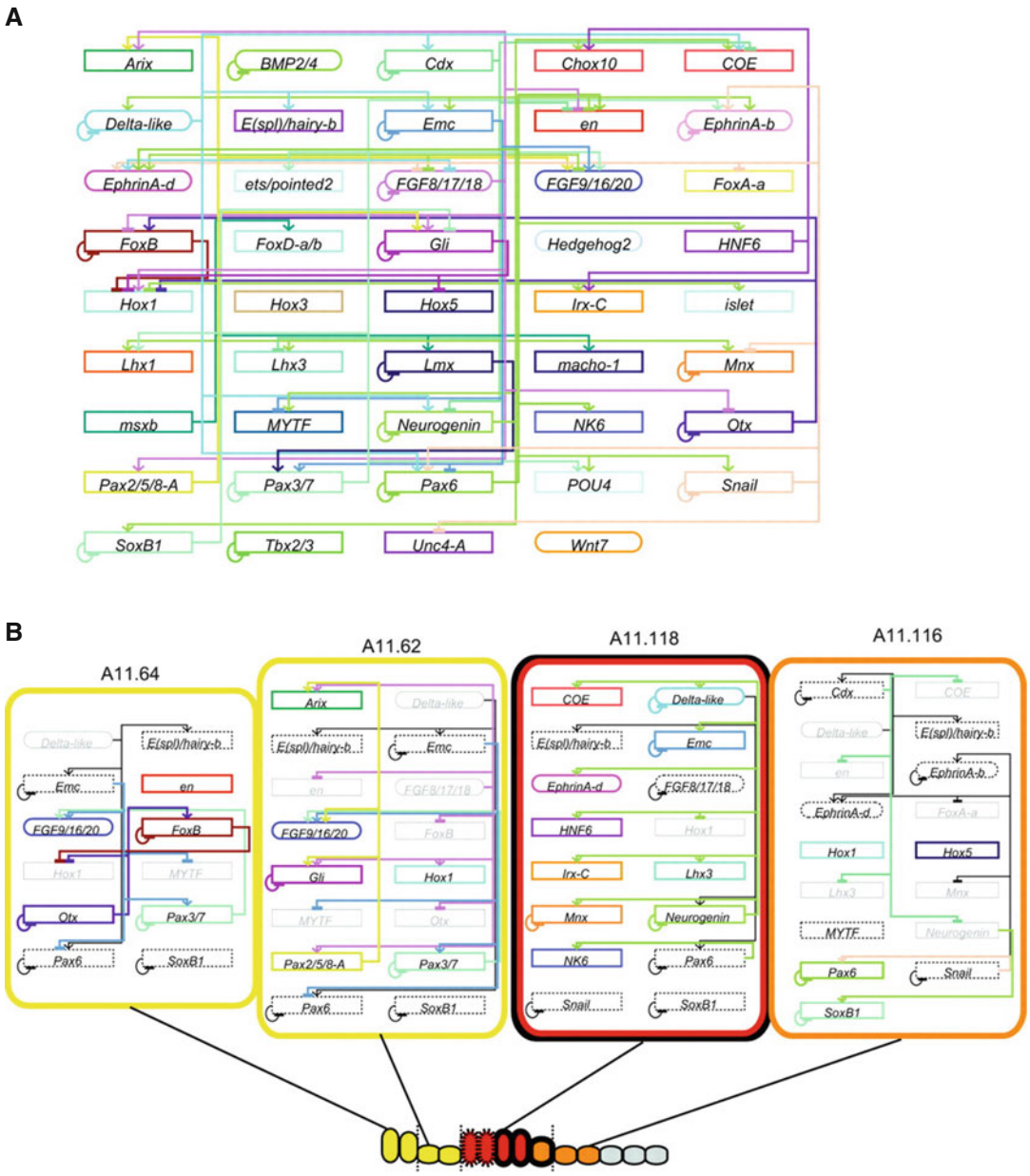

Fig. 4.5 Example of cell-specific gene regulatory networks in *Ciona intestinalis*. (**A**) Circuit diagram of overall regulatory connections between a subset of regulatory genes (transcription factors and intercellular signaling pathway components) expressed in the developing central nervous system of the *Ciona intestinalis* larva. (**B**) Cell-specific circuit diagrams of regulatory connections operating in selected cells of the posterior sensory vesicle (A11.64), neck (A11.62), motor ganglion (A11.118), and nerve cord (A11.116) (Figures adapted with permission of the authors from Imai et al. (2009))

as phylogenetic and embryological evidence suggest all extant tunicates descend from an ascidian-like common ancestor. Much is known about the early development of ascidians, which have been the intense focus of over 100 years' worth of developmental genetic studies. The vast

knowledge on the subject generated over the years can only be done justice by an extended format review, as has been elegantly done most recently by Satoh (2013). Here, we attempt to summarize a summary of what is known.

The ascidian life cycle may be separated into three or four important developmental periods: (1) embryogenesis (i.e., the formation of the larva), (2) larval development (i.e., settlement and metamorphosis), (3) growth and maturation (i.e., transition from juvenile to sexually mature adult), and (4), only for colonial species, blastogenesis (i.e., development of asexually propagated clonal generations). Considerable interspecific variation is found in egg/embryo size, reproductive strategies, and adult zooidal size (Fig. 4.6). The relative timing of the different stages of the ascidian life cycle also varies substantially from species to species, which highlights the importance of heterochrony and modularity in the evolution of developmental processes.

The Ascidian Embryo

Although ascidian embryos are greatly reduced in cell number and highly derived relative to vertebrates in strategies for cell fate specification, they are profoundly steeped in their chordate pedigree, as evidenced by highly conserved chordate-specific embryonic fate maps and gene regulatory networks. Within the ascidians, one finds great variation in the mode of development: viviparity, asexual reproduction, direct development, and adultation, i.e., the precocious differentiation of adult structures prior to hatching of the swimming larva. However, even distantly related ascidians share the same streamlined, invariant embryonic cell lineages. Therefore, phylogenetic evidence suggests that the simple, solitary ascidian embryo likely represents the ancestral condition and that all the other strikingly different modes are variations on this basic theme.

Embryonic development has been characterized in great detail in a number of indirectly developing, solitary ascidian species (reviewed in Lemaire 2009, 2011). In all species, the bilaterally symmetric embryos develop in an invariant manner, and cell division rates are tightly regulated. Unlike certain species of nematodes in which apoptosis, or programmed cell death, plays a large role in development by culling unused cells, there is no evidence that apoptosis is involved in normal embryogenesis in ascidians. All the cells that are born during the development of a typical ascidian embryo seem to be accounted for upon hatching (Hotta et al. 2007).

Quite remarkably, embryogenesis of the various solitary ascidians is perfectly conserved at least up until the neurula stage (and probably well beyond that) as far as cell lineages, divisions, and arrangements are concerned. The embryos may differ in size, developmental rate, and even gene expression, but there is a 1:1 correspondence between each and every cell in *Ciona intestinalis* and *Molgula occidentalis* gastrula embryos, in spite of the estimated 500 million years of evolutionary divergence between the two species (Fig. 4.7).

That species on opposite branches of the tunicate phylogeny have the same exact cell lineages would seem to imply that genetically they must be very conservative as well and that the *cis-regulatory* elements (or "enhancers") orchestrating the gene regulatory networks responsible for embryonic development must be highly conserved. In fact, the exact opposite is true. There is virtually no conservation between *Ciona intestinalis* and *Halocynthia roretzi* noncoding sequences (Oda-Ishii et al. 2005) nor between certain congeneric species, like *Molgula occidentalis* and *Molgula oculata* (Stolfi et al. 2014). This is consistent with the observations that the genomes of ascidians, and tunicates as a whole, are rapidly evolving (Seo et al. 2001; Tsagkogeorga et al. 2012). In some cases, a lack of sequence conservation does not necessarily imply divergent regulatory mechanisms, as some enhancers are fully compatible in cross-species transgenic assays (Johnson et al. 2004; Oda-Ishii et al. 2005; Roure et al. 2014). However, there is mounting evidence for great variation in regulatory strategies controlling identical developmental processes

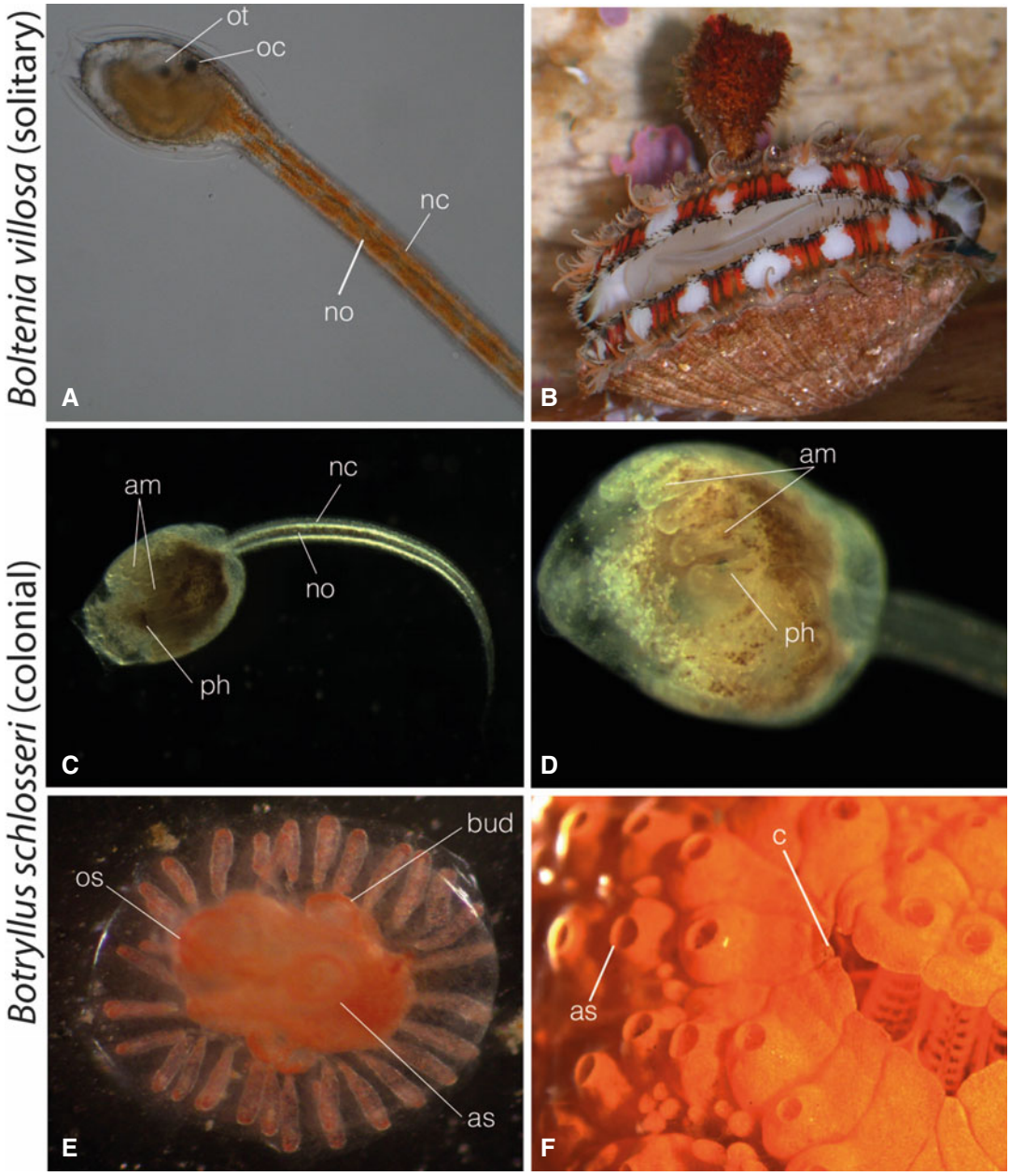

Fig. 4.6 Two styelid ascidians with different life histories: solitary *Boltenia villosa* (**A**, **B**) and colonial *Botrylloides violaceus* (**C**–**F**). (**A**) *B. villosa* orange solitary larva shows chordate features including the notochord (*no*) and the dorsal nerve cord (*nc*); these larvae present light and gravity sensing organs, i.e., ocellus (*oc*) and otolith (*ot*). Palps or adhesive papillae can be seen in the anterior (left). (**B**) An adult *Boltenia villosa* "hitchin' a ride" on a *Chlamys* scallop at Friday Harbor Laboratories. (**C**) *B. violaceus* larva also shows the characteristic chordate features in the tail, i.e., notochord (*no*) and nerve cord (*nc*), as well as a single sensory organ in the head that serves for light and gravity sensing, i.e., photolith (*ph*), and anterior protrusions known as ampullae (*am*). (**D**) Anterior magnified view of *B. violaceus* larval head, which shows the prominent ampullae and some pigmented cells before settlement of the larva. (**E**) The oozoid with open oral (*os*) and atrial (*as*) siphons after settlement shows lateral buds that will develop into the next asexual generation of blastozooids; note extended ampullae around the edges of the newly settled colony. (**F**) Magnification of a *B. violaceus* colony shows the oral openings of each zooid and the common cloacal aperture (*c*) that allows internal visualization of branchial sacs (Courtesy of J. Greer)

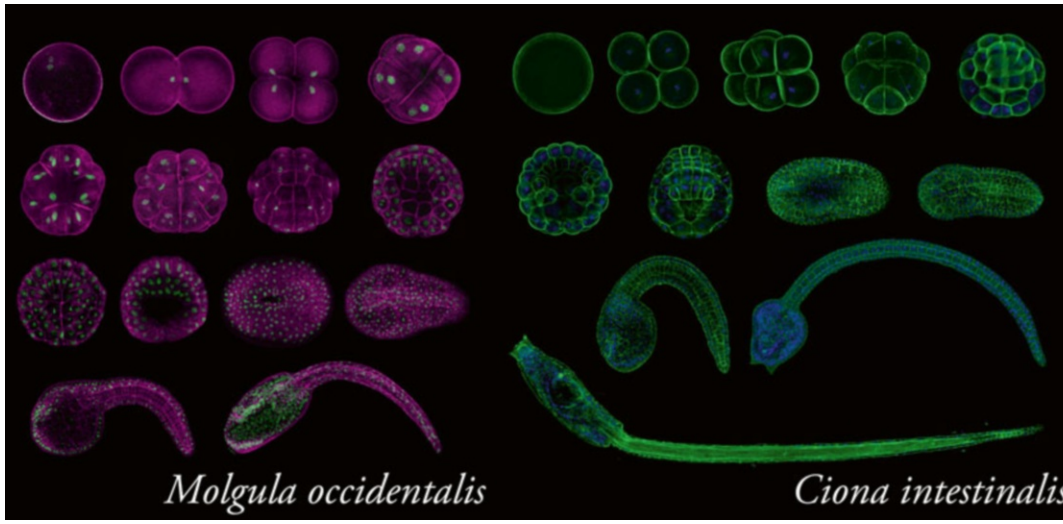

Fig. 4.7 Comparison of *Molgula occidentalis* (Stolidobranchia) and *Ciona intestinalis* (Phlebobranchia) embryogenesis. Comparative diagram of embryonic stages of *Molgula occidentalis* (*left*) and *Ciona intestinalis* (*right*), two distantly related species of solitary ascidians that share near-identical cell lineages and fate maps, in spite of negligible conservation of noncoding genomic sequences. Embryos were stained with DAPI and fluorescent phalloidin conjugates and are all at roughly the same scale (Images were adapted from Stolfi et al. (2014))

in distantly related ascidians[6] (Takahashi et al. 1999; Hudson et al. 2007, 2013; Tokuoka et al. 2007; Takatori et al. 2010).

This remarkably minimalist embryo must have evolved at a bottleneck – the last common ancestor of all extant ascidians and possibly all extant tunicates. However, the incredible derivations seen in the more unusual ascidian embryos demonstrate that, far from being an evolutionary dead end, the simplified ascidian embryo has been elaborated and reconfigured many times over. Later we will discuss the exceptional examples of derivation from this typical embryo and their impact on our understanding of the evolution of tunicate development. For now, it is this "typical" solitary ascidian embryo that will serve heavily as a reference for the general description of embryogenesis in this chapter, as it has been the workhorse of most genetic and molecular studies in the tunicates.

[6] Both examples given above are referred to as developmental system drift or DSD (see Vol. 1, Chapter 1) This refers to the divergence in molecular mechanisms governing the development of identical homologous characters in different species (True and Haag 2001). As outlined above, this can refer to the divergence in primary nucleotide sequence of orthologous enhancers that are functionally interchangeable in cross-species transgenic assays but also to the *functional* divergence of orthologous enhancers that do not drive identical gene expression patterns in their respective species of origin but are not interchangeable in cross-species assays.

The Typical Ascidian Larva

Before describing the embryonic development of ascidians, it is crucial to explain its end product: the typical solitary ascidian larva. The chordate nature of ascidians is most obvious during the larval stage (Figs. 4.6, 4.7, and 4.8). The ascidian larva is roughly divided into two parts, frequently but misleadingly termed the "trunk" and the "tail." The former is mostly composed of the anterior central nervous system (CNS), peripheral nervous system (PNS), and undifferentiated mesoderm and endoderm. From this mesodermal component are derived the adult branchiomeric muscles, heart, blood, tunic cells, and other cell types. The endoderm gives rise to the pharyngeal gill slits (later, the branchial basket), the endostyle, and the anterior digestive tract. Given the homology of these tissues and progenitor types to

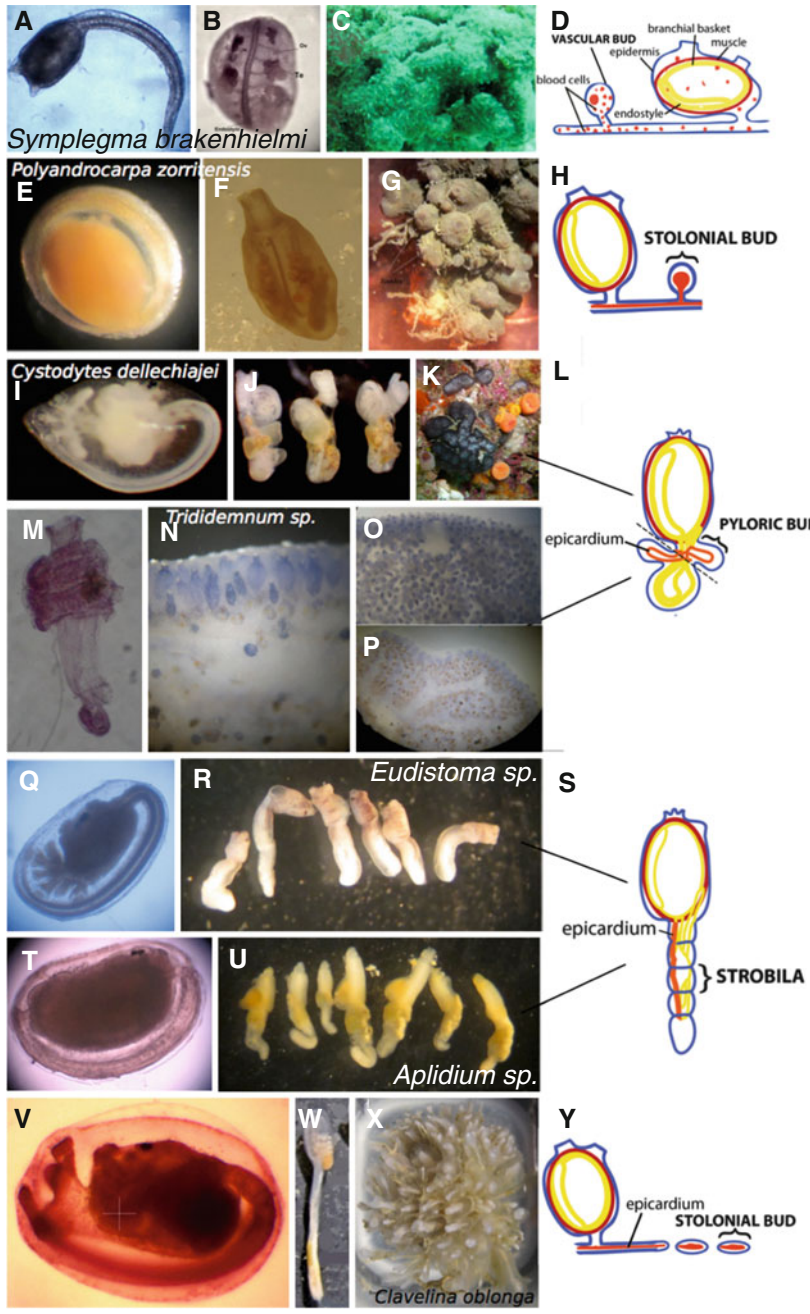

Fig. 4.8 Diversity of colonial forms and budding modes of Ecuadorean ascidians. (**A–D**) *Symplegma brakenhielmi* larva (**A**), zooid (**B**), and live colony (**C**) buds mainly by vascular budding (**D**). (**E–H**) *Polyandrocarpa zorritensis* larva (**E**), zooid (**F**), and live colony (**G**) buds mainly by stolonial budding (**H**). (**I–L**) *Cystodytes dellechiajei* larva (**I**), brooding zooids (**J**), and live colony (**K**) buds mainly by pyloric budding (**L**). (**M–P**) *Tridemnum* sp. pyloric bud during the formation of a new abdomen (**M**), lateral view of zooids and buds (**N**); dorsal view of the colony shows branchial regions of the zooids in blue and a clear common protruding cloaca (**O**), whereas a ventral view of the colony reveals the cloacal canals (**P**). (**Q–S**) *Eudistoma* sp. larva (**Q**) and zooids (**R**) bud by abdominal strobilation (**S**). (**T**, **U**) *Aplidium sp*. larva (**T**) and zooids (**U**) bud by strobilation (**S**). (**V–Y**) *Clavelina oblonga* larva (**V**), zooid (**W**), and colony (**X**) bud by stolonial budding from the abdominal region (**Y**). (**D**, **H**, **L**, **S**, **Y**) represent only symbolic/generic drawings of the distinct budding modes (*capital and bold letters*) in ascidians, but are not meant to illustrate the specific modes of budding observed for the species shown (Modified from Brown and Swalla (2012), and photo courtesy from G. Agurto (CENAIM-Ecuador))

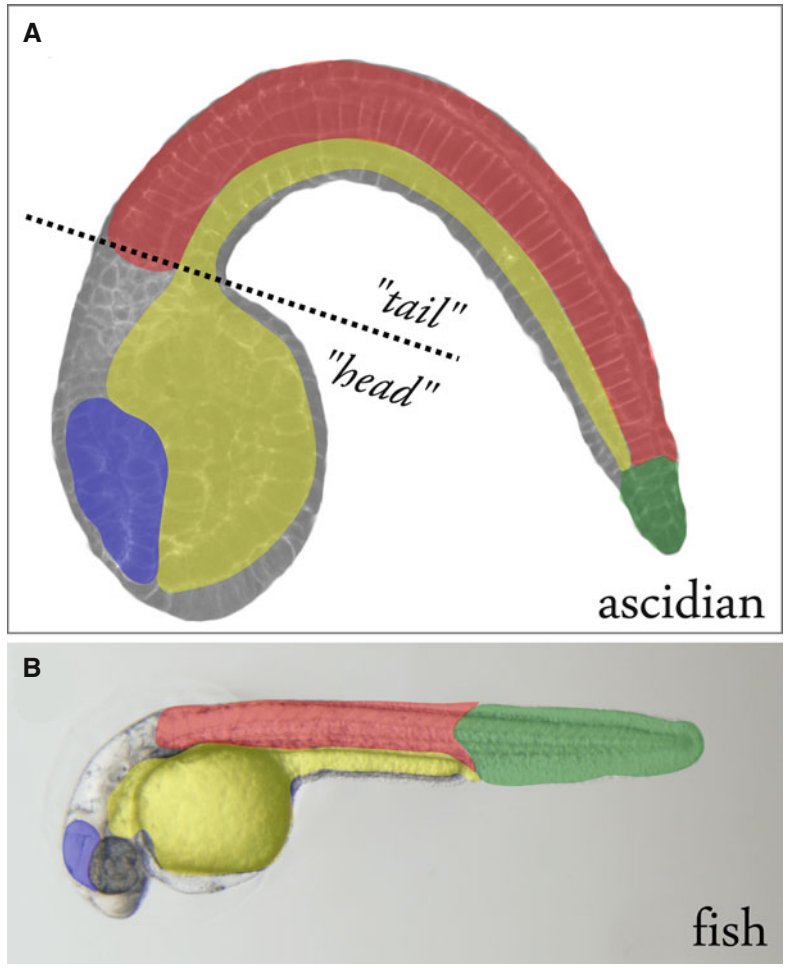

Fig. 4.9 Comparison of ascidian and vertebrate embryo anatomies. (**A**) *Ciona intestinalis* mid-tailbud stage embryo, with major tissues/territories color coded: *blue*, sensory vesicle + brain; *yellow*, endoderm; *red*, axial + paraxial mesoderm (notochord and muscle, respectively); *green*, tailbud (© Alberto Stolfi, 2015. All Rights Reserved). (**B**) Zebrafish embryo with tissues color-coded according to their homologs in *Ciona*: *blue*, forebrain; *yellow*, endoderm + yolk sac; red, trunk (notochord + paraxial muscles); *green*, postanal tail. Comparison between the two suggests the "tail" of ascidian larvae is homologous to the trunk + tail of vertebrates, and the ascidian larval "head" (formerly known as the "trunk") contains tissues and precursor cells homologous to those located in the vertebrate head (brain, endostyle/thyroid, pharyngeal endoderm). Zebrafish image is from Okuda et al. (2010)

their counterparts in vertebrates, mostly located in the head or just posterior to it, it would be more accurate to refer to this region as a "head." Therefore, this term is preferentially used herein.

The posterior half of the larva is composed mostly of caudal CNS and PNS, notochord (axial mesoderm), larval muscles (paraxial mesoderm), and a strand of undifferentiated endoderm that extends posteriorly almost to the very end of the larva. The presence of this gut rudiment, which gives rise to the adult intestine (Nakazawa et al. 2013), suggests that this "tail" is not entirely equivalent to the defining chordate postanal tail, but rather to the trunk (cervical + thoracic regions) of vertebrates, with perhaps a vestigial postanal tail at its very posterior end (Fig. 4.9). Although it would be more appropriate to refer to this structure as a "trunk-tail," it is here called "tail" for simplicity.

Thus, although the larvae of ascidians and amphibians indeed share a basic chordate body plan, as defined by the unequivocal presence of chordate-specific body structures such as the dorsal hollow neural tube and a notochord, their "tadpole" characteristics may only be superficially similar.

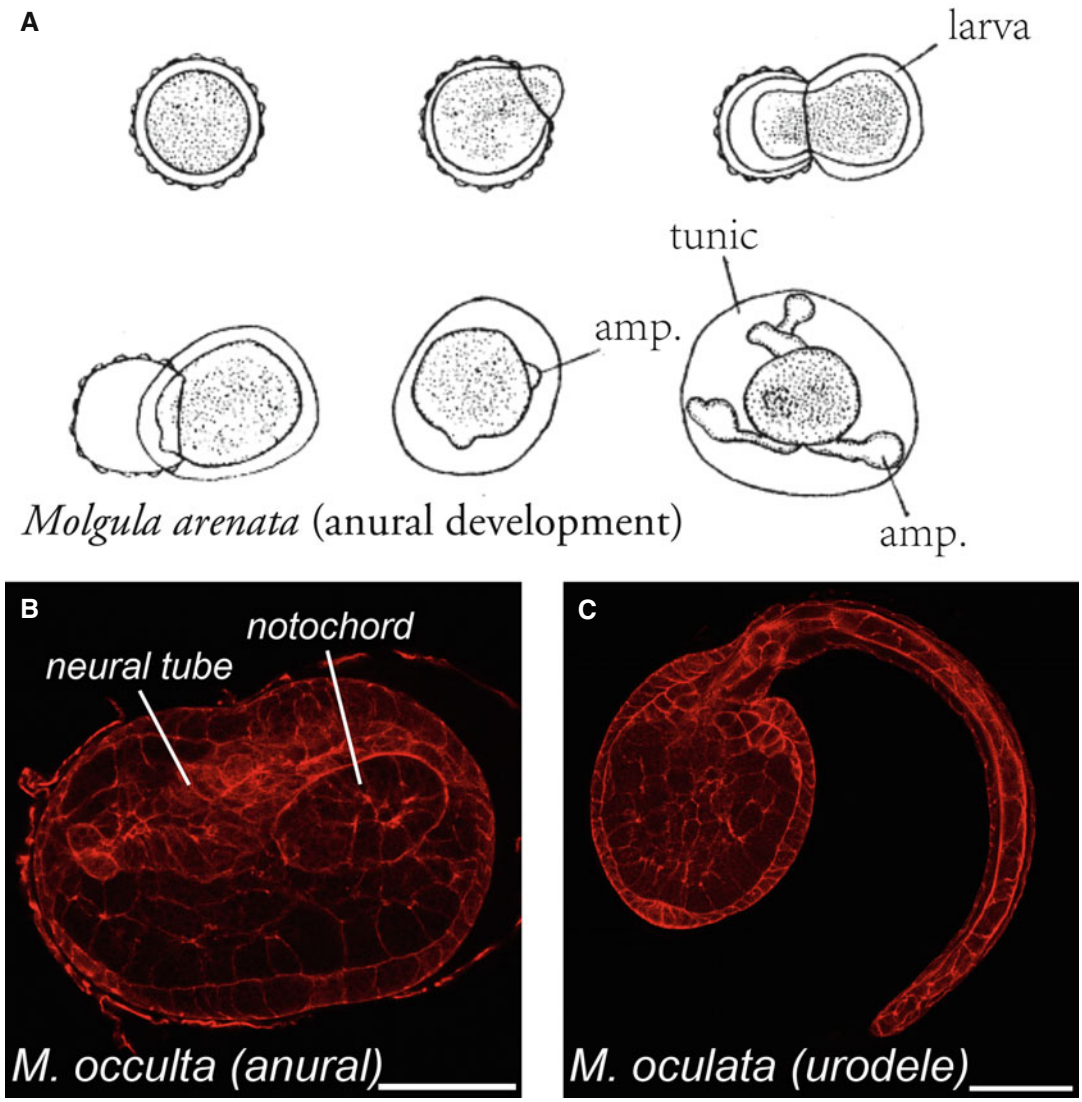

Fig. 4.10 Anural development in the Molgulidae. (**A**) Illustrations by Berrill (1931) of the development, hatching, and metamorphosis of *Molgula arenata*, an indirect-developing tailless (*anural*) species. *Amp.* epidermal ampulla. (**B**) Confocal microscopy image of a hatching larva of the anural species *Molgula occulta*. Note the presence of notochord cells that have failed to proliferate and intercalate like their counterparts in the embryos of urodele species (© Alberto Stolfi, 2015. All Rights Reserved). (**C**) Confocal image of a hatched larva of the urodele (tailed) species *Molgula oculata. M. occulta* and *M. oculata* are closely related and sympatric off the coast around Roscoff, in northern Brittany (France). Embryos were stained with a fluorescent phalloidin conjugate. Anterior is to the right in (**B**, **C**). Scale bars = 50 μm (© Alberto Stolfi, 2015. All Rights Reserved)

Anural and Direct Development

Within the ascidians, there are some curious departures from the typical tadpole-shaped larva. The incredible diversity of developmental modes was studied in detail by Berrill (1928, 1930, 1931, 1935a, 1936) and more recently reviewed by Jeffery and Swalla (1992). The best-studied case is the loss of the familiar tadpole form by larvae of diverse stolidobranchs, notably in the Molgulidae and Styelidae families (Fig. 4.10). In many of these cases, the embryo develops like a typical solitary ascidian embryo, but morphogen-

esis of the tail structures – the notochord, larval muscles, and nerve chord – is severely impaired (Fig. 4.10A). These embryos are said to be "anural" or "tailless," which are misnomers if one considers that these lost or degenerate structures correspond mostly to the axial and paraxial mesoderm of the vertebrate thoracic or cervical segments. However, in this chapter we will continue to use these terms and their opposites, "urodele" or "tailed," for lack of better words.

Anural development may occur due to improper cell fate specification, arrested differentiation, impaired morphogenetic movements, acceleration of apoptosis, or any combination of these. In the anural species *Molgula occulta*, there are fewer notochord cells (Swalla and Jeffery 1990), which remain relatively amorphous and do not extend a functional notochord through convergence and intercalation (Fig. 4.10B, C; Berrill 1931; Swalla and Jeffery 1990). Furthermore, the larval muscles of *M. occulta* fail to differentiate, in part due to recent loss of certain larval muscle-specific "structural" genes such as muscle actin (Kusakabe et al. 1996). The anural condition has independently evolved in different clades (Berrill 1931; Hadfield et al. 1995; Huber et al. 2000), although the developmental causes underlying the condition in these other species have not been extensively studied. Vestigial acetylcholinesterase activity in the muscles of some larvae but not others (Bates and Mallett 1991; Swalla and Jeffery 1992; Bates 1995; Tagawa et al. 1997) and distinct inactivating mutations in larval muscle actin pseudogenes in different anural species (Jeffery et al. 1999) suggest that the tailless conditions of different anural species are not identical.

Berrill associated the anural condition with mud- or sand-flat habitat in which larval motility may be dispensible (offering no adaptive value) and, as a result, easily lost (Berrill 1931). However, the finding of anural *Molgula* species that preferentially attach to rocky substrates along rough coastlines challenged this view (Table 4.1; Young et al. 1988; Bates and Mallett 1991; Nishikawa 1991; Bates 1995). In these cases, there is even perhaps positive selection for direct development from adhesive eggs, without the need for hatching prior to settlement. The extreme tidal changes of high latitudes have also been proposed as a factor that could make swimming at best redundant as a dispersal mechanism (Huber et al. 2000). It is likely that a combination of such biogeographical and ecological factors may have been permissive for the multiple examples of evolution of tailless larvae in the Molgulidae. Whether the molgulids are genetically predisposed to generate anural larvae is a tantalizing hypothesis that remains to be answered.

Table 4.1 Berrill's survey of development in the Molgulidae

Species	Depth found (in fathoms)
Oviparous, urodele	
Attached	
Molgula tubifera	0–3
Molgula manhattensis	0–3
Molgula simplex	20
Molgula socialis	20
Unattached	
Molgula oculata	40
Oviparous, anural	
Attached	
Molgula retortiformis	2–50
Unattached	
Molgula occulta	0–70
Molgula solenata	0–5
Molgula provisionalis	15
Molgula arenata	8
Bostrichobranchus pilularis	8
Eugyra arenosa	5–20
Ovoviviparous, urodele	
Attached	
Molgula complanata	2–10
Molgula cooperi	0–1
Molgula verrucifera	0–5
Molgula citrina	2–5
Molgula platei	–
Ovoviviparous, anural	
Attached	
Molgula bleizi	0–1

Berrill (1931) lists a detailed account of the development (urodele, anural), reproductive (oviparous, ovoviviparous), or ecological (range of depth of occurrence) strategies of each species in the Molgulidae family. Adapted from Berrill (1931)

A closely related condition found in some ascidians is direct development (Young et al. 1988; Bates and Mallett 1991; Swalla and Jeffery 1992; Tagawa et al. 1997). So similar are the two conditions that in different studies the distinction is made using different criteria and often the terms made interchangeable. In this review we distinguish direct development from anural development only by the fact that direct developers will not hatch or break through the chorion prior to the extension of the ampullae. In direct developers, it is these epidermal protrusions that penetrate the chorion and allow the juvenile to "hatch." In many of these species, the eggs themselves are adhesive, allowing for settlement prior to hatching (Young et al. 1988). In both anural and direct development, individuals are presumed to follow the normal course of embryogenesis, with specification of vestigial larval structures that may or may not differentiate. Other criteria for distinguishing direct vs. indirect development of anural species (e.g., differentiation of larval muscles) are difficult to assay and may be ambiguous depending on the assay. Further detailed characterization of the embryogenesis and morphogenesis in the Molgulidae will be needed to classify the potentially multiple gradations of anural and indirect development.

From Fertilization to Gastrulation

Fertilization and Embryonic Axis Determination

During oogenesis, the egg is polarized along an animal-vegetal (AV) axis. Unfertilized eggs are arrested in metaphase of meiosis I, with the meiotic spindle localized at the animal pole, where the polar bodies will form following fertilization. Endoplasmic reticulum-rich cortex (cER), associated maternal "postplasmic" mRNAs, and mitochondria are largely excluded from the animal pole in unfertilized eggs, but only after sperm entry the trigger of a calcium wave leads to actomyosin contraction and concentration of these maternal determinants at the vegetal pole (Prodon et al. 2008). A second phase of ooplasmic segregation occurs after meiosis is complete, shunting the cER and mitochondria toward a presumptive posterior pole, giving rise to a posterior/vegetal cytoplasmic complex (Sardet et al. 1989, 2007; Roegiers et al. 1999). Thus, the anterior-posterior (AP) axis is established roughly perpendicular to the AV axis.

Early Cleavages

The first cleavage occurs along the AP axis, equally partitioning posterior/vegetal cytoplasm into bilaterally symmetric left and right blastomeres. The second cleavage occurs perpendicular to the first, and the third cleavage occurs perpendicular to the second, resulting in a bilaterally symmetric eight-cell embryo in which each half is partitioned into four major quadrants: anterior animal ("a-line," pronounced "small a-line"), posterior animal ("b-line" or "small b-line"), anterior vegetal ("A-line" or "big/large A-line"), and posterior vegetal ("B-line" or "big/large B-line") (Fig. 4.11). Starting from these eight major octants (two halves divided into four quadrants each), the cell lineages of the embryo can be traced throughout development using Conklin's supremely elegant nomenclature system that allows for easy inference of the mitotic history of any given cell[7] (Conklin 1905b).

[7] Conklin's nomenclature system hinges on a tripartite name for each and every cell. This name is composed of a letter and two integers. Let us consider an example, the B7.5 cell. The letter indicates it is derived from the posterior vegetal ("B") blastomere of the right half (indicated by underlining) of the eight-cell embryo. The first number ("7") indicates the mitotic generation to which the cell belongs (the seventh generation, defining the first generation as the single-cell zygote). The second number is the cell's unique identifier, calculated by simple arithmetic from the identifier of its mother cell, B6.3. To derive the identifiers of its daughter cells, the mother cell's identifier ("3") is first multiplied by two ($3 \times 2 = 6$). The daughter cell closest to the original sperm-entry point receives this even number ("6") as its identifier (B7.6). The other daughter cell is then given this number minus 1 ($6 - 1 = 5$). Hence, its name is B7.5. There are some limitations to applying this nomenclature to later development. For instance, sperm-entry point becomes an untenable landmark as cells rearrange and alter their positioning relative to one another. Furthermore, all lineages eventually cease to develop in a stereotypic manner. Therefore, it is not advisable to insist upon Conklin's nomenclature beyond a certain time point in some lineages.

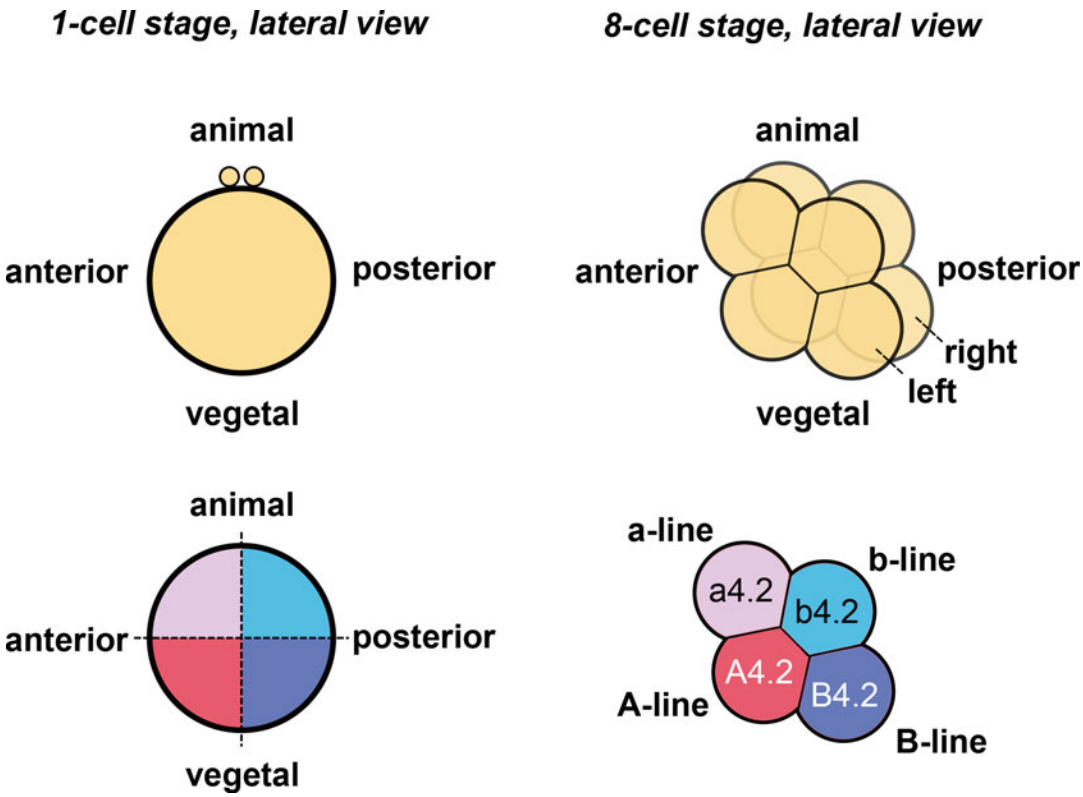

Fig. 4.11 The major cell lineages of the ascidian embryo. *Top left*: diagram of an ascidian one-cell stage embryo (zygote) viewed laterally, showing the major embryonic axes and the polar bodies at the animal pole. *Bottom left*: division of this zygote into the major quadrants of the embryo, as defined by the major axes, animal-vegetal and anterior-posterior. *Top right*: lateral view of an eight-cell stage embryo, showing *left* and *right* hemispheres of the bilaterally symmetric embryo. *Bottom right*: lateral view of only the left hemisphere of the embryo shown at top, with each blastomere labeled with its unique identifier and color-coded according to the quadrants of the one-cell stage embryo. These are the founder cells of the major lineages of the ascidian embryo: a-line (anterior/animal), b-line (posterior/animal), A-line (anterior/vegetal), and B-line (posterior/vegetal). The cells on the *right* hemisphere have the same identifiers, which are *underlined* to indicate their origin from the right hemisphere (e.g., a4.2, b4.2, A4.2, B4.2) (© Alberto Stolfi, 2015. All Rights Reserved)

Each quadrant gives rise to a multitude of cell lineages that develop according to distinct, but invariant, cleavage patterns and orientations. The only symmetry is bilateral, with right-side and left-side lineages being identical until neurulation is complete. The observations and classic experiments of Conklin (1905a, c), Whittaker (1973, 1977, 1982), and Nishida (1992, 1993, 1994a, b, 1996) indicated the presence of maternal determinants that patterned the ascidian embryo not only molecularly, through the specification of the various cell lineages and their generation of the various differentiated larval tissues, but also physically, by controlling the asymmetric cleavage patterns of the early embryos. The molecular nature of several such determinants was soon to be revealed, heralded initially by the discovery of *Macho1*, the maternal gene at the top of the regulatory cascade for the autonomous specification of primary larval muscles (Nishida and Sawada 2001).

Additional proteins were subsequently identified whose mRNAs are localized to the cER/centrosome-attracting body (CAB), comprising the postplasmic/PEM (posterior end mark) genes (Satou and Satoh 1997; Satou 1999; Sardet et al. 2003). These encode a wide variety of proteins, most of which have not been extensively studied

in ascidians. One exception is the original PEM protein, Pem1, a fascinating molecule that executes multiple functions critical for early development in multiple ascidian species. First, Pem1 is involved in the control of unequal cell cleavages through asymmetric mitotic spindle positioning (Negishi et al. 2007). Remarkably, Pem1 is also a transcriptional regulator, globally repressing transcription in early posterior blastomeres and in the germ line (Kumano et al. 2011). While the first function requires Pem1 localization to the CAB (independently of *Pem1* mRNA localization to the same structure), the second depends on Pem1 nuclear localization. These distinct functions also depend on different domains within Pem1. Furthermore, *Pem1* mRNA localization to the CAB is another important property, as it ensures an AP "gradient" of cell size and transcriptional activity, with more posterior cells being progressively smaller and transcriptionally silenced for longer, due to this asymmetric inheritance of *Pem1* mRNA at each round of cell division. The stepwise release from transcriptional silencing constitutes a "timing mechanism" that is critical for the patterning of the early ascidian embryo along the AP axis (Kumano and Nishida 2009).

Germ Layer Specification

At the vegetal pole, nuclear accumulation of maternally provided Catenin Beta-1 (Beta-catenin) helps these cells maintain mesendoderm potential and suppresses their specification as ectoderm (Imai et al. 2000), although the positional cue for the accumulation itself is not known. In *Ciona intestinalis*, *s*uppression of ectoderm fates involves antagonism of maternal Gata4/5/6 function, which is required for "naïve" ectoderm specification and later for neural induction (Rothbächer et al. 2007).

The vegetal half of the embryo at the 16-cell stage, having repressed an ectodermal fate, is then further divided into vegetal mesendoderm and a "marginal zone" by the 32-cell stage. The marginal zone refers to a ring of cells surrounding the mesendoderm proper and abutting the animal pole (ectoderm). This marginal zone does not correspond to a specific germ layer, as it includes the A-line neural/notochord progenitors. The vegetal mesendoderm in turn is largely fated to give rise to endoderm, except for A6.3, which will also give rise to the A7.6 mesenchymal lineage.

In *Ciona intestinalis*, binary fate choice between vegetal mesendoderm and marginal zone involves sustained nuclear Beta-catenin accumulation. While nuclear accumulation of maternally deposited Beta-catenin drives specification of the entire vegetal half of the embryo between the eight- and 16-cell stages, Beta-catenin nuclear localization is rapidly downregulated in the marginal zone, being restricted to their more vegetal sister cells. This differential Beta-catenin signaling is sufficient and necessary to distinguish the two layers (Hudson et al. 2013).

Surprisingly, this mechanism is not conserved in *Halocynthia roretzi*, in which marginal zone cells also show sustained nuclear Beta-catenin staining. Instead, a peculiar mechanism for asymmetric inheritance of mRNA of the marginal zone determinant *Not* seems to drive mesendoderm patterning. This mechanism involves nuclear migration, retention of locally transcribed *Not* mRNA in a Wnt5-dependent manner, and later repositioning of the nucleus at mitosis, resulting in one daughter cell inheriting all the *Not* mRNAs, which are sufficient and necessary for marginal zone specification (Takatori et al. 2010). This is a remarkable example of developmental system drift between *Ciona* and *Halocynthia*.

Gastrulation

By the 110-cell stage, the germ layers have segregated, the fate map has been established, and gastrulation commences. The endoderm cells drive gastrulation by invagination, which occurs in a two-step process in which the cells undergo first apical constriction then basolateral shortening (Sherrard et al. 2010). This is immediately followed by the involution of the cells of the marginal zone (mesoderm). Since this marginal zone is only one to two cell diameters wide, its ingression is swift and nearly concurrent with epiboly of ectodermal cells. Although this epiboly was hypothesized to push the marginal zone cells as

they ingressed, experiments revealed that the ectoderm cells were not required for proper gastrulation (Sherrard et al. 2010). Once ingressed, mesodermal cells do not immediately move great distances, the most dramatic being the inversion of the larval muscle precursors along the AP axis. Subsequent neurulation and epiboly of the epidermis effectively seal in the endoderm, mesoderm, and neural tube.

Less is known about how the different germ layers and tissues remain physically compartmentalized, though evidence from other organisms suggests that differential contractility and cortical tensions may be involved (Krieg et al. 2008). Additionally, cadherin family gene expression patterns are dynamically regulated during *Ciona intestinalis* development and may play a role in the adhesive properties of the different cell lineages of the embryo (Noda and Satoh 2008). It remains to be seen how the general principles of germ layer organization and cell sorting in larger embryos apply to the much smaller, invariant embryos of solitary ascidians.

Development of the Ectoderm

Neural Induction

The CNS is derived from two of the major quadrants of the embryo: anterior/animal (a-line) and anterior/vegetal (A-line). Either lineage gives rise to both neural and nonneural lineages. The basic mechanisms by which this induction occurs in ascidian embryos are known and differ slightly between the two lineages. In *Ciona intestinalis*, neural induction of a-line occurs at the 32-cell stage and was shown to be carried out by FGF signaling. More specifically, Fgf9/16/20 ligand expressed in vegetal-pole cells is sufficient and necessary to induce neurogenic ectoderm specifically in those a-line cells in contact with the Fgf9/16/20-expressing cells (Hudson and Lemaire 2001; Bertrand et al. 2003). Those cells that do not receive this signal go on to become epidermis and components of the PNS. While this induction still requires Gata4/5/6 activity, like earlier induction of basic ectoderm, the instructive cue is nonetheless the spatially restricted Fgf9/16/20 ligand. This induction is dependent on direct contact of inducing and induced cells, as is the case for almost every other documented FGF-dependent induction event in the *C. intestinalis* embryo.

Induction of CNS from A-line progenitors also involves FGF signaling. Surprisingly, in this lineage FGF signaling inhibits CNS specification. A-line neural precursors are specified by the absence of FGF signaling, while their sister cells are induced by FGF signaling to become notochord precursors (Minokawa et al. 2001; Yasuo and Hudson 2007). The availability of FGF ligands is not limiting, as these cells *are* the source of Fgf9/16/20 and are thus surrounded by ligand. Instead, the localized cue for differential activation cells was found to be Ephrin, which is expressed in a-line cells and antagonizes FGF-dependent ERK signaling in A-line neural progenitors in a contact-dependent manner (Picco et al. 2007). It was shown that this occurs through Ephrin/Eph-dependent localized recruitment of Rasa1 (p120 RasGAP) protein, which is an inhibitor of the Ras/ERK pathway (Haupaix et al. 2013).

Given the requirement for FGF in induction of a-line neural tissue and the conserved role for FGF in neural induction in vertebrates, this inversion in the outcomes of induction seems quite puzzling. However, FGF has since been shown to be repeatedly employed as a simple binary switch to decide between two opposing cell fates in sister cell pairs throughout ascidian embryogenesis (Davidson et al. 2006; Hudson et al. 2007; Shi and Levine 2008; Squarzoni et al. 2011; Stolfi et al. 2011; Wagner and Levine 2012). Accordingly, the role of FGF in the A-line notochord/neural decision is likely to be an ascidian-specific regulatory motif, although the induction of a-line neural progenitors may indeed be a manifestation of an ancestral FGF-dependent mechanism for neural induction.

Neurulation

Neurulation refers to the chordate-specific morphogenesis of a dorsal, hollow neural tube starting from a flat neural plate. In the typical ascidian larva, the neural plate is a flat epithelium of

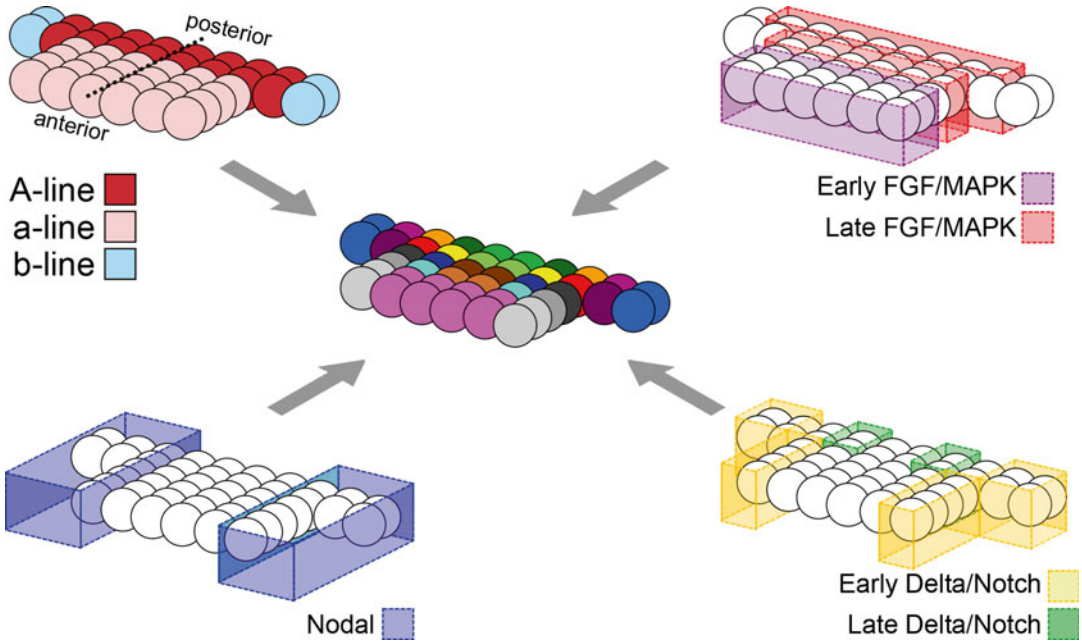

Fig. 4.12 Neural plate patterning in *Ciona*. Cartoon diagram summarizing the findings of Hudson et al. (2007) on the grid-like patterning of the *C. intestinalis* neural plate by FGF/MAPK(ERK), Nodal, and Delta-Notch signaling pathways. *Boxed cells* are under the direct influence of the indicated signals. Further input into the regulatory mechanisms for cell fate specification come from the cell lineage histories of each cell, divided into the three major lineages of the neural plate (A-line, a-line, and b-line). *Dashed line* indicates the dorsal midline. *Color coding* in the neural plate represents unique cell identities as assayed by gene expression profiles. Cell numbers and identities are accurately and realistically portrayed, but the relative sizes and positions of the cells are slightly modified for clarity. Anterior is to the *bottom left* (© Alberto Stolfi, 2015. All Rights Reserved)

neurogenic a- and A-line-derived ectodermal cells that stretch over the dorsal surface of the embryo by epiboly. It forms a highly unusual grid of rectangular cells, an organization that is critical for its proper patterning into rows and columns (Hudson et al. 2007). In *Ciona intestinalis*, this plate was shown to be under the influence of several inductive cues that pattern it into rows and columns of differently fated cells (Fig. 4.12). Namely, Delta and Nodal signals emanate from regions just lateral to the neural plate, while an intricate interplay of FGF and ephrin signals reiteratively determine the binary cell fate choices of anterior/posterior sister cell pairs, by their opposing actions on ERK pathway activation (Hudson et al. 2007; Haupaix et al. 2014).

Upon neurulation (Fig. 4.13), the rows and columns of the neural plate are precisely reorganized into the simplest of neural tubes: four AP columns or stacks of cells (one dorsal column (the neural tube roof plate, formed by the lateral-most cells of the neural plate), one ventral column (the floor plate, formed by the medial-most columns of the neural plate), and two bilaterally symmetric lateral columns, formed from the remainder of neural plate cells) (Nicol and Meinertzhagen 1988a, b; Cole and Meinertzhagen 2004). Thus, the patterning of the neural plate is critical not only for later compartmentalization of the CNS but for the actual morphogenesis of the neural tube. Neurulation is incomplete at the anterior terminus of the neural tube where it remains open, giving rise to the neurogenic portion of the larval stomodeum (Veeman et al. 2010). The neural tube is eventually internalized, after being completely covered dorsally by the epidermis.

Like in most of the embryo, the cell lineages of the neural tube are invariant through neurulation, except for the exact AP order of intercalation of the dorsal and ventral cells. Neural tube

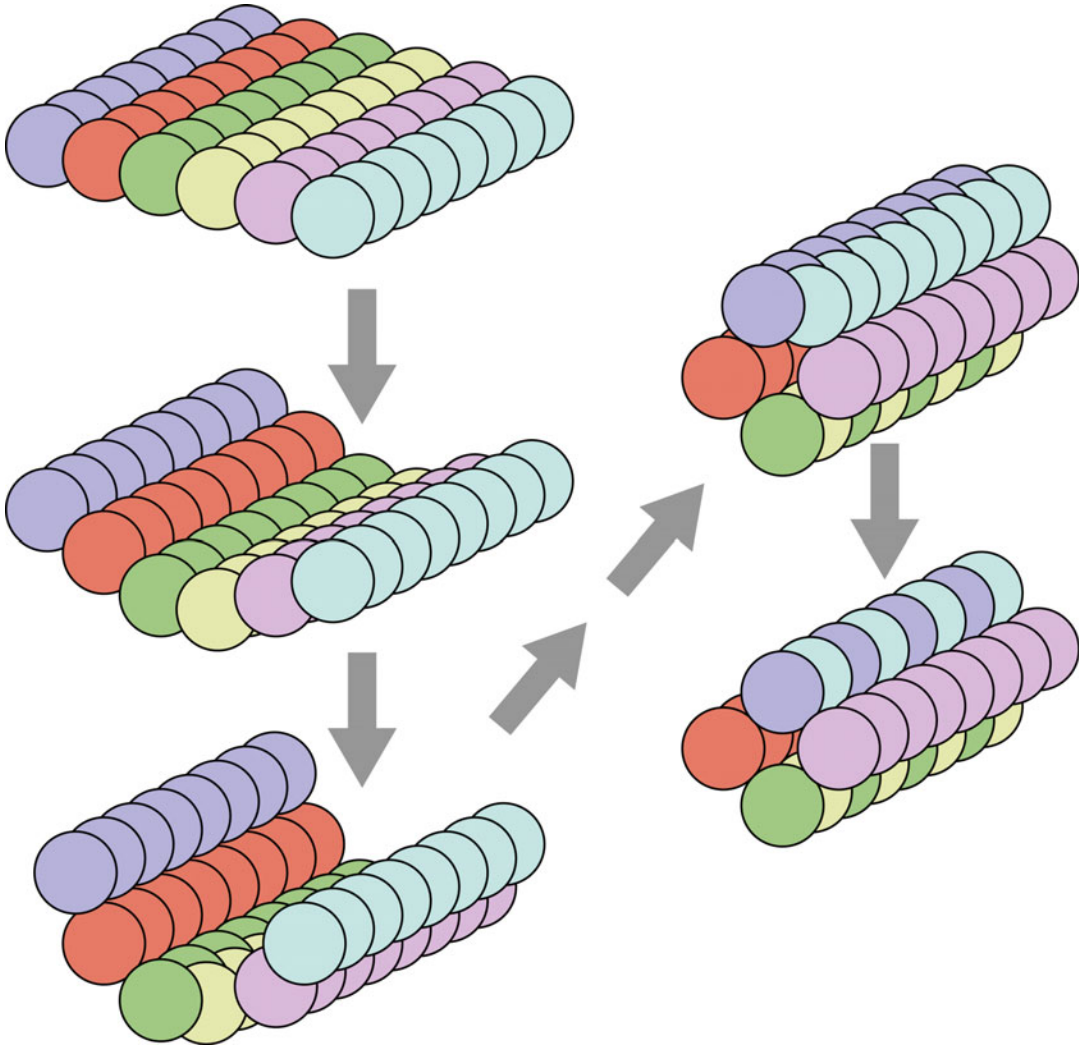

Fig. 4.13 Neurulation. Cartoon diagram depicting the mode of neurulation in solitary ascidian embryos. The flat, dorsal neural plate is a grid-like sheet of cells. The lateral and medial columns are displaced in opposite directions (dorsal and ventral, respectively) by as of yet unknown forces. The cells of the lateral columns meet at the dorsal midline and intercalate to form a single column of cells, the neural tube "roof." The cells of the medial columns also intercalate, forming a single column of cells (the "floor"). Thus, the ascidian neural tube is a simple bundle of four single-cell columns (one dorsal, one ventral and two lateral). A small lumen forms along the inside of the bundle, from the apical surfaces of the neural tube cells ()

progenitors proliferate during neurulation, but it was shown that a prolonged G2 phase in dorsal epidermal midline cells is essential for their intercalation (Ogura et al. 2011). Thus, there is a tight coordination between cell division and morphogenesis of the neural tube.

Further elaboration of the neural tube is uneven along the AP axis, foreshadowing the regionalization of the larval central nervous system. At the anterior, the neural tube lumen is engorged (Marino et al. 2007) and eventually becomes the sensory vesicle (SV), which houses the larval melanocytes and associated sensory (light- and acceleration-sensing cells). Distinct rates of proliferation and differentiation occur along the length of the AP axis, resulting in an irregularly shaped neural tube and discontinuous neural tube lumen (Cole and Meinertzhagen 2004).

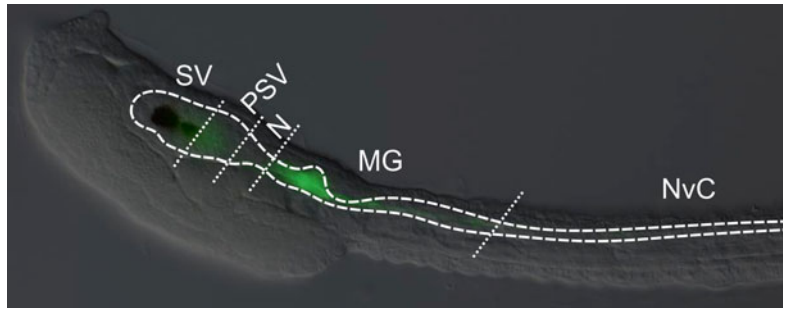

Fig. 4.14 The ascidian larval central nervous system (CNS). *Ciona intestinalis* larva electroporated with the *Vesicular acetylcholinesterase transporter* (*Vacht*)*>unc-76::eGFP* plasmid, fluorescently labeling the major neuronal centers of the larval CNS. The five major anatomical subdivisions of the CNS are demarcated, from anterior to posterior: sensory vesicle, posterior sensory vesicle (*PSV*, also known as the brain), neck (*N*), motor ganglion (*MG*), and nerve cord (*NvC*) (Adapted with permission from Stolfi et al. (2011))

Central Nervous System Patterning

At the end of larval development, the central nervous system (CNS) contains approximately 100 neurons (Imai and Meinertzhagen 2007a) and is divided into at least five anatomical compartments along the AP axis (Fig. 4.14). At the anterior end lies the sensory vesicle (SV). Immediately posterior to that is the larval "brain" or posterior sensory vesicle (PSV): a tightly bundled cluster of neurons, photoreceptors, and other putative sensory cells associated with the SV. Posterior to the brain is the neck, an undifferentiated mass of neural progenitors that will give rise to certain branchiomeric neurons of the adult (Dufour et al. 2006). Next is the motor ganglion (MG), comprised of motor neurons and interneurons that drive the swimming behavior of the larva (Bone 1992; Horie et al. 2010). Most posteriorly, along the length of the tail lies the nerve cord. Other than a few scattered neurons of uncertain function, the nerve cord is composed chiefly of elongated ependymal cells and the axons of MG neurons that project posteriorly toward the tailbud. The clonal subdivisions of the neural tube (a-line and A-line) together with cell signaling are responsible for the establishment of regionalized patterns of gene expression. These molecular domains are assumed to then specify and drive the differentiation of the anatomical subdivisions.

Gene expression patterns support a fundamentally bipartite organization of the ascidian CNS: *Otx* expression marks the larval brain and adult anterior CNS progenitors, while absence of *Otx* expression characterizes the remainder (Ikuta and Saiga 2007). However, a tripartite organization emerges when one looks at several genes expressed in the neck. Among these, *Pax2/5/8* and *Phox2* suggest homology of the neck to the vertebrate hindbrain, a claim strongly supported by the fact that these progenitors give rise to *Tbx20*$^{+}$ motor neurons innervating the pharyngeal muscles of the adult (Dufour et al. 2006). The motor ganglion (MG) progenitors express several sequence-specific transcription factor (TF) genes involved in spinal cord motor neuron specification in vertebrates such as *Pax6*, *Lhx3/4*, *Islet*, *Onecut*, and *Nk6*, such that homology of this region to the vertebrate spinal cord is hard to refute. Not enough is known about the adult anterior CNS progenitors, and whether they constitute a molecularly or physically distinct compartment apart from the larval brain, leaving us three functionally distinct regions: larval/adult brain, adult branchiomeric motor neurons, and larval tail motor neurons.

The correspondences to the major divisions of the vertebrate CNS are somewhat tenuous and controversial. There are at least three major factors that make these comparisons a dicey proposition. First, there is a drastic alteration in the positioning of CNS neural precursors and differentiated neurons. For instance, the motor ganglion, argued to be homologous to the vertebrate spinal cord based on molecular, embryological, and functional grounds, is arrayed as only a single cluster of several bilateral pairs of cells. There is no dorsoventral axis to speak of and no serial

repetition of this structure, as there is only one muscle to innervate on either side of the larva. Posterior to the motor ganglion, the nerve cord over the majority of its length contains no neurons of its own, supporting instead the axon bundles of the motor ganglion neurons. This drastic reconfiguration is no doubt a result of the extreme reduction in cell numbers and size of the larva.

Another issue complicating comparative studies is the heterochrony of larval and adult CNS differentiation. Popularly, the ascidian larval CNS is thought to simply degenerate and the adult CNS thought to be formed de novo from an unorganized mass of naïve progenitors. This view has been convincingly refuted, with lineage tracing experiments revealing the contribution to the adult CNS of progenitors from specific regions of the embryonic neural tube (Dufour et al. 2006; Horie et al. 2011). The different larval and adult-differentiating portions of the neural tube will naturally be in different genetic regulatory states, compromising the simple one-to-one pairing of static "snapshots" of gene expression patterns that tend to be emphasized.

Related to this is a third complication, namely, that many of the genes used in comparing the regionalization of the CNS are reiteratively used in different cell types at different stages, carrying out different functions. For example, although Fgf8/17/18 was shown to act as an organizing molecule in the motor ganglion and neck regions as well as at the vertebrate midbrain/hindbrain boundary (Imai et al. 2009), the repeated use of FGF signaling for cell fate decisions in *Ciona* leaves open the question as to whether this organizer is a conserved or convergent feature. Similarly, *Otx* is also a critical regulator of posterior PNS fate (Roure et al. 2014), muddling its intimate association with anterior CNS specification. Finally, given the rapid pace of development of ascidian embryos, where every cell division is potentially a binary fate choice between two completely different lineages, gene expression patterns are highly dynamic and rapidly changing over the course of embryogenesis (Ikuta and Saiga 2007). Great care must be taken to ascertain the temporal and cellular context in which gene expression is taking place before seizing these to support claims of homology.

That said, it seems that the embryological and molecular evidence thus far presented best supports a tripartite nature of the ascidian CNS (Wada et al. 1998). When comparing to vertebrates, the motor ganglion and nerve cord may correspond to the spinal cord, the neck may be homologous to the hindbrain, and the anterior *Otx*-expressing domain would encompass everything anterior to the hindbrain. The finer subdivisions seen both in ascidians and vertebrates (midbrain, midbrain/hindbrain boundary, etc.) would be lineage-specific elaborations of this basic frame, adapted to their respective specialized needs.

Motor Neuron Specification

The gene regulatory networks and inductive events governing neuronal specification in the ascidian CNS have best been studied in motor ganglion neurons (MGNs). In the *Ciona intestinalis* MG, four of the five pairs of MGNs are specified from the A9.30 blastomere (Fig. 4.15A; Cole and Meinertzhagen 2004). Each pair corresponds to a molecularly and morphologically distinct subtype (Stolfi and Levine 2011) and is born and specified in an invariant manner by a series of short-range signaling events (Fig. 4.15B, C; Stolfi et al. 2011). This is in stark contrast to subtype specification in the vertebrate spinal cord, which is patterned along the DV axis by opposing BMP and Shh morphogen gradients. It was shown that in *C. intestinalis*, although the neural tube roof plate expresses BMP and the floor plate expresses Hedgehog, these molecules have no bearing on patterning the MG (Hudson et al. 2011). This is not entirely surprising, given that all MGNs are at the same DV position and thus cannot be easily patterned by DV morphogen gradients.

The A9.29 lineage, just posterior to the A9.30 lineage, gives rise to the fifth MGN, the A10.57 motor neuron, and to the decussating GABAergic interneurons that lie at the base of the tail and presumably play a role in the left-right alternation of muscle contraction that drive swimming behavior (Nishino et al. 2010; Nishitsuji et al. 2012). Although physically removed from the rest of the MGNs, these neurons are likely an integral component of the ascidian larval motor system and should be considered as belonging to the MG.

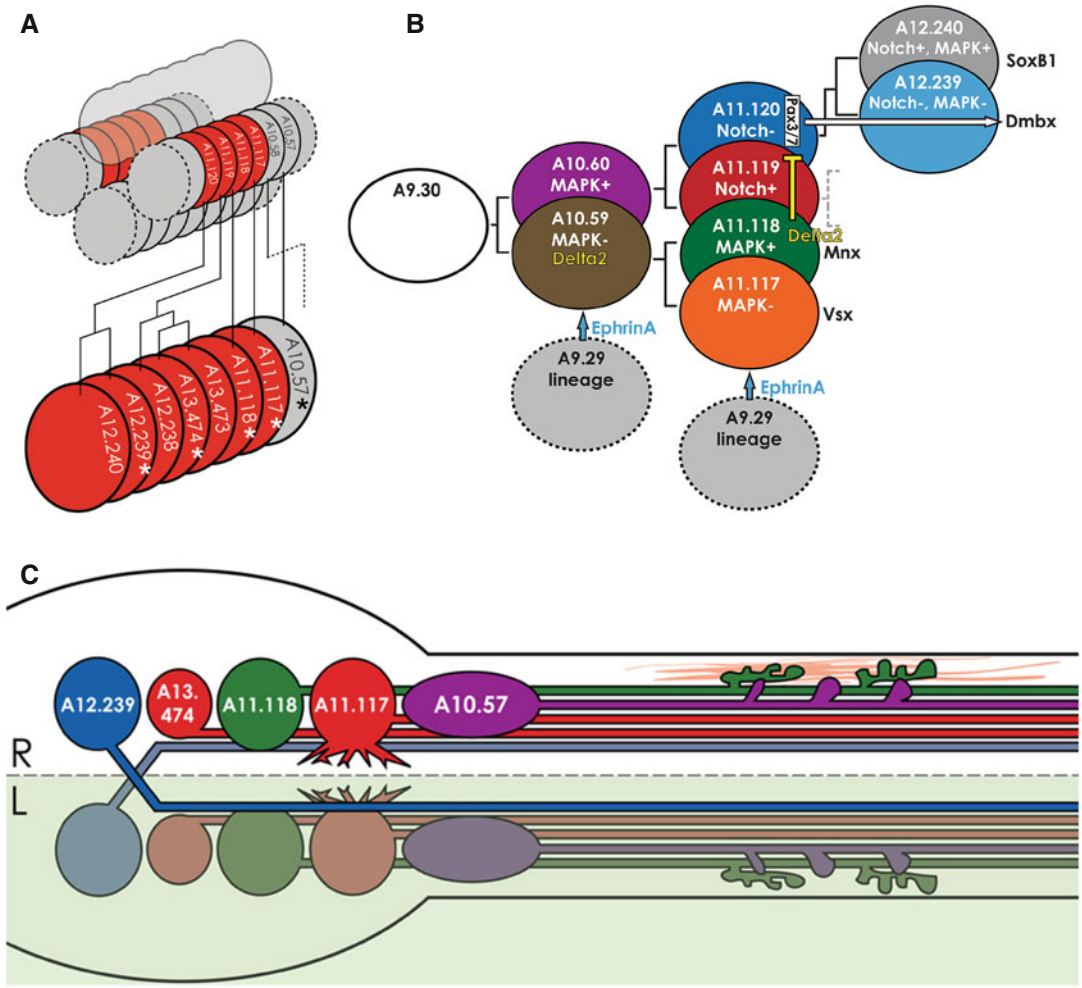

Fig. 4.15 The cell lineages, patterning, and neuronal subtypes of the *Ciona* motor ganglion. (**A**) The cell lineage of the motor ganglion. Cells in *red* are those descended from the A9.30 blastomeres of the neural plate, which gives rise to four of the five pairs of motor ganglion neurons (indicated by *asterisks*). Anterior is to the *left* (Diagram adapted from Stolfi and Levine (2011). Lineage information is from Cole and Meinertzhagen (2004)). (**B**) Summary diagram adapted from Stolfi et al. (2011) depicting the major cell signaling events that pattern the motor ganglion into specific progenitor and neuronal subtypes. Ephrin-A signals from the adjacent A9.29 lineage suppress MAPK(ERK) signaling in the posterior half of the A9.30 lineage and then in the A11.117 cell, which is specified as a *Vsx*+ interneuron. Delta2 ligand expressed in the posterior half of the lineage signals to A11.119 cell, limiting the expression of *Pax3/7* to the anterior-most cell of the lineage, which gives rise to the *Dmbx*+ interneuron (A12.239). The *Mnx*+/*Nk6*+ motor neuron (A11.118) is specified by later activation of ERK signaling, and neuronal differentiation of A12.239 is driven by stereotyped downregulation of ERK and Notch signaling in this cell by unknown means. Anterior is to the top. (**C**) Summary diagram from Stolfi and Levine (2011) of the different neuronal subtypes of the motor ganglion of *C. intestinalis*, depicting their most salient morphological features, such as decussating axons of A12.239, frondose motor end plates of A11.118, dendritic arborizations of A11.117, and elongated cell body and en passant motor end plates of A10.57. Anterior is to the left

Surprisingly, the Hox cluster genes appear to play limited functions in the larval CNS of *Ciona intestinalis*, with no obvious CNS patterning defects observed in loss-of-function experiments (Ikuta et al. 2010). Nine Hox genes have been found in *C. intestinalis* and *Oikopleura dioica*, with a nearly complete set of anterior and posterior Hox genes, but lacking a number of central Hox genes (Fig. 4.16) found in vertebrates and cephalochordates (Seo et al. 2004; Brown et al.

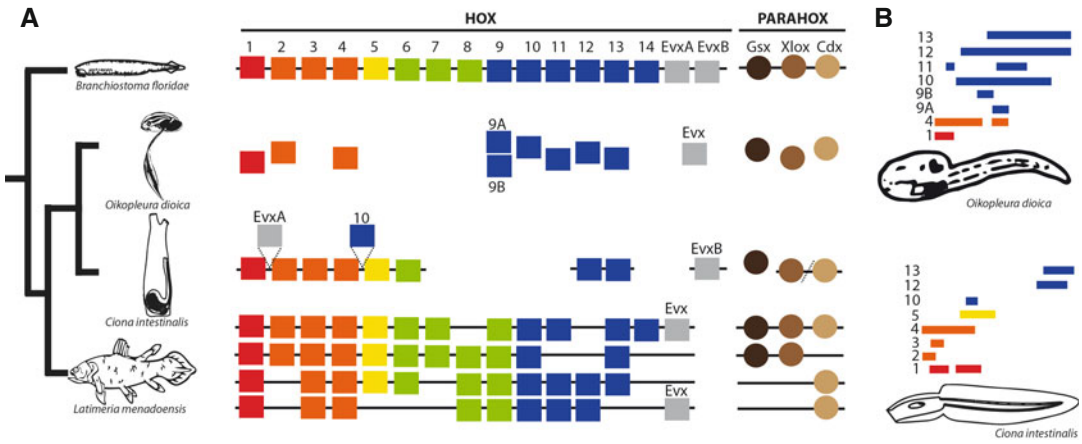

Fig. 4.16 Chordate Hox and ParaHox genes. (**A**) Evolutionary reconstruction of the Hox gene complex in chordates and cephalochordates. The complete Hox and ParaHox clusters are shown for the cephalochordate (*Branchiostoma floridae*). A disintegration in the order of the clusters and the lack of central Hox genes can be seen in the tunicates (*Oikopleura dioica* and *Ciona intestinalis*). The coelacanth (*Latimeria menadoensis*) Hox and ParaHox clusters are also shown (*dark colored circles*). Hox genes are color-coded by their relative position of expression: anterior genes, *red* and *orange boxes*; central genes, *yellow* and *green boxes*; and posterior genes, *blue boxes*. *Evx* duplications and transpositions are shown in *gray boxes*. *Dashed lines* indicate large gaps between Hox genes that remain on the same chromosome but have been dispersed. (**B**) Hox gene expression pattern relative to the anterior-posterior anatomical position of the larva of *O. dioica*. (**C**). Hox gene expression pattern relative to the anterior-posterior anatomical position of the larva of *C. intestinalis* (Figures are based on data from Ikuta et al. (2004), Seo et al. (2004), Brown et al. (2008), Amemiya et al. (2010), David and Mooi (2014), Mulley and Holland (2014))

2008; Amemiya et al. 2010; Ikuta et al. 2004; Ikuta 2011; David and Mooi 2014). The Hox complex itself is fragmented and eroded in the genomes of tunicates (Spagnuolo et al. 2003; Ikuta et al. 2004; Seo et al. 2004), with partial loss of collinearity of gene expression and cluster organization (Fig. 4.16). The same is observed for the ParaHox genes (Ferrier and Holland 2002). Those Hox cluster genes that remain are expressed in the nerve cord, notochord, and muscle of the larva (Ikuta et al. 2004; Seo et al. 2004) and undoubtedly play indispensable biological roles that have yet to be fully elucidated, but it is nonetheless stunning to see the rock stars of bilaterian embryonic patterning remain behind the scenes in the tunicates.

Neural Plate Borders, Placodes, and Neural Crest

From the lateral borders of the neural plate arise a handful of different cell types, mostly associated with the PNS. The most conspicuous of these are the melanin-containing pigment cells associated with the sensory vesicle (Fig. 4.17). In the basic larva of species covering diverse families, there are only two pigment cells. One is an otolith (also known as the statocyst or statocyte) that is required for geotaxis of the larva, presumably by acting as a weight that can activate associated mechanosensory cells, depending on the relative orientation of the larva in the water column (Tsuda et al. 2003; Jiang et al. 2005). The other is an ocellus, associated with a photoreceptor complex (Tsuda et al. 2003; Horie et al. 2008). In some species, the otolith or the ocellus may be missing. In other species (e.g., *Botryllus schlosseri* and other botryllids; Fig. 4.6C), both have been combined into a dual function pigment cell termed the "photolith" (Sorrentino et al. 2000).

In species with separate otolith and ocellus, both cell types are derived from left-right equivalent cells in the neural plate, and their differentiation into one or the other occurs mainly through relative positioning along the anterior-posterior axis after intercalation at the dorsal midline (Darras and Nishida 2001; Abitua et al. 2012). The cell that ends up more anterior invariably becomes the otolith, and the one that ends up

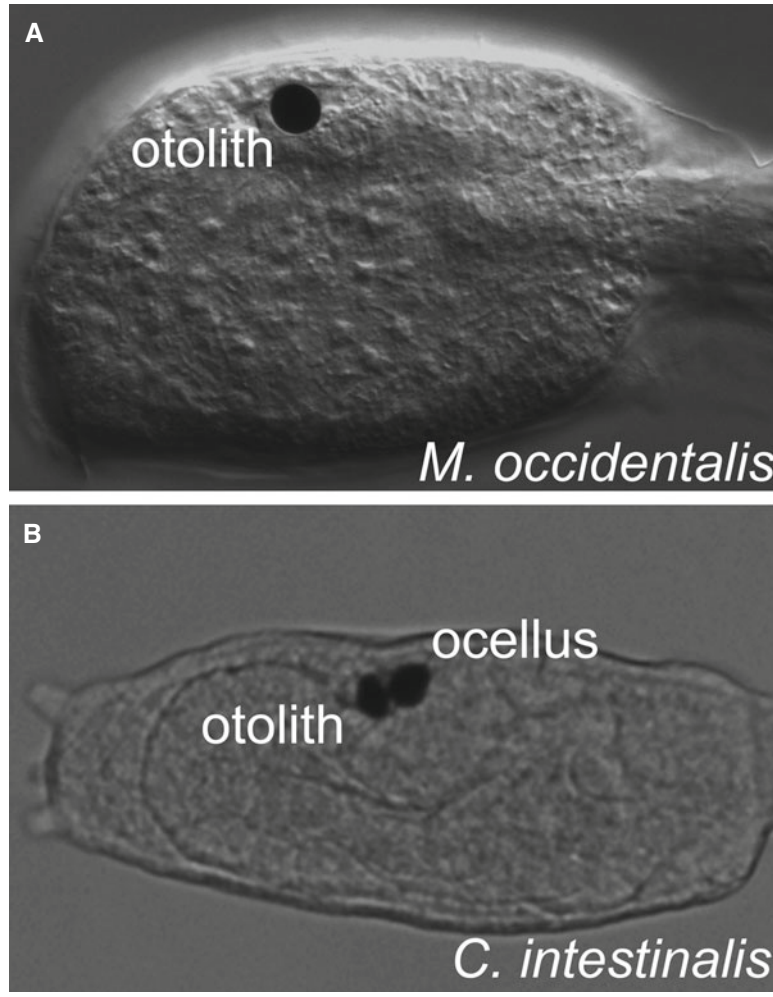

Fig. 4.17 The pigment cells of ascidian larvae. (**A**) Larva of *Molgula occidentalis*, showing a single melanocyte in the sensory vesicle, an otolith (also known as a statocyte or statocyst) associated with putative geotactic mechanoreceptory cells. (**B**) Larva of *Ciona intestinalis*, showing two melanocytes in the sensory vesicle: one otolith and one ocellus pigment cell (© Alberto Stolfi, 2015. All Rights Reserved)

more posterior is specified to become an ocellus. Both subsequently undergo an epithelial-to-mesenchymal transition as they delaminate from the neural tube epithelium and enter the sensory vesicle lumen.

Wada was the first to note that the specification of otolith/ocellus precursors from the neural plate borders closely resembles the development of neural crest-derived melanocytes in vertebrates (Wada et al. 1997; Wada 2001). Interestingly, neural plate border cells (NPBCs) express combinations of transcription factors that in vertebrates participate in the specification of neural crest cells. These include orthologs of *Pax3/7*, *Msx*, *Dlx*, *Zic*, *Snail*, *Id*, and others (Wada et al. 1997; Abitua et al. 2012). Molecularly, the expression of common neural plate border specifying genes like the ones listed above further supports the claims for homology. Later, neural plate border descendants express genes associated with more advanced neural crest developmental processes, including *Foxd* and *Mitf* orthologs (Abitua et al. 2012).

Now, are the NPBCs in fact neural crest cells? That is a trickier question to answer. Since neural crest cells were initially identified in vertebrates, they were defined by those criteria that described them in vertebrates. And there are more than a few such criteria, given the myriad embryonic origins, molecular signatures, and differentiated fates of all those cells collectively referred to as the "neural crest." As such, it is a tall order to

expect to find cells outside the vertebrates that strictly fit those multiple criteria.[8] Taking this into consideration, we venture that the answer is then ascidian NPBCs are homologous to neural crest cells, but are *not* neural crest cells.

We have seen that ascidian NPBCs share an embryological origin and certain regulatory signatures with vertebrate neural crest cells. Furthermore, like their craniate counterparts, the NPBCs give rise to melanocytes and sensory neurons. What are obviously missing are two things: (1) the capacity/propensity for long-range migration and (2) the ability to give rise to mesoderm-like differentiated cell types.

Along the descent of vertebrates, a rudimentary neural crest similar to the ascidian NPBCs must have come to express genes that conferred on them the entire suite of neural crest properties we have come to recognize. In tunicates, we find other cells that display some of these neural crest-like properties. Pigment cell precursors capable of migrating long distances were identified in the complex adultative larvae of *Ecteinascidia turbinata* (Jeffery et al. 2004). These were proposed as homologous to the A7.6-derived mesenchymal cells of *Ciona intestinalis* and *Halocynthia roretzi*, which do express some neural crest factors such as *Twist-related* genes (Jeffery et al. 2008). However, the embryological origin of the A7.6 lineage is not from the neural plate borders, being of clear endomesodermal origin. Interestingly, the forced expression of *Twist-related* genes in neural plate border cells of *C. intestinalis* was found to confer migratory properties to them, resulting in a long-range migration of pigment cell precursors, mimicking the behavior of *E. turbinata* pigment cell precursors (Abitua et al. 2012). Such an experiment may represent a very simplified reenactment of the evolutionary co-option that gave rise to *bona fide* vertebrate neural crest cells.

[8] If the forelimbs had been initially identified in birds and been strictly defined as feathery appendages that bear three digits, then one would be infallibly correct in claiming that only birds have forelimbs and that the homologous structures found in all non-avian vertebrates are *like* forelimbs, but *not* forelimbs.

Epidermis and Epidermal Sensory Neurons

The entire larva is covered by an epithelium composed of epidermal cells and related cell types that share a common clonal origin. Neurons comprising the PNS are embedded throughout the epidermis in both the head and tail regions, and other specialized structures arise at the border regions between the epidermis and neurogenic ectoderm. All these epidermis derivatives are descended from the four animal-pole octants of the eight-cell embryo. The major roles of the larval epidermis are to seal in the different tissues and organ primordia and to synthesize the tunic. The tunic, from which the tunicates derive their name, is made of cellulose. Tunicates are the only metazoans capable of synthesizing cellulose. This is made possible by epidermal expression of the cellulose synthase enzyme, thought to be derived from a gene that was horizontally transferred from an unidentified prokaryotic organism to the last common ancestor of all tunicates (Nakashima et al. 2004; Matthysse et al. 2004; Sasakura et al. 2005).

In the head, PNS neurons (including those derived from the neural plate borders) are dispersed along the anterior and dorsal regions, being absent from the ventral side of the epidermis (Imai and Meinertzhagen 2007b). In the tail, regularly interspaced epidermal cells at the dorsal and ventral midlines differentiate into caudal epidermal sensory neurons (CESNs) that form thin projections into the tunic (Fig. 4.18) and are thought to serve a mechanosensory role (Pasini et al. 2006; Imai and Meinertzhagen 2007b; Terakubo et al. 2010; Yokoyama et al. 2014).

Caudal CESNs are induced from neurogenic epidermis of the tail, which is induced at the dorsal and ventral midlines. The dorsal midline neurogenic epidermis is induced by FGF signaling, while the ventral midline neurogenic epidermis is induced by ADMP/BMP signaling (Pasini et al. 2006). Within these median stripes of neurogenic epidermis, putative mechanosensory neurons are specified through Delta-Notch lateral inhibitory signaling (Pasini et al. 2006), which controls the deployment of a core PNS neurogenic code consisting of the transcription factors Mytf,

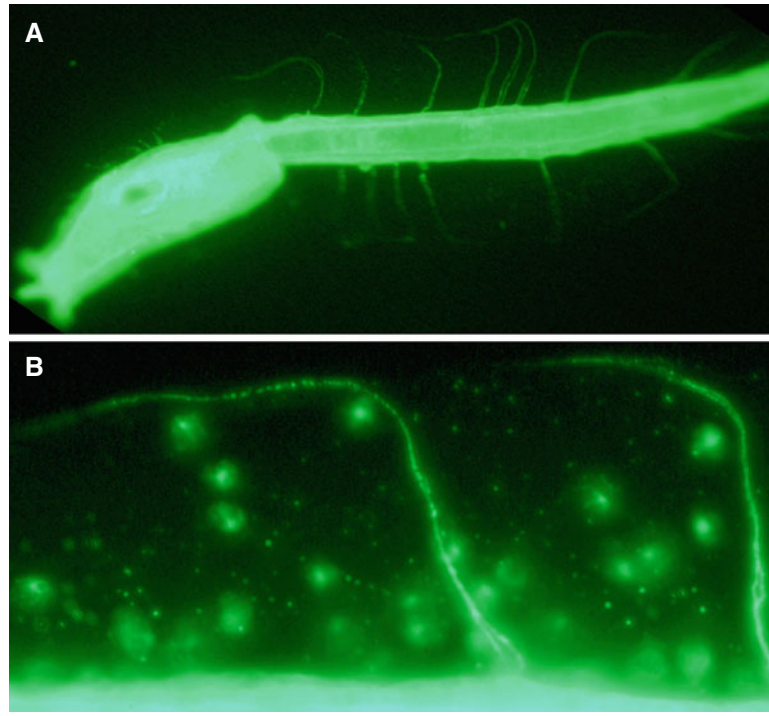

Fig. 4.18 Caudal epidermal sensory neurons of *Ciona*. (**A**) The thin ciliary projections of the caudal epidermal sensory neurons into the tunic fin revealed by beta-tubulin immunostaining. (**B**) Higher magnification view of tunic fin sensory projections (Figure is adapted from Pasini et al. (2006))

NeuroD-related, Pou4, and Atoh and the microRNA *miR-124* (Chen et al. 2011; Tang et al. 2013). Further AP patterning of these sensory neurons is achieved through antagonistic retinoic acid and FGF signals emanating from the anterior larval muscles and tailbud, respectively (Pasini et al. 2012).

Adult Siphon Primordia

Also arising from the head epidermis are the siphon primordia that give rise to the oral and aboral (or incurrent and excurrent) openings, or siphons, of the adult. The excurrent siphon is also known as the "atrial" siphon, due to its association with the peribranchial atrium or chamber. These are observed late in embryogenesis as rosettes of morphologically distinct epidermal cells. In phlebobranchs, one incurrent and two excurrent siphon primordia are specified, and initially the juveniles, or young adults, have three siphons each. Later in adult life, the two excurrent siphons fuse into a single siphon in a poorly studied process. In contrast, the excurrent siphon of stolidobranch ascidians arises from a single primordium in the larva or young juvenile.

While part of the incurrent siphon primordium is determined in a lineage-dependent manner from cells forming the neuropore[9] (Veeman et al. 2010), the excurrent siphon primordia are induced de novo from naïve epidermis by retinoic acid-dependent expression of *Hox1* in combination with later induction by FGF/ERK signaling (Kourakis and Smith 2007; Sasakura et al. 2012).

Adhesive Organ

At the most anterior end of the head is the adhesive organ, which in the majority of ascidians (one notable exception being the Molgulidae) consists of three protruding clusters of putative sensory and adhesive-secreting cells. These cell clusters are commonly referred to as "palps." The palps are remarkably elaborated in phlebobranch ascidians that undergo adultation (discussed below), perhaps because their larger, heavier larvae need to be more securely fastened to the substrate.

The adhesive organ primordium arises from the anterior borders of the neural plate and is

[9] The opening formed by the incomplete closure of the neural tube

specified in part by Foxc (Wagner and Levine 2012). Later adhesive organ development appears to require FGF/ERK signaling and an intricate interplay between the transcription factors Sp8, Emx, and Islet to specify the different cell types composing the palps and to regulate their morphogenesis (Wagner et al. 2014).

Development of the Mesoderm

Larval Muscles

The ascidian larva is specialized for dispersal, this being in fact its only role in the life cycle. Indispensable to this function are the larval muscles, arranged as bands of striated, mononucleated cells on either side of the tail. These muscle cells are divided into primary and secondary muscle lineages, according to their mode of specification. In *Ciona intestinalis*, there are 18 muscle cells per side and 21 cells per side in the slightly larger *Halocynthia roretzi* embryo. This difference in muscle cell number is entirely due to variation in the secondary lineage, while the primary lineage is invariant between the two species. It does not appear that these numbers deviate substantially among the larvae of the various solitary species. However, in those species showing extreme adultation and caudalization (explained later), larval muscles are greatly elaborated, both in terms of number of rows of cells and total numbers of cells (Cavey and Cloney 1976; Cavey 1982).

Primary muscle cells are autonomously specified, through inheritance of posterior/vegetal mitochondria-rich cytoplasm (Conklin's famous orange-yellow myogenic cytoplasm or "myoplasm"), shown by Whittaker to be sufficient and necessary for larval muscle formation (Whittaker 1973, 1982). The critical molecular component of the myoplasm was identified as maternally deposited *Macho1* mRNA, which is localized to the cER and translated into Macho1 protein in the primary larval muscle precursors (Nishida and Sawada 2001). Macho1 protein in turn activates its targets, among them the *Tbx6-related* family of genes (Yagi et al. 2005). Tbx6-related proteins then activate the myogenic regulatory factor gene *Mrf*, also known as *Myod* (Meedel et al. 1997, 2002, 2007; Imai et al. 2006). Mrf, Tbx6, and other transcription factors then cooperate to activate the expression of a battery of "differentiation" genes such as myosins, muscle actins, troponins, tropomyosins, etc. (Johnson et al. 2004, 2005; Brown et al. 2007; Izzi et al. 2013).

In contrast, secondary muscle cells are induced by extracellular signals from A- and b-line progenitors that do not inherit any maternal *Macho1*. Cell-cell signaling results in activation of *Tbx6-r* and *Mrf* independent of Macho1 (Kim and Nishida 2001; Hudson et al. 2007; Tokuoka et al. 2007). However, the exact identity of the signaling pathways used for the same inductive event differs between *Ciona intestinalis* and *Halocynthia roretzi*, representing another example of developmental system drift in ascidian evolution (Hudson et al. 2007; Tokuoka et al. 2007; Hudson and Yasuo 2008).

The variation in the *number* of secondary muscle cells being specified between *Ciona* and *Halocynthia* appears to be due to slight differences in cell positioning. In *C. intestinalis*, muscle-inducing cells are in contact with only the b7.9 blastomere, whereas in *H. roretzi* contact is made with both b7.9 and b7.10, resulting in induction of extra muscle progenitors (Kim and Nishida 2001; Hudson et al. 2007; Tokuoka et al. 2007).

Cardiopharyngeal Mesoderm

The term "cardiopharyngeal mesoderm" refers to multipotent progenitors that give rise to heart precursors and muscles of the peribranchial chamber and excurrent siphon of the adult (collectively referred to as "pharyngeal muscles"). In the embryo, four cardiopharyngeal progenitors (CPPs), two on either side of the embryo, are specified from the B7.5/B7.5 pair of blastomeres, which also give rise to anterior larval muscle cells (Fig. 4.19).

Investigations into marginal zone specification have largely ignored the B7.5 pair of blastomeres, which are situated at the posterior end of the marginal zone. Embryologically, the B7.5 cells are a confluence of vegetal and posterior endoderm and mesoderm, and this "hybrid" nature holds also true at the molecular level. In *Ciona intestinalis*, the B7.5 cells are delineated

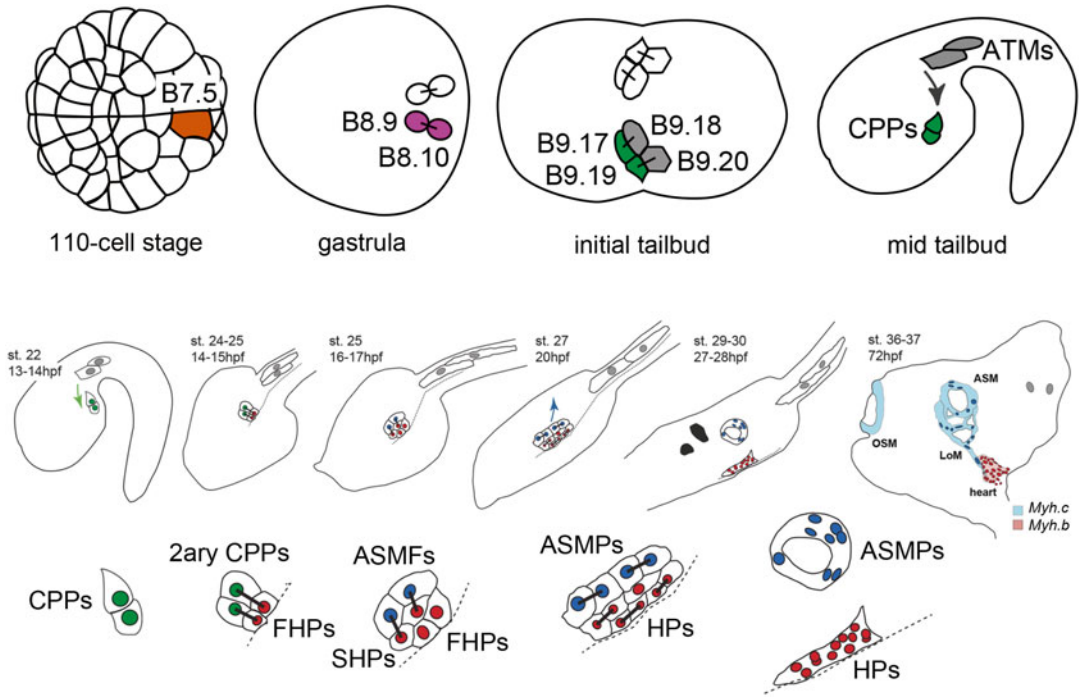

Fig. 4.19 The B7.5 lineage and cardiopharyngeal mesoderm. Diagram of the cell division and morphogenetic events of the B7.5 lineage, which gives rise to the cardiopharyngeal progenitor cells (*CPPs*) that will generate the heart and atrial siphon muscles (*ASM*) of the juvenile/adult. Refer to text for details. *ATMs* anterior tail muscles, *FHPs* first heart precursors, *SHPs* second heart precursors, *ASMFs* atrial siphon muscle founder cells, *ASMPs* atrial siphon muscle precursors, *HPs* heart precursors, *OSM* oral siphon muscles, *ASM* atrial siphon muscles, *LoM* longitudinal body wall muscles, *Myh.c* Myosin heavy chain.c (also known as *MHC3*), *Myh.b* Myosin heavy chain.b (also known as *MHC2*) (Figure is adapted from Wang et al. (2013))

by expression of the *Mesogenin*/*MesP* homolog *Mesp*, which is exclusively expressed in these cells and is necessary for the subsequent ontogenesis of lineage and its derivatives including the adult heart and pharyngeal muscles (Davidson et al. 2005; Satou et al. 2004). In *Ciona intestinalis*, *Mesp* is activated by Tbx6.b and Lhx3/4, zygotically expressed transcription factors under the direct regulatory control of beta-catenin and Macho1 maternal determinants, respectively. The expression territories of Tbx6.b (posterior) and Lhx3/4 (vegetal) overlap precisely in the B7.5, resulting in synergistic activation of *Mesp* in these cells alone (Christiaen et al. 2009). A Pem1-dependent timing mechanism has been proposed to help coordinate the precise overlap in time of these transcriptional cascades in the B7.5 (Tolkin and Christiaen 2012).

Experiments carried out in *Ciona intestinalis* and later extended to other ascidian species revealed that the CPPs are specified from the B7.5 lineage by FGF signaling (Davidson et al. 2006; Cooley et al. 2011). FGF-dependent activation of the ERK pathway and its effector, the transcription factor Ets.b, results in upregulation of a core of cardiac regulatory network genes and cell migration effector genes (Davidson and Levine 2003; Davidson et al. 2006; Beh et al. 2007; Christiaen et al. 2008). In contrast, their sister cells do not activate the ERK pathway and the cardiopharyngeal program and are instead specified as anterior primary larval muscle cells, as they inherit some myoplasm.

The CPPs detach from their sister cells and migrate anteriorly into the head (Hirano and Nishida 1997). In *Ciona intestinalis*, they migrate

along a ventral path and are thus called trunk ventral cells (TVCs), but in other species such as *Molgula* spp., these cells undertake a more lateral migration (Stolfi et al. 2014).

In the head, the CPPs undergo two rounds of asymmetric cell division to give rise to ventral/medial heart progenitors and dorsal/lateral pharyngeal muscle progenitors. The pharyngeal muscle progenitors are specified by a Tbx1/10-Ebf cascade (Stolfi et al. 2010; Wang et al. 2013; Razy-Krajka et al. 2014), which is antagonized by Nk4 in the heart precursors. The heart progenitors remain quiescent in the larva until needed for heart organogenesis during metamorphosis. On the other hand, the adult muscle progenitors migrate to dorsal regions and surround the excurrent siphon primordia while the larva is still swimming (Fig. 4.19).

During metamorphosis, cardiac and pharyngeal muscles differentiate, each expressing a unique suite of muscle structural genes (Stolfi et al. 2010; Razy-Krajka et al. 2014). The pharyngeal muscle progenitors will further migrate and proliferate to elaborate the musculatures of the excurrent siphon and the peribranchial chamber, which comprises essentially the entire body wall of the adult (Hirano and Nishida 1997; Razy-Krajka et al. 2014). Given the striking parallels in ontogeny and clonal topology between the cardiopharyngeal mesoderm in ascidians and vertebrates, it has been proposed that ascidian pharyngeal muscles are homologous to certain craniofacial muscles in vertebrates (Stolfi et al. 2010; Tzahor and Evans 2011; Tolkin and Christiaen 2012).

Notochord Formation

The notochord, one of the defining chordate traits, is the most salient feature of the ascidian larva and serves primarily as a hydrostatic skeleton required for the biomechanics of swimming (Jiang and Smith 2007). It is a single column of 40 cells, which are vacuolated late in larval development to form a hollow tube. Embryologically, the notochord has two origins (Fig. 4.20). The 32 primary notochord cells are derived from the A-line, specifically the A7.3 and A7.7 blastomeres. The remaining eight secondary notochord cells, occupying the posterior tip of the notochord, are derived from the B8.6 blastomere.

The primary notochord precursors are induced by an FGF signal and activate transcription of *Brachyury* (*Bra*). *Bra* is sufficient and necessary for notochord fate in *Ciona* and *Halocynthia* (Yasuo and Satoh 1998; Takahashi et al. 1999). Later, the secondary notochord precursors are induced by Delta-Notch signaling to also activate *Bra* (Hudson and Yasuo 2006). Upstream factors also regulating *Bra* activation in both lineages include Foxa and Foxd, while Zic-related appears to be required for *Bra* only in the primary notochord precursors (Imai et al. 2002a, b, 2006; Wada and Saiga 2002; Yagi et al. 2004; Kumano et al. 2006).

At the moment of gastrulation, notochord precursors are fate restricted and begin to ingress, prior to dividing twice to give rise to the final number of notochord cells. The cells form a notochord plate, which undergoes convergent extension, contributing to the elongation of the tail (reviewed in Jiang and Smith 2007). Final differentiation of the notochord involves the deposition of extracellular luminal matrix by each notochord cell. These lumens then fuse with each other to generate a single tube extending along the length of tail (Dong et al. 2009).

Downstream of Bra, approximately 450 genes have been identified as being upregulated in the notochord (Hotta et al. 1999; Takahashi et al. 1999). Of these, some are direct targets of Bra, with earlier-activated targets containing more Bra binding sites in upstream cis-regulatory sequences than targets activated later, which typically contain only one binding site (Katikala et al. 2013). There are also indirect targets of Bra, mediated by transcription factors that are direct Bra targets (Katikala et al. 2013). All in all, the notochord genes constitute a diverse group of proteins involved in several steps of notochord morphogenesis and differentiation.

Mesenchyme

With the exception of the anterior portion of the notochord, mesodermal cells in the head of the larva are undifferentiated and have been collectively referred to as "mesenchyme" due to their

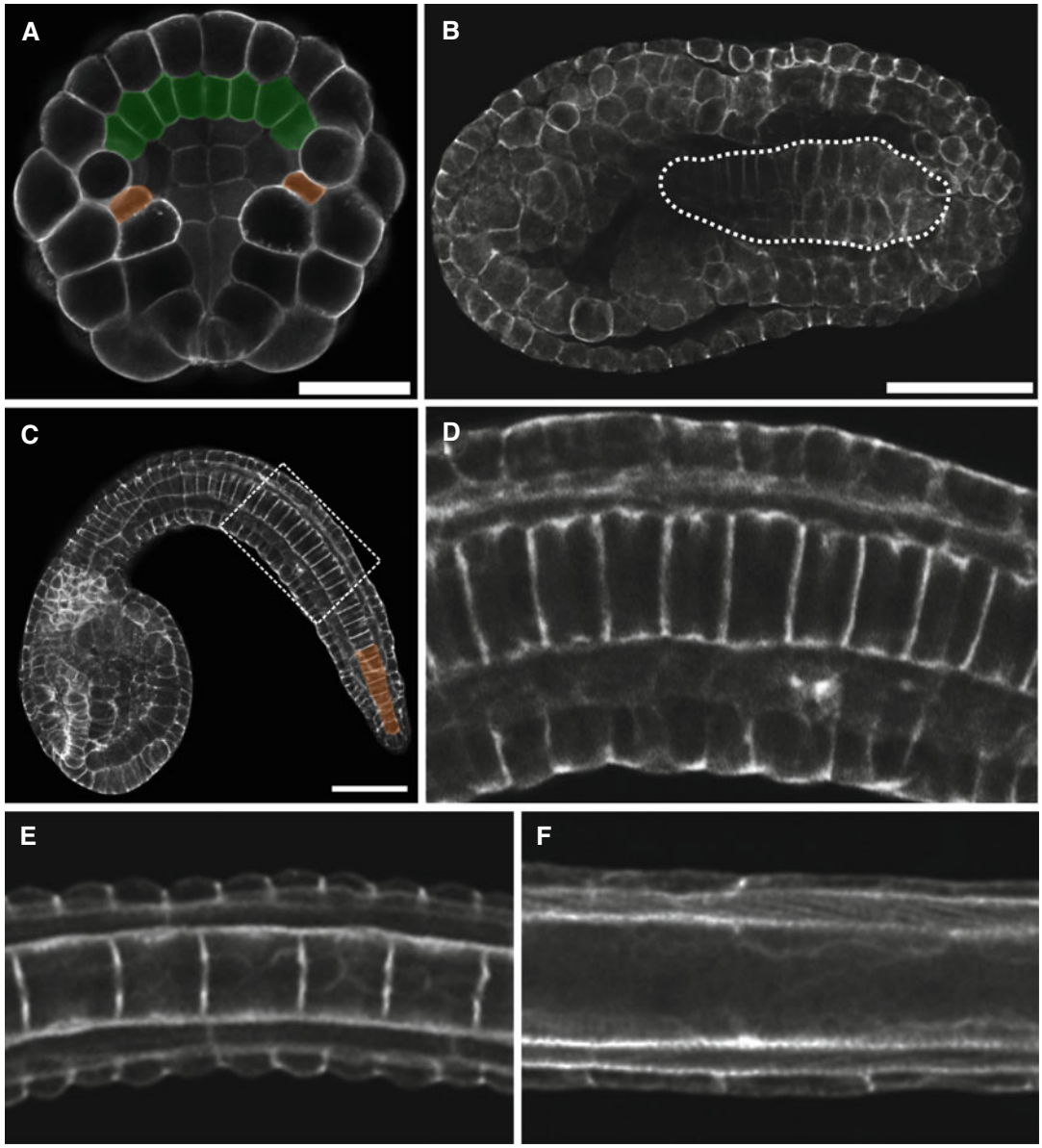

Fig. 4.20 The ascidian notochord. (**A**) 110-cell stage *Ciona intestinalis* embryo. The primary notochord precursors are false colored in *green*; the secondary notochord precursors are colored in *orange*. (**B**) Early tailbud stage embryo, with the cluster of intercalating notochord cells outlined by the *dotted line*. (**C**) Notochord in a mid-tailbud stage embryo, showing a single row of cells in the "stack of coins" configuration. Secondary notochord lineage colored in *orange*. (**D**) Magnified view of boxed area in (**C**). (**E**) Notochord cells in late tailbud stage embryo, already elongated and undergoing vacuolization. (**F**) Vacuolization of notochord cells is complete in the larva, with the unified lumens resulting in one long hollow tube running the entire length of the notochord. Scale bars in all panels equal 50 μm (© Alberto Stolfi, 2015. All Rights Reserved)

loose, seemingly disorganized distribution. These cells undergo an epithelial-to-mesenchymal transition after gastrulation and engage in proliferation and migration to varying degrees. Among these, there is usually a strong distinction made between the B7.5-derived cardiopharyngeal progenitors and mesenchyme derived from the A7.6, B7.7, and B8.5 pairs of blastomeres (Tokuoka et al. 2004).

The most anterior mesodermal lineage, the A7.6, has been reported to give rise to diverse

adult tissues including hematopoietic (blood) cells, gill slit lining, part of the stomach and peribranchial chamber, and incurrent (oral) siphon muscles (Hirano and Nishida 1997; Tokuoka et al. 2005). There were discrepancies between A7.6 tracing in different species, and new tools like photoconvertible intracellular fluorescent proteins may be needed to ascertain whether these represent true species-specific differences. The remaining mesenchymal lineages, B7.7 and B8.5, have been reported in *Ciona* as giving rise to blood cells as well as diverse cells that come to populate the adult tunic, whereas in *Halocynthia roretzi* they are described as giving rise to tunic cells only (Hirano and Nishida 1997; Tokuoka et al. 2005).

FGF signaling and the basic helix-loop-helix (bHLH) factor Twist-related were shown to be required for specification of mesenchyme (Imai et al. 2002a, 2003; Tokuoka et al. 2005), but little else is known about the developmental events and processes involved in specification and differentiation of A7.6, B7.7, and B8.5 mesenchymal derivatives of the adult.

Development of the Endoderm

Endoderm specification occurs immediately downstream of vegetally localized, stabilized maternal Beta-catenin, in part by activation of Lhx3/4 (Imai et al. 2000; Satou et al. 2001). In the *Ciona intestinalis* larva, there are approx. 500 endodermal cells, the majority of these residing in the head while a minority comprises the endodermal strand, a single column of cells that runs underneath the notochord to the posterior tip of the animal. The endoderm is largely undifferentiated upon hatching, but undergoes a process of differentiation while the larva is still swimming, in preparation for settlement and metamorphosis (Nakazawa et al. 2013).

Cell tracing experiments in *Halocynthia roretzi* revealed that the clonal boundaries of these cells in the larva were invariant and could be traced to blastomeres in the pre-gastrula embryo (Hirano and Nishida 2000). Furthermore, differentiated adult organs could be traced to specific regions of the endoderm fate map in the larva, indicating that the "anlagen" of these organs are laid out in the larva and are not significantly rearranged during metamorphosis. However, there was variation among individuals in the contributions of each blastomere to the final differentiated organs, suggesting that the endoderm is patterned at the larval stage in a position-dependent manner by extrinsic cues, and not according to deterministic, lineage-dependent processes. Late in larval development, the digestive tract rudiment can be seen to undergo tubular morphogenesis (Nakazawa et al. 2013), while in those species that show adultation, these and other organs are fully formed at the moment of larval hatching.

Primordial Germ Cells

The highly asymmetric divisions of the posterior vegetal end of the embryo eventually give rise to the B7.6/B7.6 pair of blastomeres, the smallest and most posterior cells in the pre-gastrula embryo. They are kept transcriptionally silent through inheritance of *Pem1* mRNAs and protein. They also inherit other postplasm components including the homolog of the major metazoan germ cell marker Vasa (Fig. 4.21; Takamura et al. 2002; Brown and Swalla 2007; Brown et al. 2009; Shirae-Kurabayashi et al. 2006).

After gastrulation, these cells end up in the ventroposterior portion of the larval tail. Each B7.6 cell divides and gives rise to two daughter cells: B8.11 and B8.12. *Vasa* mRNAs and protein are asymmetrically inherited by the more posterior B8.12 cell, whose descendants are eventually incorporated into the adult gonad and give rise to the animal's germ line (Takamura et al. 2002; Shirae-Kurabayashi et al. 2006). Thus, the B8.12 cells are the primordial germ cells (PGCs). Curiously, *Pem1* is asymmetrically inherited by B8.11, suggesting the PGCs are released from global transcriptional repression around this stage.

It was found that germ cells could be secondarily induced in adults generated from larvae in which the tail, and therefore the B8.12-derived primary germ cells, had been severed. This suggests that there may be mechanisms that allow for induction of secondary germ cells in case the primary germ line is somehow lost (Takamura et al. 2002).

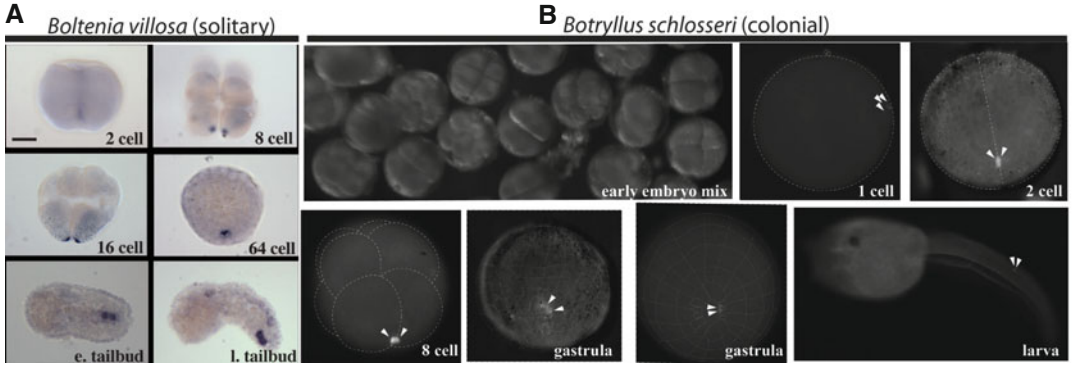

Fig. 4.21 The primordial germ cells (*PGCs*) of solitary and colonial styelid ascidians. RNA-dependent helicase *Vasa* transcripts are shown as early PGC marker. (**A**) *Vasa* transcripts in blue for the solitary *Boltenia villosa*. (**B**) *Vasa* transcripts marked by *white arrowheads* in the closely related colonial *Botrylloides violaceus*. Note that in both cases *Vasa-positive* cells are localized to a few posterior cells of the early embryos. Developmental stages are noted below each panel. Scale bar in (**A**) equals 50 μm (From Brown et al. (2007, 2009))

Taken as a whole, ascidian embryos are excellent organisms in which to observe cellular processes in vivo and investigate the function of genes involved in such processes. The gene regulatory networks of the ascidian embryo (Fig. 4.5) have been considerably annotated, but these networks so far have mostly concerned the connections among the transcription factors and signaling pathways. More recently, our knowledge of these networks has started to extend to their interface with the realm of effector genes – those that do not directly regulate transcription but rather interact with other proteins to carry out mechanical or enzymatic functions. The best-studied effector genes are those that are responsible for the unique properties of differentiated cells, also known as terminal differentiation genes. More challenging genes to study are those that are involved in transient cellular properties and behaviors like polarity, motility, adhesion, contractility, and other components of morphogenesis. There have been some notable examples where the genes controlling these processes in the ascidian embryo were discovered. For instance, forward genetic screens for notochord morphogenesis defects in *Ciona* identified genes required for the convergent extension of this tissue (Jiang et al. 2005; Veeman et al. 2008). A later phase of notochord morphogenesis, namely, the formation of the notochord tube, has been studied using a combination of sophisticated imaging of fluorescently tagged proteins and targeted disruption of candidate genes (Dong et al. 2009, 2011; Denker et al. 2013; Deng et al. 2013). Finally, cell-specific transcriptome profiling can reveal those genes upregulated during morphogenesis, which was done for the migrating CPPs and revealed several candidate migration genes (Christiaen et al. 2008). Although the tissues and cell types investigated thus far are not many, the future for research on cellular morphogenesis in ascidian embryos holds great promise.

Early Development of Other Tunicates

Recently acquired evidence suggests that the thaliaceans and larvaceans, once thought to be distinct from ascidians, appear to group within the paraphyletic Ascidiacea. Phylogenetic trees strongly support the placement of a monophyletic Thaliacea squarely within the phlebobranch ascidians, i.e., Enterogona (Tsagkogeorga et al. 2009). Phylogenetic support for a revised classification of the larvaceans as the sister group to the stolidobranch ascidians is not as strong, but embryological data suggest they may be highly derived ascidians (Stach et al 2008; Fujii et al. 2008). Here, we discuss what is known about developmental processes in these less-frequently studied groups.

Larvaceans: Reduction and Neoteny

In the larvaceans, as the name implies, there is no morphological contrast between the embryo/larva and the adult. Larvaceans are planktonic tunicates that retain a functional notochord and paraxial musculature throughout their entire adult lives. These constitute a true postanal tail that has been adapted to beat vigorously and generate water currents through the "house," an intricately sculpted cellulosic filtration apparatus (Fig. 4.22). This house is shaped through the patterning of the head epidermis into a complex landscape of specialized cells that secrete specific subsets of oikosins, the major protein component of the house (Fig. 4.22; Spada et al. 2001; Thompson et al. 2001; Hosp et al. 2012). The house is many times the size of the actual animal and utilizes a series of canals and filters to trap

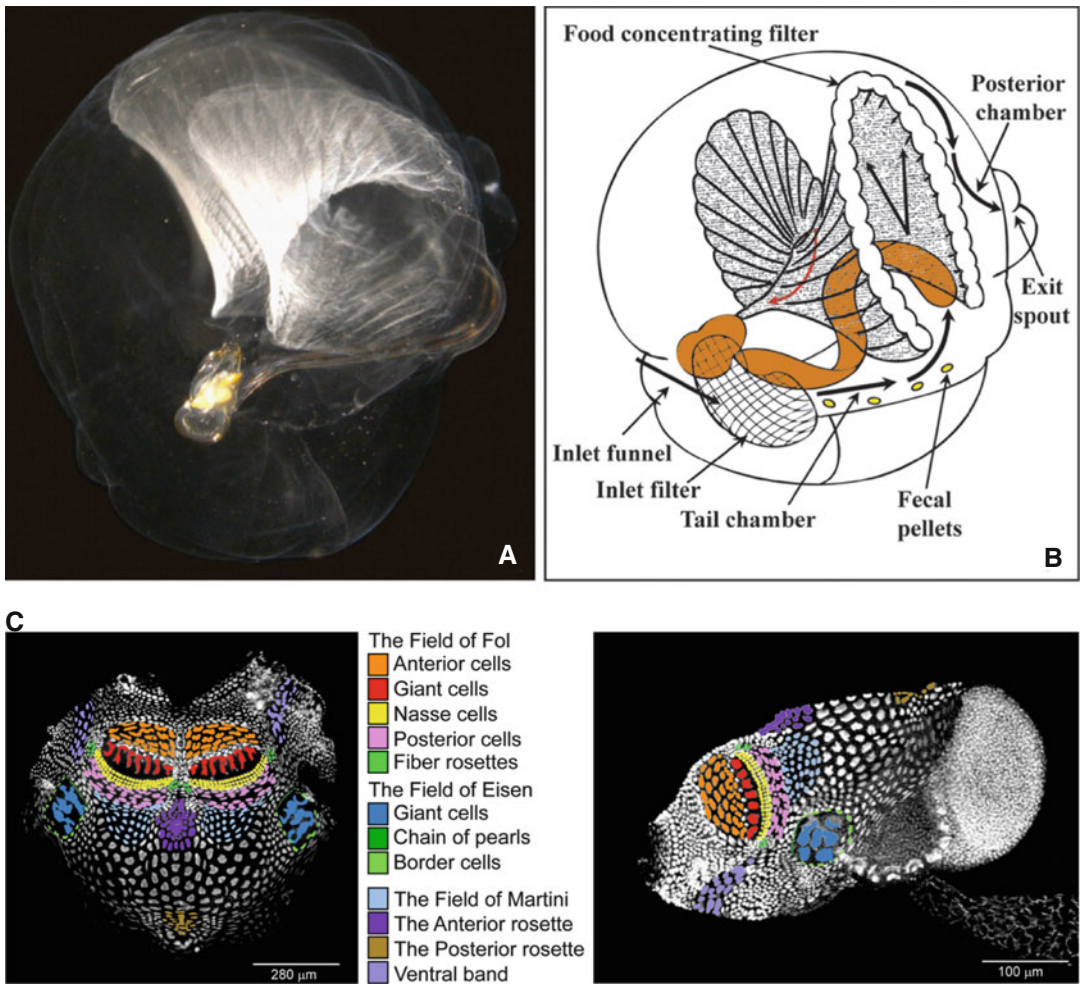

Fig. 4.22 The larvacean house. (**A**) Lateral view of an *Oikopleura dioica* individual and surrounding house. Anterior is to the *top right*. (**B**) Illustration of the animal and house depicted in (**A**). Animal is colored in *orange*. *Black arrows* indicate the direction of water currents that are swept into the house by beating of the animal's tail and through the filter apparatus of the house. *Red arrow* indicates movement of food particles toward the animal's mouth. (**C**) Oikoplastic epidermis of *O. dioica* stained with Hoechst (*left*) and To-Pro3 (*right*), revealing cell nuclei. Different fields of cells have had their nuclei false colored to highlight the different fields that shape the house through synthesis and secretion of various proteins, including oikosins (Panels (**A**, **B**) were adapted from Bouquet et al. (2009); (panel **C**) was adapted from Hosp et al. (2012))

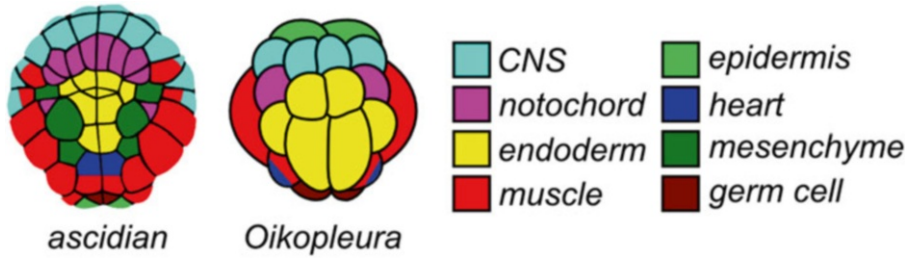

Fig. 4.23 The ascidian and larvacean fate maps. Comparison between the typical solitary ascidian and *Oikopleura dioica* (larvacean) embryonic fate maps. The ascidian fate map is largely based on the work of Nishida (1987) and the *Oikopleura* map based primarily on Stach et al. (2008) and Fujii et al. (2008)

particle food. The animal can eject from its house and does so with some regularity, some five to ten times per day, synthesizing a new one in just 10 minutes (Alldredge 1977).

Occasionally imagined as representing the common ancestor of all tunicates, these remarkable creatures likely evolved from an ascidian-like ancestor instead (Stach et al. 2008). Secondarily evolved heterochronies superimposed on the biphasic development of ascidians would have resulted in neoteny. This view is supported by recent tunicate phylogenies that place larvaceans within the ascidian tree, although these analyses are hampered by long-branch attraction problems (Tsagkogeorga et al. 2009). On the other hand, other analyses have placed the larvaceans as the sister group to all other tunicates (Delsuc et al. 2006, 2008).

The larvacean embryo and developmental times are even more reduced than those of solitary ascidians. The complete life cycle of the species *Oikopleura dioica* is only 5 days at 20 °C. Gastrulation occurs at the 32-cell stage, as opposed to gastrulation in ascidians which happens at the 110-cell stage (Fujii et al 2008). The embryo is also mostly fate restricted at this stage, and this map is very similar to the ascidian fate map, in spite of the fewer cells (Nishida 2008; Stach et al. 2008). Each cell lineage develops in a way that is very reminiscent of the homolog in ascidian embryos, albeit clearly reduced in cell numbers (Fig. 4.23). For instance, there are 20 notochord cells at the end of embryogenesis, as opposed to 40 in most solitary ascidians (Nishino et al. 2001).

Strikingly, only a fraction of the *Ciona* notochord toolkit genes are expressed in the *Oikopleura dioica* notochord (13/50), and half of them are completely absent from the *O. dioica* genome (Kugler et al. 2011). How larvaceans cope with a reduced number of genes to build a notochord is not yet clear. Since the larvacean tail is used to draw the water current through the animal's house, as opposed to a larval dispersal mechanism, it is highly elaborated during the larval and adult stages, as notochord cells proliferate to generate over 100 cells arranged into four longitudinal columns (Søviknes and Glover 2008). It is possible that this difference in gene expression underlies the adaptation of the larvacean notochord for this purpose.

Another clear example of cell count reduction during embryogenesis is seen in the neural plate, which is comprised of just two columns of four cells each when neurulation begins (Fujii et al. 2008), as opposed to the eight columns and six cells of the *Ciona* and *Halocynthia* neural plates. Additionally, larvacean tail muscles are made of only a single row of ten cells on either side of the notochord (Nishino et al. 2000), in contrast to the 18 or 21 cells per side seen in typical ascidian larvae.

Given these striking parallels with the slightly more complex embryos of solitary ascidians, it seems reasonable to conclude that larvaceans may be descended from a sessile, solitary ascidian-like ancestor, but have specialized in part through reduction in cell number, basic toolkit gene number, and acceleration of development.

Embryonic Development of Thaliaceans

Although the thaliaceans are pelagic and free swimming in their adult phase, they are very distinct from the larvaceans and represent an alternative evolutionary trajectory from an ascidian-like ancestor. They resemble pelagic ascidians, filter-feeding as they float in the water column. Salps use muscular contractions of the pharyngeal cavity to generate locomotion by jet propulsion. They constantly produce and consume mucous nets that trap particles passing through the pharyngeal cavity, which allows for simultaneous filter feeding and locomotion. As a result, they can filter a prodigious amount of water. Doliolids also move about through jet propulsion, but their feeding and swimming are separate functions, as they use cilia to draw particles through the mucous feeding net, being similar in this manner to ascidians. Pyrosome colonies move through the combined flow of each minuscule zooid, which is generated by cilia as well (reviewed in Alldredge and Madin 1982).

Pyrosomes and salps lack a caudate larval stage and both have direct developing embryos (Julin 1912; Berrill 1950a, b; Sutton 1960). Of the three main orders in Thaliacea, only certain species of the doliolids have a tadpole-like larva (Godeaux 1955), which has been used as a reminder of their ascidian pedigree and to support evidence for phylogenies that place them as the sister group to the salps + pyrosomes (Tsagkogeorga et al. 2009). However, a more recent and complete phylogeny that includes a higher number of thaliacean species supports a salp + doliolid clade with the pyrosomes in a basal position (Govindarajan et al. 2010), suggesting independent losses of the tadpole stage in pyrosomes and salps (Fig. 4.1).

A complete review of thaliacean development was last compiled by Bone (1998). Pyrosome embryogenesis is direct, giving rise to a peculiar embryo termed "cyathozooid" (Huxley 1851). The cyathozooid differentiates on top of a yolk droplet and sprouts a stolon under the droplet, which forms four buds by constriction. These buds will develop into the four initial blastozooids (called tetrazooids in this specialized case) that develop around the cyathozooid, which quickly degenerates afterward.

Perhaps the most specialized developmental mode observed in all of the tunicates occurs in the salps. In early embryogenesis, invading follicle cells separate the blastomeres, which come back together again later in development (Todaro 1880; Sutton 1960). The function of this deliberate fragmentation of the early embryo has never been ascertained.

Doliolid embryonic development occurs from internally fertilized eggs and generates a pelagic chordate-like larva, which will eventually differentiate the typical barrel-shaped form of doliolid zooids in its head, while the tail regresses to form the oozooid of the asexually reproducing generation.

Relatively little else is known about thaliacean development, and much less is known about the underlying molecular mechanisms. All three orders are capable of asexual reproduction, and salps and doliolids have complex alternation of sexual and asexual generations (see below). We can only hope that major developmental studies in the thaliaceans will be revived quite soon, in time for the next round of reviews and book chapters.

LATE DEVELOPMENT

Ascidian embryonic development, as reviewed in the previous section, is highly conserved, being nearly indistinguishable between some distantly related species. In contrast, there is a greater diversity observed in later stages of development. The following section will focus on some of these differences in late larval development, such as heterochronic shifts, the distinct modes of asexual reproduction, and blastogenesis in the colonial ascidians. Therefore, while the previous section relied heavily on studies using *Ciona intestinalis* and *Halocynthia roretzi*, the following section will mostly focus on comparative work done across several species to provide a comprehensive overview of late larval, early adult, and blastogenic development in the Tunicata.

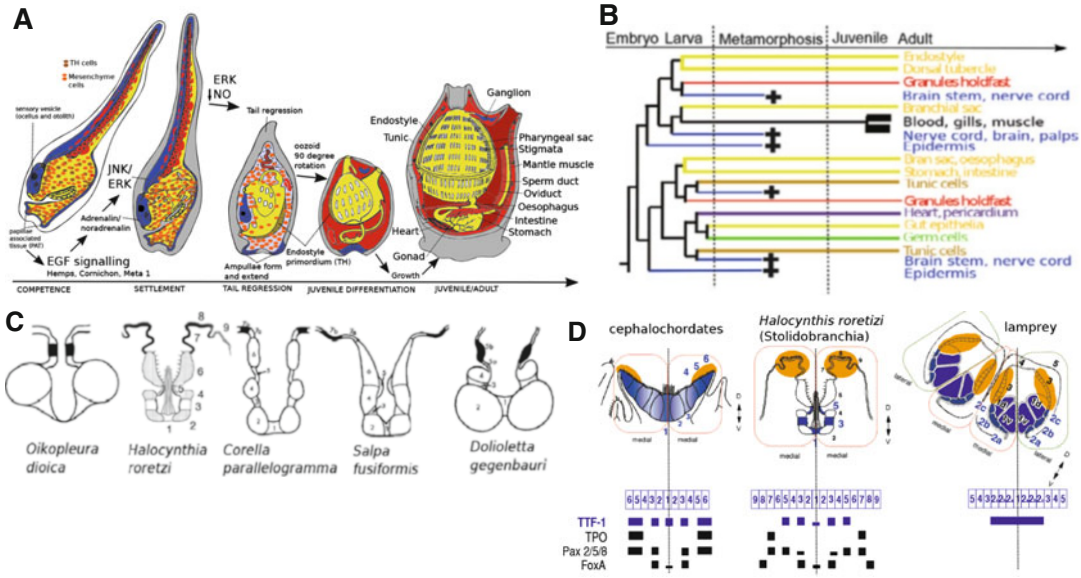

Fig. 4.24 Metamorphosis in ascidians. (**A**) Events of metamorphosis highlighting players and pathways involved (© Biodidac, 2015. All Rights Reserved). (**B**) Representation of embryonic cell lineages that contribute to the juvenile and adult; note that many cells undergo cell death (*black crosses*) and that mostly endoderm and mesoderm contribute to the adult (From Brown et al. (2012)). (**C**) Comparison of the endostyle of different tunicates shows resemblance in their organization and dorsolateral iodine-containing and peroxidase activity regions of the thyroid gland (in *black*) (Adapted from Fredriksson et al. (1988)). (**D**) Gene expression pattern supports homology between the endostyle of cephalochordates and ascidians with the endostyle of the lamprey (Adapted from Ogasawara et al. (1999, 2001), Hiruta et al. (2005), Kluge et al. (2005))

Late Larval Development

Developmental timing of embryogenesis and larval development differs between solitary and colonial ascidians. Solitary free-spawning ascidians develop rapidly: embryogenesis occurs within 8–48 h of fertilization (e.g., 15 h in *Ciona intestinalis*, 9 h in *Molgula occidentalis*), and hatched larva then swims freely for several hours or even days before settlement. In contrast, colonial species that brood have relatively longer periods of embryogenesis that can take anywhere from days to weeks (e.g., 5–6 days in *Botryllus schlosseri* or 4–6 weeks in *Botrylloides violaceus*), but present shorter larval periods that only last between several minutes to a couple of hours after they have been released (e.g., 1–2 h in *Botryllus schlosseri*). However, in both solitary and colonial ascidians, the larval period is nonfeeding and serves primarily for dispersion.

A few hours after hatching (or immediately after hatching, in the case of some colonial species), ascidian larvae acquire the ability (or "competency") to respond to settlement cues from the environment (Figs. 4.24 and 4.25). Competent larvae actively seek suitable locations and substrates on which to settle. The preferred cues will obviously vary according to the ecological niche of the species in question. For many solitary species, competent larvae seek protected and dark places, often settling on rocks or hard substrates with indirect sunlight. Biological cues, such as naturally occurring bacteria (Roberts et al. 2007), and physical cues such as trauma, crowding, or stress (Degnan et al. 1997; Davidson and Swalla 2002) have been used to artificially induce metamorphosis in different ascidian species.

Billie Swalla and collaborators found that immune genes are highly expressed at the early onset of metamorphosis in ascidians, suggesting

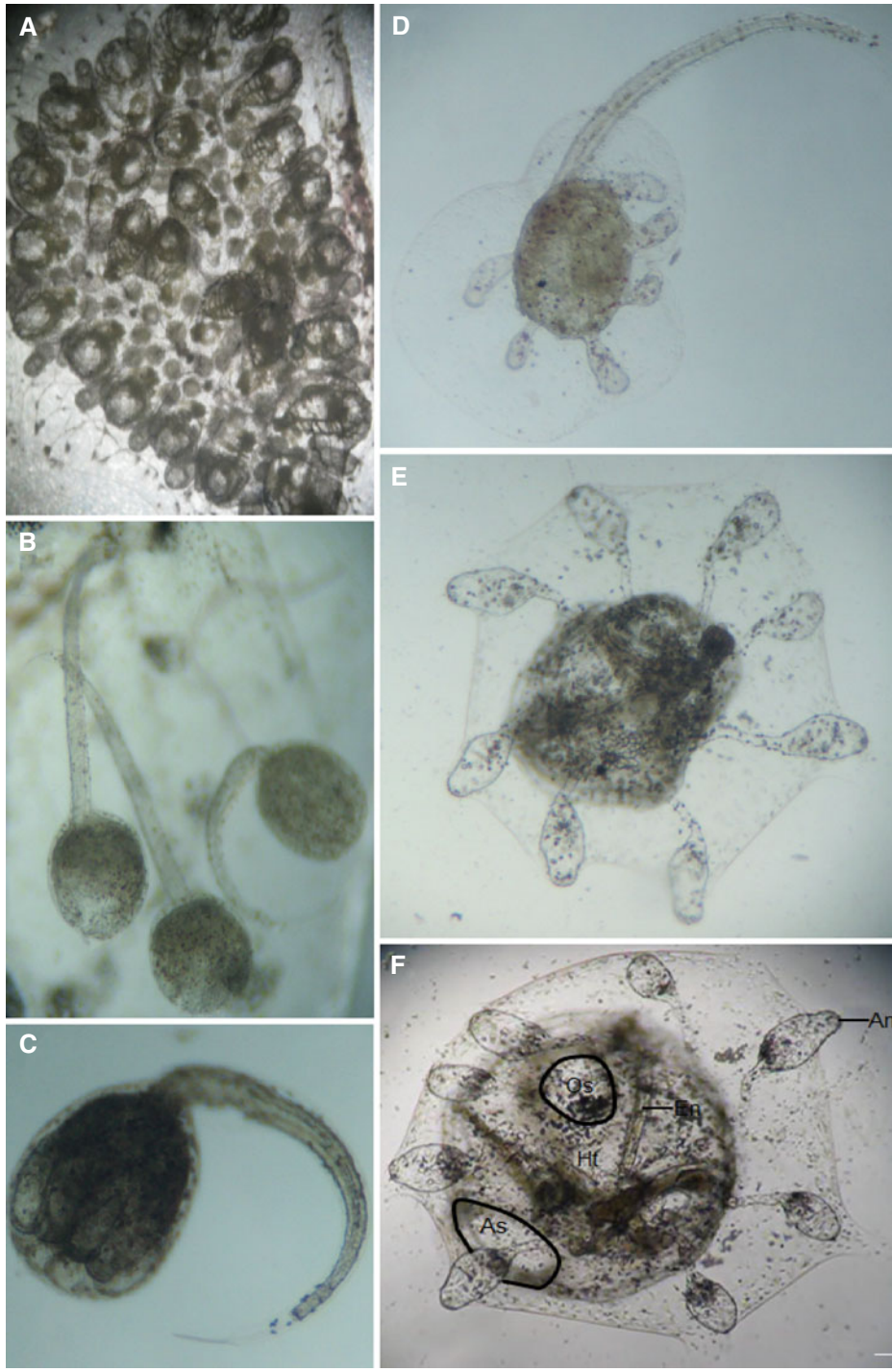

Fig. 4.25 Larval release and settlement (metamorphosis) of an unidentified *Botryllus* sp. from Santa Marta, Colombia. (**A**) Ventral view of the brooding colony hours before larval release; many round larvae can be seen in between the zooids. (**B**) Larvae right after hatching and release. (**C**) Larval head that shows the protruding ampullae (or papillae) in the anterior region of the head. (**D**) Attaching larva with extended ampullae; eye spot and tail still present. (**E**) Oozooid just before the opening of the siphons; almost regressed tail and eye spot can still be observed. (**F**) Completely differentiated oozooid; *Am* ampulla, *As* atrial siphon, *En* endostyle, *Ht* heart, *Os* oral siphon. Scale bar equals 100 μm (Courtesy of L. Restrepo (Universidad de los Andes))

that the activation of the innate immune system may occur at this stage. One intriguing explanation for this is that the innate immune system is deployed in sensing microbiota or bacterial biofilm as cues for settlement. Another possibility may be a direct involvement of immune cells in later metamorphic events including remodeling or phagocytosis of larval tissues (Davidson and Swalla 2002). One question that remains to be answered is whether the immune system response observed in these cases is specific to ascidian metamorphosis or whether it also plays a role in the metamorphic events of other tunicates or chordates.

Most solitary species' larvae have three adhesive papillae (palps) in the anterior end of the head that function in adhesion to the substrate and in responding to settlement cues. In response to environmental stimuli, the papilla-associated tissues (PATs) activate the expression of EGF signaling components (e.g., Hemps, Cornichon, Meta1) and thrombospondins. Thrombospondins are secreted extracellular proteins known to bind several ligands and are involved in many cellular processes, including tissue formation or repair (Eri et al. 1999; Davidson and Swalla 2001; Nakayama et al. 2001).

The activation and regulation of signaling pathways in PATs is followed by the release of noradrenaline/adrenaline (Kimura et al. 2003) and the activation of transduction pathways such as JNK and ERK in the larval CNS (Tarallo and Sordino 2004; Chambon et al. 2007). Further evidence supporting signaling from the PATs to the CNS comes from the disruption of sensory vesicle retraction (a key step in metamorphosis) in papilla-cut larvae of *Ciona intestinalis* (Nakayama-Ishimura et al. 2009). In summary, environmental stimuli are sensed by the PAT, which then signals to the nervous system to trigger the onset of metamorphosis.

Metamorphosis

Metamorphosis involves a radical transition in the life cycle of indirect-developing organisms. Larval body and behavior are remodeled into their final adult forms (Fig. 4.24), in order for the individual to occupy a different ecological niche. Tissue-remodeling processes during animal metamorphosis are known to occur mainly through the activation of programmed cell death in larval tissues and the differentiation of juvenile and adult tissues.

There is variation in the degree of change that results from metamorphosis among the different chordate taxa: it may be absent or minimal as in mammals or birds, subtle as in fish that undergo slight changes in fins and gut, more pronounced as in flatfish or cephalochordates that undergo rotation of parts of their bodies, or extreme as in frogs or tunicates that can lose entire larval structures and rapidly generate adult tissues and organs. However, this is not the same "catastrophic" metamorphosis of some animals such as echinoderms (cf. Chapter 1), ectoprocts (cf. Vol. 2, Chapter 11), or others, in which an entire adult body is practically generated de novo from a few cells, with little input from embryonic patterning. Even in tunicates, the majority of adult structures arise from primordia that have been specified, patterned, and primed for differentiation during the course of embryogenesis and larval development.

Because of the great diversity of metamorphic transformations observed in the chordates, these were long thought to have evolved independently. In the following, studies of metamorphosis are described for several tunicates including those on ascidian model species, focusing on how such studies have contributed to our understanding of the origins of metamorphosis in the chordates and deuterostomes in general.

Due to the dramatic transformation of the non-feeding larvae into the sessile feeding juveniles and adults of ascidians, these have been used primarily as experimental study models for metamorphosis in the tunicates. Few studies on metamorphosis have been carried out in larvaceans, which do not feature a strong contrast between the larval and adult forms, and, to our knowledge, no work has been done on metamorphosis in Thaliacea. While some species of doliolid thaliaceans present tailed larvae, all species of salps and pyrosomes have dispensed their larval

stage entirely and instead directly develop into an oozooid from the sexual cycle to reproduce asexually (Bone 1998).

Key Steps in Ascidian Metamorphosis

A rapid regression of the larval tail marks the onset of metamorphosis in the ascidians. We have already discussed the key events that precede metamorphosis, including the activation of a sensitive period that allows the larva to respond to external stimuli (i.e., competency), the secretion of adhesives by the palps to facilitate attachment to the substrate and signaling by the larval PAT and CNS (Fig. 4.24A). Upon settlement, rapid regression starting at the most posterior tip of the larval tail is mediated by a few distinct mechanisms. These include apoptosis of tunic cells, epidermis, notochord, tail muscle, and dorsal neural tube (Chambon et al. 2002), contractile morphogenetic events of either epidermal or muscle cells in the tail that generate the forces for resorption (Cloney 1982), or migration of cells of the tail (e.g., endodermal strand and PGCs) into the head, which has now become the entire body of the animal (Shirae-Kurabayashi et al. 2006; Nakazawa et al. 2013).

The relative modularity of these different steps in metamorphosis is demonstrated by the striking phenotypes of certain genetic mutants. In *Ciona intestinalis*, two mutants showing metamorphic defects have been studied: (1) *swimming juvenile* (*sj*), a transposon-generated cellulose synthase mutant strain, and (2) *tail regression failed* (*trf*), a naturally isolated mutant strain. Both mutants show that several key steps in metamorphosis can occur even in the absence of larval tail regression (Nakayama-Ishimura et al. 2009). These mutants clearly show that the developmental processes of metamorphosis are indeed decoupled from each other.

In *Ciona intestinalis*, tail regression is preceded by a decrease in endogenous nitric oxide (NO) signaling (Fig. 4.24A). While NO was found to delay metamorphosis, in part through inhibition of caspase-dependent apoptosis (Comes et al. 2007), it was also found to promote ERK signaling during the acquisition of competency (Bishop et al. 2001; Comes et al. 2007; Castellano et al. 2014). Although the same inhibitory effect of NO on metamorphosis was observed in *Boltenia villosa* and *Cnemidocarpa finmarkiensis*, the opposite was found in *Herdmania momus*, in which NO appears to promote metamorphosis (Ueda and Degnan 2013). These results point to complex roles for NO immediately prior to and after the onset of metamorphosis, which may vary from species to species.

Remodeling of the Larval Body

Metamorphosis proceeds with the remodeling of the larval body and differentiation of the juvenile tissues and organs for another 1 or 2 days (approx. 36 h in *Ciona intestinalis* or 24–36 h in *Botryllus schlosseri*) (Fig. 4.25). Some of the major events of remodeling in the larval head concern the regression of the papillae (extended during settlement), the release of the larval tunic, the formation of epidermal extensions termed ampullae, and a 90° rotation of the larval AP body axis so that the oral and atrial siphons of the juvenile come to lie opposite to the site of attachment to the substrate and sensory vesicle regression (Cloney 1982; Nakayama-Ishimura et al. 2009). Mesenchyme cells begin substantial migration within and across the epidermis of the differentiating juvenile, giving rise to their various derivatives including blood and tunic cells. Additional undifferentiated endoderm and mesoderm precursors develop into the organs and musculature of the adult.

In late embryonic and early larval development, apoptosis appears to occur in many mesenchymal and CNS progenitors (Tarallo and Sordino 2004), but these findings are in stark contrast to lineage tracing experiments that find invariant contributions of specific embryonic blastomeres to specific juvenile tissues and organs. Apoptosis is observed in mesenchymal cells that generally give rise to blood and muscle in the juvenile, although a role for programmed cell death in these progenitors is unclear (Fig. 4.24B). In the larval CNS, two waves of apoptosis have been reported, one pre-metamorphic anterior-posterior wave that progresses from the sensory vesicle in the head along

the nerve cord to the tip of the tail and a second metamorphic wave from posterior to anterior that follows regression (Tarallo and Sordino 2004).

In contrast to the extensive cell death observed in the nerve cord, the brain, and the motor ganglion, most of the anterior sensory vesicle and the neck region actually contribute to the adult CNS (Tarallo and Sordino 2004; Horie et al. 2011).

In summary, developmental processes of ascidian metamorphosis largely redeploy the cellular processes that are universal for any developing system, such as apoptosis, proliferation, migration, and differentiation. However, more work will be needed to understand exactly how they are regulated in the metamorphosing ascidian juvenile.

Thyroid Hormone Metabolism in Ascidian Metamorphosis

The series of events that occur during metamorphosis require regionalized responses to systemic signals. Therefore, one can hypothesize that a common and plesiomorphic endocrine mechanism evolved to regulate metamorphosis in all chordates. Triiodothyronine (T3) and its prohormone, thyroxine (T4), collectively referred to as thyroid hormones (THs), regulate basal metabolism in vertebrates and serve as the trigger of metamorphosis in amphibians and fish (Furlow and Neff 2006; Gomes et al. 2014). In these vertebrates, a peak in the level of T3 in the blood is associated with the onset of metamorphosis. Ever since the discovery that the thyroid gland, specifically the THs produced by its follicular cells, triggers metamorphosis in frogs (Gudernatsch 1912; Allen 1925), much research has been carried out to unravel the mechanism of TH action in other vertebrates (Holzer and Laudet 2013). However, the role of THs in the metamorphosis of invertebrates is not well understood.

Studies in ascidians and cephalochordates have revealed TH synthesis activity during metamorphosis, and T4 inhibitor treatments were found to suppress metamorphosis of competent larvae (D'Agati and Cammarata 2006). Furthermore, thyroid hormone receptor (TR) homologs have been identified both in *Ciona intestinalis* and the cephalochordate *Branchiostoma floridae*. Therefore, there is evidence to support the plesiomorphic nature of thyroid hormone metabolism in chordates. However, it was found that ascidian and cephalochordate TRs are mainly activated by TRIAC, a TH derivative that is also present in mammals but at much lower concentrations. Furthermore, these invertebrate chordate receptors cannot bind T3, the most active vertebrate thyroid hormone (Carosa et al. 1998; Paris et al. 2008). In contrast to the high sequence similarity between the DNA-binding domains of all chordate TRs, there is poor sequence conservation in the ligand-binding domains of ascidian and cephalochordate TRs. This further suggests that TRIAC, and not canonical THs, is the active ligand of basal chordate TRs. Surprisingly, recent evidence suggests that both T3 and T4 regulate the metamorphosis of sand dollars (Saito et al. 1998; Heyland and Hodin 2004), which raises the possibility that TH metabolism was involved in metamorphosis even in the last common deuterostome ancestor. Further studies are needed in the protostomes to test for TH involvement in metamorphosis of earlier bilaterians or even metazoans.

The Endostyle: Precursor to the Thyroid Gland

The endostyles of tunicates and cephalochordates have long been recognized as homologous to the thyroid gland of vertebrates, a connection first suggested by A. Dohrn at the Stazione Zoologica in Naples, Italy (Dohrn 1886).[10] In both ascidians and cephalochordates, the endostyle forms a groove along the ventral edge of the pharynx and contains distinct functional "zones" of specialized cells. The general organization of functional zones in the endostyles of ascidians and cephalochordates is essentially the same, although the overall number of zones may vary (Fig. 4.24C,

[10] Curiously, the Stazione Zoologica has an old tradition of TH research. It was the same place where in 1910 J.F. Gudernatsch made the initial observations that the thyroid gland acted on the induction of metamorphosis, but as he did not trust his original results because the organs he used were not fresh, he published his findings a couple of years later from research done in Prague (Gudernatsch 1912; Brown and Cai 2007).

D): the zones in the bilateral dorsal-most crest-like region of the endostyle closer to the pharynx concentrate iodine and contain peroxidase activity essential for thyroid-like activity, whereas the ventral-most inner groove region contains alternating zones that serve either as support elements or secrete mucoproteins that coat the pharynx to facilitate capture of food particles (Bone et al. 2003; Hiruta et al. 2005; Sasaki et al. 2003). Physiological similarities that support homology of the endostyle and the thyroid gland are backed by conserved gene expression patterns in the developing endostyle. Orthologs of the vertebrate thyroid markers TPO, TTF-1, Pax2/5/8, FoxE4, FoxQ1, and FoxA have been shown to be expressed in the endostyles of both ascidians and cephalochordates (Fig. 4.24D; for details, see Hiruta et al. 2005).

The adult solitary ascidian endostyle of *Ciona intestinalis* derives from an endostyle primordium formed by anterior and ventral endodermal cells in the head of the larva. Within a day of metamorphosis, this primordium elongates and differentiates (Jacobs et al. 2008). The rapid and anticipatory differentiation of the endostyle observed in *C. intestinalis* and other phlebobranchs that show a relatively delayed onset of metamorphosis suggests that TH production may be crucial for the completion of metamorphic differentiation. However, in stolidobranchs (e.g., *Herdmania momus*), the endostyle differentiates only at the end of metamorphosis along with all other juvenile structures, arguing against an important role for the endostyle in metamorphosis.

This apparent incongruence might be disentangled if other cell types, before endostyle differentiation, produced THs. Seemingly resolving this issue, D'Agati and Cammarata (2006) reported that THs are produced by mesenchyme cells of mesodermal origin, completely unrelated to the endostyle. These cells were found scattered throughout the head, particularly behind the papillae and at the basal and posterior region of the head of several phlebobranch ascidian species.

Although further characterization of the specific roles and targets of THs is necessary, a comparative study of TH larvae of different species may reveal whether endocrine mechanisms are employed to modulate heterochronic development in ascidians (i.e., adultation). In summary, ascidian metamorphosis relies on information-carrying systems such as the nervous system, the endocrine system, and particularly the immune system, in order to coordinate a response to environmental cues, which involves an intricate and highly regulated redeployment of developmental processes to drastically reconfigure the individual's body.

Asexual Reproduction: Modes of Budding (Blastogenesis)

The considerable variation observed in the developmental modes of budding in the tunicates (ascidians and thaliaceans) is indicative of the independent evolution of asexual reproduction and coloniality. Several evolutionary transitions to colonialism have been identified in the tunicates, which are accompanied by several morphological, developmental, and reproductive changes, such as miniaturization of individual body size, primarily asexual reproduction by budding and brooding (Davidson et al. 2004). Fully developed larvae are released from the colony to rapidly metamorphose and begin the asexual cycle of development, otherwise known as budding or blastogenesis. In all modes of budding, the epidermis of new individuals derives from preexisting epidermal progenitors, suggesting that mechanisms of epidermal cell replenishment may act locally at the sites of budding and may not differ all that much between solitary and colonial species. In contrast, the endodermal (pharynx, gut, etc.) and mesodermal (muscle, heart, etc.) derivatives originate from distinct precursor tissues in different species. In an attempt to identify homologous developmental mechanisms of budding, a comparison of bud precursor tissues and cells involved in this process will be reviewed next for several species of ascidians.

Budding in Ascidians

In colonial stolidobranchs (specifically in *Polyandrocarpa misakiensis*, *Botryllus schlosseri*, and *Symplegma reptans*), the endoderm-derived

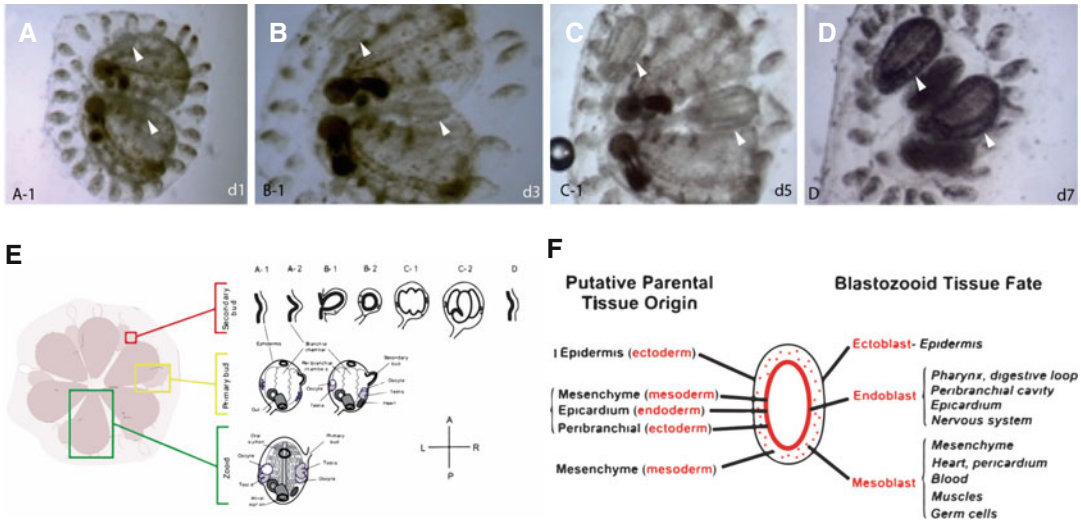

Fig. 4.26 Blastogenic stages in the botryllid ascidians. (**A**–**D**) Developmental events of budding in *Botrylloides violaceus*, stage is shown below to the *left*, and the time in days is below to the *right*. (**E**) Representation of botryllid development. *Arrowheads* point to primary buds. (**F**) Representation of the origin and contribution of the double vesicle stage that is recapitulated during embryogenesis and blastogenesis of botryllids (Adapted from Brown et al. (2007, 2009) and Tiozzo et al. (2008))

outer epithelium surrounding the branchial sac (known as the peribranchial epithelium) contributes to the formation of mesendodermal tissues of the peribranchial buds. Circulatory mesenchymal cells or hemoblasts also contribute to these buds. Evaginations of the lateral peribranchial epithelium and epidermis form an early bud that resembles a double vesicle (Fig. 4.26). The inner vesicle derived from the peribranchial epithelium undergoes a series of folds that will generate most organ primordia. In between the double vesicle, mesenchymal progenitors or hemoblasts are thought to contribute to the differentiation of several tissues and organs, including the pharynx, muscles, and mantle (Sabbadin et al. 1975). One well-documented example includes the participation of hemoblasts in the differentiation of muscle cells near the oral siphon primordium, presumably induced by the oral epidermis (Sugino et al. 2007).

An extensive amount of research demonstrating somatic stem cell exchange in chimeric colonies of *Botryllus schlosseri* suggests that circulatory mesenchymal progenitors are responsible for the differentiation of zooids with distinct genotypes in the same colony (Pancer et al. 1995; Stoner and Weissman 1996). Serial transplantations of circulatory stem cells between different colonies showed that at least two distinct populations of progenitors occur in the circulatory cells of the colony, including germ line and at least one somatic stem cell lines. It was also shown that a minimum of 5.000 transplanted circulatory mesenchyme cells was sufficient to establish a new genotype in the chimera. From this we can estimate the occurrence of one stem cell for every 5.000 mesenchymal cells in the blood[11] (Laird et al. 2005). In certain species of stolidobranchs such as *Botryllus* and *Botrylloides* spp., the double vesicle stage is also observed in vascular buds. In these buds, the outer vesicle is formed from the evagination of the ectodermal vasculature (Fig. 4.26), which connects the zooids of the colony, whereas the inner vesicle is formed from the accumulation and differentiation of circulatory mesenchymal cells within the outer vesicle instead originating from an epithelium (Brown

[11] A stem cell ratio of 1:5.000 in the blood is a relatively high number of circulatory stem cells; for comparison, in humans 1:5.000–10.000 bone marrow cells are stem cells and 1:100.000 nucleated blood cells are stem cells.

et al. 2009). Three possible mechanisms have been suggested for the origin of circulatory mesenchymal progenitors in the stolidobranchs: (1) dedifferentiation of the atrial epithelium and transdifferentiation of these cells into new epithelia, e.g., intestinal epithelial cells (Kawamura and Fujiwara 1995; Kawamura et al. 2008), (2) self-renewal of pluri- or multipotent cells in the circulatory system that may differentiate into distinct cell fates (Freeman 1964; Laird and Weissman 2004; Laird et al. 2005; Kürn et al. 2011; Brown and Swalla 2012), and (3) self-renewal of pluri- or multipotent cells in stem cell niches that circulate and differentiate into distinct cell fates (Voskoboynik et al. 2008; Rinkevich et al. 2013; Jeffery 2014).

In aplousobranchs that are exclusively colonial, bud development is strictly associated with the presence of the epicardium, an endoderm-derived epithelium that extends from the base of the pharynx to the pericardium, covering the entire abdominal or postabdominal regions of the zooid. Thus, colony propagation by budding is generally activated after settlement of the larva and specifically when the oozooid has differentiated. However, the most precocious case of budding in colonial ascidians has been documented in the Holozoidae (i.e., *Distaplia* and *Hypsistozoa*), in which zooids can already differentiate in the larval head of the swimming larva (see below) and also generate larval buds or probuds that can self-replicate or differentiate into new zooids. Other mechanisms of bud formation documented in the aplousobranchs include strobilation (specifically in *Aplidium* spp., *Eudistoma* spp., and *Pycnoclavella* spp.), stolonial budding (specifically in *Clavelina lepadiformis*), and pyloric budding (specifically in *Diplosoma listerianum* and *Didemnum* spp.).

Strobilation occurs by the constriction of abdominal or postabdominal segments (Nakauchi 1982, 1986; reviewed in Brown and Swalla 2012). Each segment generates an independently developing bud that detaches from the parental zooid and begins to differentiate in neighboring areas of the tunic. As each segment develops from distinct regions along the length of the abdomen or postabdomen, bud primordia may vary according to the amount of initial tissue and cell types they inherit. In stolonial budding of *Clavelina lepadiformis* (Brien and Brien-Gavage 1927), budding stolons sprout radially from the base of the zooid, specifically from the post-thoracic region containing the epicardium. Each of the stolons undergoes an enlargement of the tip, which later detach from the parental zooid to form independently developing stolonial buds (Berrill 1951). In contrast, pyloric buds form between the thoracic and abdominal regions of the zooid where the esophagus, stomach, and pyloric gland are located. This corresponds to the site where the epicardium of the zooid prevails (reviewed in Brown and Swalla 2012; Nakauchi 1982). The thoracic region of the parental zooid develops a new abdomen, whereas the parental abdomen develops a new thoracic region. Therefore, this budding mode forms two daughter zooids from one single parental zooid.

In colonial phlebobranchs (specifically *Perophora viridis* and *P. japonica*), buds form at regular intervals along tubular structures also known as stolons, which connect the zooids of the colony. The stolons consist of epidermal diverticula that project from the base of each zooid and spread through the substrate, thus expanding the reach of the colony. Both the stolons of *Perophora* and the colonial vasculature of *Botryllus* are ectodermally derived but differ greatly in form and function. In *Perophora*, stolons are covered by a thin tunic and grow external tubular networks in direct contact with the substrata, whereas the vasculature of *Botryllus* generates a network of canals within a common and more solid tunic of the colony. Within the lumen of a stolon, there is a single-layered epithelium derived from mesenchyme or from the septum that partitions the stolon, allowing for blood flow in opposite directions (Freeman 1964; Mukai et al. 1983).

Since the earliest observations of budding in *Perophora*, Kowalevsky (1874) already noted the contribution of the septum for the formation of stolonial buds; he wrote: "… die innere Haut der Knospe durch eine Verdickung der Scheidewand der Wurzeln …", i.e., "… the inner layer of the bud is formed from a thickening of the stolonial

septum ….” In fact, cuboidal cells in the budding zone of the septum acquire a columnar shape and form a small vesicle on the upper part of the septum at a close distance (approx. 100–200 μm) to the tips of the stolons; these are the earliest recognizable structures of a stolonial bud (Deviney 1934; Kawamura et al. 2008).

As the vesicle grows, several circulatory mesenchymal cells are incorporated, the epidermis of the stolon protrudes, and organ primordia continue to differentiate (Deviney 1934). Among the circulatory mesenchymal cells that were observed to integrate in the developing bud, a lymphocyte-like undifferentiated cell type – similar in cytological characteristics to the hemoblasts in botryllids – was also seen. Some cellular characteristics of these undifferentiated lymphocyte-like cells have also been observed in the budding zone cells of the septum, including a large nucleolus and a mitochondria-rich cytoplasm, demonstrating the possible mesenchymal origin of bud progenitor cells (Kawamura et al. 2008). Furthermore, the stem cell potential of these cells alone was demonstrated by the rescue of irradiated colonies after transplantation of isolated lymphocytes (Freeman 1964). Therefore, this experiment unequivocally demonstrates that circulatory lymphocytes in phlebobranchs are necessary and sufficient for budding. Attempts to rescue irradiated botryllids after hemoblast transplants have not been successfully achieved (Laird and Weissman 2004), which may be suggestive of distinct stem cell potentiality in these two populations of undifferentiated circulatory mesenchymal cells. The homology between these two stem cell types remains to be tested.

Another mode of budding known as “terminal budding” has been reported in *Perophora japonica* and includes the participation of the septum and the incorporation of many circulatory mesenchymal cells at the tip of the stolon to form a terminal stellate bud that serves as a propagule (Mukai et al. 1983). The stellate buds develop three to six epidermal projections, detach from the stolon, and drift away by currents. These pelagic buds will eventually settle again; the stellate projections of the pelagic bud turn into stolonial primordia that grow and begin to form new zooids by stolonial budding. Therefore, a limited input of circulatory mesenchymal cells into the bud occurs at a very early stage before detachment cuts off this mesenchymal cell source, in contrast to constant contribution of mesenchymal cells to the stolonial buds.

Budding in Thaliaceans

In colonial, pelagic thaliaceans, stolonial budding is used to rapidly multiply when environmental conditions are optimal for growth. Salps form chains of buds that emerge by terminal constriction of internal stolons in the oozooid, which undergo differentiation into long chains of blastozooids that often remain attached. The stolons specifically form from the pericardium and are organized into epidermis, endoderm derived from tissues of the endostyle, and mesodermal tissues surrounding the heart. As the stolon grows, constriction occurs in several terminal segments forming a series of blastozooids that will develop and mature synchronously. As chains of blastozooids differentiate, older segments of blastozooids in the most distal parts of the chain release sperm and fertilize the eggs of the younger, more proximal blastozooids. However, blastozooids can survive either as chains or as solitary forms when detached from the chains (Brooks 1893).

In contrast, pyrosomes begin to bud by stolonial budding during embryonic development, when the developing embryo (or cyathozooid, see above) gives rise to an initial colony of four blastozooids (the tetrazooids) (Bone 1998). These blastozooids continue to generate stolons, which undergo constriction to form additional blastozooids, thus expanding the colony. There is no solitary phase, as pyrosomes are obligate colonials.

Doliolids have the most complex life cycles of all thaliaceans. Fertilization and embryonic development occur internally in the gonozooid. After the larvae are released, a metamorphic-like event results in the development of the oozooid. The oozooid next forms a posterior-dorsal stolonial primordium that will continue to grow and undergo stolonial budding by terminal constriction. These buds then migrate independently to the posterior ventral edge of the doliolid and align

to form three rows of buds, which will eventually develop into specialized blastozooids. These include trophozooids, specialized for feeding and responsible for nurturing the entire colony, and phorozooids which develop into the free-living hermaphroditic sexual gonozooids. At this stage, the original oozooid ceases feeding, being nurtured by its trophozooids, and becomes specialized for navigating and transporting the colony (Bone 1998; Paffenhöfer and Köster 2011).

Life History Evolution

On the Biphasic Nature of Ascidian Development

Of the major chordate-specific traits, the notochord, dorsal hollow nerve cord, and somites (represented as a single iteration of paraxial mesoderm that gives rise to the larval muscles) are only present at the larval stage. In contrast, other chordate characters such as the endostyle, the pharyngeal gill slits, and the branchiomeric muscles are fully formed only in the juvenile. Thus, the claim that metamorphosis "replaces" the chordate body plan of the larva with an ascidian-specific adult plan is not accurate at a detailed anatomical level. Either stage features a unique subset of chordate-specific anatomical structures. In this way, the chordate body plan in ascidians is biphasic in time, but ever (partially) present through the life of the individual. The continuity of the chordate body plan in tunicates is clearest in larvaceans, for obvious reasons, and in those ascidian species that undergo anural development or adultation (discussed below).

From an ontological point of view, this biphasic nature does not mean the larval and adult phases are discontinuous. On the contrary, there is a clear linear ontological progression of all the major adult structures from primordia that are specified and patterned during the course of embryogenesis and undergo morphogenesis and differentiation even as the larva is swimming. As such, it is more akin to a "swimming embryo" than a true larva.

The contrast between motile, nonfeeding larva and sessile, filter-feeding adult is likely a result of heterochrony relative to the ancestral chordate, with larval structures quickly differentiating and adult structures being slower to differentiate. Even this heterochrony is not absolute. As will be explained below, in perhaps the majority of ascidian species, this boundary between larva and adult is not clearly defined (due to widespread occurrence of adultation) and in some cases does not exist at all (i.e., in direct developing species).

Ultimately, the evolution of the tunicates from a vermiform ancestor must have involved the acquisition of a biphasic developmental mode through heterochrony, with later secondarily derived heterochronies (adultation and direct development). With the exception of the germ cells, the intestine, and the nervous system, this partitioning between adult and larval components correlates with their location in either the head (mostly adult) or tail (mostly larval). The germ cells are set aside prior to gastrulation and are physically contained within the tail during the larval phase. Immediately upon settlement, the germ cells and surrounding endoderm cells migrate into the head during tail retraction, which precedes all other events that occur during metamorphosis. Within the nervous system, the fractured rudiment of the adult CNS can be found interspersed with the fully differentiated components of the larval CNS along the AP axis (Dufour et al. 2006; Horie et al. 2011). This is probably due to historical contingency, the result of descent from an ancestor with a brain-like structure anterior to those compartments controlling homochronic feeding and locomotion functions.

In contrast, the separation of adult feeding/respiration and larval locomotor functions in time mirrors the strict separation of the mesoderm into anterior (head: branchial/pharyngeal muscles, vasculature, heart, blood cells) and posterior (tail: swimming muscles, notochord) compartments. Whether or not this spatial compartmentalization was already partially completed in the last common ancestor of tunicates and vertebrates and whether this could have represented a precondition for additional temporal compartmentalization are two of the more intriguing questions surrounding the origins of tunicates.

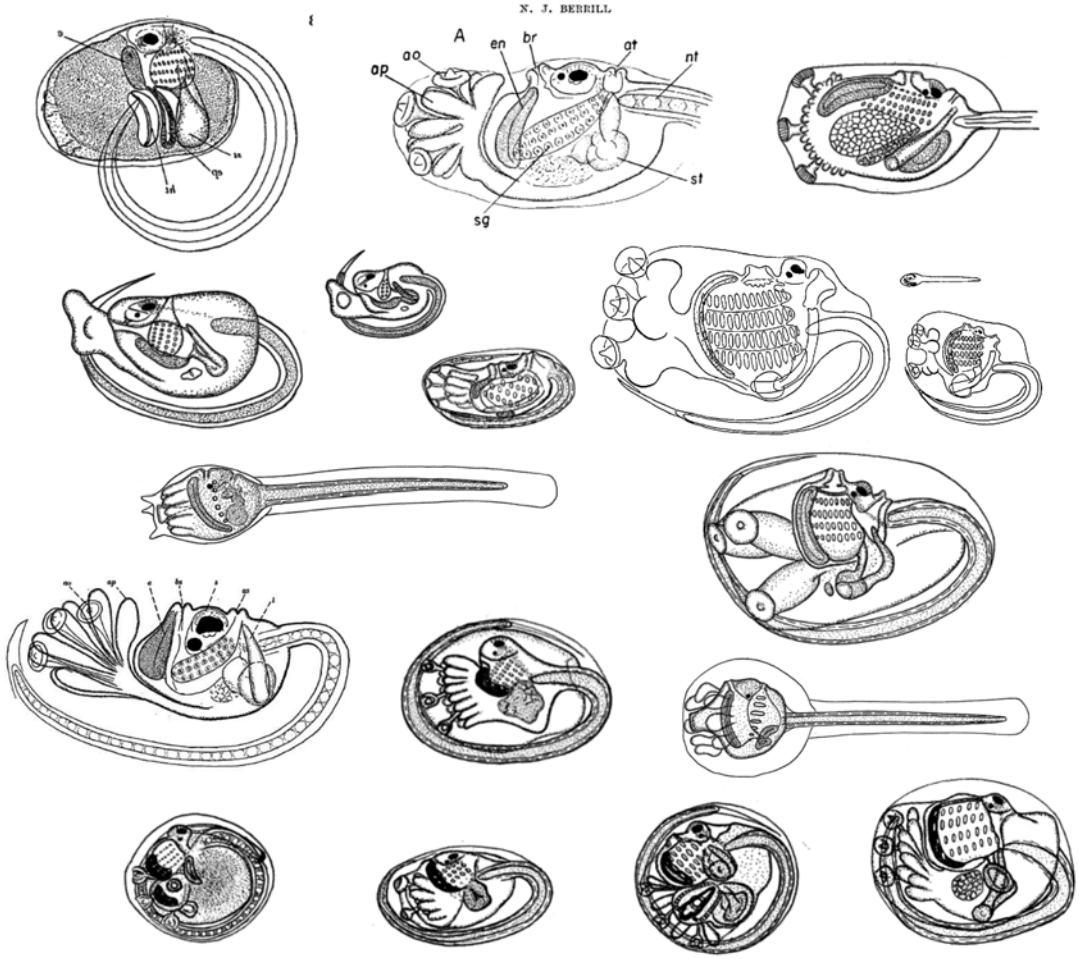

Fig. 4.27 Adultation of ascidian larvae. A composite of several illustrations of works by N. J. Berrill on larvae of several species of ascidians showing varying degrees of adultation or premature differentiation of the juvenile stage while the larva is still swimming (From Berrill, various works)

Fig. 4.28 Evolutionary reconstruction of ascidian adultation, brooding, and budding modes. *Left*: head anatomy of ascidian swimming larvae shows different degrees of adultation (see text for details). With some variation, solitary ascidian larvae show a lower degree of adult differentiation in the head compared to colonial forms (*shaded box*). Exceptional cases include (1) two cases of anural development (direct development) in the stolidobranchs (*squared brackets*); (2) *Molgula citrina* that presents the highest degree of adultation among solitary species (*solid rectangle*), a labeled cross section of the head that has been included to show detail of the internal anatomy (Adapted from Grave 1926); (3) the Diazonidae that present the lowest degree of larval adultation among colonial species (*dashed rectangle*). *Center*: species that brood their embryos irrespective of species-specific differences are marked with the "brood" symbol (*gray* individual with *black* spots representing the embryos); note that *Molgula citrina* and other solitary styelids can brood in the peribranchial cavity. *Right*: schematic representation of the distinct budding modes (*bold* and *capital letters*) is shown; color code represents tissues of endodermal (*yellow*), mesodermal (*red*), and ectodermal origins (*blue*); the epicardium (important tissue for budding, see text for details) of the Enterogona is shown in *orange*; germ layer derivatives shown for every case of budding have only been labeled in *Botrylloides leachi*. *Minus* (−) signs represent absence of that character, and *question marks* (*?*) show cases in which some controversy occurs in the literature regarding the trait (Modified from Millar (1971) and Brown and Swalla (2012))

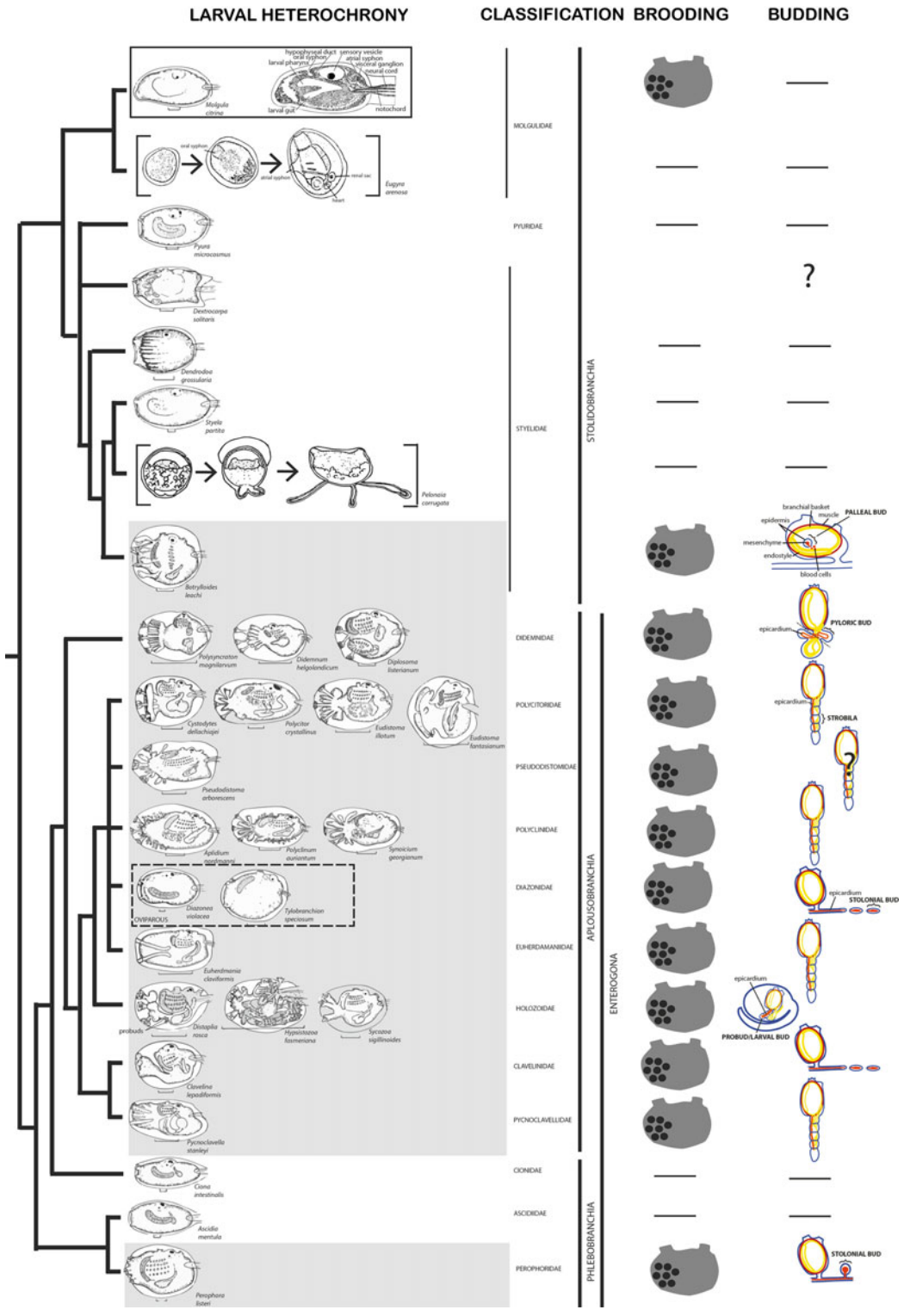
LARVAL HETEROCHRONY
CLASSIFICATION
BROODING
BUDDING
Molgula citrine
Eugyra arenosa
Pyura microcosmus
Dextrocarpa solitaris
Dendrodoa grossularia
Styela partita
Pelonaia corrupata
Botryllioides leachi
Polyzoncratos magnilarvum
Didemnum helgolandicum
Diplosoma listerianum
Cystodytes dellachiajei
Polycitor crystallinus
Eudistoma illotum
Eudistoma fantasianum
Pseudodistoma arborescens
Aplidium variabile
Polyclinum aurantium
Synoicium georgianum
OVIPAROUS
Diazona violacea
Tylobranchion speciosum
Euherdmania claviformis
probuds
Distaplia rosea
Hypsistozoa fasmeriana
Sycozoa sigillinoides
Clavelina lepadiformis
Pycnoclavella stanleyi
Ciona intestinalis
Ascidia mentula
Perophora listeri
MOLGULIDAE
PYURIDAE
STYELIDAE
DIDEMNIDAE
POLYCITORIDAE
PSEUDODISTOMIDAE
POLYCLINIDAE
DIAZONIDAE
EUHERDMANIIDAE
HOLOZOIDAE
CLAVELINIDAE
PYCNOCLAVELLIDAE
CIONIDAE
ASCIDIIDAE
PEROPHORIDAE
STOLIDOBRANCHIA
APLOUSOBRANCHIA
PHLEBOBRANCHIA
ENTEROGONA
?
branchial basket
epidermis
mesenchyme
endostyle
muscle
blood cells
PALLEAL BUD
PYLORIC BUD
epicardium
STROBILA
STOLONIAL BUD
PROBUD/LARVAL BUD
STOLONIAL BUD

Adultation and Heterochrony in Development

The precocious differentiation of adult structures during the embryonic or larval stages is known as adultation (Fig. 4.27). This heterochrony in development, which blurs the line between larva and adult, can be observed in different ascidian species, having likely evolved independently multiple times.

Among ascidians, one sees variation in the extent of adultation (Fig. 4.28), with some species, like *Molgula citrina*, showing limited adultation, while others, like *Ecteinascidia turbinata*, showing extensive growth and differentiation of adult structures, supported by highly elaborated larval structures such as a tail with increased number of muscle cells, required for the larva to swim in spite of its greater mass. This increase in size and complexity of larval structures (muscle, notochord, motor ganglion) is termed "caudalization." In some species of colonial ascidians that undergo adultation, larvae may already be carrying asexually reproducing buds, or blastozooids, and thus constitute a "swimming colony." It is tempting to speculate that this odd configuration of an oozooid larva carrying a blastozooid bud might be an evolutionary forerunner to the acquisition of "catastrophic" metamorphosis. A simple heterochrony could result in the senescence of the larva/oozooid before the initiation of metamorphosis and in the initiation of the adult stage by the blastozooid.[12] This would lead to the discontinuity between embryonic patterning and adult body seen in echinoderms, entoprocts, and other taxa.

In one recent study, three non-adultative phlebobranch ascidian species were found to be prone to slight adultation if metamorphosis was artificially delayed, while there was no such regulative adultation seen in the three stolidobranch ascidians assayed (Jacobs et al. 2008). This suggests that adultation may be dynamically regulated.

[12] This is technically what occurs in pyrosomes, in which the oozooid generates a few blastozooids and immediately senesces. However, because pyrosomes are direct developers and the oozooids and blastozooids share a common body plan, this is not seen as a catastrophic metamorphosis.

Table 4.2 Egg sizes of primitive (non-adultative) and adultative species of ascidians

Primitive (non-adultative) developers	
Species	Size of egg (μm)
Ascidiella aspersa	170
Boltenia echinata	170
Ciona intestinalis	160
Diazona violacea	160
Halocynthia pyriformis	260
Molgula manhattensis	110
Phallusia mammillata	160
Styela canopus	150

Adultative developers	
Species	Size of egg (μm)
Aplidium nordmanni	380
Clavelina lepadiformis	260
Dendrodoa grossularia	480
Distomus variolosus	590
Hypsistozoa fasmeriana	25*
Molgula citrina	200
Stolonica socialis	720

Modified from Berrill (1930). Top: egg size of species that develop into "primitive"-type larvae that do not undergo adultation. This is considered the ancestral condition, due to the nearly identical embryos of distantly related species that develop in this manner (e.g., *Ciona* vs. *Halocynthia*). Bottom: egg sizes and species whose larvae show adultation. Most adultative species develop from larger and more yolk-laden eggs. Asterisk (*) indicates the exception to this, the viviparous *Hypsistozoa fasmeriana*, whose eggs are entirely devoid of yolk and are nurtured by the parental colony through a placenta-like structure (see text, Fig. 4.29, and Brewin (1956) for more details

Such a capacity to "anticipate" metamorphosis could compensate for the negative consequences of delayed metamorphosis, which might happen if the right environmental cues for settlement are not present. While this conclusion was supported by the correlation between length of competency period and tendency toward adultation, the phylogenetic significance of this finding awaits a larger sampling of species.

Adultation goes hand in hand with increased egg size and ovoviviparity, in which eggs, embryos, and hatchlings are brooded inside the parental individual or colony (Table 4.2). This is probably due to an increased threat of predation on the energetically rich, yolky eggs that are required to sustain the development of adultative larvae. There is also a strong association between adultation and coloniality, which has also arisen

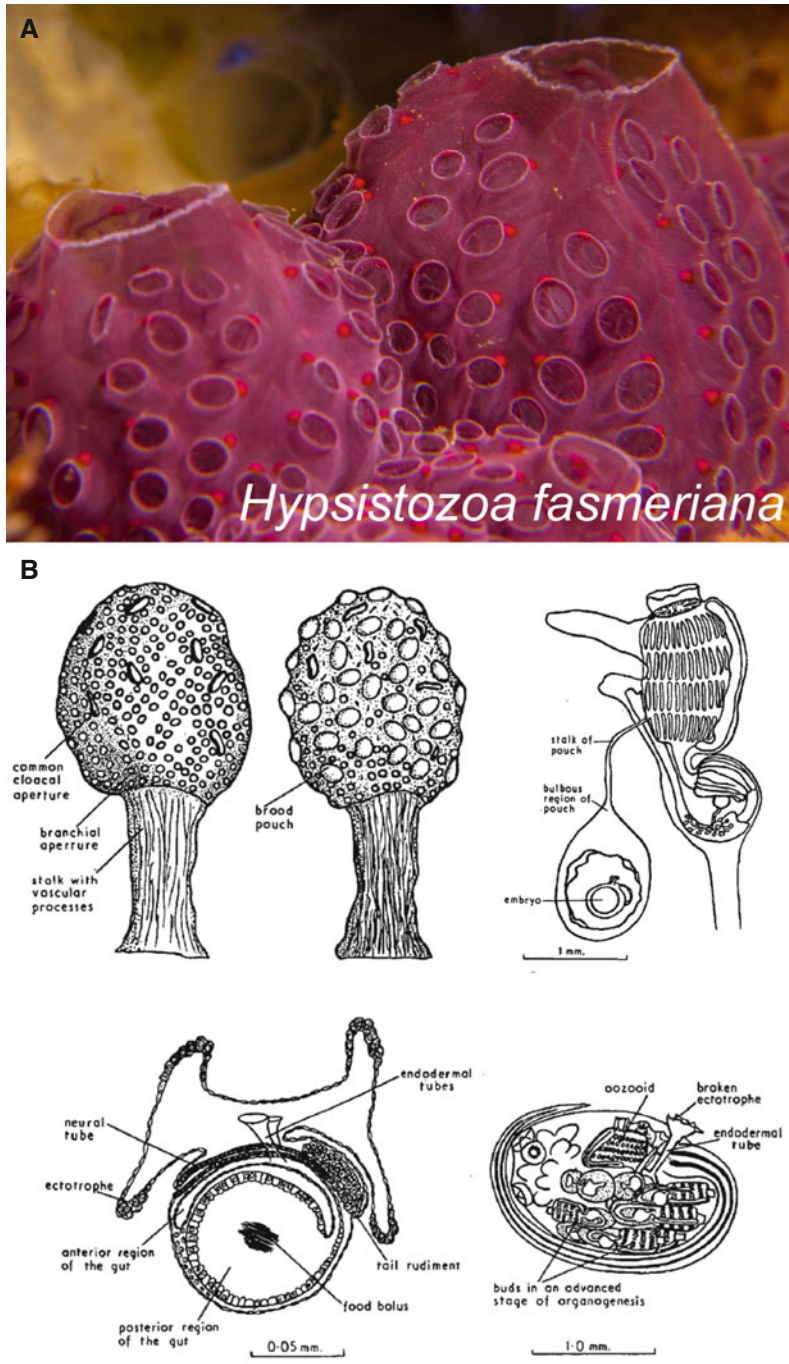

Fig. 4.29 True viviparity in *Hypsistozoa fasmeriana*. (**A**) Colonies of *Hypsistozoa fasmeriana* (Photograph by Paul Caiger) (© Paul Caiger, 2015. All Rights Reserved). (**B**) Illustrations of *H. fasmeriana* colonial and embryonic development. *Top left*: young colony. *Top middle*: senescing colony, preparing for shedding of larvae. *Top right*: anatomy of *H. fasmeriana* zooid showing embryo being brooded in attached brood pouch. *Bottom left*: structure of *H. fasmeriana* embryo and associated ectotroph, an extra-embryonic tissue. Endodermal tubes connect the brood pouch with the lumen of the gut of the embryo, presumably to transfer food and nutrients from the parent to the embryo. *Bottom right*: large larva with numerous buds in an advanced stage of differentiation (a swimming colony) (Illustrations in (**B**) are reproduced with permission from Brewin (1956): http://jcs.biologists.org/content/s3-97/39/435.short)

independently in different ascidian families (Fig. 4.28). There are, however, some notable exceptions, such as the adultative solitary *Molgula citrina* or non-adultative colonial *Diazona* spp. Possible explanations for the association between coloniality and adultation are discussed below.

Some adultative species appear to have evolved true viviparity, with secondary reduction in egg size since nutrients now can be passed from parent to daughter during development. This appears to be the case between the closely related *Botryllus* and *Botrylloides* genera (Berrill 1935). A more extreme example of viviparity is found in *Hypsistozoa fasmeriana*, which has extremely small eggs (approx. 25 μm diameter), whose growth into large "swimming colonies" or compound larvae, each comprising an oozooid plus several blastozooids in various stages of development, depends on transfer of food through a connection between the colony's brood pouch and the embryo's gut (Fig. 4.29; Brewin 1956).

Maximum Direct Development

There are some very rare examples in which direct development and adultation have been combined in a process of "direct adultation," also called "maximum direct development," in which early embryonic development may truly bypass the formation of a larva (urodele or anural) prior to differentiation of adult structures. The maximum direct developers potentially include *Polycarpa tinctor* (Millar 1962), *Pelonaia corrugata* (Fig. 4.28; Millar 1954), and *Molgula pacifica* (Young et al. 1988; Bates 2002), although in all these cases a detailed stage-by-stage description of development is lacking and we are left without any certainty about how development in these species occurs. It is hypothesized that the various species with anural development find themselves at different stages of an evolutionary transition toward maximum direct development.

Embryogenesis vs. Blastogenesis

Only after metamorphosis do ascidians begin to feed and grow. In solitary species, the settled juvenile grows and matures as a single individual. In colonial species, the settled juvenile is called the oozooid (Fig. 4.25), i.e., the founding individual of a colony derived from sexual reproduction. The oozooid then activates asexual budding cycles (i.e., blastogenesis) to generate blastozooids, individuals derived from asexual generations or blastogenesis (Fig. 4.26). Although oozooids and blastozooids show certain anatomical differences, such as different arrangement of the pharyngeal slits of the branchial sac, the general organization and body plan are maintained. Also, expression patterns of many developmental genes that are expressed in embryogenesis are redeployed during the development of the bud. For example, *Botryllus schlosseri* orthologs of *Six*, *Eya*, and *FoxI* (transcription factors associated with the vertebrate placode network) expressed in anterior and posterior placodal regions in the metamorphosing larva are also expressed in corresponding anterior and posterior regions of the developing bud (Tiozzo et al. 2005; Gasparini et al 2013). The anterior placode region will eventually differentiate into cells of the oral siphon, ciliated duct, and cerebral ganglion, whereas the posterior placode region will differentiate into cells of the atrial siphon of both oozooid and blastozooid, similar to their development in solitary ascidians (Mazet et al. 2005) and larvaceans (Bassham and Postlethwait 2005).

Contrary to the reported effects of thyroid hormone inhibitors on *Ciona intestinalis* juveniles during metamorphosis, the thyroid hormone inhibitor thiourea was found to accelerate bud development and inhibit stolon growth in the colonial phlebobranch *Perophora orientalis*. Conversely, the thyroid derivative thyroxine inhibited bud development but induced stolon growth (Fukumoto 1971). These results provide an exciting opportunity to compare modular effects of endocrine signaling during zooid differentiation between metamorphosis and blastogenesis. However, the expression patterns of the main thyroid pathway genes remain to be elucidated in ascidians.

Future work is needed to compare developmental mechanisms of the earliest stages of embryogenesis vs. blastogenesis, in order to identify similarities and differences in patterning events between bud progenitors and early blastomeres. In sum, the existence of dual developmental

trajectories (sexual vs. asexual) to generate the same body form in a single species provides an excellent opportunity to address questions about developmental pathway co-option in evolution.

Evolution of Coloniality

Within the deuterostomes, the hemichordate pterobranchs (Chapter 2) and many species of tunicates have a colonial stage in their life cycle. Colonies are defined as aggregates of individuals that are "connected together, either by living extensions of their bodies, or by material that they have secreted" (Barrington 1967). In the tunicate literature, colonies with living extensions that interconnect the individuals have been referred to as "social forms," whereas colonies that secrete material to embed the individuals have been referred to as compound forms (Milne-Edwards 1841; Pérez-Portela et al. 2009). In deuterostomes, the colonial life stage is generally initiated after metamorphosis. Asexual reproduction of the colony occurs by clonally generating new individuals from preexisting juvenile or adult tissues. Curiously, individuals of most species that form colonies are (1) smaller in size than their closely related solitary species clades, (2) able to brood and release larvae with a high degree of adultation (see above), and (3) imbued with highly regenerative and propagative potentials (Davidson et al. 2004; Brown and Swalla 2012).

The current phylogeny of Deuterostomia supports the idea that coloniality in this group has evolved independently multiple times but that the ability to regenerate was likely present in the ancestral deuterostome. In the clade comprised by the questionable Xenacoelomorpha + Ambulacraria (Fig. 4.1), coloniality only occurs in the pterobranchs, but regenerative potential has also been documented for the harrimaniids, ptychoderids, echinoderms, and xenacoelomorphs (see Chapters 1 and 2; Vol. 1, Chapter 9). Among the Chordata, ascidians are the only subphylum that show convergent evolution of coloniality in several species that also have full regenerative potential (i.e., whole body regeneration). Regenerative potential, albeit much more modest (i.e., tissue, organ, and structure regeneration), has also been reported in solitary ascidians, cephalochordates (Somorjai et al. 2012), some Craniata/Vertebrata, and, most remarkably, platyhelminths (see Vol. 2, Chapter 4 for a detailed account on regeneration in the latter). Therefore, we can speculate that developmental mechanisms of asexual reproduction and regeneration preceded the establishment of colonial lifestyles.

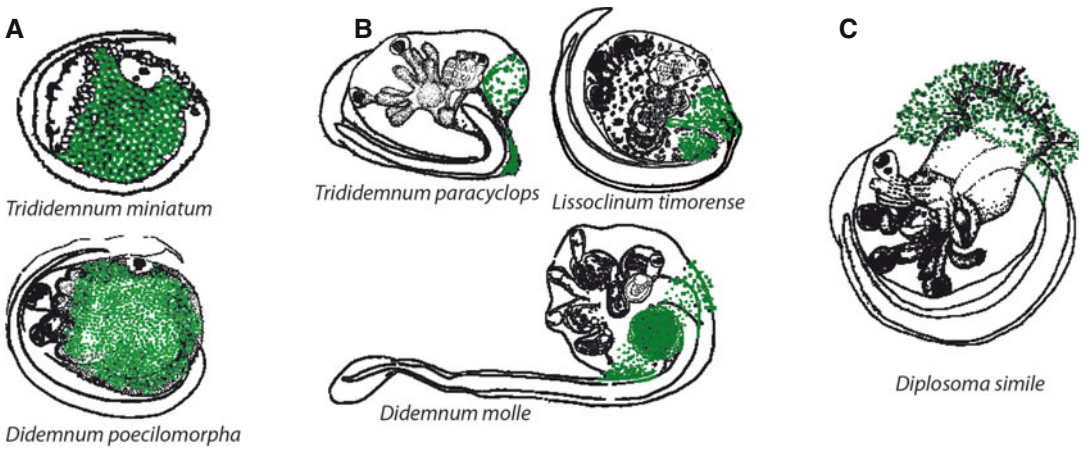

Fig. 4.30 Vertical transmission mechanisms of photosymbionts in didemnid ascidian larvae. (**A**) Prochloron cyanobacteria (*green*) embedded within the larval tunic. (**B**) Prochloron attached to hairlike projections and tunic folds in the posterior region of the larval head that does not contain larval tunic. (**C**) Prochloron attached and inserted into the rastrum, a T-shaped extension of larval ectoderm in the posterior-dorsal region of the larval head (Modified from Kott (2001))

Conceptual arguments on life history tradeoffs between individual forms and cooperative entities such as colonies are starting to emerge (see recent published books edited by Calcott and Sterelny 2011; {Inserting} Bouchard and Huneman 2013). However, we are far from understanding how selective forces act to co-opt developmental modules in the evolution of such higher-level organized forms. To begin to address this question, it is necessary to first identify the developmental processes associated with coloniality.

Photosymbiosis in Colonial Didemnid Ascidians

Last, but not least, symbiosis occurs between an oxygenic photosynthetic cyanobacteria and several tropical colonial ascidian species of the Didemnidae. The symbiont *Prochloron* spp. (Kühl et al. 2012) is found associated, almost exclusively, with four different genera of didemnids: *Diplosoma*, *Lissoclinum*, *Didemnum*, and *Tridemnum* (Yokobori et al. 2006). *Prochloron* is usually present in the outer surface of the tunic, within the common cloacal system of the colony, or embedded in the tunic as either free-living cells or intracellularly in tunic cells. *Prochloron* is transmitted vertically from the mother colony to the daughter colonies by three distinct mechanisms: (1) by direct attachment into a sticky posterior region of the larval head before the larvae are released, (2) by encapsulating into a specialized pouch-like organ in the posterior head of the larvae, or (3) by the transmission of *Prochloron-containing* tunic cells with intracellular *Prochloron* from the mother colony to the developing larval tunics while brooding (Fig. 4.30; Kott 2001; Yokobori et al. 2006; Hirose and Hirose 2007).

The evolution of vertical transmission mechanisms of the host species suggests an obligate symbiotic interaction in which the didemnid ascidians provide shelter for the symbiont and the prochloron provides protection. Two protection mechanisms have been suggested: (1) UV screening mechanisms by producing mycosporine-like amino acids (MAAs) (Kühl et al. 2012) and (2) cyanobactins (toxins) to protect the ascidians from predators or parasites (Donia et al. 2011). In sum, didemnid ascidians provide an opportunity to study the effects of symbiosis in development and the recurrence and particular adaptations of this biological interaction across several species.

OPEN QUESTIONS

Tunicate/Chordate Origins

- What was the tunicate ancestor like?
- How did it evolve from the olfactorean ancestor?
- Which (if existing) are the autapomorphies of Olfactores (Tunicata + Vertebrata)?

Tail Loss in the Molgulids

- How much do the multiple, independent cases of evolutionary loss of the larval tail structures in the Molgulidae have in common at the molecular or cellular levels?
- Is there a common point of evolutionary convergence for the different anural species?
- Did those species exhibiting direct development evolve from indirectly developing tailless species?

Adultation of Colonial Ascidian Larvae

- How are the much bigger larvae of certain colonial ascidians formed?
- How have they evolved presumably from a simple larva of the solitary kind?
- Do the mechanisms involved in patterning and growth of these larger embryos resemble in any way perhaps those lost in the, presumably, drastically reduced ascidian ancestor?

Evolution of Larvaceans

- Did Appendicularia evolve from an ascidian-like stock or did they evolve directly from free-swimming, pelagic ancestors?
- If they evolved from a sessile ascidian ancestor, what were the embryological and gene

regulatory hurdles that needed to be overcome in order for larvaceans to break free from the constraints of the typical solitary ascidian embryo archetype?
- What are the mechanisms that regulate larvacean metamorphosis, and how conserved are these with the rest of the tunicates?

Evolution and Development of Thaliaceans
- What are the relationships among the thaliacean orders (pyrosomes, salps, and doliolids?
- How did complex life cycles evolve in this class?
- How far do metamorphic events in the thaliaceans resemble those of other tunicates?
- What are the underlying molecular and genetic mechanisms of thaliacean development?

Regeneration and Coloniality
- How closely do the mechanisms of blastozooid patterning resemble those that pattern the embryo/oozooid?
- How is the formation and regression of zooids modulated in colonial species?
- What are the signaling mechanisms that orchestrate the synchronized differentiation of blastozooids in certain species?
- When do bud progenitors first reorganize themselves into a new individual with a body plan that corresponds to an embryonic stage, and which stage would that be?
- Is there an analogous "phylotypic" stage for blastogenesis?
- How closely do the mechanisms of blastozooid patterning resemble those that pattern the embryo/oozooid?
- Given that of embryonic patterning are set up by localized maternal determinants that presumably would be very difficult to redeploy in a blastogenic bud, at what point(s) in the gene regulatory network(s) do the embryonic and blastozooid programs converge?
- Was the last common ancestor of all tunicates imbued with the remarkable regenerative potential of colonial tunicates and subsequently lost from the less regenerative solitary ascidians?

Gene Expression and Function
- Why has the Hox complex fragmented or its regulation become less cohesive in tunicates?
- Has the presumed loss of segmentation in tunicate body plans relaxed the constraints on Hox cluster integrity?
- Do the Hox genes play a more peripheral role in gene regulatory networks governing embryonic development in the tunicates, relative to their role in other phyla?
- What were the genes potentially co-opted by the neural plate border cells in the craniate ancestor that might have modified these into *bona fide* neural crest cells?
- How are metamorphic processes of apoptosis, proliferation, migration, and differentiation regulated in the tunicates, and to what extent are these regulatory mechanisms redeployed in ascidians, larvaceans, and thaliaceans?

Developmental System Drift
- How pervasive is developmental system drift among the tunicates, especially those with very conservative, simplified embryos like most solitary ascidians?
- Are the genomes of tunicates rapidly evolving in order to adapt to the various other environmental and ecological concerns faced by them, such as feeding, temperature, salinity, predation, reproduction, etc.?
- If so, do species-specific *cis*/*trans* compensatory mechanisms evolve in order to maintain the same exact embryo?
- Is this invariant embryo required due to the lack of regulative developmental processes that might allow for the ontogenesis of a viable sea squirt via a very different embryo?
- Is embryonic development more variable among the colonial species (not related to the separate issue of adultation) because these have evolved/retained greater developmental plasticity, as evidenced by their blastogenic mode of reproduction?

Prochloron Photosymbiosis

- Why is prochloron present only in some species of didemnids?
- How did host-symbiont interaction become obligatory?
- How does obligate symbiosis trigger the evolution of specific mechanisms and organs for vertical transmission in the host?
- Does intracellular prochloron within tunic cells represent a causative event of an older symbiotic interaction of particular lineages?
- Did prochloron diversify after symbiosis with the host?

Acknowledgments Many thanks to Andreas Wanninger and Ivan Dias for comments on the manuscript and to Florian Razy-Krajka for thoughtful discussions. Thanks to Leda Restrepo, Gabriela Agurto, Joanna Greer, and Paul Caiger for contributing with some figures. We would also like to thank all the authors who have granted us permission to modify and adapt figures from their excellent papers. This work was supported by an "Apoio aos Novos Docentes" Grant from Universidade de São Paulo, an Assistant Professor Grant from Universidad de los Andes and a Prometeo Research Award from the Secretaría Nacional de Ciencia, Tecnología e Innovación (Senescyt-Ecuador) to F. D. B., and by a National Science Foundation Postdoctoral Research Fellowship (under grant NSF-1161835) to A. S.

References

Abbott CL, Ebert D, Tabata A, Therriault TW (2011) Twelve microsatellite markers in the invasive tunicate, *Didemnum vexillum*, isolated from low genome coverage 454 pyrosequencing reads. Conserv Genet Resour 3:79–81

Abitua PB, Wagner E, Navarrete IA, Levine M (2012) Identification of a rudimentary neural crest in a non-vertebrate chordate. Nature 492:104–107

Alldredge AL (1977) House morphology and mechanisms of feeding in the Oikopleuridae (Tunicata, Appendicularia). J Zool 181:175–188

Alldredge A, Madin L (1982) Pelagic tunicates: unique herbivores in the marine plankton. Bioscience 32: 655–663

Allen BM (1925) The effects of extirpation of the thyroid and pituitary glands upon the limb development of anurans. J Exp Zool 42:13–30

Amemiya CT, Powers TP, Prohaska SJ, Grimwood J, Schmutz J, Dickson M, Miyake T, Schoenborn MA, Myers RM, Ruddle FH (2010) Complete HOX cluster characterization of the coelacanth provides further evidence for slow evolution of its genome. Proc Natl Acad Sci 107:3622–3627

Barrington EJW (1967) Invertebrate structure and function. Thomas Nelson Sons Ltd., London, p 550, First Edit

Bassham S, Postlethwait JH (2005) The evolutionary history of placodes: a molecular genetic investigation of the larvacean urochordate *Oikopleura dioica*. Development 132:4259–4272

Bates WR (1995) Direct development in the ascidian *Molgula retortiformis* (Verrill, 1871). Biol Bull 188:16–22

Bates WR (2002) The phylogenetic significance of maximum direct development in the ascidian, *Molgula pacifica*. Invertebr Reprod Dev 41:185–192

Bates WR, Mallett JE (1991) Anural development of the ascidian *Molgula pacifica* (Huntsman). Can J Zool 69:618–627

Bateson W (1884) Memoirs: the early stages in the development of *Balanoglossus* (sp. incert.). Q J Microsc Sci 2:208–236

Bateson W (1886) Continued account of the later stages in the development of *Balanoglossus kowalevskii*, and of the morphology of the enteropneusta. Q J Microsc Sci 26:511–534

Beh J, Shi W, Levine M, Davidson B, Christiaen L (2007) FoxF is essential for FGF-induced migration of heart progenitor cells in the ascidian *Ciona intestinalis*. Development 134:3297–3305

Berrill NJ (1928) The identification and validity of certain species of ascidians. J Mar Biol Assoc U K N Ser 15:159–175

Berrill NJ (1930) Studies in tunicate development. Part I. General physiology of development of simple ascidians. Phil Trans R Soc Lond Ser B 218:37–78, Containing Papers of a Biological Character

Berrill NJ (1931) Studies in tunicate development. Part II. Abbreviation of development in the Molgulidae. Phil Trans R Soc Lond Ser B 219:281–346, Containing Papers of a Biological Character

Berrill NJ (1932) The mosaic development of the ascidian egg. Biol Bull 63:381–386

Berrill NJ (1935a) Studies in tunicate development. Part IV. Asexual reproduction. Philos Trans R Soc Lond B Biol Sci 225:327–379

Berrill NJ (1935b) Studies in tunicate development. Part III. Differential retardation and acceleration. Philos Trans R Soc Lond B Biol Sci 225:255–326

Berrill NJ (1936) Studies in tunicate development. Part V. The evolution and classification of ascidians. Philos Trans R Soc Lond B Biol Sci 226:43–70

Berrill NJ (1947a) The developmental cycle of *Botrylloides*. Q J Microsc Sci 3:393–407

Berrill NJ (1947b) The structure, development and budding of the ascidian, *Eudistoma*. J Morphol 81: 269–281

Berrill NJ (1947c) The structure, tadpole and budding of the ascidian *Pycnoclavella aurilucens* Garstang. J Mar Biol Assoc U K 27:245–251

Berrill NJ (1948a) Budding and the reproductive cycle of *Distaplia*. Q J Microsc Sci 3:253–289

Berrill NJ (1948b) The development, morphology and budding of the ascidian *Diazona*. J Mar Biol Assoc U K 27:389–399

Berrill NJ (1948c) The gonads, larvae, and budding of the polystyelid ascidians *Stolonica* and *Distomus*. J Mar Biol Assoc U K 27:633–650
Berrill NJ (1948d) The nature of the ascidian tadpole, with reference to *Boltenia echinata*. J Morphol 82:269–285
Berrill NJ (1948e) Structure, tadpole and bud formation in the ascidian *Archidistoma*. J Mar Biol Assoc U K 27:380–388
Berrill NJ (1950a) Budding and development in *Salpa*. J Morphol 87:553–606
Berrill NJ (1950b) Budding in *Pyrosoma*. J Morphol 87:537–552
Berrill NJ (1951) Regeneration and budding in tunicates. Biol Rev 26:456–475
Berrill NJ (1955) The origin of vertebrates. Clarendon, Oxford, p 257
Bertrand V, Hudson C, Caillol D, Popovici C, Lemaire P (2003) Neural tissue in ascidian embryos is induced by FGF9/16/20, acting via a combination of maternal GATA and Ets transcription factors. Cell 115:615–627
Bishop CD, Bates WR, Brandhorst BP (2001) Regulation of metamorphosis in ascidians involves NO/cGMP signaling and HSP90. J Exp Zool 289:374–384
Bone Q (1992) On the locomotion of ascidian tadpole larvae. J Mar Biol Assoc U K 72:161–186
Bone Q (1998) The biology of pelagic tunicates. Oxford University Press, Oxford
Bone Q, Carre C, Chang P (2003) Tunicate feeding filters. J Mar Biol Assoc UK 83:907–919
Bouchard F, Huneman P (2013) From groups to individuals: evolution and emerging individuality. MIT Press, Cambridge, MA
Bouquet J, Spriet E, Troedsson C, Otterrå H, Chourrout D, Thompson EM (2009) Culture optimization for the emergent zooplanktonic model organism Oikopleura dioica. J Plankton Res 31:359–370
Brewin BI (1956) The Growth and Development of a Viviparous Compound Ascidian, Hypsistozoa fasmeriana. Q J Microsc Sci 97:435–454
Brien P, Brien-Gavage E (1927) Contribution a l'etude de la blastogenese des Tuniciers. III. Bourgeonnement de *Clavelina lepadiformis* Müller. Rec Inst Zool Torley-Rousseau B31–81
Brooks WK (1893) The genus salpa. The Johns Hopkins Press, Baltimore, p 523
Brown DD, Cai L (2007) Amphibian metamorphosis. Dev Biol 306(1):20–33
Brown FD, Swalla BJ (2007) Vasa expression in a colonial ascidian, *Botrylloides violaceus*. Evol Dev 9:165–177
Brown FD, Swalla BJ (2012) Evolution and development of budding by stem cells: ascidian coloniality as a case study. Dev Biol 369:151–162
Brown CD, Johnson DS, Sidow A (2007) Functional architecture and evolution of transcriptional elements that drive gene coexpression. Science 317: 1557–1560
Brown FD, Prendergast A, Swalla BJ (2008) Man is but a worm: chordate origins. Genesis 46:605–613
Brown FD, Tiozzo S, Roux MM, Ishizuka K, Swalla BJ, De Tomaso AW (2009) Early lineage specification of long-lived germline precursors in the colonial ascidian *Botryllus schlosseri*. Development 136:3485–3494
Calcott B, Sterelny K (eds) (2011) The major transitions in evolution revisited. The MIT Press, Cambridge, MA, 319
Cameron CB, Garey JR, Swalla BJ (2000) Evolution of the chordate body plan: new insights from phylogenetic analyses of deuterostome phyla. Proc Natl Acad Sci U S A 97(9):4469–4474
Carosa E, Fanelli A, Ulisse S, Di Lauro R, Rall JE, Jannini EA (1998) Ciona intestinalis nuclear receptor 1: a member of steroid/thyroid hormone receptor family. Proc Natl Acad Sci U S A 95(19):11152–11157
Castellano I, Ercolesi E, Palumbo A (2014) Nitric oxide affects ERK signaling through down-regulation of MAP kinase phosphatase levels during larval development of the ascidian *Ciona intestinalis*. PLoS One 9:e102907
Cavey MJ (1982) Myogenic events in compound ascidian larvae. Am Zool 22:807–815
Cavey MJ, Cloney RA (1976) Ultrastructure and differentiation of ascidian muscle. Cell Tissue Res 174:289–313
Chabry L (1887). Embryologie normale et teratologique des Ascidie. In: Alcan F (ed). Paris, p 161
Chambon J-P, Soule J, Pomies P, Fort P, Sahuquet A, Alexandre D, Mangeat P-H, Baghdiguian S (2002) Tail regression in *Ciona intestinalis* (Prochordate) involves a Caspase-dependent apoptosis event associated with ERK activation. Development 129:3105–3114
Chambon J-P, Nakayama A, Takamura K, McDougall A, Satoh N (2007) ERK-and JNK-signalling regulate gene networks that stimulate metamorphosis and apoptosis in tail tissues of ascidian tadpoles. Development 134:1203–1219
Chen JS, San Pedro M, Zeller RW (2011) miR-124 function during *Ciona intestinalis* neuronal development includes extensive interaction with the notch signaling pathway. Development 138:4943–4953
Christiaen L, Davidson B, Kawashima T, Powell W, Nolla H, Vranizan K, Levine M (2008) The transcription/migration interface in heart precursors of *Ciona intestinalis*. Science 320:1349
Christiaen L, Stolfi A, Davidson B, Levine M (2009) Spatio-temporal intersection of Lhx3 and Tbx6 defines the cardiac field through synergistic activation of *Mesp*. Dev Biol 328:552–560
Cloney RA (1982) Ascidian larvae and the events of metamorphosis. Am Zool 22:817–826
Cole AG, Meinertzhagen IA (2004) The central nervous system of the ascidian larva: mitotic history of cells forming the neural tube in late embryonic *Ciona intestinalis*. Dev Biol 271:239–262
Collins AG, Valentine JW (2001) Defining phyla: evolutionary pathways to metazoan body plans. Evol Dev 3:432–442
Comes S, Locascio A, Silvestre F, d'Ischia M, Russo GL, Tosti E, Branno M, Palumbo A (2007) Regulatory

roles of nitric oxide during larval development and metamorphosis in *Ciona intestinalis*. Dev Biol 306:772–784
Conklin EG (1905a) Mosaic development in ascidian eggs. J Exp Zool 2:145–223
Conklin EG (1905b) Organ-forming substances in the eggs of ascidians. Biol Bull 8:205
Conklin EG (1905c) The organization and cell-lineage of the ascidian egg. Academy of Natural Sciences of Philadelphia, Philadelphia, p 175
Cooley J, Whitaker S, Sweeney S, Fraser S, Davidson B (2011) Cytoskeletal polarity mediates localized induction of the heart progenitor lineage. Nat Cell Biol 13:952–957
Corbo JC, Levine M, Zeller RW (1997) Characterization of a notochord-specific enhancer from the *Brachyury* promoter region of the ascidian, *Ciona intestinalis*. Development 124:589–602
D'Agati P, Cammarata M (2006) Comparative analysis of thyroxine distribution in ascidian larvae. Cell Tissue Res 323:529–535
Darras S, Nishida H (2001) The BMP/CHORDIN antagonism controls sensory pigment cell specification and differentiation in the ascidian embryo. Dev Biol 236:271–288
David B, Mooi R (2014) How Hox genes can shed light on the place of echinoderms among the deuterostomes. EvoDevo 5:22
Davidson B, Levine M (2003) Evolutionary origins of the vertebrate heart: specification of the cardiac lineage in *Ciona intestinalis*. Proc Natl Acad Sci 100:11469–11473
Davidson B, Swalla BJ (2001) Isolation of genes involved in ascidian metamorphosis: epidermal growth factor signaling and metamorphic competence. Dev Genes Evol 211:190–194
Davidson B, Swalla BJ (2002) A molecular analysis of ascidian metamorphosis reveals activation of an innate immune response. Development 129:4739–4751
Davidson B, Jacobs M, Swalla B (2004) The individual as a module: metazoan evolution and coloniality. In: Schlosser G, Wagner GP (eds.) Modularity in development and evolution. University of Chicago Press, Chicago, pp 443–465
Davidson B, Shi W, Levine M (2005) Uncoupling heart cell specification and migration in the simple chordate *Ciona intestinalis*. Development 132:4811–4818
Davidson B, Shi W, Beh J, Christiaen L, Levine M (2006) FGF signaling delineates the cardiac progenitor field in the simple chordate, *Ciona intestinalis*. Genes Dev 20:2728
Degnan B, Souter D, Degnan SM, Long SC (1997) Induction of metamorphosis with potassium ions requires development of competence and an anterior signalling centre in the ascidian *Herdmania momus*. Dev Genes Evol 206:370–376
Dehal P, Satou Y, Campbell RK, Chapman J, Degnan B, De Tomaso A, Davidson B, Di Gregorio A, Gelpke M, Goodstein DM (2002) The draft genome of *Ciona intestinalis*: insights into chordate and vertebrate origins. Science 298:2157
Delsuc F, Brinkmann H, Chourrout D, Philippe H (2006) Tunicates and not cephalochordates are the closest living relatives of vertebrates. Nature 439:965–968
Delsuc F, Tsagkogeorga G, Lartillot N, Philippe H (2008) Additional molecular support for the new chordate phylogeny. Genesis 46:592–604
Deng W, Nies F, Feuer A, Bočina I, Oliver D, Jiang D (2013) Anion translocation through an Slc26 transporter mediates lumen expansion during tubulogenesis. Proc Natl Acad Sci 110:14972–14977
Denker E, Bočina I, Jiang D (2013) Tubulogenesis in a simple cell cord requires the formation of bi-apical cells through two discrete Par domains. Development 140:2985–2996
Denoeud F, Henriet S, Mungpakdee S, Aury J-M, Da Silva C, Brinkmann H, Mikhaleva J, Olsen LC, Jubin C, Cañestro C (2010) Plasticity of animal genome architecture unmasked by rapid evolution of a pelagic tunicate. Science 330:1381–1385
Deviney EM (1934) The behavior of isolated pieces of ascidian (Perophora viridis) stolon as compared with ordinary budding. J Elisha Mitchell Sci Soc 49(2):185–224
Dohrn A (1886) Thyroidea bei *Petromyzon*, *Amphioxus* und den Tunicaten. Mitt Zool Sta Neapel 6:49–92
Dong B, Horie T, Denker E, Kusakabe T, Tsuda M, Smith WC, Jiang D (2009) Tube formation by complex cellular processes in *Ciona intestinalis* notochord. Dev Biol 330:237–249
Dong B, Deng W, Jiang D (2011) Distinct cytoskeleton populations and extensive crosstalk control *Ciona* notochord tubulogenesis. Development 138: 1631–1641
Donia MS, Fricke WF, Partensky F, Cox J, Elshahawi SI, White JR, Phillippy AM, Schatz MC, Piel J, Haygood MG (2011) Complex microbiome underlying secondary and primary metabolism in the tunicate-Prochloron symbiosis. Proc Natl Acad Sci 108:E1423–E1432
Dufour HD, Chettouh Z, Deyts C, de Rosa R, Goridis C, Joly J-S, Brunet J-F (2006) Precraniate origin of cranial motoneurons. Proc Natl Acad Sci 103:8727–8732
Eri R, Arnold JM, Hinman VF, Green KM, Jones MK, Degnan BM, Lavin MF (1999) Hemps, a novel EGF-like protein, plays a central role in ascidian metamorphosis. Development 126:5809–5818
Ferrier DE, Holland PW (2002) *Ciona intestinalis* ParaHox genes: evolution of Hox/ParaHox cluster integrity, developmental mode, and temporal colinearity. Mol Phylogenet Evol 24:412–417
Field KG, Olsen GJ, Lane DJ, Giovannoni SJ, Ghiselin MT, Raff EC, Pace NR, Raff RA (1988) Molecular phylogeny of the animal kingdom. Science 239:748–753
Fischer JL (1992) The embryological oeuvre of Laurent Chabry. Dev Genes Evol 201:125–127
Fredriksson G, Öfverholm T, Ericson LE (1988) Iodine binding and peroxidase activity in the endostyle of Salpa Fusiformis, Thalia Democratica, Dolioletta Gegenbauri and Doliolum Nationalis (Tunicata, Thaliacea). Cell Tissue Res 253(2):403–411

Freeman G (1964) The role of blood cells in the process of asexual reproduction in the tunicate *Perophora viridis*. J Exp Zool 156:157–183

Fujii S, Nishio T, Nishida H (2008) Cleavage pattern, gastrulation, and neurulation in the appendicularian, *Oikopleura dioica*. Dev Genes Evol 218:69–79

Fukumoto M (1971) Experimental control of budding and stolon elongation in *Perophora orientalis*, a compound ascidian. Develop Growth Differ 13:73–88

Furlow JD, Neff ES (2006) A developmental switch induced by thyroid hormone: xenopus laevis metamorphosis. Trends Endocrinol Metab 17(2):40–47

Garstang W (1894) Preliminary note on a new theory of the phylogeny of the Chordata. Zool Anz 17: 122–125

Garstang W (1928) Memoirs: the morphology of the Tunicata, and its bearings on the phylogeny of the Chordata. Q J Microsc Sci 2:51–187

Gasparini F, Degasperi V, Shimeld SM, Burighel P, Manni L (2013) Evolutionary conservation of the placodal transcriptional network during sexual and asexual development in chordates. Dev Dyn 242:752–766

Gerhart J, Lowe C, Kirschner M (2005) Hemichordates and the origin of chordates. Curr Opin Genet Dev 15:461–467

Godeaux J (1955) Stades larvaires du *Doliolum*. Acad Roy Belg Bull CI Sci 41:769–787

Gomes AS, Alves RN, Rønnestad I, Power DM (2014) Orchestrating change: the thyroid hormones and GI-tract development in flatfish metamorphosis. Gen Comp Endocrinol (in press) doi:10.1016/j.ygcen.2014.06.012

Govindarajan AF, Bucklin A, Madin LP (2010) A molecular phylogeny of the Thaliacea. J Plankton Res 33:843–853

Grave C (1926) Molgula citrina (Alder and Hancock). Activities and structure of the free-swimming larva. J Morphol 42(2):453–471

Grobben K (1908) Die systematische Einteilung des Tierreiches. Verh Zool Bot Ges Wien 58:l–5

Gudernatsch J (1912) Feeding experiments on tadpoles. Arch Entwicklungsmechanik Organismen 35:457–483

Gudo M, Syed T (2008) 100 years of deuterostomia (Grobben 1908): cladogenetic and anagenetic relations within the Notoneuralia domain. arXiv preprint arXiv:08112189

Hadfield KA, Swalla BJ, Jeffery WR (1995) Multiple origins of anural development in ascidians inferred from rDNA sequences. J Mol Evol 40:413–427

Haeckel EH (1866) Generelle Morphologie der Organismen allgemeine Grundzuge der organischen Formen-Wissenschaft, mechanisch begründet durch die von Charles Darwin reformirte Descendenz-Theorie von Ernst Haeckel: allgemeine Entwickelungsgeschichte der Organismen, vol 2, Kritische Grundzuge der mechanischen Wissenschaft von den entstehenden Formen der Organismen, begründet durch die Descendenz-Theorie. Verlag von Georg Reimer, Berlin

Haeckel EH (1869) Ueber Arbeitstheilung in Natur und Menschenleben. Lüderitz, Berlin

Haeckel EH (1874) Anthropogenie oder Entwickelungsgeschichte des Menschen: gemeinverständliche wissenschaftliche Vorträge über die Grundzüge der menschlichen Keimes- und Stammes-Geschichte. Wilhelm Engelmann, Leipzig

Halanych KM (2004) The new view of animal phylogeny. Annu Rev Ecol Evol Syst 35(1):229–256

Haupaix N, Stolfi A, Sirour C, Picco V, Levine M, Christiaen L, Yasuo H (2013) p120RasGAP mediates ephrin/Eph-dependent attenuation of FGF/ERK signals during cell fate specification in ascidian embryos. Development 140:4347–4352

Haupaix N, Abitua PB, Sirour C, Yasuo H, Levine M, Hudson C (2014) Ephrin-mediated restriction of ERK1/2 activity delimits the number of pigment cells in the *Ciona* CNS. Dev Biol 394(1):170–180

Helmkampf M, Bruchhaus I, Hausdorf B (2008) Phylogenomic analyses of lophophorates (brachiopods, phoronids and bryozoans) confirm the Lophotrochozoa concept. Proc R Soc B Biol Sci 275:1927–1933

Heyland A, Hodin J (2004) Heterochronic developmental shift caused by thyroid hormone in larval sand dollars and its implications for phenotypic plasticity and the evolution of nonfeeding development. Evolution 58:524–538

Hirano T, Nishida H (1997) Developmental fates of larval tissues after metamorphosis in ascidian Halocynthia roretzi. I. Origin of mesodermal tissues of the juvenile. Dev Biol 192(2):199–210

Hirano T, Nishida H (2000) Developmental fates of larval tissues after metamorphosis in the ascidian, Halocynthia roretzi. II. Origin of endodermal tissues of the juvenile. Dev Genes Evol 210(2):55–63

Hirose E, Hirose M (2007) Morphological process of vertical transmission of photosymbionts in the colonial ascidian *Tridemnum miniatum* Kott, 1977. Mar Biol 150:359–367

Hiruta J, Mazet F, Yasui K, Zhang P, Ogasawara M (2005) Comparative expression analysis of transcription factor genes in the endostyle of invertebrate chordates. Dev Dyn 233:1031–1037

Holzer G, Laudet V (2013) Thyroid hormones and postembryonic development in amniotes. Curr Top Dev Biol 103:397–425

Horie T, Sakurai D, Ohtsuki H, Terakita A, Shichida Y, Usukura J, Kusakabe T, Tsuda M (2008) Pigmented and nonpigmented ocelli in the brain vesicle of the ascidian larva. J Comp Neurol 509:88–102

Horie T, Nakagawa M, Sasakura Y, Kusakabe TG, Tsuda M (2010) Simple motor system of the ascidian larva: neuronal complex comprising putative cholinergic and GABAergic/glycinergic neurons. Zool Sci 27: 181–190

Horie T, Shinki R, Ogura Y, Kusakabe TG, Satoh N, Sasakura Y (2011) Ependymal cells of chordate larvae are stem-like cells that form the adult nervous system. Nature 469:525–528

Hosp J, Sagane Y, Danks G, Thompson EM (2012) The evolving proteome of a complex extracellular matrix, the *Oikopleura* house. PLoS One 7:e40172

Hotta K, Takahashi H, Erives A, Levine M, Satoh N (1999) Temporal expression patterns of 39 Brachyury-downstream genes associated with notochord formation in the Ciona intestinalis embryo. Dev Growth Differ 41:657–664

Hotta K, Mitsuhara K, Takahashi H, Inaba K, Oka K, Gojobori T, Ikeo K (2007) A web-based interactive developmental table for the ascidian *Ciona intestinalis*, including 3D real-image embryo reconstructions: I. From fertilized egg to hatching larva. Dev Dyn 236:1790–1805

Huber JL, da Silva KB, Bates WR, Swalla BJ (2000) The evolution of anural larvae in molgulid ascidians. Semin Cell Dev Biol 11(6):419–426

Hudson C, Lemaire P (2001) Induction of anterior neural fates in the ascidian *Ciona intestinalis*. Mech Dev 100:189–203

Hudson C, Yasuo H (2006) A signalling relay involving nodal and delta ligands acts during secondary notochord induction in *Ciona* embryos. Development 133:2855–2864

Hudson C, Yasuo H (2008) Similarity and diversity in mechanisms of muscle fate induction between ascidian species. Biol Cell 100:265–277

Hudson C, Lotito S, Yasuo H (2007) Sequential and combinatorial inputs from Nodal, Delta2/Notch and FGF/MEK/ERK signalling pathways establish a grid-like organisation of distinct cell identities in the ascidian neural plate. Development 134:3527–3537

Hudson C, Ba M, Rouvière C, Yasuo H (2011) Divergent mechanisms specify chordate motoneurons: evidence from ascidians. Development 138:1643–1652

Hudson C, Kawai N, Negishi T, Yasuo H (2013) β-catenin-driven binary fate specification segregates germ layers in ascidian embryos. Curr Biol 23:491–495

Huxley TH (1851) Observations upon the anatomy and physiology of *Salpa* and *Pyrosoma*. Philos Trans R Soc Lond 141:567–593

Hyman L (1959) The invertebrates: smaller coelomate groups, Chaetognatha, Hemichordata, Pogonophora, Phoronida, Ectoprocta, Brachiopoda, Sipunculida, the coelomate Bilateria, vol V. McGraw-Hill Book Company, New York

Ikuta T (2011) Evolution of invertebrate deuterostomes and Hox/ParaHox genes. Genomics Proteomics Bioinforma 9:77–96

Ikuta T, Saiga H (2007) Dynamic change in the expression of developmental genes in the ascidian central nervous system: revisit to the tripartite model and the origin of the midbrain–hindbrain boundary region. Dev Biol 312:631–643

Ikuta T, Yoshida N, Satoh N, Saiga H (2004) *Ciona intestinalis* Hox gene cluster: its dispersed structure and residual colinear expression in development. Proc Natl Acad Sci U S A 101:15118–15123

Ikuta T, Satoh N, Saiga H (2010) Limited functions of Hox genes in the larval development of the ascidian *Ciona intestinalis*. Development 137:1505–1513

Imai JH, Meinertzhagen IA (2007a) Neurons of the ascidian larval nervous system in *Ciona intestinalis*: I. Central nervous system. J Comp Neurol 501:316–334

Imai JH, Meinertzhagen IA (2007b) Neurons of the ascidian larval nervous system in *Ciona intestinalis*: II. Peripheral nervous system. J Comp Neurol 501:335–352

Imai K, Takada N, Satoh N, Satou Y (2000) (beta)-catenin mediates the specification of endoderm cells in ascidian embryos. Development 127:3009–3020

Imai KS, Satoh N, Satou Y (2002a) Early embryonic expression of *FGF4/6/9* gene and its role in the induction of mesenchyme and notochord in *Ciona savignyi* embryos. Development 129:1729–1738

Imai KS, Satoh N, Satou Y (2002b) An essential role of a *FoxD* gene in notochord induction in *Ciona* embryos. Development 129:3441–3453

Imai K, Satoh N, Satou Y (2003) A Twist-like bHLH gene is a downstream factor of an endogenous FGF and determines mesenchymal fate in the ascidian embryos. Development 130:4461–4472

Imai KS, Hino K, Yagi K, Satoh N, Satou Y (2004) Gene expression profiles of transcription factors and signaling molecules in the ascidian embryo: towards a comprehensive understanding of gene networks. Development 131:4047–4058

Imai KS, Levine M, Satoh N, Satou Y (2006) Regulatory blueprint for a chordate embryo. Science 312:1183

Imai KS, Stolfi A, Levine M, Satou Y (2009) Gene regulatory networks underlying the compartmentalization of the *Ciona* central nervous system. Development 136:285

Izzi SA, Colantuono BJ, Sullivan K, Khare P, Meedel TH (2013) Functional studies of the *Ciona intestinalis* myogenic regulatory factor reveal conserved features of chordate myogenesis. Dev Biol 376:213–223

Jacobs MW, Degnan BM, Bishop JD, Strathmann RR (2008) Early activation of adult organ differentiation during delay of metamorphosis in solitary ascidians, and consequences for juvenile growth. Invertebr Biol 127:217–236

Jeffery WR (2014) Closing the wounds: one hundred and twenty five years of regenerative biology in the ascidian Ciona intestinalis. Genesis 00:1–18

Jeffery WR, Swalla BJ (1992) Evolution of alternate modes of development in ascidians. Bioessays 14:219–226

Jeffery WR, Swalla BJ, Ewing N, Kusakabe T (1999) Evolution of the ascidian anural larva: evidence from embryos and molecules. Mol Biol Evol 16:646–654

Jeffery WR, Strickler AG, Yamamoto Y (2004) Migratory neural crest-like cells form body pigmentation in a urochordate embryo. Nature 431:696–699

Jeffery WR, Chiba T, Krajka FR, Deyts C, Satoh N, Joly J-S (2008) Trunk lateral cells are neural crest-like cells in the ascidian *Ciona intestinalis*: insights into the ancestry and evolution of the neural crest. Dev Biol 324:152–160

Jiang D, Smith WC (2007) Ascidian notochord morphogenesis. Dev Dyn 236:1748–1757

Jiang D, Munro EM, Smith WC (2005) Ascidian *prickle* regulates both mediolateral and anterior-posterior cell polarity of notochord cells. Curr Biol 15:79–85

Johnson DS, Davidson B, Brown CD, Smith WC, Sidow A (2004) Noncoding regulatory sequences of *Ciona*

exhibit strong correspondence between evolutionary constraint and functional importance. Genome Res 14:2448–2456

Johnson DS, Zhou Q, Yagi K, Satoh N, Wong W, Sidow A (2005) De novo discovery of a tissue-specific gene regulatory module in a chordate. Genome Res 15:1315–1324

Julin C (1912) Recherches sur le développement embryonnaire de *Pyrosoma giganteum*. Zool Jahrb Suppl 15: 775–863

Katikala L, Aihara H, Passamaneck YJ, Gazdoiu S, José-Edwards DS, Kugler JE, Oda-Ishii I, Imai JH, Nibu Y, Di Gregorio A (2013) Functional brachyury binding sites establish a temporal read-out of gene expression in the *Ciona* notochord. PLoS Biol 11:e1001697

Kawamura K, Fujiwara S (1995) Establishment of cell lines from multipotent epithelial sheet in the budding tunicate, *Polyandrocarpa misakiensis*. Cell Struct Funct 20:97–106

Kawamura K, Sugino Y, Sunanaga T, Fujiwara S (2008) Multipotent epithelial cells in the process of regeneration and asexual reproduction in colonial tunicates. Develop Growth Differ 50:1–11

Kim GJ, Nishida H (2001) Role of the FGF and MEK signaling pathway in the ascidian embryo. Develop Growth Differ 43:521–533

Kimura Y, Yoshida M, Morisawa M (2003) Interaction between noradrenaline or adrenaline and the β_1-adrenergic receptor in the nervous system triggers early metamorphosis of larvae in the ascidian, *Ciona savignyi*. Dev Biol 258:129–140

Kluge B, Renault N, Rohr KB (2005) Anatomical and molecular reinvestigation of lamprey endostyle development provides new insight into thyroid gland evolution. Dev Genes Evol 215(1):32–40

Kott P (2001) The Australian Ascidiacea part 4, Aplousobranchia (3), Didemnidae. Mem Queensland Mus 47:1–408

Kourakis MJ, Smith WC (2007) A conserved role for FGF signaling in chordate otic/atrial placode formation. Dev Biol 312:245–257

Kowalevsky A (1874) Ueber die knospung der Ascidien. Arch Mikrosk Anat 10:441–470

Kowalewski AO (1866) Entwicklungsgeschichte der einfachen Ascidien. In: mémoires de L'Académie Impériale des Sciences de St.-Pétersbourg, vol. 10. St. Petersburg: commissionäre der Kaiserlichen Akademie der Wissenschaften

Kozloff EN (1990) Invertebrates. Saunders College Pub, Philadelphia, p 866

Krieg M, Arboleda-Estudillo Y, Puech P-H, Käfer J, Graner F, Müller D, Heisenberg C-P (2008) Tensile forces govern germ-layer organization in zebrafish. Nat Cell Biol 10:429–436

Kugler JE, Kerner P, Bouquet J-M, Jiang D, Di Gregorio A (2011) Evolutionary changes in the notochord genetic toolkit: a comparative analysis of notochord genes in the ascidian *Ciona* and the larvacean *Oikopleura*. BMC Evol Biol 11:21

Kühl M, Behrendt L, Trampe E, Qvortrup K, Schreiber U, Borisov SM, Larkum AWD (2012) Microenvironmental ecology of the chlorophyll b-containing symbiotic Cyanobacterium Prochloron in the didemnid ascidian Lissoclinum patella. Front Microbiol 3:402

Kumano G, Nishida H (2009) Patterning of an ascidian embryo along the anterior–posterior axis through spatial regulation of competence and induction ability by maternally localized PEM. Dev Biol 331:78–88

Kumano G, Yamaguchi S, Nishida H (2006) Overlapping expression of *FoxA* and *Zic* confers responsiveness to FGF signaling to specify notochord in ascidian embryos. Dev Biol 300:770–784

Kumano G, Takatori N, Negishi T, Takada T, Nishida H (2011) A maternal factor unique to ascidians silences the germline via binding to P-TEFb and RNAP II regulation. Curr Biol 21:1308–1313

Kürn U, Rendulic S, Tiozzo S, Lauzon RJ (2011) Asexual propagation and regeneration in colonial ascidians. Biol Bull 221:43–61

Kusakabe T, Swalla BJ, Satoh N, Jeffery WR (1996) Mechanism of an evolutionary change in muscle cell differentiation in ascidians with different modes of development. Dev Biol 174:379–392

Kusakabe T, Yoshida R, Kawakami I, Kusakabe R, Mochizuki Y, Yamada L, Shin-i T, Kohara Y, Satoh N, Tsuda M (2002) Gene expression profiles in tadpole larvae of *Ciona intestinalis*. Dev Biol 242:188–203

Laird DJ, Weissman IL (2004) Telomerase maintained in self-renewing tissues during serial regeneration of the urochordate *Botryllus schlosseri*. Dev Biol 273:185–194

Laird DJ, De Tomaso AW, Weissman IL (2005) Stem cells are units of natural selection in a colonial ascidian. Cell 123:1351–1360

Lamarck JB (1816) Histoire Naturelle Des Animaux Sans Vertèbres. Verdière, Paris

Lankester ER (1877) Memoirs: notes on the embryology and classification of the animal kingdom: comprising a revision of speculations relative to the origin and significance of the germ-layers. Q J Microsc Sci 2:399–454

Lemaire P (2009) Unfolding a chordate developmental program, one cell at a time: invariant cell lineages, short-range inductions and evolutionary plasticity in ascidians. Dev Biol 332:48–60

Lemaire P (2011) Evolutionary crossroads in developmental biology: the tunicates. Development 138(11):2143–2152

Marino R, Melillo D, Di Fillippo M, Yamada A, Pinto M, De Santis R, Brown ER, Matassi G (2007) Ammonium channel expression is essential for brain development and function in the larva of Ciona intestinalis. J Comp Neurol 503:135–147

Matthysse AG, Deschet K, Williams M, Marry M, White AR, Smith WC (2004) A functional cellulose synthase from ascidian epidermis. Proc Natl Acad Sci U S A 101:986–991

Mazet F, Hutt JA, Milloz J, Millard J, Graham A, Shimeld SM (2005) Molecular evidence from *Ciona intestinalis* for the evolutionary origin of vertebrate sensory placodes. Dev Biol 282:494–508

Meedel TH, Farmer SC, Lee JJ (1997) The single MyoD family gene of *Ciona intestinalis* encodes two

differentially expressed proteins: implications for the evolution of chordate muscle gene regulation. Development 124:1711–1721
Meedel TH, Lee JJ, Whittaker J (2002) Muscle development and lineage-specific expression of *CiMDF*, the MyoD family gene of *Ciona intestinalis*. Dev Biol 241:238–246
Meedel TH, Chang P, Yasuo H (2007) Muscle development in *Ciona intestinalis* requires the b-HLH myogenic regulatory factor gene *Ci-MRF*. Dev Biol 302:333–344
Millar R (1954) The breeding and development of the ascidian *Pelonaia corrugata* Forbes and Goodsir. J Mar Biol Assoc U K 33:681–687
Millar R (1962) The breeding and development of the ascidian *Polycarpa tinctor*. Q J Microsc Sci 3:399–403
Millar RH (1971) The biology of ascidians. Adv Mar Biol 9:1–100. doi:10.1016/S0065-2881(08)60341-7, Elsevier
Milne-Edwards H (1841) Observations sur les ascidies composées des côtes de la Manche. Chez Fortin-Masson et Cie, Paris
Milne-Edwards H (1843) Élémens de Zoologie, Ou, Leçons Sur L'anatomie, La Physiologie, La Classification et Les Moeurs Des Animaux. Fortin Masson, Paris
Minokawa T, Yagi K, Makabe KW, Nishida H (2001) Binary specification of nerve cord and notochord cell fates in ascidian embryos. Development 128:2007–2017
Mochizuki Y, Satou Y, Satoh N (2003) Large-scale characterization of genes specific to the larval nervous system in the ascidian *Ciona intestinalis*. Genesis 36:62–71
Mukai H, Koyama H, Watanabe H (1983) Studies on the reproduction of three species of *Perophora* (Ascidiacea). Biol Bull 164:251–266
Nakashima K, Yamada L, Satou Y, Azuma J, Satoh N (2004) The evolutionary origin of animal cellulose synthase. Dev Genes Evol 214:81–88
Nakauchi M (1982) Asexual development of ascidians: its biological significance, diversity, and morphogenesis. Am Zool 22:753–763
Nakauchi M (1986) Oozooid development and budding in the polyclinid ascidian, *Parascidia flemingii* (Urochordata). J Zool 208:255–267
Nakayama A, Satou Y, Satoh N (2001) Isolation and characterization of genes that are expressed during *Ciona intestinalis* metamorphosis. Dev Genes Evol 211:184–189
Nakayama-Ishimura A, Chambon J-p, Horie T, Satoh N, Sasakura Y (2009) Delineating metamorphic pathways in the ascidian *Ciona intestinalis*. Dev Biol 326:357–367
Nakazawa K, Yamazawa T, Moriyama Y, Ogura Y, Kawai N, Sasakura Y, Saiga H (2013) Formation of the digestive tract in *Ciona intestinalis* includes two distinct morphogenic processes between its anterior and posterior parts. Dev Dyn 242:1172–1183
Negishi T, Takada T, Kawai N, Nishida H (2007) Localized PEM mRNA and protein are involved in cleavage-plane orientation and unequal cell divisions in ascidians. Curr Biol 17:1014–1025
Nicol D, Meinertzhagen I (1988a) Development of the central nervous system of the larva of the ascidian, *Ciona intestinalis* L: I. The early lineages of the neural plate. Dev Biol 130:721–736
Nicol D, Meinertzhagen I (1988b) Development of the central nervous system of the larva of the ascidian, *Ciona intestinalis* L: II. Neural plate morphogenesis and cell lineages during neurulation. Dev Biol 130:737–766
Nielsen C (1995) Animal evolution: interrelationships of the living phyla. Oxford University Press, Oxford
Nielsen C (2002) The phylogenetic position of entoprocta, ectoprocta, phoronida, and brachiopoda. Integr Comp Biol 42:685–691
Nishida H (1987) Cell lineage analysis in ascidian embryos by intracellular injection of a tracer enzyme III. Up to the tissue restricted stage. Dev Biol 121:526–541
Nishida H (1992) Regionality of egg cytoplasm that promotes muscle differentiation in embryo of the ascidian, *Halocynthia roretzi*. Development 116:521–529
Nishida H (1993) Localized regions of egg cytoplasm that promote expression of endoderm-specific alkaline phosphatase in embryos of the ascidian *Halocynthia roretzi*. Development 118:1–7
Nishida H (1994a) Localization of determinants for formation of the anterior-posterior axis in eggs of the ascidian *Halocynthia roretzi*. Development 120:3093–3104
Nishida H (1994b) Localization of egg cytoplasm that promotes differentiation to epidermis in embryos of the ascidian *Halocynthia roretzi*. Development 120:235–243
Nishida H (1996) Vegetal egg cytoplasm promotes gastrulation and is responsible for specification of vegetal blastomeres in embryos of the ascidian *Halocynthia roretzi*. Development 122:1271–1279
Nishida N (2008) Development of the appendicularian Oikopleura dioica: culture, genome, and cell lineages. Dev Growth Differ 50:S239–S256
Nishida H, Sawada K (2001) *macho-1* encodes a localized mRNA in ascidian eggs that specifies muscle fate during embryogenesis. Nature 409:724–729
Nishikawa T (1991) The ascidians of the Japan sea. II. Publ Seto Mar Biol Lab 35:25–170
Nishino A, Satou Y, Morisawa M, Satoh N (2000) Muscle actin genes and muscle cells in the appendicularian, *Oikopleura longicauda*: phylogenetic relationships among muscle tissues in the urochordates. J Exp Zool 288:135–150
Nishino A, Satou Y, Morisawa M, Satoh N (2001) *Brachyury* (*T*) gene expression and notochord development in *Oikopleura longicauda* (Appendicularia, Urochordata). Dev Genes Evol 211:219–231
Nishino A, Okamura Y, Piscopo S, Brown ER (2010) A glycine receptor is involved in the organization of swimming movements in an invertebrate chordate. BMC Neurosci 11:6

Nishitsuji K, Horie T, Ichinose A, Sasakura Y, Yasuo H, Kusakabe TG (2012) Cell lineage and cis-regulation for a unique GABAergic/glycinergic neuron type in the larval nerve cord of the ascidian *Ciona intestinalis*. Develop Growth Differ 54:177–186

Noda T, Satoh N (2008) A comprehensive survey of cadherin superfamily gene expression patterns in *Ciona intestinalis*. Gene Expr Patterns 8:349–356

Oda-Ishii I, Bertrand V, Matsuo I, Lemaire P, Saiga H (2005) Making very similar embryos with divergent genomes: conservation of regulatory mechanisms of *Otx* between the ascidians *Halocynthia roretzi* and *Ciona intestinalis*. Development 132:1663–1674

Ogasawara M, Di Lauro R, Satoh N (1999) Ascidian homologs of mammalian thyroid peroxidase genes are expressed in the thyroid-equivalent region of the endostyle. J Experimental Zool 285(2):158–169

Ogasawara M, Shigetani Y, Suzuki S, Kuratani S, Satoh N (2001) Expression of thyroid transcription factor-1 (TTF-1) gene in the ventral forebrain and endostyle of the agnathan vertebrate, Lampetra japonica. Genesis 30(2):51–58

Ogura Y, Sakaue-Sawano A, Nakagawa M, Satoh N, Miyawaki A, Sasakura Y (2011) Coordination of mitosis and morphogenesis: role of a prolonged G2 phase during chordate neurulation. Development 138:577–587

Okuda Y, Ogura E, Kondoh H, Kamachi Y (2010) B1 SOX coordinate cell specification with patterning and morphogenesis in the early zebrafish embryo. PLoS Genet 6:e1000936

Paffenhöfer G-A, Köster M (2011) From one to many: on the life cycle of *Dolioletta gegenbauri* Uljanin (Tunicata, Thaliacea). J Plankton Res 33:1139–1145

Pancer Z, Gershon H, Rinkevich B (1995) Coexistence and possible parasitism of somatic and germ cell lines in chimeras of the colonial urochordate *Botryllus schlosseri*. Biol Bull 189:106–112

Paris M, Brunet F, Markov GV, Schubert M, Laudet V (2008) The amphioxus genome enlightens the evolution of the thyroid hormone signaling pathway. Dev Genes Evol 218:667–680

Pasini A, Amiel A, Rothbächer U, Roure A, Lemaire P, Darras S (2006) Formation of the ascidian epidermal sensory neurons: insights into the origin of the chordate peripheral nervous system. PLoS Biol 4:e225

Pasini A, Manenti R, Rothbächer U, Lemaire P (2012) Antagonizing retinoic acid and FGF/MAPK pathways control posterior body patterning in the invertebrate chordate *Ciona intestinalis*. PLoS One 7:e46193

Pérez-Portela R, Bishop J, Davis AR, Turon X (2009) Phylogeny of the families Pyuridae and Styelidae (Stolidobranchiata, Ascidiacea) inferred from mitochondrial and nuclear DNA sequences. Mol Phylogenet Evol 50:560–570

Perrier E (1898) Note sur la Classification des Tuniciers. CR Acad Sci Paris 124:1758–1762

Picco V, Hudson C, Yasuo H (2007) Ephrin-Eph signalling drives the asymmetric division of notochord/neural precursors in *Ciona* embryos. Development 134:1491–1497

Prodon F, Sardet C, Nishida H (2008) Cortical and cytoplasmic flows driven by actin microfilaments polarize the cortical ER-mRNA domain along the a–v axis in ascidian oocytes. Dev Biol 313:682–699

Raff RA, Love AC (2004) Kowalevsky, comparative evolutionary embryology, and the intellectual lineage of evo-devo. J Exp Zool B Mol Dev Evol 302:19–34

Razy-Krajka F, Lam K, Wang W, Stolfi A, Joly M, Bonneau R, Christiaen L (2014) Collier/OLF/EBF-dependent transcriptional dynamics control pharyngeal muscle specification from primed cardiopharyngeal progenitors. Dev Cell 29:263–276

Rinkevich Y, Voskoboynik A, Rosner A, Rabinowitz C, Paz G, Oren M, Douek J, Alfassi G, Moiseeva E, Ishizuka KJ (2013) Repeated, long-term cycling of putative stem cells between niches in a basal chordate. Dev Cell 24:76–88

Roberts B, Davidson B, MacMaster G, Lockhart V, Ma E, Wallace SS, Swalla BJ (2007) A complement response may activate metamorphosis in the ascidian *Boltenia villosa*. Dev Genes Evol 217:449–458

Roegiers F, Djediat C, Dumollard R, Rouvière C, Sardet C (1999) Phases of cytoplasmic and cortical reorganizations of the ascidian zygote between fertilization and first division. Development 126:3101–3117

Romer AS (1967) Major steps in vertebrate evolution. Science (New York, NY) 158(3809):1629–1637

Rothbächer U, Bertrand V, Lamy C, Lemaire P (2007) A combinatorial code of maternal GATA, Ets and β-catenin-TCF transcription factors specifies and patterns the early ascidian ectoderm. Development 134:4023–4032

Roure A, Lemaire P, Darras S (2014) An Otx/Nodal regulatory signature for posterior neural development in ascidians. PLoS Genet 10:e1004548

Sabbadin A, Zaniolo G, Majone F (1975) Determination of polarity and bilateral asymmetry in palleal and vascular buds of the ascidian *Botryllus schlosseri*. Dev Biol 46:79–87

Saito M, Seki M, Amemiya S, Yamasu K, Suyemitsu T, Ishihara K (1998) Induction of metamorphosis in the sand dollar *Peronella japonica* by thyroid hormones. Develop Growth Differ 40:307–312

Sander K, Fischer J-L (1992) How to dart ascidian blastomeres: the embryological micro-tools of Laurent Chabry (1855–1893). Dev Genes Evol 201:191–193

Sardet C, Speksnijder J, Inoue S, Jaffe L (1989) Fertilization and ooplasmic movements in the ascidian egg. Development 105:237–249

Sardet C, Nishida H, Prodon F, Sawada K (2003) Maternal mRNAs of PEM and macho 1, the ascidian muscle determinant, associate and move with a rough endoplasmic reticulum network in the egg cortex. Development 130:5839–5849

Sardet C, Paix A, Prodon F, Dru P, Chenevert J (2007) From oocyte to 16-cell stage: cytoplasmic and cortical reorganizations that pattern the ascidian embryo. Dev Dyn 236:1716–1731

Sasaki A, Miyamoto Y, Satou Y, Satoh N, Ogasawara M (2003) Novel endostyle-specific genes in the ascidian *Ciona intestinalis*. Zool Sci 20:1025–1030

Sasakura Y, Nakashima K, Awazu S, Matsuoka T, Nakayama A, Azuma J, Satoh N (2005) Transposon-mediated insertional mutagenesis revealed the functions of animal cellulose synthase in the ascidian *Ciona intestinalis*. Proc Natl Acad Sci U S A 102:15134

Sasakura Y, Kanda M, Ikeda T, Horie T, Kawai N, Ogura Y, Yoshida R, Hozumi A, Satoh N, Fujiwara S (2012) Retinoic acid-driven *Hox1* is required in the epidermis for forming the otic/atrial placodes during ascidian metamorphosis. Development 139:2156–2160

Satoh N (2013) Developmental genomics of ascidians. Wiley-Blackwell, Hoboken, p 216

Satou Y (1999) *posterior end mark 3* (*pem-3*), an ascidian maternally expressed gene with localized mRNA encodes a protein with *Caenorhabditis elegans* MEX-3-like KH domains. Dev Biol 212:337–350

Satou Y, Satoh N (1997) *posterior end mark 2* (*pem-2*), *pem-4*, *pem-5*, and *pem-6*: maternal genes with localized mRNA in the ascidian embryo. Dev Biol 192:467–481

Satou Y, Takatori N, Yamada L, Mochizuki Y, Hamaguchi M, Ishikawa H, Chiba S, Imai K, Kano S, Murakami SD (2001) Gene expression profiles in *Ciona intestinalis* tailbud embryos. Development 128:2893–2904

Satou Y, Takatori N, Fujiwara S, Nishikata T, Saiga H, Kusakabe T, Shin-i T, Kohara Y, Satoh N (2002) *Ciona intestinalis* cDNA projects: expressed sequence tag analyses and gene expression profiles during embryogenesis. Gene 287:83–96

Satou Y, Kawashima T, Kohara Y, Satoh N (2003) Large scale EST analyses in *Ciona intestinalis*. Dev Genes Evol 213:314–318

Satou Y, Imai KS, Satoh N (2004) The ascidian *Mesp* gene specifies heart precursor cells. Development 131:2533–2541

Seo HC, Kube M, Edvardsen RB, Jensen MF, Beck A, Spriet E, Gorsky G, Thompson EM, Lehrach H, Reinhardt R (2001) Miniature genome in the marine chordate *Oikopleura dioica*. Science 294:2506

Seo H, Edvardsen RB, Maeland AD, Bjordal M, Jensen MF, Hansen A, Flaat M, Weissenbach J, Lehrach H, Wincker P, Reinhardt R, Chourrout D (2004) Hox cluster disintegration with persistent anteroposterior order of expression in Oikopleura dioica. Nature 431:67–71

Sherrard K, Robin F, Lemaire P, Munro E (2010) Sequential activation of apical and basolateral contractility drives ascidian endoderm invagination. Curr Biol 20:1499–1510

Shi W, Levine M (2008) Ephrin signaling establishes asymmetric cell fates in an endomesoderm lineage of the *Ciona* embryo. Development 135:931–940

Shirae-Kurabayashi M, Nishikata T, Takamura K, Tanaka KJ, Nakamoto C, Nakamura A (2006) Dynamic redistribution of *vasa* homolog and exclusion of somatic cell determinants during germ cell specification in *Ciona intestinalis*. Development 133:2683–2693

Small K, Brudno M, Hill M, Sidow A (2007) A haplome alignment and reference sequence of the highly polymorphic *Ciona savignyi* genome. Genome Biol 8:R41

Somorjai IM, Somorjai RL, Garcia-Fernàndez J, Escrivà H (2012) Vertebrate-like regeneration in the invertebrate chordate amphioxus. Proc Natl Acad Sci 109:517–522

Sorrentino M, Manni L, Lane N, Burighel P (2000) Evolution of cerebral vesicles and their sensory organs in an ascidian larva. Acta Zool 81:243–258

Søviknes AM, Glover JC (2008) Continued growth and cell proliferation into adulthood in the notochord of the appendicularian *Oikopleura dioica*. Biol Bull 214:17–28

Spada F, Steen H, Troedsson C, Kallesøe T, Spriet E, Mann M, Thompson EM (2001) Molecular patterning of the oikoplastic epithelium of the larvacean tunicate *Oikopleura dioica*. J Biol Chem 276:20624–20632

Spagnuolo A, Ristoratore F, Di Gregorio A, Aniello F, Branno M, Di Lauro R (2003) Unusual number and genomic organization of *Hox* genes in the tunicate *Ciona intestinalis*. Gene 309:71–79

Squarzoni P, Parveen F, Zanetti L, Ristoratore F, Spagnuolo A (2011) FGF/MAPK/Ets signaling renders pigment cell precursors competent to respond to Wnt signal by directly controlling *Ci-Tcf* transcription. Development 138:1421–1432

Stach T, Winter J, Bouquet J-M, Chourrout D, Schnabel R (2008) Embryology of a planktonic tunicate reveals traces of sessility. Proc Natl Acad Sci 105:7229–7234

Stefaniak L, Zhang H, Gittenberger A, Smith K, Holsinger K, Lin S, Whitlatch RB (2012) Determining the native region of the putatively invasive ascidian *Didemnum vexillum* Kott, 2002. J Exp Mar Biol Ecol 422:64–71

Stolfi A, Christiaen L (2012) Genetic and genomic toolbox of the chordate *Ciona intestinalis*. Genetics 192:55–66

Stolfi A, Levine M (2011) Neuronal subtype specification in the spinal cord of a protovertebrate. Development 138:995–1004

Stolfi A, Gainous TB, Young JJ, Mori A, Levine M, Christiaen L (2010) Early chordate origins of the vertebrate second heart field. Science 329:565

Stolfi A, Wagner E, Taliaferro JM, Chou S, Levine M (2011) Neural tube patterning by Ephrin, FGF and Notch signaling relays. Development 138:5429–5439

Stolfi A, Lowe EK, Racioppi C, Ristoratore F, Brown CT, Swalla BJ, Christiaen L (2014) Divergent mechanisms regulate conserved cardiopharyngeal development and gene expression in distantly related ascidians. eLife. doi:10.7554/eLife.03728

Stoner DS, Weissman IL (1996) Somatic and germ cell parasitism in a colonial ascidian: possible role for a highly polymorphic allorecognition system. Proc Natl Acad Sci 93:15254–15259

Sugino YM, Matsumura M, Kawamura K (2007) Body muscle-cell differentiation from coelomic stem cells in colonial tunicates. Zool Sci 24:542–546

Sutton MF (1960) The sexual development of *Salpa fusiformis* (Cuvier) Part I. J Embryol Exp Morpholog 8:268–290

Swalla B (2006) Building divergent body plans with similar genetic pathways. Heredity 97:235–243

Swalla BJ, Jeffery WR (1990) Interspecific hybridization between an anural and urodele ascidian: differential expression of urodele features suggests multiple mechanisms control anural development. Dev Biol 142:319–334

Swalla BJ, Jeffery WR (1992) Vestigial brain melanocyte development during embryogenesis of an anural ascidian. Develop Growth Differ 34:17–25

Swalla BJ, Cameron CB, Corley LS, Garey JR (2000) Urochordates are monophyletic within the deuterostomes. Syst Biol 49:52–64

Tagawa K, Jeffery WR, Satoh N (1997) The recently-described ascidian species *Molgula tectiformis* is a direct developer. Zool Sci 14:297–303

Takahashi H, Mitani Y, Satoh G, Satoh N (1999) Evolutionary alterations of the minimal promoter for notochord-specific *Brachyury* expression in ascidian embryos. Development 126:3725–3734

Takamura K, Fujimura M, Yamaguchi Y (2002) Primordial germ cells originate from the endodermal strand cells in the ascidian *Ciona intestinalis*. Dev Genes Evol 212:11–18

Takatori N, Kumano G, Saiga H, Nishida H (2010) Segregation of germ layer fates by nuclear migration-dependent localization of *Not* mRNA. Dev Cell 19: 589–598

Tang WJ, Chen JS, Zeller RW (2013) Transcriptional regulation of the peripheral nervous system in Ciona intestinalis. Dev Biol 378:183–193

Tarallo R, Sordino P (2004) Time course of programmed cell death in *Ciona intestinalis* in relation to mitotic activity and MAPK signaling. Dev Dyn 230:251–262

Tassy O, Dauga D, Daian F, Sobral D, Robin F, Khoueiry P, Salgado D, Fox V, Caillol D, Schiappa R (2010) The ANISEED database: digital representation, formalization, and elucidation of a chordate developmental program. Genome Res 20:1459–1468

Tatián M, Lagger C, Demarchi M, Mattoni C (2011) Molecular phylogeny endorses the relationship between carnivorous and filter-feeding tunicates (Tunicata, Ascidiacea). Zool Scr 40:603–612

Telford MJ, Copley RR (2011) Improving animal phylogenies with genomic data. Trends Genet 27:186–195

Terakubo HQ, Nakajima Y, Sasakura Y, Horie T, Konno A, Takahashi H, Inaba K, Hotta K, Oka K (2010) Network structure of projections extending from peripheral neurons in the tunic of ascidian larva. Dev Dyn 239:2278–2287

Thompson EM, Kallesøe T, Spada F (2001) Diverse genes expressed in distinct regions of the trunk epithelium define a monolayer cellular template for construction of the oikopleurid house. Dev Biol 238:260–273

Tiozzo S, Christiaen L, Deyts C, Manni L, Joly JS, Burighel P (2005) Embryonic versus blastogenetic development in the compound ascidian *Botryllus schlosseri*: insights from *Pitx* expression patterns. Dev Dyn 232:468–478

Tiozzo S, Brown FD, De Tomaso AW (2008) Regeneration and stem cells in ascidians. In: Bosch TCG (ed) Stem cells from hydra to man. Springer, Dordrecht, pp 95–112

Todaro F (1880) Sui primi fenomeni dello sviluppo delle Salpe. Atti R Accad Lincei 3 Trans 4(3):86–89

Tokuoka M, Satoh N, Satou Y (2005) A bHLH transcription factor gene, *Twist-like1*, is essential for the formation of mesodermal tissues of *Ciona* juveniles. Dev Biol 288:387–396

Tokuoka M, Kumano G, Nishida H (2007) FGF9/16/20 and Wnt-5α signals are involved in specification of secondary muscle fate in embryos of the ascidian, *Halocynthia roretzi*. Dev Genes Evol 217:515–527

Tolkin T, Christiaen L (2012) Development and evolution of the ascidian cardiogenic mesoderm. Curr Top Dev Biol 100:107

Treen N, Yoshida K, Sakuma T, Sasaki H, Kawai N, Yamamoto T, Sasakura Y (2014) Tissue-specific and ubiquitous gene knockouts by TALEN electroporation provide new approaches to investigating gene function in *Ciona*. Development 141:481–487

True JR, Haag ES (2001) Developmental system drift and flexibility in evolutionary trajectories. Evol Dev 3:109–119

Tsagkogeorga G, Turon X, Hopcroft RR, Tilak M-K, Feldstein T, Shenkar N, Loya Y, Huchon D, Douzery EJ, Delsuc F (2009) An updated 18S rRNA phylogeny of tunicates based on mixture and secondary structure models. BMC Evol Biol 9:187

Tsagkogeorga G, Cahais V, Galtier N (2012) The population genomics of a fast evolver: high levels of diversity, functional constraint, and molecular adaptation in the tunicate *Ciona intestinalis*. Genome Biol Evol 4:852–861

Tsuda M, Sakurai D, Goda M (2003) Direct evidence for the role of pigment cells in the brain of ascidian larvae by laser ablation. J Exp Biol 206:1409–1417

Tzahor E, Evans SM (2011) Pharyngeal mesoderm development during embryogenesis: implications for both heart and head myogenesis. Cardiovasc Res 91:196–202

Ueda N, Degnan SM (2013) Nitric oxide acts as a positive regulator to induce metamorphosis of the ascidian *Herdmania momus*. PLoS One 8:e72797

Veeman MT, Nakatani Y, Hendrickson C, Ericson V, Lin C, Smith WC (2008) Chongmague reveals an essential role for laminin-mediated boundary formation in chordate convergence and extension movements. Development 135:33–41

Veeman MT, Newman-Smith E, El-Nachef D, Smith WC (2010) The ascidian mouth opening is derived from the anterior neuropore: reassessing the mouth/neural tube relationship in chordate evolution. Dev Biol 344:138–149

Vinson JP, Jaffe DB, O'Neill K, Karlsson EK, Stange-Thomann N, Anderson S, Mesirov JP, Satoh N, Satou Y, Nusbaum C (2005) Assembly of polymorphic genomes: algorithms and application to *Ciona savignyi*. Genome Res 15:1127–1135

Voskoboynik A, Soen Y, Rinkevich Y, Rosner A, Ueno H, Reshef R, Ishizuka KJ, Palmeri KJ, Moiseeva E, Rinkevich B (2008) Identification of the endostyle as a stem cell niche in a colonial chordate. Cell Stem Cell 3:456–464

Voskoboynik A, Neff NF, Sahoo D, Newman aM, Pushkarev D, Koh W, Quake SR (2013) The genome

sequence of the colonial chordate, Botryllus schlosseri. eLife 2:e00569–e00569
Wada H (1998) Evolutionary history of free-swimming and sessile lifestyles in urochordates as deduced from 18S rDNA molecular phylogeny. Mol Biol Evol 15:1189–1194
Wada H (2001) Origin and evolution of the neural crest: a hypothetical reconstruction of its evolutionary history. Develop Growth Differ 43:509–520
Wada S, Saiga H (2002) *HrzicN*, a new Zic family gene of ascidians, plays essential roles in the neural tube and notochord development. Development 129:5597–5608
Wada H, Holland PWH, Sato S, Yamamoto H, Satoh N (1997) Neural tube is partially dorsalized by overexpression of *HrPax-37*: the ascidian homologue of *Pax-3* and *Pax-7*. Dev Biol 187:240–252
Wada H, Saiga H, Satoh N, Holland P (1998) Tripartite organization of the ancestral chordate brain and the antiquity of placodes: insights from ascidian *Pax-2/5/8*, *Hox* and *Otx* genes. Development 125:1113–1122
Wagner E, Levine M (2012) FGF signaling establishes the anterior border of the *Ciona* neural tube. Development 139:2351–2359
Wagner E, Stolfi A, Choi YG, Levine M (2014) Islet is a key determinant of ascidian palp morphogenesis. Development 141:3084–3092
Wang W, Razy-Krajka F, Siu E, Ketcham A, Christiaen L (2013) NK4 antagonizes Tbx1/10 to promote cardiac versus pharyngeal muscle fate in the ascidian second heart field. PLoS Biol 11:e1001725
Whittaker J (1973) Segregation during ascidian embryogenesis of egg cytoplasmic information for tissue-specific enzyme development. Proc Natl Acad Sci 70:2096–2100
Whittaker J (1977) Segregation during cleavage of a factor determining endodermal alkaline phosphatase development in ascidian embryos. J Exp Zool 202:139–153
Whittaker J (1982) Muscle lineage cytoplasm can change the developmental expression in epidermal lineage cells of ascidian embryos. Dev Biol 93:463–470
Wicht H, Lacalli TC (2005) The nervous system of amphioxus: structure, development, and evolutionary significance. Can J Zool 83:122–150
Willey A (1894) Amphioxus and the ancestry of the vertebrates. Macmillan, New York, p 316
Winchell CJ, Sullivan J, Cameron CB, Swalla BJ, Mallatt J (2002) Evaluating hypotheses of deuterostome phylogeny and chordate evolution with new LSU and SSU ribosomal DNA data. Mol Biol Evol 19:762–776
Yagi K, Satou Y, Satoh N (2004) A zinc finger transcription factor, *ZicL*, is a direct activator of *Brachyury* in the notochord specification of *Ciona intestinalis*. Development 131:1279–1288
Yagi K, Takatori N, Satou Y, Satoh N (2005) *Ci-Tbx6b* and *Ci-Tbx6c* are key mediators of the maternal effect gene C*i-macho1* in muscle cell differentiation in *Ciona intestinalis* embryos. Dev Biol 282: 535–549
Yasuo H, Hudson C (2007) *FGF8/17/18* functions together with *FGF9/16/20* during formation of the notochord in *Ciona* embryos. Dev Biol 302:92–103
Yasuo H, Satoh N (1998) Conservation of the developmental role of *Brachyury* in notochord formation in a urochordate, the ascidian *Halocynthia roretzi*. Dev Biol 200:158–170
Yokobori S, Kurabayashi A, Neilan BA, Maruyama T, Hirose E (2006) Multiple origins of the ascidian-Prochloron symbiosis: molecular phylogeny of photosymbiotic and non-symbiotic colonial ascidians inferred from 18S rDNA sequences. Mol Phylogenet Evol 40:8–19
Yokoyama T, Hotta K, Oka K (2014) Comprehensive morphological analysis of individual peripheral neuron dendritic arbors in ascidian larvae using the photoconvertible protein kaede. Dev Dyn 243:1362–1373
Young CM, Gowan RF, Dalby J, Pennachetti CA, Gagliardi D (1988) Distributional consequences of adhesive eggs and anural development in the ascidian *Molgula pacifica* (Huntsman, 1912). Biol Bull 174:39–46
Zeng L, Swalla BJ (2005) Molecular phylogeny of the protochordates: chordate evolution. Can J Zool 83:24–33
Zeng L, Jacobs MW, Swalla BJ (2006) Coloniality has evolved once in stolidobranch ascidians. Integr Comp Biol 46:255–268
Zimmer R, Larwood G (1973) Living and fossil bryozoa. Academic, Lawrence

Index

A
Abdomen, 61, 150, 183
Aboral, 3, 14, 15, 17, 19, 20, 33–35, 38–40–44, 70, 72, 166
Aboral field, 70, 72
Acoela, 139
Acorn worm, 60, 61, 63, 74, 78, 79
Acrosome, 12, 97
Actin, 153, 167
Actomyosin, 154
Adhesive organ, 166–167
Adultation, 147, 166, 167, 171, 181, 185, 186, 188–193
Adult muscle progenitor, 169
Agassiz, 62, 70, 73–75
Ambulacraria, 2, 6, 30, 31, 60, 63, 75, 77, 78, 80–82, 139, 140, 191
Amphioxus, 77, 92, 141
Ampulla, 3, 43, 148, 152, 154, 177, 179
Anatomy, 43, 62, 64, 72, 73, 110, 115, 121, 142, 151, 160, 163, 185, 186, 189, 190
Ancestral, 6–8, 49, 76, 77, 79, 94, 105, 106, 111, 114–116, 118, 120–122, 137, 140, 141, 147, 157, 185, 188, 191
Animal-vegetal (AV) axis, 15, 17, 26, 66, 154, 155
Annelid, 43, 62, 99, 115, 118, 119, 121, 139
Anterior ectoderm, 66, 69, 117
Anterior endoderm, 23, 83
Anterior-posterior (AP) axis, 39–41–44, 48, 66, 79, 81, 106, 115, 118, 154–157, 159, 160, 163, 185
Antibodies, 20, 22, 75, 76, 117
Anural, 152–154, 185, 186, 190, 192
Anus, 3, 6, 15, 16, 20, 22, 23, 28, 30, 41, 42, 60, 61, 67, 69, 71, 72, 108, 138
AP axis. *See* Anterior-posterior (AP) axis
Apical constriction, 156
Apical organ, 17, 28, 73, 75, 76, 78
Apical tuft, 70, 76
Aplidium, 150, 183, 188
Aplousobranchia, 136
Aplousobranchs, 136, 141, 183
Apomorphy, 3
Appendage, 43, 120, 165
Appendicularia, 136, 137, 141, 192
Aquaculture, 96
Archenteron, 11, 15–18, 20, 22, 26, 28, 30–32, 37, 41, 44, 63, 66, 69, 77, 79, 95, 100
Arm, 15, 18, 24, 25, 43–46, 65
Arthropod, 115, 116, 118, 121
Ascidiacea, 136, 172
Ascidian, 79, 83, 93, 97, 99, 101, 103, 104, 118, 136, 137, 139–141–143–145–147–157, 159–161, 164–170, 172, 174–176, 178–180–183, 185, 186, 188, 190–193
Ascidiella, 142, 188
Asexual, 45, 46, 144, 147, 148, 175, 181–185, 188, 190, 191
Asexual reproduction, 45, 147, 175, 181–185, 191
Asteroidea, 2, 4, 8, 20–26, 38
Asterozoa–Echinozoa hypothesis, 6, 7
Asymmetric cell division, 169
Asymmetron, 92–94, 122
Asymmetry, 4, 5, 17, 20, 37, 82, 122, 156, 169, 171
Asynchronous, 66
Atria, 96, 108, 148, 166, 168, 177, 179, 183, 190
Atrium, 96, 166
Atubaria, 64
Auricularia, 6–8, 23–28, 31–33, 37, 140
Axial mesoderm, 151
Axial organ, 3
Axis, 15–19, 26, 38–45, 48, 66, 79, 81–83, 105, 106, 111, 118, 154, 156, 157, 159–161, 163, 179, 185

B
Balanoglossus, 60, 62, 69–71, 73–77, 82, 83
BarH, 82
Basal, 3, 6, 15, 16, 31, 71, 79, 92, 93, 121, 138, 139, 141, 175, 180, 181
Basic helix-loop-helix (bHLH) factor, 171
Basolateral shortening, 156
Bateson, W., 61–63, 66, 77, 79, 83, 118, 138
Beta-catenin (β-catenin), 34, 36, 79, 105, 106, 113, 156, 168, 171
bHLH factor. *See* Basic helix-loop-helix (bHLH) factor
Bilaterality, 38
Bilateral symmetry, 40, 44, 76, 147, 154, 155, 158
Bilateria, 9, 41, 48
Bilaterian, 18, 37, 41–43, 79, 80, 105, 116, 118–119, 121, 122, 163, 180
Bipartite organization, 160
Bipinnaria, 6, 8, 20–22, 26, 28, 31, 35, 62

A. Wanninger (ed.), *Evolutionary Developmental Biology of Invertebrates 6: Deuterostomia*
DOI 10.1007/978-3-7091-1856-6, © Springer-Verlag Wien 2015

Blastema, 24, 25, 45, 46
Blastocoel, 13–15–17, 19, 20, 22, 26, 30–32, 72, 74, 95, 100, 105
Blastocoelar cell, 14, 17, 19, 20, 22, 26
Blastogenesis, 144, 145, 147, 175, 181, 182, 190–191, 193
Blastomere, 10, 12, 13, 16, 20, 26, 29, 30, 37, 79, 94, 95, 98, 99, 101, 103, 104, 142, 143, 154–156, 161, 162, 167, 169–171, 175, 179, 190
Blastomere isolation, 79
Blastoporal, 30, 41, 95, 104, 105
Blastopore, 16, 17, 26, 30–32, 66, 69, 95, 97–101, 103–107, 138
Blastozooid, 148, 175, 184, 185, 188, 190, 193
Blastula, 13–16, 18–20–22, 26, 27, 29, 30, 36, 66, 69, 77, 95, 97, 99, 100, 104
Blood, 60, 71, 149, 171, 179, 180, 182, 183, 185
Blood cell, 171, 182, 185
Bmp2/4, 79–81–83
BMPs. *See* Bone morphogenic proteins (BMPs)
Body plan, 2–4, 10, 31, 37, 38, 40, 41, 78, 83, 121, 136, 138, 140, 151, 185, 188, 190, 193
Body wall, 3, 42, 43, 47, 61, 69, 108, 168, 169
Boltenia, 148, 172, 179, 188
Bone morphogenic proteins (BMPs), 105
Botryllus, 144, 145, 163, 176, 177, 179, 181–183, 190
Bra, 36, 82, 169
Brachiolaria, 8, 20, 26
Brachiopod, 137, 139
Brachyury, 35, 169
Brain, 3, 35–37, 61, 108–116, 118, 122, 151, 160, 161, 180, 185
Branchial basket, 149
Branchial nerve, 62, 73, 75
Branching, 48
Branchio-genital region, 61
Branchiomeric neurons, 160
Branchiostoma, 92–95, 97–100, 104, 105, 107, 108, 111, 122, 163, 180
Brittle star, 2, 7, 28–30, 33, 37
Brood, 6, 176, 186, 188–191
Brooding, 150, 177, 181, 186, 192
Buccal, 40, 71, 96
Buccal cavity, 71
Bud, 44, 98, 106, 107, 118, 150, 160, 170, 181–184, 186, 188, 190, 193
Budding, 61, 107, 144, 150, 181–186
Burrowing, 61, 69

C

CAB. *See* Centrosome-attracting body (CAB)
Cadherin, 157
Caenorhabditis, 9
Caenorhabditis elegans (C. elegans), 9
Calyx, 42
Cambrian, 4, 5, 42, 61–63
Canonical Wnt, 84
Cardiopharyngeal mesoderm, 167–169
Catastrophic metamorphosis, 178, 188
Caudal, 114, 151, 165, 166
Caudal epidermal sensory neurons (CESNs), 165, 166
Caudalization, 167, 188
Cdx, 24
Cell, 3, 60, 93, 137
Cell adhesion, 26
Cell division, 16, 30, 98, 104, 143, 147, 156, 158, 159, 161, 168, 169, 171
Cell junction, 13
Cell labeling, 22, 66
Cell lineage, 15, 18, 22, 30, 36, 37, 48, 142–144, 147, 149, 154, 155, 157, 158, 162, 174, 176
Cell type, 15, 17, 18, 22, 26, 35, 47, 75, 115, 149, 161, 163, 165, 167, 172, 181, 183, 184
Cellulose, 136, 137, 165, 179
Cellulose synthase, 165, 179
Central canal, 71
Central nervous system (CNS), 35, 40, 44, 45, 73, 79, 82, 83, 103, 107–118, 121, 122, 146, 149, 151, 157–162, 178–180, 185
Centrosome, 97, 155
Centrosome-attracting body (CAB), 155, 156
Cephalochordate, 77, 78, 92, 93, 122, 138, 140, 141, 162, 163, 176, 178, 180, 181, 191
Cephalodiscus, 60, 62, 64, 65
cER. *See* Endoplasmic reticulum-rich cortex (cER)
Cerebral, 96, 108–111, 114, 190
CESNs. *See* caudal epidermal sensory neurons (CESNs)
Chaetopterus, 119
Change, 3, 8–10, 15–17, 35, 38, 46–48, 72, 74, 93, 113, 121, 140, 141, 153, 178, 181
Chemistry, 78
Chordata, 2, 6, 63, 77, 78, 92, 138, 139, 141, 191
Chordate, 163, 169, 175, 178, 180, 185, 192
Chorion, 154
Cidaroid, 38, 39
Cilia, 15, 16, 20, 22, 30, 66, 107, 109, 175
Ciliary band, 6, 8, 15, 17, 20, 22, 25, 26, 28–30–33, 35, 62, 63, 66, 69, 70, 72–74–76, 78, 139, 140
Ciliary photoreceptor, 75, 109
Cilium, 75, 100, 103, 109, 117
Ciona, 35, 93, 142–147, 149, 151, 156–158, 160–172, 174–176, 178–181, 188, 190
Circulatory system, 183
Cirri, 92, 96, 108
Cis-regulatory element, 147
Cis-regulatory module, 37
Clavelina, 150, 183, 188
Cleavage, 13, 15, 16, 18–20, 22, 26, 27, 30, 31, 33, 62, 65, 66, 69, 76, 77, 95, 98–101, 105, 154, 155
Cleavage pattern, 66, 69, 77, 155
Clonal, 147, 160, 165, 169, 171, 191
Cnemidocarpa, 179
Cnidarian, 45, 105
CNS. *See* central nervous system (CNS)
Cocoon, 65
Coeloblastula, 66, 69, 77
Coelom, 3, 17, 20, 23, 26, 28, 38, 39, 41–43, 74, 77
Coelomic, 3, 14, 15, 17, 19, 21, 23, 25, 27–30, 38, 40–44, 46, 47, 63, 66, 70, 72–74, 77
Coelomic cavity, 63, 66, 70, 72–74, 77
Coelomic pouch, 15, 17, 19, 40, 77

Coenecium, 60, 61, 64, 65
Collar, 60–63, 66–68, 70–76, 82, 83
Collinearity, 163
Colonial, 60, 61, 63, 136, 137, 139, 144, 145, 147, 148, 150, 172, 176, 181, 183, 184, 186, 188–193
Coloniality, 181, 188, 190–193
Colony, 60–65, 136, 137, 139, 141, 144, 145, 147, 148, 150, 172, 175–177, 181–186, 188–190–193
Column, 2, 6, 8, 22, 40, 68, 72, 74, 93, 109, 112, 115, 116, 158, 159, 163, 169, 171, 174, 175, 184
Competency period, 188
Competent, 40, 48, 70, 74, 176, 180
Compound cilia, 66
Conklin, E.G., 97, 99, 101, 103, 104, 107, 108, 142, 143, 154, 155, 167
Connective, 3
Convergence, 16, 28, 153, 161, 169, 172, 191, 192
Convergent extension, 16, 169, 172
Co-opted, 37, 44, 118–120, 122, 193
Co-option, 35, 42, 165, 191
Cord, 3, 10, 47, 61–63, 68, 71–73, 75, 76, 82, 83, 93, 95, 96, 105, 108, 111, 112, 114, 115, 139, 146, 148, 160, 161, 163, 180, 185
Cortex, 99, 154
Craniata, 139–141, 191
Craniate, 140, 165, 193
Creeping-type larva, 66
Crinoidea, 2–4, 6, 8, 23, 24, 31–33, 38
Crustacea, 136
Crustacean, 136
Cryptic species, 92
Cryptosyringida hypothesis, 6, 7
Cut, 108, 178
Cyathozooid, 175, 184
Cyst, 145, 163, 164
Cytoplasm, 97, 104, 143, 154, 167, 184

D
Degeneration phase, 40
Delamination, 16, 17, 26, 164
Delay, 179, 181, 188
Delta, 22, 33–36, 103, 113, 117, 118, 158, 162, 165, 169
Delta-Notch pathway, 33, 34, 113, 118, 158, 165, 169
Determinant, 10, 101, 143, 154–156, 168, 193
Deuterocerebrum, 112
Deuterostome, 11, 16, 41–45, 63, 64, 66, 76–79, 81, 118, 119, 122, 137, 139–141, 178, 180, 191
Deuterostomia, 9, 63, 78, 138–140, 191
Development, 3, 62, 94, 137
Developmental biology, 10, 12, 37, 136, 142–144
Developmental evolution, 136
Developmental gene, 44, 93, 101, 111, 121, 140, 143, 146, 190
Developmental system drift (DSD), 149, 167, 193
Diazona, 188, 190
Didemnum, 145, 183, 192
Differentiation, 15, 17, 28, 30, 31, 35, 45, 47, 61, 66, 71, 77, 116, 117, 143, 144, 153–155–157, 159–161–163–165, 167, 169, 171, 172, 175, 177–179–181–183–186, 188, 190, 193
Digestive system, 15, 20, 26, 29, 46
Digestive tract, 17, 22, 26, 30, 40, 41, 47, 61, 69, 71, 73, 74, 96, 149, 171
Dipleurula, 6, 31, 63, 78, 139, 141
Diplosoma, 183, 192
Direct development, 137, 152–154, 185, 186, 190
Distalless, 43, 104, 116, 120
Division, 12, 13, 16, 26, 29, 30, 97, 104, 143, 147, 155, 159–161, 168, 169, 171
Dlx, 79, 80, 83, 111, 113, 114, 116, 164
Doliolaria, 8, 28, 31–33
Doliolid, 175, 184, 193
Doliolida, 136
Dorsal ectoderm, 69, 80–82, 103
Dorsal nerve cord, 61, 68, 71, 73, 82, 148
Dorso-ventral (DV) axis, 17, 39, 79, 81–83, 115, 160, 161
Drosophila, 9, 112, 115, 116, 121
DSD. *See* Developmental system drift (DSD)
D/V patterning, 16, 79–83, 106, 112, 114–116

E
EAT. *See* Extraxial-axial theory (EAT)
Echinodermata, 1–49, 63, 77, 78, 139, 140
Echinoidea, 2, 4, 8, 12–20, 23, 24, 38
Echinopluteus, 8, 28, 30, 37
ECM. *See* Extracellular matrix (ECM)
Ecteinascidia, 165, 188
Ectoderm, 14–17, 19–22, 24–27, 29, 33–36, 38–41, 44, 66, 67, 69, 72, 77, 79–82, 84, 95, 100, 101, 103–105, 107, 109, 112–114, 116–119, 156–167, 182, 183, 191
Ectoneural, 3, 44, 47
Ectoproct, 178
EGF, 178
Egg, 6, 7, 11–13, 28, 32, 65, 66, 93–95, 97–99, 103–105, 143, 144, 147, 153, 154, 175, 184, 188, 190
Elav, 82, 103, 117
Embryo, 3, 65, 95, 138
Embryogenesis, 9–11, 15, 20, 26, 28, 30, 48, 67, 84, 142, 143, 147, 149, 154, 157, 161, 166, 174–176, 178, 185, 190
Embryology, 17, 26, 66–69, 79, 93, 94, 138, 142, 143, 146, 160, 161, 165, 167, 169, 172, 192
Embryonic, 11–12, 15, 18, 19, 23–25, 29, 34, 41, 48, 65, 69, 78, 79, 82, 83, 94, 105, 143, 145, 147, 149, 154, 155, 161, 163, 164, 174–176, 178, 179, 184, 188–190, 193
Emx, 167
Endocrine, 180, 181, 190
Endoderm, 14–19, 21–24, 26, 27, 29, 33–37, 60, 66–69, 77, 82, 83, 100, 101, 104, 119, 122, 149, 151, 156, 157, 167, 171, 176, 179, 181, 183–186, 189
Endodermal, 16, 18, 22, 33–37, 60, 77, 82, 171, 179, 181, 186, 189
Endomesoderm, 11, 14, 18–20, 22–26, 29, 31–36, 66, 69, 79, 122, 165
Endoplasmic reticulum, 99
Endoplasmic reticulum-rich cortex (cER), 154, 155, 167

Endoskeleton, 3
Endostyle (en), 96, 107, 108, 140, 143, 151, 162, 176, 177, 180–181, 184, 185
Engrailed, 44, 82, 113, 114, 118–122
Enhancer, 116, 147, 149
Enterocoely, 63, 119, 120
Enteropneust, 60–77, 79–84, 118, 141
Enteropneusta, 61, 63
Entoproct, 188
Epiboly, 156–158
Epicardium, 183, 186
Epidermis, 3, 40, 69, 71, 76, 157, 158, 165–166, 173, 179, 181, 182, 184
Epimorphic, 45
Epithelial cell, 16, 71, 183
Epithelium, 3, 13, 15, 17, 22, 23, 39, 46, 47, 69, 157, 164, 165, 182, 183
Equal cleavage, 65
Equal division, 13
Esophageal, 17
Esophagus, 3, 15, 17, 20, 22, 26, 28–30, 47, 71, 183
Ets, 46
Eudistoma, 150, 183
Eve. See Even skipped (Eve)
Even skipped (Eve), 121
EvoDevo, 10, 48, 63, 94, 104, 110, 118, 121–122, 144–145
Evolution, 4, 63, 110, 137
Evolutionary change, 10
Evolutionary novelties, 140
Evolution of novelty, 37
Evolution of segmentation, 118
Evx, 163
Excretory system, 3, 60, 71
Expressed gene, 26, 82
Extracellular matrix (ECM), 3, 13, 15, 61, 71
Extra-embryonic tissue, 189
Extraxial-axial theory (EAT), 42, 43
Eya, 190
Eye, 72, 74–76, 96, 108–110, 114, 115, 143, 177
Eye spot, 72, 74–76, 177

F
Fate map, 20, 29, 30, 69, 78, 100–105, 147, 149, 156, 171, 174
Feather star, 2, 8, 31–33, 47
Feeding, 6–9, 12, 13, 17, 18, 20, 22, 30, 31, 39–41, 60–62, 93, 108, 136, 137, 139, 140, 175, 178, 185, 193
Fertilization, 6, 12, 13, 15, 22, 26, 28, 31–33, 93, 95, 97–99, 107, 108, 154–157, 176, 184
Fertilization envelope, 13, 22, 26, 31, 32, 95, 107
Fertilization membrane, 15
Fez, 113, 114, 116
FGFR signaling, 79
FGF signaling, 79, 105, 157, 161, 165, 168, 171
Filter-feeding, 60, 61, 93, 109, 136, 137, 140, 141, 175, 185
Flagellum, 97
Flask-shaped, 28
Flatworm, 45
Floor plate, 113, 115, 158, 161
Fluorescent protein, 171
Fng, 113
Follicle cell, 93
Foregut, 17, 19, 20, 28
Fossil, 4–6, 10, 41–44, 48, 61, 62
Fossilization, 61
FoxA, 24, 33–37, 82, 169, 181
FoxC, 167
FoxD, 116, 121, 164, 169
FoxQ2, 113
Free-swimming, 93, 136, 140, 141, 175, 192
Fushi-tarazu, 121

G
GABAergic, 161
Gain-of-function, 79
Gamete, 10, 12, 13, 93, 94
Ganglia, 30, 109, 117
Ganglion, 146, 160–162, 180, 188, 190
Gap gene, 121
Garstang hypothesis, 140
Gastrula, 9, 14, 20, 26, 28–32, 67–68, 71, 93, 95, 98–101, 103–107, 147
Gastrulation, 11, 15, 16, 18, 20, 22, 26, 28–30, 35, 37–39, 66, 69, 77, 79, 99–101, 104–106, 138, 154–157, 169–171, 174, 185
Gata4/5/6, 24, 156, 157
GATA factor, 46
Gene, 3, 71, 93, 139
Gene duplication, 122
Gene expression, 9, 15, 17, 20, 26, 31, 37, 41, 44, 78–79, 82–84, 94, 99, 107, 110–111, 113–115, 119–120, 122, 143, 145, 147, 158, 160, 161, 163, 174, 193
Gene expression pattern, 20, 80, 84, 105, 121, 141, 149, 157, 160, 161, 163, 176, 181
Gene function, 145
Gene knockdown, 47, 48, 79, 94
gene network, 35, 94, 116, 118–122
Gene regulatory network, 10, 11, 22, 33–37, 45, 48, 122, 146, 147, 161, 172, 193
Gene regulatory network (GRN), 10–12, 33, 35–37
Genital wing, 60, 63, 64
Genome, 9–12, 20, 47, 48, 51, 78, 82, 92, 93, 105, 111, 116, 117, 121, 122, 141–145, 147, 163, 174, 193
Genotype, 182
Germ cell, 3, 98, 99, 122, 171–172, 185
Germ cell determination, 3
Germ layer, 15, 19, 29, 41, 79, 106, 156, 157, 186
Germ line, 3, 122, 145, 156, 171, 182
Giant neuron, 61, 71
Gill, 139, 141
Gill pore, 64, 66–68–69, 71, 73, 74
Gill slit, 60–64, 67, 68, 70, 71, 73–75, 78, 84, 93, 94, 96, 107, 108, 122, 141, 149, 171, 185

Glandiceps, 69, 72, 77
Glia, 47, 48
Glomerulus, 60, 61, 68, 71, 73, 74, 77
Gonad, 3, 7, 60, 64, 92, 94, 99, 136, 171
Gonoduct, 3
Gonozooid, 184, 185
Gradient, 13, 83, 106, 156, 161
Gradual, 71, 75, 78, 108
Graptolithina, 62
Grid, 105, 158, 159
GRN. *See* Gene regulatory network (GRN)
Growth, 41, 44, 46, 47, 79, 96, 147, 184, 188, 190, 192
Growth zone, 38, 43–44
Gut, 3, 6–7, 15, 16, 22, 24, 26, 29–31, 35, 40–42, 47, 95, 96, 105, 107, 108, 117, 136, 137, 151, 178, 181, 189, 190

H
Haeckel, E.H., 93, 137, 138, 140, 141
Hairy, 106, 121
Halocynthia, 136, 143–145, 147, 156, 165, 167, 169, 171, 174, 175, 188
Harrimaniidae, 60, 63
Hatching, 22, 65, 68, 71, 72, 83, 100, 107, 147, 152–154, 171, 176, 177
Hatchling, 64, 67, 68, 188
Head mesoderm, 119
Head segment, 112, 119–121
Heart, 60, 66, 68, 71, 73, 77, 107, 149, 167–169, 177, 181, 184, 185
Hedgehog (hh), 83, 113, 121, 122, 161
Heliocidaris, 7–9, 18, 39
Hemichordata, 2, 4, 6, 59–84, 138–140
hemichordate, 28, 30, 60, 63, 71, 76–80, 82–84, 118, 138, 140, 191
Hepatic region, 61, 75
Herdmania, 179, 181
Hermaphrodite, 94
Hermaphroditic, 185
Heterochronic, 39, 175, 181
Heterochrony, 39, 140, 147, 161, 174, 175, 181, 185, 188
hh signaling, 83, 122
Hindgut, 17, 22, 28, 35, 71
Holoblastic, 13, 31, 65, 66, 76
Holoblastic cleavage, 65, 76–77
Holopelagic, 141
Homeobox, 40, 46
Homeobox-containing genes, 40, 46
Homolog, 31, 37, 43, 45–47, 96, 105, 107, 110, 111, 113–117
Homologous, 30, 40, 75, 77, 78, 83, 107, 108, 110, 112, 114–118, 120
Homology, 43, 44, 61, 76–78, 83, 110, 111, 115–116, 120–122, 149–150, 160, 161, 164, 176, 181, 184
Host, 105, 192, 194
Hox cluster, 48, 49, 82, 111, 162, 163
Hox gene, 23, 31, 32, 35, 40–42, 44, 49, 82, 106, 111, 112, 114, 116, 118, 162, 163, 166, 193
Hunchback, 121
Hydra, 45
Hydrocoel, 2, 23, 25, 31, 32, 38–41, 43
Hydropore, 17, 28, 31, 69, 72, 77
Hydroporic canal, 17, 28
Hyponeural, 3, 47
Hypsistozoa, 183, 188–190

I
Identity, 15, 40, 105, 106, 116, 158, 167
Immunocytochemical, 63, 76
Immunostaining, 20, 166
Indirect development, 154
individuality
Induction, 79, 105, 113, 143, 156, 157, 166, 167, 171, 180
Ingression, 15, 20, 28, 29, 33, 37, 156
Innovation, 18, 48, 119
Insect, 119–121
In situ hybridization, 23, 47, 103, 104
Intercalation, 6, 153, 158, 159, 163
Invagination, 16, 22, 26, 30, 31, 33, 35, 38, 39, 95, 99, 100, 156
Inversion, 83, 139, 157
Involution, 99–101, 104, 156
Islet, 115, 117, 160, 167

J
Jelly, 12
JNK, 178
Juvenile, 6, 8, 9, 17, 18, 23–26, 38–40, 43, 44, 62, 64, 65, 67–71, 73–76, 78, 137, 147, 154, 166, 168, 176, 178–181, 185, 186, 190, 191

K
Kernel, 35, 122
Knockdown, 11–12, 47, 48, 79, 80, 94, 113, 122
Kowalevsky, 62, 94, 107, 137, 142, 183
Krohn, A., 62, 74
Krüppel, 121

L
Lab, 34, 46, 48, 94, 97, 122, 143, 144, 148
Labial, 112
Lamella, 108–110, 114
Lamina, 15, 16
Lancelet, 92
Larva, 6, 61, 94, 136
Larvacean, 136, 139–141, 145, 172–175, 178, 185, 190, 192–193
Larval, 6, 62, 94, 137
Larval development, 11–12, 17, 26, 28, 30, 69, 74, 147, 160, 169, 171, 175–179
Larval phase, 6, 185
Lateral protocerebrum, 112
Lattice organ, 3
Lecithotrophy, 6–8, 39

Left-right axis, 18, 39, 81, 122, 161, 163
Lhx3/4, 160, 168, 171
Life cycle, 63, 136, 140, 141, 147, 167, 174, 178, 184, 191, 193
Life history, 6–8, 139, 185–192
Ligament, 3
Limb, 43, 45–47, 122
Limb bud, 43
Lineage, 15, 18, 19, 22, 29, 30, 33, 35–37, 48, 49, 142–144, 147, 149, 154, 155, 157, 158, 161, 162, 165–171, 174, 176, 179, 194
Lineage tracing, 161, 176
Lipid, 12
Liver sac, 60, 61, 63, 64
Longitudinal muscle, 69, 71
Longitudinal patterning gene, 112, 116
Lophophorate, 138, 140
Lophophore, 139, 140
Lophotrochozoa, 139
Lumen, 71, 107, 159, 164, 169, 170, 183, 189

M
Macho1, 155, 167, 168
Macromere, 13, 15, 18
Mantle, 137, 182
Marginal zone, 156, 167
Maternal determinant, 143, 154, 155, 168, 193
Maternal mRNA, 154
Matrix metalloproteinase, 100
Maximum direct development, 190
Mechanosensory, 163, 165
Meioglossus, 63, 76
Meiosis, 154
Melanin, 163
Meridional cleavage, 66
Mesenchymal, 3, 26, 28, 31, 156, 164, 165, 170, 171, 179, 182, 184
Mesenchyme, 15, 16, 18–20, 22, 26–30, 33, 37, 169–171, 179, 181, 183
Mesendoderm, 95, 104, 106, 118, 156, 182
Mesocoel, 60, 64, 71–74, 77
Mesocoel pore, 60, 64, 73
Mesoderm, 15, 17–20, 22–26, 33–35, 37, 39, 41, 43, 46, 66, 67, 72, 77, 79, 81, 83, 95, 101, 103, 104, 106, 107, 116, 118–120, 149, 151, 153, 156, 165, 167–171, 179, 185
Mesodermal, 15, 18, 19, 22, 26, 34–36, 43, 44, 99, 100, 103, 149, 157, 169, 170, 181, 184, 186
Mesogenin, 168
Mesomere, 13, 15
Mesosoma, 61
Mesp, 168
Metacoel, 66–68, 71–74, 77
Metamere, 40, 44
Metamorphic, 178–181, 184, 193
Metamorphosis, 7, 8, 17, 38–41, 48, 62, 65, 69, 70, 75, 78, 83, 94, 96, 103, 107–108, 117, 140, 141, 147, 152, 169, 171, 176–181, 185, 188, 190, 191, 193
Metasoma, 60, 64
Metasome, 65
Metazoa, 138
Metazoan, 18, 31, 79, 165, 171, 180
MG. *See* Motor ganglion (MG)
MGNs. *See* Motor ganglion neurons (MGNs)
MHB. *See* Midbrain-hindbrain boundary (MHB)
Microbial symbiont, 192
Micromere, 13–15, 18–20, 22, 33–37
Midbrain-hindbrain boundary (MHB), 110–115, 161
Midgut, 26, 28, 76
Midline, 71, 74, 83, 95, 96, 100, 103, 104, 107, 108, 115, 117, 158, 163, 165
Midline cell, 100, 103, 159
miRNA, 115, 139
Mitf, 164
Mitochondria, 92, 98, 99, 139, 154, 167, 184
Mitochondrial genome, 92
Mitosis, 47, 156
Mitotic spindle, 156
Model organism, 9, 10, 48, 144, 145
Model species, 46, 143, 178
Modification, 10, 17, 74, 140
Molgula, 136, 145, 147, 149, 152, 153, 164, 169, 176, 186, 188, 190
Molgulid, 153, 192
Molgulidae, 136, 152–154, 166, 192
Mollusk, 92, 139, 142
Mononucleate, 167
Monophyletic, 139
Monophyly, 139
Morphallaxis, 45
Morphogen, 106, 161
Morphogenesis, 9, 15, 18, 39, 41, 48, 142, 152–154, 158, 169, 171, 172, 185
Morphogen gradient, 161
Morpholino, 12
Morphology, 2, 17, 20, 22, 28, 30, 35, 37, 38, 41, 43, 45, 46, 48, 60, 63, 67, 68, 74, 78, 93, 94, 109, 114, 121, 136–139, 161, 162, 166, 173
Mosaic, 97, 101, 142, 143
Mosaic development, 143
Motor ganglion (MG), 146, 160–162, 188
Motor ganglion neurons (MGNs), 161, 162
Motor neuron, 110, 114, 115, 160–163
Mouth, 3, 6, 15, 17, 20, 22, 26, 28, 29, 31–33, 39, 41–44, 60, 61, 63, 65, 67, 69, 70, 72–74, 92, 96, 107, 108, 117, 138, 173
Mouth shield, 60, 61, 65
Msh, 112, 116
Msx, 83, 112, 114, 116, 117, 164
Multipotent, 167, 183
Muscle, 15, 17, 19, 20, 28, 34, 44, 47, 69, 71, 107, 115, 116, 118–121, 137, 138, 143, 149, 151, 153–155, 157, 160, 161, 166–169, 171, 174, 179, 181, 182, 185, 188
Muscle founder cell, 155, 168
Muscle precursor, 157, 167, 168
Musculature, 69, 71, 99, 169, 173, 179
MyoD, 167
Myogenic regulatory factor, 167

Myoplasm, 99, 103, 142, 167, 168
Myosin, 167
MyTF, 165

N
Nanos, 3, 98, 99
Nematode, 147
Nemertea, 62
Nemertean, 62
Neoteny, 118, 173–174
Neotroch, 62, 63, 69, 70, 72, 74, 75, 78
Nephridia, 77, 78
Nephridium, 78, 107
Nerve, 3, 10, 44, 61–62, 78
Nerve cord, 3, 10, 47, 61, 68, 71–73, 75, 76, 82, 83, 93, 95, 96, 105, 108, 111, 112, 115–116, 139, 146, 148, 160, 161, 163, 179–180, 185
Nerve net, 61, 68, 71, 75, 76, 82, 122
Nerve ring, 3, 24, 25, 73, 75, 76
Nervous system, 3, 15, 17, 18, 26, 35, 39, 40, 42–48, 61–62, 68, 73, 75, 76, 78, 79, 82–84, 110–116, 145, 146, 178, 181, 185
Neural crest, 109, 116–118, 121, 163–165, 193
Neural plate, 72, 83, 95, 99–101, 103, 104, 107, 113–117, 157–159, 162–166, 174, 193
Neural plate border cells (NPBCs), 164, 165
Neural tube, 61, 83, 100, 108, 112, 137, 140, 141, 151, 157–161, 164, 166, 179
Neurite, 71, 75, 76
Neurite bundle, 75, 76
Neuroanatomy, 110
Neuroblast, 109, 112, 116
NeuroD, 165–166
Neuroectoderm, 105, 112, 113, 117
Neurogenesis, 22, 23, 71, 75–76, 80, 82, 84, 110–111
Neuropeptide, 115
Neuropil, 61, 71, 72, 75, 78
Neuropore, 95, 107, 109, 166
Neurotransmitter, 46, 75–76
Neurotroch, 70, 72
Neurula, 95, 101, 103, 106–108, 111, 113, 114, 117, 147
Neurulation, 71, 72, 155, 157–159, 174
Nitric oxide (NO), 179
NK2.1, 22, 25
NK4, 169
Nodal, 81, 82, 84, 105, 158
Non-skeletogenic mesoderm (NSM), 15–19, 24, 25, 33–34
Notch/Delta, 22, 33–36, 113, 118, 158, 165, 169
Notch pathway, 34, 106
Notch signaling pathway, 162
Notochord, 61, 83, 93, 95, 96, 99–101, 103–105, 113, 115, 116, 137, 138, 141, 148, 151–153, 156, 157, 163, 169–174, 179, 185, 188
Notoneuron, 141
Novelties, 37, 140, 141
NPBC. *See* Neural plate border cells (NPBCs)
NSM. *See* Non-skeletogenic mesoderm (NSM)
Nuclei, 95, 173
Nucleus, 13, 95, 97, 98, 156

O
Ocellus (oc), 148, 163, 164
Ocular, 44
Oikopleura, 93, 145, 162, 163, 173, 174
Oikosins, 173
Olfactorean, 141, 144, 192
Olfactores, 139, 141, 192
Ontogenetic, 43, 77
Ontogeny, 5, 43, 45, 69, 78, 168, 169, 193
Onychophoran, 121
Oocytes, 20, 29, 66, 79, 93, 95, 97
Oogenesis, 12, 154
Oozooid, 175, 177, 179, 183–185, 188, 190, 193
Ophiopluteus, 8, 28, 29
Ophiuroidea, 2, 4, 8, 23, 24, 28–30, 46
Opisthotroch, 66, 67, 69, 70, 72–76
Oral-aboral axis, 15, 17, 38–40, 43
Oral field, 17, 70, 72, 75
Ordovician, 6
Organizer, 79, 105–107, 110–114, 161
Organogenesis, 122, 169
Orthologous, 149
Orthologs, 22, 82, 164, 181, 190
Osmoregulation, 3
Ossicle, 3, 26, 28, 37, 44
Otolith (ot), 148, 163, 164
Otx, 24, 31, 37, 39, 40, 111, 113, 114, 116, 160, 161
Ovary, 12, 93, 145

P
Paedomorphosis, 118
Paired, 66, 71, 74, 77, 110, 114, 121, 153
Pair rule gene, 121
Palp, 148, 166, 167, 178, 179
ParaHox, 20, 22, 163
Parapodia, 43
Parasite, 192
Paraxial mesoderm, 151, 153, 185
PAT, 178, 179
Patched, 83
Pattern, 7, 16, 72, 77, 83, 113, 117, 138, 145, 158, 162, 163, 176, 193
Patterning, 16, 18, 22, 23, 31, 40, 78–84, 105, 106, 111, 112, 114–116, 122, 156, 158, 160–163, 166, 173, 178, 188, 190, 192, 193
Pax3/7, 83, 115, 116, 162, 164
Pax6, 25, 31, 83, 108, 111, 113, 117, 160
Pelagic, 62–66, 72, 136, 139–141, 175, 184, 192
Pelonaia, 190
Pentamer, 2, 6, 37, 38, 40–45, 48, 78
Pentaradial, 5, 8
Peribranchial atrium, 166
Peribranchial chamber, 167, 169, 171
Pericardium, 60, 61, 66, 68, 70, 72–74, 77, 78, 183, 184
Perihaemal, 73, 74
Peripheral nervous system (PNS), 40, 61, 149, 151, 157, 161, 163, 165
Perophora, 183, 184, 190
Phalloidin, 149, 152

Phallusia, 142, 145, 188
Pharynx, 61, 69, 73, 74, 96, 108, 119, 180–183
Phenotype, 7, 8, 179
Phlebobranch, 136, 141, 144, 145, 149, 166, 172, 181, 183, 184, 188, 190
Phlebobranchia, 136, 149
Phoronid, 139
Photolith, 148, 163
Photoreceptor, 75, 96, 103, 108–111, 115, 160, 163
Phylogenetic, 4–6, 8, 38, 62–64, 77, 78, 92, 93, 122, 136, 139–141, 146, 147, 172, 188
Phylogenetic analysis, 4, 63, 64, 92, 93
Phylogenetic tree, 5, 92, 172
Phylogeny, 6, 38, 64, 136, 142, 147, 175, 191
Phylotypic, 37, 193
Pigment cell, 17, 19, 20, 22, 34, 108, 109, 163–165
Placenta, 188
Placode, 109, 116–118, 163–165, 190
Planarian, 45
Planktonic, 7, 8, 17, 66, 173
Planktotrophic, 6, 39
Plasticity, 5, 193
Plate, 3, 14–16, 18–20, 22, 26, 30, 35, 41, 44, 63, 72, 83, 95, 99–101, 103, 104, 107, 113–115–117, 153, 157–159, 161–163–166, 169, 174, 193
Platyhelminthes, 45, 191
Platynereis, 119
Plesiomorphic, 5, 6, 77, 78, 180
Pluteus, 7, 8, 13–15, 17, 18, 22, 28–30
Polar bodies, 29, 93, 95, 97, 98, 101, 154, 155
Polarity, 37, 79, 121, 172
Pole cell, 157
Pole plasm, 98, 99, 103
Polyandrocarpa, 150, 181
Polycarpa, 190
Postanal field, 66
Postanal tail, 67–69, 71, 151, 173
Postembryonic development, 41, 48
Posterior ectoderm, 66, 69
Posterior end mark (PEM), 155, 156
Posterior endoderm, 167
Posterior growth zone, 44
Posterior lobe, 31
Posterior sensory vesicle (PSV), 146, 160
Postplasmic mRNA, 154
Precambrian, 4
Primary germ cell, 171
Primary lobe, 70, 72
Primary mesenchyme cells (PMCs), 15, 16, 20, 22, 33
Primordial germ cells (PGCs), 171–172, 179
Primordium, 40, 166, 181, 182, 184
Prism stage, 17
Proboscis, 60, 61, 63, 66–76
Proboscis pore, 60, 69–71, 73, 74
Proboscis skeleton, 63, 68, 71, 73, 75
Proboscis stalk, 61, 71
Proboscis stem, 61, 68, 71, 73, 75, 76
Proboscis vesicle, 72, 74
Programmed cell death, 147, 178, 179
Proliferation, 47, 159, 170, 180, 193
Prosoma, 60
Protocerebrum, 112
Protocoel, 60, 66, 68–70, 72, 74, 77
Ptc, 83, 113
Pterobranch, 60–66, 84, 139, 140, 191
Pterobranchia, 61–62
Ptychodera, 62, 63, 67, 69, 72, 77–82
Ptychoderidae, 60, 63, 66
Pycnoclavella, 183
Pyrosome, 175, 178, 184, 188, 193
Pyrosomida, 136

R
Radial cleavage, 66, 76, 77
Ras/ERK pathway, 157
Recapitulation, 140–142, 182
Reconstruction, 16, 68, 73, 77, 94, 111, 114, 121, 140, 141, 163, 186
Redundancy, 153
Regeneration, 9, 10, 24, 25, 45–48, 108, 191, 193
Regionalization, 17, 20, 26, 28, 35, 84, 110–111, 115, 159–161, 180
Regressive change, 74, 144, 175, 177, 179, 180, 193
Regulation, 9–11, 18, 22, 26, 33–37, 41–43, 45, 48, 78, 97, 101, 104–106, 113, 114, 116, 117, 121, 122, 142, 143, 145–147, 155–158, 161, 162, 165, 167–169, 172, 178, 180, 181, 188, 193
Regulative capacities, 188
Regulative development, 183
Regulatory network, 10, 145, 168
Remodelling, 47, 69, 74, 75, 103, 108, 178–180
Respiration, 47, 61, 185
Retina, 111, 115
Retinoic acid (RA), 105, 106, 166
Retractor, 16, 178, 185
Rhabdomeric photoreceptor, 75
Rhabdopleura, 62, 64, 65
Ring canal, 40
Romer hypothesis, 139, 140
Roof plate, 115, 158, 161
Roughest, 32, 153
Row, 61, 67, 96, 108, 142, 170, 174
Rudiment, 8, 15, 16, 18, 23, 38–40, 44, 47, 110, 151, 165, 171, 185
Run, 71
Runt, 121

S
18S, 93, 136, 140
Saccoglossus, 60, 62, 64, 66–69, 71, 72, 75, 77–84
Salpida, 136
Salps, 175, 178–179, 184, 193
Schistocerca, 121
Schizocardium, 63
Schizocoely, 66, 77, 94, 107, 119, 120
Sea cucumber, 2, 7, 26–28, 30, 31, 33
Sea lily, 2, 8, 31–33
Sea stars, 2, 3, 7–8, 20–26, 35–40, 46, 48, 62

Sea urchin, 2, 7, 9–20, 22–23, 26, 28, 30, 33, 35–42, 44, 69, 75, 105, 122, 143
Secondary cell, 167, 169, 171
Secondary lobe, 62, 72
Secondary mesenchyme cells (SMCs), 16–17, 19, 20
Segment, 18, 44, 106, 112, 118–122, 138, 153, 183, 184, 193
Segmentation gene, 44, 118–121
Segment polarity, 121
Segment polarity gene, 121
Sensory organ, 65, 141, 148
Sensory vesicle (SV), 146, 151, 159, 160, 163, 164, 178–180
Serial homology, 120
Seriality, 16, 44, 68, 73, 75, 97, 111, 114, 120, 160–161, 182
Serotonergic, 17, 22, 28, 30, 61, 71, 76, 114, 115
Serotonin, 28, 75–76, 82
Sessile, 60, 61, 63, 118, 136, 140, 141, 174, 178, 185, 192
Sessility, 141
Settlement, 40, 65, 70, 73–75, 147, 148, 153, 154, 171, 176–179, 183, 185, 188
Sex determination, 144
Sexual, 7, 45, 46, 61, 93, 94, 141, 144, 147, 148, 175, 179, 181–185, 188, 190–191
Shell, 62
Shh, 113, 115, 122, 161
Shield, 60, 61, 65
Short gastrulation, 38, 39
Sicyonia
Signal, 18, 19, 22, 33–36, 39, 40, 79–84, 103–106, 113, 117, 118, 121, 122, 143, 145, 146, 156–158, 160–162, 165–169, 171, 172, 178–180, 190, 193
Signalling pathway, 79, 81
Siphon, 136, 137, 148, 166–169, 171, 177, 179, 182, 190
siRNA, 79
Six3, 22, 25, 31, 82
Six3/6, 111, 113, 114, 117
Skeletogenic cells, 15, 17–19, 22, 24–26, 29, 33, 37
Skeleton, 3, 15, 16, 18, 20, 22, 25–26, 28–30, 35, 37, 39, 42–43, 63, 68, 71, 73, 75, 169
Slit, 60–64, 67, 68, 70, 71, 73–75, 78, 84, 93, 94, 96, 107, 108, 122, 140, 141, 149, 171, 185, 190
Smoothened, 74, 92, 104, 107
Snail, 79, 164
Solitary, 60, 63, 136, 137, 141, 143, 144, 147–149, 152, 157, 159, 167, 172, 174, 176, 179, 181, 184, 186, 190–193
Somatocoel, 23, 31, 32, 38, 41–43
Somite, 43, 95, 98–101, 103–108, 110, 111, 115, 118–120, 185
Somitogenesis, 119
SoxB1, 22
Sp8, 167
Spawning, 6, 28, 29, 66, 78, 93–97, 176
Specification, 3–6, 10–12, 15, 17–20, 22, 23, 26, 28, 29, 33–37, 40, 42, 43, 45, 47–49, 62, 72, 74–76, 78, 79, 83, 106, 113, 115, 116, 122, 140–147, 150, 151, 153–158, 160–164, 167, 169, 171–173, 178–181, 183–186, 193, 194
Spemann's organizer, 105
Spengelidae, 63, 66, 69, 77
Spengel, J.W., 61, 63, 69, 70, 72–74, 77
Sperm, 12, 13, 93, 97–99, 154, 184
Spicule, 3, 16, 17, 26, 28–30, 37
Spinal cord, 111, 112, 114, 115, 160, 161
Spine, 23, 39
Spiral, 4
Stalk, 4, 31, 40, 60–62, 64, 65, 71
Stalked crinoid, 31
Statocyst, 163, 164
Stellate cell, 184
Stem cell, 144, 182–184
Stereom, 3, 4
Stolidobranch, 136, 144, 145, 149, 152, 166, 172, 181–183, 186, 188
Stolidobranchia, 136, 144, 145, 149, 152, 166, 172, 181–183, 186, 188
Stolon, 175, 183, 184, 190
Stolonial budding, 150, 183, 184
Stomochord, 60–63, 67, 68, 70, 71, 73–75, 83
Stomodeum, 17, 158
Stripe, 118–120, 165
Strobilation, 150, 183
Strongylocentrotus, 2, 8–12, 15, 17, 20, 22, 33, 34, 39, 48
Styela, 142, 143, 188
Superficial, 28, 30, 60, 151
Symbion, 192, 194
Symmetry, 4, 38–45, 48, 76, 82, 99, 147, 154–156, 158
Symplegma, 150, 181–182
Synapomorphy, 60, 78, 136, 138, 141
Synapticle, 63, 64
Synchronous, 10, 26, 30, 78, 97, 144, 145, 184, 193
Syncytium, 93, 145

T

Tailbud, 98, 106, 107, 118, 151, 160, 166, 170
Tailless, 152, 153, 192
Target gene, 79, 145, 172
Tbx1/10, 119, 120, 169
Tbx6, 167, 168
Tentacle nerve, 61–62
Tentacles, 40, 47, 60–62, 64, 65, 72, 74, 139, 140
Terminal budding, 184
Terrestrialisation, 144
Test, 65, 76, 139, 180
Tetrazooid, 175, 184
Thaliacea, 136, 137, 141, 172, 175, 178, 181, 184–185, 193
Thoracic, 151, 153, 183
Thrombospondins, 178
Thyroid gland, 107–108, 140, 176, 180–181
Thyroid hormone (TH), 75, 108, 180, 181, 190
Thyroxine (T4), 180, 190
Tinman, 107
Tongue bar, 71, 73, 74
Tornaria, 6, 28, 62, 63, 66, 69, 70, 72–76, 78, 84, 140
Torquaratoridae, 63

Transcription, 9, 10, 33, 46–48, 78, 80, 82, 141, 145, 156, 168, 171, 172
Transcription factor (TF), 23, 33, 34, 37, 46, 82, 83, 106, 113, 145, 146, 160, 164–169, 172, 190
Transcriptome data, 9, 78
Transcriptomes, 9, 141, 172
Transdifferentiation, 47, 183
Transforming growth factor (TGF), 46, 79
Transgenesis, 12, 48, 122, 143, 147, 149
Transmission, 72, 97, 104, 107, 111, 191, 192, 194
Transplantation, 105, 111, 113, 182, 184
Tree, 5, 47, 92, 172, 174
TRIAC, 180
Tripartite organisation, 65, 160
Tritocerebrum, 112
Trochaea hypothesis, 141
Trophozooids, 185
Tropomyosin, 167
Troponin, 167
Trunk, 60, 61, 63–71, 73–76, 149, 151, 169
Tube foot, 3, 40
Tuft, 15, 70, 72, 76
Tunic, 137, 144, 149, 165, 166, 171, 179, 183, 185, 191, 192, 194
Tunicata, 135–194
Tunicate, 43, 92, 93, 97, 101, 103, 118, 136–147, 149, 163, 165, 172–176, 178, 180, 181, 185, 191–193
Twist, 165, 171

U
Unequal cleavage, 13, 15, 30, 156
Unequal division, 13, 15
Urbilateria, 121–122
Urochordata, 138
Urodele, 152, 153, 190
U-shaped, 61, 71, 73, 74, 137

V
Vasa, 98, 99, 171, 172
Vegetal (Veg), 13–20, 22, 26, 29–33, 35, 36, 66, 69, 79, 95, 97–99, 103, 104, 142, 154–157, 167, 168, 171
Ventral midline, 74, 83, 96, 103, 104, 108, 115, 117, 165
Ventral nerve cord (VNC), 61, 68, 71, 75, 76, 83, 108, 112
Ventral stalk nerve, 61–62
Vermiform, 60–62, 141, 185
Vertebrata, 138–141, 191, 192
Vertebrates, 43–45, 48, 79, 82, 83, 92–94, 99, 105–108, 110–121, 138, 140–142, 145, 147, 151, 153, 157, 160–162, 164, 165, 169, 180, 181, 185, 190
Vestibule, 23, 31, 32, 38–40
Visceral, 45–47
Visceral muscle, 47
Vitellaria, 8, 30, 31, 33
Vitelline, 12, 13, 66, 95
Vitelline membrane, 13, 66
Viviparity, 147, 189, 190
Viviparous, 188

W
Wada Hypothesis, 139, 140
Walking leg, 100, 116
Water vascular system (WVS), 2, 3, 38, 40, 42
Web, 9, 34, 104
Wings, 60, 63, 64
Wnt, 40, 84, 105, 106, 113, 114, 118, 119, 121, 122
Wnt6, 47
Wnt8, 113
Wnt/β-catenin signaling pathway, 34, 105, 106, 113
Wnt gene, 119
Wnt signaling, 106, 113, 118, 122
Wound healing, 47

X
Xenacoelomorpha, 2, 64, 191
Xenoturbella, 139

Y
Yellow, 15, 20, 26, 29, 32, 65, 80, 101, 143, 151, 163, 167, 186
Yolk, 12, 18, 26, 30, 65, 66, 77, 97, 99, 103, 151, 175, 188

Z
Zooids, 61, 64–66, 144, 147, 148, 150, 175, 177, 182–184, 189, 190, 193
Zygote, 7, 13, 34, 65, 66, 95, 97, 98, 103, 154, 155, 168